The Spectrum of Molecular Nitrogen

Alf Lofthus

Institute of Physics, University of Oslo, Oslo, Norway

and

Paul H. Krupenie

Optical Physics Division, National Bureau of Standards, Washington, D.C. 20234

This is a critical review and compilation of the observed and predicted spectroscopic data on the molecule N_2 and its ions N_2^-, N_2^+, N_2^{2+}, and the molecule N_3. Each electronic band system is discussed in detail, and tables of band origins and heads are given. In addition to the gas phase electronic, electron and Raman spectra, there are also examined the spectra of condensed molecular nitrogen as well as the pressure- and field-induced infrared and microwave absorption. Dissociation energy of N_2, predissociations, and perturbations are discussed. Potential energy curves are given, as well as radiative lifetimes, *f*-values, and Franck-Condon integrals. Molecular constants are listed for the known electronic states. Electronic structure and theoretical calculations are reviewed.

Key words: Critical review; Franck-Condon integrals; molecular constants; molecular nitrogen; potential energy curves; radiative lifetimes; spectrum.

Contents

	Page
1. Introduction	117
2. Electronic Structure of N_2, N_2^+, N_2^{2+}, and N_2^-	118
2.1. Molecular Orbitals	118
2.2. Electronic Structure of N_2; Rydberg States	120
2.3. Electronic Structure of N_2^+	121
2.4. Electronic Structure of N_2^{2+}	122
2.5. Theoretical Calculations	122
3. Electronic Spectrum of N_2, N_2^+, N_2^{2+}, and N_3	123
3.1. $a^1\Pi_g - X^1\Sigma_g^+$ Lyman-Birge-Hopfield System (2600–1000 Å) R	124
3.2. $a'^1\Sigma_u^- - X^1\Sigma_g^+$ Ogawa-Tanaka-Wilkinson-Mulliken System (2000–1080 Å) R	126
3.3. $w^1\Delta_u - X^1\Sigma_g^+$ Tanaka Absorption System (1400–1140 Å) R	126
3.4. $a''^1\Sigma_g^+ - X^1\Sigma_g^+$ Dressler-Lutz System (1010.5 Å)	127
3.5. $b^1\Pi_u - X^1\Sigma_g^+$, $b'^1\Sigma_u^+ - X^1\Sigma_g^+$, $c_n{}^1\Pi_u - X^1\Sigma_g^+$, $c_n'^1\Sigma_u^+ - X^1\Sigma_g^+$, and $o_n{}^1\Pi_u - X^1\Sigma_g^+$ Systems (1300–800 Å) R; Absorption Spectrum of Vibrationally Excited N_2	127
a. Historical	128
b. $b^1\Pi_u - X^1\Sigma_g^+$ System (1110–850 Å) R	130
c. $b'^1\Sigma_u^+ - X^1\Sigma_g^+$ System (1290–820 Å) R	131
d. $c_n{}^1\Pi_u - X^1\Sigma_g^+$ System (960–860 Å)	131
e. $c_n'^1\Sigma_u^+ - X^1\Sigma_g^+$ System (960–860 Å)	131
f. $o^1\Pi_u - X^1\Sigma_g^+$ System (950–880 Å)	133
g. Absorption Spectrum of Vibrationally Excited N_2 (1900–600 Å)	133
3.6. $^1\Sigma_u^+ - a^1\Pi_g$ and $^1\Pi_u - a^1\Pi_g$ Gaydon-Herman Singlet Systems (3670–2220 Å) R,V	133
3.7. $x^1\Sigma_g^- - a'^1\Sigma_u^-$ Fifth Positive System (3070–2030 Å) V	135
3.8. $y^1\Pi_g - a'^1\Sigma_u^-$ and $y^1\Pi_g - w^1\Delta_u$ Kaplan First and Second Systems (2860–2070 Å) V	136
3.9. $k^1\Pi_g - a'^1\Sigma_u^-$ and $k^1\Pi_g - w^1\Delta_u$ Carroll-Subbaram First and Second Systems (2700–2300 Å) V	136
3.10. $a^1\Pi_g - a'^1\Sigma_u^-$ and $w^1\Delta_u - a^1\Pi_g$ McFarlane Infrared Systems (30,000–85,000 Å)	137
3.11. $A^3\Sigma_u^+ - X^1\Sigma_g^+$ Vegard-Kaplan System (5325–1250 Å) R	137
3.12. $B^3\Pi_g - A^3\Sigma_u^+$ First Positive System (25,310–4780 Å) V	138
3.13. $C^3\Pi_u - B^3\Pi_g$ Second Positive System (5460–2680 Å) V	139
3.14. $B^3\Pi_g - X^1\Sigma_g^+$ Wilkinson System (1685–1640 Å) R	140
3.15. $B'^3\Sigma_u^- - X^1\Sigma_g^+$ Ogawa-Tanaka-Wilkinson System (2240–1120 Å) R	140

Copyright © 1977 by the U.S. Secretary of Commerce on behalf of the United States. This copyright will be assigned to the American Institute of Physics and the American Chemical Society, to whom all requests regarding reproduction should be addressed.

Page

3.16. $C^3\Pi_u - X^1\Sigma_g^+$ Tanaka System (1130-1070 Å) R 140
3.17. $B'^3\Sigma_u^- - B^3\Pi_g$ Infrared Afterglow System (8900–6050 Å) R 140
3.18. $W^3\Delta_u \rightleftarrows B^3\Pi_g$ Wu-Benesch Infrared System (22,000–43,000 Å) R,V 141
3.19. $W^3\Delta_u - X^1\Sigma_g^+$ Saum-Benesch System (1505–1440 Å) R 141
3.20. $C'^3\Pi_u - B^3\Pi_g$ Goldstein-Kaplan System (5080–2860 Å) R 141
3.21. $D^3\Sigma_u^+ - B^3\Pi_g$ Fourth Positive System (2900–2250 Å) V 142
3.22. $E^3\Sigma_g^+ - A^3\Sigma_u^+$ Herman-Kaplan System (2740–2130 Å) V 142
3.23. $H^3\Phi_u - G^3\Delta_g$ Gaydon-Herman Green System (6370–5040 Å) V 143
3.24. Herman Infrared System (9100–7000 Å) V 144
3.25. Rydberg Series (960–490 Å) 144
a. $(N_2^+ X^2\Sigma_g^+)\, c_n{}^1\Pi_u \leftarrow X^1\Sigma_g^+$ Worley-Jenkins Rydberg Series (960–780 Å) 145
b. $(N_2^+ X^2\Sigma_g^+)\, c_n'{}^1\Sigma_u^+ \leftarrow X^1\Sigma_g^+$ Carroll-Yoshino Rydberg Series (960–805 Å) 145
c. $(N_2^+ X^2\Sigma_g^+)\, c_n{}^1\Pi_u \leftarrow a''{}^1\Sigma_g^+$ Ledbetter Rydberg Series (865–820 Å) 146
d. $(N_2^+ A^2\Pi_u) \leftarrow X^1\Sigma_g^+$ Rydberg Series: $^1\Pi_u - X$ (950–685 Å); $^3\Pi_u - X$ (785–685 Å); $o_n{}^1\Pi_u - X$ Bands (950–815 Å) 146
e. $(N_2^+ B^2\Sigma_u^+) \leftarrow X^1\Sigma_g^+$ Hopfield Series (725–660 Å) 147
f. $(N_2^+ C^2\Sigma_u^+) \leftarrow X^1\Sigma_g^+$ Codling Rydberg Series (555–490 Å) 148
3.26. $B^2\Sigma_u^+ - X^2\Sigma_g^+$ First Negative System of N_2^+ (5870–2860 Å) V, R 148
3.27. $C^2\Sigma_u^+ - X^2\Sigma_g^+$ Second Negative System of N_2^+ (2230–1270 Å) R 149
3.28. $A^2\Pi_{u1} - X^2\Sigma_g^+$ Meinel System of N_2^+ (17,700–5500 Å) R 150
3.29. $^4\Sigma_u^+ - X^2\Sigma_g^+$ d'Incan-Topouzkhanian System of N_2^+ (3920–3820 Å) V 150
3.30. $D^2\Pi_g - A^2\Pi_{u1}$ Janin-d'Incan System of N_2^+ (3070–2050 Å) R 150
3.31. $D^1\Sigma_u^+ - X^1\Sigma_g^+$ Carroll System of N_2^{2+} (1590 Å) 151
3.32. $^2\Sigma_u^+ - X^2\Pi_{g1}$ System of N_3 (2765–2670 Å) V 151
3.33. Unclassified Bands 152
4. Raman Spectrum 153
5. Spectra of Condensed N_2, and N_2 in Matrices; Pressure- and Field-Induced Infrared and Microwave Absorption 154
6. Electron Spectroscopy 155
6.1. Photoelectron Spectroscopy 155

Page

6.2. Auger Electron Spectroscopy; States of N_2^{2+} 156
6.3. Electron Impact Spectroscopy 157
6.4. Penning Ionization 159
6.5. Resonances in Electron Impact; Unstable States of N_2^- 159
7. Perturbations and Splittings 160
7.1. Perturbations in Singlet States 160
7.2. Triplet Splittings in the $A^3\Sigma_u^+$ and $B'^3\Sigma_u^-$ States 163
7.3. Triplet Splittings in the $B^3\Pi_g$, $C^3\Pi_u$, and $C'^3\Pi_u$ States 164
7.4. Λ-Doubling in the $B^3\Pi_g$ and $C^3\Pi_u$ States 164
7.5. Doublet Splittings in the $A^2\Pi_u$ and $D^2\Pi_g$ States of N_2^+ 164
7.6. Rotational Perturbations in the $B^2\Sigma_u^+$ and $A^2\Pi_{u1}$ States 164
7.7. Rotational Perturbations in the $C^2\Sigma_u^+$ State of N_2^+ 165
7.8. Vibrational Perturbations in the $B^2\Sigma_u^+$ and $C^2\Sigma_u^+$ States of N_2^+ 165
8. Dissociation Energies and Predissociations 165
8.1. Dissociation Energy of N_2 and N_2^+ 165
8.2. Predissociations and Dissociation Limits 166
8.3. Predissociation of the $a^1\Pi_g$ State 166
8.4. Predissociation of the $B^3\Pi_g$ State 167
8.5. Predissociation of the $C^3\Pi_u$ and $C'^3\Pi_u$ States 167
8.6. Predissociation of the $b^1\Pi_u$, $c^1\Pi_u$, and $o\,^1\Pi_u$ States 168
8.7. Predissociation of the $b'^1\Sigma_u^+$ and $c'^1\Sigma_u^+$ States 168
8.8. Predissociation of the $x^1\Sigma_g^-$ State 169
8.9. Predissociation of the $y^1\Pi_g$ and $k^1\Pi_g$ States 170
8.10. Predissociation of the $D^3\Sigma_u^+$ State 170
8.11. Predissociation of the $E^3\Sigma_g^+$ State 170
8.12. Predissociation of the $C^2\Sigma_u^+$ State of N_2^+ 170
9. Potential Energy Curves 171
10. Transition Probability Parameters 173
10.1. Franck-Condon Factors and Transition Moments R_e 174
a. $a^1\Pi_g - X^1\Sigma_g^+$ 176
b. $B^3\Pi_g - A^3\Sigma_u^+$ 177
c. $W^3\Delta_u - B^3\Pi_g$ 177
d. $C^3\Pi_u - B^3\Pi_g$ 177
e. $N_2^+\, A^2\Pi_u - X^2\Sigma_g^+$ 177
f. $N_2^+\, B^2\Sigma_u^+ - X^2\Sigma_g^+$ 178
g. Ionization 178
10.2. Radiative Lifetimes and f-values 178
a. $A^3\Sigma_u^+ - X^1\Sigma_g^+$ 179
b. $W^3\Delta_u - B^3\Pi_g$ 179
c. $B^3\Pi_g - A^3\Sigma_u^+$ 180
d. $B'^3\Sigma_u^- - B^3\Pi_g$ 181
e. $a'^1\Sigma_u^-$ 181

Page

f. $a^1\Pi_g$ ... 181
g. $w^1\Delta_u$ ... 182
h. $^5\Sigma_g^+ - B^3\Pi_g$ ... 182
i. $C^3\Pi_u - B^3\Pi_g$ (2+) ... 182
j. $E^3\Sigma_g^+$ ... 183
k. $a''^1\Sigma_g^+ - X^1\Sigma_g^+$ ... 183
l. $b^1\Pi_u - X^1\Sigma_g^+$ ... 184
m. $D^3\Sigma_u^+ - B^3\Pi_g$ ... 184
n. $b'^1\Sigma_u^+ - X^1\Sigma_g^+$ ... 184
o. $c_3{}^1\Pi_u - X^1\Sigma_g^+$ ... 184
p. $H^3\Phi_u - G^3\Delta_g$ ... 184
q. $c_4'{}^1\Sigma_u^+ - X^1\Sigma_g^+$ ... 184
r. Hopfield Rydberg Series ... 184
s. $N_2^+ A^2\Pi_u - X^2\Sigma_g^+$ ... 184
t. $N_2^+ B^2\Sigma_u^+ - X^2\Sigma_g^+$ ... 185
u. $N_2^+ {}^4\Sigma_u^+$ State at 21 eV ... 185
v. $N_2^+ C^2\Sigma_u^+$ ... 186
w. Miscellaneous ... 186

10.3. Absorption in the Extreme Ultraviolet ... 186

11. Miscellaneous; Electric and Magnetic Properties ... 189
12. Summary ... 190
13. Acknowledgments ... 291
14. References ... 291

Appendix A: Notation and Terminology ... 306

Appendix B: Physical Constants and Conversion Factors ... 307

List of Tables

Page

1. Molecular constants, electron configurations, and dissociation products for the electronic states of N_2, N_2^+, and N_2^{2+} ... 194
2. Molecular constants for the electronic states of N_3 ... 198
3. Binding energies (eV) of core and valence electrons in N_2 ... 198
4. Possible Rydberg states for N_2 ... 199
5. Comparison of some calculated and observed Rydberg terms ... 200
6. A–X Rydberg series limits from band head measurements (cm^{-1}) ... 202
7. Band heads and origins of the $a^1\Pi_g - X^1\Sigma_g^+$ Lyman-Birge-Hopfield system (R) ... 203
8. Band heads and origins of the $a^1\Pi_g - X^1\Sigma_g^+$ Lyman-Birge-Hopfield system of $^{14}N^{15}N$ (R) ... 205
9. Band heads and origins of the $a'^1\Sigma_u^- - X^1\Sigma_g^+$ Ogawa-Tanaka-Wilkinson-Mulliken system (R) ... 206
10. Band heads of the $w^1\Delta_u - X^1\Sigma_g^+$ Tanaka absorption system (R) ... 206
11. Bands of the $a''^1\Sigma_g^+ - X^1\Sigma_g^+$ Dressler-Lutz system ... 207
12. Band heads and origins of the $b^1\Pi_u - X^1\Sigma_g^+$ system (R) ... 207
13. Band heads and origins of the $b'^1\Sigma_u^+ - X^1\Sigma_g^+$ system (R) ... 209
14. $(N_2^+ X^2\Sigma_g^+) c_n{}^1\Pi_u - X^1\Sigma_g^+$ Worley-Jenkins Rydberg series ... 212
15. Band heads and origins of the $(N_2^+ X^2\Sigma_g^+)$ $c_n'{}^1\Sigma_u^+ - X^1\Sigma_g^+$ Carroll-Yoshino Rydberg series ... 213
16. $(N_2^+ X^2\Sigma_g^+) c_n{}^1\Pi_u \leftarrow a''^1\Sigma_g^+$ Ledbetter Rydberg series (5980–4360 Å) ... 214
17. Rydberg series converging to the $N_2^+ A^2\Pi_u$ state ... 214
18. Rydberg series converging to the N_2^+ $B^2\Sigma_u^+$ state ... 219
19. Observed bands of the Codling Rydberg series $(C^2\Sigma_u^+) \leftarrow X^1\Sigma_g^+$ (555–490 Å) ... 219
20. Band heads and origins of the $^1\Sigma_u^+ - a^1\Pi_g$ and $^1\Pi_u - a^1\Pi_g$ Gaydon-Herman systems ... 220
21. Band heads and origins of the $x^1\Sigma_g^- - a'^1\Sigma_u^-$ Fifth Positive system (V) ... 221
22. Band heads and origins of the $y^1\Pi_g - a'^1\Sigma_u^-$ Kaplan First system (V) ... 221
23. Band heads and origins of the $y^1\Pi_g - w^1\Delta_u$ Kaplan Second system (V) ... 222
24. Band heads and origins of the $k^1\Pi_g - a'^1\Sigma_u^-$ Carroll-Subbaram I system ... 222
25. Band heads and origins of the $k^1\Pi_g - w^1\Delta_u$ Carroll-Subbaram II system ... 222
26. Observed lines of the McFarlane Infrared systems ... 223
27. Band heads and origins of the $A^3\Sigma_u^+ - X^1\Sigma_g^+$ Vegard-Kaplan system (R) ... 224
28. Band heads and origins of the $B^3\Pi_g - A^3\Sigma_u^+$ First Positive system ... 225
29. Band heads and origins of the $C^3\Pi_u - B^3\Pi_g$ Second Positive system (V) ... 226
30. Observed bands of the $B^3\Pi_g - X^1\Sigma_g^+$ Wilkinson system ... 227
31. Band heads and origins of the $B'^3\Sigma_u^- - X^1\Sigma_g^+$ Ogawa-Tanaka-Wilkinson system (R) ... 227
32. Band heads and origins of the $C^3\Pi_u - X^1\Sigma_g^+$ Tanaka absorption system (R) ... 228
33. Band heads of the $B'^3\Sigma_u^- - B^3\Pi_g$ infrared afterglow system (R) ... 228
34. Bands of the $W^3\Delta_u - X^1\Sigma_g^+$ system (1500–1440 Å) ... 228
35. Band origins of the $W^3\Delta_u - B^3\Pi_g$ system (R, V) ... 229
36. Band heads of the $C'^3\Pi_u - B^3\Pi_g$ Goldstein-Kaplan system (R) ... 229
37. Band heads and origins of the $D^3\Sigma_u^+ - B^3\Pi_g$ Fourth Positive system (V) ... 230
38. Band heads and origins of the $E^3\Sigma_g^+ - A^3\Sigma_u^+$ Herman-Kaplan system (V) ... 230
39. Bands of the $H^3\Phi_u - G^3\Delta_g$ Gaydon-Herman green system (V) ... 231
40. Band heads of the Herman Infrared system (V) ... 231
41. Band heads and origins of the $A^2\Pi_u - X^2\Sigma_g^+$ Meinel system of N_2^+ (R) ... 232

Page

42. Band heads and origins of the $B^2\Sigma_u^+ - X^2\Sigma_g^+$ First Negative system 233
43. Bands of the $^4\Sigma_u^+ - X^2\Sigma_g^+$ d'Incan-Topouzkhanian system 234
44. Band heads and origins of the $C^2\Sigma_u^+ - X^2\Sigma_g^+$ Second Negative system (R) 235
45. Band heads and origins of the $D^2\Pi_g - A^2\Pi_u$ Janin-d'Incan system of N_2^+ (R) 237
46. Unclassified bands 238
47. Band heads of the $^2\Sigma_u^+ - X^2\Pi_{gi}$ system of N_3 240
48. Rotational constants for the N_2 ground state from Raman spectra 241
49. Rotational constants for the $X^1\Sigma_g^+$ state .. 242
50. Rotational constants for the $A^3\Sigma_u^+$ state .. 242
51. Rotational constants for the $B^3\Pi_g$ state ... 242
52. Rotational constants for the $B'^3\Sigma_u^-$ state .. 243
53. Rotational constants for the $a'^1\Sigma_u^-$ state .. 243
54. Rotational constants for the $a^1\Pi_g$ state ... 244
55. Rotational constants for the $w^1\Delta_u$ state ... 244
56. Rotational constants for the $G^3\Delta_g$ state ... 244
57. Rotational constants for the $C^3\Pi_u$ state ... 244
58. Rotational constants for the $E^3\Sigma_g^+$ state .. 244
59. Rotational constants for the $C'^3\Pi_u$ state .. 245
60. Rotational constants for the $a''^1\Sigma_g^+$ state .. 245
61. Rotational constants for the $b^1\Pi_u$ state ... 245
62. Rotational constants for the $D^3\Sigma_u^+$ state .. 245
63. Rotational constants for the $b'^1\Sigma_u^+$ state .. 245
64. Rotational constants for the $c_n{}^1\Pi_u$ Rydberg states 246
65. Rotational constants for the $c_n'^1\Sigma_u^+$ Rydberg states 246
66. Rotational constants of the $H^3\Phi_u$ state ... 246
67. Rotational constants for the $o_n\ ^1\Pi_u$ states. 247
68. Rotational constants for the $x^1\Sigma_g^-$ state ... 247
69. Rotational constants for the $y^1\Pi_g$ state ... 247
70. Rotational constants for the $k^1\Pi_g$ state ... 247
71. Rotational constants for the $z^1\Delta_g$ state ... 247
72. Rotational constants for the $X^2\Sigma_g^+$ state of N_2^+ 248
73. Rotational constants for the $A^2\Pi_u$ state of N_2^+ 248
74. Rotational constants for the $N_2^+ B^2\Sigma_u^+$ state 248
75. Rotational constants for the $^4\Sigma_u^+$ state of N_2^+ 248
76. Rotational constants for the $D^2\Pi_g$ state of N_2^+ 249
77. Rotational constants for the $C^2\Sigma_u^+$ state of N_2^+ 249
78. RKR potentials for electronic states of N_2 below 11 eV: X, A, B, B', a', a, w, and C states 249
79. RKR potentials for high lying singlet states of N_2: b, c, o, b', c_4', and c_5' states 251

Page

80. RKR potentials for states of N_2^+: X, A, B, and C states 252
81. RKR potential for the D state of N_2^+ 253
82. Radiative lifetimes and f-values 254
83. Franck–Condon factors: $A^3\Sigma_u^+ - X^1\Sigma_g^+$, $B^3\Pi_g - X^1\Sigma_g^+$, $B'^3\Sigma_u^- - X^1\Sigma_g^+$, $a^1\Pi_g - X^1\Sigma_g^+$, $a'^1\Pi_g - X^1\Sigma_g^+$, $w^1\Delta_u - X^1\Sigma_g^+$, $C^3\Pi_u - X^1\Sigma_g^+$, and $a^1\Pi_g - X^1\Sigma_g^+(^{14}N^{15}N)$ .. 256
84. Franck–Condon factors: $B^3\Pi_g - A^3\Sigma_u^+$, $B'^3\Sigma_u^- - B^3\Pi_g$, $C^3\Pi_u - B^3\Pi_g$, $a^1\Pi_g - a'^1\Sigma_u^-$, and $w^1\Delta_u - a^1\Pi_g$ 263
85. Franck-Condon factors for $W^3\Delta_u - B^3\Pi_g$ ... 268
86. Franck-Condon factors for $W^3\Delta_u - X^1\Sigma_g^+$ .. 268
87. Franck-Condon factors for the $A^2\Pi_u - X^2\Sigma_g^+$ transition in N_2^+ 268
88. Franck-Condon factors and r-centroids for the $B^2\Sigma_u^+ - X^2\Sigma_g^+$ First Negative band system of N_2^+ 269
89. Franck-Condon factors and r-centroids for the $C^2\Sigma_u^+ - X^2\Sigma_g^+$ Second Negative band system of N_2^+ 271
90. Franck-Condon factors for ionization of the N_2 molecule 272
91. r-centroids: $A^3\Sigma_u^+ - X^1\Sigma_g^+$, $B^3\Pi_g - X^1\Sigma_g^+$, $B'^3\Sigma_u^- - X^1\Sigma_g^+$, $a'^1\Sigma_u^- - X^1\Sigma_g^+$, $a^1\Pi_g - X^1\Sigma_g^+$, $w^1\Delta_u - X^1\Sigma_g^+$, $C^3\Pi_u - X^1\Sigma_g^+$, $B^3\Pi_g - A^3\Sigma_u^+$, $B'^3\Sigma_u^- - B^3\Pi_g$, $C^3\Pi_u - B^3\Pi_g$, $a^1\Pi_g - a'^1\Sigma_u^-$, $w^1\Delta_u - a^1\Pi_g$ 273
92. r-centroids for the $W^3\Delta_u - X^1\Sigma_g^+$ transition (Å) 283
93. Oscillator strengths, transition probabilities and band origin wavelengths for the $A^2\Pi_u - X^2\Sigma_g^+$ Meinel system of N_2^+ 284
94. Einstein A coefficients, absolute band strengths, and band oscillator strengths for the $B^2\Sigma_u^+ - X^2\Sigma_g^+$ first negative bands of N_2^+ 285
95. Absolute transition probabilities for the $N_2\ C^3\Pi_u - B^3\Pi_g$ system (in units of $10^6\ s^{-1}$) .. 286
96. Absolute transition probabilities of the N_2 First Positive system 287

List of Figures

1. Potential energy curves for N_2 and N_2^+ 288
2. Potential energy curves for the $W^3\Delta_u$ and $B^3\Pi_g$ states 289
3. Potential curves for states involved in transitions to and interactions with the $k^1\Pi_g$ and $y^1\Pi_g$ states 289
4. Energy level diagram for the highly excited singlet states of N_2 arranged according to the new interpretations 290

1. Introduction

This report is devoted to the spectrum of N_2 and its ions (and N_3), and contains a compilation of critically evaluated numerical data on band positions, molecular constants, potential energy curves, and transition probability parameters. Though emphasis is on the gas phase, some discussion of condensed N_2 is included, because some forbidden transitions were first observed in the solid. Discussions of the various aspects of the spectrum are based on a comprehensive review of the literature. The bibliography, however, includes only those references cited in the text and tables. The present work is a revision of "The Molecular Spectrum of Nitrogen" by A. Lofthus [20].[1]

Spectroscopically, one of the most thoroughly studied diatomic molecules is nitrogen. It is only recently, however, that many complexities regarding some transitions have been understood theoretically. The energy levels and electronic structure seem now to be basically understood. There remain, however, numerous details to be worked out, especially for excited states in the neighborhood of the first ionization limit. Numerical data on intensities, lifetimes, and such are in a less satisfactory status than the data on transition frequencies (wavenumbers).

As the principal constituent of air, the nitrogen molecule plays a significant role in atmospheric phenomena including aurorae and airglows. (See e.g., Chamberlain [6], McCormac [23] and Vallance Jones [39].) The N_2^+, A–X Meinel bands were first identified in the aurora at wavelengths longer than 9000 Å. Other auroral emissions include N_2^+, B–X (1−), and N_2 systems B–A (1+), C–B (2+), A–X (VK), and a–X (LBH). Rocket or satellite observations are necessary for study of UV emissions below 3100 Å. Balloon or rocket measurements are useful for IR bands beyond 20000 Å. In the region 10000–20000 Å aircraft observations become feasible. Comet tails show the spectrum of the N_2^+, B–X (1−) bands.

Nitrogen spectra are produced in a variety of laboratory discharges and afterglows (see Pearse and Gaydon [26]; Wright and Winkler [43]). R. J. Strutt (Lord Rayleigh) in 1911 described a "chemically active modification" of nitrogen, produced by an electrical discharge in flowing nitrogen. The yellow-green afterglow following such discharge is labeled the Lewis-Rayleigh afterglow; other afterglows have also been studied. No entirely satisfying explanation has yet been advanced to account for all the spectroscopic features of active nitrogen in terms of simultaneous excitation mechanisms.

The experimental and theoretical facets of this subject have been reviewed numerous times, and remain replete with contradictions. (See the books and papers by Mitra [24], Manella [22], Bass and Broida [63], Oldenberg [504–6], Wright and Winkler [43], and Anketell and Nicholls [2].) Wright and Winkler have commented: "Moreover, apparent contradictions in observations and interpretations are indicated as reflecting a greater sensitivity of the system to experimental conditions than has generally been appreciated. As a consequence, assessment of much of the available data, at the present time, is likely to be arbitrary." Wright and Winkler therefore attempted only to organize the literature on active nitrogen. Anketell and Nicholls, in contrast, have attempted to develop a self-consistent picture of various processes occurring in active nitrogen, despite a paucity of unambiguous experimental data. Young [676] has proposed a more recent theory of active nitrogen which attempts to fill a gap in earlier work (see his references 3 and 8).

Kaplan [377] first noticed the similarity between features in active nitrogen and those in the aurora and airglow.

Golde and Thrush [261], in a series of papers, have explored the vacuum uv emission by active nitrogen. Afterglows are extensively reviewed in a separate work by the same authors [9].

Cramarossa and Ferraro [181] and Cramarossa et al. [182] have produced N_2 spectra in high power-density rf discharges in flowing nitrogen operated at pressures below 50 torr (6 kPa), and have compared the various methods of determining the rotational temperature.

Numerous laser stimulated N_2 lines have been observed, notably in the B–A (1+) and C–B (2+) systems, and in the a–a' and w–a McFarlane systems. (See Mathias and Parker [440], Kaslin and Petrash [378], Kasuya and Lide [379], Parks et al. [519], McFarlane [447–50]. See also Massone et al. [438], Girardeau-Montaut [259], and Tocho et al. [617], and references cited therein.)

A rich spectrum is known for N_2 and its positive ion. Observed transitions, both allowed and forbidden by symmetry and multiplicity, span the wavelength region from 600 to 85000 Å. A fragmentary spectrum has even been observed for N_2^{2+}, as well as some structure for a state of N_2^-.

Many perturbations are known in molecular nitrogen. These are often accompanied by complex intensity irregularities. The in depth explanation of these features in terms of the mixing of electronic states is not yet complete. Recent ab initio calculations of potential energy curves, principally for valence states of N_2, have been done by Michels [459]. These offer the basis for a qualitative understanding of many of the features just mentioned. A tabular review of the energy levels of the nitrogen molecule by Mulliken [473], now nearly two decades old, has served largely to focus attention on electronic states in nitrogen that are not known reliably. A useful graphical summary of many potential curves has been given by Gilmore [258].

[1] Figures in brackets indicate literature references at the end of the paper.

The study of the spectrum of molecular nitrogen can be traced back to 1858–9, when the first attempts were made to describe parts of this spectrum by investigators studying electric discharges in gases.[2] Beginning in 1885, Deslandres [194–5] published a series of detailed investigations on the vibrational structure and general appearance of the nitrogen spectrum, leading to his dividing the spectrum into different systems, and each system into different sequences, and to his constructing what is now known as the Deslandres table of band heads.

The nitrogen spectrum in the vacuum ultraviolet region was first investigated by Schumann [566] in 1903, and later by Lyman [430, 21], Birge and Hopfield [81–2] and others. Significant progress following development of the early quantum theory of molecular spectra was due mainly to Hopfield, Worley, Watson, Koontz, Kaplan, Vegard, Herman, and Gaydon. Of the recent work, special attention should be given to the systematic absorption measurements under high resolution by Tilford and collaborators, and to Dressler [210], Carroll [130, 132], and Lefebvre-Brion [412] for the creation of some order out of the chaos of what appeared to be numerous singlet states.

An extensive discussion of the determination of the dissociation energy of N_2, now firmly established, has been given by Gaydon [8].

The present report includes no spectrograms (but see table 1 for references to papers with reproductions of spectra). Several sources of published spectra include papers by Tilford and collaborators, and the reference works of Pearse and Gaydon [26] and Tyte and Nicholls [37, 38]. Prior compilations which include spectroscopic data on molecular nitrogen are the works by Herzberg [12], Wallace [40], and Rosen et al. [29].

2. Electronic Structure of N_2, N_2^+, N_2^{2+}, and N_2^-

The early work of Mulliken [471], largely intuitive and semi-empirical, has laid the foundation for our understanding of the electronic structure and spectroscopic properties of the nitrogen molecule. In a later review article Mulliken [473] gave an extensive list of observed and predicted energy levels, with configuration assignments and probable dissociation limits and dissociation products. Gilmore [258] constructed potential energy curves for observed and some predicted states of N_2 and its ions, and discussed electronic structure. However, both these latter works have been to some extent superseded by later important experimental and theoretical data.

Michels [459] has recently made ab initio calculations of potential curves assumed accurate to 0.1 eV, for more than 100 valence states of N_2. Strong mixing between the higher excited states is evident. Several as yet unobserved stable states were predicted. Michels' work has become the most comprehensive single source of qualitative information on such curves for the nitrogen molecule.

All non-Rydberg states up to $^4S+^4P$ at 20 eV were included. The full CI wavefunctions asymptotically connected with the correct atomic limits, but showed an increasing error for shorter r because of nonoptimization of the inner-shell basis. A correction for this was obtained from a comparison between the calculated and experimental potentials for the lowest state of a given symmetry. This correction was then applied to the excited states of this symmetry, with the implicit assumption that the CI calculation gave the correct relative energies for the excited states. Only graphical representation of the potentials has been given in Michels' unpublished report [459].

A spin-free, non-relativistic electrostatic Hamiltonian was used in the Born-Oppenheimer approximation. Double occupancy of spatial orbitals was not imposed. Slater-type orbitals were used in an iterative solution to the Hartree-Fock equations. Details have not appeared in print.

Mulliken [478] has recently computed a correlation diagram for the occupied orbitals as a function of r, from 0 to r_e. The SCF MO calculation gives the relative energies of the orbitals as a function of r, replacing the semi-empirical ones deduced from intuition. For the lowest $^3\Pi_g$ and $^3\Pi_u$ states of N_2, it is shown in a companion paper [479], that the $1\pi_g$ orbital is nearly pure valence-shell MO at r_e, and nearly pure Rydberg $3d\pi$ MO near 0.5 Å. See also Mulliken [480]. Briggs and Hayns [93a] have calculated the correlation diagram over the whole range of inter-nuclear separation from zero to infinity. The results are less accurate than those of Mulliken, though they are presumed adequate for use in scattering calculations.

2.1. Molecular Orbitals

The relative energetic order of the molecular orbitals for the nitrogen molecule is usually given as follows:

$$\sigma_g 1s < \sigma_u 1s < \sigma_g 2s < \sigma_u 2s < \pi_u 2p < \sigma_g 2p < \pi_g 2p < \sigma_u 2p \quad \text{(i)}$$

or

$1\sigma_g$	$1\sigma_u$	$2\sigma_g$	$2\sigma_u$	$1\pi_u$	$3\sigma_g$	$1\pi_g$	$3\sigma_u$	(ii)
K	K	b	a	b	a	a	a	

Orbital designation (i) specifies the atomic origin of the molecular orbitals in the separated atom approximation (SA). This designation is not always adequate in characterizing a molecular orbital. The use of simply numbered symbols $1\sigma_g$, $2\sigma_g$, . . . as in (ii) is more suitable when dealing with extended basis set expansions for the molecular orbitals. Designation (i) is then often employed instead to denote the individual symmetry basis functions, as will be explained below.

The bonding character of the orbitals is specified above as b (bonding) or a (antibonding). The $1\sigma_g$ and $1\sigma_u$ orbitals virtually retain their purely atomic

[2] The early history of the study of the nitrogen spectrum has been summarized by Kayser [16] and von der Helm [640].

character and are often called K or inner shell orbitals. Mulliken [477] has discussed the bonding characteristics of diatomic molecular orbitals. Observed and calculated orbital energies are given in table 5.

In the LCAO approximation it is convenient to form the MO's in (i) as a linear combination of the following set of "primitive symmetry MO's" [114]:

$$\sigma_g 1s = 1s_a + 1s_b$$

$$\sigma_u 1s = 1s_a - 1s_b$$

$$\sigma_g 2s = 2s_a + 2s_b$$

$$\sigma_u 2s = 2s_a - 2s_b$$

$$\sigma_g 2p = 2p\sigma_a + 2p\sigma_b$$

$$\sigma_u 2p = 2p\sigma_a - 2p\sigma_b$$

$$\pi_u 2p = 2p\pi_a + 2p\pi_b$$

$$\pi_g 2p = 2p\pi_a - 2p\pi_b$$

where $1s$, $2s$, $2p\sigma$ and $2p\pi$ are known atomic orbitals (AO) centered around atoms a and b. Most often Slater-type orbitals (STO) are used in actual calculations. This list can be readily extended to include $3s$, $3p$, $3d$, $4s$, $4p$, $4d$, $4f$, . . . orbitals (atomic orbitals). An extended basis set must be used for an adequate description of Rydberg states; for valence states it usually gives improved numerical results.

From the available symmetry MO's as basis, molecular orbitals of a given symmetry type can be formed by linear combinations. For example, the MO's of the σ_g symmetry type are given by

$$\text{m } \sigma_g = C_{m1}(\sigma_g 1s) + C_{m2}(\sigma_g 2s) + C_{m3}(\sigma_g 2p) + \ . \ . \ .,$$

where the expansion coefficients usually are found by some Hartree-Fock method. Where more than one orbital configuration is necessary to properly describe an electronic state, the dominant configuration, if there is one, is often given as a shorthand (but incomplete) description of that state.

The assignment of orbitals for the excited electron in Rydberg states gives rise to special problems. The term values of Rydberg series can to a good approximation be represented by a formula of the type

$$T = T_{ion} - R/(n-\delta)^2,$$

where T_{ion} is the energy of the ion core to which the series converges, R is the Rydberg constant, n runs through integers (principal quantum number), and δ is the quantum defect. The quantum defect depends on the type of Rydberg orbital, but is nearly constant within a given series of terms.

The form of the term formula suggests that the Rydberg orbitals are essentially hydrogenic in character; i.e., to a good approximation the Rydberg electron moves in the field of a point charge. Accordingly one should be able to specify Rydberg orbitals by a set of hydrogenic quantum numbers (n, ℓ, λ) (united atom approximation). However, the very existence of the quantum defect shows that the Rydberg orbitals deviate from the simple hydrogenic picture. A better description would then be to form a molecular Rydberg orbital by a linear combination of two or more Rydberg atomic orbitals. This conclusion is strongly supported by ab initio calculations.

Observation of Rydberg series gives values only for the effective quantum numbers, $n^* = n - \delta$. The principal quantum number n is not uniquely determined unless the magnitude of the quantum defect can be estimated by other means, such as an ab initio calculation which includes configuration mixing. For the same orbital, values of n in the literature may differ by unity.[3] The absolute value of n is useful mainly in identifying the first term in a Rydberg series.

The electronic states of nitrogen may be conveniently divided into four groups (although this classification may be blurred by configuration mixing):

(1) Normal valence states, both repulsive and stable, which dissociate into configurationally unexcited atoms (i.e. ^{4}S, ^{2}D, ^{2}P).

(2) Valence hole states, where a $2\sigma_u$ (or deeper) electron is excited (see, e.g., Gilmore [258]). These states show strong bonding and dissociate or tend to dissociate into configurationally excited atoms (e.g. ^{4}P).

(3) Ionic valence states which dissociate or tend to dissociate into configurationally unexcited atomic ions.

(4) Rydberg states, which mainly dissociate into atoms one of which is in an excited state. These molecular states have vibrational and rotational constants and internuclear separation similar to those of the ionic state which is the convergence limit of a series of Rydberg states.

Using the ten available valence-shell MO's,[4] the electronic structure of the valence states of N_2 and its ions may be described in terms of the configurations expressed by

$$(1\sigma_g)^2(1\sigma_u)^2(2\sigma_g)^2(2\sigma_u)^2(1\pi_u)^a(3\sigma_g)^b(1\pi_g)^c(3\sigma_u)^d,$$

where the values of a, b, c, and d are specified for each single configuration: (a b c d). In some cases a $2\sigma_u$ electron is excited; the resulting configurations are denoted by (a b c d; $-2\sigma_u$) (hole states). $1\pi_g$ and $3\sigma_u$ are the unoccupied orbitals.

The electron configuration of Rydberg states can be described by (a b c d; Ry), where 'Ry' stands for some symbols characterizing the Rydberg orbital in question, usually in the united atom limit.

[3] Quantum number assignments of Rydberg orbitals and their correlation between the united atom and the separated atom approximations are discussed by e.g., Mulliken [473], Duncan [214], Carroll and Collins [130, 132], Dressler [210], and Lefebvre-Brion and Moser [413]. In this review Mulliken's usage will largely be followed, though both UA and SA descriptions are used in table 5.

[4] The MO assignment refers to small and moderate internuclear distances. At larger internuclear distance this configuration might give a poor description of the actual state, due to configuration interaction between states of the same symmetry.

Table 4 lists possible Rydberg states for N_2. In table 5 is presented a comparison of some calculated and observed Rydberg terms.

2.2. Electronic Structure of N_2; Rydberg States

The dominant orbital configurations for states of N_2 are taken from the review by Gilmore [258]. Those states not labeled by a letter have not been observed directly, but remain known only from perturbations of other states. Additional orbital information on many states as yet unobserved has been given by Mulliken [473]. Potential curves of observed and many unobserved valence states have been calculated by Michels [459]. (See section 9 for an extended discussion and additional references.)

The problem of assigning MO's to observed and unobserved Rydberg states has been the subject of much controversy in the past. However, the recent theoretical calculations on Rydberg states by Lefebvre-Brion and Moser [413] have greatly facilitated the understanding of the Rydberg states and their electronic structure.

To calculate the energy levels of the Rydberg states of N_2 they assumed that the m'th member of a Rydberg series of a certain symmetry which converges to a given state of N_2^+ could be described by the dominant configuration for the state to which it converges:

$$(4100;\ \mathrm{Ry}_{m\lambda}) \text{ for } X\,^2\Sigma_g^+ \text{ of } N_2^+,$$

$$(3200;\ \mathrm{Ry}_{m\lambda}) \text{ for } A\,^2\Pi_u \text{ of } N_2^+,$$

$$(4200;\ -2\sigma_u \mathrm{Ry}_{m\lambda}) \text{ for } B\,^2\Sigma_u^+ \text{ of } N_2^+,$$

where $\mathrm{Ry}_{m\lambda}$ is the m'th Rydberg orbital of symmetry λ such that the correct symmetry for the Rydberg states can be obtained by the usual multiplication rules. The core orbitals were taken from the ground state orbitals of N_2. The configurations which describe the N_2^+ cores of symmetry $X\,^2\Sigma_g^+$, $A\,^2\Pi_u$, and $B\,^2\Sigma_u^+$ were found by removing, respectively, one electron from the $3\sigma_g$, $1\pi_u$, and $2\sigma_u$ orbitals of the $X\,^1\Sigma_g^+$ ground state of N_2.

The energy corresponding to the wavefunction of each Rydberg state was written in the form $E(\psi_m) = E(\mathrm{core}) - \epsilon(\mathrm{Ry}_m)$, where the expression $\epsilon(\mathrm{Ry}_m)$ depends on the symmetry of the Rydberg function. The orbital Ry_m was found by minimizing this energy, $\epsilon(\mathrm{Ry}_m)$, in the field of the fixed core. The orbital thus obtained is a linear combination of the unoccupied orbitals which are available from the calculation of the SCF orbitals of the ground state of N_2.

In the energy formula above, the core energy was replaced by the experimental Rydberg series limit, and by use of the calculated $\epsilon(\mathrm{Ry}_m)$'s, the heights of the Rydberg levels above the ground state were determined with an estimated uncertainty of 0.2 eV.

As mentioned in section 2.1, it is necessary to include in the basis set several Rydberg orbitals of the nitrogen atom. In the work discussed here, three different basis sets were used, consisting of selections of ns, np, and nd Slater-type orbitals:

For σ_g—orbitals: $\sigma_g 3s$, $\sigma_g 4s$, $\sigma_g 3p$, $\sigma_g 4p$, $\sigma_g 3d$, $\sigma_g 4d$,
σ_u—orbitals: $\sigma_u 3s$, $\sigma_u 4s$, $\sigma_u 3p$, $\sigma_u 4p$, $\sigma_u 3d$, $\sigma_u 4d$,
π_u—orbitals: $\pi_u 3p$, $\pi_u 4p$, $\pi_u 3d$, $\pi_u 4d$.

The nature of the Rydberg orbitals was determined from an atomic population analysis; for σ_g Rydberg orbitals it was found that the atomic orbital which had the greatest population was in some cases not uniquely determined, which indicated that, e.g., the $4s\sigma_g$ orbital is nearly degenerate with the $4d\sigma_g$ orbital. When the basis set was extended, the expression of Rydberg orbitals as linear combination of Slater orbitals (and consequently the atomic population) was changed somewhat, but not the corresponding energy.

Lefebvre-Brion and Moser presented tables of calculated positions of the first few members of Rydberg series of states converging to $X\,^2\Sigma_g^+$, $A\,^2\Pi_u$, and $B\,^2\Sigma_u^+$ states of N_2^+, and compared them with observations. Recent new experimental findings have, however, made it necessary to revise their tables slightly. The important revisions are:

(a) The lowest singlet Rydberg state is identified as $a''\,^1\Sigma_g^+$, the upper state of the a''–X Dressler-Lutz system [212].

(b) The state $c_4'\,^1\Sigma_u^+$ formerly called $(p'\,^1\Sigma_u^+)$ is the first member of Carroll-Yoshino's Rydberg series, not of the Worley-Jenkins' series as formerly believed.

(c) The first member of Worley-Jenkins' series is the e state (now called $c_4\,^1\Pi_u$), formerly believed to be $^1\Sigma_u^+$ in type.

Betts and McKoy [77] used a simple model potential (see section 2.5) to calculate Rydberg series in N_2 and some other molecules. Orbitals of symmetry types $ns\sigma_g$, $np\sigma_u$, $np\pi_u$, $nd\sigma_g$, and $nd\pi_g$ were considered. In the model used it was assumed that the three cores $X\,^2\Sigma_g^+$, $A\,^2\Pi_u$, and $B\,^2\Sigma_u^+$ were identical.

In table 5 we compare energies of some of the Rydberg states calculated by Lefebvre-Brion and Moser [413] and Betts and McKoy [77] with observed values.

The use of pseudopotentials (model potentials) in the quantum theory of atoms and molecules has recently been reviewed by Weeks et al. [646] and by Duncan [7].

In a series of papers on Rydberg series in small molecules Lindholm [419] discussed in a more qualitative way the expected magnitudes of the quantum defects. It was pointed out that for diatomic molecules built up from atoms from the first period, the quantum defect of a Rydberg state should depend mainly on the Rydberg orbital and be approximately independent

of the nature of the molecule. A list of quantum defects as function of the type of Rydberg orbitals for a series of small molecules was given. The Rydberg series in N_2 were discussed using the similarity with the Rydberg series in CO. This simplified analysis of Rydberg series has been applied to recent results of photoelectron impact spectroscopy. The subtleties of configuration mixing that may show up as unexpected magnitudes of the quantum defect are not considered in this model.

2.3. Electronic Structure of N_2^+

Recent theoretical calculations (see section 2.5) have substantially altered and extended Mulliken's [473] and Gilmore's [258] discussions on the electronic structure of the ion N_2^+, though the X, A, B, D, and C states remain the only ones extensively studied by optical spectroscopy.

A summary of the electron configurations of observed and predicted states is given below. The configurations listed are those believed to be the dominant contributors near the potential minimum of each state.

Electron configuration

Molecule	State	$1\pi_u$	$3\sigma_g$	$1\pi_g$	$3\sigma_u$	Other
N_2^-	$X\,^2\Pi_g$	4	2	1	0	
N_2	$X\,^1\Sigma_g^+$	4	2	0	0	
	$A\,^3\Sigma_u^+$	3	2	1	0	
	$W\,^3\Delta_u$	3	2	1	0	
	$B\,^3\Pi_g$	4	1	1	0	
	$B'\,^3\Sigma_u^-$	3	2	1	0	
	$a'\,^1\Sigma_u^-$	3	2	1	0	
	$a\,^1\Pi_g$	4	1	1	0	
	$W\,^1\Delta_u$	3	2	1	0	
	$^5\Sigma_g^+$	2	2	2	0	
		3	1	1	1	
	$^7\Sigma_u^+$	2	1	2	1	
	$C\,^3\Pi_u$	4	2	1	0	$-2\sigma_u$
	$^5\Pi_u$	3	1	2	0	
	$E\,^3\Sigma_g^+$	4	1	0	0	$3s\sigma_g$
	$C'\,^3\Pi_u$	3	1	2	0	
	$b'\,^1\Sigma_u^+$	3	2	1	0	
N_2^+	$X\,^2\Sigma_g^+$	4	1	0	0	
	$A\,^2\Pi_u$	3	2	0	0	
	$B\,^2\Sigma_u^+$	4	2	0	0	$-2\sigma_u$
		3	1	1	0	
	$^4\Sigma_u^+$	3	1	1	0	
	$^4\Delta_u$	3	1	1	0	
	$D\,^2\Pi_g$	2	2	1	0	
		4	0	1	0	
	$^4\Sigma_u^-$	3	1	1	0	
	$^4\Pi_g$	2	2	1	0	
	$C\,^2\Sigma_u^+$	3	1	1	0	
		4	2	0	0	$-2\sigma_u$
	$^2\Delta_u$	3	1	1	0	
	$^4\Pi_u$	1	2	2	0	
		3	0	2	0	
	$^4\Sigma_g^+$	2	1	2	0	
	$^2\Sigma_u^-$	3	1	1	0	
	$^2\Pi_u$	1	2	2	0	
		3	0	2	0	
	$^2\Phi_g, {}^2\Pi_g$	2	2	1	0	
	$^2\Delta_u, {}^2\Sigma_u^-$	3	1	1	0	
		3	2	1	0	$-2\sigma_g$
	$^2\Phi_u, {}^2\Pi_u$	2	1	1	1	
		1	2	2	0	
	$^2\Delta_g$	2	1	2	0	
	$^2\Sigma_g^+$	2	1	2	0	
		4	1	0	0	
	$^2\Gamma_g$	2	1	2	0	

In particular, the $^2\Delta_u$ state predicted from the configuration (3 1 1 0) is shown in Gilmore's curves tending to dissociate into $N(^4S°) + N^+(^1D)$ atoms. Gucrin [275], however, has derived two $^2\Delta_u$ states from the same configuration, both tending to dissociate into $N(^2P°) + N^+(^3P)$ at 28.2 eV. Potential curves for these $^2\Delta_u$ states, as well as for the known $A\,^2\Pi_u$ (3 2 0 0) and $D\,^2\Pi_g$ (2 2 1 0 + 4 0 1 0) states, were calculated using LCAO MO SCF functions, and in this approximation the states do not dissociate to the correct products. Except for the dissociation energy, good agreement with experiment was obtained for the spectroscopic and spin-orbit constants of the A and D states.

Stallcop [583] used a valence-bond method to determine a set of relations between the potential energies of those states of N_2^+ having dissociation products, ground state N and ground state N^+. The potential curves of the sextet and the quartet states are calculated at intermediate internuclear separation distances (2–3.5 Å) from these relations and the experimental curves of the doublet states (X, A, B, D).

There are twelve different N_2^+ states that can be derived from $N(^4S°) + N^+(^3P)$. Accurate potential curves for the four doublet states are known near equilibrium from experimental data. The potential curves for the remaining eight states have been calculated for large r (see Gilmore [258]), but, according to Stallcop [583], these were based on wavefunctions that do not transform properly under inversion. Stallcop's wavefunctions that do conform to molecular symmetry give an opposite order of the quartet states; i.e. the $^4\Sigma_g^+$ and $^4\Pi_u$ lie above the $^4\Sigma_u^+$ and $^4\Pi_g$ states. This is consistent with Gilmore's prediction that these latter two are bound states. In addition, when the quartet potential curves are extended to smaller r, one finds that the minimum of the $^4\Sigma_u^+$ potential would occur at $r \sim 1.3$ Å and that of the $^4\Pi_g$ state at $r < 1.3$ Å, in good agreement with Gilmore's estimated value. Beyond 2.5 Å it is expected that more extensive multiconfiguration calculations may not lead to the strictly monotonic behavior of these potential curves as deduced by Stallcop.

Andersen and Thulstrup [47] have calculated potential curves and molecular constants for low-lying

quartet states in N_2^+. Thulstrup and Andersen [608] and Cartwright and Dunning [148] have made similar CI calculations for doublet states.

2.4. Electronic Structure of N_2^{2+}

States of the N_2^{2+} ion have been observed in mass spectrometers, and one electronic transition, the $D^1\Sigma_u^+$–$X^1\Sigma_g^+$ Carroll system (see section 3.31), has been observed spectroscopically.

Hurley and Maslen [329] developed a theory which enabled the potential curves for doubly positive diatomic ions to be calculated in terms of the corresponding curves for a related isoelectronic molecule (in this case C_2). The appearance potentials of a number of such ions, including N_2^{2+}, were calculated and compared with values obtained from electronic impact measurements. (Extensive recent CI calculations by Thulstrup and Andersen [608] are discussed in section 2.5).

Hurley [328] used this theory to predict potential curves and spectroscopic constants for a number of states of N_2^{2+}, O_2^{2+}, and NO^{2+}. The calculations provided an accurate description of Carroll's band which Carroll and Hurley [134] assigned to the transition $d^1\Sigma_u^+$–$a^1\Sigma_g^+$ of N_2^{2+}, (now labeled D–X) and suggested that a number of other band systems may be observed for these ions under suitable experimental conditions.

Mass spectrometers have been used to study cross sections for ionization of N_2 to form N_2^{2+} by electron impact. A recent value of the appearance potential is 42.7 ± 0.2 eV [202, 487].

Auger electron spectroscopy[5] has been applied by Stalherm et al. [582] to the study of excited states of N_2^{2+}. The states were investigated via the K Auger spectrum of N_2. The Auger electrons gave direct evidence for six states of the ion whose relative energies were measured. The energy to ionize N_2 twofold in the ($\sigma_g 2s$) orbital was determined to be (96.5 ± 1.0) eV.

Thulstrup and Andersen [608] predicted spectroscopic constants for N_2^{2+}; the predicted potential curves are shown in their figure 2.

2.5. Theoretical Calculations

Much of the early work on N_2 quantum mechanical calculations was semiempirical, where not all electrons were considered. The more recent calculations have used mainly the Hartree-Fock approach with the n-electron wave function built from a linear combination of atomic orbitals (SCF LCAO MO). With the use of extended basis sets, the Hartree-Fock limit is approached. Cade et al. [114] have assessed the success and limitations of the recent Hartree-Fock results; the next level of complexity would include configuration mixing. Numerous properties have been calculated including orbital energies, terms values, spectroscopic constants, and potential curves. Summaries of the numerical results and references to the literature can be found in reviews by Nesbet [486], Krauss [18] (who includes many unpublished results), and Richards et al. [28]. The early term calculations, now only of historical interest, can be found in the papers cited in the reviews. Magnetic properties have been calculated by Laws et al. [405]. For earlier calculations see references cited by Richards et al. [27].

Methods other than molecular orbital have also been used in calculations on N_2. Recknagel [541], long ago, used the Thomas-Fermi-Dirac statistical model to calculate excitation energies; Gombas [264–5] later used the same model for discussing binding in N_2. Huber and Thorson [321] used the valence-bond approach to estimate the A–X separation. Öpik and Thomas [511] estimated excitation energies by a semi-empirical method. All these results have been supplanted by more recent calculations.

Cade et al. [114] have calculated molecular constants and potential curves in the Hartree-Fock limit, for the ground state of N_2 and the X, A, and B states of N_2^+. Calculated vibrational frequencies larger than experiment, smaller r_e than experiment, and incorrect long range asymptotes display the typical limitations of the H–F approximation and point out the need to include electron correlation for a chemically significant description of these states. References to earlier calculations can be found in Cade's paper. Schaefer [30] mentions additional calculations on N_2 in his survey of current techniques for molecular ab initio calculations. (See also Goodisman [10].)

Using the equations-of-motion method, Rose et al. [547] have calculated the term values for eleven low lying states of N_2. Coughran et al. [177] have calculated potential curves for these states in the region 0.9 to 1.4 Å. Both papers also present calculated oscillator strengths and transition moments.

Guerin [275], using a limited configuration interaction (CI), calculated potential curves and molecular constants for N_2^+ states $A\,^2\Pi_u$, $D\,^2\Pi_g$, $2\Delta_u(^2D+^3P)$, and $^2\Delta_{u1}(^2D+^3P)$. The two stable $^2\Delta_u$ states, with r_e about 1.3 Å, had a calculated separation of only 0.3 eV. It seems more likely that they are separated by about 1 eV. Lorquet and Desouter [427] performed a CI calculation on $^2\Sigma_u^+$ states of N_2^+, calculating energy differences. The results showed strong configuration mixing between the B and C states, as had been suggested by Douglas [204] and Mulliken [473]. Higher lying $^2\Sigma_u^+$ states were predicted to lie above 40 eV, all seemingly repulsive between 0.99 and 1.2 Å. Calculations showed that the C state is crossed in two places by the $^4\Pi_u$ state, the latter having a shorter r_e. The next higher $^4\Pi_u$ state drops rapidly in energy as r increases, and indicates an avoided crossing with the lower state of the same symmetry, giving rise to a maximum in the lower state. The calculations of Stallcop [583] had shown

[5] See section 6.2.

earlier that the lower $^4\Pi_u$ state approached its dissociation products, $N(^4S)+N^+(^3P)$, with negative slope. Energies of $^4\Sigma_u^+$ and $^4\Delta_u$ were calculated, and are in agreement with earlier predictions [473]. Predissociation of $^4\Pi_u$ by these latter quartet states is indicated, but it could not be determined whether crossing occurs at the left or right limb of the potential.

In addition to the very illuminating ab initio Rydberg calculations by Lefebvre-Brion and Moser [413], as mentioned in section 2.2, there have appeared a number of recent papers concerning various aspects of the theoretical interpretation of Rydberg states. We refer here mainly to those which have had some bearing on the understanding and interpretation of the Rydberg series of N_2.

Of particular interest is the broad discussion of the general theory of atomic and molecular Rydberg states by Mulliken [476]. In addition, Kotani [392] has presented a formal theory of Rydberg states for the general case of nonspherically symmetric core field, which can be used for the evaluation of quantum defects and orbital functions of higher members of Rydberg series of states.

A one-center approximation has been applied to the problem of suitable radial forms of Rydberg functions. Duncan [214] and Duncan and Damiani [215] developed a simplified model in terms of one-center functions for calculating Rydberg terms, and applied it to the lowest terms of the Worley-Jenkins series. Some variation in core function parameters significantly improved the calculated term values. Hazi and Rice [287], using a model potential with adjustable parameters, have calculated term values of $np\sigma\ ^1\Sigma_u^+$ states whose limit is the ground state of N_2^+. The core was represented by the ground state.

Formation of N_3^+ by ion-molecule reactions proceeds from exited states of N_2^+. Cermak and Herman [154] studied $N_2+N_2^+$ reactions and found an unusual shape for the ionization efficiency curve, which resembles the form expected for transitions involving a change of multiplicity. It was speculated that the appearance potential observed near 21 eV could correspond to a long lived $^4\Sigma_u^+$ state of N_2^+. It was asserted by Maier and Holland [433] that ultraviolet emissions produced in transition from long-lived states of N_2^+ might possibly be associated with quartet states of the ion. Later work by Maier and Holland [434, 436] could not confirm an observation of quartet states, and a new interpretation of N_2^+A state is involved in the process, not quartet states.

Andersen and Thulstrup [47] have made ab initio valence shell CI calculations of potential curves for quartet states of N_2^+ and find that the several bound states have lower energies and larger internuclear distances than earlier estimates made by Gilmore [258] from fragmentary experimental data. Gilmore, however, had already pointed out that these quartets could indeed have even lower energies and larger r_e's than he had assumed.

Thulstrup and Andersen [608] have made complete valence shell CI calculations of many valence states of N_2^-, N_2, N_2^+, and N_2^{2+}. Potential curves and molecular constants were determined which provide a qualitative description of these states. Several new states are predicted. A minimum set of Slater orbitals (1*s*, 2*s*, and 2*p* on each atom) is used as basis. For N_2 only $^1\Sigma_g^+$ and $^1\Sigma_g^-$ states were considered. For N_2^- many doublet and quartet states were calculated, many of which were bound. The minimum basis CI method over-estimates the equilibrium distances by about 0.05 Å, and also gives too high asympototic limits which tends to give too-deep binding energies.

Their calculations on N_2^{2+} predict a number of low-lying states that were not calculated by Hurley [328], whose results were based on corresponding states of the isoelectronic molecule C_2. The electronic transition in N_2^{2+} observed by Carroll [124] and shortly thereafter identified as the *d–a* system would in current notation, by analogy with C_2 (see Can. J. Phys. **47**, 2740 (1969)), be labeled *D–X*. Experimental data on doubly ionized N_2 has been obtained by a variety of techniques; references to the literature are cited by Thulstrup and Andersen [608].

Potentials were calculated for low-lying states of N_2^+; these generally lay at energies below the prior estimates. The results dispute identifications by Asbrink and Fridh [54] who attributed features observed in their photoelectron spectra as vibrational levels of the *C* state up to $v=17$.

Cartwright and Dunning [148], using a CI method, have calculated potentials for doublet states of N_2^+ that arise from the first six dissociation limits. Because a larger basis set was used than that employed by Thulstrup and Andersen [608], these calculations are assumed to be more reliable. These results which show many doublet states to be bound, and the calculations of Andersen and Thulstrup [47] on quartets, offer tentative explanations for many features observed experimentally in the energy range 21–28 eV above the ground state of N_2. Maier [432] has also used some of these results in a study of reactions between isotopically labeled N_2^+ and N_2.

Whalen and Green [652] have used an independent particle model to calculate the energies of Rydberg states. Additional calculations with this model have been performed by Miller and Green [461] for valence and Rydberg states.

3. Electronic Spectrum of N_2, N_2^+, N_2^{2+}, and N_3

Molecular nitrogen possesses one of the richest spectra of any diatomic molecule. Numerous band systems corresponding to electronic transitions of N_2 and N_2^+ span the spectral region from 490 Å to 85,000 Å. Stimulated emission spectra (30,000 to 85,000 Å) observed by McFarlane [447–50], only partially analyzed, include transitions $a^1\Pi_g-a'^1\Sigma_u^-$, $w^1\Delta_u-a^1\Pi_g$,

and hints of $W^3\Delta_u - B^3\Pi_g$, later confirmed and developed more extensively by Wu and Benesch [670] in the region 22,000–43,000 Å. An infrared afterglow transition $B'^3\Sigma_u^- - B^3\Pi_g$ has been observed in the region 8900–6050 Å.

The whole visible region and part of the near ultraviolet (down to about 2800 Å) and the near infrared regions are dominated by the very strong $B^3\Pi_g - A^3\Sigma_u^+$ First and $C^3\Pi_u - B^3\Pi_g$ Second Positive systems, and only under rather special excitation conditions can these systems be sufficiently suppressed to permit observation of weaker systems. The other systems in this region include the $B^2\Sigma_u^+ - X^2\Sigma_g^+$ First Negative and the $A^2\Pi_u - X^2\Sigma_g^+$ Meinel systems of ionized nitrogen, but part of the $A^3\Sigma_u^+ - X^1\Sigma_g^+$ Vegard-Kaplan system and some other peculiar systems are also observed. The rest of the near ultraviolet region (from 2800 to 2000 Å) is free from any really strong structure. Here part of the Vegard-Kaplan system, the $D^3\Sigma_u^+ - B^3\Pi_g$ Fourth Positive system and a series of different singlet systems are observed.

Herzberg [14] has observed absorption spectra of diatomic molecular ions using flash discharge. For N_2^+ the 0–0 band of the B–X $(1-)$ system was obtained at low resolution. The absorption spectrum has also been observed using a flash radiolysis technique, but at low resolution. Clerc and Lesigne [161] have also observed absorption in N_2^+ by means of pulse radiolysis produced by a Febetron.

In the vacuum ultraviolet region the most prominent emission features are the $a^1\Pi_g$–$X^1\Sigma_g^+$ Lyman-Birge-Hopfield system extending down to 1200 Å, and the $C^2\Sigma_u^+$–$X^2\Sigma_g^+$ Second Negative system of the ion extending down to 1370 Å. Between 1650 and 795 Å are observed numerous bands from states of species $^1\Sigma_u^+$ and $^1\Pi_u$. At 1590 Å a single band attributed to N_2^{2+} is observed.

The absorption spectrum of N_2 should begin at about 2025 Å with the $A^3\Sigma_u^+$–$X^1\Sigma_g^+$ Vegard-Kaplan system. This system is extremely weak and only in the region 1730–1280 Å has absorption been observed. In the region 1520–1060 Å there is also observed weak absorption to the states $a\,^1\Pi_g$, $a'^1\Sigma_u^-$, $w^1\Delta_u$, $B^3\Pi_g$, $B'^3\Sigma_u^-$, $C^3\Pi_u$, and $W^3\Delta_u$, and some weak absorption at about 1010 Å is due to the $a''^1\Sigma_g^+$ state. The corresponding transitions are all electric dipole-forbidden.

The strong absorption in the region 1000–796 Å (i.e., up to the first ionization limit), shows a large number of bands arising from electric dipole-allowed transitions to the states of species $^1\Sigma_u^+$ and $^1\Pi_u$. Some of these bands form Rydberg series, but otherwise they appear irregularly spaced, in contrast to the forbidden absorption bands at longer wavelengths. Some of the upper levels have also been reached in absorption from vibrationally excited ground state levels in the afterglow. (See section 3.5 for details of these singlet transitions.) Worley's group of three bands attributed to a system $i-X(0)$ is now known to be the (0–1), (1–1), and (2–1) bands of the $b-X$ system.

Below 796 Å the ionization continuum appears. This region is also crowded with many intense bands, most of which belong to Rydberg series converging to excited states of the ion. These bands usually appear diffuse due to auto-ionization.

In total 40 transitions are found among the known states of N_2. Five states of N_2^+ partake in four observed electronic transitions. One transition is attributed to N_2^{2+} and one to N_3. Details of the observed transitions are discussed below. Equilibrium molecular constants are given in table 1.

3.1. $a^1\Pi_g - X^1\Sigma_g^+$ Lyman-Birge-Hopfield System (2600–1000 Å) R

The Lyman-Birge-Hopfield system is the most extensive and promiment singlet system of nitrogen. As it represents an electric dipole forbidden transition, it is not a strong system, but nevertheless occurs readily in emission from various sources, as well as in absorption at relatively long paths (~0.025 m·atm). The stronger part of the system consists of numerous bands in the vacuum region down to about 1200 Å, but there are also numerous weaker bands in the near ultraviolet region up to about 2600 Å. Altogether 125 bands have been observed. The absorption bands extend from 1450 Å down to about 1100 Å. All bands are degraded to longer wavelengths.

Table 7 lists the observed band heads and band origins for $^{14}N_2$; table 8 gives the band data for $^{14}N^{15}N$. Tables 49 and 54 list the rotational constants in states X and a.

The Lyman-Birge-Hopfield system has been the subject of numerous investigations, and is now one of the best known systems of nitrogen. A detailed analysis of this system provides the most reliable data for the ground state as well as for the important $a\,^1\Pi_g$ state. These two states are the lower states for several other transitions, for which a reliable analysis is more difficult to make.

The system was first studied by Lyman [430], who observed and measured 21 emission bands in the region 1870–1380 Å in a high voltage transformer discharge through pure nitrogen at low pressure. Later Sponer [580] obtained 9 bands of this system in absorption, but these bands were first incorrectly attributed to NO. Then Birge and Hopfield [83] reported a large number of bands of this system both in emission and in absorption, and analyzed the vibrational structure in detail; insufficient dispersion prevented a rotational analysis.

Appleyard [52], R. Herman and L. Herman [299] and R. Herman [294] observed several new bands in the region 2500–2000 Å, thus extending the vibrational levels of the ground state up to $v=27$. At the same

time Herman [294–5] observed a predissociation in the $a\,^1\Pi_g$ state above $v=6$, but at higher pressures this predissociation disappeared. This predissociation was later confirmed by Herzberg and Herzberg [306], and reinvestigated under higher resolution by Douglas and Herzberg [206] and Lofthus [421]. It was observed that for lower pressures a clear breaking-off of the rotational structure above $v'=6$, $J'=13$ was present, whereas for increasing pressure the breaking off became less sharp (see section 8.3).

At first it was believed that the a–X transition was allowed, and consequently that the $a\,^1\Pi$ state was of u-symmetry type. The early rotational analyses were based on measurements that did not resolve the Λ-doubling. (See Appleyard [52], Watson and Koontz [645], and Spinks [579]). However, as Mulliken [471] pointed out rather early, on the basis of electron configuration theory, it seemed very difficult to account for the existence of a $^1\Pi_u$ state at this energy. In addition, Herman [295] pointed out that in the cycle of the observed singlet transitions h–X, h–a, and a–X, (where h is now known to belong to $c'\,^1\Sigma_u^+$) one of them must be forbidden. Based on this constraint and the fact that the absorption intensity of the system is rather low, Herzberg [305] finally concluded that the transition was $a\,^1\Pi_g$–$X\,^1\Sigma_g^+$, allowed as a magnetic dipole transition.

Tanaka [597] extended the absorption progression up to $v'=13$; peak intensities were for $v'=3$, 4.

Until 1956 rotational and vibrational data for the system were not very precise due to the limited resolution of the spectrographs used. Then Wilkinson and Houk [660], using a 6.6 m grating vacuum spectrograph (dispersion 1.33 Å/mm, resolving power 90000), photographed and analyzed selected bands: (0–2), (0–3), (0–4), and (1–5). Subsequently, Lofthus [421] photographed in the 3rd order of a 6.6 m spectrograph (dispersion 0.43 Å/mm; resolving power 350000) 13 bands in the region 2220–1940 Å. The (2–10), (3–11), (4–11), (4–12), (5–13), (5–14), (6–14) and (6–15) bands were analyzed in detail. Only a Q branch was analyzed for the 5–12 and 6–13 bands. Wilkinson [655] obtained the (0–0), (1–0) and (2–0) bands in absorption in the 4th order of a vacuum spectrograph (dispersion 0.30 Å/mm; resolving power 300,000). Combining the results of these high resolution studies and the results of Stoicheff's [590] high resolution Raman spectrum of nitrogen (see section 4), molecular constants were derived for both the $a\,^1\Pi_g$ and the $X\,^1\Sigma_g^+$ states.

In addition to the predissociation already mentioned, there is another type of perturbation in the $a\,^1\Pi_g$ state. As noticed by Wilkinson and Houk [660], both components of the rotational levels above $v=0$, $J=34$, are shifted upwards, and exhibit at the same time a large Λ-splitting (see section 7).

Certain weak absorption lines observed on high-resolution photographs were shown by Wilkinson and Mulliken [661] to belong to an electric quadrupole transition, being the first known example of such a transition in molecules. Since the selection rules allow an electric quadrupole concurrently with a magnetic dipole transition, the observed quadrupole lines can be regarded as conclusive proof that the Lyman-Birge-Hopfield system is due to a $^1\Pi_g$–$^1\Sigma_g^+$ transition.

Low resolution measurements of this system have recently been made by several authors. Tanaka et al. [599] studied emission from the Lewis-Rayleigh afterglow and absorption from the pink afterglow; Bass [61] observed absorption bands originating from $v''=0$ to 3 in the nitrogen pink afterglow; Tanaka et al. [604] resolved both R and S heads in absorption studies using rare gas continuua as background; Crosswhite et al. [187] observed a–X bands in the 1800–2200 Å region of the aurora by use of rockets. Campbell and Thrush [117] observed a number of bands in active nitrogen. Holland [314] observed bands of this system in the vacuum UV under low resolution; these were produced by a beam of electrons in nitrogen.

Vanderslice, Tilford, and Wilkinson [627] obtained the absorption spectrum of this system at very high resolution in the region 1098–1450 Å. Bands involving $v''=0$, and $v'=1$–15 have been analyzed. Their observed bands are listed in table 7.

The predissociation observed in emission above $J=12$, $v=6$ of $a\,^1\Pi_g$ was not observed in absorption, in agreement with the interpretation that the predissociation is a weak one involving interaction with the $^5\Sigma_g^+$ state. The combination defect was found to be quite negligible below $J=30$, within experimental error, in agreement with theoretical expectations.

Very accurate vibrational and rotational data were obtained for $v=0$ of the $X\,^1\Sigma_g^+$ state, and for $v'=1$–15 of the $a\,^1\Pi_g$ state.

Shortly thereafter Vanderslice et al. [629] studied the intensity distribution of the five branches in the bands in detail. The results were in agreement with theory and, with calculated line strengths from the theory of Chiu [159], gave a ratio $Q/D=0.33$ for the relative transition probabilities of electric quadrupole (Q) to magnetic dipole (D) branches.

Vanderslice, Tilford, and Wilkinson [628] observed at high resolution the absorption spectrum of $^{14}N^{15}N$ in the region 1098–1450 Å. The vibrational and rotational structures for the (3–0) through (11–0) bands of the system were analyzed. The Dunham isotope correction formulae were shown to be valid for both the vibrational and rotational structure indicating no observable interaction of $a\,^1\Pi_g$ with $^1\Sigma_g$ states.

In the emission from an ordinary discharge through flowing pure nitrogen at low pressure (~1/2 mm), Miller [464] observed in the region 1380–1810 Å ten bands of this system, and analyzed them under very high resolution: (0–0), (0–4), (0–5), (0–6), (1–0), (1–4),

(1–5), (1–6), (2–0), and (2–6). Very accurate rotational constants and band origins were obtained.

McEwen [445–6] recently repeated the band head measurements of Birge and Hopfield [83] in the region 2150–1450 Å. New bands observed were (0–7), (0–8), (3–1), and (7–1). From the relative intensities, measured photoelectrically, and simplifying assumptions in the theory, a roughly constant transition moment was deduced, based on Franck-Condon factors from Zare et al. [678], and r-centroids from (at that time) unpublished values of Nicholls. The electric quadrupole intensity was found to be 13% of the total band intensity. The results of Vanderslice et al. [629] indicate that this contribution would be about 25%.

McEwen's measured intensities were assumed accurate to ±20%; accuracy of ±5% was assumed for relative intensities at a given wavelength. McEwen has given an extensive discussion of his calibration methods.

3.2. $a'\,^1\Sigma_u^- - X\,^1\Sigma_g^+$ Ogawa-Tanaka-Wilkinson-Mulliken System (2000–1080 Å) R

Employing a 2-m vacuum spectrograph and an ordinary transformer-excited discharge with several torr of argon and a small amount of nitrogen, Ogawa and Tanaka [497–8] observed six new bands, all degraded to longer wavelengths, in the region 2050–1600 Å. From a vibrational analysis of these bands, they showed that the bands formed a single progression to $v=3-8$ of the ground state. They assumed that the upper level was $v=0$.

Comparing their results with theoretical predictions as to the existence of a $^1\Sigma_u^-$ state at about 70000 cm^{-1}, and with the absorption work of Wilkinson and Mulliken [662], they concluded that their new transition could be assigned as $a'\,^1\Sigma_u^- - X\,^1\Sigma_g^+$, and thus represents a forbidden transition.

About the same time as Ogawa and Tanaka observed their emission progression, Wilkinson and Mulliken [662] observed at high gas pressure (3.4 atm.) and under high resolution, a progression of four absorption bands at 1444, 1414, 1358, and 1331 Å, which they attributed to the transition $a'\,^1\Sigma_u^- - X\,^1\Sigma_g^+$. These bands consisted of Q-branches only, and were all degraded to longer wavelengths. That the bands of the a'–X transition have been observed, even though they should be strictly forbidden by the usual selection rules, was accounted for by rotational perturbations with the nearest $^1\Pi_u$ states lying between about 98000 and 109000 cm^{-1} above the ground state. The intensity distribution in the Q branches was found to be in agreement with theory.

Low resolution observations (absorption) were later extended to higher vibrational levels ($v'=0-15$) by Tanaka, Ogawa and Jursa [604]. Campbell and Thrush [117] have observed under low resolution the 0—1 to 0—6 emission bands in active nitrogen, along with some a–X Lyman-Birge-Hopfield bands.

Recently, Tilford, Wilkinson, and Vanderslice [615] observed twenty bands ($v'=0-19$) in absorption at high resolution. A complete analysis was made, providing very accurate vibrational and rotational constants for the upper state. Mixing of the $^1\Sigma_u^-$ state with $^1\Pi_u$ states permits observation of only a Q branch and shifts the maximum intensity of the lines in the bands from $J=6$ to $J=14$.

Observed bands are listed in table 9. Rotational constants for the a' state are in table 53.

3.3. $w\,^1\Delta_u - X\,^1\Sigma_g^+$ Tanaka Absorption System (1400–1140 Å) R

This weak and strongly forbidden system was first observed by Tanaka and discussed in a preliminary report of low resolution absorption measurements of forbidden systems in nitrogen (see ref. 8 in the paper by Tanaka et al. [604]). Tanaka, Ogawa, and Jursa [604] reinvestigated and extended the system. Ten bands ($v'=1-11$) were observed; individual bands were red-degraded with somewhat loosely defined heads. With a 4-m optical path, a nitrogen pressure of about 100 torr (130 kPa) was required for the observation of the strongest bands in the system. The intensity of this system was found to increase with pressure more rapidly than for other systems. For example, at high pressure, it appeared much stronger than the $a'-X$ system, while the appearance pressure for the two systems were approximately equal.

The observed band heads are listed in table 10. The heads can be represented by the formula

$$\sigma_H = 70963.6 + 1559.26(v+1/2) - 11.63(v+1/2)^2.$$

Band positions, calculated from known molecular constants of the $w\,^1\Delta_u$ state are 35–40 cm^{-1} smaller than the observed values, despite the close agreement between the vibrational constants deduced by Tanaka et al. [604] and the more reliable values known from the fine structure analysis of the Kaplan 2 system [425]. Rotational constants for the w state are in table 55.

It was mentioned by Tanaka et al. [604] that a rotation uncoupling could cause the $^1\Delta_u$ to mix with a $^1\Pi_u$ state. Then the bands should take on the appearance of a $^1\Pi_u - {}^1\Sigma_g^+$ transition with P, Q, and R branches, having negligibly low intensities for low J values, while higher J's should have intensities higher than those in normal bands, so that the intensity of J_{max} is higher than in normal bands. (This behavior is observed for the $a'\,^1\Sigma_u^- - X\,^1\Sigma_g^+$ system.)

Dressler [209] and Brith and Schnepp [96] have observed part of this system in absorption by condensed nitrogen. The absorption was investigated in the wavelength region 1600–1150 Å. Two electronic transitions were observed:

$a\,^1\Pi_g - X\,^1\Sigma_g^+$; 8 bands,

$w\,^1\Delta_u - X\,^1\Sigma_g^+$; 11 bands.

These two systems in the solid were almost equal in intensity. In the gas phase the intensity of $w-X$ was only about 5×10^{-3} times that of the $a-X$ transition. The $w-X$ transition should be expected to be intensified in the solid since it becomes dipole allowed in the crystal symmetry.

Roncin, Damany, and Roman [546] extended the absorption progression up to $v'=17$ (no band positions were published). It was found that whereas the intensity was enhanced in the pure solid, this was not the case for N_2 contained in a matrix. The $w\,^1\Delta_u - X\,^1\Sigma_g^+$ transition remains dipole forbidden in the matrix. The bands appeared sharper in the matrix than in the solid.

Ching et al. [158], using a scanning monochromator at low resolution, measured the absorption spectrum in the 1450–1050 Å region at pressures up to 40 atmospheres. For the $w-X$ system the integrated absorption coefficient was found to increase with pressure.

Tilford et al. [610] studied the system at high resolution in hopes of directly observing the rotational structure of the bands. No rotational structure was observed, even though discrete rotational lines were apparent for all other band systems photographed. The bands appeared diffuse even at the lowest pressure for which they could be observed. Further, it was observed that the intensity of the bands increased quadratically with pressure even up to pressures as high as 11 atmospheres, whereas the pressure dependence was linear for both the $a'-X$ and $B'-X$ systems. The experimental evidence indicates a pressure-induced transition.

Both the extreme width of the lines as well as the quadratic dependence of the intensity on pressure suggest that this system is pressure induced. For such a transition an S branch is permitted; this brings the calculated heads in better agreement with the observed ones. And, since the observed lines must possess a halfwidth of at least 20 cm^{-1}, the differences between the observed and calculated positions is less than 5 cm^{-1} for the band heads.

3.4. $a''\,^1\Sigma_g^+ - X\,^1\Sigma_g^+$ Dressler-Lutz System (1010.5 Å)

Mulliken [473] predicted a state of type $^1\Sigma_g^+$ at about 98300 cm^{-1} above the ground state, which should be the Rydberg state arising from the association of of $3s\sigma_g$ electron with the core $N_2^+\,X\,^2\Sigma_g^+$. The triplet counterpart, $E\,^3\Sigma_g^+$, is known as the upper state of the $E-A$ Herman-Kaplan system.

Lefebvre-Brion and Moser [413], from SCF–MO calculations on Rydberg states in N_2, placed a $^1\Sigma_g^+$ Rydberg state at 100,800 cm^{-1} (Rydberg orbital, $(3s+4p)\sigma_g$). The predicted state can combine with the ground state only through quadrupole or pressure-induced dipole radiation, and the transition should be observable in the far-ultraviolet absorption at sufficently high pressures and long pathlengths.

In an absorption spectrum of N_2 at pressures from 10 to 80 torr (1–10 kPa) Dressler and Lutz [212] and Lutz [429], employing a 3-m spectrograph in first and second orders, observed a new diffuse band centered around a Q-branch line at 1010.5 Å, corresponding to a term value of 99005 cm^{-1} or 12.275 eV. The new state was designated $a''\,^1\Sigma_g^+$.

The increasing intensity with rising pressure appears to show that the observed band arises as a pressure-induced dipole transition. The large bandwidth observed (400 cm^{-1}) is attributable to the short duration of the dipole-inducing collisions.

This optically-observed new state at 12.275 eV seems to be the one that had been observed as a peak at 12.26 eV in the energy loss spectrum of nitrogen by Heideman et al. [292], and determined to have arisen from an electric quadrupole transition by Lassettre et al. [401]. Using higher resolution that has resolved rotational structure, Ledbetter [408] has more recently studied the absorption of a Rydberg series whose lower state is the lowest $^1\Sigma_g^+$ state, but whose term value lies 165 cm^{-1} below that cited by Lutz (table 11). The pressure shift of this amount is not incompatible with Lutz's interpretation. See section 3.25(c) for a discussion of this Rydberg series, and table 60 for the a'' rotational constants.

3.5 $b\,^1\Pi_u - X\,^1\Sigma_g^+$, $b'\,^1\Sigma_u^+ - X\,^1\Sigma_g^+$, $c_n\,^1\Pi_u - X\,^1\Sigma_g^+$, $c_n'\,^1\Sigma_u^+ - X\,^1\Sigma_g^+$, and $o_n\,^1\Pi_u - X\,^1\Sigma_g^+$ Systems (1300–800 Å) R; Absorption Spectrum of Vibrationally Excited N_2

In the wavelength region below 1100 Å numerous strong dipole-allowed, irregularly spaced absorption bands have been observed. Most of the corresponding upper levels have also been reached in absorption from vibrationally excited ground state levels. Some, but not all of them have been observed in emission to the ground state $X\,^1\Sigma_g^+$, or to the excited state $a\,^1\Pi_g$.

These bands have traditionally been interpreted in terms of some twenty-five $^1\Sigma_u^+$ and $^1\Pi_u$ states, denoted by arbitrary letter symbols. Some of these states are clearly members of a few Rydberg series, whereas others must be classified as valence states. However, from theoretical considerations of possible valence configurations only a small number of $^1\Sigma_u^+$ and $^1\Pi_u$ states can be expected.

Only recently has this part of the spectrum been understood in principle. The current interpretation, due to Dressler [210] and to Carroll and Collins [130, 132] is that the observed levels can be ordered into six vibrational progressions of three valence states

$b\,^1\Pi_u$, $b'\,^1\Sigma_u^+$, and d' ($^1\Sigma_u^-$ or $^1\Delta_u$),

and the three Rydberg states

$$c\,^1\Pi_u,\ c'\,^1\Sigma_u^+,\ \text{and}\ o\,^1\Pi_u.$$

The d' level is known only through emission to the $a^1\Pi_g$ state.

The observed irregularities of the vibrational intervals, rotational constants, isotope shifts, and intensity distribution within these progressions can be interpreted qualitatively on the basis of homogeneous interactions between Rydberg and valence states of the same species.

Figure 4, reproduced from Carroll and Collins [130], shows the energy level diagram for the excited states $^1\Sigma_u^+$ and $^1\Pi_u$ arranged according to the new interpretation described above. The relation between the old and new designations is also shown.

The study of the systems involving these $^1\Sigma_u^+$ and $^1\Pi_u$ states has a long and confusing history. Since the old designations and much of the confusion still persist in recent literature, it is appropriate to give a fairly detailed account of this history, in a somewhat chronological order.

At the conclusion of this section, a survey of the more recent and reliable observations and conclusions is given for the individual transitions. Observed Rydberg series of bands are discussed more fully in section 3.25; however, since transitions between the lowest level of each Rydberg series and the ground state give rise to resolvable bands, they will be treated in this section as separate band systems.

The Gaydon-Herman systems, originating from the same upper levels, but terminating at $a^1\Pi_g$, are discussed in section 3.6.

a. Historical

In their low-dispersion investigation of the vacuum ultra-violet band spectrum of nitrogen, Birge and Hopfield [83] recognized in emission three distinct ground state progressions of bands, each apparently coming from a different electronic level, and labeled them the b, b', and c series. The bands observed in the region 1650–1000 Å, were all degraded to longer wavelengths:

b–$X(v''=1$–$5,\ 7$–$15)$; new designation $b(1)$–X

b'–$X(v''=4$–$18,\ 20$–$21)$; new designation $b'(0)$–X

c–$X(v''=5$–$13)$; new designation $b'(1)$–X.

The bands of the b and b' series were single-headed, whereas each band of the c series apparently consisted of a sharply defined and essentially symmetrical doublet. This, together with the intensity distribution, seemed to indicate that the c series consisted of double-headed bands, the second head being possibly a Q head.

The new series were observed in the emission from an ordinary transformer discharge through nitrogen. When the excitation conditions were changed, Birge and Hopfield [83] noted the complete absence of the b' progression, and speculated as to the possibility of its being due to NO rather than N_2 even though the vibrational intervals agreed fairly well with those of the N_2 ground state.

Watson and Koontz [645], using somewhat higher dispersion, observed the b' progression in the emission from a helium discharge containing a trace of nitrogen. A clear intensity alternation among the rotational lines of the bands definitely decided in favor of N_2 as the emitter. Several of their bands seemed to consist of a single branch emanating from the head, and each had one rotational line at some distance from the head showing a marked intensity perturbation. They concluded (erroneously) that the b' progression consisted of a set of single Q-branches, the upper state of which should be $^1\Pi_u$ with $B=1.147$ cm^{-1}. The absence of R and P branches was attributed to predissociation.

In addition to the b' progression, Watson and Koontz [645] also observed in the emission from an ordinary discharge through pure nitrogen at low pressure, five new progressions of bands, degraded to longer wavelengths, from upper states which they labeled d, e, f, g, and h, to the ground state:

d–$X(v''=3$–$11)$; new designation $b(5)$–X

e–$X(v''=10$–$13)$; new designation $c_4(0)$–X

f–$X(v''=1$–$9,\ 11$–$12)$; new designation $b'(9)$–X

g–$X(v''=1$–$9,\ 11$–$13)$; new designation $b'(7)$–X

h–$X(v''=5$–$9,\ 11$–$14)$; new designation $c_4'(4)$–X.

Tschulanowsky [618] observed in a high-voltage transformer discharge through nitrogen nine bands of Birge-Hopfield's b'-progression ($v''=13$–21), under medium dispersion. Birge-Hopfield's b and c progressions did not show up under these conditions. The observed intensity alternation in the branches clearly showed that N_2 was the emitter.

A partial rotational analysis revealed clearly that the transition was $^1\Sigma$–$^1\Sigma$ in type. In some of the bands there was a near coincidence of P and R lines. At lower dispersion this had led Watson and Koontz to believe that the $b'-X$ bands consisted of Q-branches only.

In addition to the $b'-X$ bands, Tschulanowsky observed and analyzed four new bands that could very very well be part of the $v'=1$ progression ($v''=18$–21). The d and e progressions of Watson and Koontz were ascribed to $v'=2$ and 3, respectively, of b'.

In a very extensive and thorough study of the absorption spectrum of nitrogen between 1020–730 Å, Worley [666] observed a large number of relatively strong bands. Data were presented for a very extensive Rydberg series, and the rest of the bands were ar-

ranged into a number of groups, labeled i, j, k, ℓ, m, n, o', p, q, r, s, t, u, and v. Of these groups, k was found to consist of bands from $v=0$, 1, 2, and 3 of Birge and Hopfield's state b (these vibrational numbers must be increased by one unit; see below), and group ℓ of bands from $v=4$ and 5 of the same state. (Worley's $b(4)$ level is now known to be $c_3(0)$; see below.) Group n was found to consist of the bands from $v=4$, 5, 6, and 7 of state b' (Worley's $b'(7)$ is now known to be $c_4'(2)$; see below). According to Carroll and Collins [130], the i group consists of hot bands of the $b-X$ system: 0–1, 1–1, and 2–1.

Worley observed that lower members of his new Rydberg series showed two heads of about equal intensity. The first member was listed in Worley's table as

$$c\begin{cases} R_o'(2)\ 958.625\ \text{Å},\ 104316.1\ \text{cm}^{-1} \\ R_o(2)\ 958.170\ \text{Å},\ 104365.6\ \text{cm}^{-1} \end{cases}$$

and was identified (erroneously) as the c state of Birge and Hopfield, who obtained the heads of the 0–0 band by extrapolation at 958.60 and 957.90 Å.

Setlow [568] observed in a condensed discharge in flowing nitrogen several bands of the b' and c progressions and made a partial rotational analysis. The analysis of the $v'=0$ bands confirmed Tschulanowsky's designation of this upper b' state as a $^1\Sigma$ state. The previous designation as $^1\Pi$ by Watson and Koontz [645] was due to the almost exact superposition of the P and R branches in the bands they measured. Further, Birge-Hopfield's c-progression was found to originate in $v'=1$ of the b' state. The rotational constants obtained by Tschulanowsky [618] were $B_o=1.144$ and $B_1=1.142$ cm^{-1}, in good agreement with values obtained later by Setlow.

Incorporating the Watson and Koontz' d and e states as the levels $v=2$ and 3, respectively, of the b' state, Setlow drew up a Deslandres table for the $b'-X$ system. For the b' state $T_e=103678.9$ cm^{-1} was obtained.

Setlow discussed a possible correlation of the $v=1$ level of the b' state with other observed states. There were three other known states of N_2 of about the same energy:

(1) p' (Gaydon's p) [249]
$T=104327.9$, $B=1.93$ cm^{-1}

(2) c (Worley)
$T_R=104365.6$, $B=1.92$ cm^{-1}
$T_Q=104316.1$

(3) c (Birge-Hopfield)
$T_R=104394.6$ cm^{-1}
$T_Q=104318.7$ cm^{-1}

As far as the states p' and c (Worley) are concerned, the B values precluded any possibility of their being $v=1$ of b'. Furthermore, it seemed highly probable that these states were identical. By using Gaydon's data [249] to calculate the position of the head of the 0–0 band of $p'-X$ and also the position of the strong lines of the P branch, Setlow obtained $\sigma_{head}=104377$, $\sigma_P=104320$ cm^{-1} which is in good agreement with Worley's c state. This is in agreement with Herzberg [305], who also suggested that the far ultraviolet data could also be accounted for on the assumption that p' and c were identical and of type $^1\Sigma_u^+$.

The difficulty in correlating Birge and Hopfield's c state with the first vibrational level of b' lies in their observation that the $c-X$ system was comprised of double-headed bands. From Setlow's higher dispersion spectrograms, evidence was found that this apparent double-headed structure was due to an intensity anomaly caused by a perturbation from the nearby p' state of the same species. This perturbation was discussed in some detail. Setlow observed also a small perturbation in $b'(1)$ at $J=10$, and identified the p' state as the perturbing state.

Wilkinson and Houk [660] observed under higher resolution 38 bands of the $b'-X$ system in the emission from an electrodeless discharge of 1% nitrogen in helium or in pure nitrogen alone. Rotational analyses were carried out for the well-resolved 0–11, 0–12, 1–7, 1–8, 1–9, and 2–8 bands, which yielded reliable values of the rotational constants. From the less resolved 3–5, 1–6, and 2–6 bands, reasonable values of $B'-B''$ were also obtained. Band head measurements were made for the remaining bands which were either badly overlapped or poorly resolved. All these bands are included in table 13.

The known rotational perturbations were confirmed and discussed. Vibrational perturbations were found in the $v=4$, 5, and 6 levels, and a new predissociation at $v=4$, $J=9$.

Carroll [127] studied some of Worley's progressions under higher resolution, and gave a summary of some preliminary results obtained. Some of the progressions are now known to be part of the $b'-X$ system.

Tilford and Wilkinson [613] investigated the emission spectrum of molecular nitrogen obtained from an electrodeless discharge in $Ar-N_2$, $Ne-N_2$, and $He-N_2$ mixtures at high resolution in the 1130–900 Å region. Altogether 80 bands were observed, degraded to longer wavelengths.

Transitions to the ground state, $X^1\Sigma_g^+$, were identified for the first time for the electronic states $r'^1\Sigma_u^+$, $s'^1\Sigma_u^+$, and $k^1\Sigma_u^+$ (now called $c_4'(1)$, $c_4'(3)$ and $c_4'(2)$, respectively), and also extensive additional bands for the following states: $p'^1\Sigma_u^+$, $f^1\Sigma_u^+$, $g^1\Sigma_u^+$, $b^1\Pi_u$, $b'^1\Sigma_u^+$, and $h^1\Sigma_u^+$ (now called $c_4'(0)$, $b'(9)$, $b'(7)$, $b(1)$, $b'(0)$, and $c_4'(4)$, respectively).

Some of these bands appeared to have only one branch. A rotational analysis showed that in these cases P and R branches were coinciding. The rotational analysis showed conclusively that both the f and g

states were $^1\Sigma_u^+$ in type. In the f-bands there was an intensity drop following $P(14)$; this was attributed to a weak predissociation process. Similarly, a weak predissociation in the g-state was observed between $J=9$ and 10.

Bands of the individual systems sometimes appeared with very different relative strengths when excited in the different carrier gases. As an example, the $b'-X$ transition was much stronger in the argon mixture than in the helium mixture.

The $b'(2)-X$ bands, when excited in a mixture of argon and nitrogen, showed an intensity anomaly not observed with other gas mixtures or in pure nitrogen. It was not clear whether this was caused by a predissociation or by a collison of the second kind with metastable argon atoms.

In the neon mixture there was a regular decrease in intensity as J increased, while in the argon mixture, there was a sharp intensity drop at $P(13)$ and also $R(11)$. A similar anomaly was observed in each band involving $v'-2$, $J'-12$ when the $b'-X$ bands were excited in this way.

In a subsequent paper Tilford and Wilkinson [614] discussed the observation of an unusual enhancement in emission bands involving the $b'(5)$ level near 13.336 eV. A progression of five weak emission bands shaded to longer wavelengths was observed with vibrational quantum numbers $v''=2$, 3, 4, 5, and 6, respectively. The intensity distribution in the 5−4, 5−3, and 5−2 bands was most unusual. The intensities of all eighteen lines in these bands involving rotational levels $J'=13$, 14, and 15 were abnormally large. It was proposed that this pronounced intensity enhancement resulted from an increased population of the levels by an inverse predissociation process involving $^4S+^2P$ atoms.

Tanaka and Nakamura [602] extended the investigation on intensity anomalies in the $b'-X$ system. A small amount of nitrogen mixed with an excess of rare gas was excited with an uncondensed transformer discharge to yield specific progressions of N_2 bands which were selectively enhanced. The progressions observed were the $b'(0)-X(v'')$ and $g-X(v'')$ in the Kr-discharge, and $b'(2)-X(v'')$ in the Ar-discharge. In addition to the enhancement, the individual bands also showed either an unusually narrow appearance or an anomalous intensity distribution in their rotational structure. Resonance fluorescence is a generally satisfactory explanation, but collisions of the second kind can be considered a possible explanation as well. However, rather little evidence for such collisions involving metastable states of the rare gas was observed in their work.

The observed bands in the $b'(0)$, $b'(2)$, and $g-X(v'')$ progressions were extended to $v''=21$, 27, and 24, respectively.

Ogawa, Tanaka, and Jursa [500] and Mahon-Smith and Carroll [431] studied the isotope shift of nitrogen bands from the several $^1\Sigma_u^+$ and $^1\Pi_u$ levels in the 100000–120000 cm^{-1} region. In particular, the vibrational quantum numbers of the b' levels were found to be correct, whereas the numbering of the b levels had to be increased by one. The $j\,^1\Sigma_u^+$ level at 100824 cm^{-1} was found to have $v=0$; it is now known to be $^1\Pi_u$, and the lowest level of the b state. The l, m, p, q, s, t, and other levels were shown to have high vibrational quantum numbers (due to perturbations, numbering is difficult to determine without ambiguity), thus indicating that some of them could very well be higher vibrational levels of the b and b' states.

The h, s', and r' levels all had $v>0$. These levels are now known to be the $v=4$, 3, 1 vibrational levels of the $c_4'\,^1\Sigma_u^+$ Rydberg state.

The observed vibrational isotope shifts are given in table 15c.

A number of weak emission bands in the region 1300–1000 Å, formerly thought to belong to CO, though with some misgivings, have now been unambiguously identified by Tilford and Simmons [609] as belonging to N_2 systems $b-X$, $b'-X$, and $c'-X$.

b. $b\,^1\Pi_u-X\,^1\Sigma_g^+$ System (1110–850 Å) R

The strong $b-X$ system has been observed in absorption up to $v'=24$, and rotationally analyzed by Carroll and Collins [130]. Ogawa et al. [500] observed the same system in absorption at lower resolution for both $^{14}N_2$ and $^{15}N_2$, and determined isotope shifts. Absorption from ground state vibrationally excited levels has been observed by Bass [61] in a study of active nitrogen.

Emission from the $b\,^1\Pi_u$ state ($b-X$ and $b-a$) has been observed only for $v'=1$, 5 and 6. The missing emission from other vibrational levels clearly indicates predissociation.

The pronounced irregularities in the rotational and vibrational structure observed in these bands were attributed by Carroll and Collins [130] and Dressler [210] to a homogeneous interaction between the $b\,^1\Pi_u$ state and the first member of the $c\,^1\Pi_u$ Rydberg states. Diffuseness in the rotational lines of several bands was also observed and attributed to predissociation by a $^3\Pi_u$ repulsive state.

Leoni and Dressler [415] derived quantitative measures of the natural linewidths by fitting computed band profiles to photoelectric scans of the absorption bands. The resulting linewidths were used to derive information on the continuum state or states causing the predissociation.

Yoshino et al [675] have extended the known spectrum of the 7–0, 12–0, and 15–0 bands and also revised prior analysis of the 9–0 band. For these bands, rotational quantum assignments for $J<7$ differ from those given earlier by Carroll and Collins [130].

For the $b(7)$ level, all rotational levels suffer homogeneous perturbation with $o_3(0)$. The deperturbed $B_7=1.310$ cm^{-1}, is to be compared with the unperturbed value of Carroll and Collins [130], 1.340. The homogeneous perturbation in $b(9)$ is considered in the reanalysis of the 9–0 band. The 12–0 band is extended beyond the position of the homogeneous perturbation. By extending the 15—0 band, a homogeneous perturbation was found for J about 25.

Table 12 lists heads and origins for (a) emission, (b) absorption bands at high resolution, and (c) isotope shift of band heads. Rotational constants for the b state are in table 61.

c. $b'^1\Sigma_u^+-X\,^1\Sigma_g^+$ System (1290–820 Å)

The strong b'–X system has been observed in absorption up to $v'=28$, and the high resolution spectra have been analyzed by Carroll, Collins and Yoshino [132]. Simultaneously, twelve bands of the $c_n{}^1\Sigma_u^+$ (Rydberg)$-X\,^1\Sigma_g^+$ system were studied. Ogawa et al. [500] observed the same system in absorption for both $^{15}N_2$ and $^{14}N_2$ and determined isotope shifts. Absorption has also been observed in active nitrogen from ground state vibrationally excited levels by Bass [61].

In emission, numerous bands are observed for the b'–X and b'–a transitions (see Gaydon-Herman systems; section 3.6) for v' up to 9. The more reliable measurements of the b'–X emission system appear to be those of Wilkinson and Houk [660], and of Tilford and Wilkinson [613].

Carroll et al. [132] and Dressler [210] found that the $c_n{}'^1\Sigma_u^+$ Rydberg and the $b'^1\Sigma_u^+$ valence states suffer pronounced mutual perturbation, showing up as irregularities of varying magnitude, in both the vibrational and rotational structure.

The b' state is predissociated at higher vibrational levels. In particular the 20–0, 21–0 and 22–0 bands showed decided diffuseness in their rotational structure.

Table 13 lists band heads and origins for (a) emission, (b) emission at moderate resolution, (c) absorption bands at high resolution, and (d) isotope shifts of band heads. Perturbed rotational constants for the b' state are included in table 63.

d. $c_n{}^1\Pi_u$–$X\,^1\Sigma_g^+$ System (960–860 Å)

The $c_n{}^1\Pi_u$ states are members of the Worley-Jenkins Rydberg series (subscript n refers to the principal quantum number of the Rydberg electron) converging to the ground state of N_2^+. This Rydberg series is discussed more fully in section 3.25.

$c_3(0)=\ell_1$

Worley [666] observed in absorption a band labeled ℓ, at 960.206 Å, with a rotational constant $B'=1.482$ cm^{-1}. Ogawa et al. [500] observed the same band for $^{15}N_2$ as well as $^{14}N_2$. The rotational structure of this level has also been studied in the ℓ–$a\,^1\Pi_g$ transition (see Gaydon-Herman systems; section 3.6).

There is a very strong homogeneous perturbation between this level and $b(5)$, and consequently neither level can be uniquely determined. Only formally can the ℓ_1 level be assigned to the $c_3(0)$ Rydberg level.

$c_3(2)=d''$

Worley [666] observed a band at 920.04 Å, which he labeled $R_2(2)$; n. No rotational analysis was made; however, the rotational structure is partly known from the d''–$a\,^1\Pi_g$ transition (see Gaydon-Herman systems; section 3.6) from which are obtained $B_o'=1.796$ cm^{-1} and $T_o=108696$ cm^{-1}.

$c_4(0)=e$

The e state is the second member of the Worley-Jenkins Rydberg series. Worley observed a double-headed band

$R_o'(3)$ 865.324 Å, 115563.6 cm^{-1},

$R_o(3)$ 865.060 Å, 115598.9 cm^{-1},

which probably originated in the e level. No rotational analysis was made. Ogawa and Tanaka [499] observed the same band at 115565.2, 115600.3 cm^{-1}.

The e level is also known from the $e-a\,^1\Pi_g$ transition (see Gaydon-Herman systems; section 3.6). A partial rotational analysis indicated a B' value of about 1.92 cm^{-1}, which is normal for a Rydberg state converging to the ground state of N_2^+. It was (erroneously) concluded that the e level was of type $^1\Sigma_u^+$. Later it was shown by Carroll and Yoshino [141] that it was in fact of type $^1\Pi_u$.

Observed c_n-X bands are listed in table 14. Rotational constants for the c_n states are in table 64.

e. $c_n{}'^1\Sigma_u^+-X\,^1\Sigma_g^+$ System (960–860 Å)

The $c_n{}'^1\Sigma_u^+$ states are members of the Carroll-Yoshino Rydberg series (subscript n refers to the principal quantum number of the Rydberg electron). This Rydberg series is discussed more fully in section 3.25.

$c_4'(0)=p'$

The well known p' level has for a long time been identified as the first member of Worley-Jenkins' Rydberg series. It is now known to be the first member of Carroll-Yoshino's Rydberg series. The earlier studies of this level are discussed in section 3.5.a.

Tilford and Wilkinson [613] observed for the first time in emission the rotational structure for the $p'-X$ transition. There were a number of unusual features in the $p'-X$ bands, the most outstanding of which was the appearance of three heads. The intensity alternation was observed to be disrupted at $P(12)$, and the $P(19)$ line was very weak. In the R branch all lines were found to be very close together with the exception of the $R(9)$ and $R(10)$ lines. This is the exact position where the center 'head' of the band was

observed; this third 'head' resulted from the perturbation in the upper state and was not a real head.

The rotational structure of the p' level has also been studied in the $p'-a\,^1\Pi_g$ transition (see Gaydon-Herman systems; section 3.6).

$c_4'(1)=r'$

Tilford and Wilkinson [613] observed a progression of five bands ($v''=1-5$). Each band had a very condensed R branch and was degraded toward longer wavelengths. This progression extrapolated to $\sigma_H=$ 106379.8 cm^{-1} for $v''=0$, in good agreement with prediction from the $r'-a\,^1\Pi_g$ transition (see Gaydon-Herman systems; section 3.6).

Ogawa et al. [500] observed this band in absorption at 106381.4 cm^{-1} for $^{14}N_2$ and 106319.0 cm^{-1} for $^{15}N_2$, and from the observed isotope shift the vibrational quantum number appeared to be $v'=1$. From observed isotope shift in the $r'-a$ transition, Mahon-Smith and Carroll [431] came to the same conclusion.

$c_4'(2)=k$

Tilford and Wilkinson [613] observed a progression of four bands ($v''=1$–4), all degraded to longer wavelengths and possessing a similar structure with pronounced intensity alternation. This progression extrapolated to $\sigma_H=108547.7$ cm^{-1} for $v''=0$, in good agreement with predictions from the known $k-a$ $^1\Pi_g$ transition.

Ogawa et al. [500] observed this band in absorption at 108549.4 cm^{-1}, and 108400.3 cm^{-1} for $^{15}N_2$, and from the isotope shift the vibrational quantum number appears to be $v'=2$.

$c_4'(3)=s'$

Tilford and Wilkinson [613] observed in the region 1010–920 Å a new progression of five bands ($v''=1-5$), all degraded to longer wavelengths. The progression extrapolated to $\sigma_H=110664.9$ cm^{-1} for $v''=0$, in good agreement with prediction from the known $s'-a\,^1\Pi_g$ transition.

Ogawa et al. [500] observed this band at 110664.2 cm^{-1} for $^{14}N_2$ and 110482.3 cm^{-1} for $^{15}N_2$, and from the isotope shift the vibrational quantum number could be $v'=3$. The same conclusion was drawn by Mahon-Smith and Carroll [431] from observed shifts in the $s'-a\,^1\Pi_g$ transition.

The upper state is strongly perturbed, giving the bands an irregular appearance.

$c_4'(4)=h$

The $h-X$ transition was first studied in emission by Watson and Koontz [645], and in absorption by Worley [666]. The bands were degraded to longer wavelengths.

Tilford and Wilkinson [613] observed a progression of six bands in emission ($v''=4-9$) in the region 1080–960 Å. The progression extrapolated to $\sigma_H=112778.7$ cm^{-1} for $v''=0$, in good agreement with prediction from the known $h-a\,^1\Pi_g$ transition.

Ogawa and Tanaka [499] observed this band in absorption at 112777.4 cm^{-1} for $^{14}N_2$ and 112542.8 cm^{-1} for $^{15}N_2$, and from the isotope shift the vibrational quantum number could be $v'=5$. Carroll and Mahon-Smith [135] and Mahon-Smith and Carroll [431] favored the assignment $v'=4$, because of the observed isotope shift in the $h-a\,^1\Pi_g$ transition.

Tilford and Wilkinson's bands were overlapped so that no rotational analysis could be obtained. However, there appeared to be a sharp intensity break-off in the P branch; a similar intensity break-off was known beyond $J'=10$ in the $h-a\,^1\Pi_g$ transition (see Gaydon-Herman systems; section 3.6).

$c_4'(5)=h'$, $c_4'(6)=h''$, and $c_4'(7)=h'''$

Ogawa, Tanaka and Jursa [500] observed in the absorption spectrum three new bands at 870.8, 856.0, and 841.9 Å for $^{14}N_2$, and 873.1, 858.4, and 844.9 Å for $^{15}N_2$, and assigned them to new levels h', h'', and h'''. From the isotope shifts they concluded that the vibrational quantum numbers were likely $v'=5$, 6, and 7, respectively.

Many of these bands, as well as some new ones, have recently been studied under high resolution by Carroll et al. [132].

The observed bands and isotope shifts for the $c_n'\,^1\Sigma_u^+-X\,^1\Sigma_g^+$ are listed in table 15. Rotational constants for the c_n' states are in table 65.

An extensive list of term values and rotational constants for the c_n' Rydberg states has been given by Carroll et al. [132].

The rotational analysis of the c_n-c_{n+1}' complexes is discussed by Carroll and Yoshino [142]. The c_5' levels are strongly mixed with high-v levels of the $b'\,^1\Sigma_u^+$ valence state (homogeneous perturbation). Levels $c_4(1)\,^1\Pi^+$ and $c_5'(1)\,^1\Sigma_u^+$ interact strongly because of l-uncoupling; the coupling conditions vary with principal quantum number n.

For $n>9$ the heads in each complex blend and form a single peak, coinciding with the R head of the $^1\Pi_u$ band. Johns and Lepard [360] account theoretically for the formation of a single peak for large n, as the separation between the components of the Rydberg complex becomes smaller because of l-uncoupling and the rotational structure collapses. For n beyond 12 the single-headed series members in the new measurements nearly coincide with the lower resolution values of Ogawa and Tanaka [499] (see table 15).

Carroll [129] has examined the changing structure arising from changing coupling conditions of some N_2 c_n-c_{n+1}' p-complexes. In particular, he considered the $5p$ and $8p$ complexes which involve Rydberg series that converge to the ground state of N_2^+. For

higher n the rotational structure is not resolved, but theoretical profiles can be compared with experiment, enabling structural changes to be interpreted. Resolution for $n > 8$ becomes more difficult, partly because of the contraction of the complex. The application of the theory of p-complexes to N_2 is complicated by the homogeneous perturbations of the Rydberg states by non-Rydberg states (see section 7).

f. $o^1\Pi_u - X^1\Sigma_g^+$ System (950–880 Å) R

The $o^1\Pi_u$ state is the lowest member of Worley's Rydberg series converging to the $A^2\Pi_u$ state of N_2^+. This Rydberg series is discussed more fully in section 3.25.

The o–X system (originally labeled o'–X) was first observed in absorption by Worley [666] for $v'=0$–3. Ogawa, Tanaka and Jursa [500] observed the same progression for both $^{14}N_2$ and $^{15}N_2$. Although the vibrational spacing in $^{14}N_2$ is quite regular, the isotope shift of the $^{15}N_2$ 0–0 band deviated somewhat from the expected value.

In activated nitrogen more than sixty bands have been observed in absorption from excited ground state vibrational levels (see Tanaka et al. [599]).

The $o^1\Pi_u$ state is also the upper state of the o–a $^1\Pi_g$ transition (see Gaydon-Herman systems; section 3.6). From an analysis of this transition the following constants were obtained: $B_o'=1.694$, $T_o=105682$ cm^{-1}. The state does not appear to be strongly perturbed.

Table 17 lists the observed absorption bands for $^{14}N_2$ and $^{15}N_2$. Rotational constants for the o state are in table 67.

g. Absorption Spectrum of Vibrationally Excited N_2 (1900–600 Å)

Kaufman and Kelso [380] were the first to report strong physical evidence for the presence in active nitrogen of appreciable concentrations of N_2 in the first vibrationally excited level. Subsequently Dressler [208] identified this level in active nitrogen by means of its vacuum ultraviolet absorption spectrum. In addition to nine bands of the $v''=0$ progression of the $a-X$ system, four bands with $v''=1$ were observed. Bass [61] observed additional $a-X$ bands from $v''=1$, 2, and 3 in the absorption spectrum of the 'pink' afterglow.

In addition to these bands, Bass [61], Ogawa et al. [501], Tanaka et al. [601], and Huffman et al. [324] observed a large number of absorption bands originating in high vibrational levels of the ground state. The various sources include the 'pink' and Lewis-Rayleigh afterglows, and other discharges through N_2. The upper states include the various valence and Rydberg states of symmetry $^1\Sigma_u^+$ and $^1\Pi_u$ (b, b', c, c', o). The bands are too numerous to be listed here.

These absorption bands give no new information on the upper levels. For the ground state they do extend the vibrational term values from $v''=15$ to $v''=20$. The latter term values ($v''=16-29$), however, are derived from band head measurements, whereas for $v''=0-15$ they are derived from band origins.

Appleton and Steinberg [51] measured absorption coefficients of shock-heated nitrogen over a temperature range from 3500 to 10000 K at four wavelengths: 1086, 1176, 1247, and 1334 Å. The temperature dependence of the absorption coefficients obtained at each wavelength indicated that the absorption was due to photoexcitation of molecules from within one or two adjacent vibrational levels of the ground state to the $b'\,^1\Sigma_u^+$ (12.849 eV) and $b\,^1\Pi_u$ (12.575 eV) states, and probably other levels of comparable energy. Upper limits for the values of the electronic f numbers for the $b'-X$ and $b-X$ transitions were deduced from the experimental data using previously calculated values of the absorption coefficients.

3.6. $^1\Sigma_u^+ - a^1\Pi_g$ and $^1\Pi_u - a^1\Pi_g$ Gaydon-Herman Singlet Systems (3670–2220 Å) R, V

The band systems called the Gaydon-Herman singlet systems arise from emission transitions from various upper levels (valence and Rydberg) of type $^1\Sigma_u^+$ and $^1\Pi_u$ to the $a^1\Pi_g$.

Such states can combine equally well with the ground state $X\,^1\Sigma_g^+$, and such transitions are indeed observed (see section 3.5). The two types of transitions should give the same information about the upper levels. However, the Gaydon-Herman systems fall in the near ultraviolet region where higher resolution spectra are easier to obtain, providing, in certain cases, valuable information about the upper levels.

Most of these systems were first studied by Gaydon [249–51] and by Herman [295, 298], who assigned eight new systems to this group (e, h, s', d', r', m, d, and p'). Some of the systems were also studied by Janin [341–6] (m, b' and d) and by Janin and Crozet [347], who added three new systems to this group (o, ℓ, and d''). Lofthus [423] remeasured most of the bands at higher resolution, and added two new transitions (g and k).

The Gaydon-Herman systems are rather weak, but are nevertheless observed fairly readily in a mildly condensed discharge through pure nitrogen (Gaydon) and in ordinary discharges at low pressure (Herman, Lofthus). Janin obtained most of his bands in a special high pressure discharge, and some bands (ℓ, o, d'') in a high voltage discharge through NH_3.

In the past these systems have been treated more or less as independent systems, the upper levels of which have been designated by a large number of arbitrary letter symbols. Recent studies by Dressler [210], Carroll and Collins [130], and Carroll and Mahon-Smith [135], made it quite clear that all these levels are vibrational levels of only a small number of independent states. These states are heavily affected by perturbations, accounting for the observed irregu-

larities in the vibrational and rotational structure, and in intensities.

The vibrational structure of the upper states involved in the Gaydon-Herman systems are clearly shown in figure 4. In the same figure the connection between the old and new designation is also shown. In the following, the various bands of the Gaydon-Herman systems are discussed. The new notation for the upper states is that of Dressler [210] and Carroll and Collins [130].

$b\,^1\Pi_u(1)$

Janin [345] observed two red-degraded bands originating in a common upper level, with lower levels $a\,^1\Pi_g$, $v''=0$ and 1, respectively. The stronger band was at 3075.1 Å and the weaker one was at 3241.3 Å. The position and rotational constants of the upper level were found to agree with those of the $b(1)$ level of the known b–X transition.

Rajan [538] has observed the 1–0 band at high resolution.

$b\,^1\Pi_u(5) \equiv \ell_2(d)$

Herman [295] and Janin [342] observed in the region 3420–2740 Å two progressions of bands, degraded to longer wavelengths, which they atrributed to the same system, labeled d–a. The first progression originates from $b(5)$ and terminates at $v''=0$–4 of the $a\,^1\Pi_g$ state. The second progression is identical with Gaydon's m-progression (see below). No rotational analysis exists for this progression. Observed isotope shifts [431] indicated that $v=5$ or 6 for the upper level.

$b\,^1\Pi_u(6) \equiv m$

Gaydon [249] observed three bands, degraded to longer wavelengths, with heads at 2746.2, 2878.0, and 3020.3 Å, and with $v''=0$, 1, and 2, respectively. The structure was found to be consistent with a $^1\Pi_u$-type upper level (originally called q by Gaydon). There was some indication of a perturbation and Λ-doubling from about $J'=12$. Herman [295] and Janin [342] have observed the band going to $v''=3$, at 3175.0 Å.

Lofthus [423] analyzed these bands at higher resolution, and obtained band origins and rotational constants. Due to badly masked bands, nothing more definite could be said about possible perturbations in the upper level.

Measured isotope shifts [431] in the m–a transition indicated that $v=5$ or 6 for the upper level.

$b'\,^1\Sigma_u^+(7) \equiv g$

Lofthus [423] observed a new band, degraded to longer wavelengths, at 2498.6 Å, the analysis of which showed that it was due to a transition from an upper level $^1\Sigma_u^+$ to $v=0$ of $a\,^1\Pi_g$. The position of the upper level was found to coincide with the g level of Watson and Koontz [645].

There seemed to be a breaking-off of all branches above $J'=11$, but the lines from $J'=10$ and 11 were already somewhat weakened, indicating the presence of a weak predissociation. An irregular rotational structure was also observed.

$c_3\,^1\Pi_u(0) \equiv \ell_1$

Janin [345–6] observed two new bands, degraded to longer wavelengths, at 2839.4 and 2980.1 Å. A partial rotational analysis [346] showed that the common upper level was $^1\Pi_u$ in type, showing a large Λ-doubling.

Janin concluded that the upper level of this transition was identical with Worley's state ℓ, also showing a large Λ-doubling. Further, Worley [666] found $B'=1.484$ cm^{-1}, compared with 1.492 cm^{-1} by Janin.

$c_3\,^1\Pi_u(2) \equiv d''$

Janin [346] and Janin and Crozet [347] observed in the region 3010–2510 Å a progression of five bands ($v''=0$–4), all degraded to shorter wavelengths. The 2–0 and 2–1 bands were partially analyzed. There was an indication of a perturbation in the upper state; the rotational lines were displaced, and the Λ-doubling became large at about $J'=13$.

$c_4\,^1\Pi_u(0) \equiv e$

Herman [295] observed in the region 2700–2220 Å a progression of six apparently single-headed bands ($v''=1$–6), all degraded to shorter wavelengths, but none of them were analyzed in detail.

Janin [345] suggested that the upper level, called e, probably was the second member of the Worley-Jenkins Rydberg series. A partial rotational analysis of two of the bands indicated a B-value of about 1.92 cm^{-1}.

$c_4'\,^1\Sigma_u^+(0) \equiv p'$

A progression of six bands ($v''=0$–5), degraded to shorter wavelengths, was observed in the region 3670–2820 Å, and was assigned to this system by Gaydon [249] and Janin [343].

Gaydon [249] analyzed the 0–0 band and found indications of a perturbation in the upper level about $J=10$; the same perturbation was also noted by Janin [344] and by Setlow [568], the latter in the $p'-X$ system. Gaydon concluded from his analysis that the upper level was $^1\Sigma_u^+$ in type.

Lofthus [423] also analyzed the 0–0 band, but at higher resolution. The perturbation in the p' level was readily observed, maximum perturbation lying between $J=10$ and 11. Conclusive evidence was found that this perturbation was caused by the $v=1$ level of the $b'\,^1\Sigma_u^+$ state.

The $c_4\,^1\Sigma_u^+$ state is now known to be the first member of the Carroll-Yoshino Rydberg series, not Worley-Jenkins series as believed in the past.

$c_4'\,^1\Sigma_u^+(1) \equiv r'$

Gaydon [249] observed two bands slightly degraded to shorter wavelengths, at 2671.7 and 2696.0 Å (Q-heads), terminating at $v''=0$ and 1, respectively of the $a\,^1\Pi_g$ state. The upper level was clearly $^1\Sigma_u^+$ in type, and a predissociation was indicated.

Lofthus [423] analyzed the first of these bands under higher resolution. The predissociation showed up very clearly as a cutting-off of all branches above $J'=11$; at least the intensities had decreased so much that the branches could not be followed after this point.

Measured isotope shifts in the $r'-a$ transition indicated that $v=1$ in the upper level [135, 431].

$c_4'\,^1\Sigma_u^+(2) \equiv k$

Lofthus [423] observed two bands, degraded to longer wavelengths, at 2524.9 and 2753.8 Å. The rotational analysis showed that they originated from the same upper level, and that the lower levels were $v=0$ and 2 of the $a\,^1\Pi_g$ state. The upper level was clearly $^1\Sigma_u^+$ in type. Indication of a transition from case b' to d' coupling was observed.

$c_4'\,^1\Sigma_u^+(3) \equiv s'$

Gaydon [249] observed three bands, slightly degraded to longer wavelengths, at 2397.1, 2496.8, and 2603.3 Å ($v''=0$, 1, and 2), and showed that the common upper level was $^1\Sigma_u^+$ in type.

Lofthus [423] observed the same bands at higher resolution, and made a rotational analysis. An anomalous intensity distribution among the branches of the bands was observed. The R branch was very weak, and the P and Q branches had about the same overall intensity, whereas in normal cases $Q>P>R$ should be expected.

Measured isotope shift in the $s'-a$ transition indicated that $v=3$ in the upper level [135,431].

$c_4'\,^1\Sigma_u^+(4) \equiv h$

Gaydon [249] and Herman [295] observed a progression of five bands ($v''=0$, 1, 3, 4, and 5), all slightly degraded to longer wavelengths (Q-heads). Gaydon analyzed the 4–0 and 4–3 bands and concluded that the upper level was $^1\Sigma_u^+$ in type. Lofthus [423] analyzed the 4–0, 4–1 and 4–3 bands under higher resolution, and obtained reliable band origins and rotational constants.

A transition from case b' to d' coupling was indicated in the upper level. There was also a clear indication of a not too sharp predissociation in the upper level. The branches had normal intensity up to $J'=10$, after which the intensity dropped markedly.

Measured isotope shift in the $h-a$ transition [135, 431] indicated that $v=4$ in the upper level.

$o\,^1\Pi_u(0)$

Janin and Crozet [347] observed two new bands at 2723.6 and 2853.3 Å, degraded to longer wavelengths. These bands were identified as 0–0 and 0–1, respectively, of the $o\,^1\Pi_u-a\,^1\Pi_g$ transition, where $o\,^1\Pi_u$ is identical with Worley's o-level, and is the first member of Worley's Rydberg series. Later, Janin [346] made a partial rotational analysis of the 0–0 band.

d'

Herman [295] observed a progression of three bands, 2358.8, 2455.1, and 2558 Å, which were assigned as 0–0, 0–1, and 0–2 bands of a new transition $d'-a$. No rotational analysis of this system exists, and the symmetry type of the upper level is thus unknown. Dressler [210] points out that this level (111333 cm^{-1}) does not fit into any other progression and that no trace of it has been found in absorption. This could well mean that the d' level, if real, belongs to a state of type $^1\Sigma_u^-$ or $^1\Delta_u$, though the calculations by Michels [459] do not indicate a state of either species near 13.8 eV. These features remain a puzzle.

The 49 observed bands of the Gaydon-Herman systems are given in table 20.

3.7. $x\,^1\Sigma_g^- - a'\,^1\Sigma_u^-$ Fifth Positive System (3070–2030 Å) V

The Fifth Positive System, though weak, remains the most prominent singlet system in N_2 above the vacuum region, and occurs readily in discharges in pure nitrogen at low pressures. Twenty-five bands have been observed in the region 3070–2030 Å, all degraded to shorter wavelengths (table 21).

This system was labeled Fifth Positive by Gaydon [249], because these bands are produced under conditions similar to those for exciting the stronger $D-B$ Fourth Positive system.

Most of the bands of this system were first observed by Duncan [216] in his study of electron impact spectra of nitrogen. Appleyard [52] observed two bands in a strong discharge, but made no assignments.

Van der Ziel [631] first analyzed the rotational structure of bands produced in a transformer discharge, and concluded that the transition was likely $^1\Sigma_g^- - {}^1\Sigma_u^-$. Herman also observed these [295], and discussed the vibrational structure. Gaydon [249], in a weak, condensed discharge, observed a new progression in addition to those seen by Van der Ziel, which required a change in v' numbering. From the rotational analysis of the (0–1) band, Gaydon concluded that the transition was either $^1\Sigma_u^+ - {}^1\Sigma_g^+$ or $^1\Sigma_g^- - {}^1\Sigma_u^-$.

More recently Lofthus [422] observed 19 bands under high resolution, including two new bands. The

detailed analysis provided vibrational and rotational constants for the x and a' states, though based on numerous blended lines. The observed bands are listed in table 21. Rotational constants for the a' and x states are in tables 53 and 68, respectively. The observed intensity alternation (even J, strong; odd J, weak) was consistent with either of Gaydon's possible assignments. Theoretical considerations [473] favored interpretation of the transition as $^1\Sigma_g^- - ^1\Sigma_u^-$.

Rajan [538] observed two new bands (1–10 and 2–12) in a discharge, and carried out a rotational analysis.

No bands with $v'>2$ have so far been observed, though some of them, according to the Frank-Condon principle, should be strong enough to be seen. Lofthus [424] attributed the absence of these bands to a predissociation (see section 8). See also section 7.

The vibrational numbering of Gaydon [249] has been confirmed by the isotope shift of $^{15}N_2$ bands produced in emission by Mahon-Smith and Carroll [431] (table 21).

Lefebvre-Brion and Moser [413] have shown from SCF MO calculations that the $x\,^1\Sigma_g^-$ state is the first term in a Rydberg series converging to $N_2^+ A\,^2\Pi_u$.

3.8. $y^1\Pi_g - a'^1\Sigma_u^-$ and $y^1\Pi_g - w^1\Delta_u$ Kaplan First and Second Systems (2860–2070 Å) V

Kaplan [374, 376] first reported the now so-called Kaplan First and Second systems of nitrogen, suggesting that they might involve a transition to the same level (a') as that involved in the Fifth Positive system. (Some of these bands had already been observed by Duncan [216] in a study of nitrogen by electron impact.)

Gaydon [249] made a rotational analysis of the (0–2) band of Kaplan's First system and proved that the lower state was identical with the lower state (a') of the Fifth Positive system, and suggested that the transition was either $y^1\Pi_u - a'^1\Sigma_g^+$ or $y^1\Pi_g - a'^1\Sigma_u^-$.

The Second system was obtained relatively strongly by Herman [295], who showed that the transition did not involve the lower state of the Fifth Positive system, and that the upper state might be identical with the upper state of the First System.

Lofthus and Mulliken [425] remeasured these systems under high resolution (two new bands were observed) and the final conclusion as to their nature seems to have been resolved. The First system was found to involve a transition $y^1\Pi_g - a'^1\Sigma_u^-$ as suggested by Gaydon, and the Second system, a transition $y^1\Pi_g - w^1\Delta_u$, as suggested by Herman, where $w^1\Delta_u$ was a state not known from other transitions. Recently, Carroll and Subbaram [140] have observed emission from the new state $k^1\Pi_g$ to the a' and w states, and for the first time, observed Kaplan bands with $v'=2$. Their rotational analysis indicated that the new k state perturbs the structure of the $y^1\Pi_g$ state.

Kaplan's systems are rather weak, and most of the bands, which lie in the region 2860–2070 Å, are more or less obscured by stronger structures. The systems were observed by Kaplan [374, 376] in a special tube for producing the afterglow, by Herman [352] in an ordinary discharge at low pressure in a long tube, and by Lofthus and Mulliken [425] in an ordinary transformer-excited discharge through pure nitrogen in a short tube at gas pressures about 0.5 torr (0.06 k Pa). Altogether eight bands of the First system (table 22) and thirteen bands of the Second system (table 23) are observed.

The analysis of the First system yielded constants for the $a'^1\Sigma_u^-$ state in complete agreement with those from the Fifth Positive system. The analysis of the Second system yielded new and accurate data for the $w^1\Delta_u$ state. Rotational constants for the y and w states are in tables 69 and 55, respectively.

No perturbations in the lower states $a'^1\Sigma_u^-$ and $w^1\Delta_u$ were revealed; by contrast, the upper state $y^1\Pi_g$ showed peculiar structure. An apparently clear breaking-off of the branches coming from the Π^+ levels of the y state above $v'=0$, $J'=10$, and a perturbation of the remaining Π^- levels was observed. This breaking-off of the rotational structure was originally interpreted by Lofthus and Mulliken [425] as an allowed predissociation by a $^1\Sigma_g^+$ state dissociating to two ^2D atoms; however, after the exact location of the $y^1\Pi_g$ state was determined by Wilkinson and Mulliken [662] from an observation of the $a'^1\Sigma_u^- - X^1\Sigma_g^+$ transition, a revision of this view became necessary (section 8). A large Λ-splitting in the $y^1\Pi_g$ state (section 7) was also observed.

Mahon-Smith and Carroll [431], observing five emission bands for $^{15}N_2$ (tables 22 and 23), have confirmed the vibrational numbering for the states involved.

Lefebvre-Brion and Moser [413] have shown from SCF MO calculations that the $y^1\Pi_g$ state is the first term in a Rydberg series converging to $N_2^+ A\,^2\Pi_u$.

3.9. $k^1\Pi_g - a'^1\Sigma_u^-$ and $k^1\Pi_g - w^1\Delta_u$ Carroll-Subbaram First and Second Systems (2700–2300 Å) V

Carroll and Subbaram [140] have observed two very weak emission systems of N_2 in the near UV. The upper state is a new $^1\Pi_g$ Rydberg state having configuration . . . $(1\pi_u)^4\,(2\sigma_g)3d\pi_g$ and the lower states are $a'^1\Sigma_u^-$ and $w^1\Delta_u$. Conventional fine structure analysis showed the k state levels to be perturbed in a manner similar to that of the y state (section 7.1); the c levels of the new state are predissociated in an unusual way (section 8.9). Deperturbed constants for this state place it very close to the $y^1\Pi_g$ state with which it suffers a strong homogenous interaction that explains the observed irregularities.

Observed bands of the $k-a'$ system and $k-w$ system are given respectively in tables 24 and 25. Rotational constants for the k state are in table 70.

3.10. $a^1\Pi_g - a'^1\Sigma_u^-$ and $w^1\Delta_u - a^1\Pi_g$ McFarlane Infrared Systems (30,000–85,000 Å)

The stimulated emission spectrum of the nitrogen molecule was examined by McFarlane [447–50] between 30000 and 85000 Å using a pulsed gas discharge laser. One hundred-twenty lines were observed of which 36 were identified as arising from the transitions $a^1\Pi_g - a'^1\Sigma_u^-$ and $w^1\Delta_u - a^1\Pi_g$. These lines are given in table 26.

The remaining lines observed fall into four groups:

Group I	1866.89–1803.01 cm^{-1}	24 lines
Group II	1692.84–1600.44 "	24 "
Group III	1543.82–1482.71 "	16 "
Group IV	1314.37–1239.90 "	20 "

No definite assignment was made by McFarlane, although he pointed out that the lines could possibly belong to a $^3\Delta_u - B^3\Pi_g$ transition. This suggestion was recently confirmed by Wu and Benesch [670] who, in their arrays of calculated band positions in their newly observed infrared system, $W^3\Delta_u - B^3\Pi_g$, identified McFarlane's Groups I–IV as the (1–2), (0–1), (1–0), and (2–1) bands of this system. (See Wu-Benesch System, section 3.18.)

The high relative accuracy in line position measurements made it possible to specify very precisely, differences in B-values for the states involved in the transitions. Also, for the first time it was possible to observe in the unperturbed region at low J values the Λ-type doubling in $v=0$ of the $a^1\Pi_g$ state [448].

Term differences between the a, a', and w states could also be determined with higher accuracy than before. However, there is a discrepancy ranging from 0.25 cm^{-1} to 0.45 cm^{-1} between the observed infrared lines and those that can be calculated from known lines and constants from the vacuum UV spectra involving the same states (see Benesch et al. [70]).

The absolute accuracy quoted by McFarlane is $1:10^4$ in the 80000 Å region, and $5:10^5$ in the 30000 Å region; consequently there should be an absolute wavenumber uncertainty of about 0.15 cm^{-1} for the observed lines and the deduced term differences.

On the other hand, Vanderslice et al. [627] quote an absolute wavenumber uncertainty of about 0.30 cm^{-1}. It then turns out that the apparent discrepancy is within experimental error.

By combining the w–a 0–0 band origin with the term value of the a state from UV measurements [627], an improved term value is obtained for the w state: $T_0 = 71698.44 \pm 0.33$ cm^{-1}. The prior determination was based on a three-step process.

Averaged rotational constants when Λ-doubling is not apparent are [449]: $B_0(w^1\Delta_u) = 1.4870$ cm^{-1}; $B_0(a^1\Pi_g) = 1.6065$ cm^{-1}.

3.11. $A^3\Sigma_u^+ - X^1\Sigma_g^+$ Vegard-Kaplan System (5325–1250 Å) R

The important Vegard-Kaplan system, which fixes the relative energies of the singlet and triplet states, is the weakest of the known intercombination systems, and is observed in the aurora and in laboratory sources only under rather special conditions of excitation [561].

Vegard [633–4] was the first to observe this system, and found 120 red-degraded bands in the region 6700–1700 Å in the luminescence of solid nitrogen. Shortly thereafter, Kaplan [373] observed the system of single-headed bands in gaseous nitrogen in the laboratory. In the region 3500–2300 Å, 14 bands were observed in a special discharge in which the afterglow was present.

Bernard [76] produced additional bands by electron bombardment of a mixture of argon and nitrogen. Altogether 26 new bands were observed in the region 5400–3600 Å ($v'=0-7$, $v''=10-18$).

Wulf and Melvin [671] made a partial resolution of the rotational structure of four bands in emission (1–4), (1–5), (0–5) and (0–6), and found satisfactory agreement between calculated and measured line positions, thus making more certain the identification of the system.

Janin [344] studied the system in a high-voltage discharge through pure nitrogen at atmospheric pressure, and obtained 13 bands, 11 of which could be partially resolved, thus yielding approximate rotational constants of the two states involved.

In a laboratory source Herman [296, 300] observed 45 bands, many of which were for higher v' and v'' values ($v'=0-5$, $v''=12-15$).

The Vegard-Kaplan system had for a long time escaped detection in absorption (Herzberg [13]). Wilkinson [656], however, succeeded in observing two bands in absorption (9–13 m·atm). These weak bands, at 1689 (7–0) and 1276 Å (6–0), were incompletely resolved, but showed intensity alternation and distribution in agreement with theory. Later, Tilford and Wilkinson [614] reported that the Vegard-Kaplan bands had been observed in absorption up to $v'=22$, corresponding to 9.67 eV., but no further details were given.

Tanaka and Jursa [600], using a new method for producing the auroral afterglow, observed this system with more intensity than did Kaplan [373], and were able to make extended observations in the region 3425–2200 Å.

Miller [462] developed a special light source which emitted the Vegard-Kaplan system with sufficient intensity for a high dispersion, high resolution spectrograph, and the (0–4), (0–5), and (0–6) bands were analyzed in detail. The absolute energy of the triplet levels in nitrogen could now be obtained by adding to the values of band origins the corresponding energy of the $v=4$, 5, and 6 levels of the ground state as obtained by Miller [462–3] from an analysis of the more intense Lyman-Birge-Hopfield system [464].

Carleton and Papaliolios [120] have measured relative intensities of eight bands in the 2470–3425 Å region. The emission from a pulsed discharge was measured photoelectrically; a tungsten filament was used for calibration. Chandraiah and Shepherd [156] observed this system emitted from a low-current discharge through a xenon-nitrogen mixture. Photoelectric measurements of relative intensities were made on 18 bands (2340–4324 Å). Calibration was with respect to an ultraviolet low brightness source, which was calibrated against a tungsten ribbon filament lamp. In both above cases, there was some overlap by C–B (2+) bands.

Shemansky [570] has observed bands (6−0) to (12−0) in absorption through 12 m·atm. of nitrogen. His absorption intensities are included in table 27 which lists the observed A–X bands. Rotational constants for the A state are given in table 50.

Numerous authors have observed the A–X Vegard-Kaplan system in aurorae, including Petrie and Small [525], Broadfoot and Hunten [98], and Crosswhite, Zipf, and Fastie [187], the latter from a rocket at a height of 125 km.

Wright and Winkler [43] discuss in detail the excitation of this system, especially in the afterglow.

3.12. $B^3\Pi_g - A^3\Sigma_u^+$ First Positive System (25310–4780 Å) V

The First Positive System is the most prominent band system of nitrogen. It appears readily in most types of discharges, notably in the positive column, and it consists of numerous multiple-headed bands degraded to shorter wavelengths, extending from the infrared to the blue. Because of its strong intensity, this system was the first to be studied by the early investigators, and has since been the subject of many detailed investigations.

The visible part of the First Positive System was already investigated by Deslandres [194] and von der Helm [640], and under somewhat higher resolution by Birge [79–80], who made the first vibrational analysis. Some bands were also identified by Fowler and Strutt [136], and by Birkenbeil [84].

Poetker [531] photographed the system in the infrared region 10500–7500 Å, and thermocouple measurements extended the known part of the system up to 15000 Å. On the basis of his study, Poetker reassigned the vibrational numbering given by Birge.

Until then (1927) little was known about the rotational structure of the bands and of the nature of the transition involved. Then Naudé [484] obtained bands at higher dispersion and resolution by means of a powerful discharge in pure nitrogen, and analyzed in detail two bands: (5–2) and (6–3). On the basis of his analysis, Naudé concluded that the transition was $^3\Pi - {}^3\Sigma$ in type, the $^3\Pi$ state probably conforming to Hund's case a for lower J values, and going over to case b for higher J values. From the Λ-type doubling, it was concluded that the $^3\Pi$ state was normal. The branch lines showed alternating intensities in the ratio 2:1, approximately, in conformity with theory. The rotational levels of the $^3\Sigma$ state having odd N values were found to have the greater statistical weight, and thus this state could be either $^3\Sigma_g^-$ or $^3\Sigma_u^+$. The observed spin fine structure of the lower $^3\Sigma$ state agreed closely with theory (section 7.2). Some rotational constants were given.

Van der Ziel [630] analyzed two bands, (12–8) and (12–7) in order to study the predissociation above $v'=12$, first observed by Kaplan [370–1].

Feast [223] analyzed the (1–0) band under high resolution. From his measurements the spin splitting in the $A^3\Sigma_u^+$ state and the Λ-doubling in the $B^3\Pi_g$ state could be evaluated. Herman and Weniger [301] studied the same band under conditions which excited higher rotational levels, and analyzed it in some detail.

Hepner and Herman [293] extended the known part of the system farther into the infrared by studying the emission spectra of nitrogen in the region 9000–26000 Å using a spectrometer equipped with a lead sulfide cell. Fifteen new bands were observed.

Carroll [123] analyzed the rotational structure of the (0–1), (2–1) and (3–2) bands, and calculated rotational constants. The observed Λ-doubling in the levels $v=1$, 2 and 3 of the $B^3\Pi_g$ state was found to follow the trend predicted theoretically for a $^3\Pi$ state conforming to Hund's case a at low J values and tending to case b with increasing J. Carroll also measured the spin splitting in the $A^3\Sigma_u^+$ state.

Carroll and Sayers [139] remeasured some bands in the photographic infrared, and gave improved wavelengths for the band heads. They also recorded 14 bands in the blue, until then only observed in the afterglow (see Herman [295]). From their measurements, combined with data from Birge [79–80] and Birkenbeil [84], Carroll and Sayers obtained improved vibrational constants.

In a very extensive and detailed work, Dieke and Heath [196] measured the positions of a large number of bands, and made a very accurate rotational analysis of 21 of them. By cooling the discharge with liquid nitrogen, and using a spectrograph of high resolution, they obtained band structure for this system to a higher degree of accuracy than had been obtained before. Except for the predissociation above $v=12$ in the $B^3\Pi_g$ state (section 8.4), no irregularities in the band structure of the First Positive System have been observed.

The observed bands and band origins of the B A First Positive System are listed in table 28. Rotational constants for the A and B states are given in tables 50 and 51, respectively.

Tanaka and Jursa [600] have observed 60 bands with high v' (up to 26) in the auroral afterglow. Only a few bands are new (P_{11} heads are included in table 28). Intensity measurements have been made by

Turner and Nicholls [619]. Mathias and Parker [440], Kasuya and Lide [379], Andrade et al. [48], Massone et al. [437], and Tocho et al. [617] have observed numerous stimulated emission lines of the system, produced by a molecular nitrogen pulsed laser.

Wright and Winkler [43] discuss in detail the excitation conditions under which the $B-A$ (1+) system is produced. (See also Heath [289] on excitation of the B–A and C–B systems.)

Bullock and Hause [107] have obtained equilibrium molecular constants for the A and B states from a non-linear least squares analysis of the data on the $B-A$ (1+) bands observed by Dieke and Heath [196]. The main feature of these new results is that the constants for both states were obtained simultaneously, thereby acknowledging the correlation among the coefficients of the two states. In some instances there are large differences from the results of Dieke and Heath.

The published values differ from those in the thesis by Bullock because revised formulas for the $^3\Pi$ state were used (these being supplied by Kovacs). Two unexpected results suggest that these constants are tentative: There was found no v-dependence for the centrifugal distortion parameter D, and the revised constants for the A state are the same as the thesis values.

3.13. $C\,^3\Pi_u - B\,^3\Pi_g$ Second Positive System (5460–2680 Å) V

The Second Positive System appears readily in most sources, notably in ordinary discharges through pure nitrogen and air. The known part of the system consists of some fifty triple-headed bands, all degraded to shorter wavelengths.

Although observed and described since 1869, it was not before the 1920's that the rotational structure of this system became a subject of systematic study. Mecke and Lindau [451], Lindau [418] and Hulthen and Johansson [327] all measured rotational structure and band positions, and set up a vibrational scheme. These authors also observed a sharp cutting-off of the rotational levels in $v'=4$, which Herzberg [304] attributed to a predissociation. Perturbations of various types in the upper state were also observed (see section 7.4).

Herzberg [303], and Coster, Brons and van der Ziel [175] observed some weak bands of the isotope molecule $^{14}N^{15}N$, and measured the displacement of the (1–0) and (2–0) bands relative to those of $^{14}N_2$, confirming the vibrational numbering.

In the early 1930's a detailed rotational analysis of the system was undertaken. Coster, Brons and van der Ziel [175] analyzed six bands and evaluated some rotational constants. Their analysis indicated that the transition was $^3\Pi$–$^3\Pi$ in type. In both states Hund's coupling case a was approached for small J, and case b for large J. For the state $B^3\Pi$ this was in conformity with previous observations of the B–A First Positive System. Guntsch [276] analyzed 18 bands. These authors all observed and discussed the predissociation and the various perturbations in the $C^3\Pi_u$ state.

In order to study more fully the type of predissociation, Büttenbender and Herzberg [112] analyzed the rotational struture of the (2–0), (3–0), (3–1), (3–5), (4–1), (4–2) and (4–6) bands, and offered improved rotational constants. Coster, van Dijk, and Lameris [176] observed some bands at very high resolution, and gave line positions of the (0–0) band for higher J-values ($J=40-91$). Budó [106] developed a general formula for term values for $^3\Pi$ states in intermediate coupling between Hund's cases a and b. By using data in the literature for the B–A and C–B systems, he derived revised equilibrium rotational and spin splitting constants for the B and C states.

Pankhurst [514] remeasured the wavelengths of heads of the system, reliable to 0.1 Å. Carroll and Sayers [139] added five new bands in the green. Janin [344] observed new branches in some bands, and discussed perturbations.

At very high resolution, Dieke and Heath [196] measured bands of this system and made a detailed rotational analysis of nine of them. By combining these results with those from the First Positive System, they obtained improved molecular constants for the $A\,^3\Sigma_u^+$, $B\,^3\Pi_g$ and $C\,^3\Pi_u$ states. Rotational constants for the A, B and C states are in tables 50, 51, and 57, respectively. Observed bands for the C–B transition are in table 29.

A number of satellite branches of very low intensity were found which had not been observed before. (Satellite branches are those for which $\Delta J \neq \Delta N$; they cannot occur in exact case a or exact case b coupling.) Dieke and Heath also measured and discussed Λ-doubling and triplet separations in these states, as well as various perturbations in the $C^3\Pi_u$ state (see section 7.4).

Pannetier et al. [515], in a study of the atomic flame spectra with aliphatic amines in active nitrogen, observed the (3–3) and (4–4) bands of this system. An additional band, with head at 3259.2 Å, was interpreted as (5–5). Tanaka and Jursa [600], studying the (2+) system with high intensity in the auroral afterglow, observed for the first time four weak, red-degraded triplet bands which were all believed to originate from $C^3\Pi_u$ ($v=5$). The term value for this level lay higher by 140 cm^{-1} than that obtained by Pannetier et al.

Carroll and Mulliken [136] examined the strong "non-crossing rule interaction" between levels of the $C^3\Pi_u$ and $C'^3\Pi_u$ states and concluded that the Pannetier level was mostly C, and the Tanaka-Jursa level mostly C'. (Details are discussed more fully in section 7 and section 8.)

$C-B$ stimulated lines in a nitrogen pulsed laser have been observed by Kaslin and Petrash [378],

Kasuya and Lide [379], Parks et al. [519], and Tocho et al. [617]. These results all concern lines of the 0–0 band.

Wright and Winkler [43] have surveyed in some detail the appearance and occurrence of this system, especially in the afterglow. An identification atlas by Tyte and Nicholls [37] includes vibrationally identified spectrograms, a compilation of molecular data on the B and C states, and a selected bibliography.

3.14. $B\,^3\Pi_g - X\,^1\Sigma_g^+$ Wilkinson System (1685–1640 Å) R

Wilkinson [659] observed two new weak band heads in absorption at 1685.8 and 1638.7 Å (table 30). These heads appear to coincide with the predicted positions of the 0–0 and 1–0 heads ($^3\Pi_1$ component) of the $B\,^3\Pi_g - X\,^1\Sigma_g^+$ transition. As with the $a\,^1\Pi_g - X\,^1\Sigma_g^+$ transition, the $B-X$ must be partly magnetic dipole and partly electric quadrupole in nature.

The transition is an intercombination one, made possible by violating the spin selection rule $\Delta S=0$. The $B\,^3\Pi_g$ and the $a\,^1\Pi_g$ states have the same electron configuration and symmetry properties and lie rather close together. An expected interaction between these states leads to increased strength of the $B\,^3\Pi_g - X\,^1\Sigma_g^+$ transition.

3.15. $B'\,^3\Sigma_u^- - X\,^1\Sigma_g^+$ Ogawa-Tanaka-Wilkinson System (2240–1120 Å) R

By using a transformer discharge through a mixture of nitrogen and xenon, Ogawa and Tanaka [497–8] observed 16 double-headed, red-degraded bands in the region 2240–1590 Å. The bands were attributed to the transition $B'\,^3\Sigma_u^- - X\,^1\Sigma_g^+$, the upper state of which was known from the observation of the $B'\,^3\Sigma_u^- - B\,^3\Pi_g$ infrared afterglow system. Wilkinson [657] observed in absorption four bands to $v=0$ to 3 of the $B'\,^3\Sigma_u^-$ state (then called Y). Ogawa and Tanaka did not observe Wilkinson's bands in emission, but from their vibrational data the position of these bands could be calculated, and good agreement was found with Wilkinson's data.

Tanaka et al. [604] observed the absorption spectrum with low resolution for $v'=0$–20. Individual bands consisted of two sharply defined heads of S and Q branches, both degraded to longer wavelengths. Tilford et al. [611] observed the same system for $v'=0$–18 at high resolution, and made a complete rotational and vibrational analysis.

Five branches: ^OP, ^QQ, ^SR, and ^QR and ^QP were expected for a $^3\Sigma_u^- - ^1\Sigma_g^+$ transition as a result of the $^3\Sigma_u^-$ mixing with $^1\Pi_u$ and $^1\Sigma_u$ states. The observed ^QR and ^QP branches were not resolved. Spin-spin and spin-orbit coupling, and line intensities were discussed. The line intensity distribution in the various branches is accounted for by revised formulas due to Watson [643] (see also Kovacs [394]). In particular, the sum of the overlapped ^QP and ^QR branches agrees with experiment, whereas the formulas used by Tilford et al. [611] give results too high by nearly a factor of two.

The observed emission and absorption bands are listed in table 31. Rotational constants for the B' state are in table 52.

3.16. $C\,^3\Pi_u - X\,^1\Sigma_g^+$ Tanaka System (1130–1070 Å) R

In absorption Tanaka [597] observed three new double-headed, red-degraded bands at about 1076, 1099, and 1123 Å. Considerations of their relative intensities, appearance, and wavelengths led Tanaka to suggest that the bands probably belonged to the intercombination transition $C\,^3\Pi_u - X\,^1\Sigma_g^+$. With higher resolution, individual bands of this system were resolved into five heads by Tanaka et al. [604].

The system was remeasured at very high resolution by Tilford et al. [612]. Only the 0–0, 1–0, and 2–0 bands could be observed; these show nine branches. The analysis, together with the intensity distribution, confirmed the upper state as $C\,^3\Pi_u$. A few minor perturbations were observed. A branch intensity formula for a $^3\Pi_u - X\,^1\Sigma_g^+$ transition was derived, following a method of Chiu [159]. This system has not been observed in emission.

The observed bands are listed in table 32.

3.17. $B'\,^3\Sigma_u^- - B\,^3\Pi_g$ Infrared Afterglow System (8900–6050 Å) R

In the infrared spectrum of a high-voltage transformer discharge, Carroll and Sayers [139] observed a new multi-headed band, degraded to longer wavelengths; the strongest head was located at 8310 Å.

In the spectrum of a nitrogen afterglow, Brook [104] observed four new bands at 6897, 7788, 8247 and 8459 Å, all degraded to longer wavelengths. Kistiakowsky and Warneck [387] observed four additional bands of similar type (which they called the Y bands) at 6934, 7823, 8949 and 10434 Å, the first two of which probably correspond to the long wavelength heads of the 6897 and 7788 Å bands of Brook. The corresponding $^{15}N_2$ bands were also seen.

LeBlanc et al. [407] observed in the afterglow many more bands (14 in all) in the region 8700–6000 Å, including the first two of Kistiakowsky and Warneck's bands and the first of Brook. These authors found excellent agreement between the vibrational spacings for the lower state of the new system and those for the $B\,^3\Pi_g$ state, and concluded that the new system does indeed terminate on the $B\,^3\Pi_g$ state. They further pointed out that, according to Mulliken's [473] predictions, there should be two electronic states, $^3\Delta_u$ and $^3\Sigma_u^-$, which could account for the upper state of the system.

Carroll and Rubalcava [137] remeasured with higher resolution the 8265.5 Å band (long wavelength head 8310 Å) previously observed by Carroll and Sayers [139], and concluded that it was identical

with one of the bands observed by LeBlanc et al. [407]. They were also able to analyze the rotational structure of the band. Subsequently Carroll and Rubalcava [138] reported a more detailed study of the same band. An observation of the isotope shifts showed that the band was in fact 5–1 of the $B'^3\Sigma_u^- - B^3\Pi_g$ system. Dieke and Heath [197] analyzed the rotational structure of the 8–3 band of the normal isotope.

Khvostikov and Megrelishvili [385] observed two nitrogen bands in the twilight sky spectrum. They are believed to be the 7–1 and 6–0 bands of this afterglow system.

Mahon-Smith and Carroll [431] reconfirmed the vibrational scheme for this system from an observation of the isotope shift in $^{15}N_2$. Earlier Bayes and Kistiakowsky [64] observed the afterglow spectrum in $^{15}N_2$, and although their work was apparently carried out at quite low resolution, their results left little doubt as to the vibrational numbering in the B' state.

Wright and Winkler [43] have surveyed in detail the appearance and occurrence of this system, especially in the afterglow.

Observed bands are given in table 33.

3.18. $W^3\Delta_u \rightleftarrows B^3\Pi_g$ Wu-Benesch Infrared System (22,000–43,000 Å) R, V

The triplet counterpart to the well-established $w^1\Delta_u$ state, called $W^3\Delta_u$, has been predicted to lie at about 7.5 eV by Mulliken [473]. Evidence for the importance of this state in discharges and afterglows in nitrogen mixed with rare gases has been given experimentally by Kenty [383], who concluded that the energy for the $v=0$ level of this state must be close to 7.35 eV. The state has also been invoked in a discussion of the mechanism of the Lewis-Rayleigh afterglow by Bayes and Kistiakowsky [64].

In a discharge through 2 to 10 torr (0.3 to 1.3 kPa) of flowing nitrogen gas, using an infrared spectrometer, Wu and Benesch [670] observed eleven bands in the 22,000–41,000 Å region. Seven of these were assigned to the $W^3\Delta_u \rightleftarrows B^3\Pi_g$ system. The bands attributed to the W–B transition were arranged in a Deslandres array with only relative vibrational quantum numbers assigned. ΔG's for the vibrational levels of the lower state coincided with those for the $B^3\Pi_g$ state. Several choices of v' were made, and that one selected which gave a T_e nearest the prediction of Mulliken [473]. The most compelling reason for the v' selected was that there could be drawn a reasonable Condon locus consistent both with the observed bands as well as with groups of unidentified laser-induced emission lines, observed by McFarlane [448], but suspected of belonging to a $^3\Delta_u$–B system.

Saum and Benesch [556] extended the number of bands to fifteen, seven of which belong to the $W \rightarrow B$ transition, and eight to the $W \leftarrow B$ transition. In addition, two bands, 4435 cm^{-1} and 4134 cm^{-1}, of a group observed by Hepner and Herman [293] were found to be the 3–0 and 4–1 bands of the W–B system.

The emission bands come about as a result of a transition between two electronic states which lie so close to one another in energy that intra-system cascading becomes prevalent. The W–B system can thus appropriately be regarded as two band systems, W–B and B–W. This feature is clearly illustrated in figure 1 of Benesch and Saum [67], showing the potential curves of the two states involved. (See figure 2 of this report.)

The resolution (0.5 cm^{-1}) did not allow a complete rotational analysis. Benesch and Saum [67] instead constructed a computer-generated model to obtain values of the band origins given here in table 35. They are considered accurate to ± 2 cm^{-1}.

Combining the information from both the W–B and W–X systems (for the latter see Saum and Benesch [557]), Benesch and Saum [67] calculated vibrational constants for the $W^3\Delta_u$ state (see table 1). The location of the $W(0)$ level, $T_o = 59378$ cm^{-1} (i.e., 7.362 eV) was in very close agreement with the observation of Kenty [383].

3.19. $W^3\Delta_u - X^1\Sigma_g^+$ Saum-Benesch System (1505–1440 Å) R

From the known spectroscopic constants for the $W^3\Delta_u$ state, obtained from the $W^3\Delta_u$—$B^3\Pi_g$ system, it is possible to calculate the location of bands of the $W^3\Delta_u - X^1\Sigma_g^+$ system. This is a forbidden transition which can become observable due to mixing with neighboring $^1\Pi_u$ states. Saum and Benesch [557] calculated Deslandres and Franck-Condon arrays which together with the relevant potential energy curves (see fig. 1) for the system indicate which bands of the system are likely to occur most readily.

Saum and Benesch in fact found three weak unanalyzed bands in a compendium of ultraviolet absorption by Tilford et al. [34] (table 34) (see Benesch and Saum [67]).

Since only the $v=0$ level of the $W^3\Delta_u$ is expected to be appreciably populated because of intrasystem cascading, only the $v'=0$ progression will occur in emission. The 0–4, 0–5, and 0–6 W–X bands should be the strongest, but so far they have not been observed.

3.20. $C'^3\Pi_u - B^3\Pi_g$ Goldstein-Kaplan System (5080–2860 Å) R

The Goldstein-Kaplan system is a relatively weak one consisting of a number of complex red-degraded bands in the region 5080–2860 Å. A few of these bands were first recognized by Goldstein [263] in an induction-coil discharge in nitrogen at a few cm pressure at liquid-air temperature, but no measurements of any precision were made. Kaplan [374–5] rediscovered these bands, together with some new

ones, apparently belonging to the same system. He identified them as probably belonging to a transition from an unknown state to the $B^3\Pi_g$ state.

In the afterglow of a 3.5 kV dc discharge in a special tube at gas pressures of a few mm to a few cm, at liquid-air temperature, Hamada [284–5] observed and measured positions of 13 bands, and arranged them into two progressions, the one labeled $v'=1$ being very feeble compared with the $v'=0$ progression. Gaydon [247–8] observed part of the system in various sources, the best source being a Tesla-coil discharge at high gas pressures. The bands also appeared quite readily in the ozonizer-type discharge and in normal discharge tube sources, provided the gas pressure was about 100 torr (13 k Pa). Only the bands at 4166, 4432, and 4728 Å were well developed, but weaker bands at 5059 and 5450 Å were also visible on Gaydon's plates. Gaydon considered the possibility that these bands might constitute two systems, one in the blue-green, one in the near ultraviolet region.

Tanaka and Jursa [600] observed twelve bands of the system in a special light source designed to produce the auroral afterglow. Their measured band heads constitute the bulk of table 36.

Crosswhite, Zipf, and Fastie [187] observed two bands of this system in a rocket probe measurement of the aurora, and Pleiter [530] observed a number of them in the spectrum from a radio-frequency-excited nitrogen jet.

Carroll [128] obtained the 0–3, 0–4, and 0–11 bands under high resolution in a conventional transformer discharge through pure N_2 at pressure of a few Torr. He showed conclusively that the blue-green Goldstein bands and the ultraviolet Kaplan bands form a single system having the well known $B^3\Pi_g$ as the lower state. The upper state C' was identified as $^3\Pi_u$, in coupling case b. Rotational constants for the $v=0$ level are given in table 59. The C' state had an unusual structure in which spin-spin interaction appeared to play an important role. To account for the unusual properties of the state, Carroll suggested that it arises from a mixture of two or more MO configurations. The vibrational structure indicated that either predissociation occurred or that the state had a very small dissociation energy. Interaction of states C and C', both $^3\Pi_u$, was suggested as responsible for the observed irregularities in the C state.

Carroll and Mulliken [136] examined in fuller detail the strong "non-crossing rule interaction" between the C and C' states. The two bands at 3026 and 3178 Å, observed by Hamada [284–5] and Tanaka and Jursa [600], and assigned as the 1–4 and 1–5 bands of the Goldstein-Kaplan system, were reassigned with $v'=2$ by Carroll and Mulliken, who further suggested that the C' state had a potential maximum, and tended to dissociate to $^4S+^2D$. Sections 7 and 8 contain a fuller account of these considerations.

Mahon-Smith and Carroll [431] confirmed the vibrational numbering of this system from observation of the isotope shifts in $^{15}N_2$ (table 36). Carroll [128] had provided a hint that the labeling of bands with $v'=1$ might be in error, since the ΔG (approximately ω) for the C' state, using Hamada's quantum numbering [284–5] gave a vibrational frequency about twice that obtained from the B and D coefficients.

3.21. $D^3\Sigma_u^+ - B^3\Pi_g$ Fourth Positive System (2900–2250 Å) V

In a condensed discharge producing the afterglow in pure nitrogen, Fowler and Strutt [234] observed a new system of seven bands, all degraded to shorter wavelengths. Each of the bands showed five principal heads. This new system has been labeled "Fourth Positive."

Heurlinger [311] showed that the bands belonged to a v''-progression and it was readily seen from the measured positions that the bands terminated at the $v=0$ to 6 levels of the $B^3\Pi_g$ state.

Gerö and Schmid [257] analyzed the rotational structure of the 0–1 and 0–2 bands, and concluded that the transition was $^3\Sigma - {}^3\Pi$.

The nature of the intensity alternation, and the identification of the lower state as $B^3\Pi_g$ indicated that the upper state was $^3\Sigma_u^+$. No noticeable spin-splitting in the upper state was observed.

Only a single upper vibrational level has been observed, and this level has tentatively been assigned to $v'=0$. The absence of higher vibrational levels may indicate a predissociation.

Wentink et al. [650] observed this system readily in the spectrum from a pulsed discharge in flowing pure nitrogen.

Lefebvre-Brion and Moser [413] showed that the $D^3\Sigma_u^+$ state coincided in energy with a theoretically predicted first member of a triplet Rydberg series converging to the ground state of N_2^+.

Observed bands are listed in table 37. Rotational constants for the D state are in table 62.

3.22. $E^3\Sigma_g^+ - A^3\Sigma_u^+$ Herman-Kaplan System (2740–2130 Å) V

In a special discharge tube in which the afterglow was present, Kaplan [376] observed a new system consisting of four bands at 2242, 2316, 2392, and 2472 Å. These bands were only present at the lowest pressure which would support a discharge.

Herman [295] extended this system to twelve bands, and made a tentative vibrational analysis (table 38). The vibrational spacings clearly indicated that the lower state of this system was $A^3\Sigma_u^+$. If the transition is allowed, the upper state must be $^3\Sigma_g^+$ or $^3\Pi_g$. Mulliken [473] had pointed out that the location of the state, the vibrational data, and the absence of observed bands of a transition $E - {}^3\Delta_u$, made the identification $E^3\Sigma_g^+$ probable.

Lefebvre-Brion and Moser [413] showed that the E state coincided in energy with a theoretically predicted first member of a triplet Rydberg series converging to the ground state of N_2^+.

Heidman et al. [292] observed a resonance at 11.87 eV in a high resolution electron spectrometer, which is coincident in energy with the $E^3\Sigma_g^+$ state.

Carroll and Doheny [133] have observed the rotational structure of this system for the first time. Their rotational analysis of bands 0–2,3,4,5 has determined the upper state to be, unambiguously, $^3\Sigma_g^+$, as initially suggested by Mulliken. This Rydberg state is obtained by adding a $3s\sigma_g$ electron to the $N_2^+ X\,^2\Sigma_g^+$ core. No spin splitting was observed in the E state, within experimental error.

This very weak system was produced in a 10,000 volt ac discharge. Each band showed a triplet R branch and a head-forming triplet P branch. The observed bands are included in table 38. Rotational constants for the E state are in table 58.

Rotational constants had been derived for each band. Since only low N values were observed, the D values are not very accurate. The constants given in table 58 were obtained from a fit to the calculated rotational levels of the E state.

The $E-A$ transition is allowed by electric dipole selection rules, but it involves a two-electron change in orbital configuration: $(1\pi_u)^4(2\sigma_g)(3s\sigma_g)$ to $(1\pi_u)^3(2\sigma_g)^2(1\pi_g)$. The long lifetime of the E state adds support to the description of this state as metastable.

3.23. $H^3\Phi_u - G^3\Delta_g$ Gaydon-Herman Green System (6370–5040 Å) V

The known part of Gaydon's Green system consists of 17 weak, complex bands, degraded to shorter wavelengths. In ordinary discharges the bands are, if present, completely masked by bands of the $B-A$ First Positive system. The system can therefore only be studied in special sources where the First Positive system is weak or absent.

Gaydon [248] first observed seven bands of this system in an ozonizer-type discharge at atmospheric pressure and in a Tesla discharge at a pressure of a few cm, and arranged them into a provisional vibrational scheme. The general appearance of the bands was very similar to that of the $D-B$ Fourth Positive system, suggesting that the bands may be due to a $^3\Sigma - {}^3\Pi$ transition.

Herman [295] observed three bands of this system. Carroll and Sayers [139], using a Tesla discharge and a transformer-excited discharge, observed all of Gaydon's bands in addition to a new one (3–1) at 5062 Å.

Grün [273] produced this system by electron bombardment of a molecular beam. In this source, most completely free of the $B-A$ bands, 17 bands of this system were observed and measured. Contrary to Gaydon, who selected five heads or outstanding features in the bands, Grün observed under higher dispersion, only three different maxima (denoted α, β, and γ, respectively), the relative intensities of which were strongly dependent on excitation conditions.

Pleiter [530] observed a number of bands of this system in the spectrum of a radio-frequency excited nitrogen jet. Mahon-Smith and Carroll [431] confirmed the vibrational scheme for this system from an observation of the isotope shifts in $^{15}N_2$ (table 39).

In table 39 are listed wavelengths of the maxima observed by Grün [273]. The vibrational constants derived for this system indicate that the states involved are not identical with any other known states (see however Herman's infrared system, section 3.24).

Carroll et al. [131] have studied the rotational structure of the Gaydon-Herman green bands. The analyzed bands include 0–0, 1–0, 2–1, 2–0 and 3–1. Strong molecular orbital arguments are presented to support the identification of this system as $H^3\Phi_u - G^3\Delta_g$, the letters being simply selected to bear the initials of those for whom the system is named. The lower state has virtually pure case b coupling; the upper state, inverted, is case a below $N=7$, and case b, beyond.

The spectrum was produced in a Geissler discharge in pure nitrogen; this was run at currents below 15 mA; pressures were below 2 torr (0.3 kPa). Though the spectrum was observed in first order of a 10 m concave grating spectrograph (resolving power above 200,000), numerous lines remained blended. Of the 27 predicted branches, only the $^NP_{13}$ and $^TR_{31}$ were not detected.

Both states were found to originate from simultaneous excitation of two electrons. The $^3\Delta_g$ state, dissociating to $^4S+{}^2D$, arises from the configuration $(1\pi_u)^2(3\sigma_g)^2(1\pi_g)^2$; the $^3\Phi_{ul}$ state, converging to $^2D+{}^2D$, arises from the configuration $(1\pi_u)^3(3\sigma_g)(1\pi_g)^2$. Ab initio calculations by Michels [458–9] also indicate that both states in this transition are stable.

The absolute term values of the H and G states can only be estimated, since the only known transition involving these states is the transition between them. Approximate potentials for the G and H states are given by Carroll et al. [131] and reproduced here in figure 1.

Band origins are included in table 39. Rotational constants for the G and H states are given in tables 56 and 66, respectively.

Veseth [637] has obtained the molecular constants for the G and H states from a numerical diagonalization of the perturbation matrix combined with a least squares fit to the term values calculated from the spectra. The constants so derived would appear to be more reliable than those obtained by Carroll et al., but since correlation of the term values has been neglected, the uncertainties are underestimated. Veseth's results of the simultaneous fit differ negligibly

from those of Carroll et al., an indication that the approximate treatment introduces very small errors compared with the matrix approach in this instance.

3.24. Herman Infrared System (9100–7000 Å) V

In a low current discharge through pure nitrogen at liquid air temperature, Herman [297] observed a system of eight new bands, degraded to shorter wavelengths.

Carroll and Sayers [139] obtained the same system in a Tesla discharge, and in a high-voltage transformer discharge through pure nitrogen at pressures between 2 and 20 torr (0.3 and 3 kPa), and remeasured the bands under somewhat higher resolution. Six close heads were resolved at this resolution (where lower resolution showed only a simple structure), indicating that the bands could result from a triplet or possibly a quintet transition.

The vibrational intervals (from band heads) for the upper state of this system are seen to be very similar to those of the upper state of the Gaydon-Herman Green system [139] (see also section 3.23.):

		$v=0$	$v=1$	$v=2$
$\Delta G\left(v+\frac{1}{2}\right)$	Green	896.0	872.0	843.8
$\Delta G\left(v+\frac{1}{2}\right)$	Infrared	888.1	864.3	833.7

However, as pointed out by Carroll and Sayers, ambiguities remained so that the conclusion could not be drawn that the new system had the upper state in common with the Green system. Mahon-Smith and Carroll [431] have confirmed the vibrational scheme for the IR system from an observation of the isotope shifts in $^{15}N_2$ (table 40).

Pleiter [530] observed a number of these bands in the spectrum of a radio-frequency excited nitrogen jet. Davidson and O'Neil [190] have excited the Herman Infrared system by bombardment of N_2 with high energy electrons. Two new bands were observed: 0–2, 9071 Å; 0–3, 9629 Å. Uncertainty for these shortest wavelength heads is about ±3 Å.

The observed bands are listed in table 40.

3.25. Rydberg Series (960–490 Å)

Below 1000 Å several Rydberg series of bands can be observed converging to the ground and excited states of the molecular ion N_2^+. Below the first ionization limit (i.e., for wavelengths above 796 Å) the bands are usually sharp and have a line-like structure, whereas above this energy (i.e., below 796 Å) the structure may become diffuse due to pre-ionization.

The Rydberg series of N_2 which have been observed are mainly of species $^1\Sigma_u^+$ and $^1\Pi_u$. Observed absorption series originate from states $X^1\Sigma_g^+$ and $a''^1\Sigma_g^+$; emission has been observed to the $a^1\Pi_g$ state. These are all allowed by electric dipole selection rules. Weak absorption from the ground electronic state has been observed to the $v=0$ level of the lowest lying Rydberg state a'' (see the Dressler-Lutz system, section 3.4). The $^3\Pi_u$ series have also been observed in absorption. Rydberg states have been observed in emission to some lower state other than the ground state. Such Rydberg states known to be the first members of Rydberg series include $x^1\Sigma_g^-$, $y^1\Pi_g$, $k^1\Pi_g$, $D^3\Sigma_u^+$, $z^1\Delta_g$, and $E^3\Sigma_g^+$.

In this section the observed Rydberg series of bands are discussed. In some cases where the rotational fine structure of Rydberg states has been analyzed, the states are considered further under the corresponding electronic transitions (e.g., $c'-X$, etc.). The electronic structure of Rydberg states and related theoretical calculations are summarized in section 2.

Leoni [414] has shown that a matrix representation of the perturbations between valence and Rydberg states of like species leads to an understanding of the observed vibrational intervals and also the observed irregular rotational constants for the $^1\Sigma_u^+$ and $^1\Pi_u$ states lying above 100,000 cm^{-1}. The heterogeneous perturbations between the $^1\Sigma_u^+$ and $^1\Pi_u^+$ levels are also treated by a reexamination of the experimental data of Carroll and Collins [130], Ledbetter [408], and Carroll et al. [132].

An attempt is made by Leoni to represent predissociation of $^1\Pi_u$ levels, by considering interaction with neighboring $^3\Pi_u$ states. A partial explanation of the line broadening of levels of the b state is proposed in terms of interaction with the continuum of $C'^3\Pi_u$. This simple model is incapable of explaining the very broad nature of the bands $b(3)-X$, $b(2)-X$, and $b(4)-X$. A more complete understanding of these features requires consideration of interaction with $F^3\Pi_u(0)$ and $C^3\Pi_u(7)$. There are speculations about the causes of other broadened features; the rather large broadening of $b(11)-X$ is still a puzzle.

The relative vibronic intensities of Geiger and Schröder [253] are used by Leoni to obtain an approximate deperturbed transition moment for $b-X$. A weakly r-dependent R_e was obtained.

Leoni has given deperturbed term values and B_v values together with the Dunham coefficients fitted to the singlet states discussed. Leoni and Dressler [416] have published some results of the quantitative deperturbation.

The notation used in describing the Rydberg states is a mixture of the old and the new. The old notation retains continuity with usage that goes back decades; the new is based on a more cohesive picture of these states and was introduced by Dressler [210] and Carroll and Collins [130]. Figure 1 of the latter paper which illustrates the two notations is reproduced here as figure 4.

a. ($N_2^+X^2\Sigma_g^+$)$c_n{}^1\Pi_u \leftarrow X^1\Sigma_g^+$ Worley-Jenkins Rydberg Series (960–780 Å)

In the absorption spectrum of N_2 below 1000 Å, Worley and Jenkins [668] observed bands forming a Rydberg series, converging to the $X^2\Sigma_g^+$ ($v=0$) ground state of N_2^+. Later Worley [666], in his extensive study of the absorption spectrum of N_2, tabulated the observed series terms up to $n=27$ (then labeled $m=26$ where $m=n-1$). Meanwhile, Tanaka and Takamine [605] had observed 1–0 bands of the same series; i.e., bands converging to $v=1$ of the X state of N_2^+. This series was of appreciably lower intensity than the 0–0 series.

Ogawa and Tanaka [499] observed and extended the $v'=0$ series to $n=32$, and also observed $v'=1$ members up to $n=20$. Several lower members showed two heads, as in Worley's observations, and their separation became smaller as the principal quantum number (n) increased. Rydberg formulas were fitted to the series of bands heads, with considerable deviations from the calculated positions of the short wavelength heads only for $n=7$ and 12. Table 14 lists the observed members of the Worley-Jenkins series. Recent results by Johns and Lepard [360] on Rydberg complex theory is applied to the analysis of the Worley-Jenkins Rydberg series.

In absorption the most probable Rydberg series correspond to transitions $^1\Pi_u - X^1\Sigma_g^+$ and $^1\Sigma_u^+ - X^1\Sigma_g^+$. The Rydberg states can be represented by the simplified electron configurations as

$$\ldots\ (\sigma_g 2p)(np\pi_u)^1\Pi_u,$$

$$\ldots\ (\sigma_g 2p)(np\sigma_u)^1\Sigma_u^+.$$

For the observed series the former configuration was proposed by Worley [666], who explained the double heads as R and Q heads of a $^1\Pi_u - X^1\Sigma_g^+$ transition. The latter configuration was adopted by Herzberg [12] and by Mulliken [473] after the observation that the $p'{}^1\Sigma_u^+$ and $e^1\Sigma_u^+$ states seemed to coincide in energy with the first and second members, respectively, of the Worley-Jenkins series. Ogawa and Tanaka [499] suggested that each of the two heads belonged to different electronic transitions.

Based on new high resolution spectra, Carroll and Yoshino [141] (see following sub-section) showed that whereas the first member of the Worley-Jenkins series, as originally listed by Worley [666] and by Ogawa and Tanaka [499], was the well-known $p'{}^1\Sigma_u^+$ state, the higher members ($n \geq 4$), however, showed strong Q branches and therefore had $^1\Pi_u$ upper states. This also applied to the e state, formerly believed to be $^1\Sigma_u^+$ in type, which was found to coincide in energy with the $n=4$ member of the series. The double-headed structure was thus easily accounted for. As for the $p'{}^1\Sigma_u^+$ state, the apparent double-headed structure has been shown to result from a perturbation, (see sections 3.25b, 3.25c, 7.1).

Carroll and Yoshino [141] further concluded that the p' state was in fact the first member of a new Rydberg series, and they were also able to observe the next few members of this series (see following sub-section). The first member of the Worley-Jenkins series, should according to them be the $\ell_1{}^1\Pi_u$ state with $T_o=104139$ cm^{-1}. This ℓ_1 state (now called $c_3(0)^1\Pi_u$, where $n=3$ and $v=0$) is strongly mixed with the valence state ℓ_2(or d, now called $b(5)^1\Pi_u$), and these states are quite anomalous in B-values: $B_v=1.50$ and 1.93 cm^{-1}, respectively.

The final conclusion is that the Worley-Jenkins Rydberg series is formed by the transition

$$\ldots\ (np\pi_u),\ c_n{}^1\Pi_u - X^1\Sigma_g^+,\ n=3,\ 4,\ \ldots,$$

and the Carroll-Yoshino series by

$$\ldots\ (np\sigma_u),\ c_n'{}^1\Sigma_u^+ - X^1\Sigma_g^+,\ n=4,5,\ \ldots,$$

both converging to the $X^2\Sigma_g^+$ ground state of N_2^+.

Band origins of $c_3 - X$: 1–0, 2–0, and 3–0 transitions were given by Carroll and Yoshino [141]. An extensive rotational analysis of the $c_n - c_{n+1}'$ complexes has been carried out by Carroll and Yoshino [142] who have published additional band origins and have tabulated many band heads of the Worley-Jenkins series. More recent measurements at somewhat higher resolution have been made by Ledbetter [408]. He observed $c_n - X$, $n=4$, 5, 6. This is discussed in section 3.25c, which refers to the $c_n - a''$ series. Rotational constants for the $c_n{}^1\Pi_u$ Rydberg states are listed in table 64.

b. ($N_2^+X^2\Sigma_g^+$)$c_n'{}^1\Sigma_u^+ \leftarrow X^1\Sigma_g^+$ Carroll-Yoshino Rydberg Series (960–805 Å)

In the absorption spectrum of N_2 in the region 960–805 Å, Carroll and Yoshino [141] observed a new Rydberg series converging to the $X^2\Sigma_g^+$ ground state of N_2^+. Three members of the series were observed, each lying to the short-wavelength side of the corresponding member of the Worley-Jenkins series converging to the same limit. Each band showed a resolved P and R branch. The upper states were therefore of species $^1\Sigma_u^+$. Following the single-electron orbital description of Mulliken [473], Carroll and Yoshino designated the electron configuration of the new $^1\Sigma_u^+$ series as $(3\sigma_g)\ np\sigma_u$, $n=4,5,\ \ldots$

The same spectra enabled the rotational structure of the Worley-Jenkins series to be studied. The first member of this series was assumed to be the well-known $p'{}^1\Sigma_u^+$ state (now called $c_4'(0)$). The higher members ($n \geq 4$), however, showed strong Q branches and therefore had $^1\Pi_u$ upper states. Consequently, the p' state can no longer be correlated with the higher Worley-Jenkins bands, but is interpreted as the first member of the new $^1\Sigma_u^+$ series [141].

An extensive discussion of these Rydberg states, their vibrational structure, electronic structure, and

interactions with other states is given by Carroll and Collins [130], Dressler [210], and Lefebvre-Brion [412]. (See also Worley-Jenkins series, previous subsection, and the systems $b-X$, $b'-X$, and $c'-X$; section 3.5). Observed bands of the $c_n'-X$ Rydberg series are in table 15; rotational constants for the Rydberg states are in table 65.

Carroll [129] has discussed some features of p-complex theory as applied to the $^1\Sigma_u^+$ and $^1\Pi_u$ absorption Rydberg series that converge to the ground state of N_2^+. Relative line strengths are calculated for lower complexes with schematic illustrations given for the $5p$ and $8p$ complexes. Johns and Lepard [360] have used a more elaborate theory to fit new measurements on several of these bands.

c. (N_2^+ $X^2\Sigma_g^+$)$c_n{}^1\Pi_u \leftarrow a''{}^1\Sigma_g^+$ Ledbetter Rydberg Series (865–820 Å)

Ledbetter [408] has observed under high resolution a new Rydberg series in the visible region. The three new bands arise through absorption from $a''{}^1\Sigma_g^+$, the lowest Rydberg state of this species (see section 3.4), to the states $c_n{}^1\Pi_u$, $n=4,5,6$, upper states of the Worley-Jenkins Rydberg series. The new series constitutes a $v'=0$ progression (table 16).

The corresponding c_n-X Worley-Jenkins bands were also observed in the vacuum UV (table 14).

In the Ledbetter bands, the Q branch is most intense. The relative intensities in the branches suggested either a $\Pi\leftarrow\Sigma$ or $\Delta\leftarrow\Pi$ transition, but the first lines in the P and R branches pointed to the former. The Q branch in these bands is violet degraded while the P and R branches are red degraded; this indicates large Λ-doubling in the $^1\Pi$ states. Some spectra taken with the $^{15}N_2$ isotope confirm the vibrational numbering. Rotational constants for the a'' state are given in table 60; the rotational constants for the c_n states are included in table 64. Several perturbations were observed; these are discussed in section 7.1.

d. (N_2^+ $A^2\Pi_u$)$\leftarrow X^1\Sigma_g^+$ Rydberg Series: $^1\Pi_u-X$ (950–685 Å); $^3\Pi_u-X$ (785–685 Å); $o_n{}^1\Pi_u-X$ Bands (950–815 Å)

Shortly after the $A^2\Pi_u$–$X^2\Sigma_g^+$ Meinel system of N_2^+ had been observed [452], Worley [667] identified five distinct bands (in the 930–730 Å region), which belonged to a Rydberg series whose limit was the A state of N_2^+. He called it the third Rydberg series of N_2, since two previous series had been observed whose respective limits were the X and B states of N_2^+.

The bands were rather narrow, degraded to longer wavelengths, and showed one head. The series limit corresponds to the $v=1$ level of the $A^2\Pi_{u,\,1/2}$ state of N_2^+. It is reasonable that this Rydberg series would correspond to $v'=1$ since the $A^2\Pi_u$ state has a larger internuclear distance than the ground state of N_2^+, and the Franck-Condon principle favors a $v'=1$ series.

For the higher Rydberg terms, Worley found a few heads corresponding to $v'=0$, and a few possible heads for $v'=2$. Worley also observed that the first member of the series was the known $o^1\Pi_u$ state. Ogawa and Tanaka [499] extended Worley's series for $v'=0$, 1, 2 and observed in addition the $v'=3$ series up to $n=17$. The $v'=1$ series was the most intense. Some of the lower members ($n\leq 7$) appeared as close doublets with a separation of about 14 cm^{-1}. Members with $n\geq 8$ consisted of two bands whose head separation was about 80 cm^{-1}, the same as the separation between the $^2\Pi_{1/2}$ and $^2\Pi_{3/2}$ levels of the A state of N_2^+.

In the same wavelength region as Worley's series, Ogawa and Tanaka [499] observed four additional Rydberg series, also converging to the $v=0$, 1, 2 and 3 levels of the $A^2\Pi_{u,1/2}$ state. The bands had an appearance similar to those of Worley's series, but they were weaker. The bands of the new series were found to practically merge, at $n=8$, with the long wavelength heads of the members of Worley's series.

The electron configuration for Worley's series is given by Mulliken [473] as

$$KK(\sigma_g 2s)^2(\sigma_u 2s)^2(\pi_u 2p)^3(\sigma_g 2p)^2(ns\sigma_g),{}^1\Pi_u,\ n=3,4,5.$$

The narrow double heads ($\Delta\sigma\sim 20$ cm^{-1}) observed in some lower members of the series could represent R and Q heads in the transition $^1\Pi_u-X^1\Sigma_g^+$. From the same electron configuration, one could also expect $^3\Pi_u$ states and Ogawa and Tanaka suggested that the upper states of the new series correspond to these states.

It seems that Worley's original series includes two series, one consisting of the shorter wavelength heads ($^1\Pi_u-X^1\Sigma_g^+$) and converging to the $A^2\Pi_{u,\,1/2}$ state, and the other, which consists of the longer wavelength heads ($^3\Pi_u-X^1\Sigma_g^+$) of table 17 ($n\geq 8$), to which is added Ogawa and Tanaka's new series ($n\leq 7$), and converging to the $A^2\Pi_{u,\,3/2}$ state.

Ogawa [495] investigated the absorption spectra of $^{14}N_2$ and $^{15}N_2$ in the 830–720 Å region. The observed vibrational isotope shifts confirmed the previous assignment given by Ogawa and Tanaka for the Rydberg series converging to the $A^2\Pi_u$ state of N_2^+. The $^{15}N_2$ isotopic bands are given in tables 2 and 3 of Ogawa [495]. In addition to the Rydberg series, four new progressions were observed, but they remain unclassified; these are listed in table 46. It is seen that the ΔG values are almost the same as those of the $A^2\Pi_u$ state of N_2^+. (See section 3.33 for mention of additional unidentified bands observed by Ogawa.)

Ogawa, et al. [502] have extended the Worley third Rydberg series and the Ogawa-Tanaka series to both higher members and higher v'. Both series converge to the A state of N_2^+. The second series, labeled $A-X$(II), converges to a limit about 80 cm^{-1} below that of the $A-X$(I) series; the former limit is $A^2\Pi_{1/2}$ and the latter is $^2\Pi_{3/2}$. The new work provides im-

proved values for the series limits, which are in-general in close agreement with those obtained from the spectrum of the ion.

The new measurements were made at a dispersion of 0.63 Å/mm. The nitrogen was cooled by liquid nitrogen. Ar II lines were used as wavelength standards in this spectral region.

The new observations reported span the spectral region 946–685 Å. All bands with wavelength less than 796 Å (i.e., lying at energies above the first ionization potential) become increasingly diffuse as v' increases. The lower members of both Rydberg series show double heads (R and Q branches) with an average separation of about 11 cm^{-1}. The R heads decrease in intensity as the principal quantum number increases, and they disappear at $n=11$. The derived limits are then based on Q head measurements. The diffuse heads become blurred for $v'=7$.

The $v'=1$ series are now known till $n=45$ (I), $n=41$ (II). The $v'=3$ series are known till $n=32$ (I), $n=34$ (II). The observed series are given in table 17. The series limits are also summarized in table 6. The separation between corresponding members of the I and II series (for a given n and v') give an approximate separation between the Rydberg $^1\Pi_u$ and $^3\Pi_u$ states.

Yoshino et al. [675] have made a rotational analysis of several Rydberg transitions having as upper levels, vibrational levels of o_3 and $o_4{}^1\Pi_u$, the two lowest members of the Worley third Rydberg series. Measurements were made in second order of a 6.65 m vacuum spectrograph, with a He continuum as background source. Resolving power was as high as 180,000. All the observed bands showed three branches P, Q, R, the latter two forming red degraded heads. Many perturbations were observed, both heterogeneous and homogeneous (for details see section 7).

In addition to the new results on the $o-X$ bands there are extensions of prior results on $b-X$ bands (table 12), which has required some revision of rotational assignments and modification of earlier reported B_v values which are now obtained from deperturbed data. New data is also available on the $c_6'(1)$ level (table 15).

For the $o_n(v)$ states molecular constants are now obtained, in part derived from deperturbed data (table 67). A more complete deperturbation of the $o_3(0)$ level requires consideration of homogeneous interaction with both $b(6)$ and $b(7)$. The irregularity in $\Delta G(1/2)$ and B_0 reveal that more than one perturbation affects $v=0$.

e. ($N_2{}^+B^2\Sigma_u{}^+$)←$X^1\Sigma_g{}^+$ Hopfield Series (725–660 Å)

As the first to find a molecular Rydberg series in other than H_2 and He_2, Hopfield [319] observed a series of bands in absorption, and another seemingly in emission in the region 730–660 Å, both converging to the common limit 18.6 eV. Configuration mixing of discrete and continuum spectra is responsible for line shapes that give the appearance of emission features in an absorption spectrum. This is discussed at the end of this subsection.

Mulliken [471a] suggested that each band of the absorption series was a 0–0 band, and that the $B^2\Sigma_u{}^+$ state of $N_2{}^+$ represented the limit of the series. That each band should be 0−0 is readily understood, because the ground state of N_2 and the B state of $N_2{}^+$ have about the same internuclear distance.

Takamine, et al. [594] also observed these series, and extended the absorption series to $m=11$ ($n=12$) and the apparent emission series to $m=7$. Ogawa and Tanaka [499] extended the Hopfield absorption series to $m=20$. In addition, they observed another absorption series converging to $v=1$ of the $B^2\Sigma_u{}^+$ state. The measurements for these two series are listed in table 18. The observed wavenumbers of the Hopfield $v'=0$ absorption series are reproduced within 15 cm^{-1} by the expression

$$\sigma_m=151233-R/(m-0.0701-0.0412/m)^2,\ m=3-20.$$

In the same work, Ogawa and Tanaka observed another absorption series whose individual members appeared immediately to the longer wavelength side of each member of the emission series. The measurements for the series are listed in table 18, and the members are expressed by the equation

$$\sigma_m=151231-R/(m+0.1405-.199/m)^2,\ m=3-11.$$

Carbonneau and Marmet [118] have for the first time detected autoionizing states of N_2 in the ionization efficiency curve of N_2. The Rydberg states converging to the A state of $N_2{}^+$ have been observed before, but some of the $ns\sigma$ states converging to the B state of the ion are new.

Mulliken [471a] suggested the following possible electron configurations for the Hopfield series:

$$KK(\sigma_g2s)^2(\sigma_u2s)\ (\pi_u2p)^4(\sigma_g2p)^2(ns\sigma_g),\ ^1\Sigma_u{}^+,$$

or

$$KK(\sigma_g2s)^2(\sigma_u2s)(\pi_u2p)^4\ (\sigma_g2p)^2\ (nd\sigma_g),\ ^1\Sigma_u{}^+.$$

Ogawa and Tanaka [499] observed two series converging to the same level; one of them was assumed to correspond to the transition . . . $(ns\sigma_g)\ ^1\Sigma_u{}^+-X^1\Sigma_g{}^+$ and the other to . . . $(nd\sigma_g)\ ^1\Sigma_u{}^+-X^1\Sigma_g{}^+$. Lefebvre-Brion and Moser [413] found from theoretical calculations that both Rydberg orbitals must be considered as a linear combination of $ns\sigma_g$ and $nd\sigma_g$.

There had been some speculations in the literature as to the nature of the emission series. Tanaka and Takamine [605], as well as Worley [666] suggested that there might exist a triplet state lying close to the singlet state, such that the emission series could correspond to a transition $^3\Sigma_u{}^+-X^1\Sigma_g{}^+$. This transition is actually forbidden by the spin selection rule; however, as n increases, uncoupling of the spin is

expected and the distinction between $^1\Sigma$ and $^3\Sigma$ states would diminish.

Rydberg apparent emission series have been observed coexisting with absorption series in linear triatomic molecules.

Similar features are known for atoms, and can be understood in a general way as due to the interaction of a discrete state with adjacent continua [221] producing windows in the continuous absorption [162].

Huffman et al. [326] tried to observe the emission series without the associated absorption series, but were unable to do so.

They therefore concluded that the Hopfield emission series is not due to emission from the discharge, but originates from an intensity depression in the ionization continuum, most likely caused by preionization. The apparent emission bands are more diffuse than the Hopfield absorption series.

f. ($N_2^+C^2\Sigma_u^+$)←$X^1\Sigma_g^+$ Codling Rydberg Series (555–490 Å)

As pointed out by Weissler et al. [648], the existence of the $C^2\Sigma_u^+$ state of N_2^+ at 22 eV (526 Å) suggested the possibility that there are some weak Rydberg bands in the region 660–525 Å. These authors observed a rapid variation of the absorption coefficient in this region, indicating the prescence of such bands.

Codling [162] photographed the absorption spectrum of N_2 in the 600—100 Å region, utilizing the continuum radiated by a 180 MeV electron synchrotron as a background source. Discrete structure was observed only in the 570—470 Å region. This structure appeared to correspond to a long v'-progression belonging to a single state of N_2 having vibrational spacings very similar to those of the known $C^2\Sigma_u^+$ state of N_2^+. There were fragments of a second state; the two states appeared to be members of an autoionized Rydberg series of states converging to the C state. The observed bands are listed in table 19. One band of a possible third Rydberg state was also observed.

The vibrational quantum assignments are not unambiguous, nor is the identification of the second Rydberg state. The core C state has a mixed configuration and it is assumed that so do the Rydberg states converging to it. The new Rydberg states are tentatively designated as $(\pi_u 2p)^3\ 4s\sigma_g$ and $(\pi_u 2p)^3\ 5s\sigma_g\ ^1\Sigma_u^+$. The absence of the $3s$ member of the series could be accounted for by an assumed interaction with the Rydberg states converging to $D\ ^2\Pi_g$ which lie below the C state.

3.26. $B^2\Sigma_u^+ - X^2\Sigma_g^+$ First Negative System of N_2^+ (5870–2860 Å) V, R

The First Negative System is one of the most prominent band systems of nitrogen, and consists of numerous single-headed bands in the region 5870–2860 Å. For low v' the bands are degraded to shorter wavelengths; for high v' they are degraded to longer wavelengths; a few bands even appear headless (table 42).

As its name indicates, this system is observed in the negative column of a discharge through nitrogen, but is also readily produced in various sources, such as Tesla and ordinary transformer-excited discharges through helium containing traces of nitrogen or pure nitrogen at low pressure, in discharges produced by microwaves, and in hollow cathode tubes. The bands are often overlapped by the stronger $C—B$ Second Positive System of N_2; consequently, to study the $B—X$ system, it is necessary to develop a source in which overlapping can be suppressed.[6]

Although the system has been observed and described since 1886, a detailed study of its fine structure was first undertaken in 1924 by Fassbender [222], who made a partial rotational analysis of a few bands and gave a list of 36 band head positions. Merton and Pilley [456] and Herzberg [302] observed many more bands under low resolution. Further rotational analyses of bands were made by Coster and Brons [173–4], Brons [102–103], Childs [157], Parker [516–17] and Crawford and Tsai [183]. Douglas [204], in an extensive study of the First Negative bands, succeeded in finding a number of new bands of higher vibrational numbers, and analysed them in detail. Janin and Eyraud [353] produced the system by microwave excitation of a neon-nitrogen mixture, and observed many band heads. (The kinetics of both emission and absorption of the 0–0 transition have been observed by Clerc and Lesigne [161]. Excitation was by pulsed electrons.)

Wood and Dieke's analysis of the structure of some of the B–X bands of the isotopic molecules $^{14}N^{15}N^+$ and $^{15}N_2^+$ confirmed the vibrational numbering [664–5]. Shvangiradze et al. [576] also measured isotope shifts for this band system.

Stoebner et al. [587–8] have observed several bands in a high-voltage discharge through nitrogen and methane; the new bands include 5–3, 24–15, 11–33 and 15–10.

Janin et al. [351] have expanded the preliminary results of Janin and Eyraud [353] and have reported rotational analysis for many red-degraded bands having high v. R branches are in general not observed, though in some instances short branches were detected.

Tyte [622–3] has excited the B–X system in a cooled discharge through a helium-nitrogen mixture. The following new bands were observed: 11–6, 18–12, 12–9, 11–9, 17–13, 5–5, 7–7 and 17–18. Rotational analyses were made for 10–6,7,8,9 and 11–6,7,10. Tyte has pointed out that in a Deslandres table listing observed bands, there is a pronounced gap in one arm of the Condon locus, and a less marked one in the other (see Tyte and Nicholls [38]). Franck-Condon factors indicate that the missing bands should be as intense as

[6] For further references concerning excitation conditions for the First Negative System, see Herzberg [302], Douglas [204], Parker [516-18], Wright and Winkler [43], Tyte and Nicholls [38].

many of the observed. The few bands observed in the region of the gap are 8–6, 9–8, which are headless and the 10–9 and 10–8 which have no definite heads on weak exposures. The missing bands (weakly degraded) coincide with strong bands of either (1–) or (2+) systems, and are consequently difficult to detect.

The analysis of B–X bands have clearly shown the transition to be $^2\Sigma_u^+ - ^2\Sigma_g^+$, the lower state being the ground state of N_2^+.

Table 42 gives positions of the observed bands. Rotational constants for the X and B states are given in tables 72 and 74, respectively. Whereas the vibrational and rotational constants run quite normal for the $X^2\Sigma_g^+$ state, this is not at all the case for the $B^2\Sigma_u^+$ state. Both the B_v and $\Delta G(v)$ versus v curves have unusual shapes. According to Douglas [204] this arises from an unusually shaped potential curve, which in turn is caused by a homogeneous interaction between the $C^2\Sigma_u^+$ and $B^2\Sigma_u^+$ states.

In addition to this homogeneous perturbation there are also observed numerous rotational perturbations in the First Negative System, caused by an interaction between the $A^2\Pi_u$ and $B^2\Sigma_u^+$ states. (See a fuller discussion in section 7).

The conditions under which this system is produced are discussed by Wright and Winkler [43] (p. 43–50). An atlas for this system, including spectrograms, a compilation of molecular data, and a selected bibliography has been prepared by Tyte and Nicholls [38].

Klynning and Pages [390] have recently analyzed the rotational structure of several bands of the B–X (1–) system of N_2^+ under high resolution. The observed bands include: 0–2, 2–5, 3–6, 4–7, 5–8, 6–9. Åslund's term value method was used to evaluate molecular constants. The spectra were taken in the region of 5500–4500 Å, with a linear dispersion of 1.4 Å/mm. Iron lines from a hollow cathode were used as standard wavelengths. In the fitting use was made of data obtained by prior authors. The rotational constants for the N_2^+ X state are included in table 72. An examination of the perturbation of $v=3$ of the B state showed that a complete deperturbation requires more than just interaction with one vibrational level. The equilibrium vibrational constants for the X state are also included in table 1.

3.27. $C^2\Sigma_u^+ - X^2\Sigma_g^+$ Second Negative System of N_2^+ (2230–1270 Å) R

The Second Negative System consists of a large number of single-headed bands in the region 2230–1270 Å, all degraded to longer wavelengths (table 44). Part of this system was first observed by Hopfield [319], who reported 14 new bands in a helium-nitrogen mixture.

Watson and Koontz [645] extended the known system to 37 bands, and assigned them to a transition of N_2^+, the lower state of which was found to be the lower state of the First Negative System, $B^2\Sigma_u^+ - X^2\Sigma_g^+$. A tentative vibrational analysis was later corrected by Setlow [568] and by Baer and Miescher [56–7], who, by observing the isotope shifts in these bands with enriched nitrogen-15, verified Setlow's analysis. Takamine et al. [595], observed some of these bands in both helium and neon discharges, and proposed a mechanism that would account for the difference in intensity distribution in both discharges. Tanaka [596] reinvestigated the band system in both a condensed discharge in pure nitrogen and pure NO, and in a mixture of a trace of these gases with a large amount of helium. Tanaka made additional comments on the intensity distribution in various sources.

Setlow [568] made a partial rotational analysis of a few bands; he assigned the system to a $^2\Sigma_u^+ - X^2\Sigma_g^+$ transition and gave provisional rotational constants for the upper state. Wilkinson [654] made a complete rotational analysis under high resolution of six bands for $v'=3$ and 4, and presented rotational constants. Carroll [125] analysed under high resolution 15 bands having $v'=0$–6. From his analysis, accurate rotational constants were derived. Carroll also briefly discussed various methods for producing the C–X system. The rotational constants for the C state are given in table 77.

In a high voltage ac condensed discharge, Joshi [366] produced about 90 bands and made a vibrational analysis. Joshi [367] also studied the same system for $^{15}N_2^+$. A vibrational analysis was made of about 80 bands. A few of these had already been observed by Namioka et al. [482].

The $C-X$ (2–) system shows a number of unusual features. Watson and Koontz had observed that the system was very sensitive to excitation conditions [645]. In a nitrogen-helium mixture, bands for which $v'<3$ were very weak; bands for $v'\geq 3$ were strong and appeared readily. It was pointed out that since the position of the $v'=3$ level of the $C^2\Sigma_u^+$ state is slightly below the ionization potential of helium (24.332 eV against 24.587 eV), collisions of the second kind between ionized helium and N_2 might be responsible for the production of N_2^+ excited to $v=3$ of $C^2\Sigma_u^+$.[7]

According to Douglas [204], this effect may also be interpreted in a different manner. He argued that since the $v=3$ level is only 820 cm^{-1} above the dissociation limit at 70358 cm^{-1} ($N(^4S)+N^+(^3P)$), it should be possible that a nitrogen ion and a nitrogen atom coming together at this limit could undergo a radiationless transition into the $v=3$ level of the C state potential curve. The excitation mechanism may thus be a case of inverse predissociation. (The corresponding predissociation was discussed by Carroll [125]).

In a high voltage ac condensed discharge in flowing helium, and in neon with a trace of nitrogen added, Tanaka et al. [603] observed strong bands of the

[7] $v'=4$ is even closer: 24.578 eV. With the same argument the $v'=4$ level should be most strongly populated.

system. The intensity distribution turned out to be quite different in the two cases. (See figure 1b of this reference.)

Joshi [366] observed a similar behavior. When the discharge was passed through a mixture of helium and nitrogen, bands having $v' \geq 3$ were the only ones observed. When neon was used as a foreign gas, bands having $v' \leq 2$ also appeared quite strongly. Details of the excitation mechanism for this system were discussed following the same lines of arguments as above.

As mentioned in the discussion of the B–X $(1-)$ system, the B_v and $\Delta G(v)$ curves for the B state have unusual shapes, a fact that Douglas [204] attributed to a homogeneous interaction between the $B\,^2\Sigma_u^+$ and $C\,^2\Sigma_u^+$ states.

It is seen that the $C\,^2\Sigma_u^+$ state also has these unusual B_v and $\Delta G(v)$ curves, as expected. However, whereas the B state has been studied up to $v=29$, the C state is not yet known beyond $v=10$, so that a more detailed study of the mutual interaction cannot be made (see section 7).

Several small rotational perturbations in the C state have been observed by Carroll [125].

3.28. $A\,^2\Pi_{u1}$–$X\,^2\Sigma_g^+$ Meinel System of N_2^+ (17,700–5500 Å) R

The Meinel system, though rather weak, is often seen and studied in the aurora. Vegard and Kvifte [635] observed some of these bands, but misassigned them as members of the N_2 $B-A$ Second Positive System because of wavelength coincidences. The doublet bands bear the name of Meinel because he correctly assigned to the $A\,^2\Pi_u-X\,^2\Sigma_g^+$ transition in N_2^+ the six bands he photographed during an auroral storm in 1950 [452–4]. Meinel [455] later revised his provisional vibrational quantum numbering. The new numbering was confirmed by Liu [351], who studied the isotope effect in the spectra of $^{15}N_2^+$.

More recently, the Meinel system has been observed beyond the photographic infrared in the aurora, and band intensities have been measured. For details see the work of Federova [224] and references cited therein.

The production of the Meinel system in the laboratory was first accomplished by Dalby and Douglas [189], who studied the bands produced in a mixture of helium and nitrogen in a hollow cathode tube. Earlier, Herman [297] had claimed to have obtained this system in low pressure discharges, but published no numbers. Sayers [560] obtained the Meinel bands by electron bombardment of nitrogen, as well as in a hollow cathode.

Douglas [205] analyzed the rotational structure of the 1–0, 4–2, 3–1, and 2–0 bands, and found conclusive evidence that Meinel's initial electronic assignment was correct. The A state is inverted. (Several misprints in Douglas' paper have been corrected.)

Band heads and origins are listed in table 41; rotational constants for the A state are in table 73.

van de Runstraat et al. [550] have observed emission from a nitrogen ion beam in the spectral region 4800—6000 Å. Many features seem to belong to the N_2^+ $A-X$ transition, with $v'=5$—17. Only low resolution observations were made, and no wavelengths were published.

3.29. $^4\Sigma_u^+-X\,^2\Sigma_g^+$ d'Incan-Topouzkhanian System of N_2^+ (3920–3820 Å) V

By bombarding N_2 with high energy molecular hydrogen ions d'Incan and Topouzkhanian [199, 200] have produced the first strong evidence for an intercombination transition in N_2^+. Rotational analysis of the 0–0 and 1–1 bands supports the designation of this system (3920−3820 Å) as $^4\Sigma_u^+-X\,^2\Sigma_g^+$. The observed doublets lie near the 0–0 and 1 1 bands of the N_2^+ $B-X$ system; long exposure times (24 hours) were needed to observe the bands. The rotational constants and energies lie close to those of the N_2^+ B state. Many branches are blended, and the analysis of the structure of the states accounts for the doublet appearance of the spectra. The more intense and more extensive band is assumed to be 0–0. An excitation mechanism is proposed for the production of this quartet state which arises from $^4S+^3P$.

Observed bands of the new system are in table 43; rotational constants for the quartet state are in table 75. (See Note Added in Proof.)

3.30. $D\,^2\Pi_g-A\,^2\Pi_{u1}$ Janin-d'Incan System of N_2^+ (3070–2050 Å) R

In a pulsed microwave discharge in nitrogen-neon mixtures at about 3 torr (0.4 kPa) pressure, Janin and d'Incan [348–9] observed 21 weak bands belonging to a new system. The double headed bands were degraded to the red. The transition was identified as $^2\Pi-^2\Pi$, the lower state being identical with the upper state of the Meinel system. A provisional v' numbering was suggested which was later increased by 3 as a result of intensity studies by Grandmontagne et al. [268]. The early work of the group collaborating with d'Incan is fully described in d'Incan's thesis [198].

Tanaka produced these bands in an ac condensed discharge in neon containing a few percent of nitrogen; in this source the bands were more intense than in an uncondensed discharge. Grandmontagne's revised numbering was adopted by Tanaka et al. who observed 38 bands of the system at about the same time as Janin and d'Incan did their work, but did not publish results until several years later [603]. In addition to the new system, several bands were observed whose weakness prevented their being

identified with certainty as members of this system. (table 46).

Namioka et al. [482] verified the revised quantum numbering from measured isotope shifts using $^{15}N_2^+$. In addition, they calculated an RKR potential curve for the upper state now labeled D. In the interim, Nicholls [489] had calculated Morse-based Franck-Condon factors and r centroids for the $D-A$ transition. An extended rotational analysis by Janin et al. [352] has provided revised molecular constants for the D and A states and slightly improved band origins for the $D-A$ system. Only a partial list of observed lines has been published. The possibility was mentioned that $v=6$, 7 may be feebly perturbed.

Brömer et al. [100] observed 17 $D-A$ bands in the pink afterglow of nitrogen, including unambiguous identification of members of the $v'=2$ progression which had not been seen before. Two new band heads with $v'=3$ were also found.

The observed band heads and origins are given in table 45. Rotational constants for the A and D states are given in tables 73 and 76, respectively.

The D state dissociates to $N(^4S°)+N^+(^3P)$. By analogy with the isoelectronic molecule CN, this state would be inverted. The A coefficient for spin-orbit coupling has been determined by Janin and d'Incan [349] as either 20.5 or -16.5 cm^{-1}; Janin et al. [352] have no doubt that it is inverted. Vibrational dependence of the A coefficient was not determined. Configuration interaction calculations by Guerin [274–5] show that the predominant configuration is $\pi_u^2\sigma_g^2\pi_g$ which requires an inverted state, but that other configurations with which this mixes, principally $\pi_u^4\pi_g$, allows only a regular state. The spin-orbit coupling for the D state can then be expected to show irregularities (M. Krauss, unpublished results).

3.31. $D^1\Sigma_u^+-X^1\Sigma_g^+$ Carroll System of N_2^{2+} (1590 Å)

In a hollow cathode discharge through pure nitrogen at low pressure, Carroll [124] discovered a new headless band with origin at 1589.745 Å. A complete rotational analysis led to the following constants: $\sigma_0=62903.18$, $B'=1.8644$, $B''=1.8801$, $D'=7.1\times10^{-6}$, and $D''=6.9\times10^{-6}$ cm^{-1}.

The band was clearly due to a singlet or doublet $\Sigma-\Sigma$ transition of nitrogen, but could not be correlated with any known levels of N_2 and N_2^+. By analogy with the observed $^1\Sigma-^1\Sigma$ transition for the isoelectronic molecules C_2 and CN^+, it seemed possible to assign the new band to N_2^{2+}, most likely as the 0–0 band. Herzberg [14] believes that there still remains a slight uncertainty in the identification of this doubly ionized molecule.

Hurley and Maslen [329] developed a theory, relating the binding energy of the doubly charged ion (in this case N_2^{2+}) to the binding energy of the corresponding state of the isoelectronic molecule C_2, which enabled potential curves for the doubly positive diatomic ions to be calculated empirically. This theory was used by Carroll and Hurley [134] and by Hurley [328] to obtain potential curves for the ground state and some excited states of N_2^{2+}, and to assist in the identification of Carroll's transition as $d^1\Sigma_u^+-a^1\Sigma_g^+$; a more recently proposed notation would label the transition $D-X$ (see Herzberg et al., Can. J. Phys. **47,** 2735–43 (1969)). Electron configurations of the states were discussed. Predicted spectroscopic constants were presented and compared with available experimental data. Recently Thulstrup and Andersen [608] have made ab initio calculations of potential curves for states of N_2^{2+}.

For further discussion of N_2^{2+}, see section 9.

3.32. $^2\Sigma_u^+-X\,^2\Pi_{g1}$ System of N_3 (2765–2670 Å) V.

Following flash photolysis of N_3H in the presence of an excess of inert gas, Thrush [607] detected a diffuse complex absorption in the region 2730–2670 Å. This was attributed to N_3 on chemical grounds. The prominent spectral features consisted of diffuse absorption regions and lines of various degrees of diffuseness. Two violet degraded heads were found at 2719.5 and 2708 Å. The head separation was assumed to correspond to the multiplet splitting of the $^2\Pi_{g1}$ ground state (by analogy with the isoelectronic molecule CO_2^+), and the diffuseness was presumed to arise from predissociation of the upper state.

Douglas and Jones [207] also produced this spectrum in a flash photolysis experiment, and studied the absorption at high resolution. The analysis of rotational structure for the strongest band proved it to be the 000–000 band of the $^2\Sigma_u^+-X\,^2\Pi_{g1}$ transition of N_3, and confirmed the assignment given by Thrush. One of the two strongest bands was headless and the other nearly so (table 47).

Since the spin splitting of the $^2\Pi$ state is large and that of the $^2\Sigma$ state is small (it could not be resolved) the band consists of two subbands, each of which has four branches: R_{21}, Q_{21}; R_{11}, P_{11} and Q_{11}, R_{21}. Λ-doubling of the ground state was too small to be determined. The intensity alternation of the branch lines is characteristic of a symmetric molecule, and the absence of K structure corresponds to a linear molecule. No progression was observed, suggesting little change in geometry in going from one electronic state to the other: this also made it plausible to assign the strongest band to the 000–000 transition. The molecular parameters obtained from the analysis are given in table 2.

The strong diffuse heads at 2700.1 and 2700.8 Å cannot be assigned with confidence. They could be due to 020 subbands which are displaced by Fermi resonance, though their strength and position suggest rather that they might belong to another electronic transition, $^2\Pi_u-^2\Pi_g$. This assignment would place the

$^2\Pi_u$ state slightly above the $^2\Sigma_u^+$ state, but unexpectedly close.

Zamanskii et al. [677] have observed under low resolution almost all of the bands seen by Douglas and Jones, in addition to some others which they attribute to $0v_20$ transitions. The ω_2 values of $\approx$ 200 to 300 cm^{-1} obtained from a fit to these bands seems too low by more than a factor of two, casting doubt on the assignments of the bands, so the bands are included in table 47, but are not classified.

Archibald and Sabin [53] have made ab initio calculations on the ground states of N_3 and its positive and negative ions using LCAO MO SCF wave functions. Contracted gaussian basis sets were used in this open shell calculation. The main results showed that N_3 has a small inversion barrier and that the linear ground state is asymmetric. A barrier height about one third of the asymmetric stretch fundamental of roughly 2000 cm^{-1} would not perturb the vibrational levels sufficiently to have been detected by Douglas and Jones [207], but it would require direct observation of the excited vibrational states to have it confirmed experimentally.

3.33. Unclassified Bands

Under low resolution, spectral features may appear which are accidental clusters of lines that give the appearance of band heads. Such features have been reported in measurements on absorption coefficients, and only later higher resolution work has uncovered their true structure. Occasionally, amidst bands observed in a spectrum are some which are weak or diffuse or seem to fit no known states. Attempts to fit such bands to known systems can sometimes lead to fortuitous agreement with some formula for band heads, especially when the two states in the transition have rather different r_e and the spectrum is spread throughout a broad Condon locus. In such instances details concerning fine structure are fragmentary or non-existent.

In section 3 there are occasional references to observed bands which were unclassified. In this section attention is drawn to observations that sometimes include a partial analysis or where plausible tentative assignments have been given. Various unclassified bands are listed in table 46.

(a) In a transformer discharge through flowing nitrogen Lofthus [354] observed a number of singlet systems. Along with these were bands at 6895.5 and 8937.0 Å, both violet degraded. They gave the appearance of belonging to singlet transitions, but were strongly overlapped by $B-A$ (1+) emission.

Klynning [389] has found some near coincidences in wavenumber for some of the lines of these two long unidentified bands and with satellite branches of the 1–0 and 3–0 bands of the $B\,^3\Pi_g-A\,^3\Sigma_u^+$ bands observed by Dieke and Heath [196]. Perhaps because the lines fall on such branches they give the appearance of belonging to possible singlet transitions. In some instances the Lofthus and the Dieke and Heath measurements are very close; for the 3—0 band lines there seems to be a systematic difference of 0.15 cm^{-1}.

(b) While studying the N_2 $B-A$ bands in a discharge, Hepner and Herman [293] observed parts of five triple-headed bands in the region 19000–30000 Å (table 46a). These strong, red-degraded bands were assumed to originate from an allowed transition possibly between quintet states, both with ω_e less than 1000 cm^{-1}. These bands remain unclassified.

(c) Tilford and Wilkinson [613] studied the spectrum of nitrogen produced by an electrodeless discharge in He+Ar and He+Ne mixtures. Though numerous singlet transitions were analyzed in detail, 15 bands were observed that could not be classified: 1123.6, 1105.1, 1088.1, 1086.7, 1065.6, 1052.6, 1015.8, 992.9, 988.9, 967.5, 948.4, 948.2, 932.7, 905.4 and 900.9 Å. Many of these bands are overlapped. The band at 932.7 Å is red-degraded and seems to consist of a single branch (really two branches superimposed). The upper state is presumed to be $^1\Sigma_u^+$ at about 13.3 eV, with a rotational constant of about 1.3 cm^{-1}.

(d) Wilkinson [659] observed two new weak band heads (red-degraded) in absorption at 1685 Å and 1638 Å. These lie close to predicted positions of the $^3\Pi_1$ components of the $B^3\Pi_g-X^1\Sigma_g^+$ transition.

(e) Ogawa [495] had observed a number of Rydberg series in the region 805–702 Å. The bands which remained unclassified (for both $^{14}N_2$ and $^{15}N_2$) that were observed in the same spectra are given in table 46b. The progressions are only tentative. Progression (1) is comprised of red-degraded bands, strong and diffuse. The bands of progression (2) are line-like. The latter two progressions are weak, with the last progression double headed, unlike all the others.

All four progressions have similar ΔG values, and these are close to that of the A state of N_2^+. The separation of 40 cm^{-1} between the two heads of progression (4) would appear to be too large to be P and Q branches, and it may be that this progression is really two.

(f) Cook and McNeal [167] have observed the photoionization spectrum of N_2 in the region 795–842 Å together with an underlying continuum. More than 50 new preionized bands were reported, many of which are attributed to absorption from N_2 X, $v=1$–4 to Rydberg states converging to the X or A states N_2^+. The strongest features were at 800.4, 804.6, 806.6, and 809.6 Å. Many identifica-

ions are tentative, with numerous bands as yet unclassified.

(g) Carroll and Sayers [139] have observed an unassigned band amid the $B-A$ bands of N_2. This complex band is red-degraded and shows at least four heads: 8265.5, 8283.8, 8293.3, and 8310.6 Å, with the latter being the strongest. It was assumed that N_2 was the emitter.

(h) Along with bands of the $D-A$ system of N_2^+, Tanaka et al. [603] observed a number of additional doublet bands which could not be assigned with certainty to the same transition. The weak bands are listed in table 46 (vacuum wavelengths) together with tentative assignments which differ little from calculated values based on Tanaka's formula.

(i) In the absorption spectrum of N_2 in the vacuum region Bass [61] identified many band heads with the well known systems whose upper states were a, b, and b'. A number of additional bands were observed in the region 1570–1370 Å which remain unidentified.

(j) Huffman et al. [293] have listed many non-Rydberg bands in the region 940–800 Å which remain unclassified. Some of these had been observed earlier by Worley [666].

(k) Among Codling's observations of Rydberg series converging to the N_2^+ C state, were some unclassified bands [162].

4. Raman Spectrum

The rotational Raman spectrum of nitrogen was first photographed by Rasetti [539–40], and subsequently by Miller [460], who recorded and discussed line frequencies and intensities, and derived values for B_0 and $\Delta G(1/2)$. In a high resolution study of the Raman spectrum, using a mercury lamp as excitation source, Stoicheff [590] photographed the pure rotational spectrum, together with the Q branch of the 1—0 band. Up to 35 lines were observed, with gas pressures of 2 atmospheres. The moderately intense lines were assumed measured to an accuracy of ± 0.03 cm^{-1}. Stoicheff was limited to a resolution of 0.3 cm^{-1} because of the breadth of the mercury emission lines used to excite the spectra.

Butcher et al. [111] excited the Raman spectra by use of a dc argon-ion laser, and by use of a Fabry-Perot etalon crossed with a low dispersion spectrograph, obtained a resolution of 0.1 cm^{-1}. The measurement accuracy was 0.003 cm^{-1}. Their D_v value lies below the value 5.74×10^{-6} cm^{-1} calculated by the Dunham formula. Butcher et al. also attempted to fit the data by including an H_0 coefficient; this gave larger values for B_0 and D_0, but the H_0 obtained was 100 times larger than that calculated from the Dunham formula and was also not statistically significant.

Barrett and Adams [59] have used photoelectric detection rather than photographic to record the 1—0 vibration-rotation Raman band. Q branch lines were unresolved, but O and S lines were resolved. No line positions were published, only a graphical display of the spectrum.

Butcher and Jones [110] have measured the rotational Raman spectra of $^{14}N^{15}N$ and $^{15}N_2$. By a different technique Bendtsen [66] has measured the rotational and vibration-rotation Raman spectra of all three isotopes of N_2. The uncertainty in the absolute wavenumbers of Bendtsen's measurements is at least 0.01 cm^{-1}. There are differences between the observed Raman lines in the experiments of Butcher and of Bendtsen, and also in their B values and D values. The new vibration-rotation spectra provide an improved value for $\Delta G(1/2)$, the fundamental, and also for the difference B_0–B_1.

The molecular coefficients obtained from the Raman measurements are summarized in table 48, together with various derived equilibrium coefficients. The equilibrium coefficients obtained indirectly from the Raman results [110, 66] depend on parameters obtained from electronic spectra. The coefficients fitted to the data from electronic spectra are fitted by assuming a value for B_0 from Raman measurements.

The largest uncertainty introduced in determining B_e and r_e from Raman spectra comes from the value of α that is assumed. At times this has involved taking such a value from electronic spectra, or calculating one by taking a value for γ which has been derived from electronic spectra.

Barrett and Harvey [60] have developed an interferometer method whereby many rotational Raman lines are simultaneously observed, since prefiltering is not used to separate overlapping orders. Using this technique, they have determined a value for α (table 48). It seems preferable to assume both α and γ from the direct fitting to the B_v data obtained from electronic spectra, because the coefficients are correlated.

Pinter [529] has measured the widths of rotational Raman lines in N_2 at pressures of 1–10 atmospheres. For J values from 4 to 12, the observed widths are larger by a factor of three than the calculated values. The experimental values decreased by 25% over this range of J; the theoretical values decreased by half. The discrepancy is attributed by Pinter to neglect of interactions other than quadrupole-quadrupole. Jammu et al. [340] measured self broadening at pressures of 7–43 atmospheres and found broadening was proportional to pressure. However, for J up to 16, there was observed a decrease in self broadening as J increased. Values calculated by the theory of Fiutak and Van Kranendonk [228–9] were about 20% higher. Theory is not yet in accord with experiment.

The Raman spectrum of solid α-N_2 was investigated by Brith et al. [95], Cahill and Leroi [115], Anderson et al. [46], and Mathai and Allin [439].

Bridge and Buckingham [92] and Rowell et al. [548]

measured the polarization of light scattered by gaseous N_2. They obtained for the depolarization ratio, ρ, a value near 10^{-2}, about half that of previous experimental values. This quantity refers to depolarization of both Rayleigh and rotational Raman lines together; each paper used a separate incident frequency, but both used unpolarized incident light. (See these papers for the exact values obtained.)

For incident unpolarized light, Yoshino and Bernstein [674] have measured the depolarization ratio for the Raman vibrational band. They obtained 0.18, in close agreement with prior values obtained at lower resolution. May et al. [441] observed the narrowing of the vibrational Raman bands for densities of 10–360 Amagat. The widths decrease by half over this range of densities.

Recently, Nelson et al. [485] recorded for the first time Raman spectra of N_2 excited in an electrical discharge. Both the vibrational Stokes and anti-Stokes features were observed for the first three vibrational quanta.

The vibrational Raman effect in liquid nitrogen observed by Crawford et al. [184] showed a sharp, intense Q branch associated with isotropic Raman scattering. The rotational wings associated with anisotropic scattering showed no discrete structure, even when narrow slits were used. This is an indication of free rotation in the liquid.

Hyatt et al. [330] have measured the absolute Raman scattering cross sections of the N_2 fundamental Q branch in gaseous nitrogen, for two different incident laser wavelengths. Absolute rotational Raman cross sections have been measured by Penney et al. [523]. Absolute cross sections for vibration have been measured by Fenner et al. [225].

An extensive review of Raman studies of gases has been given by Weber [41]. A review by Jones [363] concentrates on the uses of Fabry-Perot interferometers for high resolution Raman studies of gases.

5. Spectra of Condensed N_2, and N_2 in Matrices; Pressure and Field-Induced Infrared and Microwave Absorption

Only a brief summary will be given concerning the spectra of compressed and condensed nitrogen.

Brith and Schnepp [96] studied absorption spectra of N_2 in the solid, in order to examine the perturbation of the electronic and vibrational states by the crystal field. Preliminary work of this sort had been done by Dressler [209]. Absorption in the region 1600–1200 Å was studied, at temperatures of 20–30 K. Two electric-dipole forbidden transitions were observed: $a\,^1\Pi_g - X$ and $w\,^1\Delta_u - X$. The crystal field split the bands and shifted the $a-X$ bands to lower energies by 200–270 cm^{-1}; for $w-X$ the shift was about twice as much.

Roncin et al. [546] and Roncin [545] considered the perturbation of electronic transitions in the solid and in solid rare-gas matrices. They found that the $a-X$ bands were perturbed in the solid but not in the matrix; the intensities of the $w-X$ bands were enhanced in the pure solid, but not in the matrix. Boursey and Roncin [90] observed a progression below 1000 Å, and attributed it to the $b-X$ transition. It appeared slightly diffuse in the solid, and a bit sharper in Ne and CF_4 matrices. The regular intensity distribution led the authors to conclude that the Rydberg $c-X$ transition was absent (the c state and b state interact strongly in the gas phase).

Tinti and Robinson [616] observed emission from N_2-doped rare-gas solids irradiated by X-rays. In the spectral region 2300–5000 Å two systems were found: $A-X$ Vegard-Kaplan bands and the $C-B$ 2+ system. Both showed emission from $v'>0$. Vibrational relaxation time was found to be at least as large as the radiative lifetime of the bands.

Bass and Broida [62] have summarized much of the work on properties of condensed nitrogen and energy shifts in matrices. Numerous references are given in their review of work on free radicals at low temperature. Schnepp [563] has surveyed the work on lattice vibrations of solid α-N_2. In a review of some topics on matrix isolation spectroscopy, Dressler [211] has offered a new interpretation of prior observations of vibrational satellites to the N emission in pure N_2 matrices.

N_2 has no permanent electric dipole moment, and consequently under normal conditions it has no vibration-rotation absorption spectrum. Absorption can be observed, however, in the gas at high pressure or in the liquid. Crawford et al. [185] were the first to observe absorption at 2331 cm^{-1}. The intensity-pressure relation for pressures up to 60 atmospheres showed that the absorption was not due to stable complexes or to quadrupole transitions. The effect was interpreted as having its origin in electric dipole moments induced in the molecules during collisions.

Since then, the collision-induced fundamental and first overtone bands have been observed over a range of pressures up to 1500 atmospheres. The theory of collision-induced IR absorption by homonuclear molecules, developed largely by Van Kranendonk and collaborators (see, e.g., Poll and Van Kranendonk [534]), has been applied to these absorption coefficient studies, yielding values for the quadrupole moment Q and its derivative with respect to internuclear distance Q', good to about 10%: 1.1 ea_0^2 and 0.95 ea_0, respectively. The same value for Q is obtained by Ho et al. [313] from the observed pressure-induced microwave absorption. The theory has been reviewed once again by Van Kranendonk [17].

Reddy and Cho [542] remarked that the shape of the absorption profiles, namely, pronounced Q and S branches with a hint of an O branch, confirm the selection rule for an induced-dipole transition: $\Delta J=0, \pm 2$. For details see the papers by Heastie and Martin

[288], Gebbie et al. [252], Poll [533], Ketelaar and Rettschnick [384], Bosomworth and Gush [89], Reddy and Cho [373], and Shapiro and Gush [569]. Sheng and Ewing [574] studied the collision induced nitrogen fundamental at low temperature.

The extensive literature on the determinations of the molecular quadrupole moment is included in reviews by Stogryn and Stogryn [589], Krishnaji [19], and Birnbaum [85].

The N_2 fundamental at 4.3 μm was observed by Oxholm and Williams [513] in absorption by liquid air and liquid nitrogen. Buontempo et al. [108] measured the absorption coefficient in liquid nitrogen and N_2+Ar mixtures at a temperature of 90 K. The plot of absorption coefficient versus wavenumber showed essentially the same shape for both, an indication that even in pure nitrogen, simultaneous transitions in two colliding molecules do not play a significant role. In their study of the pressure-induced bands, Shapiro and Gush [569] did find significant contribution to the intensity from simultaneous transitions.

Buxton and Duley [113] have, for the first time, measured the reflection spectrum of solid α-N_2 at 4.2 K over the wavelength range 550–1550 Å. Photographic recording was used. The dominant feature was a group of discrete bands between 12.5 and 13.8 eV which were readily identified as the vibrational levels of the $b^1\Pi_u - X^1\Sigma_g^+$ transition. It was found that Rydberg levels still exist in the solid as a perturbing influence on the $b^1\Pi_u$ levels even though they were not directly observable in the solid. Haensel et al. [277], with an improved experimental arrangement, measured the same reflection spectrum up to 23 eV using photoelectric detection and a synchrotron radiation source.

Mass spectral data by Leckenby and Robbins [408] indicated the presence of the dimer $(N_2)_2$ in the gas phase at low temperature, bound by van der Waals interaction. Long et al. [426] examining the infrared spectrum of gaseous nitrogen at 77 K, found a relatively strong diffuse band which could be assigned as a collision-induced absorption. Weak, but discrete features overlaying the observed band are assigned to vibration-rotation absorption by $(N_2)_2$ van der Waals molecules.

Courtois et al. [179] have observed the field-induced Q-branch of N_2 at 2331 cm^{-1}, at an electric field strength of 160 kV/cm. Courtois and Jouve [178] observed the N_2 fundamental vibration-rotation band (branches O, S were resolved, Q branch remained unresolved), induced by an alternating electric field of up to 140 kV/cm. The vibrational polarizability matrix elements which were deduced from intensity measurements are comparable to the values obtained from Raman intensities. The $k=0$ vibrational spectrum for solid α-N_2 has been discussed by Raich [537]. These results are compared with prior calculations and experiments.

6. Electron Spectroscopy

In the last decade, electron spectroscopy has become an important new field which can sometimes provide information about molecular electronic structure and electron binding energies not readily attainable by conventional spectroscopic methods.

The main branches of electron spectroscopy include: photoelectron spectroscopy, Auger spectroscopy, electron impact spectroscopy, and Penning ionization spectroscopy. All use energy analysis of electrons, rather than energy analysis of photons, as the primary source of information. But they differ in the manner by which excitation is induced, and in the kind of information obtained. The nitrogen molecule has been the object of numerous investigations using all these methods.

It is outside the scope of this work to cover the vast field of electron spectroscopy. The merits of the methods will briefly be mentioned; elucidation of the specific problems concerning the nitrogen molecule are discussed in this work. Otherwise references will be made to recent review articles and books.

6.1. Photoelectron Spectroscopy

In photoelectron spectroscopy the structure of a molecule is probed by analyzing the kinetic energy of electrons emitted following the impact of monochromatic photons. Selected keV X-rays have been used to probe core and valence electrons in the method labeled ESCA (Electron Spectroscopy for Chemical Analysis). The valence electrons have also been studied by use of photons having energies below 30 eV, namely, at wavelengths of 584 Å, 736–744 Å (doublet), and 304 Å. The techniques which use lower energy photons have higher resolution.

The intensity distribution among the experimentally observed peaks constitutes a measure of the relative transition probabilities. The nature and extent of the observed progressions of vibrational structure of the states of the ions also indicates the nature of the ionized electron. A sharp single term progression indicates a 0–0 band, and removal of a non-bonding electron; removal of a bonding electron is shown by a long progression, with maximum intensity for some high v'; a shorter progression with peak intensity above $v'=0$ is a sign of an anti-bonding electron being ionized.

From ESCA measurements are obtained the orbital energies. Those not normally available from other techniques include: $\sigma_g 2s$ at 37.3 eV and the $1s$ K shell energy at 409.9 eV [32]. An unusually fine example of the photoelectron spectrum of nitrogen, showing the structure of the $A^2\Pi_u$ vibrational progression is given in figure I:26 of the first review of ESCA by Siegbahn et al. [32].

Summaries of the experimental techniques, results, and references to prior work can be found in a review by

Berry [4], the book by Turner et al. [36], and a review of ESCA by Siegbahn et al. [32].

Collin and Natalis [163] were the first to observe the somewhat different intensity distribution in the photoelectron spectra when two different energy photons are used. Berkowitz and Chupka [75] have studied the photoelectron distribution from autoionizing states of N_2. It seems that the two-step process of autoionization always accompanies the direct photoionization and indicates that the intensity distribution of the photoelectron spectra observed by Collin and Natalis can be accounted for.

Using 304 Å photons, Edqvist et al. [217] were unable to observe the $C^2\Sigma_u^+$ state of N_2^+ at 23.6 eV.

In examining the relative intensities for transitions to the $v=0,1$ levels of the X state of N_2^+, Carlson [121] found a strong angular dependence, over the range 20 to 140 degrees. This he interpreted as due to a possible breakdown in the Born-Oppenheimer approximation.

Natalis et al. [483] have used the Ne I doublet (736–744 Å) to excite the photoelectron spectrum of N_2. All vibrational levels of the ground state of the ion were observed below the $v=0$ level of the first excited electronic state of the ion. The enhanced intensity of these vibrational peaks relative to those produced by the use of 584 Å photons is accounted for by a two-step autoionization mechanism (see also Samson [553]). Relative intensities of vibrational peaks with the 584 Å photons conform to direct excitation rather than a two-step process.

The $N_2^+C^2\Sigma_u^+$ state is formed by ionizing one electron and exciting another; consequently, its intensity in PES is low. Åsbrink and Fridh [54] claim to have observed this state up to $v=18$, i.e., up to 27.5 eV. Only graphical results have been published. A Birge-Sponer extrapolation tentatively points to a new dissociation limit for the C state at 28.5 eV, $N(^2D^\circ)+N^+(^1D)$. This contradicts earlier theoretical potential curves deduced for this state [258, 427, 47]. There appears to be coincidence between the new PES measurements and peaks observed in the mass spectrum of N_2 as reported by Newton and Sciamanna [487] and Fournier et al. [230, 233]. A small discontinuity in vibrational spacing for levels above $v=13$ is attributed to crossing of the C state potential by a repulsive state whose separated atom limit is $^2D^\circ+^3P$ at 26.7 eV [54]. Åsbrink and Fridh's interpretation of their photoelectron spectrum is questioned by Thulstrup and Andersen [608].

Gardner and Samson [243] have observed the PES for N_2 with 304 Å photons; their resolution was about half that of Natalis et al. In addition to the usual features they observed the following states: 28.2 eV, $D^2\Pi_g$; 36.5 eV, $^2\Sigma_u^-$ or $^2\Pi_u$; and 38.7 eV, $^2\Sigma_g^+$. Adiabatic energies are given. The identification of the states is tentative.

Gardner and Samson [244] obtained the PES of N_2 with Ne I radiation (736 and 744 Å); they were able to separate N_2^+X, $v=4$ from A, $v=0$ but could not resolve the small spin-orbit splitting of the A state. They also observed the PES involving the first three states of N_2^+ by use of 584 Å and 537 Å radiation [245]. In the latter experiment the vibrational intensities, corrected for transmission of the analyzer, were compared with Franck-Condon factors; the deviations were interpreted as possibly indicating r-dependence of the transition moment.

Okuda and Jonathan [503] used CI calculations to interpret weak bands in the PES of N_2.

By use of He II 304 Å radiation Potts and Williams [536] observed PES spectra, including transitions that arise from two-electron processes. The bands at 28.8 eV and 32.8 eV are assumed to arise from overlapping states involving configuration mixing. The vertical IP at 36.6 eV is associated with ionization of a $1\sigma_g$ electron. The observed peaks are tentatively identified in terms of a model that overestimates the energies.

Comes and Speier [166] have irradiated nitrogen, using the He I 584 Å line to produce the $N_2^+B^2\Sigma_u^+$ state, which then is de-excited by transition to $N_2^+X^2\Sigma_g^+$. Franck-Condon factors for both transitions are deduced from experiment and compared with earlier determinations.

La Villa [402] obtained the $K\alpha$ emission from gaseous neutral N_2 excited by electron bombardment. A contribution to the intensity on the high-energy side of the main spectral feature was attributed to resonance emission from neutral states. Werme et al. [651] have produced the X-ray emission spectrum of N_2 by bombardment with 10-keV electrons, and have for the first time observed fine structure that is due to vibrational splitting. From a comparison with ESCA results they are able to identify the observed lines.

6.2. Auger Electron Spectroscopy; States of N_2^{2+}

Auger spectroscopy may be considered a variant of photoelectron spectroscopy. In this case the ionization of an inner shell is caused by photon or electron impact, followed by ejection of an additional electron, the Auger electron, resulting in a doubly ionized molecular state.

An Auger process is one in which an initial inner shell hole is filled by an outer shell electron while a second outer shell electron is emitted with kinetic energy equal to the total energy difference between the final and initial states of the system. This energy difference is the observable in Auger electron spectroscopy.

The Auger spectrum can be complex and consist of many lines and bands. Satellite lines originate when the vacancy is coupled with a simultaneous excitation of a second electron. The nomenclature for such

transitions is given by Moddeman et al. [468]. The *K-LL* Auger spectrum, for example, refers to an initial *K* vacancy and a final ion with two *L* vacancies.

Stalherm et al. [582] have analyzed the *K* Auger electrons whose energies have given evidence for several states of N_2^{2+}. Also determined was the energy needed to ionize N_2 two-fold in the ($\sigma_g 2s$) orbital as (96.5±1.0) eV.

The two lines with highest observed kinetic energy, about 384 eV, were ascribed by Stalherm et al. as arising not from a normal *K-LL* Auger process, but from excitation of a *K* shell electron into an excited state (of the neutral molecule), followed by autoionization. This was verified by Carlson et al. [122].

Moddeman et al. [468] have measured the *K-LL* Auger spectrum of N_2 produced by electron impact, and have identified a number of normal and satellite lines. In addition, the second and third ionization potentials were obtained, the latter value being estimated as 41 eV above the ground state of N_2^{2+}, giving 84 eV above the ground state of N_2 for its appearance potential.

Energies (in eV) of the lowest states of N_2^{2+} (at r_e for the N_2 ground state) from theory and experiment are compared below. CI calculations are from Thulstrup and Andersen [608]; measured values are from (a) Carroll [124], (b) Stalherm et al. [582], (c) Moddeman et al. [468], and (d) Appell et al. [50]. The new notation for the electronic states is by analogy with proposed new notation for C_2 (Herzberg et al., Can. J. Phys. 47, 2740 (1969)).

New	Old	Theory	Experiment			
			(a)	(b)	(c)	(d)
$X\,^1\Sigma_g^+$	(*x*) $a\,^1\Sigma_g^+$	0.0(+0.2−0.0)	0.0	0.0	0.0	0.0
$a\,^3\Pi_u$	(*X'*) $X\,^3\Pi_u$	1.2(+0.8−0.4)			1.5	
$c\,^3\Sigma_u^+$	$A''\,^3\Sigma_u^+$	1.7(+0.2−0.0)				
$A\,^1\Pi_u$	$b\,^1\Pi_u$	3.5(+0.6−0.4)		2.9±0.4	3.0	2.1±1.0
$b\,^3\Sigma_g^-$	$A'\,^3\Sigma_g^-$	4.3(+1.0−0.8)		3.9±0.4	4.0	
$d\,^3\Pi_g$	$A\,^3\Pi_g$	4.5(+0.6−0.4)				
	$^1\Sigma_g^+(2)$	5.2(+0.8−0.6)		6.4±0.3	6.3	
	$^1\Delta_g$	5.6(+1.1−0.9)				
	$^3\Sigma_u^+(2)$	7.8(+0.6−0.4)				
$C\,^1\Pi_g$	$c\,^1\Pi_g$	8.5(+0.6−0.4)				
$D\,^1\Sigma_u^+$	$d\,^1\Sigma_u^+$	8.5(+0.3−0.0)	7.80	7.9±0.25	7.8	
	$^3\Delta_u$	8.9(+0.9−0.7)				
$e\,^3\Pi_g(2)$	$B\,^3\Pi_g(2)$	9.0(+1.0−0.8)		9.5±0.25	9.4	
$E\,^1\Sigma_g^+(3)$	$e\,^1\Sigma_g^+(3)$	10.3(+0.8−0.5)				

The maximum energy of observed *K* Auger electrons is (366.5±0.2) eV. The calculated value of this quantity is 366.8 eV, obtained from the difference between the *K* orbital energy of 409.5 eV, from the accurate measurement of Nakamura et al. [481] and the energy to doubly ionize N_2 into the N_2^{2+} ground state, (42.7±0.2) eV. The latter value is from appearance potential measurements of Dorman and Morrison [202] and the mass spectra work of Newton and Sciamanna [487].

Nakamura et al. [481] have measured the *K* electron energy in a study of the absorption spectrum in the 30 Å region, with 1.3×10^9 eV electron synchrotron radiation as background source. Resolution was better than 0.03 Å (0.1 eV). Their results included a broad, flat band at 400.8 Å. This feature appeared sharp in the *K* shell energy loss spectra observed by Van der Wiel [629a]. Both N^+ and N_2^{2+} contribute to this feature (see [629a] for further discussion).

Vinogradov et al. [638] have studied the X-ray *K* absorption spectrum of N_2 and have obtained a *K* shell limit in agreement with the value of Nakamura. In addition, a number of $^1\Sigma_u^+$ and $^1\Pi_u$ X-ray excited states were observed; the relative energies and suggested electron configurations (by analogy with NO) are also given.

In the Auger spectra produced by 50–500 keV proton impact, Stolterfoht [591] observed strong satellite lines arising from double ionization. The initial double ionization is explained by either successive inner and outer shell ionizations, or by an inner ionization followed by capture of an outer shell electron.

Appell et al. [50] have studied the double charge transfer spectroscopy of several molecules and have measured vertical energies of several states of N_2^+.

6.3. Electron Impact Spectroscopy

In electron impact spectroscopy the energy of the scattered electrons from a monoenergetic beam is analyzed. The energy loss of the scattered electrons gives information on which molecular states have been excited in the process. (See, e.g., reviews by Berry [4], Trajmar et al. [35], and Hasted [11]).

This method applied to nitrogen has two important advantages: it permits easy access to the region of transition energies above 11 eV; and by use of low-energy incident electrons (20 eV or less), it permits the excitation of optically forbidden transitions. In this way singlet-triplet transitions can be conveniently studied, but not at sufficient resolution to give details on rotational structure. For high energy electrons (over 100 eV), the selection rules closely resemble the optical ones, and cross sections are related to optical absorption coefficients.

The electron impact excitation of N_2 has been studied extensively at different scattering angles and at a number of incident energies. Many electronic states have been observed, and comparisons of relative intensities in electron impact and ultraviolet absorption for both allowed and forbidden transitions have been made.

A spectral transition at 12.26 eV was first observed in electron impact spectra (see Heideman et al. [292], Meyer and Lassettre [457a]). The corresponding state, $a'\,{}^1\Sigma_g^+$, was later observed in ultraviolet absorption (a''–X Dressler-Lutz system; see section 3.4) at 12.28 eV.

The transition to the $E^3\Sigma_g^+$ state at 11.87 eV has been studied extensively (see Heideman et al. [292], Meyer and Lassettre [457a]). This state is the parent state for some observed resonances in N_2^-.

Freund [239] used electron-impact excitation of a molecular beam of nitrogen to produce the metastable $E^3\Sigma_g^+$ state, and studied the emission from the beam. In addition to bands of the E–A Herman-Kaplan system, the following bands of the E–B transition were observed: (0−0) 2740, (0−1) 2880, (0−2) 3020, and (0−3) 3180 Å. Simultaneously a few bands of the C–B second positive system appeared.

The E–C transition will fall in the infrared region (0−0 band at ~1.47 μm). However, assuming that the C–B bands observed in the beam experiment were solely populated from the E–C transition, Freund estimated the relative intensities as

$$E\rightarrow A=5.9\pm0.5,$$

$$E\rightarrow C=3.7\pm0.5,$$

$$E\rightarrow B=1.0\pm0.5.$$

The radiative lifetime of the E state was estimated as (270 ± 100) μs, and the equilibrium internuclear distance as (1.16 ± 0.02) Å.

Hall et al. [279] have measured the electron impact spectrum of N_2 in the 6–12.5 eV range by the trapped electron method. The experiments in the threshold region largely favored excitation of triplet states. Energy resolution of 0.01 eV enabled observation of vibrational structure of the states $A^3\Sigma_u^+$, $B^3\Pi_g$, $C^3\Pi_u$, $E^3\Sigma_g^+$, and $a''\,{}^1\Sigma_g^+$. The A and B intensity distributions showed agreement with calculated Franck-Condon factors. For the C state, significant differences were observed, a possible indication of the effect of non-constant transition moment. (See however Williams and Doering [663] for a survey of intensity distribution as a function of incident electron energy.)

A broad feature between 9.6 and 11.6 eV (peak at 9.75 eV) does not correspond to any known repulsive or stable state, either from experiment or from the calculated potentials by Michels [459].

Level $E^3\Sigma_g^+$, $v=2$ identified at 12.41 eV is uncertain.

Geiger and Schroeder [253] have used 25 keV electrons to study the energy loss spectrum in range 12.5–14.9 eV. Numerous states were observed with a resolution of 0.01 eV. It is in this range that energy loss and UV spectra had often disagreed. (See section 10 for a discussion of the resolution of these apparent discrepancies.) At this resolution rotational structure is not resolved.

Williams and Doering [663] have used 9–50 eV electrons impacting on nitrogen, and concluded that the dominant electron impact processes in the atmosphere occur in the 15 eV range, with the principal emissions from a–X, B–A, and C–B.

Lassettre [400] has extensively reviewed the work on inelastic scattering of electrons having kinetic energy from 15 eV to 40 keV. Numerous transitions have been observed, including some triplet-singlet systems, as well as transitions involving high lying singlet states. Relative intensities have been studied as a function of scattering angle; for high energies these should be governed by the optical selection rules. In section 10 these topics are considered at greater length. Many of the states observed are known from photon absorption studies.

Chutjian et al. [160] have produce energy loss spectra at 20.6 eV for a range of scattering angles. They were the first to identify in the impact spectra the states $W^3\Delta_u$, $w^1\Delta_u$, $B'^3\Sigma_u^-$, and $a'^1\Sigma_u^-$.

Hicks et al. [312] have observed autoionizing transitions following low energy electron impact. Many of the states observed are known from photon absorption studies. Some new bands were seen with energies of 18.282, 18.375 and 18.477 eV, a possible vibrational progression belonging to a Rydberg state whose series limit is the $D^2\Pi_g$ state of N_2^+. This identification is only tentative.

Wight et al. [653] have observed the K-shell energy loss spectra produced by the scattering of 2.5 keV electrons. (Compare the ESCA and optical work as discussed in section 6.1.)

Goddard et al. [260] have discussed selection rules for transitions induced by electron impact and have provided an explanation for the absence of certain transitions; these are used to estimate relative transition strengths. Cartwright et al. [151] also mention the variation of transition strength with scattering angle.

Joyez et al. [368] used two methods to study electron scattering by N_2 in the energy range 11.8–13.8 eV, energy loss spectra for various scattering angles and fixed incident energy of 14.3 eV, and threshold excitation for zero residual energy for the same scattering angles. Angular behavior of the peaks enabled singlet-singlet and singlet-triplet transitions to be distinguished. $F^3\Pi_u$ and $G'^3\Pi_u$ Rydberg states, predicted by Leoni and Dressler [415], were observed. Unidentified triplets should be Rydberg states: 13.155 eV, N_2^+ X core; 13.395 eV, 13.635 eV, N_2^+ A core.

Fournier et al. [232] have studied collisions of keV N_2^+ ions on noble gases, and among other features, observed two thresholds of especial interest at 21.2 and 22.8 eV. The first they identified as possibly a $^4\Sigma_u^+$ state of N_2^+ with configuration $\pi_u^3\sigma_g\pi_g$. The second could be either another quartet state from the same configuration, e.g., $^4\Sigma_u^-$ or $^4\Pi_g$, or one of the more familiar N_2^+ states D or C.

El-Sherbini et al. [220] have obtained oscillator-strength spectra for the production of N_2^+. At 22.5 eV is a feature that is likely an unresolved pre-ionizing Rydberg series whose limit is the N_2^+ C state.

6.4. Penning Ionization

In Penning ionization electron spectroscopy there is measured the energy distribution of electrons ionized from an atom or molecule by an electronically excited long-lived neutral species. Controlled energy electrons excite the neutral species, and a (molecular) beam of these excited species then undergoes a reaction of the form $N_2^*+M=M^+ + N_2+e$. Ionization occurs when $N_2^* \geq IP(M)$. $E(N_2^*)=E_e+IP(M)+E_{kin}(M^+ + N_2)$, the latter term normally being negligible.

Using this technique Cermak [152–3] detected the $v=0,1$ levels of the $E^3\Sigma_g^+$ state of N_2, and an amorphous feature interpreted as the higher vibrational levels of the $a^1\Pi_g$ state.

6.5. Resonances in Electron Impact; Unstable States of N_2^-

During electron impact, when an electron is temporarily captured by the molecule, there are formed temporary compound states also called temporary negative ions or resonances. Sharp structure in scattering cross section indicates a relatively long-lived compound state; broad structure indicates a rather short-lived compound state.

For electron energies less than 4 eV, attachment to the ground state of N_2 results in a shape resonance. Core-excited resonances indicate association with an electronically excited parent state. Core excited resonances can lie at higher or lower energies than the parent. If below, this means a positive electron affinity, and is labeled a Feshbach resonance; if above the parent, there occurs a core-excited shape resonance. According to Weiss and Krauss [647] Feshbach resonances are associated with Rydberg states. Resonances having valence excited parent states do not display sharp structure in their cross sections.

These topics will be considered only briefly, for they have been discussed at great length in reviews by Bardsley and Mandl [3] and Schulz [31], among others.

Dominating the low energy electron impact cross sections in N_2 is some resonance structure in the range 1.8 eV to about 3.8 eV. Gilmore [258] was the first to propose that the impacting electron temporarily finds itself in the $\pi_g 2p(3d\pi_g UA)$ orbital, forming the short-lived N_2^- ion in its ground state. Thus is formed the $^2\Pi_g$ shape resonance from the $N_2X\,^1\Sigma_g^+$ parent state.

Vibrational cross sections for $v=1$ to 8 of the N_2 ground state show structure of a compound state that is independent of angle of observation (see, e.g., Ehrhardt and Willmann [218], Schulz [565], and Herzenberg [307]). An excellent fit to the observed cross sections has been obtained by Birtwistle and Herzenberg [85], with similar parameters obtained in ab initio calculations by Krauss and Mies [395]. Rotational broadening in the 2 eV resonant scattering has been observed by Comer and Harrison [164].

A potential curve for this state has been sketched by Gilmore [258]. The potential-energy curve calculated for N_2^- [395] predicts a shift of 0.20 a_0 (0.10 Å) in r_e from N_2 to N_2^- and $\omega_e=1960$ cm^{-1} for N_2^-. An analysis of the scattering by Herzenberg [307] determined this shift to be about 0.3 a_0 (0.15 Å).

There exist numerous core-excited resonances in the region 11–15 eV. Heideman et al. [292] and Comer and Read [165] and later others observed a progression of resonances beginning at 11.48 eV. This lies less than half a volt below the parent N_2 state $E'^3\Sigma_g^+$, the lowest Rydberg state of this species. The various experimental determinations are summarized by Schulz [31]. This Feshbach resonance is identified as having $^2\Sigma_g^+$ symmetry.

Electron transmission measurements by Heideman et al. [292] and Hall et al. [279] showed that structure exists in the scattering of electrons from N_2 between 11 and 12.5 eV. The observed resonances were at 11.48, 11.75, 11.87, and possibly also at 12.02 and 12.26 eV. With the assumption that $E^3\Sigma_g^+(0)$ is the parent state of the 11.48 eV peak, which would give a reasonable electron affinity of 0.39 eV, the three resonances at 11.48, 11.75, and 12.02 eV would then belong to the same vibrational series and have, respectively, the $v'=0,1,2$ vibrational levels of the $E^3\Sigma_g^+$ state as parents. Also, the resonance at 11.87 eV, which produced the strong threshold excitation of the $E(0)$ level, could have the $a''^1\Sigma_g^+(0)$ state at 12.25 eV as parent state and an electron affinity of 0.39 eV.

Some broad structure between 9.6 eV and 11.6 eV observed by Hall et al. [279] does not correspond to any observed state. It was loosely suggested that the shallow $^5\Sigma_g^+$ state could reasonably explain this structure.

Comer and Read [165] observed the same resonances, and concluded that they were vibrational levels of a temporarily bound state of N_2^-. From the vibrational levels and the relative cross sections for the individual peaks, a Morse potential curve was derived:

Symmetry $^2\Sigma_g^+$ (parent, $E^3\Sigma_g^+$),

$$r_e = 1.115 \pm 0.01 \text{ Å},$$

$$\omega_e = 2180 \pm 160 \text{ cm}^{-1},$$

$$\omega_e x_e = 20 \pm 20 \text{ cm}^{-1}$$

This state lies 11.345 eV in energy above $N_2 X$, $v=0$. Eliezer and Moualem [219] have calculated the binding energy of the $^2\Sigma_g^+$ resonance state relative to the $E^3\Sigma_g^+$ state and obtained a value about half the experimental value.

Apart from the series already discussed, Comer and Read [165] observed two other features in the elastic scattering, at 11.87 and 12.205 eV. These are both present for scattering at 40° and both absent on the 85° spectrum. They may be members of another series. The feature at 11.87 eV has been previously observed at 0° by Heideman et al. [292] and it has been suggested that it affects threshold excitation spectra (Hall et al. [279]) by enhancing excitation to the E state which is nearly coincident in energy. Hall has also suggested that if a resonance exists at 11.87 eV, it would have the $v=0$ level of the $a'' {}^1\Sigma_g^+$ state at 12.28 eV as parent. As in the case of the E state, the a'' is a Rydberg state so this would also be consistent with the conclusion of Weiss and Krauss [647].

Following the prior work on structure observed in a transmission experiment by Sanche and Schulz [555], Mazeau et al. [442] observed broad, core-excited shape resonances associated with the $A^3\Sigma_u^+$ and $B^3\Pi_g$ valence states as parents. These resonances occur for impact energies of 8.2 to 11 eV for the A state, and for 9 to 11.5 eV for the B state. In both cases, the structure seems to be due to overlapping processes.

Only approximate information is then available for the N_2^- states which are formed. These include: $A+(3p\pi_u)$ to form Π_g, and $B+(3p\sigma_u)$ to form Π_u. $r_e \sim$ 1.42 Å, $T_e \sim 7.1$ eV, $\Delta G(1/2) \sim 0.1$ eV. Crude potentials can be sketched from the estimated parameters: Π_u $r_e \sim 1.40$ Å, $T_e \sim 7.4$ eV, $\Delta G \sim 0.15$ eV.

Mazeau et al. [443] have made an angular analysis of the structure in the excitation function of the $N_2 E^3\Sigma_g^+$ state. Four transient states of N_2^- have thereby been identified: $E+3p\sigma_u {}^2\Sigma_u^+$ lying above the E state by 20 meV, $E+3p\pi_u {}^2\Pi_u$, N_2^+ $A+(3s\sigma_g)^2 {}^2\Pi_u$ responsible for core excited resonances, and a Σ_u^+ state of unknown triplet parentage. Krauss and Neumann [396] have calculated $^4\Pi_u$, $^2\Phi_u$, and $^4\Sigma_g^-$ resonance valence states of N_2^-. T_e values above $N_2 X$ are estimated as 6.8, 8.5, and 8.8 eV, respectively. These play a role in the resonance excitation of the A and B states of N_2, though not the entire role.

Pavlovic et al. [520] have observed a broad maximum near 22 eV in the vibrational cross section. This was studied as a function of scattering angle and electron energy, and the feature is attributed to a possible overlap of several short-lived compound states whose spacing is too close to be resolved. The identity of these states remains obscure. Previously, only the shape resonance at 2 eV had been observed.

Streets et al. [592] have observed anomalous peaks in the photoelectron spectra of N_2 which are attributed to formation of N_2^- by collisions between emitted photoelectrons and N_2.

In the 11 to 15 eV energy region numerous features in the electron impact spectrum observed by Golden et al. [262] are attributed to decay of states of N_2^- to the E state of N_2.

7. Perturbations and Splittings

In section 3 where the individual electronic transitions are discussed, perturbations and splittings are mentioned. In the present section some of these local perturbations and splittings will be considered in more detail. Many of the levels discussed are mixed so intimately that the division of topics in this section seems somewhat arbitrary, but an attempt is made to broadly isolate discussion of the different effects.

7.1. Perturbations in Singlet States

$a\,{}^1\Pi_g$

For low J the Λ-doubling in the $a\,{}^1\Pi_g$ state is very small. With the assumption that the doubling in the $w\,{}^1\Delta_u$ state is negligible, McFarlane [449] determined from the w–a transition that the c levels (Π^+) lie above the d levels (Π^-). A value of the difference $B_{oc}-B_{od}=(1.0\pm0.3)\times10^{-4}$ cm^{-1} was found for $v=0$.

In a high resolution study of the 0–3 and 0–4 bands of the a–X transition, Wilkinson and Houk [660] observed that the Λ-doubling above $J=34$ increased rapidly due to a perturbation. Both Λ-components were shifted upwards, an indication that the perturber is not a $^1\Sigma_g$ state. Also $F_c >> F_d$. The most likely level to cause this perturbation is $v=6$ of $B\,{}^3\Pi_g$, but no direct observations exist for the high J-values in question.

$x\,{}^1\Sigma_g^-$

In the 0–1 and 0–0 x–a' bands are observed anomalous intensity distributions. In the 0–1 band the first P and R branch lines are rather strong, but there is a rapid drop in intensity, and no lines were observed beyond $J'=11$ [422]. The 0–0 band was weaker, but a similar intensity decrease was noted by Lofthus. Gaydon [249] mentioned no such anomaly in his study of the 0–1 band. It is not certain whether this intensity distribution results from perturbations or predissociation.

$k\,^1\Pi_g$

Carroll and Subbaram's conventional analysis of bands involving this new state [140] led to anomalous B values and vibrational quantum $\Delta G(1/2)$; similar anomalies had been observed in the $y\,^1\Pi_g$ state. (See section 3.9). It was found that the deperturbed $v=1$ levels of the k and y states nearly coincide in energy.

$y\,^1\Pi_g$

This state shows a rather peculiar structure (see Lofthus and Mulliken [425]. (See sections 3.8 and 8).

Large Λ-doubling is observed in $v=0$. This is fitted by $\Delta\sigma_{cd}(J)=(B_c-B_d)J(J+1)$, where $B_c-B_d=0.022$ cm^{-1}. The Λ-splitting cannot be accounted for in terms of interaction with a single Σ state [425]. A plot of $\Delta_2F_c(J)/4(J+1/2)$ vs. $(J+1/2)^2$ showed marked curvature for $v=1$, and only by extrapolating this curve for higher J is there obtained $B_1<B_0$.

Bands with $v=0$ were short and blended; observed branches for $v=1$ bands were longer.

Carroll and Subbaram [140] have observed the $v=2$ level for the first time, in the $y-w$ and $y-a'$ bands. A homogeneous interaction with the new $k\,^1\Pi_g$ state has accounted for the anomalies observed previously. Deperturbed B values and term values show strongest interaction between the $v=1$ levels; no deperturbation was carried out for the $v=2$ level, but the level position and B value suggest only a small homogeneous interaction.

$a'\,^1\Sigma_u^-$

No perturbations are observed, but the $C\,^3\Pi_u$ state ($v=0$) may cause some perturbations in the $v=16$ level, as suggested by Dieke and Heath [196].

$w\,^1\Delta_u$

No perturbations are observed, but Dieke and Heath [196] found it possible that the $v=13$ level of this state could account for some observed perturbations in the $C\,^3\Pi_u$ state.

$b\,^1\Pi_u$, $c\,^1\Pi_u$, $c'\,^1\Sigma_u^+$ and $b'\,^1\Sigma_u^+$

In the spectral region 1000–796 Å are found many strong and irregularly spaced bands of molecular nitrogen. Some of these bands had been arranged into Rydberg series by Worley [666], while many others had been grouped into progressions assigned arbitrary letters. These progressions had seemingly each represented states having small binding energies, although far more states were so indicated than could be accounted for by theory. The strength of these bands made it certain that the upper states of these bands were of species $^1\Sigma_u^+$ or $^1\Pi_u$.

In the summary that follows it is mainly the results of Dressler and of Carroll and colleagues that will be emphasized, and these papers can be referred to for details and the notation used [210, 130, 132]. (See section 3.5 and figure 4).

$b\,^1\Pi_u$

Irregularities in structure of the $b\,^1\Pi_u$ valence state are accounted for by the strong interaction with the first member ($n=3$) of the $(3\sigma_g)np\pi_u\,^1\Pi_u$ Rydberg series, labeled c_3. Three levels of the b state show observable Λ-doubling, which is attributed to interaction with vibrational levels of the first member ($n=4$) of the $(3\sigma_g)np\sigma_u\,^1\Sigma_u^+$ Rydberg series, labeled c_4'. Carroll and Collins [130] and Carroll et al. [132] observed many of these effects in their high resolution absorption spectra. A mix of the new and old designations for these levels will be used in describing them. See figure 4 for the notation used.

2–0, b_3

This band is among the strongest in the spectrum of N_2. Diffuse rotational structure was observed in the head region. Perturbations for $J<12$ are indicated by the levels being lower than expected; maximum displacement is about 5 cm^{-1} for $J=1$.

4–0, b_4

This is the first band in this state to show some small Λ-doubling. Analysis yielded D values larger than expected due to perturbation of higher J levels. The D value obtained then includes a perturbation component, and only fortuitously does this fit the observed spectra.

5–0, ℓ_1 and ℓ_2

Either level ℓ_1 or ℓ_2, if assigned to state b or c, would have an anomalous B value. Both levels share valence and Rydberg character: the ℓ_2 level is more valence-like and is formally assigned as $v=5$ of $b\,^1\Pi_u$. ℓ_1 is formally assigned as $v=0$ of $c_3\,^1\Pi_u$. A small perturbation for low J depresses both Λ-components.

6–0, m_1

There seems to be a small perturbation at high J. Lofthus [423] had observed some hint of a perturbation around $J=12$.

7–0, m_2

A strong perturbation is indicated.

8–0, m_3

At J above 12 there begins a sharp drop in intensity accompanied by a level shift. At high J the intensity increases once more.

9–0, p_1

Worley [666] had indicated a small Λ-splitting.

11–0, p_3

At $J=21$ the Λ-doubling amounts to 4 cm^{-1}. At higher J values both Λ-components are perturbed.

14–0, q_3

$F_e(17)$ and $F_e(18)$ levels seem to be shifted about 0.5 cm^{-1}. In figure 1 are shown approximate potential curves which suggest the nature of the vibrational perturbations whereby levels b, $v \leq 4$ are depressed, and $v \geq 5$ lie higher in energy than the unperturbed values. (See also the approximate deperturbed potential curves in figure 1 of Dressler [210].) The b state vibrational quanta are smaller than those of the c_3 Rydberg state so that one vibrational level of c_3 may affect several levels of the b state. (See table 1 in ref. [210].)

The ΔG's for the b state are very irregular. $\Delta G(4\frac{1}{2})$ is nearly twice as large as others in this progression [210]. This occurs because the ℓ_1 level (having the largest B value) is assigned to the Rydberg c state rather than to b.

The b,c interaction is centered about 104000 cm^{-1} (T_0). Above the energies for $b(8)$ and $c_3(1)$ the interaction is very weak.

In the reflection spectrum of solid nitrogen observed by Buxton and Duley [113], there are indications of the presence of Rydberg states that presumably perturb the b state, though these states are not directly observed. Compare also the reflectance spectrum of Haensel et al. [277].

$c_3\,{}^1\Pi_u$

$c_3(0)$, ℓ_1

Janin [346] observed a large Λ-splitting in the ℓ_1 level ($F_e > F_d$) and attempted to interpret this splitting as arising from interaction with the nearby p', $c_4(0)$ level. The $v=1$ level of the b' state may also play a role (see e.g., results of Wilkinson and Houk [660], which showed a permanent shift in high J levels, possibly due to a ${}^1\Pi_u$ perturbation). Observed Λ-splittings observed by Janin can be fitted by: $\Delta\sigma_{cd} = (B_c - B_d)J(J+1)$ with $B_c - B_d = 0.016$ cm^{-1}.

$c_3(2)$, d''

Janin [346] found some indication of a perturbation; lines were weakened near $J=13$ and large Λ-splitting centered about $J=13$.

Deperturbation of c_3 is referred to in the discussion of c_n', next.

$c_n'\,{}^1\Sigma_u^+$

The Rydberg levels c_n' show numerous perturbations resulting from interaction with levels of the b' valence state. The old notation for these levels identified the upper state in transitions to the X or a states.

$c_4'(0)$, p'

Lofthus [423] observed a weak perturbation in this level; maximum displacement occurred between $J=10$ and 11. The perturber is $b'(1)$.

$c_4'(2)$, k

Worley [666] found evidence of a transition from Hund's coupling case b' to d'.

$c_4'(3)$, s'

In the s'–a bands Gaydon [249] and Lofthus [423] observed anomalously low intensity of the R branch, with roughly equal intensity for P and Q. Normally $Q > P > R$. A transition from coupling case b' to d' is indicated.

$c_4'(4)$, h

Both Gaydon [249] and Lofthus [423] observed the oddity that the h–a band with $v''=2$ was absent even though h–0, h–1, and h–3 were all strong. For the h–3 band the Q branch was sufficiently resolved to be measured; the R branch was unexpectedly weak, as was the case for the h–0 and h–1 bands. This intensity anomaly might originate in an unusual form of rotational structure of the upper state. This shows some similarity to the $c_4'(3)$ level.

Lefebvre-Brion [412] has made an approximate deperturbation calculation for the ${}^1\Sigma_u^+$ states of interest here. Morse potentials were assumed to describe the deperturbed potentials of the interacting states. By a matrix diagonalization, the perturbed levels were obtained by a fit to the observed values.

Carroll et al. [132] point out that nearly all ${}^1\Sigma_u^+$ levels show some perturbation. The low vibrational levels of the $b'\,{}^1\Sigma_u^+$ state are irregular because of a homogeneous perturbation with the first ${}^1\Sigma_u^+$ Rydberg state, c_4': $(3\sigma_g)4p\sigma_u$. At higher v are even stronger interactions with c_5'. The unperturbed potential energy curves for b' and c_4' intersect between $b'(4)$ and (5) and just above $v=1$ of c_4'. Above b', $v=16$ there is also a strong perturbation.

The Worley-Jenkins Rydberg series is comprised of two series having upper states $c_n\,{}^1\Pi_u$ and $c_n'\,{}^1\Sigma_u^+$. The lowest members of the series with $n<4$ are strongly perturbed by the valence states $b\,{}^1\Pi_u$ and $b'\,{}^1\Sigma_u^+$. Leoni and Dressler [416] have made a quantitative deperturbation of states c_3 and c_3' and c_4'. The representation of the ${}^1\Sigma_u^+$ states is an extension of an earlier treatment by Lefebvre-Brion [412]. The results account for the Λ-doublings discussed in detail by Carroll and Collins [130].

$b'\,{}^1\Sigma_u^+$

$b'(0)$

Tschulanowsky [618] commented that in the b'–X bands with $v'=0$, $P(23)$ and $R(21)$ were unusually

weak or missing. This was also observed by Wilkinson and Houk [660]. Further, Wilkinson and Houk found a positive shift of 2.35 cm^{-1} for both lines from the smooth course of other branch lines. This very sharp perturbation results from a perturber state having a much different B value from that of the b' level. The level $v=0$ of b seems to be the likely perturber.

$b'(1)$

Setlow [568] observed a small perturbation in $v'=1$ at $J'=10$. Wilkinson and Houk [660] detected the perturbation in several bands with $v'=1$. Above the perturbation they observed that the branch lines for higher J were shifted to lower energy by 0.45 cm^{-1}, an indication that the perturber might be $^1\Pi_u$, not $^1\Sigma_u^+$, as had been suggested by Setlow. Later Lofthus [423] determined conclusively that the perturber is p', $c_4'(0)$.

Dressler [210] (see his figure 2) shows the irregular $\Delta G(v+\frac{1}{2})$ curve for the b' state. The strongest deviations from a smooth curve are found near Rydberg levels. The maximum perturbations between b' and c' occur for $b'(7)$ and $c_3'(2)$. Lofthus [423] and Tilford and Wilkinson [613] have detailed the deviation in rotational structure in $c_4'(0)$, p'; $c_4'(1)$, r'; $c_4'(2)$, k; $b'(7)$, g; and $b'(19)$, as arising from homogeneous perturbations.

For high J, $c_4'(0)$ has a strong interaction with b', $v\geq 2$ so that $B_2(b')$ is larger than normal.

$b'(18)$ and $c_5'(0)$ both show mixed valence and Rydberg character [130].

An apparent $B_0(c_4'(0))$ from low J values is 1.929 cm^{-1} [423]. This should be corrected for the heterogeneous interaction with the ℓ_1 level below it. This interaction is likely the principal contribution to the observed Λ-doubling of the ℓ_1 level (see Janin [346]). Correction for this interaction indicates that the level $c_4'(0)$, p' is nearly unperturbed Rydberg in character at low J.

Wilkinson and Houk [660] found line shifts of 27 to 50 cm^{-1} in levels b', $v=4,5,6$ relative to their extrapolated values from $v=0$ to 3 (vibrational perturbation). The interaction between these levels and $c_4'(1)$ accounts for the unexpectedly low B value for $c_4'(1)$, r' and the rather large B values for b' (4,5). A rather strong interaction has been found between $b'(7)$ and $c_4'(2)$ which also shows up in $b'(8)$ and $b'(6)$ [210].

In $b'(14)$, r_5 there is a distinct perturbation. Lines $R(17)$ and $P(18)$ both indicate a shift in energy of 10 cm^{-1} for $J'=18$ (see Worley [666] for details). Some intensity anomalies were also observed for $b'(15)$, r_6 by Worley.

Yoshino et al. [675] have examined the o_n–X transitions (see section 3.25d) and have uncovered some perturbations.

o_3-X:0−0 A rotational perturbation occurs in the $R(17)$ and $P(19)$ lines, but not in the Q branch. Only the $^1\Pi_u^-$ sublevel is affected and the perturber is $b'(3)$ $^1\Sigma_u^+$. At $J=28$ there occurs a homogeneous perturbation by $b(7)$ $^1\Pi_u$.

1−0 This is the strongest band of the $o-X$ system. The $b-X$ 9−0 band lies close to the $o-X$ 1−0. A perturbation between $J=3$ and 4 arises from homogeneous interaction with $b(9)$. A heterogeneous perturbation at $J=18$ is due to $b'(6)$.

2−0 The $b'-X$ 8−0 transition lies close to the o_3-X 2−0. There is no evidence of a perturbation for $J<20$. A homogeneous perturbation is expected near $J=2$. Weak Λ-doubling of the $o_3(2)$ level is observed near $J=25$.

3−0 $o_3(3)$ and $b'(11)$ cross between $J=14$ and 15, resulting in irregular intensities and spacing. At higher J there is a further perturbation by $b(15)$.

4−0 The weak 4–0 band is overlapped by the strong b–X 14–0 band; irregular line spacing occurs around $J=18$ in the P branch. A homogeneous perturbation by $b(18)$ is expected at higher J.

$o_4(0)-X$ This is the only band analyzed that belongs to the second member of the Worley third Rydberg series. The band has a weak R branch head and a strong Q branch head. Irregular line positions and intensities are observed from $P(13)$ to $P(16)$. Weak extra lines arise from P branch transitions of $c_6'(1)^1\Sigma_u^+$–$X(0)$.

7.2. Triplet Splittings in the $A^3\Sigma_u^+$ and $B'^3\Sigma_u^-$ States

For $^3\Sigma$ states the splittings $\Delta_{12}=F_1(N)-F_2(N)$ and $\Delta_{32}=F_3(N)-F_2(N)$ are usually discussed by the well-known formulas of Schlapp (see e.g., p. 223 of [12]).

For a more fundamental approach to the splittings in $^3\Sigma$ states see, e.g., Veseth [636]. For large B/λ values these formulas can be approximated by simpler formulas due to Kramers.

Dieke and Heath [196] measured the splittings in the $A^3\Sigma_u^+$ state for $v=0$–8, and found only a weak decrease with increasing v (see their table 4). Carroll [123] had earlier obtained both parameters λ and γ for $v=0$–2. Miller [462] obtained the same value ($\lambda=-1.33$, $\gamma=-0.003$ cm^{-1}) from the Schlapp formula fitted to splitting in the A state for $v=0$. Miller has also given a brief discussion of coupling in the A state and line strengths for the A–X bands [465].

Carroll and Rubalcava [138] observed the triplet splitting in the $v=5$ level of $B'^3\Sigma_u^-$, and Kramers' formulas were used to determine the splitting con-

stants. From Δ_{12} they obtained $\lambda=0.63$ cm^{-1}, $\gamma=-0.0052$ cm^{-1}, and from Δ_{32}, $\lambda=0.60$ cm^{-1}, $\gamma=0.0014$ cm^{-1}. This apparent discrepancy in that both splittings do not lead to the same numerical coefficients was further discussed by Kovacs [393] who developed more extensive formulas, the additional parameters arising from perturbation of the $^3\Sigma$ state by a $^3\Pi$ state. (Both A and B' states are so affected.) These perturbations are brought about in part by spin-orbit interaction.

Tilford et al. [611] showed that, if a single set of constants, $\lambda=0.66$ cm^{-1} and $\gamma=-0.0030$ cm^{-1}, were used in connection with Schlapp's formulas, good agreement exists between the observed and calculated splittings.

7.3. Triplet Splittings in the $B\,^3\Pi_g$, $C\,^3\Pi_u$, and $C'\,^3\Pi_u$ States

For a $^3\Pi$ state the rotational term values for any degree of spin uncoupling (intermediate between case (a) and (b)) are usually discussed in terms of the Budó formulas [106] (see also ref. [12] p. 235) and $Y=A/B_v$, the coupling constant which measures the strength of the coupling of spin to the internuclear axis.

For strict case a (no interaction between the electronic and rotational motion), the splittings F_2-F_1 and F_3-F_2 are approximately constant and equal to A. For strict case b, however, there is in the first approximation no multiplet splitting, and all the terms can be expressed by $F(N)=B_vN(N+1)$ . . .

From Dieke and Health's data [196] it is seen that the $B\,^3\Pi_g$ and $C\,^3\Pi_u$ states correspond to coupling intermediate between case a and case b.

Budó's values for the coupling constants Y and A (see [106]) were fitted to prior observations on the $B-A$ system by Naudé [484] and for the $C-B$ system by Büttenbender and Herzberg [112]. For the B state, the coefficient A ($\sim$42 cm^{-1}) decreased slightly with increase in v. For the C state $A(A_0=3.90)$ decreased more than 10% in going from $v-0$ to $v-4$.

The fine structure of the $C'\,^3\Pi_u$ state was studied by Carroll [128]. The splitting was found to be very small, the overall width being less than 0.90 cm^{-1} over the whole range of N studied ($N<35$). Clearly the state shows case b coupling conditions. However, the $c-d$ splitting was not found to be proportional to $N(N+1)$ as expected for case b, suggesting incomplete understanding of the Λ-doubling in $^3\Pi$ states. It was concluded that the fine structure of the $C'\,^3\Pi_u$ is best interpreted in terms of spin-orbit and spin-spin effects.

7.4. Λ—Doubling in the $B\,^3\Pi_g$ and $C\,^3\Pi_u$ States

The Λ-doubling in the B and C states has been studied by many authors (see First and Second Positive systems). Dieke and Health [196] resolved the Λ-doubling in all multiplet components of these states, except $\Pi_2(F_3)$ of $C\,^3\Pi_u$. See e.g., figure 10 of [196].

The Λ-doubling in $B\,^3\Pi_g$ is to a good approximation independent of v. In $C\,^3\Pi_u$ this is also the case for $v=0-3$. For $v=4$ the doubling is noticeably smaller, a fact that is probably due to a perturbation in this level.

7.5. Doublet Splittings in the $A\,^2\Pi_u$ and $D\,^2\Pi_g$ States of N_2^+

The rotational term values of the components of a $^2\Pi$ state are usually discussed in terms of the Hill and Van Vleck formulas (see ref. [12], p. 232). The Λ-doubling is not considered in these equations, and it has indeed been found that it is negligible within experimental accuracy for both the $A\,^2\Pi_u$ and $D\,^2\Pi_g$ states.

In his analysis of the $A\,^2\Pi_u-X\,^2\Sigma_g^+$ Meinel system, Douglas [205] discussed the doublet splitting in the $A\,^2\Pi_u$ state. The following coupling constants were obtained (these values correct some misprints in the original paper):

v	A	
2	−74.62	
3	−74.60	
4	−74.58	$A_e=-74.67$

Similarly Jain et al. [352] obtained $A=-16.5$ cm^{-1} for the $D\,^2\Pi_g$ state, from an analysis of the $D\,^2\Pi_g-A\,^2\Pi_u$ system.

The $A\,^2\Pi_u$ and $D\,^2\Pi_g$ states are both inverted.

7.6. Rotational Perturbations in the $B\,^2\Sigma_u^+$ and $A\,^2\Pi_{u1}$ States

In the bands of the $B\,^2\Sigma_u^+-X\,^2\Sigma_g^+$ First Negative system there have been observed numerous rotational line displacements and intensity anomalies arising from perturbations in the upper state, where one or both of the spin components may be affected. The perturbing state is $A\,^2\Pi_{u1}$; unfortunately, however, this state has been observed only up to $v=9$, whereas $v=10$–30 would be required to see the mutual perturbations.

The perturbed levels of the B state are $v=0,1,3,5,9$ and 13. The perturber levels of the A state are, respectively, $v=10,11,14,17,23$, and 29, based on extrapolation (see Brons [102] and Douglas [205]). Only some highlights of these perturbations will be given here; details can be found in Childs [157], Parker [516–18], Coster and Brons [173–4], Brons [102–3], Crawford and Tsai [183], Gerö and Schmid [256], and Douglas [204–5]. A general theoretical discussion has been given by Ittmann [333] on perturbations between $^2\Sigma$ and $^2\Pi$ states. For a unified discussion of the $A\,^2\Pi_u$ state and its influence on the $B\,^2\Sigma_u^+$ state see d'Incan [198] and Janin et al. [350].

Childs [157] observed that B, $v=0$ was perturbed at $N=39$ and 66, this being likely due to successive vibrational levels of the perturber state, affecting both spin components. Fassbender [222], Coster and Brons [174], and Childs [157] found the F_2 components of the $v=1$ level showed a maximum displacement at $N=13$, perturbed likely by the same level causing the perturbation at high N in $v=0$.

Lazdinis and Carpenter [406] observed perturbations by the A state in B, $v=1$ in a study of electron-beam induced spectra. Anomalous behavior of rotational lines in the observed B–X bands begins with $N'=12$.

For perturbations of $v=3$ it is the 3–5 band that has been studied. Coster and Brons [174] found both spin components displaced, and also several extra lines. Brons' analysis of this band revised these results [103]. Crawford and Tsai [183] measured a displacement in F_1 at $N=9$ of about 11 cm^{-1}; the F_2 component was displaced by only 1 cm^{-1}.

Parker [518] found F_1 components in $v=5$ displaced at low N, with maximum at $N=4$. Extra lines were observed in the 5–8 band. Brons [103] analyzed the 5–7 band and found $N=2$ and 6 of the upper level perturbed by $^2\Pi_{3/2}$, the lower N level being less disturbed than the higher. For some N value about 20 the $^2\Pi_{1/2}$ perturbation is expected, but observations did not extend that far.

Brons [102] observed the $v=9$ level to be perturbed. His resolution was too small to enable his seeing the doublet splitting of the $B\,^2\Sigma_u^+$ state, except near the regions of maximum perturbation at $N=22$ and 45. For $N=22$ only the F_2 component is affected; for $N=45$ only the F_1. Extra lines were observed near the maximum perturbations. These represent $^2\Pi_{u1}$—$^2\Sigma_u^+$ transitions which become visible when the $^2\Pi$ state borrows intensity from the B state. The $A\,^2\Pi_{u1}$ state was thus first known from its perturbations of the B state, before it had been observed directly.

Parker [517–18] found large doublet separation for low N in the 13–15 band arising from a perturbation. He assumed the perturbation to be only in the F_2 levels. Extra lines were observed.

The general course of the mutual perturbations between the B and the A states finds this order: first a crossing at low N affecting only one spin component, then two close perturbations affecting both spin components, and then a fourth one affecting only one component. (See Childs [157].) The relative strengths of these is discussed by Brons [102].

7.7. Rotational Perturbations in the $C\,^2\Sigma_u^+$ State of N_2

Carroll [125] observed three small perturbations in the observed rotational structure of C–X bands from $v'=2$, 3, and 6, due to displacements of rotational levels in the upper state.

$v=2$: Displacement of both components by about 0.30 cm^{-1} for $N=23$.

$v=3$: A displacement of one of the doublet components by -0.21 cm^{-1} for $N=17$, and by -0.31 cm^{-1} for $N=18$ was observed. A $^2\Sigma_u^-$ state having the same electron configuration as the C state was assumed to be the perturber.

$v=6$: Displacement of both doublet components by about -0.40 cm^{-1} for $N=24$.

According to Carroll [125], the perturbations in $v=6$ could be due to a state $^4\Sigma_u^-$ or $^2\Delta_u$ (case b); both have the same configuration as the C state. It is possible that the perturbation in $v=2$ could be due to high vibrational levels in the $B^2\Sigma_u^+$ state.

7.8. Vibrational Perturbations in the $B\,^2\Sigma_u^+$ and $C\,^2\Sigma_u^+$ States of N_2^+

It has been noted by many authors (see Carroll [125] and references cited therein) that for both the B and C states the ΔG_v and B_v versus v curves have unusual shapes. According to Douglas [204] this can be interpreted as caused by a strong mutual vibrational perturbation between the two states. As this perturbation is homogeneous (i.e. $\Delta\Lambda=0$), the shifts in both levels will be nearly independent of J [12, p. 292].

Figure 4 of reference [204] shows this effect schematically. From these curves Douglas [204] concluded that the effect of the perturbation is such as to cause the $B^2\Sigma_u^+$ potential curve to flatten out in the middle of its energy range, and hence to cause the ΔG_v values to decrease rapidly in this region. The B_v values should follow the same trend.

The minimum of the $C^2\Sigma_u^+$ potential curve should at the same time be moved to smaller internuclear distance, leading to an abnormally large B_0 value. On the contrary, Carroll [125] found that B_0 was abnormally small. (The values of B_0 and B_1 may not be known with sufficient accuracy to determine with certainty the course of the B_v curve.) It was therefore concluded that an upward displacement of the lower part of the $C^2\Sigma_u^+$ state was much more pronounced than any lateral displacement of the potential minimum. Unfortunately, the detailed analysis of the C state is not yet extended beyond $v=6$, so that a further discussion of the mutal interaction between the B and $C^2\Sigma_u^+$ state cannot be given.

8. Dissociation Energies and Predissociations

8.1. Dissociation Energy of N_2 and N_2^+

The dissociation energy D_0^0 of a diatomic molecule is defined as the energy required to dissociate the molecule from the lowest vibrational level of the ground state into normal atoms (see Herzberg [12], p. 437).

If in a molecular spectrum the vibrational levels of the ground state can be followed up to the dissociation limit, the dissociation energy is found directly as $D_0^0=hc\sum_v \Delta G_{v+\frac{1}{2}}$. For most molecules, the vibrational

levels cannot be followed all the way to dissociation, and consequently the dissociation energy cannot be determined in this way. In such cases one may try to extrapolate the ΔG curve to the dissociation limit (e.g. Birge-Sponer extrapolation), but if only a few levels are observed, this extrapolation may not be very accurate.

For molecular nitrogen, transitions to the ground state have been observed only for v'' up to about 30, whereas about 40 would be necessary to provide an unambiguous value for D^0. Similarly, for N_2^+, bands involving ground state v'' up to 20 have been observed, whereas about 35 would provide an unambiguous D^0.

For an excited state the dissociation energy D^0, relative to the lowest level of that state may involve dissociation products that may include excited as well as ground state atoms. Every combination of states of the two atoms corresponds to a definite dissociation limit, to which, in general, several molecular states belong (Herzberg [12], p. 437).

The atomic term values being known, the relative energies of the various dissociation limits can easily be determined. Some of the lowest relative dissociation limits for N_2 and N_2^+ are thus

N_2	cm^{-1}	eV	N_2^+	cm^{-1}	ev
$^4S+^4S$	0	0	$^4S+^3P$	0	0
$^4S+^2D$	19224	2. 383	$^4S+^1D$	15316	1. 899
$^4S+^2P$	28839	3. 576	$^2D+^3P$	19224	2. 383
$^2D+^2D$	38449	4. 767			

Data from Moore [25].

By the use of these dissociation limits and the term value of the $v=0$ level of a state, its dissociation energy can readily be determined if the dissociation products and vibrational quantum numbering are unambiguous, which may sometimes not be the case.

The dissociation energy of N_2 had been controversial for many years. The spectroscopic determination of possible values of the dissociation energy of nitrogen rests on a careful study of several predissociations. Neither the dissociation products nor the dissociation energy could be determined with certainty, but a very thorough discussion of the spectroscopic data led to the conclusion that only two possibilities needed to be considered, namely 9.759 eV and 7.373 eV.

The preponderance of evidence supports the higher value of the dissociation energy of N_2, though the direct evidence is still lacking. The value near 9.8 eV had been difficult to reconcile with the spectrum of N_2^+ unless an irregular potential curve was assumed for the $B\,^2\Sigma_u^+$ state. It has been shown by Douglas [204] that indeed the B state had such a curve.

For a long time the lower value of the dissociation energy was believed to be the correct one, but with the weight of other spectroscopic data, and thermodynamic and electron impact data, all in favor of the higher value,

$$D_0^0 = 9.759 \pm 0.005 \text{ eV (limit } 78714 \pm 40 \text{ cm}^{-1}),$$

has now generally been accepted as the correct value for the dissociation energy of N_2.

The dissociation energy of N_2^+ is given by the equation $D(N_2^+) = D(N_2) - I(N_2) + I(N)$. Inserting $I(N_2) = 125667.5$ cm^{-1} [K. Yoshino, unpublished (tentative)] and $I(N) = 117225.4$ cm^{-1} [25], one gets the value

$$D_0^0 = 8.713 \pm 0.005 \text{ eV (limit } 70273 \pm 40 \text{ cm}^{-1}).$$

The arguments leading to these results are mainly due to Gaydon, and are masterfully summarized in his book [8] to which reference is made for further details. See also Herzberg [12], Douglas and Herzberg [206], Brewer and Searcy [5], and Tilford and Wilkinson [614].

Recently Moore and Hansen [470] have measured N atoms produced by thermal dissociation of N_2 interacting with a tungsten catalyst. The results are consistent with the 9.8 ev dissociation energyof N_2.

8.2. Predissociations and Dissociation Limits

Several predissociations are observed in nitrogen, the study of which has established a number of predissociation and dissociation limits. The most important of these, which have played a decisive role in the discussions as to the correct dissociation energy of nitrogen, are:

(a) One at 97938 ± 40 cm^{-1}, derived from an observed predissociation of the $C\,^3\Pi_u$ state. This limit coincides exactly with a dissociation limit, now established to be $^4S+^2D$. The lowest dissociation limit $^4S+^4S$ should thus be 19224 cm^{-1} lower; i.e., at 78714 ± 40 cm^{-1}, which is now the accepted value for the dissociation energy of N_2.

(b) One at 78828 ± 50 cm^{-1} derived from an observed predissociation of the $a\,^1\Pi_g$ state, which goes to $^4S+^4S$ via a potential hill.

(c) One at about 78380 cm^{-1}, derived from an observed predissociation of the $B\,^3\Pi_g$ state, which goes to $^4S+^4S$ via a potential hill.

Predissociations of most bands in the spectral region 800–960 Å play a role in atmospheric processes (see Hudson and Carter [322]).

Some of the predissociations observed under high resolution are discussed in detail below.

8.3. Predissociation of the $a\,^1\Pi_g$ State

In a study of the Lyman-Birge-Hopfield system, $a\,^1\Pi_g - X\,^1\Sigma_g^+$, Herman [294–5] was the first to observe the predissociation in the $a\,^1\Pi_g$ state above $v=6$. At higher pressures this predissociation disappeared. Herzberg and Herzberg [306] also observed it in emission at low pressure. It is not observed in absorption.

Later this predissociation was reinvestigated under higher resolution by Douglas and Herzberg [206] and by Lofthus [421]. It was observed that for lower pressures a clear breaking-off of the rotational structure above $v'=6$, $J'=13$ was present, whereas for increasing pressure this breaking-off became less sharp. All branches were terminated; consequently the predissociation must occur in both Λ-components of the $a\,^1\Pi_g$ state.

The predissociation limit was found to be at 78828 ± 50 cm^{-1}. There is thus a small remaining difference of 114 cm^{-1} (assumed to be halfway between $J'=13$ and 14) between this limit and the dissociation limit at 78714 cm^{-1}. Douglas and Herzberg [206] pointed out that this was undoubtedly due to a slight potential hill separating the undissociated from the dissociated state. Such a hill will arise when the potential curves of the two states intersect at a point above the asymptote of the state causing the predissociation (case Ic; ref. [12], Fig. 186), or, if the point of intersection is below the asymptote, it may arise on account of the rotation of the molecule (case Ib). Taking the 'effective curve' into account, they argued that the state causing the predissociation cannot be a purely repulsive state. The difference, 114 cm^{-1}, mentioned above might therefore be due to a rotational potential hill.

Applying similar considerations to the predissociation of the $B^3\Pi_g$ state, Douglas and Herzberg concluded that the point of intersection would lie about 350 cm^{-1} below the asymptote of the state causing the predissociation, which also cannot be a pure repulsive state. They also concluded that this predissociation is forbidden, though which state was responsible could not be definitely decided.

Gaydon [8] has advanced arguments which favor predissociation of the $a^1\Pi_g$ state by a slightly stable $^5\Sigma_g^+$ state derived from ground state atoms $^4S+^4S$.

8.4. Predissociation of the $B^3\Pi_g$ State

The predissociation in the $B^3\Pi_g$ state was first observed by Kaplan [370–2] who also studied its dependence on pressure (induced predissociation). A detailed study was first undertaken by van der Ziel [630, 632] who analyzed the 12–8 and 12–7 bands of the $B^3\Pi_g-A^3\Sigma_u^+$ First Positive system. It was found that this predissociation in $v'=12$ was not of the usual type for which the band lines at a certain J-value totally disappeared. In this case the lines in the P, Q, and R branches became suddenly less intense, but were still visible. The bands with $v'=14$ and 15 were on the whole weakened, but for still higher v the predissociation could not be seen.

The predissociating state crosses just above Π_0 at $J=34$, and just below Π_1 at $J=33$, which levels differ by only a few cm^{-1}. Van der Ziel chose $^3\Pi_1$, $J=33$ as the limit of the predissociation (with an uncertainty of only a few cm^{-1}), and calculated the predissociation limit to be 20070 cm^{-1} above $B^3\Pi_1$, $v=0$, ($\approx{}^4S+{}^4S$) whereas the energy of dissociation in $C^3\Pi_u$ was 38770 cm^{-1} above the same level ($^4S+^2D$). The difference between the atomic terms ^4S and ^2D is 19224 cm^{-1}. The energy difference between the C state dissociation limit and the predissociation limit of the B state is 18700 cm^{-1}. The difference 524 cm^{-1} (19224–18700) was taken as evidence that the state causing predissociation in $B^3\Pi_g$ at $v=12$ was repulsive. Finally, van der Ziel concluded that the observations indicated a $^3\Delta_g$-type perturbation. This has been proved to be incorrect; it is now well established that the $^5\Sigma_g^+$ state (S^4+S^4) is the predissociating state (see Gaydon [8]). See also some critical remarks to van der Ziel's analysis by Dieke and Heath [196]. Polak et al. [532] have measured predissociation probabilities for $B^3\Pi_g$, $v=13$–18. The results are interpreted as confirming predissociation by a radiationless transition to the repulsive part of the $^5\Sigma_g^+$ potential curve.

8.5. Predissociation of the $C^3\Pi_u$ and $C'^3\Pi_u$ States

Kaplan [370] long ago pointed out that no bands of the $C^3\Pi_u-B^3\Pi_g$ Second Positive system having $v'>4$ could be observed, a fact that was attributed to a predissociation in the upper state.

This predissociation was examined in detail by Büttenbender and Herzberg [112], and their analysis forms the basis for the currently accepted value of the dissociation energy of N_2. They analyzed under high resolution the rotational structure of several bands, and observed a sharp breaking-off of the rotational structure in the vibrational levels $v'=4$, 3, 2, and (with less certainty) 1. A similar breaking-off was also observed in $^{15}N_2$ by Frackowiak [237]. The positions of these breaking-off limits are:

$^{14}N_2$	v	N_{max}	Term value relative to $v=0$	
			Last unpredissociated levels	First predissociated levels
	1	65 (less certain)	9589.8	9819.8
	2	55	9316.2	9509.6
	3	43	9070.8	9221.3
	4	28	8961.3	9058.9
$^{15}N_2$	0	80	10758.68	11021.79
	1	68	9667.30	9891.12
	2	57	9209.32	9396.61
	3	46	9113.25	9263.63
	4	32	9033.01	9137.03

Plotting these energies against $N(N+1)$, and extrapolating to $N(N+1)=0$, one obtains for the pre-

dissociation limit above $v'=0$, $N'=0$ (F_2) the values 8960 ± 40 cm^{-1} for $^{14}N_2$, and 9065 ± 45 cm^{-1} for $^{15}N_2$. The slope of these limiting curves tends to zero at $N(N+1)=0$, corresponding to the fact that the potential curve in the rotationless state has no maximum and the predissociation limit coincides with the dissociation limit ($^4S+^2D$).

The energy of this limit above $v=0$, $J=0$ of the ground state is, since $T_0(C)=88978$ cm^{-1} for $^{14}N_2$, and 88983 cm^{-1} for $^{15}N_2$ (calculated isotope shift), 97938 ± 40 cm^{-1} for $^{14}N_2$, and 98048 ± 45 cm^{-1} for $^{15}N_2$. Subtracting $E(^2D)=19224$ cm^{-1}, one gets for the dissociation limit 78714 ± 40 cm^{-1} for $^{14}N_2$, and 78824 ± 45 cm^{-1} for $^{15}N_2$. By using the $^{14}N_2$ dissociation limit and the isotope shift in zero point energy for the ground state, the two isotopes lead to a consistent value for the N_2 dissociation energy.

Hori and Endo [320] observed that the predissociation described by Büttenbender and Herzberg could be suppressed by increasing the pressure. As emphasized by Carroll and Mulliken [136] this suggests that the predissociation is not of the strongest kind which one would expect if it were of the homogeneous type $^3\Pi_u-{}^3\Pi_u$. Further support for this interpretation is given by the fact that Hori and Endo observed a complete breaking-off in the rotational structure at higher N-values which is presumably due to a second and considerably stronger predissociation. Worth mentioning is that Coster et al. [176] observed no predissociation in the 0–0 band, although rotational levels up to $J=90$ were observed (pressure was not specified).

In the following table, Hori and Endo's N-values and energies are given together with those of Büttenbender and Herzberg.

v'	N_{max}		Term value relative to $v'=0$	
	B–H	H–E	B–H	H–E
1	(65)	>99	9590	>19174
2	55	80	9316	15155
3	43	67	9071	13627
4	28		8961	

The N_{max} value 65 for $v'=1$ was obtained from an analysis of the 1–3 band, and was considered less certain. Hori and Endo's spectrum of the 1–0 band showed for $R(66)$ a clear intensity drop. They therefore considered it more likely that the first breaking-off for $v'=1$ occurred above $N=67$.

In a detailed and thorough discussion, Carroll and Mulliken [136] concluded that the predissociation of Büttenbender and Herzberg [112] is due to a $^5\Pi_u$ state and not to a $^3\Pi_u$ state as had been formerly believed. The second predissociation of Hori and Endo [320] was interpreted as being in all probability due to the $C'\,^3\Pi_u$ state. This explanation requires that the C' state have a maximum in its potential curve at an internuclear distance of about 2.0 Å. The behavior of the C and C' potential curves, which should apparently intersect at about 1.4 Å, was interpreted as a noncrossing rule interaction. The vibrational structure of the region of interaction was discussed.

The resulting C' curve is of a form such as is expected when a crossing between two states of the same species is avoided. For increasing internuclear distance starting with its equilibrium distance, the C' state may be supposed to tend toward some higher dissociation limit, here taken as $^4S+^2P$, while the second state involved in the crossing must be a repulsive $^3\Pi_u$ state derived from $^4S+^2D$. Refer to figure 2 in the paper by Carroll and Mulliken [136].

While considering the predissociation of the C state by the C' state Carroll and Mulliken [136] examined the likely vibrational structure of these two states. Rotational data exist only for the $v=0$ level of C'. It appears that this level is little mixed with the C state.

The vibrational levels of the C state display a vibrational perturbation that increases with increasing v. For details on the mixing of these vibrational levels as to combined C and C' character see Carroll and Mulliken [136]. This topic is briefly mentioned in section 3.13, with the caution that some reserve is necessary in this interpretation. The various levels observed by Pannetier et al. [515], Tanaka and Jursa [600], and Hamada [285] show different degrees of C and C' character.

8.6. Predissociation of the $b\,^1\Pi_u$, $c\,^1\Pi_u$, and $o\,^1\Pi_u$ States

In absorption most of the bands involving the b, c, and $o\,^1\Pi_u$ states show greatly varying degrees of diffuseness, thus indicating predissociation. Exceptions are bands $b(1, 5, 6,)$, $c_3(0, 2)$, $c_4(0)$, and $o(0)$, where there is no evidence of diffuseness. In the $b(6)$–$a\,^1\Pi_g$ emission bands there appears to be a clear intensity drop from $J'=12$ on. This may indicate a local predissociation at about 105560 cm^{-1} (13.08 eV), or about 7650 cm^{-1} (0.95 eV) above $^4S+^2D$.

The predissociation that produces this diffuseness cannot be an allowed one since neither a $^1\Pi_u$ continuum (homogeneous predissociation) nor $^1\Sigma_u$ or $^1\Delta_u$ continua (heterogenous predissociation) can exist at these energies. According to Dressler [210] and Carroll and Collins [130] the predissociations of the several $^1\Pi_u$ levels are likely caused by the $^3\Pi_u$ continuum which is associated with the atomic products $^4S+^2D$ at 97938 cm^{-1}. This is the same continuum which also causes the predissociation of the higher levels of the states $C\,^3\Pi_u$ and $C'\,^3\Pi_u$. Detailed and comprehensive discussions of predissociations in the $^1\Pi_u$ states are given in the references just cited.

8.7. Predissociation of the $b'\,^1\Sigma_u^+$ and $c'\,^1\Sigma_u^+$ States

In contrast to $^1\Pi_u$, the $^1\Sigma_u^+$ levels show no strong predissociations at low J-values. Emission bands are

in fact observed at least up to $v=9$ for b' and up to $v=4$ for c'.

According to Carroll et al. [132], the $b'\ ^1\Sigma_u^+$ state is predissociated at higher vibrational levels. In particular the 20–0, 21–0, and 22–0 b'–X absorption bands show rather diffuse rotational structure at energies above the $^2D+^2D$ limit so that a singlet state derived from these products may be responsible for the predissociation. The $c_5'(1)$ absorption band was also observed to be somewhat diffuse, and is assumed also to be subject to predissociation.

By analogy with the singlet-triplet interaction proposed above for the $^1\Pi_u$ states, one might have expected predissociation of the $^1\Sigma_u^+$ states by a $^3\Sigma_u^+$ continuum which must be associated with $^4S+^2D$ at 97938 cm^{-1} (in addition to the continuum of the $A\ ^3\Sigma_u^+$ state). Possible explanations as to why such a predissociation is absent are discussed in some detail by Dressler [210].

In emission bands of the systems b', $c'\rightarrow a\ ^1\Pi_g$ and b', $c'\rightarrow X\ ^1\Sigma_g^+$ a number of weaker predissociations have been observed, giving rise to breaking-off of the rotational structure, or to intensity anomalies. These are discussed in the following.

$b'(2)$

The $b'(2)$–X bands, when excited in a mixture of argon and nitrogen, show an intensity anomaly; there is a sharp intensity decrease at $F'(12)$. In a neon mixture there is a regular decrease in intensity as one goes to higher J-values. The energy value where the intensity peculiarities begin is at 105315.5 ± 14.2 cm^{-1} or 13.058 ± 0.002 eV. It was not clear whether this is caused by a predissociation or by a collision of the second kind with metastable argon atoms (see Tilford and Wilkinson [613], and also Tanaka and Nakamura [602]).

The observed (possible) predissociation limit is 7378 cm^{-1} (0.915 eV) above the dissociation limit of $^4S+^2D$ at 97938 cm^{-1}.

$b'(5)$

An unusual intensity enhancement is observed in an emission band involving rotational levels $J'=13$, 14, and 15 of probably the $b'\ ^1\Sigma_u^+(v=5)$ state near 107569 cm^{-1}=13.337 eV, and attributed to a two-body recombination along a slightly attractive potential curve (inverse predissociation) (see Tilford and Wilkinson [614]). If 9.76 eV is assumed to be the correct dissociation energy of N_2, a dissociation limit at 107554 ± 44 cm^{-1} (13.335 ± 0.006 eV) can be predicted, corresponding to $^4S+^2P$. Evidence was found suggesting that a slightly stable $^3\Pi_u(T_e\sim13.2$ eV), originating from $^4S+^2P$, could be the predissociating state, though $^5\Sigma_u^-$ and $^5\Pi_u$ cannot be entirely ruled out.

$b'(7)$, g

Intensity anomalies and breaking-off of the rotational structure of the $b'(7)$–X bands between $J'=9$ and 10 indicate a predissociation at 109089.8 ± 14.0 cm^{-1} or 13.526 ± 0.002 eV [613]. The same predissociation was observed in the $b'(7)$–$a\ ^1\Pi_g$ bands by Lofthus [423]; weak lines from $F'(10)$ and $F'(11)$ were observed, indicating a weak predissociation.

The observed predissociation is 1537 cm^{-1} (0.191 eV) above the dissociation limit of $^4S+^2P$ at 107553 ± 44 cm^{-1}.

$b'(9)$, f

b'–X bands with this upper level show a sudden drop in intensity after $P(14)$. In the 9–1 b'–X band the lines are weak, but $R(12)$ and subsequent lines in this branch are abnormally weak. A weak predissociation could account for these intensity effects. T_0 of the predissociation is at $110{,}389.9\pm14.6$ cm^{-1} (13.687 ± 0.002 eV), assumed to lie midway between $F'(12)$ and $F'(13)$ (see Tilford and Wilkinson [613]).

$c_4'(0)$, p'

After the maximum perturbation in this level, the line intensities of the $c_4'(0)$–$a^1\Pi_g$ transition decreased abruptly, and the branches could not be followed after $J=12$; i.e., 104410 cm^{-1} [423]. This observed predissociation limit is 6605 cm^{-1} (0.819 eV) above the dissociation limit $^4S+^2D$ at 97938 cm^{-1} (see also Tilford and Wilkinson [613]).

$c_4'(1)$, r'

A sharp breaking-off of the rotational structure of the $c_4'(1)$–$a^1\Pi_g$ system is observed above $F(11)$; i.e., 106611 ± 20 cm^{-1} (13.218 ± 0.003 eV) [194, 354]. This predissociation limit is thus 8673 ± 20 cm^{-1} (1.075 ± 0.003 eV) above $^4S+^2D$. Tilford and Wilkinson [613] observed P branch lines above this J value in b'–X absorption bands and did not observe such a predissociation.

$c_4'(4)$,h

In this level there is a clear indication of a sharp predissociation. In the $c_4'(4)$–$a^1\Pi_g$ bands branches have normal intensities up to $J=10$, from where the intensities decrease markedly as observed by Lofthus [423].

In the $c_4'(4)$–X bands there appears to be a sharp intensity breaking-off in $P(J)$ $\approx9\pm2$. The predissociation limit is estimated by Tilford and Wilkinson [613] as 112940 ± 80 cm^{-1} (14.003 ± 0.010 eV), or 5387 cm^{-1} (0.668 eV) above the dissociation limit $^4S+^2P$.

8.8. Predissociation of the $x^1\Sigma_g^-$ State

An anomalous intensity distribution in the 0–1 band of the x–a' transition is observed (see Lofthus

[424]). The first lines of the P and R branches are relatively strong, but intensities decrease rapidly with J, and no lines can be seen for $J'>11$. The same tendency has been seen in the 0–0 band, but in this case the band was too weak to be measured completely. The predissociation limit is about 113210 cm^{-1} (14.036 eV), or 5657 cm^{-1} (0.708 eV) above $^4S+^2P$.

Another predissociation in the $x^1\Sigma_g^-$ state is indicated by the fact that no bands from $v'>2$ have been observed, although some of them, according to the Franck-Condon principle, should be strong enough to be seen.

Not only are bands from $v'>2$ not observed, but there is also a breaking-off of the rotational structure in the $v'=2$ level itself. From J' around 13–15 the lines became weakened, and from $J'=25$ on the lines could not be observed. The corresponding predissociation limit can thus be placed at about 117210 cm^{-1} (14.532 eV); i.e., very close to the dissociation limit $^2D+^2D$ at 117163 cm^{-1}.

8.9. Predissociation of the $y^1\Pi_g$ and $k^1\Pi_g$ States

In Kaplan's First and Second systems, $y^1\Pi_g - a'^1\Sigma_u^-$ and $y^1\Pi_g - w^1\Delta_u$, respectively, Lofthus and Mulliken [425] observed that there was a breaking off of all branches coming from the Π^+-levels of the $^1\Pi_g$ state, above $v=0$, $J=10$. This was interpreted as an allowed predissociation by a $^1\Sigma_g^+$ state dissociating to $^2D+^2D$. Assuming the dissociation energy of nitrogen to be 9.759 eV, $^2D+^2D$ is at 14.526 eV. Then $y^1\Pi_g$ was thought to have energy >14.526 eV for $v=0$, $J=10$, hence >14.51 eV for $v=0$, $J=0$.

Following this work, Wilkinson and Mulliken [662] observed the $a'^1\Sigma_u^- - X^1\Sigma_g^+$ system in absorption, and were able to give the electronic energy for the states $a'^1\Sigma_u^-$, $w^1\Delta_u$, $x^1\Sigma_g^-$, and $y^1\Pi_g$. Thus for the $y^1\Pi_g$ state, $T_0=114165.18$ cm^{-1} (14.155 eV), 0.35 eV lower than the minimum value found above. It seemed obviously necessary to reinterpret this predissociation, and Wilkinson and Mulliken deduced that it most probably was an accidental one resulting in the formation of $^2P+^4S$ instead of $^2D+^2D$ atoms as formerly assumed.

Two new band systems have been observed in the near UV by Carroll and Subbaram [140]: $k^1\Pi_g - a'^1\Sigma_u^-$ and $k^1\Pi_g \quad w^1\Delta_u$. In the upper state, a Rydberg state with N_2^+ X core, only the Π^- (d) levels were observed. The absence of the c levels was attributed to an indirect predissociation involving a stable $^1\Sigma_u^+$ state (going to $^2D+^2D$) predicted by Michels [458] but not yet observed directly; this state was considered predissociated by a state that was assumed repulsive, $^3\Sigma_g^-$ (coming from $^4S+^2P$). For strong spin-orbit interaction, the $^3\Sigma_g^-$ state, in the limit of Hund's coupling case c, becomes states $\Omega=1_g$ and 0_g^+, the latter then causing a homogeneous predissociation of the $^1\Sigma_g^+$ state (see Mulliken [474]).

Ab initio calculations by Michels [459] show the $^3\Sigma_g^-$ state to be stable. Its left limb is in about the right place so that it can either act directly on the k state or effect predissociation through an intermediate state (figure 3). This is also true for the $^3\Delta_g$ state which arises from the same configuration $\pi_u^2\pi_g^2$, but dissociates to $^4S+^2D$. The question remains unanswered as to why the k-state Π^- Λ-components are not also predissociated by the 1_g components of the triplet states. Even more complex is the predissociation of the y state, and the above considerations do not apply to that state [140].

8.10. Predissociation of the $D^3\Sigma_u^+$ State

The fact that no bands of the $D^3\Sigma_u^+ - B^3\Pi_g$ Fourth Positive system with $v'>0$ have been observed may indicate a predissociation.

8.11. Predissociation of the $E^3\Sigma_g^+$ State

Only bands with $v'=0$ and 1 have been observed for the $E^3\Sigma_g^+ - A^3\Sigma_u^+$ transition (Herman-Kaplan system). The $v'=1$ level is at 97955 cm^{-1}; i.e., just above the dissociation limit $^4S \mid ^2D$ at 97938 cm^{-1}. In this case $^3\Sigma_g^+$, $^5\Sigma_g^+$, and $^5\Pi_g$ states might act on the $E^3\Sigma_g^+$ state (see Mulliken [413]).

8.12. Predissociation of the $C^2\Sigma^+$ State of N_2^+

The $C^2\Sigma_u^+ - X^2\Sigma_g^+$ system of N_2^+ shows an anomalous intensity distribution depending on the excitation conditions. In a nitrogen-helium mixture, bands with $v'<3$ are very weak, whereas bands with $v'\geq 3$ are strong and appear readily. Douglas [204] suggested that this might be explained by the fact that the $v=3$ level is just above the dissociation limit at 70272 cm^{-1} ($N(^4S)+N^+(^3P)$); consequently it should be possible that a nitrogen ion and a nitrogen atom coming together at this limit could undergo a radiationless transition into the $v\geq 3$ levels of the C potential curve. The excitation mechanism should thus be a case of inverse predissociation.

In a nitrogen-helium mixture a large number of ions and atoms should be present, and then by this process of inverse predissociation highly populated $v\geq 3$ levels might be expected. On the other hand Douglas [204] concluded that if one is dealing with a source in which the $C^2\Sigma_u^+$ state is excited from the ground state by electron collisions and there are only a very few ions and atoms present, one should expect the C state to be predissociated at the $v=3$ level. Following these suggestions, Carroll [125] studied the $C-X$ bands in a discharge through pure nitrogen. A breaking-off in the rotational structure in $v'=2$ was not found in the observed region ($N\leq 31$; i.e. 517 cm^{-1} below $v'=3$), but it was clearly seen that bands with $v'=0$, 1, and 2 were well developed while only a faint trace of bands with $v'\geq 3$ could be detected. Carroll then interpreted this behavior in terms of predissociation.

Preceding these works, Watson and Koontz [645] noticed that this $v'=3$ level (24.336 eV above the ground state of N_2) is in near resonance with the ionization potential of helium (24.588 eV) and on the basis of this, proposed that charge transfer between He^+ and N_2 may preferentially excite this level. However, Takamine, Suga and Tanaka [595] have pointed out that, in fact, the $v'=4$ level (24.581 eV) is in much closer resonance. Thus, it was reasoned that if the proposed charge transfer is indeed the mechanism whereby the $C\,^2\Sigma_u^+$ state is excited, then the transitions originating from $v'=4$ should be more intense than those from $v'=3$, in contrast to what has been actually observed.

Recently, Albritton, Schmeltekopf, and Ferguson [44] have reported simultaneous optical and mass spectrometric studies of the reactions

$$He^+(^2S)+N_2(X\,^1\Sigma_g^+)\rightarrow He(^1S)+N_2^+(C\,^2\Sigma_u^+),$$

$$N_2^+(C\,^2\Sigma_u^+)\rightarrow \begin{cases} N_2^+(X\,^2\Sigma_g^+)+h\nu \text{ (2nd Neg.)}, \\ N^+(^3P)+N(^4S), \end{cases}$$

which have identified the operative mechanism as well as the predissociating level of the $C\,^2\Sigma_u^+$ state. Their main conclusions are:

(a) Inverse predissociation is not the mechanism for populating the $N_2^+\,C\,^2\Sigma_u^+$ state, (b) the mechanism is in fact a charge transfer which is resonant from $v=0$ of the $N_2X\,^1\Sigma_g^+$ state to $v=4$ and $v=3$ (rotationally excited) of the $C\,^2\Sigma_u^+$ state, (c) the occurrence of $N_2^+\,C\,^2\Sigma_u^+-X\,^2\Sigma_g^+$ Second Negative bands from high v'-levels in discharges through He-N_2 mixtures is due to charge transfer with highly vibrationally excited N_2, (d) a forbidden predissociation of the $N_2^+\,C\,^2\Sigma_u^+$ state at $v=4$ is the source of the N^+ ions, and (e) the ratio of the radiative to predissociative lifetimes for the $v=4$ level of the $N_2^+\,C\,^2\Sigma_u^+$ state is about 20:1.

Emission spectroscopy and collision experiments have clearly indicated a competition between two decay modes for vibrational levels $v'\geq 3$ of the C state: emission of the C–X Second Negative system, and predissociation into $N(^4S°)+N^+(^3P)$, the lowest pair of dissociation products of N_2^+. A large number of investigations in the past few years have tried to describe the observed phenomena in terms of the relative probabilities for radiative decay and predissociation.

Fournier et al. [231] measured the translational energy spectrum of N^+ fragments from unimolecular dissociation of N_2^+ ions and concluded that several vibrational levels of $C\,^2\Sigma_u^+$ contributed to the predissociation. The identification is tentative, and it remains possible that other states are responsible for the observed predissociation. Fournier et al. [233] also made an analysis of the laboratory velocity distribution of forward and backward scattered N^+ fragments produced by the impact of a 10 keV N_2^+ beam of He. The discrete structure observed is ascribed to a collision-induced population of the C state, followed by a predissociation of its levels with $v'\geq 3$. The lifetime of the levels $v'\geq 4$ is estimated to be 5×10^{-9} s; that for $v'=3$ is considerably longer.

Lorquet and Desouter [427] made an ab initio theoretical study of the C state. Their calculation indicated that the C state might be predissociated by a $^4\Pi_u$ state which has a minimum but goes through a maximum at larger r. The potential curve of the C state is crossed twice by that of the $^4\Pi_u$ state, giving rise to the possibility of a rather complex (accidental) predissociation mechanism. Govers et al. [266–7] observed that the ratio between the probabilities for radiative decay and predissociation are subject to an unexpectedly large isotope effect. More recent calculations by Lorquet and Lorquet [428] indicate that this isotope effect could be interpreted in terms of an accidental predissociation.

In an extensive investigation of the excitation and decay of the C state of N_2^+ in the case of electron impact on N_2, van de Runstraat et al. [551] studied the competition between the two decay modes mentioned above. Their data are consistent with the recent proposal by Lorquet and Desouter [427] that the C state can be excited through "intensity borrowing" by configuration interaction. For $^{14}N_2^+$ the ratio of the probability for predissociation to that for $C-X(2-)$ emission is found to increase significantly from $v'=3$ to $v'=7$. For $^{14}N^{15}N^+$ predissociation becomes about 6 times less probable and and for $^{15}N^{15}N^+$ about 10 time less. These observations could possibly be explained by the accidental predissociation mechanism suggested by Lorquet and Desouter [427].

Tellighuisen and Albritton [606] discussed two mechanisms for the predissociation of the C state—the accidental mechanism and a direct, homogenous process $C-B\,^2\Sigma_u^+$. They pointed out limitations to both, but considered the direct process more plausible.

Roche and Lefebvre-Brion [544] have performed ab initio calculations for several states of N_2^+ with $^2\Sigma_u^+$, $^2\Sigma_u^-$, and $^4\Pi_u$ symmetry. Their results indicate that the $^4\Pi_u$ state cannot be the intermediate state involved in an accidental mechanism. On the other hand, their calculations of the electronic part of the vibronic interaction between the C and B states lends support to the direct predissociation mechanism as proposed by Tellinghuisen and Albritton [606], whereby the C state is predissociated by the B state continuum through nuclear momentum coupling.

9. Potential Energy Curves

The potential energy curves for many states of N_2 and N_2^+ have been determined by the RKR method which requires as input data the vibrational quanta and B_v values. Following the pioneer calculation for N_2 by Vanderslice et al. [625–6], curves were published

by Jain [334] and then by Gilmore [160], whose extensive results were based largely on the data compiled by Wallace [40]. Benesch et al. [70] calculated improved RKR potentials for the observed N_2 states lying below 11 eV (table 78), using data from newer high resolution absorption measurements.

The state labelled $E\,^3\Sigma_g^+$ lying at 11.8 eV has been the subject of controversy; i.e., the identity of the state was uncertain. The definitive evidence, rotational analysis of bands involving that state, has recently been obtained by Carroll and Doheney [133]; earlier Lefebvre-Brion and Moser [413] identified this state as the lowest Rydberg state of its species whose limit is the N_2^+ ground state. Band heads attributed to the $E-A$ transition have been observed by Herman [295] but only for $v'=0$ and 1. The state is assumed to go through a maximum of undetermined size before dissociating to $^4S^\circ+^2D^\circ$. Calculations by Michels [459] show that the adiabatic potential curve would have a sizeable maximum.

In the work of Vanderslice et al. [625] approximate methods were used to estimate potentials for the $^7\Sigma_u^+$ and $^5\Sigma_g^+$ states which derive from ground state atoms. The repulsive septet state is unknown experimentally; the quintet state is slightly stable and is known only by its predissociation of the $B\,^3\Pi_g$ and $a\,^1\Pi_g$ states. A multi-configuration calculation (M. Krauss and D. Neumann) verifies that the quintet state is feebly bound; the curve also shows a potential maximum. (See Note Added in Proof.)

Earlier Carroll [126] had proposed an approximate potential for the $^5\Sigma_g^+$ state based on afterglow measurements and the known predissociations. Approximate parameters for this state included: $D^e=1100$ cm^{-1}, $\omega_e=650$ cm^{-1}, and $r_e=1.55$ Å (see his table 1). These parameters were fitted by a Morse curve which was then modified to curve more sharply near 1.98 Å as it approaches its dissociation limit. At the same time Mulliken [475] used a modified valence bond method to estimate this potential, and by also invoking molecular orbital arguments, found qualitative agreement with Carroll's estimates. This curve was included in Gilmore's curves.

The quintet state ($T_0\sim77940$ cm^{-1} or 9.66 eV), lies about 800 cm^{-1} below the dissociation limit, slightly above the term value of level $v=12$ of the B state ($T_v=77847$ cm^{-1}). Bayes and Kistiakowsky [64] had previously suggested a dissociation energy close to that suggested by Carroll.

A summary of the role of this quintet state in afterglow energy transfer is given by Anketell and Nicholls [2].

Curves for the C and C' states of N_2 show peculiar structure because they interact strongly. Gilmore joined the curves together for these two states, partly to satisfy the non-crossing rule.

High resolution measurements by Carroll et al. [131] have identified two new states, $H\,^3\Phi_u$ whose limit is $^2D+^2D$ and $G\,^3\Delta_g$ which dissociates to $^4S+^2D$. Since only four vibrational levels are known for the H state and 2 for the G state the curves were only sketched in by Carroll. The absolute energies of these states are uncertain since the only transition known involving these states is the one between them. Ab initio calculations by Michels [458] had predicted two stable $^3\Delta_g$ states, the one that has been since observed as well as one with a deeper well that dissociates to $^2D^\circ+^2D^\circ$. A stable $^3\Phi_u$ state was also predicted whose dissociation products are $^2D+^2D$.

Among the estimated curves is one for the $^5\Pi_u$ state which predissociates $C\,^3\Pi_u$. This curve is after the sketch by Carroll [128] and lies in the energy region expected theoretically (see Mulliken [473]).

An approximate potential for the $W\,^3\Delta_u$ state has been drawn by Saum and Benesch [556] (see also Benesch and Saum [67]).

Until 1969 when the work of Dressler [210] and Carroll and Collins [130] appeared, the understanding of the high energy singlet states of N_2 was chaotic. Based on the high resolution spectra that originated with these papers Leoni [414] has obtained diabatic potential energy curves (those of like symmetry that do not obey the non-crossing rule). From a first attempt at deperturbation of the data he deduced RKR curves for the following states: b, c, $o\,^1\Pi_u$ and b', c_4' and $c_5'\,^1\Sigma_u^+$. The perturbations among the various states had created irregular term values and B_v's. The p-complexes could be only partly unscrambled. States b and b' are valence. The Rydberg states are c, o, c_4' and c_5' (called e' by Leoni), the latter state being the analog of the c_4 Rydberg state which had formerly been called e. Leoni's dissociation limit for the b state, 116,670 cm^{-1}, is close to the calculated limit of $^2D+^2D$. The b' state converges to the limit $^2D+^2P$ at 126,772.7 cm^{-1} (15.72 eV).

The newly observed $k\,^1\Pi_g$ state at 14 eV lies near the y state of the same species. Carroll and Subbaram [140] have shown that the two states undergo strong homogeneous interaction; the k state also appears to be predissociated in an unusual way. Approximate potentials for the k and y states have been obtained following a deperturbation procedure. Various potentials involved in transitions to and interaction with the k and y states are shown in figure 3.

Grandmontagne and Eido [269] used the graphical Rydberg method to calculate the potential curve for the $B\,^2\Sigma_u^+$ state of N_2^+. Gilmore [258] calculated curves for the X, A, and C states of the ion by the numerical RKR method; only graphical displays were published. The A state curve was drawn by Gilmore up to high v by using data from Janin et al. [350] on perturbations of the B state by the A state which gives term values for the A state up to $v=28$. It was necessary to extrapolate the rotational constants. By extrapolating the left limb of the potential, the right limb could be approximated from the RKR formulas.

Namioka et al. [482] calculated an RKR potential for the D state of N_2^+. They used the band origin data on the $D-A$ bands and rotational constants from Janin et al. [352]. Gilmore repeated this calculation.

Singh and Rai [578] and Joshi [365] have calculated RKR curves for the X, A, B, and C states of N_2^+, the latter author only for the X and C states. The two calculations, based on slightly different data, differ by at most a few thousandths Å in the turning points at high v. Irregularities in the shape of the curves for the N_2^+ B and C states can be attributed to their strong interaction.

Additional discussion about fragmentary evidence concerning other states of N_2^+ has been given by Gilmore [258]. Some of this evidence has since been revised by newer work (see section 2.3).

During electron impact, when an electron is captured, there are formed temporary states of the negative ion called resonances. These are discussed in section 6.5. From experimental energies a Morse potential has been fitted to the $^2\Sigma_g^+$ state whose parent is the E state of N_2 (see Comer and Read [165]). Mazeau et al. [442] have fragmentary experimental data on other resonances associated with the N_2 A and B states. Krauss and Neumann [396] have calculated ab initio potentials for three states that play a role in the resonant excitation of these same states of N_2. Potentials for a number of doublet and quartet states of N_2^- have been calculated by Thulstrup and Andersen [608].

For N_2^{2+} one band of one electronic transition has been observed spectroscopically (see section 3.31). The identification of this band was aided by a theory which enabled potentials for the doubly charged ion to be approximated from the binding energies of isoelectronic molecules. Details are given by Hurley [328], and by Carroll and Hurley [134] whose work made possible the identification of the band observed by Carroll [124]. Configuration interaction calculations by Thulstrup and Andersen [608] have revised earlier model potentials for states of N_2^{2+}.

Numerical data from Benesch et al. [70] on RKR potentials for states below 11 eV is given in table 78. Figure 1 is similar to Gilmore's diagram; some states based on semi-empirical calculations have been deleted. A better approximation of the $W\,^3\Delta_u$ is now available. The H and G states are new. Deperturbed data is included for the b, c, $o\,^1\Pi_u$ states and also for the b', c_4', and $c_5'\,^1\Sigma_u^+$ states. Numerical data on these states is included in table 79.

Figure 2 shows the relation of the W state with respect to the B state which lies so near it in energy. These two states are involved in intra-system cascading. Potentials for the k and y states and other related states are given in figure 3.

Leoni and Dressler [415] have drawn some tentative potentials for deperturbed $^3\Pi_u$ states that are the triplet analogs of the Rydberg o and $c\,^1\Pi_u$ states. In their figure are included similar curves for the C and C' states, the latter having a small maximum near 2 Å, following Carroll and Mulliken [136].

Numerical data on the X, A, B, and C states of N_2^+ in table 80 is from Singh and Rai [578]. For the D state of N_2^+ the numerical potential is given in table 81 from the data of Namioka et al. [482].

Ab initio potentials have been calculated by Thulstrup and Andersen [608] for many low-lying bound states of N_2 and N_2^+. Additional calculations for N_2^+ have been made by Andersen and Thulstrup [47] Cartwright and Dunning [148], and by Roche and Lefebvre-Brion [544], the latter work devoted to states concerned with the predissociation of the $C\,^2\Sigma_u^+$ state. All calculations show a potential maximum in the C state, and figure 1 of the present work just indicates this feature qualitatively.

10. Transition Probability Parameters

The experimental quantities which measure transition probabilities include intensities of individual spectral lines, integrated intensities of electronic-vibrational bands, radiative lifetimes of rotational or vibrational levels, absorption coefficients, and inelastic scattering cross sections. These parameters can be used to deduce electronic transition moments, band or transition strengths, f-values, and Einstein A coefficients.

Experimental complications arise from overlapping structure, self-absorption, and cascading. Oft-made theoretical simplifications include assumed constancy of the transition moment, or frequency-independence of the A coefficients. In some instances, significantly different numerical results may be obtained when using wave functions based on Morse potentials rather than Rydberg-Klein-Rees (RKR) potentials. Some difficulties with the use of the r-centroid approximation for determination of electronic transition moments have been discussed by James [339] and Krupenie and Benesch [397]. Difficulties with the definition and meaning of electronic f-value (f_{el}) and electronic A coefficient for discrete spectra have been discussed by many authors, most recently by Tatum [33] and Schadee [562]. In addition to these conceptual difficulties, the use of different definitions of relevant parameters (e.g., in the use of degeneracies), lends confusion when several sets of data are compared. Wentink et al. [650] have compared the two principal conventions for transition moments for $\Delta S=0$ transitions only as follows:

R_e (Nicholls)$=\sqrt{g'G''}R_e$ (Mulliken), where g' is the degeneracy of state v' [i.e., $(2-\delta_{\Lambda,0})(2S+1)$] and G'' is the number of orbitals of state v''.[8] Values of $f_{v'v''}$

[8] $\delta_{\Lambda,0}$ is the Dirac delta function in the notation of Schadee [562]; G'' is defined by Mulliken [472].

or $\tau_{v'}$ are independent of convention since these parameters involve ratios $g'/g''=G'/G''$; but absolute values of transition moment and transition moment matrix elements depend on the convention used.

We will now summarize the data on transition probability parameters. Recall that f_{el} is an imprecisely defined quantity and is used only as an order of magnitude measure of transition probability (for discrete structure). Because of simplifying approximations there is sometimes confusion in the literature as to whether f_{el} or $f_{v'v''}$ is being discussed. Data based on Morse functions are considered tentative and should be used with caution.

In a recent review by Nicholls [492], the general concepts are briefly discussed, and a concise survey is given of recent measurements and calculations of aeronomically important transition probability parameters; his references include citations to auroral and rocket studies of nitrogen (see also reviews by Tatum [33] and Whiting and Nicholls [41]). Many references to auroral spectroscopy have been given in a brief review by Omholt [509]. An extensive review of transition probability determinations for diatomic molecules was given several years ago by Ortenberg and Antropov [512], but most of the calculations upon which this is based were done using Morse functions.

Two recent developments concerning molecular nitrogen are of special interest, and will be discussed in the following sections. Shemansky [570] has shown that vibrational levels of the $A\,^3\Sigma_u^+$ state have double lifetimes, in principle; i.e., states characterized by $\Sigma=0$ have half the lifetime of those substates with mixed $\Sigma=+1$ and -1 character. Johnson [361–2], working at low pressures, has measured J-independent lifetimes for rotational levels of N_2^+, $B\,^2\Sigma_u^+$, $v=0$.

Transition probabilities will be discussed in the next three sections, and though there is overlap in topics, the rough division will be in terms of:

(1) Franck-Condon factors $q_{v'v''}$ and transition moments R_e. (section 10.1)

(2) Radiative lifetimes and oscillator strengths $f_{v'v''}$ (section 10.2)

(3) Absorption coefficients in the extreme UV (section 10.3).

10.1. Franck-Condon Factors and Transition Moments R_e

Franck-Condon factors based on RKR potentials are available for many band systems of N_2 and N_2^+. Benesch et al. [71–2] and Jain and Sahni [263] have accounted for nearly all of the well known transitions (as well as for some not yet observed): tables 83 to 90.

Franck-Condon factors of Benesch et al. [71–2] are based on RKR potentials of Benesch et al. [70]. Franck-Condon factors were calculated as a function of J (maximum J used was 30) for transitions between excited states. It was found, unexpectedly, that J-dependent effects did not exceed 10% [72].

For several bands of the N_2 B–A, C–B, and N_2^+ B–X transitions Shumaker [575] has calculated Morse

Transition	System	Reference
N_2 $A\,^3\Sigma_u^+$–$X\,^1\Sigma_g^+$	Vegard-Kaplan	
$B\,^3\Pi_g$–X		
$B'\,^3\Sigma_u^-$–X		
$a'\,^1\Sigma_u^-$–X		Benesch et al. [71] [a]
$a\,^1\Pi_g$–X ($^{14}N_2$, $^{14}N^{15}N$)	Lyman-Birge-Hopfield	
$w\,^1\Delta_u$–X		
$C\,^3\Pi_u$–X		
$B\,^3\Pi_g$–$A\,^3\Sigma_u^+$	1+	
$C\,^3\Pi_u$–$B\,^3\Pi_g$	2+	
$B'\,^3\Sigma_u^-$–$B\,^3\Pi_g$	IR afterglow	Benesch et al. [72] [a]
$a\,^1\Pi_g$–$a'\,^1\Sigma_u^-$	McFarlane I	
$w\,^1\Delta_u$–$a\,^1\Pi_g$	McFarlane II	
$W\,^3\Delta_u$–$B\,^3\Pi_g$	Wu-Benesch	Benesch (unpublished)
$W\,^3\Delta_u$–$X\,^1\Sigma_g^+$		Saum and Benesch [557]
N_2^+ $A\,^2\Sigma_u^+$–$X\,^2\Sigma_g^+$	Meinel	Albritton et al. [1]
$B\,^2\Sigma_u^+$–$X\,^2\Sigma_g^+$	(1−) (includes r centroids)	Jain and Sahni [336]
$C\,^2\Sigma_u^+$–$X\,^2\Sigma_g^+$	(2−) (includes r centroids)	Jain and Sahni [336]
Ionization		
N_2^+, $X\,^2\Sigma_g^+$←N_2, $X\,^1\Sigma_g^+$		
$A\,^2\Pi_u$←"		Jain and Sahni [338]
$B\,^2\Sigma_u^+$←"		
$C\,^2\Sigma_u^+$←"		

[a] r-centroids are from an unpublished supplement to a paper by Benesch et al. [68] (tables 91 to 92).

based Franck-Condon factors, r centroids, and band strengths, including the effect of vibration-rotation interaction. Only little J dependence was exhibited for J values up to 100. A brief discussion is given of the band strengths, assumed to be only qualitative, because of neglect of vibration-rotation interaction. (See also Chakraborty et al. [154b].)

Jain and Sahni [337] have calculated RKR based electronic transition moments (and band strengths) for three transitions: $B\,^3\Pi_g$–$A\,^3\Sigma_u^+$, $C\,^3\Pi_u$–$B\,^3\Pi_g$, and $A\,^3\Sigma_u^+$–$X\,^1\Sigma_g^+$.

From the published graphical displays, $R_e(B–A)$ decreased by a factor of two, $R_e(C–B)$ was only weakly r-dependent, and $R_e(A–X)$ increased by a factor of five over the range of $\bar{r}$ examined. The $B–A$ calculations were based on relative intensity data of Turner and Nicholls [619] (see also Kupriyanova et al. [398] for a summary of other determinations of this transition moment). For the $C–B$ transition the intensity data of Tyte [620–1] were used; for the $A–X$ transition the intensity data of Carleton and Papaliolios [120] were used. Chandraiah and Shepherd [156] obtained a large variation of R_e with $\bar{r}$, derived from measured intensities of $A–X$ bands. Use of RKR Franck-Condon factors results in an even stronger r dependence than they obtained.

Shemansky and Broadfoot [572] measured $B–A$ band intensities at the same time as they measured lifetimes, i.e., in the same beam. In this manner the relative transition probabilities could be put on an absolute scale. Band intensities were deduced by the use of synthetic spectra to separate blends. Intensities were then used to calculate the transition moment. The electronic transition moment is represented by: $R_e(\bar{r})=[-2.25(\bar{r}-1.414)+1](3.105\times10^{-4})$ in units of $(\mathrm{cm^3\,s^{-1}})^{1/2}$ [D. E. Shemansky, private communication]. The transition moment R_e dropped by half, as $\bar{r}$ varied from 1.25 to 1.55 Å.

Jain [335] has calculated the variation in transition moment for the $B–A$ and $C–B$ systems by both the r-centroid method and the polynomial method. The same experimental data were used as had been used by Jain and Sahni [264], but with the deletion of a number of measured intensities. No reason was given for the deletion. It is of interest to compare the results, even though the experimental data upon which they were based may be open to question, as Jain has pointed out.

Jain and Sahni [337] have calculated the relative transition moment for N_2^+ $B–X$.[9] This was based on intensity measurements of Wallace and Nicholls [642]. $R_e=$const. $(1.0–18.794\,\bar{r}-12.216\,\bar{r}^2)$ for $0.978<\bar{r}<1.215$ Å. The authors point out that the B state is irregular because of perturbations by $C\,^2\Sigma_u^+$ (i.e., plots of ΔG and B_v vs. v are irregular and the B state data were fitted piecewise).

From emission intensities of bands of $C^2\Sigma_u^+$–$X^2\Sigma_g^+$ produced by He^+ bombardment of N_2, Holland and Maier [315] have obtained a rough transition moment $R_e^2\,\alpha\,\exp(0.0056\,\lambda)$ for $1400<\lambda<2060$ Å, which increases appreciably with r centroid.

Absolute electronic transition moment for the N_2 $A–X$ transition has been published by Shemansky [570]; $R_e=(1.69\times10^{-6})$ $(1–0.9850\bar{r}+0.1167\bar{r}^2)$ for $1.08<\bar{r}<1.40$ Å. (See also the relative values of Broadfoot and Maran [99] and Shemansky and Carleton [573]. Compare also the results of Jain and Sahni [337] and the relative intensities measured by Chandraiah and Shepard [156] and Carleton and Papaliolios [120].)

Generosa et al. [255] have calculated RKR potentials for the b and b' states, and Franck-Condon factors for the $b–X$ and $b'–X$ transitions from limited older data. These are considered tentative, as are parameters obtained by others from Morse function estimates.

Franck-Condon factors based on Morse potentials have been calculated for the following transitions: N_2 $b^1\Pi_u$–$X^1\Sigma_g^+$ Birge-Hopfield (see Nicholls [488], also see Dressler [210] and Carroll and Collins [130]); $H^3\Phi_u$–$G^3\Delta_g$ Gaydon-Herman-Green (see Mohamed and Khanna [469] and Nicholls [491]); $D^3\Sigma_u^+$–$B^3\Pi_g$ (4+) (see Wentink et al. [649]; Hébert and Nicholls [291]).

The D state is predissociated for $v>0$, so that ω_e was estimated from $r_e=1.108$ Å (see Mulliken [473]). Wentink et al. [649] used a Morse function; Hébert and Nicholls [291] used a harmonic oscillator to get approximate wavefunctions for the state.

For the N_2^+ $A^2\Pi_u$–$X^2\Sigma_g^+$ Meinel transition, Morse based Franck-Condon factors have been calculated by Nicholls [486], Federova [224], Koppe et al. [391], and Halmann and Laulicht [280]. A strong $\bar{r}$ dependence of the transition moment is determined by Federova; this is criticized by Koppe et al. From absolute intensity measurements Kupriyanova et al. [398] have deduced a constant transition moment (see RKR results later in this section).

For the $D^2\Pi_g$–$A^2\Pi_u$ Janin-d'Incan system see) Nicholls [489]), there is a large Δr_e, so Morse results are likely inaccurate. Franck-Condon factors based on Morse functions have been calculated (Nicholls [490]) for the ionization $N_2^+D^2\Pi_g$←$N_2X^1\Sigma_g^+$ transition. Approximate Franck-Condon factors for several bands of the N_2 $E–X$ and $D–X$ transitions have been calculated by Cartwright [145].

Zare et al. [678] have calculated RKR potentials and Franck-Condon factors for several transitions. Incorrect v numbering for the X and B states (see Benesch et al. [70]) has invalidated their numerical results, but the critical discussion of variation of transition moments remains instructive.

[9] Einstein A coefficients, oscillator strengths, and absolute band strengths were also calculated for the $B–X$ system (table 94). A nearly linear transition moment has been determined from absolute intensity measurements in an arc by Kiselyovskii and Shimanovich [386].

Halmann and Laulicht [280–3] were the first to examine the effect of isotopic substitution on Franck-Condon factors and r-centroids. Qualitatively, r-centroid is rather insensitive to isotopic substitution; for transitions with large Δr_e or for weak bands of a system, the isotopic effect on $q_{v'v''}$ is relatively large. Isotopic substitution causes shifts in maxima and minima of $q_{v'v''}$, displacing the Condon loci.

For the B–X and A–X transitions Halmann and Laulicht [283] have published RKR Franck-Condon factors and r-centroids for $^{14}N_2$ and $^{14}N^{15}N$. Complete Deslandres arrays of Franck-Condon factors are contained in an unpublished supplement. Halmann and Laulicht pointed out some significant differences between their numerical results for weak bands and those of Benesch et al., which are attributable to round-off error, and suggested that for very weak bands such calculations should be made using double precision.

Tyte [624] among others, has shown that the intensity distribution in an electronic transition can be significantly dependent on source conditions. This cautions the user against simply using measured intensities and calculated Franck-Condon factors to obtain R_e, A, τ, etc. Even the photoelectrically measured intensities upon which many transition moments are based are subject to these uncertainties.

The effect of cascading is demonstrated by a succession of papers concerning processes that populate selected states of N_2; see for example Cartwright et al. [150] and the papers cited therein. Pendleton and O'Neil [522] have presented evidence that in ionization by electron collisions, contributions to the vibrational populations may arise from processes other than direct Franck-Condon transitions. His results were for the ionization transition $N_2^+B^2\Sigma_u^+ - N_2X^1\Sigma_g^+$.

The r-centroid approximation is expressed by

$$(1) \qquad (v', R_e(r)v'') \sim R_e(\bar{r}_{v'v''})(v', v''),$$

where the left hand side is the transition moment matrix element and the factors on the right are, respectively, the transition moment as a function of r-centroid and the overlap integral (whose square is the Franck-Condon factor q) for a band v'–v''. R_e is generally assumed to be a polynomial in internuclear distance r; the r-centroid $\bar{r}_{v'v''} = (v', rv'')/(v', v'')$. A measured intensity or related parameter (proportional to $(v', R_e(r)v'')^2$ is generally used to estimate $R_e(\bar{r}_{v'v''})$ from calculated values of overlap integral and r-centroid.

Halevi [278] has attempted to improve on this approximation by introducing an additional term involving the second derivative of the transition moment as a function of r-centroid

$$(2) \qquad (v', R_e(r)v'') \sim R_e(\bar{r}_{v'v''})(v', v'') + \tfrac{1}{2}R_e''(\bar{r}_{v'v''})(v', (r-\bar{r}_{v'v''})^2 v'').$$

For the N_2 B–A transition Halevi has attempted to apply the proposed correction by using an R_e derived from (1) by addition of a term involving R_e''. This is inconsistent for it implies that the squared transition moment matrix element is simultaneously equal to $R_e^2(\bar{r})q$ and $R_e^2(\bar{r})q(1+\zeta)^2$, with ζ defined by a rearrangement of terms in equation (2). When ratios of integrals used in Halevi's equation (8) are not closely the same then $R_e(\bar{r})$ may differ markedly from $R_e(r)$ which it approximates. When the ratios of integrals are equal then Halevi's correction is 0. Instead of the usual Taylor expansion about a fixed center of expansion, Halevi's correction is based on an expansion about a variable center of expansion which depends on v' and v'', namely, $\bar{r}_{v'v''}$. The point-by-point correction so made can be erratic (e.g., as when using integrals calculated by Krupenie and Benesch [397] for the CO^+ A–X transition) and does not necessarily give a smooth correction to the result obtained by the r-centroid approximation.

James [339] has pointed out flaws in the r-centroid procedure, mainly formal. Nevertheless, it still seems to be a reasonable approximation for strong bands. Krupenie and Benesch [397] have pointed out additional limitations on the use of the r-centroid approximation, and suggest a more general approach which had been mentioned by Zare et al. [678] and James [339].

Considering the above limitations the various transition moments obtained by the r-centroid approximation should be considered only approximate, and perhaps inapplicable to weak bands in an electronic transition when quadratic terms become important.

Einstein A coefficients obtained from such approximate transition moments have been used to estimate radiative lifetimes, and are not always in disagreement with values measured directly. But it must be borne in mind that Jeunehomme and Schwenker [359] as well as James have indicated the possibly unreliable nature of the scaling procedures to obtain a single curve of transition moment as a function of r-centroid.

a. $a^1\Pi_g$–$X^1\Sigma_g^+$

The transition moment for the a–X system was deduced to be roughly constant by McEwen and Nicholls [445–6]. This result was based on the use of measured band intensities (assumed uncertain by 20%) and RKR Franck-Condon factors. Shemansky [571] measured absolute transition probabilities for this system, i.e., for the v'–0 progression, and also found the transition moment to be constant (to about 10%). The Einstein A coefficients he deduced should be considered as upper limits (Shemansky, private communication to Borst and Zipf [88]).

For the $a-X$ system, all rotational lines are allowed by electric quadrupole selection rules; some lines are also allowed by magnetic dipole selection rules. The largest contribution to the intensity is from magnetic dipole radiation. Each type of transition has a separate

frequency-dependent contribution to the transition probability, and the above considerations refer to some sort of average. Pilling et al. [527] used the curve of growth method to determine f-values for the magnetic dipole and electric quadrupole components of the a–X transition. Roughly constant transition moments were obtained with magnitudes 5.9×10^{-11} Bohr magnetons and 2.6 a_0^2e, respectively.

b. $B^3\Pi_g$–$A^3\Sigma_u^+$

Halevi [278], by expanding the B–A transition moment in a Taylor series, has attempted a correction to $R_e(\bar{r})$ which involves the second derivative of this function. He applied what turned out to be small corrections to the transition moments which had been deduced for the N_2 B–A and C–B transitions. Jansson and Cunio [354–5] have applied Halevi's correction to the Einstein A coefficients for the B–A transition. Cunio and Jansson [188] in a companion paper redetermined a transition moment for this system, obtaining a function much like that of Jeunehomme [357]. Some limitations on the use of this procedure for weak bands are mentioned. (See the preceding part of section 10.1.) The r-centroids for weak bands calculated by Jansson and Cunio differ considerably from values obtained by Benesch et al. [69].

Wurster [672] deduced a roughly constant R_e from shock tube intensity measurements. Turner and Nicholls [619] had obtained an exponential r dependence for R_e. Jeunehomme [357] obtained an r dependence similar to that of Turner and Nicholls, but from measured lifetimes. The $\bar{r}$ values used by Jeunehomme were obtained by graphical interpolation, using old values from 1956. Though Jeunehomme and Duncan [358] had been concerned about cascading, Jeunehomme [357] concluded that radiative cascading into the B state from higher energy states of longer lifetime (e.g., C,C',D) was highly unlikely. Cartwright et al. [149] have shown that cascading plays a significant role in populating vibrational levels of the A and B states in auroras.

The lifetime of the B state drops by about a factor of two in going from $v=0$ to $v=6$. This is indicative of a possibly rapid variation of the transition moment with r. The B–A system extends from the visible to the near IR, so some frequency effect is also possibly significant. RKR based Franck-Condon factors give a qualitatively different picture when applied to the measured intensities of Turner and Nicholls [619] than was obtained by Turner and Nicholls who used Morse based values. This calculation was done by Jain and Sahni [337]. Keck et al. [381] had found significant variation of R_e with r from Morse based Franck-Condon factors and their measured absolute intensities in shock heated air which were five times larger than those obtained by Wurster [672] in shock heated nitrogen. $f_{00}(B$–$A)$ of Keck was about five times that of Wurster, but had been deduced from extrapolation, and the use of R_e obtained by Turner and Nicholls. It should be borne in mind that the B–A system of N_2 is especially susceptible to modification under differing conditions of excitation.

c. $W^3\Delta_u$—$B^3\Pi_g$

Wu and Benesch [670] were the first to present solid evidence of the $^3\Delta_u$—$B^3\Pi_g$ transition. Crude molecular constants were obtained, from which Franck-Condon factors were calculated. Using revised data on this transition from Benesch and Saum [67] Benesch has recalculated (unpublished) Franck-Condon factors which are reproduced in table 85.

d. $C^3\Pi_u$—$B^3\Pi_g$

Wallace and Nicholls [642] measured photoelectrically integrated band intensities. Excitation was by means of a transformer discharge in pure N_2. Using Morse based Franck-Condon factors they obtained a quadratic expression for R_e $(\bar{r})$. RKR Franck-Condon factors are not very different and would have led to about the same expression. Keck et al. [381] normalized the transition moment by use of the C state lifetime measured by Bennett and Dalby [73].

Pillow and Smallwood [528] have shown that in a discharge, the ratio of intensities of emission bands of the 0–v'' progression was not constant, but depended on excitation conditions. It is on the assumption of a constant ratio that so much work on transition probabilities depends, even though selective excitation plays a role in many experiments.

Bleekrode [86] has discussed the cause of intensity alternations originating from non-equilibrium populations of nitrogen levels when the C–B bands are excited in Ar + N_2 mixtures. These effects should be borne in mind when intensities are used for calculating transition probabilities, etc. Fishburne et al. [227] have produced this system in several different sources, with the intensity distribution dependent on the source.

Tyte [620–1] measured relative intensities photoelectrically in a low temperature discharge. Using Morse based parameters he deduced a strongly varying transition moment, differing from the result of Wallace and Nicholls. The same intensities were used by Jain and Sahni [337] to obtain an R_e from RKR based Franck-Condon factors and r-centroids. Their R_e was nearly constant: $-1+1.9669\ \bar{r}-0.8636\ \bar{r}^2$ for $1.03<\bar{r}<1.30$ Å.

Shemansky and Broadfoot [572] have used the same intensity data to calculate absolute values of Einstein A coefficients. They used the lifetime measurement of Bennett and Dalby [73], but also used unreliable r-centroids of Wallace and Nicholls [672] whose values differed considerably from the RKR results of Benesch et al. [69]. The relative band strengths of Jain and Sahni should be used to get the A coefficients. Rescaled absolute A values are given in table 95.

e. $N_2^+A^2\Pi_u$—$X^2\Sigma_g^+$

Shemansky and Broadfoot [572] have studied transition probabilities for several transitions in N_2 and N_2^+. The results for the A–X Meinel bands are uncertain. They deduced a slightly increasing transition moment from fragmentary data and scaling to obtain absolute values by using the lifetime of O'Neil and Davidson [396]. Likely, too small a value for the lifetime was assumed (see section 10.2 for a discussion of this lifetime), and their Einstein A coefficients are upper limits.

Cartwright [146] has obtained the absolute transition moment for the N_2^+ A–X system, fitted to the radiative lifetime measurements of Peterson and Moseley [524], Holland and Maier [316], and Maier and Holland [435] (table 93). The consistency of the measurements has enabled reliable extrapolation and interpolation of the lifetimes for the A $v=0$ and 9 levels which are free from perturbations. The linear R_e decreased by half as internuclear distance varied from 0.9 to 1.38 Å. The transition moment is given by $a_0(v', v'')+a_1(v', rv'')$, with $a_0=2.675\pm0.365$, $a_1=-1.231\pm0.0336$ as obtained from a weighted non-linear least squares fit. Though a linear fit was finally used, it is instructive to see Cartwright's consideration of a quadratic expression where the transition moment is expanded in powers of r, and the r-centroid approximation is not used. For the linear result, however, this is exactly what is obtained in the r-centroid approximation.

Comparison of the fits both with and without the lifetimes for the $v'=10$ level gives a further measure of confidence in the estimate of the lifetimes of the unobserved $v'=0$, 9 levels. Comparison with these results is made with ab initio calculations of Popkie and Henneker [535] which give a transition moment too low by more than a factor of two. Band f-values and Einstein A coefficients calculated from the transition moment are given in table 93. Franck-Condon factors used were from Albritton et al. [1].

From estimates that more than 1% of N_2^+ produced by impact of 50 eV electrons is in the A state with $v\geq7$, van de Runstraat et al. [550] concluded that Franck-Condon factors alone do not account for the vibrational population of the A state, following ionization from the ground vibrational state. It is assumed that cascade from some higher state of the ion plays a role, or that perhaps pre-ionization of a high-lying neutral state is involved.

f. N_2^+ $B\,^2\Sigma_u^+$– $X\,^2\Sigma_g^+$

The transition moment of the N_2^+B–X system is marked by a varied history. For many years, determinations of the B–X transition moment were based on the photoelectric relative intensity measurements of Wallace and Nicholls [642]. The bands were produced in a high voltage discharge in helium containing nitrogen as an impurity. This is a complicated source. Broadfoot [97] and Jain and Sahni [336] have calculated such R_e's, the latter using RKR based Franck-Condon factors and r centroids. The resulting R_e increased in magnitude moderately with increase in $\bar{r}$. Jain and Sahni pointed out that the B state is irregular because of perturbations by the $C\,^2\Sigma_u^+$ state. Franck-Condon factors and r centroids calculated by Jorus-Bony et al. [364] and Generosa et al. [255] differ considerably, especially for some weak bands, as expected. This transition does display some non-monotic r centroid behavior.

Brown and Landshoff [105] remeasured the intensities of the 3–1 and 1–2 bands and then used the remaining intensities of Wallace and Nicholls [642] to obtain a revised transition moment. RKR parameters of Generosa et al. [255] were used. These results showed a significant decrease in R_e with increasing $\bar{r}$.

Most recently Lee and Judge [411] have remeasured intensities for the B–X transition, from which they deduced a virtually constant transition moment, for $0.974<\bar{r}<1.153$ Å. The fluorescence spectrum was produced by bombardment with a monochromatic photon beam which gave a simple spectrum. At pressures below 10^{-3} torr (0.1 Pa) the intensities were proportional to pressure. Koppe et al. [391], using measured cross sections, had earlier indicated a constant transition moment. Hesser [309] too, had indicated a constant transition moment.

g. Ionization

Ionization of ground state N_2 by 584 Å photons, to both N_2^+, $X\,^2\Sigma_g^+$ and $A\,^2\Pi_u$ (see Frost et al. [242]) indicates relative transition probabilities in disagreement with those expected only from Franck-Condon factors, assuming direct ionization (Jain and Sahni [338]). But as Frost et al. have cautioned, the transition probabilities may be dependent on photon energy. Also, the possibility of preionization cannot be excluded.

Schoen and Doolittle [564] found from photoionization by 771 Å photons that transitions to N_2^+, $X\,^2\Sigma_g^+$, $v=1$ contributed 34% to the ionization cross section. Franck-Condon factors (Jain and Sahni [338]), assuming direct ionization, show only 9% contribution, which indicates possible significance of autoionization. Photoelectron spectroscopy of N_2 first ionization (see refs. 195, 197, 216, 221 of Berry [4]; see p. 389 of ref. [4]) showed extremely strong 0–0 transitions with much weaker 1–0 and 2–0, as expected for removal of a non-bonding electron.

10.2. Radiative Lifetimes and f-values

This section is to be regarded principally as elaborate footnotes to table 82. There is considerable overlap in the content of this section and the preceding and succeeding sections on Franck-Condon factors and the extreme ultraviolet, respectively, and these should be referred to conjointly. Each transition or state discussed, is discussed separately where possible. Many

of the lifetimes or f-values are only approximate or estimates.

The three factors most likely to interfere with the measurements of radiative lifetime are cascading, collisions, and spectral overlap. The upper state in the transition under study may be populated by cascading from excited higher-lying states with somewhat longer lifetime, when bombarding electrons have energies far above threshold unless the experiment is especially designed to avoid this problem. From an apparent drop in lifetime with decrease in electron energy, cascading at the higher bombardment energies is inferred. For pressures below about 10×10^{-3} torr (1.25 Pa) (depending somewhat on the optical path of the experiment) collisions are likely not significant in quenching radiation. This is especially true for states having relatively long lifetimes. For excitation of the N_2 $C^3\Pi_u$ state, however, Burns et al. [109] did find pressure [collision] effects above 1.2×10^{-3} torr (0.15 Pa) pressure.

The time scale of the apparatus should be at least a factor of 4 smaller than the lifetime to be measured. The linearity of the time scale is also important. In cases where two transitions can overlap because they can both be simultaneously excited, attention must be paid to the relative cross sections for excitation at the experimental electron energy. For the N_2^+ B–X and N_2 C–B transitions, the complications can be traced through the references cited in papers by McConkey ct al. [444] and Cartwright [145].

In some instances it is not obvious whether the value of τ quoted from an experiment should be based on extrapolation to zero pressure or to the threshold energy for excitation.

a. $A^3\Sigma_u^+$–$X^1\Sigma_g^+$

Shemansky [570] has shown that the upper state of this transition has, in principle, two lifetimes: one for the substate loosely described as having $\Sigma=0$ and another for the two substates with mixed $\Sigma=\pm1$ character. (For intermediate coupling Σ is not a good quantum number.) This multiple-lifetime conclusion was based on several approximations in assessing the contributions of the four branches to the band transition probabilities, including the simplifying assumptions of Hund's case b coupling and some averaging of wavenumbers which seems reasonable because of the near spatial degeneracy of the substates.

Shemansky measured observed equivalent widths of seven absorption bands of the $v''=0$ progression ($v'=6$ to 12); from these he calculated absolute $A_{v'v''}$ values (see table 6 of ref. [570]). To estimate the lifetimes he used a nearly linear extrapolation of the (strongly r-dependent) electronic transition moment derived from emission bands, and unpublished RKR based Franck-Condon factors and r-centroids of Albritton and Zare. The calculated lifetime for $v=0$ is $\tau=1.27$ s for the F_2 component and 2.5 s for the others. The probable error in the lifetime is estimated as 20%, since the τ's were determined by extrapolation. The lifetimes for vibrational levels of the A state determined by Shemansky, though not measured directly, are considered the most reliable for this state. Confirmation of these values comes from a reanalysis by Shemansky and Carleton [573] of the ratio $\tau(A)/\tau(B)$ as determined by Carleton and Oldenburg [119], whose transition probabilities were based on calculated values for the A-state population and volume emission rate.

A useful review was given of earlier estimates and determinations of τ which had varied over several orders of magnitude. Estimates based on appearance path lengths were found fraught with danger. Earlier estimates giving $\tau\sim1$ s were obtained by Zipf [679], Phillips [526], and Noxon [494]. Tinti and Robinson [616] measured the lifetime of the A state in different solid rare-gases and obtained 0.4 to 3.3 s. The upper value obtained by use of a neon matrix was claimed to be close to the gas-phase value.

Shemansky obtained some support for multiple lifetimes from a comparison of his calculated line strengths and those measured in emission by Miller [462].

Miller [465], in more recent work, claimed to have found two discrepancies between his experimentally observed line strengths and the theoretical values of Watson [643] for the $^3\Sigma_u^+$–$^1\Sigma_g^+$ transition. Watson's parameters c_j^2 and s_j^2 show considerable curvature when plotted against J; but plots of (e.g.) c_j^2 $(2J+1)$ for the F_3 component of the triplet state show no marked curvature as thought by Miller. Thus one discrepancy is eliminated. Miller's extrapolations of line strengths fitted to the experimental data did not give the same J-axis intercepts as expected from Watson's theoretical line strengths; but this is expecting too much of the experimental data.

Multiple lifetimes appear to be characteristic of transitions whose upper state has a higher multiplicity than the lower, says Shemansky [570]. For the A state, if radiative decay times were measured under conditions where collisions were negligible then with sufficient spectral resolution, each substate would display its own lifetime. If spectral resolution could not separate the substates then a decay curve would be expected which would be resolvable into two exponentials. When a lifetime measurement is made with low spectral resolution and, if further, pressure is sufficiently high to thermalize the populations of the three substates then only a single exponential decay curve is observed (as in the Carleton and Oldenburg experiment). Under the latter conditions $v=0$ has a τ of 1.9 s.

Recent absolute emission intensity measurements by Meyer et al. [457] from a known concentration of N_2 A-state molecules, provides an upper limit to the A state lifetime which favors Shemansky's value.

b. $W^3\Delta_u$–$B^3\Pi_g$

The $v=0$ level of the W state lies close to the $v=0$ level of the B state. Predominant radiation from this

W level is to the B state. Freund [239 and unpublished results], has estimated the lifetime of the W level to be in excess of 10^{-3} s. Kenty [382] had made an indirect estimate of 1–2 s for the lifetime against radiation by W–X, but this rested on a tenuous identification of a state with about 8 eV energy.

Covey et al. [180] have measured the Einstein A coefficient (A_{02}=772 s^{-1}) of the $W \leftarrow B$ $0 \leftarrow 2$ transition emitted in the infrared. (See section 3.18 for a discussion of the intra-system cascading between W and B states.) Lifetimes of the vibrational levels of the W state were calculated, assuming both constant and variable transition moment; in the latter case, the variation was assumed to be the same as for the B–A system. The calculated lifetimes were assumed accurate to better than 50% (table 82), with τ for the v=0 level being orders of magnitude larger than for higher v because of the relatively small A_{00}. In addition to the lifetimes, Covey et al. have calculated a Deslandres array of transition moment matrix elements and Einstein A coefficients. (These calculations are based in part on work concerning the B–A transition by Cunio and Jansson [188] and Jansson and Cunio [355]).

c. $B^3\Pi_g - A^3\Sigma_u^+$

The determination of the radiative lifetime of the B state and the electronic transition moment for the N_2 $B-A$ (1+) system have had a long and varied history. A number of these determinations are mentioned by Shemansky and Broadfoot [572]. Though some prior estimates indicated a constant value for R_e, there seems to be no question that R_e decreases significantly with increasing internuclear distance. The early low resolution intensity measurements of 52 bands by Turner and Nicholls [619] have been used recently by Jain and Sahni [337] to obtain R_e. Jeunehomme [357] measured relative intensities of bands emitted following excitation by the same rf discharge which he used for lifetime measurements. Most recently Shemansky and Broadfoot have excited the $B-A$ transition by electron impact and then used synthetic spectra to unravel the overlapping structure. The derived transition moment was put on an absolute scale by use of the measured lifetime of the 3–1 band (the lifetime determined was close to that obtained by Jeunehomme [357]). Franck-Condon factors and r centroids used were from unpublished calculations of Albritton et al. and were not significantly different from values of Benesch et al. [71, 69]. Absolute A values of Shemansky and Broadfoot are reproduced in table 96; lifetimes derived from the summation of these A values are in good agreement with those measured directly by Jeunehomme (table 82). Jeunehomme's values are based on extrapolation to zero pressure. (Section 10.1 discusses the transition moment.)

Jeunehomme [357] measured emission decay following a pulsed rf discharge. $B-A$ bands with v' of 0 to 10 were observed, and the derived lifetimes dropped by half over the observed range of v'. Similar results were found with the use of an electrodeless discharge. For v=0 the lifetime of 8.0×10^{-6} s was about twice that obtained from f-value determinations in a shock tube experiment by Wurster [673] and similar results by Wray and Connolly [669]. Jeunehomme's pressure range was $4\text{–}40\times10^{-3}$ torr (0.5–5 Pa). The decay was distinctly non-exponential, indicating a superposition of decays. The largest decay constant corresponds to the natural decay for the B state. Transitions populating the B state by cascading include $C-B$ (2+), $C'-B$ (Goldstein-Kaplan), and $D-B$ (4+).

Jeunehomme concluded that in his experiments the predominant means of populating the B state was not through cascade from higher energy long-lived states. Radiative lifetimes for individual vibrational levels and $B-A$ band intensities were used to determine a transition moment, which was found to decrease moderately with increasing r centroid, in qualitative agreement with results of Jain and Sahni [337]. By use of Jeunehomme's lifetime of 8×10^{-6} s, an upper limit of 4×10^{-3} is obtained for f_{00}. Jeunehomme obtained 2.23×10^{-3} by using the R_e he deduced from the lifetime measurements. Additional discussion of these results can be found in Wentink et al [649].

Benesch et al. [68] have indicated that cascading from the $C-B$ transition contributes about 10% to the emission of the $B-A$ bands in aurorae.

Hartfuss and Schmillen [286] have measured the lifetimes of several levels of the B state by monitoring the decay of the B–A bands following excitation in a pulsed rf discharge. Measurements were made over a pressure range of 10^{-2} to 1 torr (1–100 Pa), with extrapolation to zero pressure. Non-exponential decay was observed. Lifetimes were roughly half of those of Jeunehomme; they also decreased with increasing v'.

Johnson and Fowler [361–2] used an invertron to excite the B state levels in order to measure lifetimes. Pressures were about 0.03–1.4 torr (4–190 Pa), somewhat higher than those in the experiments just cited. Lifetimes were found to be independent of v', with values half that of Jeunehomme. Jeunehomme's larger values for τ were explained as due to neglect of diffusion effects. Lifetimes obtained by Hollstein [318], obtained in a time of flight experiment, agree with Jeunehomme's value. His experiment was designed to avoid many of the difficulties in prior experiments.

Breene [91] has calculated f_{00}, giving an ab initio value twice that of Jeunehomme.

The origin of the discrepancy between the two-tiered sets of lifetime measurements has not been resolved. Fowler (private communication) suggests that inclusion of diffusion corrections in Jeunehomme's analysis would have led to even longer lifetimes (too long already, he believed), and only a more careful

excitation can clarify the ambiguities, for the sources used are more complex than has generally been assumed.

d. $B'^3\Sigma_u^- - B^3\Pi_g$

This infrared afterglow system has been little studied. Only estimates of the lifetime are available. Wentink et al. [650] calculated such lifetimes assuming a constant transition moment and making use of Franck-Condon factors of Benesch et al. [72]; estimated values for $v'=0$ to 8 were in the range $25-52\times10^{-6}$ s.

e. $a'^1\Sigma_u^-$

Wilkinson and Mulliken [662] estimated the lifetime of the a' state from appearance pressure, obtaining a value of 0.04 s. Shemansky [570] has shown that such estimates may be extremely unreliable. Tilford et al. [615] have given an improved estimate based on Lichten's value of the measured lifetime of the a state; if the revised value of Borst and Zipf [88] is used, the a' lifetime is then estimated as 0.5 s. Additional discussion can be found in Tilford et al.

f. $a^1\Pi_g$

The lifetime determinations for the a state have varied by an order of magnitude. Possible intrasystem cascading effects have recently been uncovered.

From a molecular beam time-of-flight experiment Lichten [417] obtained for the radiative lifetime of the a state a value $(1.70\pm0.30)\times10^{-4}$ s. This lifetime does not correspond to an individual vibrational transition. Lichten assumed an excitation energy of ~9 eV for purposes of estimating the magnetic dipole transition moment; this energy corresponds to v' ~2. In a similar experiment but with higher resolution Olmsted et al. [508] obtained $(1.20\pm0.50)\times10^{-4}$ s.

Ching et al. [158] measured $a-X$ band intensities photoelectrically, using pressure-broadened bands. From their integrated f-values can be obtained a lifetime value of 0.30×10^{-4} s, a rather low value. Holland [314] obtained a value of 0.80×10^{-4} s from the best fit to a glow profile for the $a-X$ bands excited by a 900 eV electron beam. This value, based on extrapolation to low pressure, was thought by Holland to be an upper limit. This value would now seem to be too low. An unpublished value of Jeunehomme is a factor of 10 smaller than Holland's estimate.

The $a-X$ transition is part electric quadrupole and part magnetic dipole. Wilkinson and Mulliken [661] had tentatively estimated the ratio of transition probabilities for electric quadrupole lines relative to magnetic dipole lines to be 0.15. Vanderslice et al. [629] analyzed in detail the intensity distribution of $a-X$ lines and obtained agreement with the theory of Chiu [159]; the ratio of electric quadrupole to magnetic dipole transition probabilities was deduced as 0.33. Recently, Shemansky [571] deduced a ratio of <0.1. From measured equivalent widths (with rotational structure unresolved) a lifetime of 1.4×10^{-4} s was obtained. For the $(v'-0)$ progression of the $a-X$ transition the calculated lifetime increased by about 10% in going from $v'=0$ to 8. The calculated lifetimes are assumed uncertain by 20%.

The synthetic spectra calculated by Shemansky were based on two assumptions in the higher pressure regime: collision broadening could be described by a Lorentz profile, and the broadening coefficient is independent of J. Agreement was obtained between the observed and calculated spectral intensity distribution (for the bands showing no resolved rotational structure) when their cited ratio of quadrupole to magnetic dipole transition probabilities was adopted. This enabled absolute transition probabilities to be calculated, which led to the calculation of the lifetime for the successive levels of the a state.

Borst and Zipf [88] have studied the lifetime of the $a^1\Pi_g$ state in a time-of-flight experiment. Their diffuse-gas source was operated in the pressure range near 10^{-4} torr (0.01 Pa). The lifetime obtained was $(1.15\pm0.20)\times10^{-4}$ s, likely the best value determined directly. Shemansky's values should be considered an upper limit (private communication by Shemansky to Borst and Zipf).

Garstang [246] has extracted a quadrupole transition probability of 2000 s^{-1} from an extrapolation of generalized oscillator strengths obtained by Lassettre and coworkers (see his cited references) from studies of electron impact excitation. By using the lifetime of Borst and Zipf [88] and the relative quadrupole contribution deduced by Vanderslice et al. [629] a value 2175 s^{-1} is obtained.

Freund [240] has made a model calculation on intrasystem cascading to assess the possible effects on the lifetime determinations of levels of the a state. The $a\,^1\Pi_g$, $a'\,^1\Sigma_u^-$, and $w\,^1\Delta_u$ states were considered. The results showed that the a state decays non-exponentially, and that the lifetimes of vibrational levels of the a state may vary by a factor of two as v increases. When considering a–X decay, a–a' decay should not be neglected. Several cascade processes may affect the measurement of radiative lifetimes. A discussion is given of the various lifetime experiments and arguments given as to why their results should be described in terms of apparent lifetimes.

Pilling et al. [527] used the curve of growth method to determine (by use of some approximations) f-values for the magnetic dipole and electric quadrupole components of a–X bands in the $v''=0$ progression (table 82). From these quantities lifetimes and approximate electronic f-values were determined. The approach used is direct, though it lacks the accuracy of electron energy loss or phase shift. The authors were aware of ambiguities and inconsistencies that still exist in published f-values for this system.

g. $w^1\Delta_u$

Ching et al. [158] measured the integrated absorption coefficients for the w–X bands 3–0, 4–0, and 5–0, and found that coefficients varied quadratically with pressure. Band oscillator strengths obtained were $0(10^{-8})$. Self absorption was necessary to see these weak bands, and this required pressures of 3 to 10 atm.

The w–a transition is allowed by electric dipole selection rules. Assuming a constant transition moment of 1 Debye, Wentink et al. [650] have calculated lifetimes for the $v'=0$–4 levels, obtaining values ranging from 5×10^{-4} s to 1×10^{-4} s. These transitions span the wavelength region from 37000 to 14000 Å.

h. $^5\Sigma_g^+-B^3\Pi_g$

The quintet state at 9.5 eV is slightly stable. Its lifetime is extremely uncertain. Benson [74] has estimated an extremely short lifetime for this state as an intermediate in the formation of vibrationally excited $B^3\Pi_g$. From kinetic arguments Becker et al. [65] estimated a radiative lifetime $>10^{-3}$ s.

i. $C\,^3\Pi_u$–$B\,^3\Pi_g$ 2(+)

Bennett and Dalby [73] measured the lifetime of the $v=0$ level of the C state from a study of the C–B, 0–0 and 0–1 bands. Excitation was by impact of electrons with energies of 185–25 eV; the cited lifetimes were those extrapolated to the threshold energy of 11 eV. Pressures were $5\text{–}0.2\times10^{-3}$ torr (0.7–0.03 Pa), to avoid collisional quenching. From the [then] known cross sections for excitation of N_2 and N_2^+ [585–6], overlap between these two transitions was assumed insignificant. Bennett and Dalby concluded that their observed drop in τ with decreasing electron energy represented cascading.

Fink and Welge [226] interpreted the decrease in τ with decrease in electron energy as implying cascading at higher electron energies. (This was for a pressure of 2×10^{-3} torr (0.3 Pa).) Extrapolation to threshold energy gave τ of 3.8×10^{-8} s. An observed significant decrease in τ as pressure decreased from 10^{-2}–10^{-3} torr (1.3–0.13 Pa) was explained as arising from chemical reactions. Their graphical extrapolation to zero pressure gives 4.5×10^{-8} s, for 60 eV electron energy; the published value is 2.7×10^{-8} s.

A τ of 4.9×10^{-8} s was obtained by Jeunehomme [356], extrapolated from measurements made at pressures down to 5×10^{-3} torr (0.7 Pa). The drop in apparent τ with drop in pressure was accounted for by assuming recombination of slow electrons and molecular ions.

Desesquelles et al. [193] have obtained τ of 4.0×10^{-8} s from the 0–0 and 0–1 bands excited by impact of N_2^+ ions on H_2; ion kinetic energies were 60–150 k eV. Pressures were below 10^{-3} torr (0.1 Pa).

Nichols and Wilson [493] studied the lifetimes by the delayed coincidence technique. Use of high energy proton bombardment to excite the C state allowed measurement of lifetimes longer than 1 ns. These measurements are considered preliminary, and illustrate the capability of the technique. The long extrapolation to zero pressure from τ measured at pressures above 50 torr (6 k Pa) is not considered reliable. A drop in τ by ⅓ was obtained in going from $v=0$ to $v=1$, contrary to expectations based on a nearly constant transition moment.

Hesser [309] excited the C state by impact with 200 eV electrons. By using the phase shift method to study the 0–0 band he obtained τ of $(4.8\pm0.8)\times10^{-8}$ s. This value was based on a linear extrapolation to zero pressure from measurements made at pressures as low as 5×10^{-3} torr (0.7 Pa).

Johnson and Fowler [361–2] detected no electron energy or pressure dependence in their measured lifetimes, and hence believed that all prior observations of these effects were influenced by overlap with bands of N_2^+, B–X. Using a delayed coincidence technique they measured τ for the levels C, $v=0$ to 3. The mean τ was 3.9×10^{-8} s. Bands measured include 0–0, 1–0, 2–1, 3–2. Pressure range was 0.03–1.4 torr (4–150 Pa). (This is relatively high.) Lifetimes were measured by photometrically monitoring the excited level number densities in a pulsed invertron. Absolute Einstein A coefficients were calculated by using transition moment integrals of Zare et al. [678]. Rescaled A values are given in table 95.

Early theoretical estimates of τ and indirect determinations from shock tube and projectile experiments are summarized in a table by Johnson and Fowler.

Sawada and Kamada [559] measured τ by the time sampling technique. Excitation was by electrons with energies below 200 eV. Time resolution was about 10^{-8} s. Lifetime was found to be independent of pressure in the range of $1\text{–}5\times10^{-3}$ torr (0.1–0.6 Pa). A slight decrease in τ with decrease in electron energy down to 20 eV suggests some cascading into the C state. The quoted τ (4.8×10^{-8} s) was obtained by extrapolation to zero pressure at the threshold energy.

Wagner [641] monitored the radiation arising from impact of electron avalanches. He found τ to be pressure dependent. Extrapolation to zero pressure gave τ of 3.6×10^{-8} s for the C–B, 0–1 band. The lowest pressure used was 8 torr (1 k Pa), relatively high to consider extrapolation as reliable.

Anton [49] bombarded N_2 with 50 keV electrons and measured lifetimes which were pressure dependent; pressures used were 20–200 torr (3–30 k Pa), with the higher range necessary for observing the $C-B$ transition. His extrapolated value of τ was 3.7×10^{-8} s.

Imhof and Read [331] used the electron-photon coincidence technique to measure lifetimes. Resolving time of their apparatus was 10^{-8} s. Pressure ranged from (1 to 7)$\times10^{-2}$ torr (1–9 Pa); lifetimes for $v=0,1,2$ were independent of pressure. The problem of cascading was assumed to be eliminated in these measure-

ments. The final values are: $v=0$, $(3.56\pm0.05)\times10^{-8}$ s; $v=1$, $(3.49\pm.18)\times10^{-8}$ s; $v=2$, $(3.45\pm0.23)\times10^{-8}$ s. The quoted uncertainty is the standard error, representing 68% confidence limit. Imhof and Read assumed that the pulsed beam measurements of Johnson and Fowler [362] and the beam-gas measurements of Desesquelles et al. [193] were likely affected by cascading which leads to apparently longer lifetimes. Other measurements, they assumed, (see their succinct summary) were affected principally by overlap with the B–X $(1-)$ system of N_2^+. In their table 1 are listed, for comparison, values of τ for the C state which were obtained from early calculations and indirect measurements. Values agreeing approximately with those of Johnson and Fowler [361–2] and also assumed to be cascade-free have been obtained by Dotchin et al. [203] who excited the state by impact of 300 keV protons.

Crude f-values have been estimated by Keck et al. [381] from shock tube measurements ($f\sim9\times10^{-2}$) and by Reis [543] from hypersonic projectile measurements ($f\sim5.7\times10^{-2}$). The radiative lifetime for the C state was measured in solid Ne by Tinti and Robinson [616]; they obtained $\tau\sim5\times10^{-8}$ s. (A crude f-value for $C-X$ ($\sim10^{-6}$) has been given by Ching et al. [158]. This was based on measured absorption coefficients extrapolated to zero pressure for the 0–0, 1–0, and 2–0 bands.)

The electron-photon coincidence method for measuring τ especially eliminates problems arising from cascading and spectral overlap by other transitions. This is done by selecting the upper state of a transition with resolution of 0.05 eV. Low gas pressures ($<10^{-2}$ torr or 1 Pa) reduce errors due to radiation trapping and collisional quenching. Only those transitions are selected which have the proper photon wavelength (by use of an interference filter) and inelastic electron energy. Other experiments have been conducted at comparable or lower pressures and were also free of overlap as measured by the relative cross sections for the impact energies. Cascading from the $E^3\Sigma_g^+$ state is likely not a problem because this state has a τ larger than that of the C state by a factor of 10^4. Of course, unknown states can be invoked as responsible for cascading.

Recent lifetime determinations by Millet et al. [467] are at too high pressures to be convincing, and give a larger lifetime for $v'=1$ than for $v'=0$. Calo and Axtmann [116] have also observed τ for $v'=1$ to be larger than for $v'=0$. Their estimate for $\tau(2)$ lies between those for $v'=0$ and 1.

In principle the experiment of Imhof and Read is the cleanest for determining τ, but a number of prior experimental determinations are not that open to criticism, and not inconsistent with the results of Imhof and Read.

The recommended value in table 82, $(3.66\pm0.05)\times10^{-8}$ s, is the weighted average of measurements by Bennett and Dalby [73], Jeunehomme [356], Desesquelles et al. [193], Hesser [309], Johnson and Fowler [361–2], Sawada and Kamada [556], and Imhof and Read [331]. Tentative results by L. Kurzweg using a delayed-coincidence technique obtained τ slightly larger than the mean cited above.

j. $E^3\Sigma_g^+$

A state of N_2 was detected at 11.5 eV in Penning ionization experiments by Cermak [152]. The E state lies slightly higher than the 11.4–11.6 eV range for the feature in Cermak's experiment, but, in Penning ionization, ions can be produced with kinetic energy, and the E state at 11.87 eV is most likely the parent of the feature observed by Cermak.

Trajmar et al. [35] have summarized the electron scattering evidence, pro and con, which heavily favors interpreting the feature at 11.87 eV as a triplet state (see especially p. 46–8). For additional discussions see Heideman et al. [292] and Lassettre [400]. Additional measurements by Cermak [153] now leave no doubt that the state at 11.87 eV is $E\,^3\Sigma_g^+$.

Emission from a molecular beam of nitrogen was observed following electron impact excitation in experiments by Freund [238]. The measured upper limit of $\tau(E)$ was combined with a lower limit of Olmsted [507] to give a tentative value of $(2.7\pm1.0)\times10^{-4}$ s. The lower limit is the lifetime of the $a\,^1\Pi_g$ state; a more recent value than that assumed by Olmsted would lower the estimate for the E state. Freund calculated absolute A coefficients from the observed transitions from the E state and its lifetime; the absolute A coefficients for the E–A, E–C, and E–B transitions are uncertain by a factor of 3. The E state, a Rydberg state, has a core configuration virtually that of N_2^+, $X\,^2\Sigma_g^+$. Freund [238] briefly discusses the states which might contribute to the E–A and E–C transition by configuration mixing.

Borst and Zipf [88], from time-of-flight experiments, have obtained $\tau(E)=(1.90\pm0.30)\times10^{-4}$ s. The metastable state was produced by impact of electrons with energies from threshold to 50 eV. (The lifetimes, averages over v, were deduced from measured time-of-flight distributions.)

Freund based his lifetime estimate on an assumed lifetime for the a state of CO, and mesaured the difference τ $(E)-\tau$ $(a$, CO). By using the lifetime for the CO state as measured by Borst and Zipf, a revised value is obtained from Freund's measurement. An improved value for the CO state measured by Lawrence [403] gives a revised value of 2.2×10^{-4} s for the E state of N_2.

k. $a''\,^1\Sigma_g^+-X\,^1\Sigma_g^+$

Absorption coefficients were measured by Lutz [429] for this electric quadrupole transition which was overlapped by the b–X transition in the spectral region around 1010 Å. Measurements in the pressure range of 10 to 50 torr (1 to 7 k Pa) were converted to f-

values and for the 0–0 band, extrapolates to a value less than 10^{-7} in the limit of low pressures.

l. $b\,^1\Pi_u - X\,^1\Sigma_g^+$

Absolute absorption f-values have been measured by Lawrence et al. [404] with N_2 gas pressures in the 10^{-6} -10^{-4} torr (0.1—10 m Pa) range. 0.04 Å bandwidths were ten times smaller than what had been previously achieved (table 82). The 3–0 band at 972.02 Å was very diffuse; the 4–0 band at 965.63 Å was also diffuse, but not as much. The electron impact measurements are compatible with relative f-values obtained by Geiger and Stickel [254].

A crude measurement was made for the lifetime of the band at 1258 Å, the 1–10; the value is roughly 6×10^{-8} s. See Johnson [361]. A rough upper limit to f_{el} ($\sim$0.06) was estimated by Appleton and Steinberg [51] from high temperature absorption coefficient measurements.

m. $D\,^3\Sigma_u^+ - B\,^3\Pi_g$

The earliest theoretical estimate of the lifetime of the D state was 2.75×10^{-6} s, by Jeunehomme and Duncan [358]. This value appears to be far too large. Preliminary measurements by Jeunehomme (unpublished, but cited in reference [649]) give an estimate 8.5×10^{-8} s. Since then Wentink et al. [650] measured the radiative decay of 0–1, 0–2, and 0–4 D–B bands obtaining a value of 1.84×10^{-7} s. A value of about 6×10^{-8} s is mentioned in a report by Fowler [235] but no details are given.

Wentink et al. made crude estimates of the molecular constants of the D state (only one vibrational level has been observed) in order to estimate Franck-Condon factors and f-values for the D–B bands. An approximate potential curve was estimated for the D state by analogy with the ground state of N_2^+ which has a similar electron configuration.

Kurzweg et al. [399] have used the method of delayed coincidence with electron excitation to measure the lifetime of the D state. They obtained $(1.41\pm0.10)\times10^{-8}$ s from measurements on the decay of the 0–3 D–B (4+) band. Special efforts were made to reduce light scattering by using two monochromators in tandem. A brief discussion was given as to how use of a single monochromator might yield values five times larger.

n. $b'\,^1\Sigma_u^+ - X\,^1\Sigma_g^+$

Sroka [581] has excited the b'–X bands by bombarding N_2 with electrons having energies greater than 120 eV. Radiative decay was monitored for bands 7–2 (959 Å) and 7–3 (980 Å); approximate f-values deduced were 0.3 and 0.2, respectively. A rough upper limit for f_{el} ($\sim$0.3) was estimated by Appleton and Steinberg [51] from high temperature absorption coefficient measurements on bands in the region 1334–1086 Å.

Fowler [235] has deduced some f-values from energy loss spectra of Geiger and Stickel [254]. For the 7–0 band he obtained, as upper limit, $f=0.1$; for $v'=0$ to 6, with $v''=0$, f-values less than 0.003 were assigned.

o. $c_3\,^1\Pi_u - X\,^1\Sigma_g^+$

The level labeled $c_3(0)$ had been formerly called the ℓ_1 state. This level has been formally assigned as the $v=0$ level of the lowest term of the $^1\Pi_u$ Rydberg series though it mixes intimately with the b valence state by means of a strong homogeneous perturbation. (See Carroll and Collins [130] and Dressler [210].) The absolute f-value for the $c-X$ 0–0 band obtained by Lawrence et al. [404] is 0.040 ± 0.008.

p. $H\,^3\Phi_u - G\,^3\Delta_g$

Bombardment by 50 keV electrons produced the emission of the Gaydon-Herman green bands. The decay of light was observed in the region around 5800 Å, with a lifetime of $(2.8\pm0.5)\times10^{-8}$ s. This is likely an upper limit since the observations were made at a pressure of about 150 torr (18 kPa). At the time Anton [49] did this work, the upper state was thought to be $^3\Sigma$.

q. $c_4'\,^1\Sigma_u^+ - X\,^1\Sigma_g^+$

The upper state of this transition is a Rydberg state, formerly called p'. The absolute f-value for the $c_4'-X$, 0–0 band has been obtained by Lawrence et al. [404] as 0.14 ± 0.04. Hesser and Dressler [310] produced this band in emission by exciting with 200 eV electrons. This transition was considered cascade-free. The phase shift method was used to obtain the lifetime of the upper level as $(9\pm2)\times10^{-10}$ s.

r. Hopfield Rydberg Series

The Hopfield Rydberg series of $^1\Sigma_u^+$ states converges to the B state of N_2^+ (see section 3.25e). Cook and Ogawa [170] have measured absorption coefficients of N_2 in the region 732–668 Å (bandwidth is 0.13 Å). From these measurements were derived f-values for the bands of the $v'=0$ series (table 82).

s. $N_2^+\,A\,^2\Pi_u - X\,^2\Sigma_g^+$

Bands of the N_2^+ $A-X$ transition have been the source of information on the lifetimes of the vibrational levels of the A state of N_2^+.

In a time-of-flight apparatus, Hollstein et al. [318] measured lifetimes of decay of radiation from the A state of the ion; the values for the 3–0, 4–1, and 5–1 bands were roughly constant at about 12×10^{-6} s. In principle this was a clean experiment. O'Neil and Davidson [510] had obtained values about half as large from an experiment that wasn't as clean.

Gray et al. [271–2] bombarded N_2 at pressures down to 1.1×10^{-4} torr (16 mPa) using 1 keV electrons. For the 2–0 $A-X$ band they measured a lifetime of $(9\pm2)\times10^{-6}$ s.

In more recent time-of-flight experiments, the preliminary values of Hollstein et al. have been improved upon, with two laboratories obtaining agreement for the first time. These new values differ from the earlier work in that a vibrational dependence is observed, instead of a constant value. Peterson and Moseley [524] observed lifetimes for A levels $v=1$ to 8; lifetime decreased by half over this range of v. Holland and Maier [316] and Maier and Holland [435] made similar measurements, though over a more limited range of v, obtaining about the same values and the same v-dependence. It remains unclear why the measurements of Hollstein et al. did not show the v-dependence.

With 3 Å resolution, Maier and Holland [436] have observed radiative decay of two isotopes of N_2^+ by means of A–X emission from a nitrogen ion beam in the spectral region 3200–6000 Å. Bands with $v' \leq 19$ are identified; bands with v' up to 30 are uncertain. Of the hundreds of spectral features observed, many remain unidentified. Lifetime data has been obtained only for the $^{14}N_2$ isotope. A weakly r-dependent transition moment was deduced over the range $0.92 < r < 1.1$ Å. There is much overlapping structure, and the lifetimes above $v'=9$ are approximate but tentatively suggest that lifetimes increase above $v'=19$.

t. $N_2^+ B^2\Sigma_u^+ - X^2\Sigma_g^+$

The quoted lifetime (table 82) is the weighted mean of measurements indicated by * in the discussion below.

τ (10^{-8} s)	Reference
6. 58 ± 0. 35	Bennett and Dalby [73] *
6. 0 ⊥ 0. 4	Fink and Welge [226] *
6. 5 ± 0. 2	Sebacher [567]
7. 15 ± 0. 4	Jeunehomme [356]
6. 59 ± 1. 0	Nichols and Wilson [493]
6. 60 ± 0. 15	Desesquelles et al. [193] *
5. 9 ± 0. 6	Hesser [309]*
5. 92 ± 0. 4	Johnson and Fowler [361-2]*
6. 5 ± 0. 5	Sawada and Kamada [558]*
5. 86 ± 0. 5	Head [290]*
6. 13 ± 0. 16	Gray et al. [271]*
6. 07 ± 0. 15	Klose [388] unpublished*

Bennett and Dalby used a sampling method; their value is for impact by 185 eV electrons. Fink and Welge used the phase-shift method; their value is based on impact of 80 eV electrons, not extrapolation to threshold. Sebacher used 10 keV electrons for excitation and a sampling method. Jeunehomme used a pulsed rf discharge with electron energies of 20–28 eV; his extrapolation to zero pressure from the relatively large pressure range of his experiments is somewhat uncertain. Nichols and Wilson obtained a preliminary value in trying out the technique of delayed coincidence, using excitation by a pulsed proton beam. Their pressures of several torr did not permit a confident extrapolation to zero pressure. Desesquelles et al. used an ion beam method, with energies above 60 keV. Johnson and Fowler used an invertron with excitation energies of 40–125 eV; lowest pressures were 0.1 torr (10 Pa); their value was based on extrapolation to zero pressure.

Hesser used the phase-shift method and 200 eV electrons. Sawada and Kamada, using a time sampling technique, based their value on the virtually constant number obtained using 100–200 eV electrons. Pressures used varied from 0.001 to 0.005 torr (0.1 to 0.7 Pa) Head excited the B state by passing 20 keV N_2^+ ions through a differentially pumped gas. Gray et al. used 1 keV electrons to excite the $v=2$ level of the B state (Based on other authors' measurements for $v=1$, there would appear to be no strong dependence of lifetime on v.) Klose used excitation by a 100eV electron beam and a delayed coincidence method to measure lifetime for B, $v=0$, 1, 2 (pressure range was 0.001 to 0.016 torr (0.1 to 2.1 Pa).

The pressures used in the measurements which were averaged range from 10^{-3}—0.1 torr (0.1 to 10 Pa) Fowler and Holzberlein [236] obtained a crude value for the lifetime; the rough value of Anton [49] was derived from measurements above 1 torr (100 Pa) Several early theoretical estimates (citations are given by Klose) are of the correct order of magnitude.

Johnson [361], for $v=0$, measured the lifetime for R-branch lines having $N'=7$ to 35, and found no dependence on rotational quantum number.

Broadfoot [97] has calculated absolute Einstein A coefficients for the B–X system. He used too small a value of the radiative lifetime to put the relative values on an absolute basis, and used Morse based Franck-Condon factors which differ significantly from RKR values only for weak transitions. The relative intensities used were the photoelectric measurements of Wallace and Nicholls [642]. Using the mean value given in table 82, 6.25×10^{-8} s, means that Broadfoot's calculated A coefficients should be multiplied by a factor of 0.64; but they should still be regarded as tentative.

Dotchin et al. [203] have measured the lifetime of the $v=0$ level by monitoring the photon decay of B–X (1—) bands, following excitation by 330 keV protons. Their value, 6.04×10^{-8} s, is slightly below the mean value cited in table 82.

Dufayard et al. [213] have measured lifetimes of selected B state rotational levels (B–X bands) perturbed by the A state whose levels have much longer lifetimes. In some cases the perturbed lifetimes were 50% larger than for unperturbed levels.

u. $N_2^+ {}^4\Sigma_u^+$ State at 21 eV

The tabulated lifetime is the average of values by Cermak and Herman [154a], Cress et al. [186], Asundi

et al. [55], and Ryan [552]. Briglia [94] has estimated an upper limit for the lifetime as 10^{-6} s. These lifetimes are all obtained from studies of collision rate processes and are not the results of direct measurements. The cited value is assumed uncertain by 50%. The electron configuration for this state is (see Cermak [154]): $KK(\sigma_g 2s)^2(\sigma_u 2s)^2(1\pi_u)^3(3\sigma_g)(1\pi_g)$. This state is presumed formed by ionization of a $3\sigma_g$ electron and excitation of a $1\pi_u$ electron into its antibonding counterpart.

v. $N_2^+ C^2\Sigma_u^+$

Inn [332] estimated the lifetime of the C state to be 10^{-8} to 10^{-7} s, assuming only that the C–X transition is electric dipole allowed. Recently, van de Runstraat et al. [549] measured the lifetime in an experiment which excited the C state by keV ion-impact and obtained for $v' \leq 2$, $\tau = (9 \pm 3) \times 10^{-8}$ s.

For C $v=4$ the ratio $\tau_{rad}/\tau_{prediss}$ is 20 : 1. Albritton et al. [44] estimated $\tau_{prediss}$ as 3×10^{-9} s, assuming that the radiative lifetimes of the C and B states were about the same. This magnitude is consistent with the assumption of a forbidden predissociation of the C state. Fournier et al. [233] had estimated the lifetime of predissociated levels $v' \geq 4$ as about 5×10^{-9} s.

van de Runstraat et al. [551] have measured cross sections for emission of $C^2\Sigma_u^+$–$X^2\Sigma_g^+$ bands following high energy electron impact excitation. By considering not only (2—) radiation but also the decay from levels 3 to 7 of the C state by predissociation, they deduced approximate lifetimes for these levels (table 82). These values were normalized to the lifetimes of unpredissociated levels below $v=3$. For $v' \geq 3$, the ratio A_{predis}/A_{rad} varied from 10 to 60 in going from $v'=3$ to 7.

w. Miscellaneous

(i) Maier and Holland [433] have observed emission of metastable nitrogen ions produced by impact of 35 eV electrons. Measured lifetimes were $(4.4^{+2.0}_{1.4}) \times 10^{-6}$ s and $(44 \pm 11) \times 10^{-6}$ s. The observed radiation cannot be unambiguously identified with either quartet states of N_2^+ or the states of N_2^+ which produce N_3. They are possibly related to thresholds at 19 eV and 25 eV, and may not be radiative lifetimes at all.

(ii) Cooper [172] has measured electronic absorption f-values for several sequences of the N_2^+ B–X bands and the N_2 systems B–A and C–B. These approximate quantities were obtained from experiments in a ballistic range and a shock tube.

(iii) Dipole strengths for $^1\Sigma_g^+$–$^1\Sigma_u^+$ N_2 transitions have been calculated by Marchetti and LaPaglia [436a]. The results demonstrate the need to include configuration interaction.

(iv) Hurley [328] has estimated the lifetimes of the (metastable) states of N_2^{2+} to be greater than 1 s.

10.3. Absorption in the Extreme Ultraviolet

The absorption spectrum of nitrogen below 1000 Å consists of many strong bands, which, below the first ionization at 796 Å, are superimposed on ionization continua. Fine structure analyses of the transitions b–X, b'–X, c–X, and c'–X have been made down to 850 Å. At shorter wavelengths it becomes difficult to resolve rotational structure. In addition to extensive studies of Rydberg series in this region, emphasis has been placed on measurement of absorption and ionization cross sections as a function of wavelength.

Hudson [15] has critically reviewed the measured photoabsorption cross sections for molecules of aeronomic and astrophysical interest at wavelengths below 3000 Å. The data from the literature are presented as plots of cross section vs. wavelength Hudson discusses in detail the various techniques of measuring the cross sections. For the spectral region 800–600 Å the cross sections remain in a confused state.

A decade ago there appeared several reviews of absorption cross sections, absorption coefficients, and intensities that reflected the rather chaotic status of the measurements. Huffman et al. [325] and Cook and Metzger [168] reviewed work prior to the early 1960's. A compendium of absorption coefficients of atmospheric gases for wavelengths below 3000 Å was made by Sullivan and Holland [593]. The various measurements, often in drastic disagreement with one another, made it virtually impossible to select best values for wavelengths corresponding to discrete structure. In fact, Huffman [323], in reviewing the status of absorption cross section measurements for atmospheric gases, compiled only cross sections for continuum absorption at solar lines in the region 1215 to 10 Å. The selected wavelengths do not correspond to N_2 absorption band positions.

Often there are large discrepancies between the intensity distribution observed in optical measurements (UV absorption spectra) and those of electron energy loss spectra in the region 1000 800 Å. This is attributed to strong bandwidth-dependence of the cross sections. Hudson agrees with Lawrence et al. [404] that "the band oscillator strengths obtained from the energy-loss spectrum should be preferred over the optical results" until there are high-resolution absorption measurements.

Lawrence et al. [404] have re-examined, under lower pressure and high resolution (0.04 Å spectral bandwidth) optical absorption between 972–958 Å. The four bands they studied include $b\,^1\Pi_u$–X, 3–0, 4–0; $c_3\,^1\Pi_u$–X, 0–0 (ℓ_1 band); and $c_4'\,^1\Sigma_u^+$–X, 0–0 (p' band). The absolute oscillator strengths they obtained are confirmed by relative values deduced from measurements on electron energy loss spectra by Geiger and Schröder [253], but not by the photon absorption coefficient measurements of Huffman et al. [326], whose lower resolution work suffered from the effects

of line saturation (see discussion by Lawrence et al.). Effects of perturbations are briefly discussed, as are uncertainties in apparent f-values due to extrapolation to low pressure. The Huffman measurements give an extraordinarily large absorption coefficient to the very diffuse band at 972.07 Å (b–X, 3–0).

The close agreement between the Einstein A function and lifetime for the p' band indicates q_{00} of ~0.9.

For the 11.4–13.6 eV energy range, Lawrence et al. [404] obtain an integrated f-value of 0.40; the value of Silverman and Lassettre [577] is more than a factor of two larger.

The large ($^1\Pi_u{}^1\Pi_u$) perturbations involving the b state, make it impossible to simply compare observed intensity distribution in the b–X transition with calculated Franck-Condon factors.

The more recent photoabsorption work has used the Hopfield continuum as background source and photoelectric recording; many of the earlier measurements were made with a many-line background source. Instrumental band widths were at best 0.5 Å which corresponds to 0.006 eV to 0.017 eV in the region 1000–600 Å. The recent electron energy loss spectra have been studied with resolution of 0.010 to 0.040 eV.

Geiger and Schröder [253] have restudied in detail the electron energy loss spectra in the energy range 12.5–14.9 eV (970–870 Å), by use of 25 keV electrons. Resolution was 0.010 eV, insufficient to resolve rotational structure, but comparable to that in the photoabsorption measurements of Huffman et al. [325]. Geiger and Schröder have made a dramatic graphical comparison between their intensity distribution and that obtained by Huffman et al. [326], and have given an extensive qualitative discussion of the perturbations affecting energy levels in this region (see especially Geiger and Schröder [253], footnote ref. 19; see also Dressler [210]).

Hudson and Carter [322] have indicated that most N_2 absorption bands in the region 1130–800 Å are predissociated. Further, they stressed the caution that absorption cross sections obtained at maxima or minima can be in error up to a factor of two, because of neglect of the effect of finite instrumental band widths. In the photoionization spectrum of vibrationally-excited N_2 (842–795.8 Å) Cook and McNeal [167] observed more than 50 new pre-ionized bands lying atop the continuum.

The distribution of electronic states dictates that N_2 transmits radiation from the visible till 1000 Å, i.e., N_2 is effectively transparent above 1000 Å. Below 1000 Å, N_2 becomes a stronger absorber, with the strongest bands in the region 950–400 Å, and the onset of ionization continua at 796 Å.

Near 1300 Å is an air window with absorption coefficient $k < 10$ cm^{-1}; for 1300–1000 Å, $k < 150$ cm^{-1}; for an extensive region below 1000 Å, k is at least several hundred for absorption bands. The region 1000–796 Å (till N_2^+, $X\,^2\Sigma_g^+$) is characterized by sharp intense bands of Worley progressions (1050–820 Å) and bands of the Worley-Jenkins Rydberg series which converge to the first I.P. There is no dissociation continuum (see Cook and Metzger [168]; Huffman et al. [326]). The region 796–742 Å (till N_2^+, $A\,^2\Pi_u$) finds the ionization continuum with peak continuum absorption coefficient of 2295 cm^{-1} at 765 Å (see Samson and Cairns [553a]). Overlapping the continuum are strong bands, mostly pre-ionized, which belong to Rydberg series converging to the second I.P. (see Cook and Metzger [168], Cook and Ogawa [169]). The region 742–661 Å (till N_2^+, $B\,^2\Sigma_u^+$) finds the continuum strength increases till $k = 780$ cm^{-1} at 661 Å; pre-ionized Hopfield Rydberg series appear too. At 661 Å Huffman et al. [326] reported a sudden increase in continuum k to 980 cm^{-1}, which remained nearly constant till 580 Å. This abrupt increase was not observed in the electron impact spectrum produced by Silverman and Lassettre [577], and was later shown by Watson et al. [643] to be an artifact. Below 580 Å till 300 Å there is a general decline in k to ~90 cm^{-1}.

In general, strong continua underlie the bands for $\lambda < 820$ Å; continua are weak above 820 Å (Cook and Metzger [168]).

Fluorescence in nitrogen following absorption in the extreme ultraviolet was observed by Huffman et al. [325]. The fluorescence began at 661.3 Å and extended to at least 580 Å. It was concluded that the $B^2\Sigma_u^+$–$X^2\Sigma_g^+$ (1—) transition was responsible for the observed fluorescence. Similar fluorescence was also observed by Judge and Weissler [369] and Cook and Metzger [168].

Samson and Cairns [553a] measured photoionization and total cross sections for the region 1038–304 Å. Typical absorption coefficients were of the order of several hundred cm^{-1}.

Cook and Ogawa [169] measured absolute photoionization coefficients and ionization efficiencies of N_2 in the region 805–734 Å. Most absorption bands for wavelengths below the first I.P. at 796 Å were pre-ionized as indicated by peaks in the ion-current spectrum. Absorption coefficients were given mainly at wavelengths corresponding to minima and maxima in the absorption, including, of course, Rydberg series. Comparison with the photographic spectrum taken at somewhat better resolution showed that several absorption maxima were absent in the ion-current spectrum. A correlation between photoionization efficiency and type of electronic transition was indicated.

There exist numerous measurements of absorption coefficients for parts of the region 1100–600 Å; Huffman et al. [324, 326], Cook and Metzger [168], Cook and Ogawa [169], and Samson and Cairns [553a]. These measurements are discordant in the region 800–600 Å.

Huffman et al. [324] measured absorption from bands originating from $v > 0$ in the ground electronic state. The spectra were produced in a 2.2 m normal incidence vacuum spectrograph-monochromator; dispersion was 3.7 Å/mm in first order. Rydberg transitions spanned the region 1028–800 Å. Many unclassified non-Rydberg bands span the region 937–804 Å; there is much overlapping. Many diffuse absorption bands were observed in the region 800–740 Å. Cook and Ogawa [169] studied photoionization in the region 805–734 Å. Absorption coefficients for Rydberg bands were measured and compared with earlier measurements. Samson and Cairns [554] measured total absorption cross sections for 550–200 Å. Results are mainly in disagreement with prior measurements. (Cross sections decreased with decreasing wavelength.)

A few words are in order about absorption at solar lines (see Huffman [323]). For 1215.7 Å, Lyman α, $k \sim 0.002$ cm^{-1}. Absorption coefficients measured at this wavelength vary by a factor of 5 (Ditchburn et al. [201]). This discounts an early measurement which is a factor of 50 larger than any other reported value. For 1025.7 Å, Lyman β, $k < 0.03$ cm^{-1}. N_2 is quite transparent in this region. The reported absorption coefficients at this wavelength vary by more than an order of magnitude (Cook and Metzger [168]).

Cook et al. [171] have determined photodissociation continua cross sections for the spectral region 600–1000 Å from total absorption coefficients and ionization coefficients of Cook and Metzger [168]. The results are presented graphically.

New measurements have been made of photoabsorption coefficients by Watson et al. [644]. These span the region 300–700 Å. Accuracy of ± 3% is quoted by the authors. It is found that earlier measurements by Samson and Cairns [554] are in close agreement with the newer and more accurate values. The source is synchrotron radiation and detection was by electron multiplier photodetection. The maximum of absorption in the continuum is at 540 Å, with a shoulder at 430 Å. A sudden increased absorption coefficient at 661 Å reported by previous authors is shown to be an artifact. The continuum is overlapped by discrete structure in the region 650–680 Å. Results are presented graphically. This paper presents a brief summary of prior measurements in this region and discusses also several new features and the reasons why certain other structure is not observed because of weakness.

Carter [143] has measured the photoabsorption spectrum of N_2 (photoelectrically) in the region 984–730 Å, using a bandwidth of 0.04 Å. For wavelengths above 796 Å the peak absorption cross sections (and the f-values) were rather dependent on the number density of absorbing particles. This is caused by saturation and bandwidth effects. The cross sections obtained were, therefore, much larger than values of earlier workers. An attempt was made to extrapolate the f-values to low pressure (see table 2 of reference [143] for a list of measured f-values for over a hundred wavelength intervals and the bands with which they are identified). Using this data, Carter and Berkowitz [144] have calculated photoionization yields for the bands in the region 734–796 Å.

Lee et al. [409] have measured the absorption cross sections of N_2 photoelectrically in the region 700–180 Å using synchrotron radiation. The continuum cross sections are displayed graphically, showing no structure below 500 Å. The structure in the region 720–520 Å is accounted for by the known Rydberg series. The best data using line emission sources is consistent with the new results. References are made to the few papers that have appeared since the review by Hudson [15].

972.537 Å (Lyman γ)

A factor of 30 relates the extreme values quoted for N_2 absorption at 972.5 Å. Ogawa and Cairns [496] have summarized the measurements made prior to their reexamination of this absorption with a 3 m grating spectrograph and a 6.8 m grazing incidence spectrograph. They found that the Lyman γ wavelength is not absorbed symmetrically by N_2, so that concentrations of N_2 cannot be inferred from absorption of this radiation. There is needed yet higher resolution determination of absorption cross sections as a function of wavelength and a detailed study across the Lyman γ profile.

584.3 Å (He I)

Huffman et al. [326] obtained 980 cm^{-1} for the absorption coefficient; earlier values were more than a factor of two smaller. Cook and Metzger [168] measured 800 cm^{-1}. Brolley et al. [101] have recently determined the cross section to be 22.5±0.2 Mb (2.25×10^{-14} m^2); other recent values are also discussed. (In a study of vacuum UV fluorescence following incidence of 175–780 Å light on N_2, Lee et al. [410] observed features that could possibly include the N_2^+ C–X transition whose onset is at 525 Å.)

Absorption below 31 Å

Nakamura et al. [481] studied photographically the absorption spectrum of N_2 in the 30 Å region, using

synchrotron radiation from a 1.3-BeV electron synchrotron as the background continuum. A 2 m grazing incidence spectrograph with glass grating was used (resolution ~0.03 Å). Discrete structure was observed near the K-edge of nitrogen. On the basis of electron configuration, the absorption data obtained were compared with the optical spectroscopic data of the NO molecule and it was found that the absorption structure is well explained as arising from the excitations of a 1s electron to outer-shell orbitals of the nitrogen molecule. An energy of 409.5 ± 0.1 eV is obtained for the K level of the nitrogen molecule.

Vinogradov et al. [638–9] have observed the X-ray K absorption spectrum of N_2, with 0.6 eV resolution. The K-edge energy value they obtained, 410.3 eV, is in agreement with Nakamura's value and that obtained by electron spectroscopy (409.9 eV) [32].

11. Miscellaneous; Electric and Magnetic Properties

(a) By use of a molecular beam magnetic resonance method for studying the rf spectra corresponding to reorientations of the ^{15}N nuclear moment, Chan et al. [155] have experimentally determined the spin rotational constant for the ^{15}N nucleus in $^{15}N_2$ (c=22 kHz) and the molecular rotational magnetic moment ($g_j = 0.2593 \pm 0.0005$ nuclear magnetons). The signs of these parameters were not determined, though the latter is presumed to be negative, by analogy with O_2. De la Vega and Hameka [191] have calculated a value for g_j which is half the experimental value and has a negative sign. Paramagnetic shielding constants have been determined by Chan et al. [155] and by Baker et al. [58].

(b) Flygare and Benson [235] have surveyed the experimental and theoretical literature on the molecular Zeeman effect. Observations lead to a direct determination of g_j, magnetic susceptibility anisotropies, and molecular quadrupole moments. Included in their tabulation of experimental values are the parameters for $^{15}N_2$. Laws et al. [405] have calculated magnetic susceptibility and nuclear magnetic shielding using coupled Hartree-Fock theory.

(c) Using a molecular beam resonance method, De Santis et al. [192] have studied the rf spectrum of the N_2 $A\,^3\Sigma_u^+$ state at magnetic fields below 1 gauss. Transitions between hyperfine levels ($\Delta F = \pm 1$, $\Delta M_F = 0, \pm 1$) have been observed for v=0–12, with hyperfine frequencies accurate to ±10 kHz (see table 5 of ref. [192]). A refined theory of the fine and hyperfine structure of a $^3\Sigma$ state was developed and used to interpret the measurements. This is an extension of an earlier theory as used by Freund et al. [241] who studied the Zeeman spectrum of this state ($\Delta F = 0$, $\Delta M_F = \pm 1$) at somewhat lower resolution.

The magnetic hyperfine parameters for the A state are virtually those of the free atom. Derived molecular parameters are v-dependent with the quadrupole coupling constant varying most strongly; it decreased by 20% over the range of v studied (see their table 7).

(d) Wilkinson [658] measured the refractive index of N_2 in the region 2042–1649 Å, and Peck and Khanna [521] measured the refractive index for the region 20,586–4679 Å.

(e) Bridge and Buckingham [93] have measured polarization of light scattered from a He–Ne laser. The depolarization ratio which refers to both the Rayleigh and rotational Raman lines taken together is $(1.018 \pm .005) \times 10^{-2}$.

(f) Allen et al. [45] observed lasing of the N_2 $B-A$ (1+) system in the near infrared and the $C-B$ (2+) system in the ultraviolet. Both laser pulses occur during the risetime of the discharge current pulse for a specific range of discharge currents. For other currents only one system lases. The 13 ns long UV pulse ends 10 ns before the 35 ns IR pulse starts. The interaction between these systems by means of quenching and cascading destroys the population inversion that leads to lasing in the $B-A$ system.

(g) Bloom et al. [87] have interpreted nuclear spin measurements in earlier experiments in terms of a nuclear spin relaxation theory from which they obtained the N_2 molecular quadrupole moment Q as 1.7×10^{-26} esu. Prior experimental values range from 0.8 to 1.9. These are summarized along with calculated values in reviews by Stogryn and Stogryn [589], Krishnaji [19], and Billingsley and Krauss [78], whose recent multi-configuration value lies about 25% below the measurement of Bloom et al. [87], but is close to −1.52 (unpublished results by Buckingham recommended by Stogryn and Stogryn. The sign of the quadrupole moment is not generally obtained by experiment, but the ab initio calculations yield a negative sign. Cartwright and Dunning [147] have calculated the quadrupole moment for the ground electronic state with generalized valence bond wavefunctions. For the v=0 level they obtained −1.24; as a function of internuclear distance the quadrupole moment increased from negative values at small r to showing a slight positive maximum before going asymptotically to zero at larger r. Quadrupole matrix elements were also calculated.

(h) Gas phase energy pooling by N_2 molecules in the A state has been conclusively established by Stedman and Setser [584]. Radiative pooling which would occur at around 1400 Å lay outside the range of their detectors.

12. Summary

The spectrum of molecular nitrogen provides the data from which are obtained the energies of the observed states, molecular constants, the potential energy curves which give a shorthand description of the electronic states, and transition probability parameters. In conjunction with ab initio calculations, the spectrum also serves to elucidate the electronic structure of nitrogen. Perturbations and predissociations sometimes uncover the presence of states that are not observed directly. The following summary is concerned primarily with aspects of the spectrum that have only recently been understood, and also focuses attention on persistent problems that remain. Some current activity, experimental and theoretical, will be mentioned.

More is known about the spectrum of molecular nitrogen than for most other diatomic molecules. Though the principal features are understood considerably better than a decade ago, questions remain for a number of states.

The dissociation energy of N_2 is established, though the possibility remains that a future treatment of the long-range interactions may slightly alter the interpretation of the limiting curve of predissociation from which the dissociation energy is obtained. For no non-predissociating electronic state of N_2 are the vibrational levels known all the way to the dissociation limit.

The energies or molecular constants for some states are not known. The identity of some states that have been observed under low resolution has never been established. Even for the ground electronic state, there are still needed rotational constants for several low-lying vibrational levels. For the $D\,^3\Sigma_u^+$ state, only one vibrational level is known; this suggests a possible predissociation, but no further details are available.

Nitrogen bands in the region 1015–795 Å are characterized by irregular vibrational structure and intensities. The upper states of these transitions lying above 12 eV ($b\,^1\Pi_u$, $c_n\,^1\Pi_u$, $o_n\,^1\Pi_u$, $c_n'\,^1\Sigma_u^+$, and $b'\,^1\Sigma_u^+$), were formerly considered as numerous separate states but are now known to belong to two valence states and three Rydberg states (more properly, series). Analysis has shown that the irregularities are due largely to strong homogeneous interactions between valence and Rydberg states. In the adiabatic picture, predissociation in $b\,^1\Pi_u$ likely involves a $^3\Pi_u$ state associated with $^4S+^2P$. Predissociations have been assumed when observed levels are diffuse; requiring further examination are $b'(5, 20, 21, 22)$, c_4', and possibly c_5' (1), all $^1\Sigma_u^+$.

In the region above 12 eV, Rydberg states of both g and u symmetry remain unknown; singlets and triplets, Σ, Π, and Δ. These certainly interact with the known singlet states above 12 eV, and are likely responsible for additional nitrogen atoms that play a role in atmospheric chemistry. Many of these states, difficult to observe, may be predissociated.

The theory of ℓ-uncoupling has been applied to a limited extent to the analysis (deperturbation) of several of the Rydberg p-complexes, but strong homogeneous interactions prevent this in, e.g., c_4–c_5', and c_3–c_4' complexes. There is evidence for predissociation of c_7, c_9, and c_{12} complexes, though the exact mechanism of predissociation is not established. Deperturbation remains incomplete for an adequate description of $o_{3,4}\,^1\Pi_u$.

The lowest $^3\Sigma_g^+$ Rydberg state (E) is now established by high resolution spectroscopy, though only two vibrational levels are known. Calculations show an avoided crossing involving the E state. The lowest-lying $^1\Sigma_g^+$ Rydberg state (a'') is known, but only $v=0$ has been observed. No Rydberg series have been observed to converge to the $D\,^2\Pi_g$ state of N_2^+. Only low resolution observations have been made on $^3\Pi_u$ Rydberg states whose convergence limit is $A\,^2\Pi_u$.

Recent unpublished multiconfiguration calculations [M. Krauss, et al.] show the $C^3\Pi_u$ and $C'\,^3\Pi_u$ states to have the same adiabatic potential. The magnitude of any long-range maxima in this potential as in other potentials are speculative. Calculations indicate an avoided crossing involving the $^3\Pi_u$ state associated with $^4S+^2P$.

Observed irregularities in the $y\,^1\Pi_g$ state are now understood to arise from a strong homogeneous interaction with a new state that has been observed, $k\,^1\Pi_g$. The k state probably undergoes an accidental predissociation; the y state suffers an even more complex predissociation.

Work is in progress on new measurements of some N_2 and N_2^+ transitions [Benesch, et al.]. The $W^3\Delta_u$–$B^3\Pi_g$, $v'=2$ level is being examined. The N_2 $B'^3\Sigma_u^-$–$B\,^3\Pi_g$ 0-0 band is being reinvestigated. For N_2^+ the $B\,^2\Sigma_u^+$–$X\,^2\Sigma_g^+$ (1–) bands with low quantum number are also under study. For the $A\,^2\Pi_u$–X Meinel system of N_2^+, the 0-1 band remeasurement is expected to give an improved term value of the upper state, since both spin components can be observed. Absorption of $W\,^3\Delta_u$–X 6-0 in N_2 is expected to provide a better B value for the W state. An attempt is also being made to examine the line widths of the $a\,^1\Pi_g$–$X\,^1\Sigma_g^+$ emission to clarify the relative contributions of electric quadrupole and magnetic dipole radiation.

The $C\,^2\Sigma_u^+$ state of N_2^+ undergoes strong homogeneous interaction with the $B\,^2\Sigma_u^+$ state. To study this interaction in detail requires measurements on the C state for $v > 10$. Recent calculations identify the B state as the one responsible for predissociation of the C state, but this has not been firmly established. Only tentative explanations have been proposed for identifying states causing perturbations of low vibrational levels of the C state.

Recent calculations by Cartwright and Dunning and also by Thulstrup and Andersen show that many bound and repulsive states of N_2^+ are to be found between 7 and 12 eV above the ion ground state (23-28 eV above N_2 X). Fragmentary observations have been made on unidentified states in this energy range. The new calculations may provide a partial explanation of some of these observed features, though the current accuracy attainable may not always enable a unique identification to be made.

For most observed transitions, measured intensities are not accurate. Radiative lifetimes for some states are poorly determined.

Only one band of one transition assigned to N_2^{2+} has been observed under high resolution. Recent calculations, though not of spectroscopic accuracy, might aid in the search for more.

No entirely satisfying explanation in terms of simultaneous mechanisms has yet been advanced, to account for all the spectroscopic features of active nitrogen.

The electronic states of N_2 lying above 11 eV are characterized by strong configuration mixing. Ab initio calculations have predicted a number of these to be stable, including $H\,^3\Phi_u$ and $G\,^3\Delta_g$. Both states have recently been observed and their rotational structure analyzed. Though the H–G transition (Gaydon-Herman green system) is now known experimentally, the absolute energy of neither state has been established, because the only observed transition is the one between them. Experimentally, it might be feasible to search for the G–W transition, with the 0–0 band at around 4350 Å, though the most likely bands expected by the Franck-Condon principle would be in the red and near IR, strongly overlapped by B–A (1+). The C'–G transition, also difficult to observe, has its 0–0 transition at 6550 Å, but the strongest bands would be expected in the near IR.

The Herman infrared system (9100–7000 Å) is a group of multi-headed bands known only at low resolution. Vibrational intervals for the upper state of this system are similar to those for the $H\,^3\Phi_u$ state, the upper state of the Gaydon-Herman green system. Isotopic work has confirmed the vibrational scheme for the infrared bands, but ambiguities prevent identifying the upper state as the H state. The bands remain unclassified.

Three band heads observed in emission in the spectral region 2560–2360 Å have had quantum numbers tentatively assigned so that the vibrational spacings for the lower state seem to correspond to that of the $a\,^1\Pi_g$ state. The upper state, tentatively called d', has its lone observed vibrational level at an energy 13.8 eV above the N_2 ground state. No high resolution measurements exist for these bands; no absorption is known to the d' state, so the reality of this state has yet to be firmly established. No theoretical calculations place a state at this energy with the appropriate symmetry to expect emission to the a state.

Note Added in Proof

(1) Section 3.29 and tables 43 and 75 are to be viewed in terms of a new perspective. Bands attributed to a $^4\Sigma_u^+$–$^2\Sigma_g^+$ intercombination transition of $^{14}N_2^+$ are interpreted as $B\,^2\Sigma_u^+$–$X\,^2\Sigma_g^+$ (1−) bands of $^{14}N^{15}N^+$. See successive letters by K. Dressler, J. Chem. Phys. **64**, 3493–4 (1976) and by J. d'Incan and A. Topouzkhanian, J. Chem. Phys. **64**, 3494 (1976).

The theoretical and experimental arguments do not unambiguously favor a revised interpretation of the observed bands. But, from theory, the lowest $^4\Sigma_u^+$ state has predominent electron configuration similar to that of the $C\,^2\Sigma_u^+$ state, and is expected to have r_e somewhat the same (~1.28 Å), but also larger than that for the $B\,^2\Sigma_u^+$ state (1.08 Å). Analysis by d'Incan and Topouzkhanian [200] gives a value close to that of the B state. Ab initio calculations by Andersen and Thulstrup [47] give too large a value (1.40 Å), but improved calculations are not likely to reduce that by much more than 0.1 Å. Measurements under improved resolution are needed to separate some of the numerous blended lines to enable unambiguous branch assignments to be made.

(2) Multiconfiguration SCF calculations have shown that the bound $^5\Sigma_g^+$ state at 9.5 eV has a potential barrier nearly as large as its well depth. The calculated potential has r_e larger than the semi-empirical estimate and a somewhat smaller well depth. (Krauss, M., and Neumann, D. B., The $^5\Sigma_g^+$ States of N_2, Mol. Phys. **32**, 101–112 (1976)).

(3) An approximate and indirect method has yielded a new value of 0.013 s for the radiative lifetime of $a'\,^1\Sigma_u^-$, v=0. (Tilford, S. G. and Benesch, W. M., Absorption Oscillator Strengths for the $a'\,^1\Sigma_u^-$–$X\,^1\Sigma_g^+$ and $w\,^1\Delta_u$–$X\,^1\Sigma_g^+$ Transitions of Molecular Nitrogen, J. Chem. Phys. **64**, 3370–3374 (1976)).

(4) Complex predissociations in the $y\,^1\Pi_g$ and $x\,^1\Sigma_g^-$ Rydberg states and their likely causes have been

discussed. The location of a new $^1\Sigma_g^+$ state (x') is deduced from the analysis; it lies close to the y state in energy. (Mulliken, R. S., Predissociation and Λ-Doubling in the Even-Parity Rydberg States of the Nitrogen Molecule, J. Mol. Spectrosc. **61**, 92–99 (1976)).

(5) SCF calculations have been made for energies of Rydberg states with configurations of $1\pi_u^3 2\pi_u$, $1\pi_u^3 3\sigma_u$, and $3\sigma_g 2\pi_g$, and on valence states with configuration $1\pi_u^3 1\pi_g$. States treated include k, y, x, and x' (unobserved) as well as other states of the same electron configurations. As is the case with the k and y states, their triplet counterparts are expected to interact with one another. In support of a suggestion by Lefebvre-Brion and Moser, the calculations suggest that the $z\,^1\Delta_g$ state is observed in a vibrationally excited state, and that its term value is likely lowered to 14.12 eV. (Ermler, W. C. and Mulliken, R. S., Energies and Orbital Sizes for Some Rydberg and Valence States of the Nitrogen Molecule, J. Mol. Spectrosc. **61**, 100–106 (1976).)

(6) There is underway a joint effort by the IBM San Jose Laboratory and the University of Chicago (A. D. McLean, W. C. Ermler, R. S. Mulliken) on the computation of potential energy curves for many valence and mixed valence-Rydberg states of N_2. The method used is a combination of an MCSCF procedure with additional configuration mixing. The basis set on each atom is comprised of five s, four p, and three d Slater-type functions, and is augmented with three $3s$–, three $3p$–, and two $3d$– type STF's spanning the Rydberg region of space. (W. C. Ermler, private communication).

(7) A multi-headed band (~3246 Å) previously observed under low resolution by Tanaka and Jursa [600] has been observed in absorption under high resolution for isotopes $^{14}N_2$, $^{15}N_2$, and $^{14}N^{15}N$. Analysis confirms the upper level to be a mixture of $C'\,^3\Pi_u$, $v=1$ and $C\,^3\Pi_u$, $v=5$, mainly C', in agreement with an earlier interpretation by Carroll and Mulliken [136]. Observed and deperturbed molecular constants of the upper states are given for all isotopes. (Ledbetter, J. W., Jr., and Dressler, K., Interaction of the $C'\,^3\Pi_u$ and $C^3\Pi_u$ states in $^{14}N_2$, $^{14}N^{15}N$, and $^{15}N_2$, J. Mol. Spectrosc. **63**, 370–390 (1976).

(8) Reference [502] was used in draft form. It has appeared in print as: Yoshino, K., Ogawa, M., and Tanaka, Y., Extension of Rydberg absorption series of N_2, $A^2\Pi_u \leftarrow X^1\Sigma^+_g$. J. Mol. Spectrosc. **61**, 403–411 (1976).

(9) Selected references:

Courtois, D., and Jouve, P., Electric field induced infrared spectrum of nitrogen: Vibrational polarizability matrix elements. J. Mol. Spectrosc. **55**, 18–27 (1975).

Smith, A. J., Read, F. H., and Imhof, R. E., Measurement of the lifetimes of ionic excited states using the inelastic electron-photon delayed coincidence technique. J. Phys. B **8**, 2869–2879 (1975).

Govers, T. R., van de Runstraat, C. A., and de Heer, F. J., Excitation and decay of the $C\,^2\Sigma_u^+$ state of N_2^+ following collisions of He^+ ions with N_2 isotopes. Chem. Phys. **9**, 285–299 (1975).

Shemansky, D. E., $A\,^3\Sigma_u^+$ molecules in the N_2 afterglow. J. Chem. Phys. **64**, 565–580 (1976).

Wu, H. H., and Shemansky, D. E., Electronic transition moment of the N_2^+ ($A\,^2\Pi_u$–$X\,^2\Sigma_g^+$) system. J. Chem. Phys. **64**, 1134–1139 (1976).

Gartner, E. M., and Thrush, B. A., Infared emission by active nitrogen. I. The kinetic behaviour of N_2 ($B'\,^3\Sigma_u^-$). Proc. R. Soc. London A **346**, 103–119 (1975).

Gartner, E. M., and Thrush, B. A., Infared emission by active nitrogen. II. The kinetic behaviour of N_2 ($B\,^3\Pi_g$). Proc. R. Soc. London A **346**, 121–137 (1975).

Buontempo, U., Cunsolo, S., and Jacucci, G., The far infrared absorption spectrum of N_2 in the gas and liquid phases. J. Chem. Phys. **63**, 2570–2576 (1975).

Lee, J. S., Wong, T. C., and Bonham, R. A., Observation of a new electronic transition in N_2 at 31.4 eV by means of high energy electron impact spectroscopy. J. Chem. Phys. **63**, 1643–1645 (1975).

Bouchoux, A. M., Bacis, R., Goure, J. P., and Lambert, A. M., Relative intensities of the rotational lines of the (0,0) and (0,1) bands of the $B^2\Sigma_u^+$–$X^2\Sigma_g^+$ systems of N_2^+. J. Quant. Spectrosc. Radiat. Transfer **16**, 451–456 (1976).

Mandelbaum, D., and Feldman, P. D., Electron impact excitation of the Meinel band system of N_2^+. J. Chem. Phys. **65** 672–677 (1976).

Osherovich, A. L., and Gosrhkov, V. N., Measurement of radiative lifetimes of the $C\,^3\Pi_u$ excited state of the N_2 molecule and of the $B\,^2\Sigma_u^+$ excited state of N_2^+ by the phase shift and delayed coincidence methods. Opt. Spektrosk. **41**, 158–160 (1976).

The following items apply to table 1:

(1) [r_e] means r_o; [B_e] means B_o; [ω_e] means $\Delta G(1/2)$, as in Herzberg's book.

(2) ( ) means uncertain.

(3) T_o is the mean of the term values (in case of multiplets) relative to X, $v=0$, $J=0$.

(4) All numerical data are in units of cm^{-1} unless otherwise indicated.

(5) To avoid confusion of sign conventions several formulas are listed below:

Vibrational terms:

$$G(v)=\omega_e(v+1/2)-\omega_e x_e(v+1/2)^2$$
$$+\omega_e y_e(v+1/2)^3+\omega_e z_e(v+1/2)^4,$$

i.e., a negative value of $\omega_e x_e$ from the table would mean a positive anharmonic term.

Rotational terms:

$$F_v(J)=B_v J(J+1)-D_v J^2(J+1)^2+H_v J^3(J+1)^3,$$

where $(-D_v)$ is always <0, and

$$B_v=B_e-\alpha_e(v+1/2)+\gamma_e(v+1/2)^2+\delta_e(v+1/2)^3,$$

$$D_v=D_e+\beta_e(v+1/2),$$

$$H_v \sim H_e.$$

The Dunham coefficients are given by

$$G(v)=\sum_{i=1} Y_{i0}(v+1/2)^i,$$

and

$$B_v=\sum_{i=0} Y_{i1}(v+1/2)^i.$$

The tabulated coefficients are really $Y_{10}\sim\omega_e$, $-Y_{20}\sim\omega_e x_e$, etc.

(6) Footnotes which give supplementary information pertaining to the individual electronic states are indicated at the end of table 1 and are identified by the electronic state. Table 1 has been left free of superscripts.

Table 1. Molecular constants, electron configurations, and dissociation

State	T_o	M.O. Configuration $(1\pi_u)(3\sigma_g)(1\pi_g)(3\sigma_u)$ other	Diss. Products N + N	Dissociation Energy D^o	ω_e	$\omega_e x_e$	$\omega_e y_e$	$\omega_e z_e$
$D^1\Sigma_u^+$					(∿1910)			
$X^1\Sigma_g^+$					(∿1960)			
$C^2\Sigma_u^+$	190209.5	{3 1 1 / 4 2} $-2\sigma_u$	$^2D^o+^3P$	24954	2071.51	9.290	-0.4333	
$D^2\Pi_{gi}$	177835	{2 2 1 / 4 0 1}	$^4S^o+^3P$	18105	911.70	12.606	0.0555	
$B^2\Sigma_u^+$	151233.5	{4 2 / 3 1 1} $-2\sigma_u$	$^4S^o+^3P$	44706	2419.84	23.19		
$A^2\Pi_{ui}$	134683.9	3 2	$^4S^o+^3P$	61256	1903.53	15.011		
$X^2\Sigma_g^+$	125667.5	4 1	$^4S^o+^3P$	70273	2207.00	16.10	-0.040	
$z^1\Delta_g$	115365.4	3 2 Ry $3p\pi_u$	$^2D^o+^2P^o$	11412	(∿1700)			
$y^1\Pi_g$	114073.34	3 2 Ry $4p\sigma_u$			1906.43	37.51		
$k^1\Pi_g$	113723.58	4 1 Ry $4d\pi_g$			[2182.32]			
$x^1\Sigma_g^-$	113211.19	3 2 0 0 Ry $3p\pi_u$			1910.72	20.865		
$d'(^1\Sigma_u^-$ or $^1\Delta_u)$	111333							
$o_3\ ^1\Pi_u$	105710.4	3 2 Ry $ns\sigma_g$			1987.4	16.3		
$H^3\Phi_u$	(105,000)	3 1 2 0	$^2D^o+^2D^o$	(12163)	924.21	12.29	-0.173	
$c_4'\ ^1\Sigma_u^+$	104323.3	4 1 0 0 Ry $np\sigma_u$			2201.78	25.199	0.7874	
$c_3\ ^1\Pi_u$	104138.2	4 1 Ry $np\pi_u$			2192.20	14.70		
$b'\ ^1\Sigma_u^+$	103670.8	4 1	$^2D^o+^2P^o$	23806	760.08	4.418	0.1093	-5.42(-3)
$D^3\Sigma_u^+$	(103573)	4 1 Ry $np\sigma_u$						
$b^1\Pi_u$	100817.5		$^2D^o+^2D^o$	16345				
$a''^1\Sigma_g^+$	98840.30	4 1 0 0 Ry $3s\sigma_g$						
$c'^3\Pi_u$	97603.56	3 1 2 0	$^4S^o+^2D^o$	(334)				
$E^3\Sigma_g^+$	(95774.50)	4 1 0 0 Ry $3s\sigma_g$	$^4S^o+^2D^o$	2163	[2185]			
$^5\Pi_u$	(93200)	3 1 2 0	$^4S^o+^2D^o$					
$C^3\Pi_u$	88977.84	4 2 1 $-2\sigma_u$	$^4S^o+^2D^o$	8960	2047.178	28.4450	2.08833	-0.5350
$G^3\Delta_g$	(87100)	2 2 2	$^4S^o+^2D^o$	(10800)	765.9	11.85		
$^5\Sigma_g^+$	(77900)	{2 2 2 0 / 3 1 1 1}	$^4S^o+^4S^o$	(814)	(650)			
$w^1\Delta_u$	71698.490	3 2 1 0	$^2D^o+^2D^o$	45465	1559.496	12.0078	0.04542	
$a^1\Pi_g$	68951.210	4 1 1 0	$^2D^o+^2D^o$	48212	1694.1895	13.9480	0.007864	0.000295
$a'^1\Sigma_u^-$	67739.290	3 2 1 0	$^2D^o+^2D^o$	49424	1530.2675	12.0778	0.041534	-2.96(-3)
$B'^3\Sigma_u^-$	65852.35	3 2 1 0	$^4S^o+^2P^o$	41701	1516.883	12.1811	.041864	-7.325(-4)
$W^3\Delta_u$	59380	3 2 1 0	$^4S^o+^2D^o$	38558	1501.4	11.6		
$B^3\Pi_g$	59306.81	4 1 1 0	$^4S^o+^2D^o$	38631	1733.391	14.1221	-0.05688	3.612(-3)
$A^3\Sigma_u^+$	49754.78	3 2 1 0	$^4S^o+^4S^o$	28959	1460.638	13.8723	-0.01030	-1.965(-3)
$X^1\Sigma_g^+$	0	4 2 0 0	$^4S^o+^4S^o$	78714	2358.5685	14.3244	-0.002258	-0.000235

products for the electronic states of N_2, N_2^+ and N_2^{2+}.

r_e(Å)	B_e	α_e	$\gamma_e(10^{-5})$	D_e (10^{-6})	Zero pt. energy	Observed transition	System name	Spectral region (Å)	References
[1.1363]	[1.8644]			[7.1]		D–X	Carroll	1590	124,134
[1.1316]	[1.8801]			[6.9]					124,134
[1.2628]	[1.5098]				1033.38	C–X	2–	2230–1270	125,654
1.47082	1.113	0.020			452.872	D–A	Janin-d'Incan	3070–2050	352
1.07772	2.073	0.020			(1202.615)	B–X	1–	5870–2860	204,390,174
1.17364	1.748	0.020			948.396	A–X	Meinel	17700–5500	352
1.116384	1.9319	0.0190			1099.430				204,390
1.1693	1.761	0.0153				z–w		2480–2370	423
						y–w	Kaplan II		
1.1767	1.739	0.017			943.84	y–a'	Kaplan I	2860–2070	425,140
						k–w	Carroll-Subbaram II	2675–2385	140
1.1086	1.959	0.031				k–a'	Carroll-Subbaram I	2530–2330	140
1.172656	1.750903	0.022764			949.883	x–a'	5+	2850–2030	422
						d'–a?			210
1.17839	1.7339	0.0088			(989.63)	o_3–X		950–880	675,414
1.48808	1.0873	0.0191			(459.01)	H–G	Gaydon-Herman green	6370–5040	131
1.104	1.961186	0.04355613			(1094.69)	c_4'–X	Carroll-Yoshino Ry series	960–805	132,414
						c_n–a"	Ledbetter Ry series	865–820	408
1.112	1.932003	0.03945652			(1092.43)	c_3^n–X	Worley-Jenkins Rydberg series	960–780	130,414, K. Yoshino, (Private communication)
1.439	1.154856	7.386963(-3)	-7.498983		(378.95)	b'–X		1290–820	132,414,660
	[1.961]			[2]		D–B	4+	2900–2250	257
						(b',c,c',o,d'–a)			
						b–a	Gaydon-Herman singlet	3670–2220	
1.279	1.460133	0.02623907				b–X		1110–850	130,414
	[1.9133]					a"–X	Dressler-Lutz	1010	408
	[1.0496]			[10.9]		C'–B	Goldstein-Kaplan	5080–2860	128
[1.1177]	[1.9273]			[6.0]		E–A	Herman-Kaplan	2740–2130	133
									136
						C–B	2+	5460–2680	196,175
1.148688	1.82473	0.018683			1016.705	C–X	Tanaka	1130–1070	612
1.6107	0.9280	0.0161			(380.0)				131
(1.55)									126
						w–a	McFarlane IR	85000–30000	448–9
1.26883	1.495535	0.016200			776.857	w–X	Tanaka	1400–1140	425
						a–a'	McFarlane IR	85000–30000	448
1.220252	1.616977	0.017984	-2.438	(5.89)	843.621	a–X	Lyman-Birge-Hopfield	2600–1100	462–4,627–8
1.275422	1.480115	0.016618	2.593		762.286	a'–X	Ogawa-Tanaka-Wilkinson-Mulliken	2000–1080	615,449
						B'–B	IR afterglow	8900–6050	138
1.27838	1.47327	0.016656	0.922		755.539	B'–X	Ogawa-Tanaka-Wilkinson	2240–1120	611
					(747.8)	W–B	Wu-Benesch	43000–22000	67
						B–A	1+	25310–4780	196
1.21260	1.63745	0.017906	-7.71		863.140	B–X	Wilkinson	1685–1640	
1.28656	1.4546	0.01799	-8.79		726.809	A–X	Vegard-Kaplan	5325–1250	196,462
1.0976968	1.998197	0.017279	-3.283	(5.74)	1175.767				421,462,464,627,111

General: (a) Systematic shifts of up to 0.5 cm^{-1} occur for measurements of one band system relative to another. This has made it necessary to compromise in refitting some of the experimental data to obtain molecular constants. The singlet systems a–X and a'–X have been fitted simultaneously; singlet transitions x–a', y–a', y–w, k–a', and k–w were also fitted simultaneously. The vibrational constants for the a' state and the molecular constants for the X state are from the former fit. The constants for other states have been obtained in some instances by refitting to a set of term values (with neglect of correlation effects) and for others by quoting results from the literature. Because of the systematic and correlation effects the molecular constants obtained by refitting are quoted with the uncertain digits underlined. In some cases where literature values have been used, as for b or b', more digits are quoted than are significant in a least squares sense. Where appropriate, an entry includes in parentheses, the power of ten by which it is to be multiplied. (b) ZPE$=G(0)+Y_{00}$, when Y_{00} is explicitly given in the footnotes.

State:

$X\,^1\Sigma_g^+$: $Y_{00}=0.064$

$A\,^3\Sigma_u^+$: $Y_{00}=-0.041$

$B\,^3\Pi_g$: (a) $Y_{50}=-1.109(-4)$ (b) $Y_{00}=-0.018$ (c) Reproduction of B–A spectra, ref. [440].

$W\,^3\Delta_u$: Reproduction of W–B spectra, ref. [556].

$B'\,^3\Sigma_u^-$: (a) $Y_{00}=0.138$ (b) Reproduction of B'–X spectra, ref. [611]. (c) Reproduction of B'–B spectra, ref. [138].

$a'\,^1\Sigma_u^-$: (a) $Y_{00}=0.167$ (b) Reproduction of a'–X spectra, ref. [615].

$a\,^1\Pi_g$: (a) $Y_{00}=0.012$ (b) Reproduction of a–X spectra, ref. [627–8, 655, 463, 206].

$w\,^1\Delta_u$: $Y_{00}=0.105$

Σ_g^+: Parameters are only estimates. This state has only been observed indirectly through its perturbation of other states.

$G\,^3\Delta_g$: (a) $A=-0.19$ [131]. (b) The absolute energy of this state is uncertain by $\sim$2000 cm^{-1}.

$C\,^3\Pi_u$: (a) $\gamma_e=-2.275(-3)$, rather larger than normal. The next two coefficients in the expression for B_v's are 7.33(−1) and 1.50(−4). The five B_v's are fitted by five coefficients, so no uncertainty limits can be attached to these coefficients which likely have little mechanical significance. The C state is perturbed and predissociated. (b) Reproduction of C–X spectra, ref. [612]. (c) Reproduction of C–B spectra, ref. [519, 320, 112, 237].

$^5\Pi_u$: This state is inferred at the approximate T_0 and is assumed responsible for predissociation of the $C\,^3\Pi_u$ state.

$E\,^3\Sigma_g^+$: (a) T_0 is derived from E–A and A–X term values. (b) Reproduction of E–A spectra, ref. [133].

$C'\,^3\Pi_u$: $H_0=8.3(-10)$; see ref. [128].

$b\,^1\Pi_u$: (a) Unusual vibrational constants are obtained from a deperturbation calculation by Leoni [414]. (b) $Y_{31}=6.375667(-4)$ and $Y_{41}=-2.705698(-5)$; these are from Leoni [414]. (c) Leoni obtained an unusually large $\gamma=-3.620510(-3)$. (d) Reproduction of b–X spectra, ref. [130,613]. (e) Electron configuration is likely a mixture of 421, $-2\sigma_u$ and 312.

$b'\,^1\Sigma_u^+$: (a) $Y_{50}=5.4(-5)$; $Y_{31}=1.338124(-6)$. Molecular constants for this state are deperturbed values obtained by Leoni [414]. (b) Reproduction of b'–X spectra, ref. [142]. (c) Electron configuration is likely a mixture of 321 and 4101.

$c_3\,^1\Pi_u$: (a) Molecular constants are from a deperturbation calculation. (b) Reproduction of c_n–X spectra, ref. [142]. (c) Reproduction of c_n–a'' spectra, ref. [408].

$c_4'\,^1\Sigma_u^+$: (a) $\gamma_e=5.214827(-3)$; $Y_{31}=-2.314815(-4)$. Molecular constants for this state are the deperturbed values of Leoni [414]. (b) Reproduction of c_n'–X spectra, ref. [613].

$H\,^3\Phi_u$: (a) $A=-12.085$ (b) H–G $\sigma_0(0\text{–}0)=17897.08$. D° is only estimated since the absolute energy of this state is uncertain by $\sim$2000 cm^{-1}.

$o_3\,^1\Pi_u$: (a) Molecular constants are from a partial deperturbation by Yoshino et al. [675]. Results of an earlier deperturbation calculation by Leoni [414] are not very different. (b) Reproduction of o_3–X spectra, ref. [675].

d': It is not certain that this state belongs to N_2. The d'–a bands, generally counted among the Gaydon-Herman singlet systems, have not been unambiguously identified.

$x\,^1\Sigma_g^-$: (a) $Y_{00}=-0.261$ (b) Reproduction of x–a' spectra, ref. [422].

$k\,^1\Pi_g$: (a) Molecular constants are deperturbed values of Carroll and Subbaram [140]. (b) Reproduction of k–w spectra, ref. [140].

$y\,^1\Pi_g$: (a) Molecular constants are deperturbed values of Carroll and Subbaram [140]. (b) Reproduction of y–w spectra, ref. [425].

N_2^+:

$X\,^2\Sigma_g^+$: (a) T_0 is a tentative value derived from a Rydberg series limit [K. Yoshino, private communication]. (b) $Y_{00}=-0.040$

$A\,^2\Pi_{ui}$: (a) $Y_{00}=0.384$ (b) Reproduction of N_2^+ A–X spectra, ref. [453, 205].

$B\,^2\Sigma_u^+$: (a) $Y_{00}=-1.508$ (b) Reproduction of B–X N_2^+ spectra, ref. [588, 157, 204].

Quartets: Andersen and Thulstrup [47] have calculated molecular constants and potential curves for some bound quartet states lying 3.5–11 eV above N_2^+ X.

$D^2\Pi_{g,i}$: (a) $Y_{00}=0.167$
(b) $A=-16.5$ [352].
(c) Reproduction of D–A spectra, ref. [482, 603].

$C^2\Sigma_u^+$: (a) Observed rotational constants are somewhat irregular.
(b) $\omega_e y_e$ is larger than normal.
(c) Reproduction of C–X spectra, ref. [654, 603, 125].

N_2^{2+}:

$X^1\Sigma_g^+$: ω_0 is an estimate.

$D^1\Sigma_u^+$: (a) $\sigma_0(0\text{–}0)=62{,}903.18$ for D–X [124]. The assignment of the one band observed is tentative.
(b) ω_0 is an estimate.
(c) Reproduction of D–X N_2^{2+} spectra, ref. [124].

Reproductions of spectra: Gaydon [249]—singlet systems; Gaydon [249]—weak visible system, analysis unknown; Tilford et al. [34]—region 1520–1600 Å; Tilford and Wilkinson [613–14]—singlet systems below 1130 Å.

Spectra of Rydberg series: Ogawa et al. [502], Ogawa [495], Takamine et al. [594], Tanaka and Takamine [605], Codling [162].

Table 2. Molecular constants for the electronic states of N_3

State	Point Group	Electron configuration	T_o	B_o	D_o	r_o
$B\ ^2\Sigma_u^+$	$D_{\infty h}$	$(\sigma_u)\ (\Pi_u)^4(\Pi_g)^4$	36739.07	0.43238(10)	$1.6(10^{-7})$	---
$X\ ^2\Pi_{gi}$	$D_{\infty h}$	$(\sigma_u)^2\ (\Pi_u)^4(\Pi_g)^3$	0	0.43117(10)	$1.5(10^{-7})$	1.1815

Data from Douglas and Jones [207]. T_o is measured from halfway between $^2\Pi_{\frac{1}{2}}$ and $^2\Pi_{\frac{3}{2}}$. $A_{o;eff}$ for the X state is $-71.26\ cm^{-1}$; A_o corrected for the Renner interaction is -71.90. $\epsilon\omega_2 = -94.38$, the sign being taken the same as for BO_2. From an estimate of $\omega_2 \sim 500\pm50$ by analogy with isoelectronic molecules, $\epsilon \sim 0.19$. $D^o \approx 2.6\pm0.5$ eV for $N_3(X) \rightarrow N_2(X) + N(^2D)$, from purely thermochemical estimates following arguments of Thrush [607].

$^2\Sigma_u^+ - X\ ^2\Pi_{gi}$ system: 2765-2670 Å.

Reproduction of spectra: Zamanskii et al. [677].

Table 3. Binding energies (eV) of core and valence electrons in N_2

Orbital	State	Observed energies			Calculated energies	
		(a)	(b)	(c)	(d)	(e)
$3\sigma_g$	$X^2\Sigma_g^+$	15.5	15.61	15.576	17.28	15.99
$1\pi_u$	$A^2\Pi_u$	16.8	16.73	16.694	16.75	15.34
$2\sigma_u$	$B^2\Sigma_u^+$	18.6	18.81	18.746	21.17	19.74
	$C^2\Sigma_u^+$	25.0		23.578		
$2\sigma_g$	$^2\Sigma_g^+$	37.3			40.10	
$1\sigma_u$	$^2\Sigma_u^+$	409.9		409.5	426.61	
$1\sigma_g$	$^2\Sigma_g^+$				426.71	

Observed energies are from

(a) X-Ray photoelectron spectroscopy from Siegbahn et al. [32]. The line corresponding to $2\sigma_u$ is actually split into two components due to the strong mixing of the B and C states.

(b) UV-photoelectron spectroscopy Collin and Natalis [163]. See also Turner et al. [36].

(c) Optical spectra (this review).

Calculated energies are from Cade et al. [114]; (d) using Koopman's theorem, (e) direct calculation of ionic states.

Table 4. Possible Rydberg states for N_2

N_2^+ core	abcd	Ry	Rydberg states
$X^2\Sigma_g^+$	4100,	$ns\sigma_g$	$\underline{a''\ ^1\Sigma_g^+}$ $E^3\Sigma_g^+$
		$np\sigma_u$	$\underline{c_4'\ ^1\Sigma_u^+}$ $D^3\Sigma_u^+$
		$np\pi_u$	$\underline{c_3\ ^1\Pi_u}$ $\underline{^3\Pi_u}$
		$nd\sigma_g$	$^1\Sigma_g^+$ $^3\Sigma_g^+$
		$nd\pi_g$	$^1\Pi_g$ $^3\Pi_g$
		$nd\delta_g$	$^1\Delta_g$ $^3\Delta_g$
$A^2\Pi_u$	3200,	$ns\sigma_g$	$\underline{o\ ^1\Pi_u}$ $\underline{F^3\Pi_u}$
		$np\sigma_u$	$\underline{y\ ^1\Pi_g}$ $^3\Pi_g$
		$np\pi_u$	$\underline{z\ ^1\Delta_g}$ $^3\Delta_g$ $^1\Sigma_g^+$ $^3\Sigma_g^+$ $\underline{^1\Sigma_g^-}$ $^3\Sigma_g^-$
		$nd\sigma_g$	$^1\Pi_u$ $^3\Pi_u$
		$nd\pi_g$	$^1\Delta_u$ $^3\Delta_u$ $^1\Sigma_u^+$ $^3\Sigma_u^+$ $^1\Sigma_u^-$ $^3\Sigma_u^-$
		$nd\delta_g$	$^1\Pi_u$ $^3\Pi_u$ $^1\Phi_u$ $^3\Phi_u$
$B^2\Sigma_u^+$	[4200, $-2\sigma_u$ / 3110]	$ns\sigma_g$	$\underline{^1\Sigma_u^+}$ $^3\Sigma_u^+$
		$np\sigma_u$	$^1\Sigma_g^+$ $^3\Sigma_g^+$
		$np\pi_u$	$^1\Pi_g$ $^3\Pi_g$
		$nd\sigma_g$	$\underline{^1\Sigma_u^+}$ $^3\Sigma_u^+$
		$nd\pi_g$	$^1\Pi_u$ $^3\Pi_u$
		$nd\delta_g$	$^1\Delta_u$ $^3\Delta_u$
$D^2\Pi_g$	[2210 / 4010]	$ns\sigma_g$	$^1\Pi_g$ $^3\Pi_g$
		$np\sigma_u$	$^1\Pi_u$ $^3\Pi_u$
		$np\pi_u$	$^1\Delta_u$ $^3\Delta_u$ $^1\Sigma_u^+$ $^3\Sigma_u^+$ $^1\Sigma_u^-$ $^3\Sigma_u^-$
		$nd\sigma_g$	$^1\Pi_g$ $^3\Pi_g$
		$nd\pi_g$	$^1\Delta_g$ $^3\Delta_g$ $^1\Sigma_g^+$ $^3\Sigma_g^+$ $^1\Sigma_g^-$ $^3\Sigma_g^-$
		$nd\sigma_g$	$^1\Pi_g$ $^3\Pi_g$ $^1\Phi_g$ $^3\Phi_g$
$C^2\Sigma_u^+$	[3110 / 4200, $-2\sigma_u$]	$ns\sigma_g$	$\underline{^1\Sigma_u^+}$ (same as for $B^2\Sigma_u^+$)

Table 5. Comparison of some calculated and observed Rydberg terms

(a) Terms converging to $X^2\Sigma_g^+$ of N_2^+ (15.58 eV)

	No.	State	Term values (eV)			Orbital design.		n*	δ
			calc[a]	calc[b]	obs	SA[c]	UA[d]		
	10	$E\ ^3\Sigma_g^+$	11.9	11.78	11.87	$\sigma_g 3s$	$3s\sigma_g$	1.92	1.08
	14	$a''\ ^1\Sigma_g^+$	12.5		12.25	$\sigma_g(3s+4p)$	$3s\sigma_g$	2.03	0.97
	21	$^3\Sigma_g^+$	13.9	13.89		$\sigma_g(4s+4d)$	$4s\sigma_g$		
	22	$^1\Sigma_g^+$	14.0			$\sigma_g(4s+4d)$	$4s\sigma_g$		
Carroll-Yoshino series	15	$D\ ^3\Sigma_u^+$	13.0	12.98	12.84	$\sigma_u 4p$	$(3)4p\sigma_u$	2.23	(0)1.77
	18	$c_4'\ ^1\Sigma_u^+$	13.1		12.93	$\sigma_u 4p$	$(3)4p\sigma_u$	2.27	(0)1.73
	26	$^3\Sigma_u^+$	14.4	14.35		$\sigma_u 4s$	$(4)5p\sigma_u$		
	27	$c_5'\ ^1\Sigma_u^+$	14.4		14.32	$\sigma_u 4s$	$(4)5p\sigma_u$	3.30	(0)1.70
	31	$^3\Sigma_u^+$	14.9	14.86		$\sigma_u 4d$	$(5)6p\sigma_u$		
	32	$c_6'\ ^1\Sigma_u^+$	14.9		14.87	$\sigma_u 4d$	$(5)6p\sigma_u$	4.30	(0)1.70
		$^3\Sigma_u^+$		15.13			$(6)7p\sigma_u$		
		$c_7'\ ^1\Sigma_u^+$			15.11		$(6)7p\sigma_u$	5.38	(0)1.62
Worley-Jenkins series	16	$^3\Pi_u$	13.0	12.95	12.8	$\pi_u 3p$	$3p\pi_u$	2.2	
	19	$c_3\ ^1\Pi_u$	13.1		12.91	$\pi_u 3p$	$3p\pi_u$	2.26	0.74
	28	$^3\Pi_u$	14.4	14.32		$\pi_u 4p$	$4p\pi_u$		
	29	$c_4\ ^1\Pi_u$	14.5		14.33	$\pi_u 4p$	$4p\pi_u$	3.30	0.70
	33	$^3\Pi_u$	14.9	14.81		$\pi_u 4d$	$5p\pi_u$		
	34	$c_5\ ^1\Pi_u$	15.0		14.85	$\pi_u 4d$	$5p\pi_u$	4.3	0.7
		$^3\Pi_u$		15.11			$6p\pi_u$		
		$c_6\ ^1\Pi_u$			15.10		$6p\pi_u$	5.32	0.68

(b) Terms converging to $A^2\Pi_u$ of N_2^+ (16.70 eV)

	No.	State	Term values (eV)			Orbital design.		n*	δ
			calc[a]	calc[b]	obs	SA[c]	UA[d]		
Worley series	17	$F\ ^3\Pi_u$	13.0	12.90	12.8	$\sigma_g 3s$	$3s\sigma_g$	1.9	1.1
	20	$o_3\ ^1\Pi_u$	13.2		13.10	$\sigma_g 3s$	$3s\sigma_g$	1.94	1.06
	35	$^3\Pi_u$	15.0	15.09	15.02	$\sigma_g 4s$	$4s\sigma_g$	2.83	1.17
	36	$o_4\ ^1\Pi_u$	15.1		15.15	$\sigma_g 4s$	$4s\sigma_g$	2.96	1.04
		$^3\Pi_u$		15.82	15.78		$5s\sigma_g$	3.85	1.15
		$o_5\ ^1\Pi_u$			15.83		$5s\sigma_g$	3.95	1.05
		$^3\Pi_u$		16.17	16.12		$6s\sigma_g$	4.84	1.16
		$o_6\ ^1\Pi_u$			16.15		$6s\sigma_g$	4.97	1.03
	25	$y\ ^1\Pi_g$	14.3	14.10	14.16	$\sigma_u 4p$	$(3)4p\sigma_u$	2.31	(0)1.69
	24	$x\ ^1\Sigma_g^-$	14.2	14.07	14.04	$\pi_u 3p$	$3p\pi_u$	2.26	0.74
	23	$z\ ^1\Delta_g$	14.1	14.07		$\pi_u 3p$	$3p\pi_u$	2.38	0.62
	30	$^1\Sigma_g^+$	14.6	14.07		$\pi_u 3p$	$3p\pi_u$		
	38	$^1\Sigma_u^+$	15.2			$\pi_g 4d$			
	39	$^3\Pi_u$	15.3			$\sigma_g 4d$			
	40	$^1\Pi_u$	15.3			$\sigma_g 4d$			

Table 5. (continued)

(c) Terms converging to $B^2\Sigma_u^+$ of N_2^+ (18.75 eV)

No.	State	Term values (eV)			Orbital design.		n*	δ
		calc[a]	calc[b]	obs	SA[c]	UA[d]		
37	$^3\Sigma_u^+$	15.1	14.95		$\sigma_g 3s$	$3s\sigma_g$		
41	$^1\Sigma_u^+$	15.6			$\sigma_g 3s$	$3s\sigma_g$		
42	$^3\Sigma_u^+$	17.1	17.14		$\sigma_g(4s+4d)$	$(3)4s\sigma_g$		
43	$^1\Sigma_u^+$	17.1		17.15	$\sigma_g(4s+4d)$	$(3)4s\sigma_g$	2.92	(0)1.08
44	$^3\Sigma_u^+$	17.3			$\sigma_g(4s+4d)$			
45	$^1\Sigma_u^+$	17.4		17.31	$\sigma_g(4s+4d)$			

The identification numbers in the first column are those used in Lefebvre-Brion and Moser's tables [413]. Calculated terms values (assumed uncertain by 0.2-0.3 eV) are from (a) Lefebvre-Brion and Moser [413], and (b) Betts and McKoy [77]. Orbital designations are those for (c) Separated Atoms and (d) United Atom. The former is used by Lefebvre-Brion and Moser to define the particular linear combination of atomic orbitals used. The latter is used by Mulliken [473], Carroll and Collins [130, 132] and others. Some authors (e.g. Dressler, [210] will for some orbitals use an n value less by one unit.

The calculated values (b) refer to the mean of singlet and triplet states.

State No. 23 has been observed, but with uncertain quantum number.

State No. 43 may be the first member of the Hopfield Rydberg series. The assignments of states Nos. 37, 41, 42, 44 and 45 are uncertain.

Table 6. A-X Rydberg series limits from band head measurements (cm^{-1}).

v'	Series limits	Series limits(av)	$T_o + G_o(v)$[a]
0	134644	134683	134683.3
	134721		
1	136519	136558	136556.3
	136597		
2	138362	138401	138399.5
	138439		
3	140176	140215	140212.9
	140253		
4	141959	141997	141996.5
	142035		
5	143710	143749	143750.2
	143787		
6	145434	145472	145474.1
	145510		
7	147145[b]	147180	147168.2
	147214		

[a] Calculated from the molecular constants of the $A^2\Pi_u$ given by Douglas [205] and the σ_∞ value of the Worley-Jenkins series given by Ogawa and Tanaka [499].

[b] These values correspond probably to the limits of R-form heads instead of those of the Q-form heads and are less reliable than the data for $v' < 7$.

Data from Ogawa et al. [502].

Table 7. Band heads and origins of the $a^1\Pi_g - X^1\Sigma_g^+$ Lyman-Birge-Hopfield system (R)

(a) Emission

λ_R Å	σ_0 cm^{-1}	I	v' - v"	λ_R Å	σ_0 cm^{-1}	I	v' - v"
2601.9			15 - 27	2309.4			10 - 20
2583.7			14 - 26	(2296.1)			4 - 15
2565.2			13 - 25	2290.5			9 - 19
(2546.9)			12 - 24	2278.3			3 - 14
2528.3			11 - 23	2271.7			8 - 18
2509.7			10 - 22	2253.4			7 - 17
(2491.4)			9 - 21	2234.4			6 - 16
2481.7			14 - 25	2216.6	45086.87		5 - 15
2472.6			8 - 20	2198.7			4 - 14
2462.9			13 - 24	2181.1			3 - 13
(2454.6)			7 - 19	2162.3			7 - 16
(2444.1)			12 - 23	2144.0	46614.53		6 - 15
(2436.5)			6 - 18	2125.9	47010.84		5 - 14
2425.1			11 - 22	2108.1			4 - 13
(2418.4)			5 - 17	2090.5		.24	3 - 12
2406.3			10 - 21	2073.0	48210.20	.60	2 - 11
2387.6			9 - 20	2059.0	48538.63		6 - 14
2386.0			14 - 24	2041.2	48964.34		5 - 13
2369.0			8 - 19	2023.5	49391.85		4 - 12
2366.7			13 - 23	2006.0	49820.91	1.95	3 - 11
(2350.5)			7 - 18	1989.6	50251.55	2.75	2 - 10
(2347.6)			12 - 22	1980.1	50492.18		6 - 13
(2332.2)			6 - 17	1972.6	50683.29	1.22	1 - 9
2328.3			11 - 21	1962.4	50947.27		5 - 12
(2314.0)			5 - 16	1955.9		.31	0 - 8

Table 7 (a) Continued

λ_R Å	σ_0 cm^{-1}	I	v' - v''	λ_R Å	σ_0 cm^{-1}	I	v' - v''
1945.0	51404.11	1.85	4 - 11	1530.0		19.4	2 - 3
1927.8		4.30	3 - 10	1523.2			5 - 5
1910.9		6.68	2 - 9	1515.3		23.7	1 - 2
1894.2		4.75	1 - 8	1508.0		1.73	4 - 4
1887.9		.40	5 - 11	1500.8		72.2	0 - 1
1877.7		1.83	0 - 7	1488.6		.81	6 - 5
1870.8		1.25	4 - 10	1478.2			2 - 2
1853.8		4.99	3 - 9	1473.5		1.21	5 - 4
1837.2		12.7	2 - 8	1464.2		62.6	1 - 1
1835.0			6 - 11	1450.1	68951.24	23.7	0 - 0
1820.8		13.1	1 - 7	1444.2		5.55	3 - 2
1804.6	55402.53	6.90	0 - 6	1429.9		20.3	2 - 1
1784.4		2.83	3 - 8	1426.3		.52	5 - 3
1768.1		15.3	2 - 7	1415.9	70617.58	36.8	1 - 0
1752.0	57068.85	28.7	1 - 6	1411.9			4 - 2
1736.1	57588.64	23.7	0 - 5	1397.7			3 - 1
1719.6			3 - 7	1395.9			6 - 3
1703.1	58707.35	6.93	2 - 6	1383.8	72256.08	40.4	2 - 0
1687.4	59254.97	34.2	1 - 5	1381.6		1.21	5 - 2
1671.9	59803.71	52.9	0 - 4	1367.5			4 - 1
1657.6		3.07	3 - 6	1353.6		17.2	3 - 0
1647.3			6 - 8	1339.0		1.24	5 - 1
1626.6	61470.02	20.7	1 - 4	1325.3			4 - 0
1611.4	62047.63	92.6	0 - 3	1312.2		1.32	6 - 1
1599.7		4.86	3 - 5	1298.5		3.14	5 - 0
1591.5			6 - 7	1286.9			7 - 1
1584.4		13.7	2 - 4	1273.2		2.27	6 - 0
1575.7		.80	5 - 6	1262.9			8 - 1
1560.2			4 - 5	1249.3			7 - 0
1554.5	64319.98	100	0 - 2	1226.6			8 - 0
1544.9			3 - 4	1205.3			9 - 0

Air wavelengths are given above 2000 Å and vacuum wavelengths below 2000 Å. R-branch band head data from Herman and Herman [299], Herman [295], Pearse and Gaydon [26], Appleyard [52], and Lofthus [421]. Additional band head data and intensity data are from McEwen [445], who lists only calculated wavelengths which agree with observed wavelengths to within 0.1 Å. Band heads for 3-7, 8-0 and 9-0 are from measurements of Birge and Hopfield [831]. Band heads in parenthesis represent calculated values for bands observed but overlapped by the D-B (4+) system. A band at 1493 Å has been tentatively identified as the 3-3 transition in a low resolution study of auroral emission by Miller et al. [466]. Band origin data is from Lofthus [421], Wilkinson and Houick [660], and Miller [464]. Origins for bands 5-15, 2-11 and 1-9 were calculated from band head positions.

Table 7. (b) Absorption

λ_R Å	λ_S Å	σ_0 cm^{-1}	I	v' - v''
1500.7				0 - 1
1464.5				1 - 1
1450.125	1449.597	68951.15	45	0 - 0
1444.3				3 - 2
1427.0				5 - 3
1415.923	1415.446	70617.46	65	1 - 0
1396.0				6 - 3
1383.823	1383.398	72256.05	90	2 - 0
1382.6				5 - 2
1367.0				4 - 1
1353.664	1353.273	73866.77	100	3 - 0
1339.4				5 - 1
1325.272	1324.916	75449.78	95	4 - 0
1298.506	1298.184	77005.36	95	5 - 0
1273.249	1272.952	78533.22	90	6 - 0
1249.385	1249.116	80033.69	80	7 - 0
1226.812	1226.562	81506.84	65	8 - 0
1205.432	1205.203	82952.86	65	9 - 0
1185.191	1184.951	84371.57	70	10 - 0
1165.935	1165.739	85763.31	55	11 - 0
1147.680	1147.495	87128.12	40	12 - 0
1130.318	1130.152	88466.30	15	13 - 0
1113.807	1113.672	89777.88	5	14 - 0
1098.094		91062.81	2	15 - 0

Band heads are from data of Vanderslice et al [627] supplemented by measurements of Bass [61] and Birge and Hopfield [83]. Additional band heads only tentatively assigned to this transition were obtained by Tanaka et al [599]. Band origins are from Vanderslice et al. [627]; data for the 0-0 band are from a remeasurement of spectra taken by Wilkinson [655]. Intensities are eye estimates from Tilford et al. [34].

Table 8. Band heads and origins of the $a^1\Pi_g - X^1\Sigma_g^+$ Lyman-Birge-Hopfield system of $^{14}N^{15}N$ (R)

λ_R Å	σ_0 cm^{-1}	v' - v''
1355.021	73792.61	3 - 0
1327.019	75350.92	4 - 0
1300.580	76882.72	5 - 0
1275.616	78387.64	6 - 0
1252.007	79866.13	7 - 0
(1229.657)	81318.17	8 - 0
1208.476	82743.91	9 - 0
1188.381	84143.45	10 - 0
1169.304	85516.55	11 - 0

Data from Vanderslice et al. [628]. 8-0 band head position is calculated.

Table 9. Band heads and origins of the $a'^1\Sigma_u^- - X^1\Sigma_g^+$ Ogawa-Tanaka-Wilkinson-Mulliken system (R)

(a) Emission

λ_Q Å	I	v' - v"
1643.84	3	0 - 3
1707.00	4	0 - 4
1774.00	4	0 - 5
1845.64	3	0 - 6
1922.15	2	0 - 7
2004.17	1	0 - 8

Bandhead data from Ogawa and Tanaka [497,498].

(b) Absorption

λ (J=14)	σ_0 cm^{-1}	I	v' - v"	λ (J=14)	σ_0 cm^{-1}	I	v' - v"
1477.061*	67739.31	2	0 - 0	1225.267	81757.88	42	10 - 0
1446.481	69245.56	4	1 - 0	1206.413	83035.97	38	11 - 0
1414.661*	70727.96	8	2 - 0	1188.460	84292.24	34	12 - 0
1387.585	72186.78	16	3 - 0	1171.319	85526.93	28	13 - 0
1360.546	73622.49	22	4 - 0	1154.952	86740.18	24	14 - 0
1334.955	75034.91	30	5 - 0	1139.310	87932.24	20	15 - 0
1310.699	76424.59	38	6 - 0	1124.353	89103.06	16	16 - 0
1287.689	77791.36	52	7 - 0	1110.044	90252.89	10	17 - 0
1265.830	79135.82	60	8 - 0	1096.344	91381.93	6	18 - 0
1245.047	80457.89	48	9 - 0	1083.230	92489.95	4	19 - 0

Data from Tilford et al. [615]. Intensities (eye estimates) from Tilford et al. [34]. Column 1 lists the lines of maximum intentsity. The band head positions under low resolution [604] have wavelengths about 2 Å shorter.

* J = 8.

Table 10. Band heads of the $w^1\Delta_u - X^1\Sigma_g^+$ Tanaka absorption system (R)

λ_H Å	σ_H cm^{-1}	I	v' - v"
(1393.92)	(71740.3)		0 - 0
1364.73	73274.5	1	1 - 0
1337.14	74786.5	2	2 - 0
1311.00	76277.6	3	3 - 0
1286.25	77745.3	3	4 - 0
1262.88	79184.4	4	5 - 0
1240.56	80608.9	5	6 - 0
1219.37	82009.4	7	7 - 0
1199.34	83379.1	6	8 - 0
1180.34	84721.7	6	9 - 0
1162.12	86049.8	5	10 - 0
1144.70	87359.5	4	11 - 0

Data from Tanaka et al [604]. The 0-0 band position is calculated.

Table 11. Bands of the $a''^1\Sigma_g^+ - X^1\Sigma_g^+$ Dressler-Lutz system.

λ_Q Å	σ_0 cm^{-1}	v' - v''
1010.05	98840.30	0 - 0

Diffuse band observed by Dressler and Lutz [212] and Lutz [429]. The band origin is placed at the term value of the a'' state as obtained by Ledbetter [408] in a high resolution study of Rydberg absorption transitions originating in the a'' state. The large difference between the wavenumber of the feature observed by Lutz and the band origin is accounted for by a pressure shift, since the a''-X transition occurs as either a quadrupole transition or a pressure-induced dipole transition.

Table 12. Band heads and origins of the $b^1\Pi_u - X^1\Sigma_g^+$ system (R)

(a) Emission bands at high resolution

λ_H Å	σ_H cm^{-1}	σ_0 cm^{-1}	I	v' - v''
1008.821	99125.6		9 2	1 - 1
1032.796	96824.5	96821.8	10 8	1 - 2
1057.625	94551.5		10 10	1 - 3
1083.333	92307.3		10 10	1 - 4
1109.962	90093.2		8 10	1 - 5

Data from Tilford and Wilkinson [613]. Intensities are for nitrogen in an electrodeless discharge in helium and neon, respectively. Additional band heads, but at low resolution, were observed long ago by Birge and Hopfield [83] for transitions 1-7 to 1-15. The Birge and Hopfield wavelengths are smaller than those of Tilford and Wilkinson by an average of 0.2 Å.

Table 12. (b) High resolution absorption

λ_H Å	σ_0 cm^{-1} [a]	σ_0 cm^{-1} [b]	v' - v''	old designation
1015.316	98487.1		0 - 1	i_1
1008.809	99121.9		1 - 1	i_2
1001.729	99822.8		2 - 1	i_3
994.660	----		3 - 1	i_4
991.851	100816.9	100817.5	0 - 0	j
987.917	----		4 - 1	i_5
985.632	101451.7	101454.4	1 - 0	b_1
978.887	102151.7	102169.5	2 - 0	b_2
976.805	----		5 - 1	i_6
972.12	102863.6[c]	102919.0	3 - 0	b_3
965.687	103548.8	103688.6	4 - 0	b_4
955.066	104700.2	104473.7	5 - 0	l_2
949.217	105346.4	105268.6	6 - 0	m_1
942.390	106110.6	106064.4	7 - 0[d]	m_2
935.130	106933.3	106850.8	8 - 0	m_3
928.958	107643.5	107620.2	9 - 0[d]	p_1
922.727	108372.4	108370.9	10 - 0	p_2
916.399	109120.0	109107.0	11 - 0	p_3
910.469	109831.1		12 - 0[d]	q_1
904.725	110529.0		13 - 0	q_2
899.185	111210.4		14 - 0	q_3
893.860	111872.8		15 - 0[d]	q_4
888.806	112508.8		16 - 0	q_5
883.945	113127.9		17 - 0	q_6
879.441	113707.0		18 - 0	q_7
875.222	114255.0		19 - 0	q_8
861.839	116029.3		23 - 0	--
859.561	116337.7		24 - 0	--

[a] Data from Carroll and Collins [130]. ΔG's varied irregularly because of strong perturbations.

[b] Deperturbed values from reanalysis by Leoni [414].

[c] Extrapolated origin; perturbed rotational structure [130].

[d] Yoshino et al. [675] have made new observations on these bands. (see their table 7) which yield slightly different values than those of Carroll and Collins. Deperturbed band origins are roughly 20 cm^{-1} larger than those deduced by Leoni.

Table 12. (c) Isotope shifts

$\sigma_H(^{14}N_2)$	$\sigma_H(^{15}N_2)$	$\Delta\sigma$	v' - v''	Old design.
100823.5	100848.3	-24.8	0 - 0	j
101454.9	101459.2	-4.3	1 - 0	b_1
102159.4	102143.7	15.7	2 - 0	b_2
102873	102824	39	3 - 0	b_3
103558.8	103492.7	66.1	4 - 0	b_4
104704.5	104615.2	89.3	5 - 0	ℓ_2(d)
105349.9	105243.8	106.1	6 - 0	m_1
106114.6	105977.2	137.4	7 - 0	m_2
106938.6	----		8 - 0	m_3
107615.7	107433.1	182.6	9 - 0	p_1
108373.1	108150.9	222.2	10 - 0	p_2
109121.6	108871.8	249.8	11 - 0	p_3
109832.9	109566.3	266.6	12 - 0	q_1
110530.3	110239.9	290.4	13 - 0	q_2
111211.3	110905.6	305.7	14 - 0	q_3
111874.5	111556.2	318.3	15 - 0	q_4
112509.5	112184.7	324.8	16 - 0	q_5
113134.2	----		17 - 0	q_6

Data from Ogawa et al. [500]. The strongest band of this progression was 3-0.

Table 13. Band heads and origins of the $b'^1\Sigma_u^+ - X^1\Sigma_g^+$ system (R)

(a) Emission bands at high resolution

λ_H Å	σ_H cm^{-1}	σ_0 cm^{-1}	I	v' - v''	Old design.	λ_H Å	σ_H cm^{-1}	σ_0 cm^{-1}	I	v' - v''	Old design.
1288.301	77621.6	77618.2		0 - 12	b_1'	1057.61	94553.			0 - 4	b_1'
1255.759	79633.1	79629.7		0 - 11	b_1'	1049.604	95274.0		1 0	1 - 4	b_2'
1244.160	80375.5	82372.8		1 - 11	b_2'	1048.335	95389.4		2 0	7 - 6	g
1224.356	81675.6			0 - 10	b_1'	1042.013	95968.1		3 3	5 - 5	b_6'
1213.346	82416.7			1 - 10	b_2'	1041.604	96005.8		2 2	2 - 4	b_3'
1202.657	83149.2			2 - 10	b_3'	1034.660	96650.1	96648.2	9 7	9 - 6	f
1194.100	83745.1			0 - 9	b_1'	1034.659	96650.2			6 - 5	b_7'
1183.615	84486.9	84483.6		1 - 9	b_2'	1032.79	96825.			0 - 3	b_1'
1173.443	85219.3			2 - 9	b_3'	1024.680	97591.4	97589.5	2 2	7 - 5	g
1164.897	85844.5			0 - 8	b_1'	1018.524	98181.3	98179.0	6 2	5 - 4	b_6'
1154.918	86586.2	86583.0		1 - 8	b_2'	1017.841	98247.2		1 0	2 - 3	b_3'
1145.231	87318.6	87315.4		2 - 8	b_3'	1011.775	98836.2	98834.9	9 7	9 - 5	f
1136.719	87972.5			0 - 7	b_1'	1011.73	98841.			6 - 4	b_7'
1135.832	88041.2			3 - 8	b_4'	1010.428	98968.0		2 3	3 - 3	b_4'
1127.225	88713.4	88711.8	8 10	1 - 7	b_2'	1001.995	99800.9		2 1	7 - 4	g
1123.323	89021.6		1 2	7 - 9	g	995.774	100424.4	100421.8	4 0	5 - 3	b_6'
1117.984	89446.7		6 9	2 - 7	b_3'	995.676	100434.3			2 - 2	b_3'
1109.109	90162.5		6 6	3 - 7	b_4'	989.599	101051.0		5 1	9 - 4	f
1109.08	90165.			6 - 8	b_7'	980.45	101994.			1 - 1	b_2'
1107.863	90263.9	90262.4	8 9	9 - 9	f	979.995	102041.3		8 2	7 - 3	g
1100.467	90870.5	90867.6	4 9	1 - 6	b_2'	973.73	102698.		3 0	5 - 2	b_6'
1097.440	91121.5		4 2	7 - 8	g	968.106	103294.5		5 2	9 - 3	f
1091.654	91604.1		5 7	2 - 6	b_3'	964.564	103673.8			0 - 0	b_1'
1083.32	92309.		- -	0 - 5	b_1'	958.549	104324.4	104321.0	2 2	7 - 2	g
1083.167	92321.9		- 2	3 - 6	b_4'	957.58	(104430.)		- -	1 - 0	b_2'
1082.669	92364.3		3 1	9 - 8	f	950.85	(105169.)		- -	2 - 0	b_3'
1074.602	93057.7		3 6	1 5	b_2'	947.266	105567.0		4 2	9 - 2	f
1072.384	93250.2	93246.1	5 5	7 - 7	g	944.525	105873.3		3 0	3 - 0	b_4'
1066.270	93784.9		5 5	5 - 6	b_6'	937.866	106625.0	106621.8	3 1	7 - 1	g
1066.195	93792.4		5 5	2 - 5	b_3'	927.056	107868.4	107867.0	4 -	9 - 1	f
1058.319	94489.5		7 7	9 - 7	f	907.445	110199.6		1 -	9 - 0	f
1058.053	94513.2	94510.2	6 6	3 - 5	b_4'						

Data from Wilkinson and Houk [660] and Tilford and Wilkinson [613]. Intensities are for nitrogen in an electrodeless discharge in helium and in neon, respectively. Additional band heads, but at low resolution, are given by Birge and Hopfield [83]. This extends the progression till 0-21 at 1644 Å. Positions of the weak 1-0 and 2-0 bands are very uncertain [660]. A band reported by Wilkinson and Houk and labelled as 4-0 lies very close to the 7-1 band, and is assumed to be 7-1.

Table 13. (b) Emission at moderate resolution

λ_H (Å)	σ_H cm^{-1}	σ_0 cm^{-1}	v' - v"	λ_H (Å)	σ_H cm^{-1}	σ_0 cm^{-1}	v' - v"
1643.65	60840.2	60839.3	0 - 21	1494.57	66908.8	66905.0	1 - 18
1623.85	61582.0	61579.0	1 - 21	1470.67	67996.2	67992.9	0 - 17
1597.78	62586.8	62583.2	0 - 20	1431.32	69865.5	69863.4	0 - 16
1579.10	63327.2	63324.7	1 - 20	1393.57	71758.1	71755.9	0 - 15
1553.76	64360.0	64358.4	0 - 19	1357.18	73682.2	73679.5	0 - 14
1536.06	65101.6	65099.1	1 - 19	1322.14	75635.0	75633.3	0 - 13
1511.32	66167.3	66163.5	0 - 18				

Data in the range 1644-1322 Å are taken from Tschulanowsky [618], who mentioned a number of irregularities, line weakenings, and displacements. Many low J lines were not resolved. B'_0 had been determined only from bands with v" = 17-20 which contained the most extensive branches.

Table 13. (c) High resolution absorption bands

λ_H Å	σ_0 cm^{-1} [a]	σ_0 cm^{-1} [b]	v' - v"	Old notation	λ_H Å	σ_0 cm^{-1} [a]	σ_0 cm^{-1} [b]	v' - v"	Old notation
964.564[c]	103670.8[c]	103701.4	0 - 0	b'_1	875.875	114170.2	114184.9	15 - 0	r_6
957.634	104418.7	104452.5	1 - 0	b'_2	871.404	114754.5	114816.8	16 - 0	r_7
950.991	105151.6	105195.6	2 - 0	b'_3	866.771	115369.6	115437.8	17 - 0	r_8
944.537	105869.2	105931.2	3 - 0	b'_4	860.511	116206.6	116047.3	18 - 0	-
937.653	106646.9	106659.5	4 - 0	b'_5	857.011	116682.8	116644.7	19 - 0	s_1
931.716	107326.7	107380.8	5 - 0	b'_6	853.196	117205.2	117229.3	20 - 0	s_2
925.911	107999.3	108095.2	6 - 0	b'_7	849.738	117681.3	117800.5	21 - 0	s_3
917.805	108950.8	108802.7	7 - 0	g	843.976	118485.4	118357.6	22 - 0	t_1
912.853	109544.1	109503.1	8 - 0	-	840.552	118968.4	118900.0	23 - 0	t_2
907.447	110197.4	110196.4	9 - 0	f	837.300	119430.8	119427.2	24 - 0	t_3
901.343	110942.3	110882.1	10 - 0	r_1	834.465	119834.3	119938.6	25 - 0	-
896.187	111581.3	111560.0	11 - 0	r_2	829.282	120585.7	120433.8	26 - 0	u_1
890.946	112238.2	112229.7	12 - 0	r_3	826.190	121035.6	120911.8	27 - 0	-
885.652	112908.5	112890.8	13 - 0	r_4	823.359	121451.7	121372.9	28 - 0	-
880.743	113539.2	113542.7	14 - 0	r_5					

[a] Data from measurements of Carroll et al. [132].

[b] Deperturbed values from reanalysis by Leoni [414]. These values are based on use of an incorrect value for σ_0 (0-0).

[c] The 0-0 band head was measured by Wilkinson and Houk [660], whose value for the band origin was calculated from this head. A misprinted value too large by 3 cm^{-1} was used by Leoni in his fit.

Table 13. (d) Isotope shifts

$\sigma_H(^{14}N_2)$	$\sigma_H(^{15}N_2)$	$\Delta\sigma$	v' - v"	Old notation	$\sigma_H(^{14}N_2)$	$\sigma_H(^{15}N_2)$	$\Delta\sigma$	v' - v"	Old notation
----	----		0 - 0	b'_1	112908.7	112624.1	284.6	13 - 0	r_4
104421.9	104422.2	-0.3	1 - 0	b'_2	113541.1	113254.1	287.0	14 - 0	r_5
----	----		2 - 0	b'_3	114170.7	113868.9	301.8	15 - 0	r_6
----	----		3 - 0	b'_4	114756.0	114472.3	283.7	16 - 0	r_7
106649.1	106568.9	80.2	4 - 0	b'_5	115370.3	115053.9	316.4	17 - 0	r_8
107327.6	107227.3	100.3	5 - 0	b'_6	----			18 - 0	
108001.2	107871.9	129.3	6 - 0	b'_7	116688.0	116346.7	341.3	19 - 0	s_1
----			7 - 0	g	117204.4	116869.0	335.4	20 - 0	s_2
----			8 - 0	g'	117685.5	117352.5	333.0	21 - 0	s_3
----			9 - 0	f	118486.0	118127.0	359.0	22 - 0	t_1
110944.3	110720.5	223.8	10 - 0	r_1	118967.8	118601.0	366.8	23 - 0	t_2
111582.6	111350.4	232.2	11 - 0	r_2	119428.8	119060.7	368.1	24 - 0	t_3
112238.4	111986.5	251.9	12 - 0	r_3	119887.9	119492.5	395.4	25 - 0	t_4

Data from Ogawa et al. [500].

Table 14. $(N_2^+ X^2\Sigma_g^+)\ c_n\ ^1\Pi_u - X^1\Sigma_g^+$ Worley-Jenkins Rydberg series.

n	Q head (Å)	σ_H(cm^{-1})	R head (Å)	σ_H(cm^{-1})	σ_0(cm^{-1})	v' - v''	n	Q head (Å)	σ_H(cm^{-1})	R head (Å)	σ_H(cm^{-1})	σ_0(cm^{-1})	v' - v''
3	----		960.209	104144.0[a]	104138.2[a,b]	0 - 0	14	799.708	125045.6	799.684	125049.4		0 - 0
	----		938.564	106545.7	b	1 - 0		----		785.986	127228.7		1 - 0
	920.46	108641	920.041	108690.8	b	2 - 0	15	----		799.143	125134.0		0 - 0
	902.578	110793.7	----			3 - 0		----		785.494	127308.4		1 - 0
	886.246	112835.5	886.030	112863.0	----	4 - 0	16	----		798.711	125201.7		0 - 0
4	865.306	115566.0	865.060	115598.9	115565.53	0 - 0		----		785.079	127375.7		1 - 0
	849.284	117746.3	----		117747.3	1 - 0	17			798.359	125256.9		0 - 0
	834.100	119889.7	----		119890.0	2 - 0				784.739	127430.9		1 - 0
5	835.154	119738.4	834.939	119769.2	119739.07	0 - 0	18			798.067	125302.7		0 - 0
	820.211	121919.8	820.028	121947.1		1 - 0				784.459	127476.4		1 - 0
6	821.224	121769.5	821.100	121787.8	121770.29	0 - 0	19			797.829	125340.2		0 - 0
7	813.702	122895.1	813.626	122906.6		0 - 0				784.226	127514.3		1 - 0
	779.440	125087.5	799.373	125098.0		1 - 0	20			797.614	125374.0		0 - 0
8	808.971	123613.8	808.901	123624.5	123616.2	0 - 0				784.037	127545.0		1 - 0
	794.995	125787.0	794.922	125798.5		1 - 0	21			797.434	125402.3		0 - 0
9	805.951	124077.0	805.889	124086.6		0 - 0	22			797.284	125425.8		0 - 0
	----		792.034	126257.2		1 - 0	23			797.143	125448.0		0 - 0
10	803.853	124400.9	803.813	124407.0		0 - 0	24			797.026	125466.4		0 - 0
	----		790.004	126581.7		1 - 0	25			796.928	125481.9		0 - 0
11	802.353	124633.4	802.324	124637.9		0 - 0	26			.840	125495.7		0 - 0
	----		788.547	126815.6		1 - 0	27			.759	125508.5		0 - 0
12	----		801.147	124821.1		0 - 0	28			.686	125520.0		0 - 0
	----		787.472	126988.7		1 - 0	29			.625	125529.6		0 - 0
13	800.377	124941.1	800.347	124945.8		0 - 0	30			.564	125539.2		0 - 0
	----		786.644	127122.3		1 - 0	31			.510	125547.7		0 - 0
							32			.460	125555.6		0 - 0

Data on band heads is from Carroll and Yoshino [142], Ogawa and Tanaka [499], and Worley [666]. (See also Carroll and Yoshino [141]). The n=3, 3-0 band head was listed by Worley as an R head, though it seems to be the Q head, which lies close to the band origin. For n=12, the R head observed by Ogawa and Tanaka is about 7 cm^{-1} larger than that estimated from a Rydberg series formula. Carroll and Yoshino [142], in more recent work at higher resolution, find this region very diffuse, so this band position remains uncertain.

As n increases, the separation between Q and R band heads does not approach a constant value of about 52 cm^{-1} as might be expected from a simplified head-origin calculation. This is because of g-uncoupling. The series limit deduced from the band heads at high n likely has an uncertainty of 5 cm^{-1}. A tentative value for the series limit is 125667.5 cm^{-1} (K. Yoshino, private communication).

Band origin data is from Carroll and Yoshino [142] and Ledbetter [408]. Ledbetter's estimated precision is .1 cm^{-1}; the band origins are assumed uncertain by .07 cm^{-1}. Carroll [130] estimated the wavenumber accuracy as .5 - .8 cm^{-1} in going from 1000 to 800 Å: relative accuracy of unblended lines was about .3 cm^{-1}.

[a] The $c_3(0)$ band head is from K. Yoshino (private communication). Uncertainty in the origin is estimated as 0.2 cm^{-1}.

[b] Deperturbed origins from the results of Leoni [414] for c_3 - X(0) bands are: 0-0, 104392.4; 1-0, 106555.2; 2-0, 108690.9.

Table 15. Band heads and origins of the $(N_2^+ X^2\Sigma_g^+)$ $c_n' {}^1\Sigma_u^+ - X^1\Sigma_g^+$ Carroll-Yoshino Rydberg series.

(a) Emission

λ_H Å	σ_H cm^{-1}	σ_0 cm^{-1}	I	v' - v"	Old notation
1077.113	92840.8		8 8	4 - 9	h
1053.292	94840.4		2 2	4 - 8	h
1052.405	95020.5		- 3	1 - 5	r'
1030.141	97074.9		2 3	4 - 7	h
1028.439	97234.7		3 1	1 - 4	r'
1007.764	99229.6		3 3	4 - 6	h
1007.026	99302.3		3 4	3 - 5	s'
1005.988	99403.8		2 1	2 - 4	k
1005.266	99476.2	99465.2	4 1	1 - 3	r'
1003.089	99692.1		2 0		
1002.783	99722.5		3 1	0 - 2	p'
1002.558	99744.9		3 1		
986.037	101416.1		5 3	4 - 5	h
985.051	101517.6		8 6	3 - 4	s'
983.821	101644.5	101641.1	5 3	2 - 3	k
982.808	101749.3	101737.3	5 0	1 - 2	r'
980.502	101988.6		8 2		
980.159	102024.3	101993.1	8 2	0 - 1	p'
979.995	102041.3		8 2		
964.853	103642.7		2 1	4 - 4	h
963.721	103764.5		5 2	3 - 3	s'
962.305	103917.2		4 1	2 - 2	k
961.102	104047.2	104038.6	4 -	1 - 1	r'
943.113	106031.8	106025.6	4 2	3 - 2	s'
941.464	106217.6		1 0	2 - 1	k
923.070	108334.2	108327.2	3 -	3 - 1	s'

Emission data from Tilford and Wilkinson [613]. The 0-1 and 0-2 bands are seemingly triple-headed (see sect. 3.5). Intensities are for nitrogen in an electrodeless discharge in helium and in neon, respectively.

Table 15. (b) High resolution absorption

n	λ_H Å	σ_0 cm^{-1} a	σ_0 cm^{-1} b	v' - v"	Old notation
4	958.139	104 323.3	104 437.8	0 - 0	p'
	940.034	106 369.5	106 592.2	1 - 0	r'
	921.232	108 545.0	108 702.8	2 - 0	k
	903.630	110 657.2	110 774.5	3 - 0	s'
	886.700	112 768.9	112 812.2	4 - 0	h
	870.755	114 830.2	114 821.0	5 - 0	h'
	855.998	116 806.8	116 805.8	6 - 0	h"
	841.914	118 765.9	118 771.5	7 - 0	h"'
	828.538	120 685.3	120 723.2	8 - 0	--
5	863.158	115 849.8		0 - 0	
	846.919	118 071.6		1 - 0	
	831.984	120 191.3		2 - 0	
6		119 940.6		0 - 0	
			122 109.4[c]	1 - 0[c]	
7		121 866.7		0 - 0	
8		122 965.3		0 - 0	
9		123 659.7		0 - 0	

[a] Data from Carroll et al. [132], and Carroll and Yoshino [142]. Preliminary data had been obtained by Carroll and Yoshino [141].

[b] Deperturbed values from data of Leoni [414]. Leoni's back-calculated σ_0's differ from the observed values by 4-22 cm^{-1}.

[c] Data of Yoshino et al. [675]. In addition, a new observation on c_4 -X, 0-0 gives σ_0=104322.6; σ_0 (deperturbed) = 104138.2 ± 0.2, the latter differing considerably from Leoni's values.

Table 15. (c) Isotope shifts

$\sigma_H(^{14}N_2)$	$\sigma_H(^{15}N_2)$	$\Delta\sigma$(cm^{-1})	v' - v"	Old notation
104 365.6	104 362.6	3.0	0 - 0	p'
106 381.4	105 319.0	62.4	1 - 0	r'
108 549.4	108 400.3	149.1	2 - 0	k
110 664.2	110 482.3	181.9	3 - 0	s'
112 777.4	112 542.8	234.6	4 - 0	h
114 841.4	114 536.8	304.6	5 - 0	h'
116 819.6	116 491.8	327.8	6 - 0	h"
118 778.0	118 354.7	423.3	7 - 0	h"'

Data from Ogawa et al. [500].

Table 16. $(N_2^+ \quad X^2\Sigma_g^+)$ $c_n\ ^1\Pi_u$ + a'' $^1\Sigma_g^+$ Ledbetter Rydberg series (5980 - 4360 Å).

λ Å	σ_0 cm^{-1}	v' - v''
5977.4	16725.12	0 - 0
4783.6	20898.71	0 - 0
4359.8	22930.15	0 - 0

Data from Ledbetter [408]. The bands are headless.

The bands correspond to c_4, c_5, c_6.

Table 17. Rydberg series converging to the $N_2^+ \quad A^2\Pi_u$ state.

Bands of the $o^1\Pi_u - X^1\Sigma_g^+$ Worley third (A-X(I)) Rydberg series.

(a) High resolution absorption

n	λ_R Å	σ_0 cm^{-1}	Method	v' - v''
3	946.132	105 682.8	a	0 - 0
		105 682.7	b	
		105 710.4	c	
	928.887	107 637.5	a	1 - 0
		----		
		107 636.7	c	
	912.632	109 561.6	a	2 - 0
		----		
		109 563.0	c	
	897.193	111 447.3	a	3 - 0
		111 447.3	b	
		111 448.2	c	
	882.459	113 306.9	a	4 - 0
		113 306.3	b	

4	818.536	122 155.4	a,b	0 - 0

Data from Yoshino et al. [675]. (a) Origin without any deperturbation; (b) with heterogeneous deperturbation; (c) with homogeneous deperturbation.

An earlier value for $o_3(0)$ - X(0) can be obtained from [346].

(b) Isotope shift

$^{14}N_2$			$^{15}N_2$			
λ_H Å	σ_H cm^{-1}	I	λ_H Å	σ_H cm^{-1}	I	v' - v''
946.051	105 702.5	1	946.496	105 652.8	2	0 - 0
928.874	107 657.2	6	929.484	107 586.6	5	1 - 0
912.619	109 574.7	7	913.600	109 457.1	7	2 - 0
897.183	111 460.0	5	898.655	111 277.4	3	3 - 0
882.466	113 318.8	2	884.395	113 071.7	2	4 - 0

Data from Ogawa, Tanaka and Jursa [500].

Table 17.(c) Band heads of the $A^2\Pi_{u\frac{1}{2}}$ - X (I) $o^1\Pi_u$ Rydberg series (cm^{-1}).

	v'=0		v'=1		v'=2		v'=3	
n	σ_H	n*	σ_H	n*	σ_H	n*	σ_H	n*
3	105682.1	1.9439	107647.9	1.9469	109560.4	1.9493	111446.7	1.9518
	693.5		655.7		573.2		458.7	
4	122154.0	2.9550						
	169.4							
5	7655.0	3.9408	129597.7	3.9559	131392.3	3.9462	133239.7	3.9554
	670.7		615.9		403.3		257.0	
6	130226.9	4.9415	132102.4	4.9411	3938.9	4.9381	5762.3	4.9433
	243.1		114.1		949.8		774.6	
7	1602.8	5.932	3485.8	5.939	5326.9	5.938	7135.9	5.9333
	617.8		496.0		338.9		151.8	
8	2440.0	6.936	4310.8	6.928	6161.6	6.941	7970.7	6.9340
	451.9		323.1		169.2		979.5	
9	2981.2	7.942	4851.0	7.929	6695.2	7.932		
	988.9		862.2		706.2		8518.3	
10	3345.5	8.932	5219.1	8.924	7062.4	8.928	8875.4	8.925
	358.2		229.2		072.7		883.7	
11	3607.3	9.926	5481.7	9.919	7326.4	9.931	9138.0	9.921
	617.5		491.1		334.6			
12	3802.3	10.929	5675.5	10.913	7519.6	10.925	9331.3	10.911
					529.0			
13	3950.6	11.93	5823.1	11.91	7667.6	11.927	9478.9	11.906
14	4064.4	12.93	5937.9	12.90	7781.6	12.92	9592.6	12.890
15	4155.5	13.93	6029.3	13.90	7872.9	13.92	9684.0	13.89
16	4227.7	14.91	6102.5	14.90	7946.1	14.92		
17			6169.3	16.02	8006.9	15.94	9823.8	15.99
18			6213.8	16.92	8056.6	16.94	9873.8	17.01
19			6256.7	17.76	8098.5	17.95	9912.4	17.95
20			6291.7	18.96	8132.6	18.92	9948.0	18.97
21			6319.5	19.89	8165.4	20.03	9977.7	19.97
22			6346.0	20.91	8185.6	20.81	140002.8	20.94
23			6367.9	21.89	8212.3	22.00	0025.0	21.94
24			6388.8	22.96			0045.0	22.97
25			6406.7	24.01			0061.6	23.94
26			6422.8	25.10			0076.3	24.92
27			6434.1	25.95			0090.4	25.98
28			6446.8	27.03			0102.1	26.96
29			6457.6	28.06			0112.8	27.98
30			6466.9	29.04			0122.6	29.01
31			6475.1	30.00			0131.4	30.04
32			6483.3	31.07			0138.3	30.93
33			6489.3	31.92				
34			6496.5	33.04				
35			6502.7	34.11				
36			136508.7	35.2				
37			6513.1	36.2				
38			6517.3	37.1				
39			6521.6	38.1				
40			6526.0	39.3				
41			6529.6	40.3				
42			6532.8	41.3				
43			6535.9	42.4				
44			6538.8	43.4				
45			6541.3	44.4				

Table 17. (c) (continued)

	v'=4		v'=5		v'=6		v'=7	
n	σ_H	n*	σ_H	n*	σ_H	n*	σ_H	n*
3	113306.2	1.9544						
	319.3							
4								
5	135025.7	3.9567	136771.1	3.9549				
			782.8					
6	7552.7	4.9479	9300.0	4.9453	141025.6	4.9468	142728.9	4.946
	563.6		310.1		036.3		740.1	
7	8924.6	5.940	140680.6	5.944	2402.4	5.942		
	932.8		688.5		411.9		4098	5.934
8	9758.9	6.943	1509.3	6.941	3227.6	6.934		
	766.3		516.5		241.2		4938	6.944
9	140292.0	7.935	2045.1	7.937	3762.2	7.924		
	301.5		053.8		776.9		5471	7.935
10	0659.1	8.931	2411.9	8.933	4131.7	8.923		
	667.7		419.5		142.4		5841	8.940
11	0921.2	9.926	2669.7	9.910	4396.0	9.925		
	927.6		680.2		409.7		6101	9.952
12	1116.5	10.930	2858.3	10.870	4591.1	10.93		
13	1262.9	11.92	3015.8	11.93				
14	1377.9	12.92	3130.3	12.92				
15	1469.3	13.93	3221.0	13.92				
16	1542.5	14.93	3295.2	14.94				
17	1602.0	15.92	3355.4	15.95				
18	1652.8	16.94	3405.7	16.96				
19	1694.3	17.95	3447.3	17.97				
20	1731.3	19.01	3484.3	19.04				
21	1755.8	19.83	3513.0	20.01				
22	1782.9	20.86	3536.0	20.91				
23	1807.2	21.95						
24	1827.8	23.01						

Data from Ogawa et al. [502].

The doublets represents Q and R heads, the latter at larger wavenumbers. For the v'=0, 1, 4 and 5 series only Q heads are observed beginning with n = 12. For the v'=2 and 3 series only Q heads are given beginning with n = 13.

[a] Wavelengths of the v'=7 series were estimated from an enlarged spectrum on a graph paper. Most of the members of the v'=7 series were diffuse and R and Q heads could not be distinguished.

Table IV. (d) Band heads of the $A^2\Pi_{u\frac{3}{2}}$ - X(II) $^3\Pi_u$ Rydberg series (cm^{-1})

	v'=0		v'=1		v'=2		v'=3	
n	σ_H	n*	σ_H	n*	σ_H	n*	σ_H	n*
5	127226.9	3.8464	129113.5	3.8494	130949.7	3.8477	132773.5	3.8502
	246.8		132.0		957.1		783.4	
6	9991.9	4.857	131872.2	4.860	3719.8	4.8620	5536.6	4.8634
	130002.8		885.2		727.7		545.5	
7	1474.7	5.884	3345.5	5.880	5194.9	5.886	7005.8	5.883
	486.5		358.2				019.6	
8	2360.6	6.932	4227.6	6.920	6069.6	6.919	7892.3	6.932
	371.6		237.1		085.8		897.8	
9	2899.5	7.931	4774.6	7.931	6617.8	7.932	8430.1	7.928
	909.8		785.3		628.4		440.5	
10	3268.7	8.933	5144.2	8.934	6988.1	8.937	8794.5	8.913
	284.1		155.9		998.9		802.8	
11	3531.4	9.931	5407.3	9.935	7251.0	9.938	9064.8	9.938
					263.1			
12	3727.7	10.943	5601.6	10.937	7445.6	10.943	9258.9	10.939
					455.6			
13	3876.3	11.95			7592.9	11.94	9406.1	11.94
					602.6			
14	3987.0	12.92	5864.6	12.949	7707.9	12.95	9520.1	12.93
					714.3			
15	4076.0	13.90	5955.0	13.949	7797.7	13.94	9604.9	13.86
16	4150.4	14.91	6029.3	14.970	7872.9	14.98	9681.0	14.89
17			6085.7	15.91	7930.2	15.94	9742.2	15.91
18			6140.0	17.02	7979.5	16.94	9794.2	16.95
19			6180.0	17.99	8023.8	18.01	9835.0	17.94
20			6213.8	18.96	8056.6	18.96	9869.7	18.93
21			6244.2	19.98	8085.9	19.94	9898.7	19.89
22			6270.0	20.99	8110.2	20.88	9924.4	20.88
23			6291.7	21.97	8132.6	21.87	9946.7	21.90
24			6312.5	23.05	8151.6	21.84	9967.3	22.93
25			6328.0	23.97	8172.7	24.08	9984.8	23.96
26			masked		8185.6	24.94	9997.1	24.77
27			masked				140011.6	25.84
28			6367.9	26.95			0025.0	26.96
29			6378.7	27.97			0035.9	27.98
30			6388.8	29.03			0045.0	28.94
31			6396.6	29.94			0051.8	29.72
32			6404.0	30.89			0061.6	30.97
33			6410.9	31.86			0069.1	32.04
34			6419.2	33.16			0076.3	33.18
35			136426.5	34.44				
36			6430.4	35.2				
37			6434.1	35.9				
38			6438.5	36.9				
39			6442.0	37.7				
40			6446.8	39.0				
41			6450.9	40.2				

Table 17.(d) (Continued)

	v'=4		v'=5		v'=6		v'=7[a]	
n	σ_H	n*	σ_H	n*	σ_H	n*	σ_H	n*
5	134562.2	3.8517	136293.6	3.8446				
	570.6		309.4					
6	7317.7	4.8624	9103.3	4.8806	140772.3	4.8518		
	326.4		111.2		782.4			
7	8794.5	5.889	140549.2	5.892	2273.8	5.893		
	802.8		557.9		285.3			
8			1415.1	6.915	3143.4	6.922		
	9684.1		429.8		159.8		144854	6.921
9	140214.4	7.931	1967.9	7.937	3692.6	9.938		
	223.7		977.2		702.9		5391	7.91
10	0583.2	8.931	2338.6	8.945				
	594.0		345.4				5760	8.90
11	0842.3	9.913	2601.0	9.947	4325	9.95		
	847.6						6030	9.92
12	1036.3	10.905	2790.0	10.921	4518.8	10.95		
	042.2							
13	1183.5	11.90	2941.9	11.95				
	190.5							
14	1298.1	12.89	3050.4	12.90				
15	1396.8	13.97	3142.5	13.91				
16	1463.4	14.88						
17	1525.2	15.91	3267.6	15.75				
18	1570.9	16.82	3321.2	16.80				
19	1614.5	17.85						
20	1652.8	18.93						
21	1684.0	19.98						
22	1708.0	20.91						
23	1731.3	21.95						

Data from Ogawa et al. [502].

[a] Wavelengths of the v'=7 series were estimated from an enlarged spectrum on a graph paper. Members of the v'=7 series were diffuse, and the different heads could not be distinguished.

Table 18. Rydberg series converging to the $N_2^+ B^2\Sigma_u^-$ state.

(a) Hopfield's Rydberg series (absorption series)

	v' = 0			v' = 1		
n	$\sigma_H(cm^{-1})$	I	n*	$\sigma_H(cm^{-1})$	I	n*
4	138330	10	2.916			
5	144090	10	3.919			
6	146690	9	4.915	149062	5	4.915
7	148104	8	5.922			
8	148944	7	6.924	151015	2	6.924
9	149484	6	7.925	151856	1	7.923
10	149855	6	8.924	152226	1	8.924
11	150119	5	9.925	152490	0	9.925
12	150313	4	10.92	152672	0	10.83
13	150448	3	11.82	152821	0	11.84
14	150559	3	12.76			
15	150647	3	13.68			
16	150722	2	14.65			
17	150784	2	15.65			
18	150834	2	16.58			
19	150879	0	17.61			
20	150916	0	18.61			
21	150945	0	19.52			

σ_∞ = 151233 σ_∞ = 153604

Data from Ogawa and Tanaka [499].

(b) Series accompanied by the Hopfield "emission" series.

	v' = 0		
n	$\sigma_H(cm^{-1})$	I	n*
4	139624	6	3.075
5	144676	6	4.092
6	147009	5	5.098
7	148289	5	6.107
8	149062	4	7.113
9	149566	4	8.118
10	149900	3	9.080
11	150161	2	10.13
12	150344	1	11.12

σ_∞ = 151231

Data from Ogawa and Tanaka [499]. This absorption series appeared to the long wavelength side of the Hopfield emission series. (See section 3.25a).

Table 19. Observed bands of the Codling Rydberg Series $(C^2\Sigma_u^+) \leftarrow X^1\Sigma_g^+$ (555-490 Å).

v' - v''	λ_H Å	σ_H cm^{-1}
0 - 0		178420[a]
1 - 0	554.10[b]	180470
2 - 0	548.00	182480
3 - 0	542.11	184460
4 - 0	536.41	186420
5 - 0	530.86	188370
6 - 0	525.54	190280
7 - 0	520.46	192140
8 - 0	515.61	193950
9 - 0	510.93	195720
10 - 0	506.35	197490
11 - 0	502.02	199200
12 - 0	497.77	200900
13 - 0	493.71	202550
First Rydberg State: Effective Quantum Number n*=3.040		
3 - 0	527.33	189630
4 - 0	521.89	191610
5 - 0	516.71	193530
6 - 0	c	
7 - 0	506.71	197350
8 - 0	502.02	199200
Second Rydberg State: Effective Quantum Number n*=4.059		
8 - 0	496.15	201550
Third Rydberg State: Effective Quantum Number n*=5.05. Data from Codling [162].		

[a] Estimated (0-0) level, assuming a correct analysis of the band sytem.

[b] Estimate of the limits of error ± .08 Å for observed bands.

[c] Masked

[d] Overlaps (11-0) band of first Rydberg state.

Table 20. Band heads and origins of the $^1\Sigma_u^+ - a\,^1\Pi_g$ and $^1\Pi_u - a\,^1\Pi_g$ Gaydon-Herman systems.

λ_H Å		σ_0 cm^{-1}	v' - v''	Notation New	Old	λ_H Å		σ_0 cm^{-1}	v' - v''	Notation New	Old
3661.1	V		0 - 5	c_4'	p'	2746.2	R	36394.5	6 - 0	b	m
3463.3	V	(38874.0)	0 - 4	c_4'	p'	2744.3	V		2 - 2	c_3	d''
3416.5	R		5 - 4	b	d	2723.6	R	(36731)	0 - 0	o	o
3283.3	V		0 - 3	c_4'	p'	2699.9	V		0 - 6	c_4	e
3241.3	R		1 - 1	b	b	2678.5	RQ		4 - 4	c_4'	h
3240.8	R		5 - 3	b	d	2671.7	VQ	37417.1	1 - 0	c_4'	r'
3175.0	R		6 - 3	b	m	2626.2	V		2 - 1	c_3	d''
3118.6	V		0 - 2	c_4'	p'	2603.3	RQ	38400.5	3 - 2	c_4'	s'
3079.9	R		5 - 2	b	d	2592.8	V		0 - 5	c_4	e
3075.1	R	32500.33	1 - 0	b	b	2569.6	RQ	38901.5	4 - 3	c_4'	h
3020.3	R	33090.0	6 - 2	b	m	2558			0 - 2	d'	d'
3008.1	V		2 - 4	c_3	d''	2524.9	R	39593.5	2 - 0	c_4'	k
2980.1	R	(33522.0)	0 - 1	c_3	ℓ	2516.0	V	(39745.0)	2 - 0	c_3	d''
2967.0	V		0 - 1	c_4'	p'	2498.6	R	40000.7	7 - 0	b'	g
2932.0	R		5 - 1	b	d	2496.8	RQ		3 - 1	c_4'	s'
2877.9	R	34728.4	6 - 1	b	m	2492.4	V		0 - 4	c_4	e
2871.3	V	(34829.0)	2 - 1	c_3	d''	2455.1			0 - 1	d'	d'
2853.3	R		0 - 1	e	e	2397.8	V		0 - 3	c_4	e
2839.4	R	(35188.0)	0 - 0	c_3	ℓ	2397.1	RQ	41705.3	3 - 0'	c_4'	s'
2827.1	V	35371.2	0 - 0	c_4'	p'	2371.6	RQ	42150.5	4 - 1	c_4'	h
2796.0	VQ		1 - 1	c_4'	r'	2358.8			0 - 0	d'	d'
2795.6	RQ		4 - 5	c_4'	h	2308.6	V		0 - 2	c_4	e
2795.4	R		5 - 0	b	d	2281.5	RQ	43816.5	4 - 0	c_4'	h
2753.8	R	36288.6	2 - 2	c_4'	k	2224.4	V		0 - 1	c_4	e

R and V indicate bands degraded to longer and shorter wavelengths, respectively.

Q indicates that the Q head is listed.

Data from Gaydon [249], Herman [295], Janin [342,343,345,346], Janin and Crozet [347], Rajan [538], and Lofthus [423]. For notations, see Figure 4. The band origins in parentheses are from Janin's partial rotational analysis. A band c_4' - a, 4-2 is expected at 2467.7 Å [249]. Intensities can be found in Pearse and Gaydon [26].

Table 21. Band heads and origins of the $x^1\Sigma_g^- - a'^1\Sigma_u^-$ Fifth Positive system (V).

λ_H Å	σ_0 cm^{-1}	I	v' - v"	λ_H Å	σ_0 cm^{-1}	I	v' - v"
3065.6	32615.65		2 - 12	2411.8	41457.9	7	1 - 4
3000.6	33322.61		1 - 10	2387.9	41872.8		2 - 5
2844.6	35149.8		2 - 10	2353.6	---	4	0 - 2
2781.6	---	3	1 - 8	2331.1	42893.6	2	1 - 3
2743.2	36449.7	1	2 - 9	2274.3	43966.2	6	0 - 1
2681.5	37289.0	5	1 - 7	2235.9	44721.0	3	2 - 3
2647.1	37771.8	2	2 - 8	2198.9	45472.8	4	0 - 0
2586.6	38655.9	7	1 - 6	2181.5	45834.6	4	1 - 1
2556.2	39116.2	1	2 - 7	2165.2	46179.6	5	2 - 2
2525.6	---	2	0 - 4	2112.1	47341.2	5	1 - 0
2496.7	40045.6	3	1 - 5	2097.9		2	2 - 1
2469.9	40483.1	4	2 - 6	2033.6	49168.4	5	2 - 0

Data from Lofthus [422] and Rajan [538]. Some band heads are from Gaydon [249].

Intensities from Pearse and Gaydon [26].

Isotope shifts

$\lambda_H(^{14}N_2)$ Å	$\lambda_H(^{15}N_2)$ Å	$\Delta\sigma$(obs) cm^{-1}	$\Delta\sigma$(calc) cm^{-1}	v' - v"
2681.5	2663.5	253	251	1 - 7
2647.1	2631.3	227	223	2 - 8
2586.6	2572.7	209	210	1 - 6
2556.2	2543.7	194	192	2 - 7
a	2513.7		181	0 - 4
2496.7	2486.5	164	168	1 - 5
2469.9	2460.6	153	151	2 - 6
2411.8	2404.6	124	119	1 - 4
2331.1	2326.6	82	88	1 - 3
2274.3	2272.0	44	44	0 - 1
2235.9	2234.9	21	29	2 - 3
2198.9	2199.1	-4	-6	0 - 0
2181.5	2182.3	-17	-18	1 - 1
2165.2	2166.4	-27	-29	2 - 2

[a] Obscured in the $^{14}N_2$ spectrum.

Data from Mahon-Smith and Carroll [431].

Table 22. Band heads and origins of the $y^1\Pi_g - a'^1\Sigma_u^-$ Kaplan First system (V).

λ_H Å	σ_0 cm^{-1}	I	v' - v"
2595.36	38525.26	-	2 - 8
2507.84	39869.81	-	2 - 7
2424.72	41236.48	-	2 - 6
2466.0	----	2	0 - 4
2381.7	41979.3	3	0 - 3
2366.4	42251.5	2	1 - 4
2301.9	43437.9	4	0 - 2
2288.6	43687.2	1	1 - 3
2225.9	44920.4	5	0 - 1
2153.6	(46427.0)[a]	4	0 - 0
2077.3	(48132.8)[a]		1 - 0

Data from Lofthus and Mulliken [425], and Carroll and Subbaram [140]. Intensities from Pearse and Gaydon [26].

[a] Origin calculated from data on band head measurements [425].

Isotope shifts

$\lambda_H\,^{14}N_2$ Å	$\lambda_H\,^{15}N_2$ Å	$\Delta\sigma$(obs) cm^{-1}	v' - v"
2381.7	2374.0	136	0 - 3
2366.4	2360.2	110	1 - 4
2301.9	2297.1	92	0 - 2
2225.9	2223.8	43	0 - 1
2153.6	2154.0	-10	0 - 0

Data from Mahon-Smith and Carroll [431].

Table 23. Band heads and origins of the $y^1\Pi_g - w^1\Delta_u$ Kaplan Second System (V)

λ_H Å	σ_0 cm^{-1}	I	v' - v"
2854.9	(35022.4)[a]	-	0 - 5
2831.7	35310.6	-	1 - 6
2741.9	(36465.2)[a]	3	0 - 4
2722.0	36730.6	3	1 - 5
2695.41	37096.76	-	2 - 6
2636.2	37931.0	5	0 - 3
2619.3	38173.4	5	1 - 4
2596.0	38517.75	-	2 - 5
2536.6	39419.9	5	0 - 2
2522.3	39639.0	3	1 - 3
2431.0	41127.8	-	1 - 2
2354.5	42467.5	4	0 - 0
2263.4	44175.4	4	1 - 0

Data from Lofthus and Mulliken [425].
Data on transitions with v'=2 from Carroll and Subbaram [140].
Intensities from Pearse and Gaydon [26].
[a] Origins calculated from band head measurements [425].

Isotope shifts			
$\lambda_H\ ^{14}N_2$ Å	$\lambda_H\ ^{15}N_2$ Å	$\Delta\sigma$ (obs) cm^{-1}	v' - v"
2741.9	2728.0	186	0 - 4
2722.0	2709.4	171	1 - 5
2636.2	2626.6	138	0 - 3
2619.3	2610.3	132	1 - 4
2536.6	2530.8	90	0 - 2
2522.3	2517.2	81	1 - 3
2354.5	2355.2	-13	0 - 0
2263.4	2266.9	-69	1 - 0

Data from Mahon-Smith and Carroll [431].

Table 24. Band heads and origins of the $k^1\Pi_g - a'^1\Sigma_u^-$ Carroll-Subbaram I system.

v' - v"	λ_H(Å)	σ_0(cm^{-1})
0 - 2	2330.44	42903.09
1 - 4	2362.89	42314.39
0 - 3	2412.49	41443.90
1 - 6	2530.45	39512.32

Data from Carroll and Subbaram [140].

Table 25. Band heads and origins of the $k^1\Pi_g - w^1\Delta_u$ Carroll-Subbaram II system.

v' - v"	λ_H(Å)	σ_0(cm^{-1})
0 - 0	2384.46	41932.40
1 - 2	2427.43	41190.56
0 - 1	2475.09	40306.72
1 - 3	2518.47	39701.72
0 - 2	2571.35	38884.59
0 - 3	2673.75	37396.06

Data from Carroll and Subbaram [140].

Table 26. Observed lines of the McFarlane Infrared Systems[a-c]

	(a) $a^1\Pi_g - a'^1\Sigma_u^-$			(b) $w^1\Delta_u - a^1\Pi_g$	
	2 - 1	1 - 0	0 - 0		0 - 0
Q(2)	3011.42_5			Q(4)	2744.89_1
Q(4)	3013.05_6	2880.93_7		Q(5)	2743.69_7
Q(5)	3014.22_8	2882.11_6		Q(6)	2742.26_9
Q(6)	3015.62_2	2883.54_7	1217.99_5	Q(7)	2740.60_5
Q(7)	3017.26_8	2885.20_1		Q(8)	2738.69_3
Q(8)	3019.13_4	2887.10_3	1222.09_2	Q(9)	2736.55_0
Q(9)	3021.24_9	2889.22_3		Q(10)	2734.14_8
Q(10)	3023.58_2	2891.57_7	1227.24_6	Q(11)	2731.53_0
Q(12)	3028.93_7	2897.00_9		Q(12)	2728.63_7
Q(14)	3035.24_3			Q(13)	2725.54_9
σ_0	3010.72_6	2878.580	1212.28	Q(14)	2722.18_6
	(3010:49)	(2878.15)	(1211.84)	Q(15	2718.61_8
B'-B"	0.1167_7	0.1181_8	0.1361	R(2)	2755.50_5
	(0.1168)	(0.1183)	(0.1363)	R(3)	2757.75_2
				R(4)	2759.76_7
				σ_0	2747.29_1
					(2747.6)
				$B'_d-B''_c$	-0.11953_1
				$B'_c-B''_d$	-0.11945_7
				B'-B"	(-0.118)

(a) This is believed to be the first confirmed $^1\Pi-^1\Sigma^-$ transition for a homonuclear molecule [447]. The data in parenthesis comes from UV measurements of Vanderslice et al. [627] and Tilford et al. [615].

(b) Λ-doubling in v=0 of the $a^1\Pi_g$ state is obtained as $B_{oc}-B_{od} = (1.0 \pm 0.3)10^{-4}$ cm^{-1}, which places the c levels above the d levels. This is based on the assumption that Λ-doubling is neglible for the $w^1\Delta_u$ state [449].

(c) B'-B" for w-a is obtained from data of Vanderslice et al. [627] and Lofthus and Milliken [425].

Data from McFarlane, [448,449, and unpublished results], except those given in parentheses which are derived from vacuum UV measurements (see text). These are the longest wavelength emission measurements on N_2.

Table 27. Band heads and origins of the $A^3\Sigma_u^+ - X^1\Sigma_g^+$ Vegard - Kaplan system (R)

(a) Heads

λ_H Å	I^a	I^b	I^c	I^d	I^e	v' - v"	λ_H Å	I^a	I^b	I^c	I^d	I^e	v' - v"
5326		0				2 - 16	2722.5			3			5 - 9
5060		4				0 - 14	2710.1	0		5			2 - 7
4960		2				3 - 16	2666.6			1			4 - 8
4837		8				2 - 15	2655.5	1		0			1 - 6
4718.5		2				1 - 14	2612.8			2			3 - 7
4649.7		4				4 - 16	2603.8	10		8	1.40	2.9	0 - 5
4616.5		3				7 - 18	(2578.7)			0			10 - 11
4605.4		2				0 - 13	2576.0						5 - 8
4534.5		5				3 - 15	(2561.7)			1			12 - 12
4494.6		1				6 - 17	2560.1	2		4			2 - 6
4319.8		2		0.171		1 - 13	2523.4			3			4 - 7
4272.3						4 - 15	2509.8	6		4	0.59	0.44	1 - 5
4219		1				0 - 12	2472.5			3			3 - 6
4171.2		4				3 - 14	2468.4			1			8 - 9
4144		2				6 - 16	2461.6	9		5	0.831	1.4	0 - 4
4072.5		3				2 - 13	2441.8						5 - 7
3979.1		3		0.404		1 - 12	2424.2	0					2 - 5
3948.1						4 - 14	2377.5	7		4	0.168	0.52	1 - 4
3940.3		4				7 - 16	2346.0			3			3 - 5
3889.2		4		0.289		0 - 11	2332.8	4		3	0.224		0 - 3
3854.7		3				3 - 13	2319.7						5 - 6
3766.9						2 - 12	2300.7			0			2 - 4
3749.8		1				5 - 14	2274.0						4 - 5
3682.4				0.664		1 - 11	2257.2			2			1 - 3
3664.5		1				4 - 13	2229.9			0			3 - 4
3603.0		4		0.641		0 - 10	2215.1			0			0 - 2
3581.8						3 - 12	2207.2						5 - 5
3502.7		3				2 - 11	2187.8						2 - 3
3424.6	4		7	0.875	2.5	1 - 10	2164.5						4 - 4
3351.5				1.26		0 - 9	2146.6						1 - 2
3197.5	5		8	0.816	2.9	1 - 9	2123.5						3 - 3
3133				1.92		0 - 8	1726						6 - 0
2997.0	2		9	0.453	2.1	1 - 8	1689						7 - 0
2935.7	9			2.39		0 - 7	1654						8 - 0
2885.4			4			5 - 10	1622						9 - 0
2817.1				0.068		1 - 7	1592						10 - 0
2766.9			1			3 - 8	1563						11 - 0
2760.6	9		8	2.33	3.7	0 - 6	1536						12 - 0

(b) Band origins

σ_0 cm^{-1}	v' - v"
57934.0	6 - 0
59200.2	7 - 0
40607.246	0 - 4
38392.167	0 - 5
36206.048	0 - 6

Band head measurements from Bernard [76], Kaplan [373], Herman [296], Herman and Herman [300], Tanaka and Jursa [600], and Shemansky [570].

For band heads enclosed in parentheses identification is uncertain.

Band origins from Wilkinson [656] and Miller [462]. Uncertainty in Miller's band origins is .003 cm^{-1}.

Intensities are from: [a]Pearse and Gaydon [26]; [b]Bernard [76]; [c]Tanaka and Jursa [600]; [d]Chandraiah and Shepherd [156]; [e]Carleton and Papáliolios [120].

Table 28. Band heads and origins of the $B^3\Pi_g - A^3\Sigma_u^+$ First positive system.

	λ_H Å	σ_0 cm^{-1}	I^a	I^b	I^c	v' - v''	λ_H Å	σ_0 cm^{-1}	I^a	I^b	I^c	v' - v''
P_1	25300					0 - 4	6788.60	14766.37	335	493		4 - 1
	23400					4 - 9	6764.01					11 - 9
	23100					1 - 5	6704.79	14950.40	504	620		5 - 2
	21200					2 - 6	6671.49		34			12 - 10
	19600					3 - 7	6623.57	15133.21	548	624		6 - 3
	18900					0 - 3	6544.88	15314.58	506	256		7 - 4
	18200					4 - 8	6468.62	15494.59	408	435		8 - 5
	17700					1 - 4	6394.66	15673.30	318	319		9 - 6
	(16500)		81			2 - 5	6322.85	15850.77	211	245		10 - 7
	15700		100			3 - 6	6253.06	16027.12	131		6	11 - 8
	14983[a]					0 - 2	6186.75	16199.28				4 - 0
	14300					1 - 3	6185.18	16202.48			2	12 - 9
	13646[e]					2 - 4	6127.33		73	149	2	5 - 1
	(13000)		97			3 - 5	6119.7				1	13 - 10
	12400					0 - 1	6069.66		111	241	4	6 - 2
	11931.03		261			1 - 2	6013.54		154	327	5	7 - 3
	11790.09					9 - 12	5959.01		193	336	5	8 - 4
	11588.51					6 - 8	5906.00		218	394	6	9 - 5
	11519.99		102			2 - 3	5854.40	17115.98	210	394	7	10 - 6
	11169.74					7 - 9	5804.16	17263.76	210		9	11 - 7
	11137.86		102			3 - 4	5755.19	17410.17	170		7	12 - 8
	10781.42					4 - 5	5707.3				3	13 - 9
	10779.87					8 - 10	5660.6				2	14 - 10
	10510.04		1000			0 - 0	5632.67					5 - 0
	10493.71					9 - 11	5615.1				4	15 - 11
	10448.23					5 - 6	5592.53		13		2	6 - 1
	10217.53					1 - 1	5570.6				5	16 - 12
	10136.65					6 - 7	5553.43		17		3	7 - 2
	10075.75					10 - 12	5527.0				5	17 - 13
	9942.03		214	308		2 - 2	5515.32		29		3	8 - 3
	9841.83					7 - 8	5484.2				3	18 - 14
	9682.07		271	334		3 - 3	5478.24		39		3	9 - 4
	9564.88					8 - 9	5442.3				4	19 - 15
	9436.40		252	310		4 - 4	5442.16					10 - 5
	9303.01					9 - 10	5406.98				6	11 - 6
	9203.95		180	224		5 - 5	5401.8				2	20 - 16
	9113.57					10 - 11	5372.11	18646.81			6	12 - 7
	8983.37					6 - 6	5360.4				1	21 - 17
	8912.39	11257.15	1260			1 - 0	5339.4				2	13 - 8
	8819.70					11 - 12	5306.7				2	14 - 9
	8773.72					7 - 7	5275.1				3	15 - 10
	8723.03	11500.40	862	852		2 - 1	5244.1				5	16 - 11
	8574.20					8 - 8	5213.9				6	17 - 12
	8542.54	11742.74	305	228		3 - 2	5184.3				6	18 - 13
	8383.94					9 - 9	5177.52					6 - 0
	8370.12		95			4 - 3	5155.4				5	19 - 14
	8205.50					5 - 4	5151.32					7 - 1
	8201.87					10 - 10	5127.1				4	20 - 15
	8073.58					11 - 11	5099.54				3	21 - 16
	8047.91	12461.83	134	166		6 - 5	5072.2				2	22 - 17
	7896.92	12699.29	166	198		7 - 6	5045.7				1	23 - 18
	7860.57					12 - 12	5020.0				1	24 - 19
	7753.67	12933.31	719	719		2 - 0	5008.9					13 - 7
	7752.03					8 - 7	4994.7				0	25 - 20
	7626.76		833	786		3 - 1	4987.5				0	14 - 8
	7612.93					9 - 8	4966.5				1	15 - 9
	7504.70	13361.13	872	570		4 - 2	4946.4				2	16 - 10
	7479.04					10 - 9	4930.6				3	17 - 11
	7387.19	13572.98	590	786		5 - 3	4911.2				4	18 - 12
	7349.82					11 - 10	4892.4				4	19 - 13
	7273.98	13783.55	362	239		6 - 4	4874.2				4	20 - 14
	7262.40					12 - 11	4856.9				3	21 - 15
	7164.83		161	131		7 - 5	4840.1				2	22 - 16
	7059.48					8 - 6	4823.7				2	23 - 17
	6957.72					9 - 7	4808.4				2	24 - 18
	6875.24	14580.89	142	299		3 - 0	4794.6				1	25 - 19
	6859.33					10 - 8	4782.4				1	26 - 20

Table 28.--Continued

[a]Stimulated emission spectra observed by Massone et al. [438]. A new band (3-3) was observed at 9599 Å. In addition, rotational analysis was extended for the 1 0, 2 1, 2-0, 3-1, and 4-2 bands.

The bands have 5 heads under low resolution, the prominent ones being 1, 2, 4 proceeding from longer to shorter wavelength. Most authors give only the first head, that of the P_1 branch. The table gives the P_1 branch heads. Band heads are taken from data of Dieke and Heath [196], Hepner and Herman [293], Carroll and Sayers [139], Turner and Nicholls [619], and Tanaka and Jursa [600].

Hepner and Herman [293] list band heads in cm^{-1}. The wavelengths in this table are based on the reciprocals of these wavenumbers, rounded to three figures, because of the low precision of the measurements and uncertainty as to whether or not a vacuum spectrograph was used.

Tanaka and Jursa have a misprint. The wavelength of the 18-12 P_1 head should read 4911.2 Å, assuming the wavenumber is correct. For the feature at 5442.3 Å Tanaka and Jursa give two identifications, 19-15 and 10-5. This suggests that other bands may be similarly overlapped.

The 2-5 and 3-5 band intensities had been reported by Turner and Nicholls [619]; the approximate wavelengths for these bands listed in this table are taken from Benesch et al. [72].

Band origins are from Dieke and Heath [196]. Note that they actually list differences between lowest rotational levels, not band origins. The origins listed here are the values deduced by Benesch et al. [70] from the measurements of Dieke and Heath.

Intensities include: (a) Measured values from Turner and Nicholls [619], who used an N_2 discharge at 1.25 Torr and a current of 0.9 amp.; (b) Measured relative intensities in the same discharge used by Jeunehomme [357] to determine radiative lifetimes - the intensities were scaled arbitrarily to agree with Turner and Nicholls value for the 2-0 band.; (c) Eye estimates of intensities in the auroral afterglow of nitrogen from Tanaka and Jursa [600].

Table 29. Band heads and origins of the $C^3\Pi_u - B^3\Pi_g$ Second Positive System (V).

(a) Emission

λ_H Å	σ_0 cm^{-1}	I^a	I^b	v' - v"	λ_H Å	σ_0 cm^{-1}	I^a	I^b	v' - v"
5452.0				0 - 7	3804.9		10	22	0 - 2
5309.3				1 - 8	3755.4	26636.59	10	25	1 - 3
5179.3				2 - 9	3710.5	26958.99	8	8.6	2 - 4
5066.0				3 - 10	3671.9	27243.75	6		3 - 5
5031.5				0 - 6	3641.7		3	1.5	4 - 6
4976.4		0		4 - 11	3576.9[c]		10	67	0 - 1
4916.8	20337.67	0		1 - 7	3536.7		8	30	1 - 2
4814.7		1		2 - 8	3500.5	28577.38	4	5	2 - 3
4723.5		1		3 - 9	3469		0	5	3 - 4
4667.3		0		0 - 5	3446		0		4 - 5
4649.4		1		4 - 10	3371.3[c]	29671.05	10	100	0 - 0
4574.3		2	0.9	1 - 6	3338.9		2	3.7	1 - 1
4490.2		3	1.1	2 - 7	3309		2	1.9	2 - 2
4416.7		3	1.5	3 - 8	3285.3		3	7.5	3 - 3
4355.0		3	0.8	4 - 9	3268.1		4	6.0	4 - 4
4343.6		4	1.8	0 - 4	(3259.2)				5 - 5
4269.7		5		1 - 5	3159.3		9	67	1 - 0
4200.5		6	3.8	2 - 6	3136.0		8	29	2 - 1
4141.8		5	3.9	3 - 7	3116.7		6	18	3 - 2
4094.8	23432.04	4	2.4	4 - 8	3104.0		3	6.1	4 - 3
4059.4	24642.19	8	7.0	0 - 3	2976.8		6	12	2 - 0
3998.4	25018.20	9	12	1 - 4	2962.0		6	23	3 - 1
3943.0		8	6.3	2 - 5	2953.2		6	19.6	4 - 2
3894.6		7		3 - 6	2819.8		1		3 - 0
3857.9		5		4 - 7	2814.3		1		4 - 1
					2687				4 - 0

Principal (P_3) heads are listed from data of Pankhurst [514], Pearse and Gaydon [26], and Dieke and Heath [196]. A band head at 3259.2 Å is considered as likely due to the 5-5 transition according to Pannetier et al. [515]. Band origins are from Benesch et al. [70] whose values were based on observations by Dieke and Heath who had tabulated the lowest rotational level above the ground state, for the observed vibrational levels. Additional bands have been observed with v' > 4, in the region where the C and C' states interaction is strong. See sections 3.13, 3.20, and 7.

Estimated intensities are from (a) Pearse and Gaydon [26] and (b) Tyte [620],

(c) Extended rotational analysis has been made by Massone et al. [438].

Table 29. (b) Absorption

λ Å	σ_0 cm^{-1}	I	v' - v''
1518.059	65852.35	1	0 - 0
1484.443	67345.10	8	1 - 0
1452.771	68813.77	25	2 - 0
1422.928	70258.56	20	3 - 0
1394.742	71679.66	23	4 - 0
1368.090	73077.56	33	5 - 0
1342.845	74452.25	30	6 - 0
1318.911	75803.91	28	7 - 0
1296.212	77132.44	26	8 - 0
1274.651	78437.99	25	9 - 0
1254.154	79720.83	25	10 - 0
1234.655	80980.96	21	11 - 0
1216.081	82218.55	19	12 - 0
1198.374	83433.52	21	13 - 0
1181.499	84625.97	19	14 - 0
1165.398	85795.87	18	15 - 0
1150.025	86943.08	15	16 - 0
1135.346	88067.62	4	17 - 0
1121.323	89169.59	2	18 - 0
(1107.95)	----		19 - 0

Data from Tilford, Vanderslice and Wilkinson [611]. Head wavelengths are for the ^{S}R branch. The 19-0 band head is from low resolution measurements of Tanaka et al. [604] who also observed the 20-0 Q-branch head. Intensities are eye estimates from Tilford et al. [34].

Table 30. Observed bands of the $B^3\Pi_g - X^1\Sigma_g^+$ Wilkinson system.

H Å	H(cm^{-1})	v' - v''
1685.8	59319	0 - 0
1638.7	61023	1 - 0

Data from Wilkinson [659].

Table 31. Band heads and origins of the $B'^3\Sigma_u^- - X^1\Sigma_g^+$ Ogawa-Tanaka-Wilkinson system (R).

(a) Emission

Branch	λ_H Å	I	v' - v''
S_R	2232.18	1.5	2 - 11
Q	33.68	1.0	
	2204.02	1.0	2 - 10
	05.54	0.8	
	2176.47	0.5	0 - 9
	78.06	0.2	
	2135.09	1.0	2 - 10
	36.33	0.8	
	2081.23	0.8	0 - 8
	82.54	0.5	
	2018.60	0.8	1 - 8
	19.78	0.5	
	1993.01	1.0	0 - 7
	94.30	0.8	
	1935.37	0.5	1 - 7
	36.59	0.3	
	1881.93	0.5	2 - 7
	83.01	0.5	
	1834.17	1.5	0 - 5
	35.33	2.0	
	1808.57	0.5	2 - 6
	09.31	0.5	
	1762.64	1.5	0 - 4
	63.45	1.5	
	1717.47	1.0	1 - 4
	18.36	0.5	
	1695.61	1.0	0 - 3
	96.50	0.7	
	1653.82	1.0	1 - 3
	54.48	1.0	
	1593.94	1.0	1 - 2
	94.63	1.0	

Data from Ogawa and Tanaka [498].

Table 31 (b) Absorption

	λ_H Å	σ_0 cm^{-1}	I	v' - v''
S_R	1518.059	65852.35	1	0 - 0
	1484.443	67345.10	8	1 - 0
	1452.771	68813.77	25	2 - 0
	1422.928	70258.56	20	3 - 0
	1394.742	71679.66	23	4 - 0
	1368.090	73077.56	33	5 - 0
	1342.845	74452.25	30	6 - 0
	1318.911	75803.91	28	7 - 0
	1296.212	77132.44	26	8 - 0
	1274.651	78437.99	25	9 - 0
	1254.154	79720.83	25	10 - 0
	1234.655	80980.96	21	11 - 0
	1216.081	82218.55	19	12 - 0
	1198.374	83433.52	21	13 - 0
	1181.499	84625.97	19	14 - 0
	1165.398	85795.87	18	15 - 0
	1150.025	86943.08	15	16 - 0
	1135.346	88067.62	4	17 - 0
	1121.323	89169.59	2	18 - 0
	(1107.95)	----		19 - 0

Data from Tilford, Vanderslice and Wilkinson [611]. Head wavelengths are for the ^{S}R branch. The 19-0 band head is from low resolution measurements of Tanaka et al. [604] who also observed the 20-0 Q-branch head. Intensities are eye estimates from Tilford et al. [34].

Table 32. Band heads and origins of the $C^3\Pi_u - X^1\Sigma_g^+$ Tanaka absorption system (R).

	λ_H Å	σ_0 cm^{-1}	I	v' - v''
Q_R	1124.288	88977.84	45	0 - 0
Q	23.858			
R	23.619			
R_Q	23.449			
S_R	22.769			
	1099.577	90972.27	60	1 - 0
	99.213			
	99.018			
	98.837			
	98.283			
	1076.600	92913.15	30	2 - 0
	76.251			
	76.018			
	75.893			
	75.454			

Data from Tilford et al. [612].

Intensities from Tilford et al. [34].

Table 33. Band heads of the $B'^3\Sigma_u^- - B^3\Pi_g$ infrared afterglow system (R).

λ_H Å	σ_H cm^{-1}	I	v' - v''	λ_H Å	σ_H cm^{-1}	I	v' - v''
8899	11234			7408	13495		
8912	11218	2	8 - 4	7416	13481	6	6 - 1
8939	11184			7435	13447		
8675	11524			----	-----		
8687	11509	10	7 - 3	7239	13811	2	5 - 0
8712	11475			7256	13778		
8458	11820			6896	14496		
8469	11805	8	6 - 2	6902	14485	8	8 - 2
8493	11771			6919	14450		
8247	12122			6735	14844		
8257	12107	5	5 - 1	6740	14833	6	7 - 1
8283	12073			6756	14797		
----	-----			6578	15198		
8053	12414	2	4 - 0	6583	15187	1	6 - 0
8075	12381			6598	15151		
7780	12850			----	-----		
7787	12838	10	8 - 3	----	-----	3	8 - 1
7809	12803			6200	16125		
7533	13170			----	-----		
7598	13157	10	7 - 2	----	-----	1	7 - 0
7619	13122			6059	16501		

Data from LeBlanc, et al. [407].

Isotopic bands

λ_H ($^{15}N_2$)	σ_H (obs)	v' - v''
8402.5	11898	5 - 1
8195.1	12199	4 - 0
7924.9	12615[a]	8 - 3
7035.8	14209	8 - 2

Data from Mahon-Smith and Carroll [431].

[a]Computed from $^SR_{21}$ head; R_2 head is obscured.

Table 34. Bands of the $W^3\Delta_u - X^1\Sigma_g^+$ system (1500-1440 Å)

σ_0 cm^{-1}	v' - v''
66537	5 - 0
67900	6 - 0
69243	7 - 0

Data from Tilford et al. [34]; identifications by Saum and Benesch [557], and Benesch and Saum [67]. These band origins are based on a tentative rotational analysis. A Deslandres array of calculated band origin wavelengths for the W-X system has also been given by Saum and Benesch.

Table 35. Band origins of the $W^3\Delta_u - B^3\Pi_g$ system (R,V)

σ_0 (cm^{-1})	Δv	v' - v"
3007	+2	2 - 0
2734		3 - 1
2463		4 - 2
4439	+3	3 - 0
4139		4 - 1
3852		5 - 2
3565		6 - 3
-3310	-2	0 - 2
-3476		1 - 3
-3640		2 - 4
-3798		3 - 5
-3950		4 - 6
-4095		5 - 7
-4234		6 - 8
-4368		7 - 9

Data from Benesch and Saum [67]. These were derived from a computer-generated model.

Table 36. Band heads of the $C'^3\Pi_u - B^3\Pi_g$ Goldstein-Kaplan system (R).

λ_H Å	I	v' - v"	λ_H Å	I	v' - v"
----			3506.11		
----	-	2 - 13	3511.67	6	0 - 6
(5450)[a]			3516.44		
5059.4			3325.24		
5066.7	1	0 - 12	3329.17	5	0 - 5
5076.2			----		
4729.13			(3178.4)		
4735.90	2	0 - 11	3182.92	4	2 - 5
(4743.8)[a]			3187.46		
4432.56			(3159.2)		
4438.87	4	0 - 10	3161.93	6	0 - 4
4446.09			3166.60		
4165.97			3025.54		
4171.59	4	0 - 9	3029.59	3	2 - 4
4177.92			3033.76		
3925.00			3004.82		
3930.29	4	0 - 8	3008.00	5	0 - 3
3936.02			3012.20		
3706.21			2863.06		
3711.30	5	0 - 7	2866.01	2	0 - 2
3716.43			----		

Data from Tanaka and Jursa [600]. Intensities are in an afterglow source. Carroll and Mulliken [136] discuss the quantum numbering of bands with v'-2. $\sigma_0(0\text{-}0)$ = 38296.75 cm^{-1}; from rotational analysis of the 0 - 3, 0 - 4, and 0 - 11 bands and known lower state constants [128]. (a) Crude band heads measured by Gaydon [248]. These bands heads are overlapped by other structure, and the identity of the 5450 Å band is uncertain. (b) Crude band positions measured by Hamada [285]. (c) Gaydon [247] also measured band heads at 5333.5, 5327.3 and 5320.0 Å. Identification of these is uncertain. A very weak band at 5575 Å might be 2 - 14 of the C' - B system, but this is too heavily overlapped to be certain.

Isotope shifts

H $^{14}N_2$ Å	H $^{15}N_2$ Å[a]	$\Delta\sigma_{obs}$ cm^{-1}	$\Delta\sigma_{calc}$ cm^{-1}	v' - v"
4728.4	4613.0	529	535	0 - 11
4432.3	4335.3	505	502	0 - 10
3707.1	(3653.7)[b]	394	386	0 - 7

Data from Mahon-Smith and Carroll [431].

[a] P_1 heads.

[b] Calculated from P_3 head; P_1 head is obscured.

Table 37. Band heads and origins of the $D^3\Sigma_u^+ - B^3\Pi_g$ Fourth Positive System (V).

λ_H Å	σ_0 cm^{-1}	I^a	I^b	v' - v''
2903.9				
2902.0				
2900.3		1	----	0 - 6
2898.1				
2896.6				
2777.9				
2776.5				
2775.1		2	0.28	0 - 5
2772.8				
2771.4				
2660.5				
2659.3				
2657.9		5	0.48	0 - 4
2655.8				
2654.5				
2550.7				
2549.7				
2548.4		8	0.67	0 - 3
2546.6				
2545.3				
2448.0				
2447.0				
2445.6	40884	10	1.0	0 - 2
2444.0				
2442.8				
2351.4				
2350.3				
2349.0	42560	6	0.64	0 - 1
2347.5				
2346.4				
2260.8				
2259.6				
2258.4	44266	2	0.36	0 - 0
2257.1				
2256.0				

[a] Intensities are photographic eye estimates from Fowler and Strutt [234].

[b] Intensities refer to monochromator scans (photomuliplier detector) from Wentink et al. [650].

Band head data from Fowler and Strutt [234].

Band origins are derived from the data of Gero and Schmid [257].

Table 38. Band heads and origins of the $E^3\Sigma_g^+ - A^3\Sigma_u^+$ Herman-Kaplan system (V)

λ_H Å	σ_0 cm^{-1}	v' - v''
2733.2		0 - 7
2642.1		0 - 6
2554.9	39132.70	0 - 5
2497.8		1 - 6
2471.4	40454.49	0 - 4
2419.8		1 - 5
2391.6	41804.19	0 - 3
2315.3	43181.54	0 - 2
2272.9		1 - 3
2242.3		0 - 1
2203.8		1 - 2
2137.6		1 - 1

Band heads are from Herman [295]; origins are from Carroll and Doheny [133].

T_o' is calculated as 95774.50 cm^{-1}.

Table 39. Bands of the $H^3\Phi_u - G^3\Delta_g$ Gaydon-Herman green system (V)

λ_{max} Å	σ_0 cm^{-1} [a]	I	v' - v"	λ_{max} Å	σ_0 cm^{-1} [a]	I	v' - v"
6336.3				5574.4			
6360.4		5	0 - 3	5594.2	17897.08	9	0 - 0
.....				5602.1			
6246.3				5727.1			
6268.8		5	1 - 4	5545.5		2	1 - 1
6279.7				.....			
6160.5				5479.6			
6183.4		3	2 - 5	5498.9		6	2 - 2
6191.6				5506.3			
6068.6				5435.0			
6091.0		8	0 - 2	.....		3	3 - 3
6101.1				.....			
5994.5				5308.6			
6017.3		6	1 - 3	5327.0	18796.16	8	1 - 0
6026.8				5333.8			
5924				5272.0			
....		1	2 - 4	5290.0	18926.62	5	2 - 1
....				.....			
5815.1				5073.4			
5836.5		10	0 - 1	5090.2	19669.11	4	2 — 0
5845.4				5097.0			
5755.1				5047.0			
5776.3		3	1 - 2	(5062.7) [b]	19772.40	2	3 - 1
.....				.....			
5640							
5661		1	3 - 4				
....							

σ_{00} = 17934 cm^{-1}; from the band heads.

Data from Grun [273]. The shortest wavelength head is the strongest. Under very low dispersion the bands display 5 heads; under higher dispersion 3 heads, though the appearance changes from band to band. The quantum numbering is that of Gaydon [248,26]; this is supported by the isotopic measurements of Mahon-Smith and Carroll [431].

[a] Origins from Carroll et al. [131].

[b] Data from Carroll and Sayers [139].

Isotope shifts

λ_H $^{14}N_2$ Å	λ_H $^{15}N_2$ Å	$\Delta\sigma_{obs}$ cm^{-1}	$\Delta\sigma_{calc}$ cm^{-1}	v' - v"
5574.5	5575.3	2.6	2.6	0 - 0
5308.6	5317.4	32.3	32.1	1 - 0
5271.1	5281.9	36.8	35.6	2 - 1
5073.3	5089.0	60.1	59.9	2 - 0
5047.1	5062.6	60.6	61.6	3 - 1

Data from Mahon-Smith and Carroll [431].

Table 40. Band heads of the Herman Infrared system (V)

λ_H Å	I	v' - v"	λ_H Å	I	v' - v"
----		0 - 3 [a]	7868.5		2 - 2
----			7862.0		
----			7853.7	8	
----			7846.7		
----			7840.7		
9629			7828.5		
----		0 - 2 [a]	7558.3		1 - 0
----			7550.0		
----			7541.4	4	
----			7536.5		
----			7530.7		
9071			7521.0		
----		0 - 1	7471.8		2 - 1
----			----		
----	2		----	5	
----			----		
----			----		
8549			7435.0		
----		1 - 2	7094.4		2 - 0
----			7087.5		
----	1		7080.8	6	
----			7076.3		
----			7069.8		
8397			7061.7		
8101.1		0 - 0	7033.3		3 - 1
8094.1			7025.8		
8084.7	10		7019.3	4	
8077.6			7014.6		
8070.9			7009.2		
8057.6			7001.2		

Data from Carroll and Sayers [139]. Intensities are Gaydon's eye estimates for the overal strength of each band under low resolution [26]. The shortest wavelength heads are the strongest.

[a] Data from Davidson and O'Neil [190].

Isotope shifts

λ_H $^{14}N_2$ Å	λ_H $^{15}N_2$ Å	$\Delta\sigma_{obs}$ cm^{-1}	$\Delta\sigma_{calc}$ cm^{-1}	v'-v"
8101.4	8102.0	1.3	3.4	0-0
7869.4	7877.8	13.9	16.0	2-2
7095.4	7123.9	56.8	59.9	2-0
7033.2	7062.9	60.1	62.2	3-1
8549	8536.6	-16.9	-20.0	0-1

Data from Mahon-Smith and Carroll [431].

Table 41. Band heads and origins of the $A^2\Pi_u - X^2\Sigma_g^+$ Meinel System of N_2^+ (R).

	λ_H Å	σ_0 cm^{-1}	I^a	I^b	v' - v''	λ_H Å	σ_0 cm^{-1}	I^a	I^b	v' - v''
Q_1	17706				5 - 6	9808.9				3 - 2
R_2	17460					9733.3				
	17705				4 - 5	9502.3			21	2 - 1
	17459					9431.2				
	16927				3 - 4	9212.06	10889.49		100	1 - 0
	16703					9145.3				
	15947			25	2 - 3	8603.9		2		5 - 3
	15748					8545.7				
	15297			80	1 - 2	8348.26	12012.73	13	15	4 - 2
	15114					8293.42				
	14692		25		0 - 1	8105.35	12371.51	53	38	3 - 1
	14523					8053.64				
	13510				5 - 5	7874.62	12732.75	105	68	2 - 0
	13366					7825.73				
	13001				4 - 4	7281.8		8	7	5 - 2
	12867					7239.9				
	12369				3 - 3	7081.4		11	10	4 - 1
	12249					7036.8				
	11931.9				2 - 2	6890.5		7	11	3 - 0
	11820.2					6853.0				
	11520.6				1 - 1	6298.9		1		5 - 1
	11416.3					6267.6				
	11133.9			35	0 - 0	6136.2		1		4 - 0
	11036.2					6106.4				
	10586.8				5 - 4	5539.8				5 - 0
	10498.6					5515.6				
	10132.8				4 - 3					
	10052.2									

Band head and origin data are from Douglas [205]. Douglas measured the heads of the 2-0, 3-1, and 4-2 bands, and the long wavelength heads of the 1-0 and 3-0. For convenience in future work on identifying bands, Douglas extrapolated this table to include all bands with v' up to and including 5 for wavelengths below 20,000 Å. Band intensities are those observed in the aurora; (a) Meinel [452-3-4-5], (b) Federova [224].

Table 42. Band heads and origins of the $B^2\Sigma_u^+ - X^2\Sigma_g^+$ First Negative system

(a) Violet degraded bands

λ_H Å	σ_0 cm^{-1}	I^a	I^b	I^c	v' - v''	λ_H Å	σ_0 cm^{-1}	I^a	I^b	I^c	v' - v''
5864.7		4	0		0 - 4	4489				2	9 - 11
5754.4				0.5	1 - 5	4466.6	22406.5			20	6 - 8 8 - 10
5653.1		4	1	0.7	2 - 6	4459.3				5	7 - 9
5564.1		1	0	0.5	3 - 7	4278.1	23391.2	8	6	400	0 - 1
5485.5		5	0	1	4 - 8	4236.5	23620.5	7	5	250	1 - 2
5450.0				0.4	11 - 15	4199.1	23830.0	4	2	100	2 - 3
5420.8				0.7	5 - 9	4166.8	24013.9	3	0	30	3 - 4
5384.3				0.5	10 - 14	4140.5		2		20	4 - 5
5372.3				0.7	6 - 10	4121.3				6	5 - 6
5344.7				0.4	9 - 13	4110.9				2	6 - 7
5340.2				0.7	7 - 11	3914.4	25566.0	6	6	1500	0 - 0
5330.0				0.4	8 - 12	3884.3		3	1	250	1 - 1
5228.3	19139.7	7	2	2	0 - 3	3857.9	25939.8	2	2	40	2 - 2
5148.8	19434.7	4	3	4	1 - 4	3835.4		1	1		3 - 3
5076.6	19710.4	7	1	5	2 - 5	3818.1		1	0		4 - 4
5012.7		3	1	3	3 - 6	3808.1					7 - 7
4957.9	20182.6	5	1	5	4 - 7	3806.8					5 - 5
4913.2	20365.5			4	5 - 8	3582.1		4	3	300	1 - 0
4883.3				1	9 - 12	3563.9		4	0	300	2 - 1
4881.7	20499.0	5	0	4	6 - 9	3548.9		3		200	3 - 2
4864.4	20578.0			6	7 - 10 8 - 11	3538.3		2		100	4 - 3
4709.2	21249.0	4	2	50	0 - 2	3532.6		1	0	100	5 - 4
4651.8	21511.3	4	1	50	1 - 3	3308.0		2	1		2 - 0
4599.7	21753.7	6	2	50	2 - 4	3298.7		3	1	60	3 - 1
4554.1	21971.5	4	0	30	3 - 5	3293.4		3	0	80	4 - 2
4515.9	22158.3	6	0	35	4 - 6	3291.6	30427.6				5 - 3
4490.3	22305.4	2	1	15	5 - 7	3078.2				1	3 - 0
						3076.4				1	4 - 1

Band head data are from Merton and Pilley [456], Herzberg [302], Stoebner et al. [587-8], and Tyte [622-3].

Measurement uncertainties of about 0.5 Å and overlapping structure could mean that some of the observed bands are misidentified.

Band origin data are from Crawford and Tsai [183], Coster and Brons [173-4], Parker [517], and Stoebner et al. [587].

Intensities:

a) In a Tesla discharge in a mixture of helium and nitrogen; Merton and Pilley [456].

b) In a Tesla discharge in pure nitrogen; Merton and Pilley [456].

c) In an electrodeless ring discharge; Herzberg [302].

In order to show the great intensity variation among the bands, Herzberg used a different intensity scale than did Merton and Pilley. For the sequence $\Delta v = 4, 3, 2, 1, 0, -1, -2$, and -3, the intensity ratio was, according to Herzberg, about $I_4:I_3:I_2:I_1:I_0: I_{-1}:I_{-2}:I_{-3} = 1:5:50:400:1500:300:80:1$.

Table 42. (continued)

(b) Red degraded bands

λ_H Å	σ_0 cm^{-1}	I	v' - v"	λ_H Å	σ_0 cm-1	I	v' - v"
5721.9		1	20 - 22	3646.4	(27411.2)	5	21 - 16
5632.1		0	22 - 23	3643.2	27425.7	4	14 - 12
5551.9		1	19 - 21	3612.4	27611.3		10 - 9
5458.5	(18308.0)	2	21 - 22	3588.6	27854.6	2	16 - 13
5391.1		3	18 - 20	3534.0		0	18 - 14
5292.6	(18882.0)	7	20 - 21	3500.6		0	15 - 12
5240.2	(19065.5)	5	17 - 19	3493.4		1	12 - 10
5227.6	(19118)	3	22 - 22	3460.8			17 - 13
5136.4	(19456.0)	8	19 - 20	3447.3		1	23 - 16
5099.8	(19588.5)	3	16 - 18	3443.7		4	19 - 14
5066.2		3	21 - 21	3439.2		2	21 - 15
4988.2	(20032.5)	5	18 - 19	3433.0			11 - 9
4969.3	(20099.0)	3	15 - 17	3419.6	29226.8	1	14 - 11
4913.3	(20339.5)	4	20 - 20	3381.4	29518.5		10 - 8
4850.7	20587.4	8	14 - 16	3374.2	(29620.0)	2	16 - 12
4850.0			17 - 18	3349.6	(29836.2)	8	18 - 13
4769.3		2	19 - 19	3345.7	(29867.0)	8	22 - 15
4743.1	21044.7	5	13 - 15				13 - 10
4720.2	(21166.0)	1	16 - 17	3341.7	(29913.5)	8	20 - 14
4680.0			11 - 13	3292.4			15 - 11
4006.7		4	20 - 17	3280.0	(30460.8)		12 - 9
3994.9		3	22 - 18	3262.5	(30642.8)	8	17 - 12
3940.1	25369.5		29 - 21	3249.6	(30758.0)	8	19 - 13
3927.3	(25447)		17 - 15	3222.6	30998.7		11 - 8
(3907.6)	25583.8		27 - 20	3217.7	31063.6	3	14 - 10
3891.8		6	19 - 16	3184.6			24 - 15
3875.1		6	10 - 10	3180.9	(31422.5)	3	16 - 11
3825.1	(26125.9)	4	16 - 14	3174.0	31459.6		10 - 7
3808.9	26229.4	2	13 - 12	3162.6	(31600.0)		18 - 12
3783.4	26419.7		26 - 19	3159.0	(31641.5)	4	20 - 13
3782.8		8	18 - 15	3148.5	(31738.6)	0	13 - 9
3762.1	(26565.5)	10	20 - 16	3137.0			9 - 6
3756.1	26607.0	5	22 - 17	3065.1			15 - 10
3733.1	26754.2	6	12 - 11	3033.0	32940.1		11 - 7
3730.3	26787.5	5	15 - 13	2992.3	(33402.0)	2	18 - 11
3726.0	26827.7		29 - 20	2987.3	33435.2		10 - 6
3691.1	27081.5	7	27 - 19	2970.0		0	13 - 8
3682.5	(27141)	7	17 - 14	2918.4	(34251.5)		21 - 12
3668.1	27119.8	6	11 - 10	2912.5		3	12 - 7
3655.7	(27337.5)	7	19 - 15	2912.0	(34324.5)		19 - 11
				2861.7	34915.7		11 - 6

Band head data from Janin et al. [351], Janin and Eyraud [353], Douglas [204], Herzberg [302], Stoebner et al. [587,588], and Tyte [622-3]. Intensities are in discharge in a mixture of neon and nitrogen, excited by microwave pulses. Band positions from Janin and Eyraud [353] are uncertain by 0.5 Å. Band origins are from Douglas [204], Tyte [622-3], Brons [102], Parker [517] and Janin et al. [351]. A band head at 3783.7 Å (σ_0 = 26415.5 cm^{-1}) was identified by Janin et al. [351] as 18 - 15. This seems identical to the band listed by Douglas as 26 - 19. The broad Condon locus for this system makes it possible that some band identifications are incorrect. Janin et al. also listed the origin for the 19 - 16 band as 25,683 cm^{-1}; this was based on high N lines only, and is assumed to be of low accuracy.

(c) Headless bands

λ_0 Å	σ_0 cm^{-1}	v' - v"
3319.9	30112.0	8 - 6
3580.3	27922.5	9 - 8
3620.6	27611.8	10 - 9
3386.7	29518.8	10 - 8

Data from Coster and Brons [173-4] and Brons [102].

Table 43. Bands of the $^4\Sigma_u^+ - X^2\Sigma_g^+$ d'Incan-Topouzkhanian system.

v' - v"	λ_H (Å)	σ_0(cm^{-1})
0 - 0	3915	25563.26(3)
1 - 1	3885	25758.90(5)

Data from d'Incan and Topouzkhamian [200].

Table 44. Band heads and origins of the $C^2\Sigma_u^+ - X^2\Sigma_g^+$ Second Negative system (R)

λ_H Å	σ_0 cm^{-1}	I^a	I^b	I^c	v' - v'' (a) $^{14}N_2^+$	λ_H Å	σ_0 cm^{-1}	I^a	I^b	I^c	v' - v''
2223.0			2		3 - 13	1846.3	54152.82	6	6		3 - 8
2210.8			2		4 - 14	1843.9	(54222.4)	3	5		4 - 9
2198.3			2		5 - 15	1841.4	(54294.8)	0	4		5 - 10
2185.8			2		6 - 16	1838.9			1		6 - 11
2139.4			1		3 - 12	1834.0			1		8 - 13
2129.6			2		4 - 13						
						1784.1		1		3	0 - 4
											1 - 5
2165.6			1		5 - 14	1783.3		1		1	2 - 6
2109.7			1		6 - 15	1781.2				2	4 - 8
2059.8	(48540.1)	3	5		3 - 11	1780.0		0	2		5 - 9
2052.4		2	4		4 - 12	1778.8		0	2		6 - 10
2044.8		1	4		5 - 13	1777.6			1		7 - 11
2037.1		0	3		6 - 14	1776.4			1		8 - 12
2029.3		0	2		7 - 15						2 - 5
											3 - 6
						1721.7	58070.30	6	5		4 - 7
											5 - 8
2021.5			1		8 - 16	1720.5		0		2	0 - 3
2013.8			1		9 - 17	1665.1			2		4 - 6
2006.1			1		10 - 18	1664.2	60080.29	3	4		3 - 5
1992.2				3	0 - 7	1660.2	60225.00			3	0 - 2
1994.9		0		3	1 - 8	1611.1		5	3		4 - 5
1990.0		0		3	2 - 9	1609.5		4	4		3 - 4
1984.8	50374.18	7	6		3 - 10	1605.5				3	1 - 2
1979.2	50513.43	6	5		4 - 11	1603.2				2	0 - 1
1973.5	50658.50	5	5		5 - 12	1560.0		5	3		4 - 4
1967.8	50806.32	3	5		6 - 13	1557.5		5	5		3 - 3
1962.0		1	4		7 - 14	1554.9					2 - 2
1956.2		0	4		8 - 15	1552.2				2	1 - 1
1950.5		0	2		9 - 16	1549.2				0	0 - 0
1944.8		0	2		10 - 17	1513.9			3		5 - 4
1939.2			1		11 - 18	1511.0		2	4		4 - 3
1923.3	51986.30	0		3	0 - 6	1507.9		2	3		3 - 2
1920.4	52061.26	0		2	1 - 7	1504.8				1	2 - 1
1917.2	52148.99	0		2	2 - 8	1501.5				1	1 - 0
1913.6	52246.22	6	7		3 - 9	1464.2		3	5		4 - 2
1909.8	52350.16	5	5		4 - 10	1460.8		3	4		3 - 1
1905.8	52459.52	4	6		5 - 11	1457.1				1	2 - 0
1901.7	52571.45	3	6		6 - 12	1419.8			1		4 - 1
1897.7		0	4		7 - 13	1415.8		3	4		3 - 0
1893.6		0	3		8 - 14	1377.3		2	4		4 - 0
1889.6			2		9 - 15	1346.1			0		6 - 1
1885.7			1		10 - 16	1341.4			2		5 - 0
1881.8			0		11 - 17	1312.9			0		7 - 1
1851.6	(53995.0)	0		3	0 - 5	1307.8			1		6 - 0
1850.2	54037.36	0		2	1 - 6	1276.5			0		7 - 0
1848.4	54090.91	0		1	2 - 7						

Band origins are from Carroll [125], Wilkinson [654] and Setlow [568]. The 0 - 5 band origin has an uncertainty of ± 3 cm^{-1} [568]. Parentheses indicate band origin calculated from band head and rotational constants from data of Wilkinson [654].

Band head data are from Tanaka [596], Joshi [366], and Takamine et al. [595]. All vacuum wavelengths. Intensities are from: [a] Tanaka [596]; [b] Joshi [366], discharge in a neon-nitrogen mixture; [c] Joshi [366], discharge in a helium-nitrogen mixture.

Table 44. (continued)

(b) $^{15}N_2^+$

λ_H Å	I^b	I^c	v' - v''	λ_H Å	I^b	I^c	v' - v''	λ_H Å	I^b	I^c	v' - v''
2244.8	2		3 - 13	1932.4	0		10 - 17	1770.0	1		7 - 11
2184.6	3		4 - 14	1927.6	0		11 - 18	1769.0	0		8 - 12
2173.5	3		5 - 15	1908.3		4	0 - 6				5 - 8
								1715.8	8		4 - 7
											3 - 6
2162.3	2		6 - 16	1905.9		3	1 - 7				8 - 11
								1715.7	2		7 - 10
											6 - 9
2106.9	1		4 - 13	1903.2		2	2 - 8	1714.1		5	0 - 3
2052.2		2	1 - 9	1900.2	8		3 - 9	1663.7	3		7 - 9
2046.1		1	2 - 10	1896.7	8		4 - 10	1662.1	4		5 - 7
2039.8	6		3 - 11	1893.2	5		5 - 11	1661.2	3		4 - 6
2033.3	6		4 - 12	1889.6	3		6 - 12	1660.3	2		3 - 5
2026.4	6		5 - 13	1885.9	3		7 - 13	1656.2		3	0 - 2
2019.5	5		6 - 14	1882.3	3		8 - 14	1632.7	4		4 - 5
2012.6	3		7 - 15	1875.1	0		10 - 16	1607.5	1		3 - 4
2005.6	1		8 - 16	1839.9		4	0 - 5	1605.7		3	2 - 3
1998.7	0		9 - 17	1838.8		3	1 - 6	1603.6		2	1 - 2
1991.7	1		10 - 18	1837.2		3	2 - 7	1601.3		1	0 - 1
1980.8		1	0 - 7	1835.5	7		3 - 8	1557.3	5		3 - 3
1977.0		2	1 - 8	1833.4	7		4 - 9	1552.1		2	1 - 1
1972.7		2	2 - 9	1831.2	3		5 - 10	1517.8	0		6 - 5
1968.3	6		3 - 10	1826.7	0		7 - 12	1514.9	2		5 - 4
1963.3	6		4 - 11	1824.4	0		8 - 13	1512.0	3		4 - 3
1958.2	6		5 - 12	1775.3		5	0 - 4	1463.5	4		3 - 1
1953.0	3		6 - 13	1775.2		5	1 - 5	1419.8	3		3 - 0
1948.0	3		7 - 14	1773.2	6		4 - 8	1382.2	3		4 - 0
1942.6	2		8 - 15	1772.2	6		5 - 9	1347.1	1		5 - 0
1837.5	1		9 - 16	1771.1	1		6 - 10				

Data from Joshi [367]. All vacuum wavelengths.

Intensities: [b] Discharge in a neon-nitrogen mixture.

[c] Discharge in a helium-nitrogen mixture.

(c) $(^{14}N^{15}N)^+$

λ_H Å	I	v' - v''	λ_H Å	I	v' - v''
2049.8	0	3 - 11	1899.5	0	5 - 11
1976.4	1	3 - 10	1895.7		6 - 12
1971.2	1	4 - 11	1840.8	0	3 - 8
1965.8	0	5 - 12			3 - 6
			1718.8	0	4 - 7
1960.5		6 - 13	1718.6	0	5 - 8
1906.8	1	3 - 9	1662.1	0	3 - 5
1903.2	1	4 - 10	1610.1	1	4 - 5

Data from Joshi [367] and Baer and Miescher [57]. All vacuum wavelengths.

Table 45. Band heads and origins of the $D^2\Pi_g - A^2\Pi_u$ Janin-d'Incan System of N_2^+ (R)

	(a) $^{14}N_2^+$											
	λ_H Å	σ_0 cm^{-1}	I^a	I^b	I^c	v' - v"	λ_H Å	σ_0 cm^{-1}	I^a	I^b	I^c	v' - v"
R_2	3073.85	32566.0	1	1		7 - 9	2469.77	40516.7	6	2	8	4 - 3
R_1	3068.31						2466.38					
	2926.50			10		7 - 8	(2459.69)				1	2 - 2
	2921.59						.....					
	2913.29			2		5 - 7	2458.82	40698.3		1		9 - 5
	2908.16						2455.21					
	2865.82	34919.6	1	4		8 - 8	2422.60	41306.5	8	5	4	5 - 3
	2861.11						2419.23					
	2849.44	35119.3	1	3		6 - 7	2418.77			1		10 - 5
	2844.30						2415.50					
	2838.29			0		4 - 6	(2410.15)				3	3 - 2
	.....						.....					
	2809.70					9 - 8	2381.08			6		11 - 5
	2805.10						2377.91					
	2776.17			1		5 - 6	2378.38	42073.0	7	5	1	6 - 3
	2771.68						2374.97					
	2766.98	36166.2	3	2	8	3 - 5	2363.88	(42331)	4	1	2	4 - 2
	.....						2360.52					
	2718.39	36812.7	3	6		6 - 6	2337.07	42816.1	5	5		7 - 3
	2714.08						2332.97					
	2706.11	36979.5	1	2	5	4 - 5	2320.56	43120.0	5	4	1	5 - 2
	.....						2317.43					
	(2698.41)				5	2 - 4	2320.07			2		10 - 4
	.....						2316.86					
	2664.66	37556.1	3	6		7 - 6	2280.11	43886.8	8	7	1	6 - 2
	2660.53						2277.08					
	2649.51			2		5 - 5	2241.90	44629.6	10	10		7 - 2
	2645.39						2239.06					
	2638.99	37919.8	5	3	10	3 - 4	2227.91			4		10 - 3
	2635.22						2225.03					
	2614.58			1		8 - 6	2206.27	45350.4		7		8 - 2
	.....						2203.55					
	2583.50	38733.0	5	3	7	4 - 4	2172.93			6		9 - 2
	2579.41						2170.24					
	(2574.51)				3	2 - 3	2152.95			6		7 - 1
	.....						2150.33					
	2547.63	39279.3	2	7		7 - 5	2120.13			5		8 - 1
	2544.16						2117.55					
	2531.96	39523.2	3	2	3	5 - 4	2089.26			4		9 - 1
	2528.29						2086.73					
	(2520.29)				9	3 - 3	2060.22			3		10 - 1
	.....						2057.68					
	2501.75	40000.0	2	2		8 - 5						
	2498.32											

Band heads are from Tanaka et al. [603] and Bromer et al. [100]. Vacuum wavelengths are given. The R_2 heads are stronger than the R_1 heads.
The 2-4, 2-3, 3-3 and 3-2 heads were observed by Bromer et al., but only calculated vacuum wavelengths were published. The R_2 head of the 9-8 band is overlapped by other structure.
Band origins are from Janin et al. [352]; the 4-2 origin is from Janin and d'Incan [348] and is uncertain by 3 cm^{-1}, being slightly less accurate than the other origins.
Intensities are from: (a) Grandmontagne et al. [268], (b) Tanaka et al. [603], and (c) Bromer et al. [100].

Table 45. (continued)

	(b) $^{15}N_2^+$					
	λ_H Å	I	v' - v"	λ_H Å	I	v' - v"
R_2	2523.90	1	5 - 4	2243.70	10	7 - 2
R_1	.....			2240.84		
	2494.31	3	8 - 5	2208.90	7	8 - 2
	.....			2206.19		
	2477.30	1	6 - 4	2176.19	6	9 - 2
	.....			2173.46		
	2452.78	2	9 - 5	2157.42	4	7 - 1
	2449.47			2155.00		
	2418.40	4	5 - 3	2145.36	3	10 - 2
	2415.27			2142.88		
	2375.66	6	6 - 3	2125.22	4	8 - 1
	2372.66			2122.77		
	2335.62	7	7 - 3	2094.91	3	9 - 1
	2332.68			2092.51		
	2320.13	5	5 - 2	2066.31	2	10 - 1
	2317.17			2063.93		
	2280.69	8	6 - 2			
	2277.81					

Data from Namioka et al. [482]. Vacuum wavelengths are given.

Table 46. Unclassified bands.

(a) Unclassified triple-headed, red-dregraded emission bands (19079-29710 Å) (R)

λ(Å)	σ(cm^{-1})	v' - v"
29710	3365	
---	---	0 - 1
---	---	
24205	4130.2	
24093	4149.5	1 - 1
23930	4177.7	
22585	4426.5	
22477	4447.8	0 - 0
22335	4476.1	
20580	4857	
20480	4881.5	2 - 1
20385	4904.2	
19255	5192.0	
19178	5212.9	1 - 0
19079	5239.9	

Data from Hepner and Herman [293]. Quantum numbering is tentative States may be quintets. See sect. 3.33.

Table 46.--Continued

(b) Unclassified progressions (805-700 Å) observed in absorption along with Rydberg series.

	$^{14}N_2$		$^{15}N_2$		
	σ(cm^{-1})	I	σ(cm^{-1})	I	v' - v"
	128892	5	128894	8	0 - 0
	130741	8	130695	8	1 - 0
(1)	132584	7	132472	7	2 - 0
	134392	5	134213	6	3 - 0
	131906	4	131890	4	0 - 0
(2)	133770	5	133688	4	1 - 0
	135598	4	135454	3	2 - 0
	132650	4	132660	2	0 - 0
(3)	134523		masked		1 - 0
	136366	3	136238	3	2 - 0
	133080	1	---		0 - 0
	133119	2	133109	5	
	134937	1	134877	1	1 - 0
	134984	2	134918	2	
(4)	136773	1	136683	1	2 - 0
	136820	1	136719	2	
	138588	1	138419	1	3 - 0
	138635	2	138460	2	

Data from Ogawa [495]. See sect. 3.33.

Table 46.--Continued

(c) Unclassified bands observed with Rydberg series (795-755 Å)

	σ(cm^{-1})	I	σ(cm^{-1})	I	σ(cm^{-1})	I	σ(cm^{-1})	I
$^{14}N_2$	126106	0	126283	3	127960	1	131023(5)	1
	126153	1	126307	3	128059(2)	3	131335(6)	2
	126193	1	126386	1	128933(3)	4	131401(7)	2
	126223	3	126439(1)	3	129647(4)	4	131549(8)	0
	126250	3	127613	5	130116	2		
$^{15}N_2$	125793	2	126241	4	127985	1	130819	2
	125930	2	126274	4	128127	1	130929(5)	2
	125964	2	126303(1)	4	128810	5	131076(6) or (7)	3
	125992	1	126363	1	128848(3)	5	131129	1
	126039	1	126518	1	129455(4)	5	131549(8)	1
	126063	1	127586	4	130064	1	131957	2
	126088	1	127784	1	130142	1	132101	2
	126130	3	127910(2)	3	130302	0		

Data from Ogawa [495]. Those bands which indicate a possible correspondence between the two isotopes are designated by a number in parentheses. See sect. 3.33.

(d) Uncertain band heads

	λ_H Å	σ_H	I	v' - v''
R_1		---		10 - 0
R_2	1983.8	50409.3	0	
	2082.0	48031.9		12 - 2
	2084.2	47981.2	0	
	---	---		12 - 5
	2346.0	42625.9	5[a]	
	2659.2	37605.3		12 - 8
	2663.1	37550.8	1	
	---	---		2 - 5
	2832.6	35303.9	0	
	2898.7	34498.6		1 - 5
	2903.3	34444.2	0	
	---	---		3 - 6
	2905.8	34414.6	0	
	3051.6	32770.1		3 - 7
	3056.4	32718.1	0	or 1 - 6

[a] Superimposed with another band.

Vacuum wavelengths from Tanaka et al. [603].

See sect. 3.33.

Table 46.--Continued

(e) Strong unidentified absorption band heads in the "pink" nitrogen afterglow.

Intensity	λ_{vac}	σ
60	1372.9	72840
90	1385.4	72182
50	1399.2	71468
50	1408.9	70976
50	1410.5	70898
85	1423.6	70243
50	1432.2	69821
100	1448.0	69061
60	1454.6	68747
65	1462.8	68362
50	1470.3	68012
40	1502.5	66556
50	1504.1	66485
75	1514.1	66046
45	1525.2	65564
50	1536.0	65106
30	1537.7	65030
40	1538.5	64998
25	1543.6	64783
40	1546.8	64651
75	1567.0	63815

Data from Bass [61]. See sect. 3.33.

Table 47. Band heads of the $^2\Sigma_u^+ - X^2\Pi_{gi}$ system of N_3

λ_H Å	σ_H cm^{-1}	I	Transition	
2723.07	36712.3	9 S	010 - 010	$^2\Pi - {}^2\Sigma^-$
2721.67	36731.1	3		
2720.67	36744.7	4		
2720.00	36753.8	4		
2719.41	36761.8	10 S	000 - 000	$^2\Sigma^+ - {}^2\Pi$
2713.63	36840.1	7 S	010 - 010	$^2\Pi - {}^2\Delta_{\frac{5}{2}}$
2708.21	36913.8	9 S	010 - 010	$^2\Pi - {}^2\Sigma^+$
2706.91	36931.6	5	010 - 010	$^2\Pi - {}^2\Sigma$
2700.77	37015.5	5 D	000 - 000	$^2\Pi_u - {}^2\Pi_g$ (?)
2700.10	37024.7	6 D	000 - 000	$^2\Pi_u^- - {}^2\Pi_g$ (?)
2699.49	37033.0	4		
2698.80	37042.4	4		
2698.6[a]	37045.2	weak		
2693.88	37110.2	3 D		
2692.72	37126.2	4 D		
2691.81	37138.7	3 D		
2691.41	37144.3	2		
2690.09	37162.2	3		
2687.5	37198	1		
2685.9	37219	1		
2684.7	37236	1		
2684.04	37246.2	3 D		
2682.7	37264	2		
2678.1	37328	1		
2673.2	37496	1		

Data from Zamanskii et al [677]. (a) Indicates a band observed by Douglas and Jones [207] who first identified a number of features of the N_3 spectrum. Vibronic mixing of $^2\Sigma^+$ and $^2\Pi_{gi}$ is displayed as Renner splitting into four subbands for excited bending vibrations. The headless 010-010 $^2\Pi - {}^2\Delta_{\frac{5}{2}}$ subband may lie under the 000-000 band. The shorter wavelength bands remain unclassified. Intensities are from Zamanskii et al [677]; assignments are from Douglas and Jones. Many assignments made by Zamanskii et al (not listed in this table) should be considered speculative. D and S indicate, respectively, diffuse or sharp bands, so indicated by Douglas and Jones. A (?) indicates those bands which possibly belong to another electrinic transition.

Table 48. Rotational constants for the N_2 ground state from Raman spectra.

Isotope	B_0 (cm^{-1})	D_0(10^{-6} cm^{-1})	B_0-B_1(cm^{-1})	γ_e(10^{-5} cm^{-1})	α_e(cm^{-1})	B_e(cm^{-1})	r_e (Å)	$\Delta G(\frac{1}{2})$(cm^{-1})	References
$^{14}N_2$	1.989506(27)	5.48(06)							Butcher et al [111]
	1.989548(28)	5.72(06)[a]							
	1.989574(12)	5.76(3)	0.017384(3)		0.017292[b]	1.998232(12)	1.097700	2329.9168(3)	Bendtsen [66]
					0.017318[c]	1.998241			
						1.998222[d]			
					0.01751(22)				Barrett and Harvey [60]
				-3.28(20)	0.017279(27)	1.998197(30)[e]	1.0976968		Present work
$^{14}N^{15}N$	1.923604(20)	5.297(38)							Butcher and Jones [110]
	1.923596(9)	5.38(3)	0.016508(2)					2291.324(3)	Bendtsen [66]
$^{15}N_2$	1.857672(27)	5.201(48)							Butcher and Jones [110]
	1.857624(16)	5.08(5)	0.015667(2)					2252.1249(3)	Bendtsen [66]

Uncertainties in the last digits (standard deviations) are in parentheses, except for the data of Bendtsen, where the numbers are a measure of internal consistency and are not standard deviations.

(a) In this fit H_0 was determined as $(3.7 \pm 11.0)10^{-10}$.

(b) Obtained assuming $\gamma = -4.60(10^{-5})$.

(c) Obtained assuming $\gamma = -3.28(10^{-5})$.

(d) Assuming both α and γ from the present review.

(e) This fit assumed Bendtsen's B_0 as revised (table 49); other data came from electronic spectra.
The mean r_e of Butcher and Jones (not included in this table) is based on an old value of α taken from electronic spectra.

Table 49. Rotational constants for the $X^1\Sigma_g^+$ state.

v	B_v obs	$D_v \times 10^6$	
0	1.98950_6 [a]	5.48	D_v exp
	$\pm 0.00002_7$	±0.05	
0	1.989574(12) [a]	5.76(3)	D_v exp
0	1.989566	5.743	D_v calc
1	1.972182	5.752	D_v calc
2	---		
3	---		
4	1.9200		
5	1.9022		
6	1.8845		
7	---		
8	---		
9	---		
10	1.8131		
11	1.7956		
12	1.7771		
13	1.7590		
14	1.7406		
15	1.7223		

Observed data for $^{14}N_2$: v = 0 from Butcher et al. [111] and Bendtsen [66], derived from Raman spectrum; v = 4 - 6 from data of Miller [462-464], derived from the A - X and a - X systems; v = 10 - 15, from data of Lofthus [421], derived from the a - X system. The calculated values of D_v are based on assuming $D_e = 5.738(10^{-6})$ and $\beta_e = 9.597(10^{-9})$, calculated respectively from formulas III, 118 and III, 125 of Herzberg's book [12]. The B_v values are determined by a refit to the measurements, assuming the approximate calculated values for D_v. The equilibrium rotational constants fitted to the B_v's are obtained by weighting the data from Raman spectra somewhat arbitrarily, but more heavily than the data from electronic spectra.

[a] See table 48 and section 4.

Table 50. Rotational constants for the $A\ ^3\Sigma_u^+$ state

v	B_v obs	$D_v \times 10^6$ obs
0	1.4459	6.15 ± 0.2
1	1.4271	
2	1.4089	
3	1.3907	
4	1.3720	
5	1.3529	
6	1.3338	
7	1.3152	
8	1.2954	
9	1.2756	

Observed data from Miller [462], derived from A - X system, and from Dieke and Heath [196], derived from B - A system.

Table 51. Rotational constants for the $B\ ^3\Pi_g$ state

v	B_v obs
0	---
1	1.6105
2	1.5922
3	1.5737
4	1.5551
5	1.5368
6	1.5179
7	1.4990
8	1.4794
9	1.4602
10	1.4412
11	1.4213
12	1.4015

Observed data from Dieke and Heath [196], derived from B - A and C - B transitions.

Table 52. Rotational constants for the B' $^3\Sigma_u^-$ state

v	B_v obs
0	1.4653
1	1.4482
2	1.4316
3	1.4151
4	1.3984
5	1.3818
6	1.3652
7	1.3487
8	1.3322
9	1.3159
10	1.2996
11	1.2832
12	1.2666
13	1.2502
14	1.2338
15	1.2173
16	1.2009
17	1.1846
18	1.1681

Observed data from Tilford et al. [611], derived from B' - X system.

Table 53. Rotational constants for the a' $^1\Sigma_u^-$ state

v	B_v obs
0	1.4718
1	1.4552
2	1.4387
3	1.4224
4	1.4059
5	1.3894
6	1.3732
7	1.3570
8	1.3407
9	1.3246
10	1.3084
11	1.2925
12	1.2764
13	1.2605
14	1.2446
15	1.2286
16	1.2130
17	1.1972
18	1.1815
19	1.1660

v = 0, observed data from McFarlane [449], derived from a - a' system and is based on B_0 for a $^1\Pi_g$.
v = 1 - 19, from Tilford et al. [615], derived from a' - X system.

Table 54. Rotational constants for the $a\,^1\Pi_g$ state

v	$^{14}N_2$ B_v obs	$^{14}N^{15}N$ B_v obs
0	1.6079	
1	1.5900	
2	1.5719	
3	1.5538	1.5031
4	1.5356	1.4857
5	1.5173	1.4684
6	1.4990	1.4508
7	1.4807	1.4334
8	1.4623	1.4160
9	1.4438	1.3986
10	1.4253	1.3812
11	1.4068	1.3640
12	1.3883	
13	1.3698	
14	1.3508	
15	1.3315	

$^{14}N_2$: Observed data from Miller [464] and Vanderslice et al. [627], derived from a - X system. For v = 1 to 4 observed D_v are $\sim 6(10^{-6})$.

$^{14}N^{15}N$: Observed data from Vanderslice et al. [628], derived from a - X system.

Table 55. Rotational constants for the $w\,^1\Delta_u$ state

v	B_v obs
0	1.490
1	---
2	1.457
3	1.440
4	1.423
5	1.407
6	1.390

Observed data from Lofthus and Mulliken [425].

Table 56. Rotational constants for the $G\,^3\Delta_g$ state.

isotope	v	B_v	$D_v(10^{-6}$ cm$^{-1})$	A	ϵ [a]
$^{14}N_2$	0	0.9200±.0005	5.0±1.0	-0.21±.05	0.72±.02
	1	0.9039±.0005	6.0±1.0	-0.25±.05	0.70±.02
$^{15}N_2$	0	0.8603±.0008	6.0±1.0	-0.25±.05	0.70±.02

Data from Carroll [131].

[a] Parallel spin coupling constant.

Table 57. Rotational constants for the $C\,^3\Pi_u$ state

v	B_v obs
0	1.8149
1	1.7933
2	1.7694
3	1.7404
4	1.6999

Observed data from Dieke and Heath [196], derived from C - B system

Table 58. Rotational constants for the $E\,^3\Sigma_g^+$ state.

B_v cm^{-1}	D_v $(10^{-6}$ cm$^{-1})$
1.9273	6.0

Data from Carroll and Doheny [133].

r_0 = 1.1178 Å.

Table 59. Rotational constants for the $C'\ ^3\Pi_u$ state

v	B_v obs	D_v obs	H_v obs
0	1.0496	10.9×10^{-6}	8.3×10^{-10}

Data from [128], derived from C' - B system.

Table 60. Rotational constants for the $a''\ ^1\Sigma_g^+$ state

v	$B_v(cm^{-1})$	$D_v(10^{-6}\ cm^{-1})$
0	1.9133±.0008	6.2±2.9

Data from Ledbetter [408]. Only the v=0 level has been observed. As the first member of a Rydberg series converging to $X\ ^2\Sigma_g^+$ of N_2^+, the a" state should have a rotational constant $B_o \sim B_o(X, N_2^+) = 1.922\ cm^{-1}$.

Table 61. Rotational constants for the $b\ ^1\Pi_u$ state

v	B_v [a] (cm^{-1})	B_v [b] (cm^{-1})	D_v [a] ($10^{-6}cm^{-1}$)	v	B_v [a] (cm^{-1})	B_v [b] (cm^{-1})	D_v [a] ($10^{-6}cm^{-1}$)
0	1.4483	1.446	29	11	1.1925	1.176	c
1	1.4086	1.415	16.4	12	1.150		d
2	1.3872	1.381	16.8	13	1.117		7
3	1.3815	1.347	22.2	14	1.091		8
4	1.4213	1.316	c	15	1.065		6
5	1.437	1.288	c	16	1.039		d
6	1.360	1.263	c	17	1.008		d
7	1.340	1.243	c	18	0.967		d
8	1.324	1.226	d	19	0.935		d
9	1.2375	1.210	d	23	0.757		d
10	1.2085	1.195	16	24	0.662		d

[a] Data from Carroll and Collins [130]. These values are heavily perturbed. Recently, from analysis of the b-a 1-0 band, Rajan [538], obtained $B_1 = 1.4085$, $D_1 = 18.5\ (10^{-6})$.

[b] Deperturbed values from Leoni [414]. No D_v's are discussed.

[c] Anomalous D value; B value assumed $D = 16(10^{-6})$ [130].

[d] D value not needed to fit data [130].

Table 62. Rotational constants for the $D^3\Sigma_u^+$ state

v	B_v	D_v
0	1.961	2×10^{-5}

Data from Gero and Schmid [257], derived from D - B system.

Table 63. Rotational constants for the $b'\ ^1\Sigma_u^+$ state.

v	B_v [a]	B_v [b]	v	B_v [a]	B_v [b]
0	1.1515[c]	1.151	15	1.0475	1.027
1	1.15	1.144	16	1.30	1.019
2	1.142	1.136	17	1.104	1.010
3	1.152	1.128	18	1.315	1.001
4	1.143	1.120	19	1.089	0.992
5	1.1598	1.112	20	1.0623	0.983
6	1.1945	1.104	21	1.180	0.975
7	1.383	1.096	22	1.113	0.966
8	1.151	1.087	23	1.060	0.957
9	1.1233	1.079	24	1.0526	0.949
10	1.255	1.071	25	1.1692	0.940
11	1.097	1.063	26	1.061	0.931
12	1.0732	1.053	27	1.10	0.923
13	1.215	1.045	28	0.980	0.914
14	1.047	1.036			

[a] Data from Carroll et al. [132].

[b] Deperturbed values from reanalysis by Leoni [414].

[c] Data for v=0 from Wilkinson and Houk [660].

Table 64. Rotational constants for the $c_n\ ^1\Pi_u$ Rydberg states.

State	v	$B_v(cm^{-1})$	B_{obs}	A
c_3	0	1.971		
c_4	0	1.899[c]		
		1.919[d]		
	1	1.914[c]		
		1.904[d]		
	2	1.891[c]		
		---		
c_5	0	1.922	1.850	-197.1
c_6	0	1.921	1.790	- 91.8
c_7	0	1.922	1.64	- 64.3
c_8	0	1.914	1.71	- 39.7

c_3: Data from a deperturbation calculation by Carroll and Collins [130]. Homogeneous perturbation with b $^1\Pi_u$ prevented application of ℓ-uncoupling theory to the c_3-c_4 p complex. Values from a deperturbation calculation by Leoni [414] are v=0, 1.912; v=1, 1.873; v=3, 1.833.

c_4: Data from p-complex analysis by Carroll and Yoshino [142].

c_5-c_8: Data from Carroll and Yoshino; use of p complex theory hindered by perturbations. B_d considered close to true B value. Approximate D_v assumed as $6.0(10^{-6})$ where needed. B_c and B_d for $c_4(0)$ to $c_6(0)$ have also been obtained by Ledbetter [408], but without consideration of uncoupling theory. The B_d values lie close to the B values obtained by Carroll and Yoshino. The D values determined have no mechanical significance.

Table 65. Rotational constants for the $c_n'\ ^1\Sigma_u^+$ Rydberg states.

State	v	$B_v(cm^{-1})$ a	b	c
c_4'	0	1.929		1.941
	1	1.711		1.907
	2	1.436		1.881
	3	1.594		1.863
	4	1.635		1.850
	5	1.80		1.841
	6	1.769		1.835
	7	1.705		1.830
	8	1.670		1.826
c_5'	0	1.337	1.345	
	1	1.29	1.285	
	2	1.173	1.173	
c_6'	0		1.990	
	1		1.9627[d]	
c_7'	0		2.057	
c_8'	0		2.15	
c_9'	0		2.215	

[a] Data from Carroll et al. [132]; the levels are perturbed.

[b] B_{eff} from a p-complex analysis by Carroll and Yoshimo [142]. See ref. [142] for definitions of terms.

[c] From a model deperturbation analysis by Leoni [414].

[d] From deperturbed data of Yoshino et al. [675]. $D_1 = 3.0(10^{-5})$.

Table 66. Rotational constants of the H $^3\Phi_u$ state.

	v	B	$D\times10^6$	A	ß
$^{14}N_2$	0	1.0778±0.0005	7.0±1.0	-12.073±0.003	0.40±0.01
	1	1.0588±0.0005	4.5±1.0	-12.081±0.003	0.40±0.01
	2	1.0402±0.0005	6.0±1.0	-12.091±0.003	0.40±0.01
	3	1.0205±0.001	5.0±1.0	-12.094±0.005	0.40±0.01
$^{15}N_2$	0	1.0071±0.0005	6.0±1.0	-12.070±0.003	0.40±0.01
	1	0.9906±0.0005	5.0±1.0	-12.076±0.003	0.40±0.01

Data from Carroll et al. [131]

Table 67. Rotational constants for the $o_n\ ^1\Pi_u$ states.

n	v	$B_v(cm^{-1})$	$D_v(10^{-5}\ cm^{-1})$
3	0	1.6869[a]	1.5
		1.6915[b]	3.0
		1.7155[c]	-1.5
	1	1.7199[a]	0.1
		1.7210[c]	0.2
	2	1.7058[a]	1.3
		1.7117[c]	1.0
	3	1.701[a]	1.6
		1.7034[b]	0.9
		1.7035[c]	0.03
	4	1.7223[a]	1.2
		1.7422[b]	6.2
4	0	1.7290[a]	-0.05
		1.7338	0.4

Data from Yoshino et al. [675].

a: Perturbed

b: With heterogeneous deperturbation

c: With homogeneous deperturbation

Table 68. Rotational constants for the $x\ ^1\Sigma_g^-$ state

v	B_v obs.
0	1.739
1	1.717
2	1.694

Observed data from Lofthus [422]. (See also Rajan [538].

Table 69. Rotational constants for the $y\ ^1\Pi_g$ state

V	B_v obs	B_v (depert.)
0	1.792[c]	
0	1.770[d]	1.729
1	1.815[d]	1.715
2	1.474[d]	1.695

Data from Lofthus and Mulliken [425] for v=0,1; data from Carroll and Subbaram [140] for v=2 and also for the deperturbed values. $D = 5.8(10^{-6})$ was used for levels v=0 to 2; calculated from $D_e = 4B_e^3/\omega_e^2$.

Table 70. Rotational constants for the $k\ ^1\Pi_g$ state.

v	B_v obs	B_v(depert.)
0	1.906	1.944
1	1.824	1.913

Data from Carroll and Subbaram [140] is for the d sublevels only obtained using $D_o = 5.9(10^{-6})$, which is the N_2^+ ground state D_e.

Table 71. Rotational constants for the $z\ ^1\Delta_g$ state.

v	B_v
0	1.753
1	---
2	---
3	1.707

Data from Lofthus [423].

Table 72. Rotational constants for the $X\ ^2\Sigma_g^+$ state of N_2^+

v	B_v obs	$10^6\ D_v$
0	1.92229	5.92
1	1.90350	6.60
2	1.88422	5.93
3	1.8651	6.1
4	1.8459	6.8
5	1.8265	7.3
6	1.8060	5.6
7	1.7855	6.0
8	1.766	
9	1.740	
10	1.724	
11	1.703	
12	1.683	
13	1.663	
14	(1.64)	
15	1.62	
16	1.593	
17	1.572	
18	(1.55)	
19	1.522	
20	1.500	
21	1.475	
22	(1.45)	

Observed data from Klynning and Pages [390], and Douglas [204]. Data in parentheses from Janin et al. [351] is of lower precision than that of Douglas.

Table 73. Rotational constants for the $A\ ^2\Pi_u$ state of N_2^+

v	B_v obs
0	---
1	---
2	1.698
3	1.678
4	1.658
5	1.638
6	1.618
7	1.598
8	1.578
9	1.558

Observed data from Janin et al. [352], derived from D - A system. Klynning and Pages [390] have obtained B_v for v = 15 as 1.454 from a partial examination of the perturbation of the B, v = 3 level.

Table 74. Rotational constants for the N_2^+ $B\ ^2\Sigma_u^+$ state.

v	B_v	v	B_v
0	2.073	15	1.452
1	2.049	16	1.404
2	2.025	17	(1.365)
3	2.002	18	(1.325)
4	1.968	19	(1.290)
5	1.926	20	(1.255)
6	1.896	21	(1.220)
7	1.852	22	1.188
8	1.810	23	---
9	---	24	---
10	1.710	25	---
11	1.653	26	1.063
12	1.595	27	1.036
13	1.545	28	---
14	1.494	29	0.977

Data from Douglas [204]. Data in parentheses from Janin et al. [351] is of lower precision than that of Douglas. A value of B_3=2.0030 was obtained by Klynning and Pages [390]; this level is perturbed by more than one other vibrational level of the A state.

Table 75. Rotational constants for the $^4\Sigma_u^+$ state of N_2^+.

v	B_v	$10^6 D_o$
0	2.064(1)	5(2)
1	2.05(1)	

Data from d'Incan and Topouzkhanian [200].

Table 76. Rotational constants for the $D^2\Pi_g$ state of N_2^+

v	B_v obs
0	---
1	---
2	---
3	1.043
4	1.023
5	1.003
6	0.983
7	0.963
8	0.943
9	0.923

Observed data from Janin et al. [352], derived from D - A system.

Table 77. Rotational constants for the $C\ ^2\Sigma_u^+$ State of N_2^+

v	B_v obs	D_v obs
0	1.509_8	$4.0\ (10^{-6})$
1	1.509_6	(average)
2	1.503_5	
3	1.497_0	
4	1.489_8	
5	1.480_4	
6	1.470_0	

Data from Carroll [125], derived from C-X system.

Table 78. RKR potentials for electronic states of N_2 below 11 eV: X, A,B, B', a', a, w and C states.

$X\ ^1\Sigma_g^+$

v	V(cm^{-1})	r_{min}(Å)	r_{max}(Å)	T_e+V(ev)	T_o(cm^{-1})
0	1175.5	1.055_0	1.145_6	0.14574	0.0
1	3505.2	1.026_6	1.184_3	0.43459	2329.66
2	5806.5	1.008_3	1.213_0	0.71992	4631.23
3	8079.2	0.994_2	1.237_7	1.00170	6903.58
4	10323.3	0.982_6	1.260_0	1.27994	9147.73
5	12538.8	0.972_5	1.280_9	1.55463	11362.97
6	14725.4	0.963_6	1.300_7	1.82573	13550.7
7	16883.1	0.955_6	1.319_7	2.09325	15707.7
8	19011.8	0.948_4	1.338_2	2.35718	17836.5
9	21111.5	0.941_7	1.356_1	2.61751	19935.9
10	23182.0	0.935_5	1.373_8	2.87422	22006.1
11	25223.3	0.929_8	1.391_1	3.12732	24047.5
12	27235.3	0.924_4	1.408_2	3.37677	26059.8
13	29218.0	0.919_4	1.425_2	3.62260	28042.7
14	31171.2	0.914_6	1.442_0	3.86477	29996.2
15	33094.9	0.910_1	1.458_8	4.10328	31920.3
16	34989.0	0.905_8	1.475_5	4.33812	33812.8
17	36853.5	0.901_7	1.492_1	4.56929	35683.3
18	38688.3	0.897_8	1.508_8	4.79678	37512.8
19	40493.4	0.894_0	1.525_5	5.02058	39317.8
20	42268.6	0.890_4	1.542_3	5.24068	41093.1
21	44014.1	0.887_0	1.559_1	5.45710	42838.8

$A\ ^3\Sigma_u^+$

v	V(cm^{-1})	r_{min}(Å)	r_{max}(Å)	T_e+V(ev)	T_o(cm^{-1})
0	726.80	1.2329	1.3482	6.31460	49754.81
1	2159.67	1.1979	1.3992	6.49226	51187.72
2	3564.87	1.1758	1.4378	6.66648	52592.96
3	4942.36	1.1589	1.4715	6.83727	53970.38
4	6292.03	1.1450	1.5025	7.00461	55320.04
5	7613.75	1.1332	1.5319	7.16848	56641.76
6	8907.33	1.1229	1.5602	7.32887	57935.33
7	10172.54	1.1138	1.5877	7.48574	59200.54
8	11409.10	1.1055	1.6149	7.63905	60437.18
9	12616.69	1.0980	1.6417	7.78878	61644.87
10	13794.95	1.091_1	1.668_5	7.93486	62822.95
11	14943.47	1.084_7	1.695_3	8.07726	63971.34
12	16061.80	1.078_7	1.722_2	8.21592	65089.92
13	17149.44	1.073_2	1.749_3	8.35077	66256.07

Table 78.--Continued

$B\ ^3\Pi_g$

v	V(cm^{-1})	r_{min}(Å)	r_{max}(Å)	T_e+V(ev)	T_o(cm^{-1})
0	863.16	1.1631	1.2689	7.49891	59306.84
1	2568.14	1.1306	1.3150	7.71031	61011.96
2	4244.46	1.1099	1.3497	7.91815	62688.12
3	5891.92	1.0940	1.3798	8.12241	64335.70
4	7510.38	1.0809	1.4074	8.32307	65954.09
5	9099.74	1.0697	1.4334	8.52013	67543.36
6	10659.92	1.0599	1.4583	8.71357	69103.59
7	12190.86	1.0511	1.4825	8.90338	70634.62
8	13692.50	1.0432	1.5061	9.08957	73136.35
9	15164.76	1.0360	1.5294	9.27210	73608.63
10	16607.54	1.0294	1.5524	9.45099	75051.31
11	18020.70	1.0233	1.5753	9.62620	76464.30
12	19404.04	1.0176	1.5981	9.79771	77847.35
13	20757.31	1.012_3	1.621_0	----	----
14	22080.16	1.007_4	1.644_0	10.12951	80524.46
15	23372.16	1.002_7	1.667_2	10.28970	81815.87
16	24632.76	0.998_2	1.690_6	10.44600	83076.11
17	25861.32	0.994_0	1.714_3	10.59832	84305.19

$B'\ ^3\Sigma_u^-$

v	V(cm^{-1})	r_{min}(Å)	r_{max}(Å)	T_e+V(eV)	T_o(cm^{-1})
0	755.40	1.2254	1.3384	8.31046	65852.35
1	2248.05	1.1908	1.3879	8.49553	67345.10
2	3716.70	1.1688	1.4250	8.67762	68813.77
3	5161.56	1.1519	1.4572	8.85676	70258.56
4	6582.82	1.1380	1.4865	9.03298	71679.66
5	7980.67	1.1261	1.5141	9.20629	73077.56
6	9355.28	1.1157	1.5404	9.37672	74452.25
7	10706.78	1.1064	1.5658	9.54429	75803.91
8	12035.31	1.0979	1.5905	9.70901	77132.44
9	13340.97	1.0903	1.6148	9.87089	78437.99
10	14623.86	1.0832	1.6386	10.02995	79720.83
11	15884.06	1.0766	1.6622	10.18619	80980.96
12	17121.62	1.0706	1.6856	10.33963	82218.55
13	18336.59	1.0649	1.7089	10.49027	83433.52
14	19528.97	1.0595	1.7321	10.63811	84625.97
15	20698.79	1.0545	1.7553	10.78315	85795.87
16	21846.03	1.0497	1.7786	10.92539	86943.08
17	22970.66	1.0452	1.8019	11.06483	88067.62
18	24072.62	1.0410	1.8254	11.20145	89169.59

Table 78.--Continued

$a'\ ^1\Sigma_u^-$

v	V(cm^{-1})	r_{min}(Å)	r_{max}(Å)	T_e+V(eV)	T_o(cm^{-1})
0	762.11	1.2229	1.3354	8.54441	67739.31
1	2268.35	1.1883	1.3846	8.73116	69245.56
2	3750.80	1.1664	1.4214	8.91496	70727.96
3	5209.70	1.1495	1.4533	9.09585	72186.78
4	6645.27	1.1356	1.4824	9.27384	73622.49
5	8057.74	1.1237	1.5096	9.44896	75034.91
6	9447.32	1.1132	1.5357	9.62125	76424.59
7	10814.20	1.1039	1.5608	9.79072	77791.36
8	12158.61	1.0955	1.5852	9.95741	79135.82
9	13480.71	1.0878	1.6091	10.12133	80457.89
10	14780.71	1.0807	1.6326	10.28251	81757.88
11	16058.77	1.0741	1.6558	10.44097	83035.97
12	17315.08	1.0680	1.6788	10.59673	84292.24
13	18549.78	1.0623	1.7016	10.74982	85526.93
14	19763.05	1.0569	1.7243	10.90025	86740.18
15	20955.03	1.0519	1.7469	11.04803	87932.24
16	22125.87	1.0471	1.7695	11.19320	89103.06
17	23275.70	1.0426	1.7921	11.33576	90252.89
18	24404.65	1.0384	1.8148	11.47574	91381.93
19	25512.84	1.0343	1.8375	11.61314	92489.95

$a\ ^1\Pi_g$

v	V(cm^{-1})	r_{min}(Å)	r_{max}(Å)	T_e+V(eV)	T_o(cm^{-1})
0	843.62	1.1702	1.2772	8.69466	68951.15
1	2509.96	1.1374	1.3240	8.90127	70617.46
2	4148.47	1.1164	1.3590	9.10442	72256.05
3	5759.24	1.1004	1.3895	9.30413	73866.77
4	7342.31	1.0871	1.4173	9.50041	75449.78
5	8897.77	1.0758	1.4435	9.69326	77005.36
6	10425.70	1.0658	1.4686	9.88270	78533.22
7	11926.19	1.0570	1.4928	10.06874	80033.69
8	13399.34	1.0489	1.5165	10.25139	81506.84
9	14845.25	1.0416	1.5397	10.43066	82952.86
10	16264.02	1.0349	1.5627	10.60657	84371.57
11	17655.79	1.0287	1.5854	10.77912	85763.31
12	19020.66	1.0229	1.6080	10.94835	87128.12
13	20358.78	1.0175	1.6305	11.11426	88466.30
14	21670.28	1.0125	1.6530	11.27686	89777.88
15	22955.31	1.0078	1.6755	11.43619	91062.81

Table 78.--Continued

$w\ ^1\Delta_u$

v	V(cm^{-1})	r_{min}(Å)	r_{max}(Å)	T_e+V(eV)	T_o(cm^{-1})
0	776.7	1.215_6	1.327_1	9.03533	71698.8
1	2312.2	1.181_4	1.375_7		
2	3824.3	1.159_6	1.412_1	9.41319	74746.4
3	5313.1	1.142_9	1.443_7	9.59778	76235.3
4	6778.8	1.129_2	1.472_4	9.77951	77700.9
5	8221.6	1.117_5	1.499_4	9.95839	79143.7
6	9641.7	1.107_2	1.525_1	10.13446	80563.8

$c\ ^3\Pi_u$

v	V(cm^{-1})	r_{min}(Å)	r_{max}(Å)	T_e+V(eV)	T_o(cm^{-1})
0	1016.71	1.1030	1.2005	11.17768	88977.89
1	3011.11	1.0730	1.2438	11.42496	90972.29
2	4951.90	1.0540	1.2771	11.66559	92913.08
3	6825.93	1.0395	1.3076	11.89794	94787.11
4	8607.21	1.0282	1.3388	12.11879	96568.39

Data is from Benesch et al. [70].

Table 79. RKR potentials for high lying singlet states of N_2: b, c, o, b', c_4', and c_5' states.

$b\ ^1\Pi_u$

v	V(cm^{-1})	r_{min}(Å)	r_{max}(Å)
0	294.1	1.1994	1.3782
1	939.5	1.1581	1.4536
2	1644.8	1.1369	1.5058
3	2392.4	1.1225	1.5491
4	3167.2	1.1114	1.5878
5	3956.8	1.1018	1.6238
6	4751.2	1.0931	1.6583
7	5542.6	1.0850	1.6917
8	6325.4	1.0771	1.7247
9	7095.6	1.0696	1.7575
10	7850.4	1.0623	1.7903
11	8588.3	1.0555	1.8233
12	9308.1	1.0490	1.8566
13	10009.1	1.0431	1.8904
14	10690.5	1.0377	1.9251
15	11351.0	1.0329	1.9610
16	11988.9	1.0287	1.9985
17	12601.5	1.0250	2.0384
18	13185.5	1.0218	2.0814
19	13736.5	1.0190	2.1286
20	14249.5	1.0165	2.1815
21	14719.2	1.0142	2.2421
22	15140.1	1.0118	2.3128
23	15507.1	1.0092	2.3973
24	15816.7	1.0061	2.5001

T_e = 100521.4 (cm^{-1})

r_e = 1.279 (Å)

$c\ ^1\Pi_u$

v	V(cm^{-1})	r_{min}(Å)	r_{max}(Å)
0	1092.4	1.0732	1.1672
1	3255.2	1.0491	1.2128
2	5388.6	1.0345	1.2471
3	7492.6	1.0246	1.2776
4	9567.2	1.0171	1.3057
5	11612.4	1.0115	1.3324
6	13628.2	1.0072	1.3582

T_e = 103300.0(cm^{-1})

r_e = 1.112 (Å)

$o\ ^1\Pi_u$

v	V(cm^{-1})	r_{min}(Å)	r_{max}(Å)
0	990.9	1.1281	1.2269
1	2948.7	1.0966	1.2687
2	4874.5	1.0772	1.3010
3	6768.2	1.0621	1.3288
4	8629.9	1.0498	1.3543
5	10459.5	1.0391	1.3782
6	12257.1	1.0297	1.4011

T_e = 104693.7 (cm^{-1})

r_e = 1.169 (Å)

Table 79.--Continued

$b'\ ^1\Sigma_u^+$

v	V(cm^{-1})	r_{min}(Å)	r_{max}(Å)
0	380.5	1.3679	1.5274
1	1131.6	1.3166	1.5938
2	1874.7	1.2832	1.6426
3	2610.3	1.2572	1.6841
4	3338.6	1.2356	1.7215
5	4059.9	1.2168	1.7563
6	4774.3	1.2003	1.7891
7	5481.8	1.1853	1.8204
8	6182.2	1.1717	1.8507
9	6875.5	1.1591	1.8802
10	7561.6	1.1474	1.9090
11	8239.1	1.1365	1.9373
12	8908.8	1.1261	1.9652
13	9569.9	1.1164	1.9929
14	10221.8	1.1070	2.0205
15	10864.0	1.0981	2.0480
16	11495.9	1.0895	2.0755
17	12116.9	1.0811	2.1032
18	12726.4	1.0729	2.1311
19	13323.8	1.0649	2.1594
20	13908.4	1.0569	2.1881
21	14479.6	1.0490	2.2173
22	15036.7	1.0412	2.2472
23	15579.1	1.0332	2.2779
24	16106.3	1.0252	2.3096
25	16617.7	1.0169	2.3424
26	17112.7	1.0085	2.3765
27	17590.9	0.9998	2.4121
28	18052.0	0.9907	2.4496

T_e = 103320.9 (cm^{-1})

r_e = 1.439 (Å)

$c_4'\ ^1\Sigma_u^+$

v	V(cm^{-1})	r_{min}(Å)	r_{max}(Å)
0	1093.8	1.0701	1.1638
1	3248.2	1.0420	1.2061
2	5358.8	1.0244	1.2384
3	7430.5	1.0112	1.2664
4	9468.0	1.0007	1.2920
5	11477.0	0.9920	1.3158
6	13461.8	0.9849	1.3382
7	15427.5	0.9791	1.3594
8	17379.2	0.9743	1.3795

T_e = 103344.0 (cm^{-1})

r_e = 1.104 (Å)

$c_5'\ ^1\Sigma_u^+$

v	V(cm^{-1})	r_{min}(Å)	r_{max}(Å)
0	1051.7	1.0715	1.1670
1	3162.2	1.0425	1.2080
2	5299.9	1.0243	1.2381

T_e = 114864.9 (cm^{-1})

r_e = 1.116 (Å)

Data is from Leoni [414], and is based upon a deperturbation calculation. These results are considered provisional.

Table 80. RKR potentials for states of N_2^+: X, A, B, and C states.

$X\ ^2\Sigma_g^+$

v	V(cm^{-1})	r_{min}(Å)	r_{max}(Å)	T_e+V(cm^{-1})
0	1099.6	1.071	1.167	1099.6
1	3285.9	1.043	1.207	3285.9
2	5417.7	1.024	1.237	5417.7
3	7536.5	1.010	1.263	7536.5
4	9590.5	0.998	1.287	9590.5
5	11648.2	0.988	1.310	11648.2
6	13651.8	0.979	1.331	13651.8
7	15629.7	0.971	1.352	15629.7
8	17570.4	0.964	1.372	17570.4
9	19474.2	0.958	1.392	19474.2
10	21345.1	0.951	1.411	21345.1
11	23180.9	0.946	1.431	23180.9
12	24981.5	0.940	1.450	24981.5
13	26746.2	0.935	1.469	26746.2
14	28479.7	0.930	1.489	28479.7
15	30164.0	0.926	1.508	30164.0
16	31819.8	0.921	1.527	31819.8
17	33436.1	0.917	1.547	33436.1
18	35012.9	0.913	1.567	35012.9
19	36550.2	0.909	1.587	36550.2
20	38048.0	0.905	1.607	38048.0

$B\ ^2\Sigma_u^+$

v	V(cm^{-1})	r_{min}(Å)	r_{max}(Å)	T_e+V(cm^{-1})
0	1204.1	1.032	1.122	26665.6
1	3575.6	1.006	1.162	29037.1
2	5894.4	0.989	1.193	31355.9
3	8154.8	0.976	1.221	33616.3
4	10351.2	0.966	1.246	35812.7
5	12474.0	0.957	1.272	37935.5
6	14515.0	0.948	1.296	39976.5
7	16466.1	0.940	1.322	41927.6
8	18304.3	0.932	1.347	43765.8
9	20031.2	0.923	1.375	45492.7
10	21627.9	0.916	1.402	47089.4
11	23107.8	0.907	1.431	48569.3
12	24479.2	0.899	1.461	49940.7
13	25755.5	0.891	1.491	51217.0
14	26951.8	0.883	1.523	52413.3
15	28078.4	0.877	1.551	53539.9
16	29145.5	0.869	1.585	54607.0
17	30161.0	0.864	1.613	55622.5
18	31127.0	0.856	1.648	56588.5
19	32049.0	0.852	1.676	57510.5
20	32931.0	0.845	1.712	58392.5
21	33776.0	0.841	1.741	59237.5
22	34586.0	0.835	1.779	60047.5
23	35361.0	0.832	1.807	60822.5
24	36105.0	0.826	1.847	61566.5
25	36822.7	0.823	1.876	62284.2
26	37513.0	0.818	1.917	62974.5
27	38174.8	0.815	1.947	63636.3
28	28812.4	0.810	1.990	64273.9

Table 80.--Continued

$C\ ^2\Sigma_u^+$

v	$V(cm^{-1})$	$r_{min}(\AA)$	$r_{max}(\AA)$	$T_e+V(cm^{-1})$
0	1049.2	1.213	1.310	65671.2
1	3096.1	1.181	1.349	67718.1
2	5126.7	1.160	1.377	69748.7
3	7136.2	1.143	1.402	71758.2
4	9111.6	1.128	1.424	73733.6
5	11055.7	1.115	1.444	75677.7
6	12968.7	1.103	1.463	77590.7
7	14845.8	1.092	1.482	79467.8
8	16691.4	1.082	1.500	81313.4

$A\ ^2\Pi_u$

v	$V(cm^{-1})$	$r_{min}(\AA)$	$r_{max}(\AA)$	$T_e+V(cm^{-1})$
0	947.7	1.135	1.235	10116.1
1	2820.8	1.103	1.279	11989.2
2	4664.0	1.083	1.312	13832.4
3	6477.3	1.068	1.341	15645.7
4	8261.0	1.055	1.366	17429.4

Data from Singh and Rai [578].

Table 81. RKR potential for the D state of N_2^+

v	$T_v(cm^{-1})$	$r_{min}(\AA)$	$r_{max}(\AA)$
$-\frac{1}{2}$	51204.5	1.471	1.471
0	51658.7	1.404	1.550
1	52547.5	1.362	1.617
2	53410.8	1.335	1.670
3	54249.1	1.316	1.716
4	55062.9	1.300	1.759
5	55852.7	1.286	1.801
6	56619.0	1.275	1.841
7	57362.3	1.265	1.880
8	58083.1	1.256	1.919
9	58781.9	1.248	1.958
10	59459.1	1.241	1.997

Data from Namioka et al. [482]. It is derived from data of Janin, and depends also on extrapolation to low v. The term values are for J=0 measured from X, v=0, J=0 of the N_2 ground state.

Table 82. Radiative lifetimes and f values. [a]

Molecule	State or Transition	Level or band	Radiative lifetime (s)	Absorption f value	Comments
N_2	$A\ ^3\Sigma_u^+$	v=0	1.9		Shemansky [570].
	$W\ ^3\Delta_u$	v=0	$0.1668(10^2)$		Calculated values by Covey et al. [180], who assumed transition moment variation for W-B was the same as for B-A. Lifetimes are assumed accurate to about 50%. Freund [23°] had estimated lifetimes against radiation by W-B as $>10^{-3}$s.
		1	$0.2000(10^{-2})$		
		2	$0.4894(10^{-3})$		
		3	$0.2336(10^{-3})$		
		4	$0.1377(10^{-3})$		
		5	$0.9287(10^{-4})$		
		6	$0.6887(10^{-4})$		
		7	$0.5432(10^{-4})$		
	$B\ ^3\Pi_g$	v=0	$8.0(10^{-6})$		Decay through B-A.
		1	$7.5(10^{-6})$		Data from Jeunehomme [357]; for v=12 the data is from Hollstein et al. [318]. Uncertainty in Jeunehomme's measurements are about 15%; Hollstein's are uncertain by 5%. A Deslandres array of Einstein A coefficients for B-A bands is given by Shemansky and Broadfoot [572], in general agreement with these measured lifetimes (table 96).
		2	$7.1(10^{-6})$		
		3	$6.8(10^{-6})$		
		4	$6.5(10^{-6})$		
		5	$6.2(10^{-6})$		
		6	$6.0(10^{-6})$		
		7	$5.3(10^{-6})$		
		8	$5.1(10^{-6})$		
		9	$4.8(10^{-6})$		
		10	$4.4(10^{-6})$		
		11	---		
		12	$4.1(10^{-6})$		
	$B'\ ^3\Sigma_u^-$	0 to 8	$(25\text{-}52)10^{-6}$		Estimates by Wentink et al. [650] are for B'-B bands.
	$a'\ ^1\Sigma_u^-$		0.5		Estimate by Tilford et al. [615] as revised by the data of Borst and Zipf [88].
	$a\ ^1\Pi_g$		$(1.15\pm.20)10^{-4}$		Borst and Zipf [88]. See also Pilling et al. [527] for discussion of f values for the electric quadrupole and magnetic dipole a-X radiation. Those f values are given at the end of this table.
	$w\ ^1\Delta_u$	0 to 4	$(5\text{-}1)10^{-4}$		Calculated estimates by Wentink et al. [650]; w-a transition.
	w-X			$\sim 10^{-8}$	Ching et al. [158].
	$^5\Sigma_g^+$		---		Only crude estimates by Benson [74] and Becker et al. [65]. Transition to $B\ ^3\Pi_g$.
	$C\ ^3\Pi_u$	v=0	$(3.66\pm.05)10^{-8}$		Weighted average of many observers' values, derived from measurements of C-B bands.
	$E\ ^3\Sigma_g^+$		$(1.90\pm0.30)10^{-4}$		Borst and Zipf [88].
	$a''\ ^1\Sigma_g^+$	0-0		$<10^{-7}$	a"-X; Lutz [429].
	$b\ ^1\Pi_u$	3-0		0.02+0.01	Data on b-X bands from Lawrence et al. [404]; crude data for 1-10 is from Johnson [361].
		4-0		$0.055\pm.011$	
		1-10	$6(10^{-8})$		
	$D\ ^3\Sigma_u^+$	v=0	$(1.41\pm0.10)10^{-8}$		Data based on measurements by Kurzweg et al. [399] on the 0-3 D-B band. Values larger by a factor of 10 were obtained by Wentink et al. [649,650].

Table 82.--Continued

Molecule	State or Transition	Level or band	Radiative lifetime (s)	Absorption f value	Comments
N_2	b' $^1\Sigma_u^+$	v=0-6(v"=0)		<.003	b'-X bands. Approximate values from Sroka [581] and
		7-0		<.1	Fowler [235].
		7-2		0.3	
		7-3		0.2	
	$c_3(0)\,^1\Pi_u$	0-0		0.040±.008	c-X. Lawrence et al. [404]. Previously called the b band.
	$H\,^3\Phi_u$			<(2.8±0.5)10^{-8}	H-C. Anton [49]; from measurements at high pressure.
	$c_4'\,(0)\,^1\Sigma_u^+$	0-0		0.14±0.04	c_4'-X. Data from Lawrence et at. [404] and Hesser and
		0	(9±2)10^{-10}		Dressler [310].
	Hopfield $^1\Sigma_u^+$ Rydberg series converging to $N_2^+B\,^2\Sigma_u^+$				
		n=4		.0131	Data from Cook and Ogawa [170]. n used here is larger by
		5		.0053	unity than the m used by Cook and Ogawa to label the
		6		.0025	Rydberg terms.
		7		.0012	
		8		.0008	
N_2^+	A $^2\Pi_u$	1-0	(13.9±1.0)10^{-6}		N_2^+ A-X. Data from Peterson and Mosely [524]; lifetime
		2-0	(11.9+0.4)10^{-6}		for v'=10 is from Maier and Holland [435]. See also
		3-0	(10.7±0.4)10^{-6}		Maier and Holland [436].
		4-1	(9.7±0.4)10^{-6}		
		5-1,5-2	(9.1±0.4)10^{-6}		
		6-3	(8.4±0.5)10^{-6}		
		7-3	(7.8±0.5)10^{-6}		
		8-3	(7.3±0.5)10^{-6}		
		9	---		
		10-4	(6.2±0.4)10^{-6}		
	B $^2\Sigma_u^+$	0-0	(6.25+0.08)10^{-8}		N_2^+ B-X. Weighted average from many observers.
	$^4\Sigma_u^+$ at 21 eV		(7±3.5)10^{-6}		Based on data of Cermak and Herman [154a], Cress et al.
					[186], Asundi et al. [55], and Ryan [552].
	C $^2\Sigma_u^+$	v'≤2	(9±3)10^{-8}		C-X. Data from van de Runstraat et al. [549,551].
		3	(9±4.5)10^{-9}		Lifetime for predissociated levels with v'≥4 are
		4	(5±2.5)10^{-9}		estimated by Albritton et al. [44] and Fournier et al.
		5	(2±1)10^{-9}		[233] as 4(10^{-9})s.

a $^1\Pi_g$

v'-v"	Magnetic dipole	Electric quadrupole
0-0	3.9(10^{-7})	
1-0	12.8(10^{-7})	6.6(10^{-8})
2-0	16.3(10^{-7})	11.1(10^{-8})
3-0	16.5(10^{-7})	13.0(10^{-8})
4-0	overlapped	----
5-0	9.8(10^{-7})	10.3(10^{-8})
6-0	7.9(10^{-7})	6.0(10^{-8})

f values for a-X bands from data of Pilling et al. [527]. Uncertainty is about 50%.

[a] For amplified discussion see section 10.2.

TABLE 83. Franck-Condon factors: $A\ ^3\Sigma_u^+ - X\ ^1\Sigma_g^+$, $B\ ^3\Pi_g - X\ ^1\Sigma_g^+$, $B'\ ^3\Sigma_u^- - X\ ^1\Sigma_g^+$, $a\ ^1\Pi_g - X\ ^1\Sigma_g^+$, $a'\ ^1\Sigma_u^- - X\ ^1\Sigma_g^+$, $w\ ^1\Delta_u - X\ ^1\Sigma_g^+$, $C\ ^3\Pi_u - X\ ^1\Sigma_g^+$, and $a\ ^1\Pi_g - X\ ^1\Sigma_g^+$ ($^{14}N^{15}N$).

$A^3\Sigma_u^+ \text{——} X^1\Sigma_g^+$

v'' \ v'	0	1	2	3	4	5	6	7	8	9	10	11	12	13
0	•9777-3 2010	•5214-2 1954	•1482-1 1901	•3008-1 1853	•4863-1 1808	•6722-1 1765	•8175-1 1726	•9145-1 1689	•9457-1 1655	•9180-1 1622	•8509-1 1592	•7562-1 1563	•6525-1 1536	•5459-1 1511
1	•8180-2 2109	•3235-1 2047	•6638-1 1990	•9377-1 1936	•1004-0 1887	•8565-1 1841	•5756-1 1798	•2935-1 1758	•9065-2 1721	•4141-3 1686	•2232-2 1653	•1086-1 1622	•2231-1 1593	•3324-1 1566
2	•3230-1 2216	•8754-1 2148	•1142-0 2085	•9019-1 2027	•4117-1 1973	•6276-2 1923	•1661-2 1876	•1851-1 1833	•3852-1 1792	•4839-1 1754	•4521-1 1718	•3293-1 1685	•1836-1 1654	•6665-2 1625
3	•8019-1 2334	•1313-0 2258	•3242-1 2189	•1458-1 2125	•3107-2 2065	•3331-1 2011	•5481-1 1960	•4713-1 1912	•2280-1 1868	•3831-2 1827	•7539-3 1788	•1034-1 1752	•2338-1 1719	•3189-1 1687
4	•1408-0 2463	•1106-0 2379	•1089-1 2302	•1590-1 2231	•5954-1 2166	•5285-1 2106	•1567-1 2050	•6088-4 1998	•1446-1 1950	•3413-1 1905	•3864-1 1863	•2711-1 1824	•1110-1 1788	•1203-2 1753
5	•1854-0 2605	•3966-1 2511	•1548-1 2425	•7253-1 2347	•4067-1 2275	•7711-3 2209	•1740-1 2147	•4370-1 2090	•3727-1 2038	•1261-1 1989	•5989-4 1943	•7431-2 1901	•2214-1 1861	•2980-1 1824
6	•1910-0 2762	•6520-5 2657	•7836-1 2561	•4484-1 2474	•4966-3 2394	•3902-1 2321	•4785-1 2253	•1379-1 2191	•6938-3 2133	•1951-1 2079	•3497-1 2030	•2800-1 1983	•1039-1 1940	•3140-3 1900
7	•1569-0 2937	•3739-1 2818	•3100-1 2711	•5276-5 2614	•4965-1 2524	•4424-1 2443	•1615-2 2368	•1697-1 2299	•4078-1 2236	•2646-1 2177	•3263-2 2122	•3306-2 2072	•1928-1 2025	•2837-1 1981
8	•1056-0 3133	•1108-0 2998	•2127-1 2877	•4362-1 2767	•5280-1 2668	•4647-4 2577	•3413-1 2494	•4203-1 2418	•7146-2 2347	•4735-2 2283	•2779-1 2223	•3124-1 2168	•1326-1 2116	•3931-3 2069
9	•5806-1 3354	•1500-0 3200	•4015-2 3062	•8094-1 2938	•2044-2 2826	•4169-1 2724	•3939-1 2632	•2843-3 2547	•2311-1 2469	•3778-1 2398	•1348-1 2332	•1644-3 2271	•1443-1 2215	•2741-1 2163
10	•2661-1 3604	•1341-0 3427	•6283-1 3269	•3567-1 3129	•3153-1 3002	•5023-1 2887	•3228-4 2783	•3714-1 2689	•3287-1 2602	•9584-3 2523	•1441-1 2450	•3241-1 2383	•1911-1 2321	•1368-2 2264
11	•1025-1 3890	•8884-1 3685	•1276-0 3503	•1670-3 3342	•7624-1 3198	•1822-2 3068	•4341-1 2951	•3077-1 2845	•8674-3 2748	•3214-1 2660	•2935-1 2579	•2396-2 2505	•7567-2 2437	•2580-1 2374
12	•3301-2 4220	•4555-1 3980	•1368-0 3769	•4670-1 3583	•3702-1 3418	•3246-1 3270	•4304-1 3137	•1942-2 3017	•4281-1 2909	•2000-1 2810	•1367-2 2720	•2677-1 2638	•2726-1 2562	•4760-2 2493
13	•8968-3 4606	•1879-1 4321	•9951-1 4073	•1170-0 3857	•9779-4 3666	•7336-1 3497	•1158-3 3345	•4939-1 3209	•1807-1 3087	•8045-2 2976	•3828-1 2875	•1479-1 2783	•1109-2 2699	•2149-1 2622
14	•2032-3 5061	•6230-2 4719	•5318-1 4425	•1338-0 4171	•4705-1 3949	•2989-1 3753	•4127-1 3579	•3103-1 3424	•9788-2 3285	•4416-1 3160	•6223-2 3046	•1184-1 2943	•3302-1 2849	•1253-1 2764
15	•3850-4 5607	•1699-2 5190	•2203-1 4837	•9864-1 4535	•1165-0 4273	•1469-2 4045	•6905-1 3844	•1795-2 3666	•5299-1 3507	•5138-2 3364	•2237-1 3236	•3356-1 3120	•1940-2 3015	•1278-1 2919
16	•6378-5 6273	•3773-3 5756	•7302-2 5325	•5246-1 4961	•1307-0 4650	•5811-1 4381	•1804-1 4146	•5447-1 3939	•1550-1 3756	•2509-1 3593	•3563-1 3447	•1680-4 3316	•2771-1 3197	•2514-1 3090
17	•0081-6 7104	•6878-4 6448	•1932-2 5912	•2110-1 5467	•9232-1 5091	•1229-0 4770	•7823-2 4493	•5898-1 4251	•1195-1 4039	•4822-1 3851	•9996-4 3684	•3742-1 3534	•1811-1 3400	•2409-2 3279
18	•1549-6 8169	•9560-5 7313	•4171-3 6631	•6561-2 6076	•4619-1 5616	•1239-0 5228	•7681-1 4897	•5484-2 4611	•6570-1 4362	•2531-2 4144	•4228-1 3951	•1769-1 3779	•8704-2 3626	•3511-1 3489
19	•2235-8 9581	•1531-5 8425	•6918-4 7533	•1650-2 6825	•1748-1 6249	•8067-1 5772	•1302-0 5371	•2340-1 5030	•4083-1 4735	•3180-1 4479	•3168-1 4254	•9926-2 4056	•4061-1 3880	•2439-2 3723
20	•1548-8 1.15	•2096-6 9906	•9327-5 8696	•3273-3 7766	•5084-2 7029	•3711-1 6431	•1146-0 5937	•9988-1 5523	•1484-4 5170	•6755-1 4866	•1704-2 4602	•5052-1 4371	•2047-2 4167	•2806-1 3987

Table 83.--Continued

$B\,^3\Pi_g \longrightarrow X\,^1\Sigma_g^+$

v'' \ v'	0	1	2	3	4	5	6	7	8	9	10	11	1	13	14	15	16	17
0	.6106-1 1686	.1477-0 1625	.1554-0 1595	.1907-0 1554	.1512-0 1516	.1054-0 1481	.6587-1 1447	.3890-1 1416	.2162-1 1386	.1139-1 1359	.5893-2 1332	.2918-2 1308	.14 1285	.7187-3 1263	.3449-3 1247	.1669-3 1222	.7984-4 1204	.3787-4 1186
1	.1914-0 1755	1941-0 1704	.6542-1 1657	.6885-3 1613	.2635-1 1572	.7651-1 1533	.1038-0 1498	.1028-0 1464	.8412-1 1435	.5988-1 1403	.3953-1 1375	.2390-1 1349	.1435-1 1324	.8176-2 1301	.4487-2 1279	.2458-2 1258	.1309-2 1238	.6864-3 1220
2	.2751-0 1829	.4513-1 1774	.2410-1 1722	.1055-0 1675	.8339-1 1631	.2028-1 1590	.6286-3 1551	.2554-1 1515	.9953-1 1481	.7742-1 1450	.5748-1 1420	.6434-1 1392	.4938-1 1366	.3452-1 1341	.2151-1 1318	.1426-1 1296	.8678-2 1275	.5114-2 1255
3	.2407-0 1908	.1615-1 1848	.1300-0 1793	.3555-1 1741	.7630-2 1693	.6643-1 1649	.7442-1 1608	.3278-1 1569	.2153-2 1533	.6556-2 1499	.3083-1 1467	.5248-1 1438	.6357-1 1410	.6185-1 1383	.5111-1 1358	.4063-1 1335	.2941-1 1313	.2010-1 1292
4	.1439-0 1994	.1427-0 1928	.4728-1 1868	.3173-1 1812	.9220-1 1760	.2536-1 1712	.4073-2 1668	.4711-1 1626	.6398-1 1588	.3731-1 1551	.7574-2 1517	.6661-3 1486	.1446-1 1456	.3433-1 1427	.4429-1 1401	.5360-1 1376	.5066-1 1353	.4285-1 1331
5	.6204-1 2086	.2046-0 2014	.1032-1 1948	.1111-0 1888	.6230-2 1832	.4226-1 1780	.7014-1 1732	.1786-1 1687	.2274-2 1645	.3566-1 1607	.5390-1 1570	.3758-1 1536	.1258-1 1504	.2064-3 1474	.5447-2 1446	.2048-1 1419	.3517-1 1394	.4391-1 1371
6	.2010-1 2185	.1500-0 2107	.1263-0 2035	.2399-1 1969	.6131-1 1908	.6160-1 1852	.1325-3 1800	.4681-1 1752	.5617-1 1707	.1287-1 1665	.2769-2 1626	.2755-1 1589	.4531-1 1555	.3723-1 1523	.1436-1 1493	.2046-2 1465	.1323-2 1438	.1086-1 1413
7	.4951-2 2294	.7020-1 2207	.1864-0 2129	.2573-1 2056	.8732-1 1990	.3640-2 1929	.7381-1 1873	.2636-1 1821	.4861-2 1772	.4663-1 1727	.4460-1 1685	.9724-2 1646	.1680-2 1609	.2180-1 1575	.3111-1 1543	.3524-1 1513	.1933-1 1484	.4829-2 1458
8	.9357-3 2411	.2332-1 2316	.1335-0 2230	.1433-0 2151	.2534-2 2078	.9102-1 2012	.1601-1 1951	.3059-1 1894	.6009-1 1842	.8247-2 1793	.1120-1 1748	.4310-1 1706	.3640-1 1666	.7948-2 1630	.1077-2 1595	.1664-1 1563	.3183-1 1533	.3222-1 1504
9	.1377-3 2540	.5616-2 2435	.5013-1 2339	.1713-0 2252	.6212-1 2173	.4588-1 2101	.3950-1 2034	.5864-1 1972	.3607-3 1916	.4761-1 1863	.3957-1 1814	.1271-2 1769	.1590-1 1727	.4049-1 1687	.3050-1 1650	.7161-2 1616	.5046-3 1584	.1210-1 1554
10	.1557-4 2681	.1028-2 2564	.1803-1 2458	.1038-0 2362	.1611-0 2275	.6786-2 2196	.8725-1 2123	.1836-2 2056	.6758-1 1995	.1650-1 1938	.1280-1 1885	.4815-1 1836	.2345-1 1791	.1963-5 1748	.1116-1 1709	.3627-1 1672	.2663-1 1637	.7097-2 1605
11	.1778-5 2836	.1353-3 2705	.4024-2 2588	.4154-1 2482	.1439-0 2386	.1121-0 2299	.6829-2 2219	.8227-1 2147	.1234-1 2080	.3600-1 2018	.4793-1 1961	.5900-3 1908	.2603-1 1859	.4213-1 1813	.1101-1 1771	.6737-3 1731	.1881-1 1694	.3219-1 1660
12	.1631-6 3008	.1320-4 2861	.6588-3 2730	.1120-1 2613	.7535-1 2507	.1673-0 2411	.4851-1 2323	.4476-1 2243	.4116-1 2170	.4759-1 2103	.4232-2 2041	.5210-1 1984	.2069-1 1931	.2455-2 1882	.3150-1 1836	.3324-1 1794	.7267-2 1754	.1555-2 1717
13	.1848-7 3199	.1884-5 3033	.7675-4 2886	.2165-2 2755	.2516-1 2638	.1144-0 2532	.1544-0 2435	.6578-2 2348	.8045-1 2268	.5618-2 2195	.6555-1 2127	.4856-2 2065	.2742-1 2008	.4304-1 1955	.5061-2 1905	.9342-2 1860	.3359-1 1817	.2555-1 1777
14	.6311-8 3412	.1926-6 3224	.6768-5 3089	.3090-3 2912	.5711-2 2781	.4661-1 2685	.1477-0 2557	.1101-0 2461	.3535-2 2373	.8388-1 2293	.3824-2 2219	.4853-1 2152	.3065-1 2090	.3051-2 2032	.3989-1 1979	.2618-1 1930	.2137-3 1884	.1489-1 1841
15	.2347-7 3651	.2453-7 3437	.5693-6 3250	.2979-4 3085	.9421-3 2938	.1268-1 2807	.7580-1 2689	.1628-0 2585	.5637-1 2487	.3204-1 2399	.5426-1 2318	.3036-1 2245	.1671-1 2177	.5015-1 2115	.4:267-2 2057	.1720-1 2004	.3819-1 1955	.1311-1 1909
16	.1417-7 3923	.1648-7 3677	.3070-7 3463	.3022-5 3276	.1078-3 3111	.2407-2 2965	.2478-1 2834	.1084-0 2716	.1567-0 2609	.1474-1 2513	.6713-1 2425	.1777-1 2345	.5697-1 2271	.1035-3 2203	.4131-1 2141	.2542-1 2083	.6957-3 2030	.2761-1 1981
17	.2165-7 4232	.8882-9 3947	.5812-8 3702	.2485-6 3489	.9333-5 3303	.3192-3 3138	.5476-2 2992	.4256-1 2861	.1377-0 2743	.1245-0 2636	.1339-4 2540	.8429-1 2452	.1455-3 2371	.5935-1 2298	.1095-1 2230	.1859-1 2167	.4131-1 2110	.6525-2 2056
18	.1021-6 4588	.9550-8 4255	.3147-7 3972	.4511-7 3728	.7433-6 3516	.2901-4 3330	.8428-3 3165	.1087-1 3019	.6576-1 2888	.1578-0 2770	.7848-1 2664	.1471-1 2567	.7096-1 2479	.1087-1 2399	.3692-1 2325	.3490-1 2257	.1008-2 2195	.3495-1 2137
19	.2363-7 5003	.3670-9 4610	.1211-7 4279	.4884-8 3967	.2012-7 3754	.2690-5 3564	.8774-4 3357	.1907-2 3193	.1994-1 3047	.9466-1 2916	.1607-0 2799	.3682-1 2682	.4547-1 2595	.3987-1 2507	.3782-1 2427	.1007-1 2353	.4829-1 2285	.5857-2 2223
20	.2549-7 5490	.2086-9 5020	.8767-8 4631	.0067-8 4302	.8930-8 4022	.1703-6 3781	.7383-5 3570	.2307-3 3385	.9983-2 3221	.3865-1 3075	.1231-0 2945	.1457-0 2827	.5737-2 2721	.7306-1 2624	.1114-1 2536	.5748-1 2456	.1056-3 2382	.3851-1 2314

Table 83.--Continued

$B'^{3}\Sigma_u^- \longrightarrow X'\Sigma_g^+$

v'' \ v'	0	1	2	3	4	5	6	7	8	9	10	11	12	13	14	15	16	17	18
0	.1605-2 1519	.8083-2 1485	.2189-1 1453	.4224-1 1423	.6197-1 1395	.8541-1 1368	.9887-1 1343	.1047-0 1319	.1031-0 1296	.9431-1 1275	.8265-1 1254	.6876-1 1235	.5602-1 1216	.4414-1 1199	.3357-1 1182	.2524-1 1166	.1875-1 1150	.1350-1 1135	.969- 11
1	.1250-1 1574	.4532-1 1538	.8530-1 1504	.1089-0 1472	.1032-0 1442	.7490-1 1413	.3945-1 1387	.1244-1 1361	.5613-3 1337	.3126-2 1314	.1488-1 1292	.2937-1 1271	.4251-1 1252	.5125-1 1233	.5446-1 1215	.5386-1 1198	.5033-1 1182	.4412-1 1166	.376 11
2	.4568-1 1633	.1085-0 1595	.1206-0 1558	.7447-1 1524	.2023-1 1491	.4222-6 1461	.1472-1 1432	.4035-1 1405	.5495-1 1379	.5096-1 1355	.3459-1 1332	.1620-1 1310	.3802-2 1289	.1350-4 1269	.3678-2 1250	.1234-1 1232	.2224-1 1215	.3054-1 1199	.364 11
3	.1044-0 1696	.1382-0 1654	.5987-1 1615	.1649-2 1578	.1234-1 1544	.5578-1 1511	.5739-1 1480	.2985-1 1451	.4872-2 1424	.1360-2 1398	.1528-1 1373	.3164-1 1350	.3975-1 1328	.3634-1 1307	.2510-1 1287	.1275-1 1268	.3702-2 1249	.6174-4 1232	.167 12
4	.1679-0 1764	.8956-1 1718	.3564-3 1676	.4154-1 1636	.6978-1 1599	.3274-1 1564	.9157-3 1531	.1220-1 1500	.3807-1 1471	.4371-1 1443	.2758-1 1417	.7746-2 1392	.1927-6 1369	.6148-2 1346	.1854-1 1325	.2849-1 1305	.3134-1 1285	.2651-1 1267	.179 12
5	.2008-0 1835	.1539-1 1786	.4315-1 1741	.7644-1 1698	.1547-1 1658	.6578-2 1620	.4322-1 1585	.4583-1 1552	.1608-1 1520	.2568-5 1491	.1184-1 1463	.3024-1 1436	.3401-1 1411	.2388-1 1388	.8508-2 1365	.3895-3 1343	.2441-2 1323	.1091-1 1304	.199 12
6	.1864-0 1912	.8593-2 1859	.9531-1 1810	.1703-1 1763	.1757-1 1720	.5870-1 1680	.2768-1 1642	.2308-5 1606	.2020-1 1575	.4029-1 1541	.2907-1 1511	.6628-2 1483	.5551-3 1456	.1233-1 1431	.2580-1 1407	.2668-1 1384	.2052-1 1365	.8577-2 1342	.103 13
7	.1377-0 1984	.7696-1 1937	.5525-1 1883	.1304-1 1833	.6785-1 1787	.1668-1 1743	.7762-2 1702	.4386-1 1664	.3328-1 1628	.3298-2 1594	.6372-2 1562	.2757-1 1532	.3298-1 1504	.1719-1 1477	.2167-2 1451	.1715-2 1427	.1237-1 1404	.2231-1 1382	.241 13
8	.8198-1 2083	.1453-0 2020	.1382-2 1962	.7687-1 1908	.2153-1 1857	.1561-1 1810	.5330-1 1766	.1623-1 1725	.3271-2 1686	.3239-1 1650	.3430-1 1616	.9209-2 1584	.5462-3 1553	.1536-1 1524	.2798-1 1497	.2360-1 1471	.9572-2 1447	.4770-3 1424	.266 14
9	.3950-1 2178	.1534-0 2107	.3338-1 2046	.6408-1 1987	.8430-2 1933	.6262-1 1882	.9280-2 1834	.1634-1 1790	.4501-1 1748	.1578-1 1709	.1026-2 1673	.2295-1 1638	.3225-1 1606	.1488-1 1575	.4074-3 1546	.6114-2 1518	.2003-1 1492	.2433-1 1468	.164 14
10	.1529-1 2281	.1122-0 2206	.1119-0 2136	.5056-2 2072	.7845-1 2013	.1676-1 1958	.2327-1 1907	.4758-1 1859	.3801-2 1814	.1605-1 1772	.3823-1 1733	.1571-1 1696	.1023-3 1661	.1568-1 1628	.2848-1 1597	.1897-1 1568	.3383-2 1540	.1118-2 1514	.112 14
11	.5133-2 2392	.6151-1 2310	.1470-0 2234	.2464-1 2164	.5947-1 2099	.1356-1 2040	.5747-1 1984	.1284-2 1932	.3155-1 1884	.3567-1 1839	.1467-2 1796	.1489-1 1756	.3338-1 1719	.1620-1 1684	.1114-3 1651	.9659-2 1619	.2399-1 1590	.2121-1 1562	.773 15
12	.1397-2 2513	.2602-1 2422	.1180-0 2339	.1039-0 2263	.3041-2 2192	.7285-1 2127	.6231-2 2066	.3818-1 2010	.3353-1 1958	.7862-3 1909	.3368-1 1864	.2662-1 1821	.1785-3 1781	.1353-1 1743	.2919-1 1707	.1665-1 1674	.9247-3 1642	.5101-2 1613	.183 15
13	.3087-3 2545	.8760-2 2544	.6690-1 2453	.1428-0 2369	.3.08-1 2292	.4657-1 2220	.2758-1 2155	.4506-1 2094	.2330-2 2037	.4485-1 1984	.1568-1 1935	.4722-2 1889	.3268-1 1846	.2118-1 1805	.2968-3 1767	.1143-1 1732	.2586-1 1698	.1730-1 1666	.243 16
14	.5618-4 2789	.2334-2 2677	.2807-1 2576	.1132-0 2484	.1114-0 2399	.2173-4 2321	.7451-1 2249	.1279-5 2183	.5247-1 2121	.1217-1 2064	.1538-1 2011	.3827-1 1961	.1700-2 1915	.8540-2 1871	.2970-1 1830	.1703-1 1792	.2256-3 1756	.9182-2 1722	.223 16
15	.8333-5 2947	.5036-3 2823	.9052-2 2710	.6152-1 2608	.1191-0 2515	.4955-1 2430	.2655-1 2351	.4920-1 2279	.2290-1 2212	.1959-1 2150	.4084-1 2092	.3334-3 2038	.2564-1 1988	.2888-1 2041	.1523-2 1897	.1086-1 1856	.2731-1 1817	.1462-1 1781	.322 17
16	.1019-5 3121	.8438-4 2982	.2303-2 2857	.2439-1 2744	.1420-0 2641	.1261-0 2547	.5251-2 2461	.6504-1 2382	.9264-2 2308	.5207-1 2241	.3901-5 2178	.3798-1 2120	.2019-1 2066	.2304-2 2015	.2934-1 1968	.2025-1 1924	.1984-3 1882	.1194-1 1843	.243 18
17	.1076-6 3114	.1074-4 3158	.4548-3 3018	.7247-2 2892	.5033-1 2778	.1234-0 2676	.7962-1 2585	.6375-2 2492	.6865-1 2412	.2715-2 2339	.4478-1 2271	.1756-1 2207	.1069-1 2149	.3714-1 2094	.6218-2 2043	.8198-2 1995	.2876-1 1951	.1397-1 1909	.497 18
18	.4911-7 3329	.7647-6 3352	.7220-4 3195	.1627-2 3034	.1187-1 2927	.8381-1 2812	.1270-0 2705	.2778-1 2612	.3930-1 2524	.3701-1 2443	.2926-1 2369	.1413-1 2301	.0937-1 2237	.6041-3 2178	.2440-1 2123	.2633-1 2071	.7320-3 2023	.1304-1 1978	.255 19
19	.1839-9 3369	.1883-6 3584	.7474-5 3390	.2887-3 3232	.4690-2 3090	.3598-1 2962	.1172-0 2846	.1026-2 2741	.6826-1 2644	.5527-2 2555	.5175-1 2475	.5175-1 2400	.3377-4 2331	.3667-1 2267	.1805-1 2207	.3431-2 2152	.2976-1 2100	.1575-1 2051	.129 20
20	.1029-7 4039	.4309-7 3809	.5717-6 3607	.3771-4 3429	.9310-3 3269	.1099-1 3127	.6190-1 2998	.1383-0 2881	.6880-1 2775	.9571-2 2673	.6623-1 2589	.3153-2 2507	.1396-1 2432	.1546-1 2362	.1276-1 2297	.3688-1 2237	.3289-2 2181	.1210-1 2129	.274 20

Table 83.--Continued

$a\,{}^1\Pi_g \longrightarrow X\,{}^1\Sigma_g^+$

v'' \ v'	0	1	2	3	4	5	6	7	8	9	10	11	12	13	14	15
0	.4308-1 1450	.1155-0 1416	.1707-0 1384	.1832-0 1354	.1600-0 1325	.1217-0 1299	.8296-1 1273	.5262-1 1249	.3153-1 1227	.1784-1 1205	.9812-2 1185	.5187-2 1166	.2733-2 1148	.1408-2 1130	.7071-3 1114	.3585-3 1098
1	.1526-0 1501	.1931-0 1464	.9710-1 1430	.1232-1 1398	.6199-2 1368	.4655-1 1339	.8456-1 1312	.9919-1 1287	.9238-1 1263	.7332-1 1240	.5294-1 1219	.3506-1 1199	.2236-1 1179	.1359-1 1161	.7888-2 1144	.4551-2 1127
2	.2495-0 1555	.7983-1 1515	.3407-2 1479	.7583-1 1444	.9643-1 1412	.4658-1 1382	.4521-2 1353	.5751-2 1326	.3372-1 1301	.6077-1 1277	.7366-1 1254	.7087-1 1233	.6034-1 1212	.4631-1 1193	.3265-1 1174	.2223-1 1157
3	.2502-0 1612	.5680-3 1570	.1084-0 1530	.6866-1 1493	.4799-3 1459	.3444-1 1427	.7273-1 1396	.5616-1 1367	.1805-1 1340	.1087-3 1315	.9922-2 1291	.3194-1 1268	.5118-1 1247	.5979-1 1226	.5754-1 1207	.5001-1 1188
4	.1728-0 1672	.9050-1 1627	.8488-1 1585	.4177-2 1545	.7834-1 1508	.5501-1 1474	.2471-2 1441	.1783-1 1411	.5600-1 1382	.5440-1 1355	.2737-1 1329	.4208-2 1305	.1318-2 1282	.1448-1 1261	.3169-1 1240	.4488-1 1221
5	.8679-1 1736	.1882-0 1688	.4928-3 1642	.9685-1 1600	.3555-1 1560	.9399-2 1523	.6401-1 1489	.4583-1 1456	.3650-2 1426	.1001-1 1397	.3999-1 1370	.4862-1 1344	.3228-1 1320	.1029-1 1297	.1516-3 1275	.4744-2 1255
6	.3306-1 1805	.1755-0 1752	.6907-1 1703	.6357-1 1658	.1909-1 1616	.7899-1 1576	.1323-1 1539	.1418-1 1504	.5550-1 1472	.3844-1 1441	.4293-2 1412	.5673-2 1385	.2975-1 1359	.4277-1 1335	.3378-1 1312	.1578-1 1290
7	.9684-2 1878	.1014-0 1821	.1681-0 1768	.5541-3 1719	.9785-1 1674	.6290-2 1631	.4320-1 1592	.5590-1 1555	.3734-2 1520	.1759-1 1487	.4821-1 1456	.3286-1 1427	.4797-2 1400	.3054-2 1374	.2170-1 1350	.3622-1 1327
8	.2210-2 1956	.4104-1 1895	.1612-0 1838	.8533-1 1785	.3279-1 1736	.5127-1 1690	.5269-1 1648	.1899-2 1608	.5251-1 1571	.3658-1 1536	.4515-3 1503	.1914-1 1472	.4236-1 1443	.2914-1 1416	.5344-2 1390	.1356-2 1366
9	.3933-2 2040	.1201-1 1973	.9090-1 1911	.1668-0 1854	.1244-1 1801	.8354-1 1752	.3557-2 1707	.6886-1 1664	.1475-1 1624	.1433-1 1587	.5006-1 1552	.2239-1 1519	.4316-4 1488	.1997-1 1459	.3729-1 1432	.2643-1 1406
10	.5505-4 2130	.2674-2 2057	.3469-1 1990	.1405-0 1928	.1161-0 1871	.5291-2 1818	.8222-1 1769	.1194-1 1723	.3569-1 1681	.4834-1 1641	.8097-3 1603	.2554-1 1568	.4284-1 1536	.1397-1 1505	.5796-3 1476	.1922-1 1448
11	.7030-5 2227	.4502-3 2147	.9607-2 2074	.7124-1 2007	.1644-0 1945	.4687-1 1888	.4631-1 1835	.3804-1 1786	.5004-1 1740	.2825-2 1698	.5136-1 1658	.2318-1 1620	.1516-2 1585	.3161-1 1552	.3462-1 1521	.8689-2 1492
12	.7162-6 2331	.5839-4 2244	.1958-2 2165	.2438-1 2092	.1136-0 2025	.1472-0 1963	.3962-2 1906	.8192-1 1853	.2884-2 1804	.6449-1 1758	.8016-2 1715	.2276-1 1675	.4472-1 1638	.7767-2 1602	.6902-2 1569	.3280-1 1538
13	.1389-6 2444	.7219-5 2349	.2931-3 2262	.5959-2 2182	.4912-1 2109	.1481-0 2042	.9858-1 1981	.7572-2 1923	.7844-1 1870	.8218-2 1821	.4149-1 1775	.3678-1 1732	.8364-3 1692	.3673-1 1655	.3025-1 1620	.1238-2 1587
14	.3433-6 2567	.6019-6 2462	.3332-4 2366	.1056-2 2279	.1433-1 2200	.8134-1 2127	.1602-0 2060	.4170-1 1998	.4214-1 1941	.4286-1 1888	.3926-1 1839	.9269-2 1793	.5113-1 1750	.8838-2 1710	.1166-1 1673	.3827-1 1638
15	.1174-7 2700	.1114-6 2584	.2869-5 2479	.1367-3 2384	.2991-2 2297	.2880-1 2218	.1165-0 2145	.1431-0 2078	.5531-2 2017	.7491-1 1960	.8037-2 1906	.6049-1 1857	.9423-3 1811	.3611-1 1768	.3192-1 1728	.3129-4 1691
16	.1391-7 2846	.4265-8 2717	.2305-6 2601	.1435-4 2497	.4451-3 2402	.7055-2 2315	.5072-1 2236	.1452-0 2164	.1027-0 2097	.3162-2 2035	.8054-1 1978	.1508-2 1925	.5228-1 1876	.2005-1 1830	.1017-1 1787	.4212-1 1747
17	.1293-7 3005	.1190-7 2862	.3516-8 2734	.1252-5 2619	.4841-4 2514	.1210-2 2420	.1454-1 2333	.7830-1 2255	.1515-0 2182	.5420-1 2115	.2840-1 2054	.5681-1 1997	.2248-1 1944	.2414-1 1894	.4302-1 1848	.1461-3 1806
18	.9650-7 3181	.2830-7 3021	.1265-7 2878	.1937-6 2751	.3776-5 2636	.1451-3 2532	.2881-2 2438	.2636-1 2352	.1017-0 2275	.1428-0 2201	.1526-1 2134	.6110-1 2073	.2239-1 2016	.4884-1 1963	.2421-2 1913	.4644-1 1867
19	.1626-7 3375	.1048-7 3195	.3261-8 3036	.4969-8 2894	.2697-6 2768	.1402-4 2653	.3933-3 2550	.6026-2 2456	.4383-1 2370	.1383-0 2292	.1216-0 2220	.5740-4 2153	.7943-1 2092	.1555-2 2035	.5884-1 1982	.3951-2 1933
20	.3021-7 3590	.6828-9 3387	.1027-7 3209	.3211-8 3051	.6947-9 2911	.1008-5 2785	.3832-4 2671	.9357-3 2568	.1146-1 2474	.6646-1 2389	.1544-0 2311	.8120-1 2239	.1047-1 2172	.7303-1 2111	.5302-2 2054	.4449-1 2001

Table 83.--Continued

$a'^1\Sigma_u^- \text{—} X^1\Sigma_g^+$

v'' \ v'	0	1	2	3	4	5	6	7	8	9	10	11	12	13	14	15	16	17	18	19
0	.1905-2 1442	.9328-2 1428	.2491-1 1385	.4717-1 1305	.7116-1 1193	.9464-1 1037	.1090-0 .1308	.1080-0 1285	.1043-0 1224	.9344-1 1143	.8032-1 1023	.6551-1 1204	.5218-1 1186	.4050-1 1169	.3017-1 1153	.2226-1 1137	.1632-1 1122	.1146-1 1108	.8086-2 1094	.5559-2 1081
1	.1440-1 1529	.5044-1 1404	.9711-2 1462	.1130-0 1431	.1020-0 1403	.9261-1 1375	.3266-1 1350	.7409-2 1325	.2787-5 1302	.5763-1 1342	.2882-1 1297	.1084-1 1275	.1188-2 1255	.1013-2 1236	.7892-2 1218	.5404-1 1168	.4930-1 1152	.4178-1 1137	.3474-1 1123	.2761-1 1109
2	.5111-1 1585	.1194-0 1513	.1206-0 1480	.6723-1 1449	.1304-1 1420	.8277-3 1393	.2139-1 1368	.4722-1 1367	.5743-1 1342	.4764-1 1319	.2882-1 1297	.1084-1 1275	.1188-2 1255	.1013-2 1236	.7892-2 1218	.1809-1 1200	.2851-1 1184	.3575-1 1168	.4023-1 1153	.4084-1 1138
3	.1133-0 1644	.1385-0 1604	.5111-1 1567	.1307-3 1532	.2717-1 1499	.4132-1 1468	.5418-1 1438	.2268-1 1411	.1520-2 1384	.4664-2 1360	.2224-1 1336	.3728-1 1314	.4097-1 1292	.3334-1 1272	.1982-1 1253	.7824-2 1234	.1058-2 1217	.4653-3 1200	.4806-2 1184	.1166-1 1168
4	.1763-0 1707	.8077-1 1664	.1324-3 1624	.5095-1 1586	.6891-1 1551	.7461-1 1518	.1462-4 1486	.1957-1 1457	.4347-1 1429	.4174-2 1402	.2097-1 1377	.3196-2 1353	.1151-2 1331	.1193-1 1309	.2498-1 1289	.3225-1 1269	.3123-1 1251	.2293-1 1233	.1305-1 1216	.4803-2 1200
5	.2039-0 1774	.9268-2 1728	.5376-1 1685	.7304-1 1644	.8598-2 1606	.1318-1 1571	.4956-1 1537	.4111-1 1505	.9181-2 1476	.1261-2 1447	.1930-1 1421	.3523-1 1395	.3297-1 1371	.1767-1 1348	.3615-2 1327	.2702-3 1306	.7059-2 1286	.1724-1 1268	.2497-1 1250	.2641-1 1233
6	.1829-0 1845	.1534-1 1795	.9636-1 1749	.9567-2 1705	.2704-1 1665	.9988-1 1626	.1906-1 1590	.1425-2 1557	.2884-1 1525	.4145-1 1495	.2216-1 1466	.2016-2 1439	.3844-2 1414	.1965-1 1389	.2996-1 1366	.2675-1 1344	.1484-1 1324	.3608-2 1304	.2723-4 1285	.4047-2 1267
7	.1296-0 1922	.9075-1 1868	.4466-1 1818	.2232-1 1771	.6764-1 1727	.1774-2 1686	.1566-1 1647	.4806-1 1611	.2540-1 1577	.2719-3 1544	.1358-1 1514	.3323-1 1485	.2901-1 1458	.1011-2 1432	.3846-4 1408	.6428-2 1385	.1043-1 1362	.2578-1 1341	.4351-3 1321	.1234-1 1302
8	.7433-1 2604	.1531-0 1945	.3835-6 1891	.8326-1 1840	.1318-1 1793	.1595-1 1748	.5282-1 1707	.8104-2 1668	.9772-2 1631	.3873-1 1597	.2841-1 1564	.3201-2 1534	.4625-2 1505	.2315-1 1477	.6428-3 1451	.1780-1 1427	.3723-2 1405	.8146-2 1384	.1781-1 1360	.1781-1 1340
9	.3436-1 2092	.1503-0 2028	.4725-1 1969	.5355-1 1914	.1792-1 1863	.1131-1 1815	.2895-2 1770	.2674-1 1728	.4350-1 1689	.7603-2 1652	.5902-2 1618	.3056-1 1585	.2887-1 1554	.7418-2 1525	.6428-3 1497	.1369-1 1471	.2541-1 1446	.2221-1 1422	.1008-1 1400	.9833-3 1378
10	.1304-1 2187	.1034-0 2117	.1259-0 2052	.8283-3 1993	.7762-1 1937	.7726-2 1886	.3516-1 1838	.4135-1 1793	.2055-3 1750	.2617-1 1711	.3653-1 1674	.7491-2 1639	.3223-2 1606	.2408-1 1574	.2799-1 1545	.1134-1 1517	.1145-3 1490	.6047-2 1465	.1849-1 1441	.2445-1 1419
11	.4024-2 2284	.5349-1 2215	.1470-0 2142	.3933-1 2077	.4783-1 2017	.2556-1 1961	.5148-1 1909	.2096-3 1861	.4147-1 1815	.2648-1 1773	.1500-3 1733	.2464-1 1695	.3178-1 1660	.7828-2 1627	.1525-2 1595	.1807-1 1565	.2639-1 1537	.1580-1 1510	.1990-2 1485	.1616-2 1461
12	.1039-2 2399	.2134-1 2316	.1089-0 2259	.1187-0 2208	.6801-1 2162	.7082-1 2042	.8223-3 1986	.4733-1 1933	.2244-1 1884	.3934-1 1795	.1719-1 1753	.3934-1 1715	.8245-3 1711	.2716-2 1682	.2824-1 1654	.2073-1 1630	.4614-3 1606	.1795-1 1558	.2318-1 1551	.1732-1 1565
13	.2182-3 2519	.6788-2 2427	.5740-1 2343	.1428-0 2269	.4832-1 2206	.3252-1 2128	.4278-1 2060	.3331-1 2010	.1031-1 1957	.4646-1 1908	.6080-2 1862	.1381-1 1818	.3578-1 1778	.1142-1 1740	.1407-2 1704	.2073-1 1670	.9227-2 1637	.1302-4 1579	.9411-2 1552	
14	.3780-4 2649	.1692-2 2568	.2245-1 2485	.1037-0 2409	.1232-0 2342	.2220-2 2280	.7152-1 2214	.3107-2 2152	.5933-1 2095	.3352-2 2035	.2784-1 1982	.3768-5 1935	.4301-3 1842	.1904-1 1801	.3008-1 1762	.7855-2 1726	.1828-1 1692	.1828-1 1660	.2337-1 1629	.1008-1 1600
15	.5197-5 2782	.3247-3 2679	.5138-1 2601	.1237-0 2528	.1358-0 2459	.7057-1 2319	.1314-1 2247	.6373-1 2180	.1019-1 2118	.3772-1 2060	.3122-1 2006	.1768-2 1956	.3503-3 1909	.1938-1 1862	.4161-3 1824	.2127-1 1785	.1149-2 1749	.5806-2 1714	.1641-2 1682	.1566-1 1651
16	.5756-6 2924	.5244-4 2822	.1582-2 2705	.1877-1 2606	.8973-1 2512	.1368-0 2426	.1724-1 2347	.5269-1 2274	.2736-1 2206	.4313-1 2144	.3744-2 2086	.4427-1 2032	.9594-2 1981	.1125-1 1934	.3324-1 1889	.9917-2 1848	.2277-2 1809	.2167-1 1772	.2208-1 1737	.4766-2 1704
17	.6513-7 3119	.5975-5 2979	.2901-3 2853	.5133-2 2736	.4028-1 2635	.1247-1 2769	.1020-0 2654	.2302-3 2575	.7280-1 2501	.1748-3 2433	.5316-1 2170	.5817-2 2112	.2415-1 2057	.3193-1 2006	.2759-3 1958	.1971-1 1914	.2748-1 1872	.4476-2 1832	.4229-2 1795	.2060-1 1760
18	.4381-7 3308	.3210-6 3151	.4264-4 3011	.1052-2 2884	.1247-1 2769	.2003-1 2665	.1408-0 2570	.5007-1 2483	.2220-1 2403	.5447-1 2329	.1416-1 2260	.2982-1 2197	.3072-1 2138	.1911-2 2083	.3431-1 2031	.1541-1 1983	.1688-2 1938	.2367-1 1896	.2088-1 1856	.1738-2 1819
19	.1120-8 3518	.1121-6 3341	.3802-5 3184	.1582-3 3042	.3112-2 2915	.2717-1 2800	.1060-0 2695	.1309-0 2599	.1031-1 2511	.5646-1 2431	.1995-1 2356	.4272-1 2287	.4068-2 2223	.4299-1 2164	.5814-2 2109	.1470-1 2057	.3116-1 2009	.4942-2 1963	.6177-2 1921	.2386-1 1881
20	.1164-7 3753	.2905-7 3552	.2390-6 3376	.1993-4 3216	.5517-3 3074	.7471-2 2946	.4864-1 2830	.1313-0 2725	.9559-1 2629	.7523-3 2540	.7202-1 2459	.3503-3 2384	.5247-1 2315	.3388-2 2251	.2805-1 2191	.2632-1 2135	.2316-3 2083	.2464-1 2034	.2164-1 1989	.5741-3 1946

Table 83.--Continued

$w\,^1\Delta_u$ —— $X\,^1\Sigma_g^+$

V'' \ V'	0	1	2	3	4	5	6
0	.3063-2 1395	.1409-1 1366	.3489-1 1338	.6176-1 1312	.8727-1 1287	.1058-0 1264	.1130-0 1241
1	.2129-1 1442	.6766-1 1410	.1103-0 1381	.1198-0 1353	.9314-1 1327	.5136-1 1302	.1645-1 1278
2	.6918-1 1491	.1343-0 1458	.1143-0 1426	.4489-1 1397	.2244-2 1369	.1023-1 1342	.4049-1 1317
3	.1399-0 1543	.1327-0 1508	.2702-1 1474	.4886-2 1442	.5014-1 1413	.6765-1 1384	.3890-1 1358
4	.1980-0 1599	.5356-1 1560	.9346-2 1524	.7366-1 1491	.5644-1 1459	.6363-2 1429	.8234-2 1400
5	.2073-0 1657	.1644-3 1616	.8176-1 1578	.5405-1 1542	.5824-6 1507	.3662-1 1475	.5516-1 1445
6	.1678-0 1720	.4318-1 1676	.8700-1 1634	.5298-9 1595	.5416-1 1559	.4922-1 1525	.2297-2 1492
7	.1067-0 1786	.1274-0 1738	.1714-1 1694	.5362-1 1652	.5282-1 1613	.1162-3 1576	.4057-1 1542
8	.5470-1 1857	.1646-0 1805	.1112-1 1757	.8503-1 1712	.5669-4 1670	.5402-1 1631	.3531-1 1594
9	.2247-1 1932	.1340-0 1876	.8948-1 1825	.2270-1 1776	.5087-1 1731	.4188-1 1689	.3903-2 1649
10	.7518-2 2012	.7848-1 1952	.1488-0 1896	.7664-2 1844	.7777-1 1796	.1010-2 1750	.5894-1 1708
11	.2057-2 2099	.3482-1 2033	.1355-0 1972	.8430-1 1916	.1567-1 1864	.6087-1 1815	.2388-1 1769
12	.4566-3 2191	.1193-1 2120	.8202-1 2054	.1444-0 1993	.1425-1 1936	.6556-1 1884	.1030-1 1835
13	.8269-4 2291	.3246-2 2213	.3603-1 2141	.1288-0 2075	.9717-1 2014	.4395-2 1957	.7361-1 1904
14	.1220-4 2398	.6911-3 2313	.1182-1 2235	.7388-1 2163	.1453-0 2096	.3284-1 2035	.4362-1 1978
15	.1251-5 2514	.1182-3 2420	.2968-2 2335	.3012-1 2257	.1149-0 2184	.1191-0 2118	.5058-3 2056
16	.1300-6 2640	.1437-4 2537	.5865-3 2443	.9033-2 2367	.5935-1 2270	.1417-0 2206	.6630-1 2139
17	.2764-7 2776	.1219-5 2663	.8824-4 2560	.2023-2 2466	.2136-1 2380	.9466-1 2301	.1400-0 2228
18	.3931-7 2925	.1311-7 2800	.1108-4 2686	.3364-3 2583	.5535-2 2488	.4134-1 2402	.1267-0 2323
19	.6109-8 3088	.4343-7 2949	.6500-6 2823	.4370-4 2709	.1068-2 2605	.1264-1 2511	.6916-1 2425
20	.1311-7 3267	.1592-7 3111	.2100-7 2972	.3952-5 2846	.1507-3 2732	.2740-2 2628	.2488-1 2534

$C\,^3\Pi_u$ —— $X\,^1\Sigma_g^+$

V'' \ V'	0	1	2	3	4
0	.5466-0 1124	.3050-0 1099	.1057-0 1076	.2963-1 1055	.7573-2 1036
1	.3470-0 1154	.8096-1 1128	.2679-0 1104	.1807-0 1082	.7749-1 1061
2	.9206-1 1186	.3612-0 1158	.2416-2 1133	.1283-0 1109	.1766-0 1088
3	.1370-1 1218	.1979-0 1190	.2351-0 1163	.7438-1 1138	.2155-1 1115
4	.1290-2 1253	.4741-1 1222	.2669-0 1194	.9156-1 1168	.1507-0 1144
5	.9019-4 1288	.6513-2 1256	.9899-1 1226	.2734-0 1199	.6433-2 1174
6	.6701-5 1326	.6425-3 1292	.1967-1 1260	.1629-0 1231	.2057-0 1205
7	.6867-6 1365	.5884-4 1329	.2779-2 1295	.4738-1 1265	.2167-0 1237
8	.4665-7 1406	.7036-5 1367	.3807-3 1332	.9458-2 1300	.9822-1 1270
9	.2808-7 1448	.1007-5 1408	.4507-4 1370	.1844-2 1336	.2865-1 1305
10	.2449-7 1493	.2039-8 1450	.1141-4 1410	.3140-3 1374	.8062-2 1341
11	.3750-7 1540	.5497-7 1494	.6290-6 1452	.7696-4 1414	.2080-2 1379
12	.1681-7 1589	.3093-7 1541	.4449-7 1496	.1254-4 1455	.5658-3 1418
13	.7348-7 1641	.6481-7 1589	.2575-6 1542	.1632-5 1498	.1298-3 1459
14	.2133-7 1695	.8725-9 1640	.0001-9 1589	.9500-6 1543	.2400-4 1502
15	.1982-7 1753	.2379-7 1693	.2275-7 1640	.2113-7 1591	.9644-5 1547
16	.1103-7 1813	.1382-7 1750	.5902-8 1692	.8046-8 1640	.7741-6 1594
17	.1133-7 1876	.1783-7 1809	.1938-8 1747	.1832-8 1692	.2522-6 1642
18	.2974-7 1943	.8937-7 1871	.2832-7 1805	.9178-7 1746	.2233-6 1693
19	.1136-7 2014	.1471-7 1936	.1916-7 1866	.7278-7 1803	.3760-7 1747
20	.1298-8 2088	.2954-7 2005	.0973-9 1930	.1719-7 1862	.1250-6 1803

Table 83.--Continued $a\,^1\Pi_g \text{——} X\,^1\Sigma_g^+$ $(N^{14}-N^{15})$

v'' \ v'	0	1	2	3	4	5	6	7	8	9	10	11	12	13	14	15
0	.4087-1 1450	.1117-0 1417	.1671-0 1385	.1825-0 1355	.1606-0 1327	.1240-0 1301	.8439-1 1276	.5477-1 1252	.3337-1 1230	.1874-1 1209	.1044-1 1188	.5424-2 1169	.2938-2 1151	.1533-2 1134	.7544-3 1118	.3844-3 1102
1	.1472-0 1500	.1929-0 1464	.1014-0 1430	.1499-1 1399	.4511-2 1369	.4288-1 1341	.8075-1 1314	.9855-1 1289	.9419-1 1265	.7468-1 1243	.5487-1 1222	.3582-1 1202	.2355-1 1182	.1453-1 1164	.8280-2 1147	.4809-2 1130
2	.2449-0 1553	.8534-1 1514	.1949-2 1478	.7135-1 1444	.9670-1 1413	.5037-1 1383	.6173-2 1354	.4168-2 1328	.3099-1 1303	.5813-1 1279	.7295-1 1256	.6988-1 1235	.6172-1 1215	.4832-1 1196	.3356-1 1178	.2306-1 1160
3	.2505-0 1609	.6836-4 1567	.1037-0 1529	.7327-1 1492	.1384-2 1459	.3025-1 1427	.7033-1 1397	.5879-1 1368	.2116-1 1342	.4831-3 1317	.8029-2 1293	.2882-1 1270	.4946-1 1249	.5986-1 1229	.5724-1 1209	.5051-1 1191
4	.1767-0 1668	.8264-1 1623	.8959-1 1582	.2220-2 1543	.7414-1 1507	.5983-1 1473	.4201-2 1441	.1458-1 1411	.5195-1 1383	.5534-1 1356	.3026-1 1331	.5608-2 1307	.6700-3 1284	.1265-1 1263	.2931-1 1243	.4316-1 1223
5	.9085-1 1731	.1834-0 1683	.1614-2 1639	.9236-1 1597	.4041-1 1558	.6314-2 1522	.6003-1 1488	.4946-1 1456	.5663-2 1426	.7503-2 1397	.3726-1 1371	.4771-1 1345	.3466-1 1321	.1243-1 1299	.4937-3 1277	.3550-2 1257
6	.3550-1 1798	.1776-0 1746	.6081-1 1699	.6922-1 1654	.1440-1 1612	.7866-1 1574	.1673-1 1537	.1051-1 1503	.5418-1 1471	.4150-1 1441	.6313-2 1412	.3823-2 1385	.2701-1 1360	.4272-1 1336	.3500-1 1313	.1764-1 1292
7	.1069-1 1869	.1059-0 1814	.1628-0 1762	.7797-5 1714	.9610-1 1670	.9653-2 1628	.3757-1 1589	.5841-1 1553	.6374-2 1518	.1371-1 1486	.4695-1 1456	.3520-1 1427	.6771-2 1400	.1778-2 1375	.1890-1 1351	.3482-1 1328
8	.2519-2 1945	.4424-1 1885	.1635-0 1830	.7585-1 1778	.3908-1 1730	.4429-1 1686	.5694-1 1644	.5367-3 1605	.4892-1 1568	.3993-1 1534	.1548-2 1502	.1506-1 1471	.4155-1 1443	.3180-1 1416	.7127-2 1390	.5678-3 1366
9	.4643-3 2027	.1341-1 1962	.9612-1 1902	.1626-0 1846	.7894-2 1794	.8661-1 1746	.1415-2 1702	.6671-1 1660	.1946-1 1621	.1033-1 1584	.4867-1 1550	.2525-1 1518	.1199-3 1487	.1714-1 1459	.3628-1 1432	.2815-1 1406
10	.6749-4 2115	.3102-2 2044	.3807-1 1978	.1441-0 1918	.1068-0 1863	.9022-2 1811	.7771-1 1763	.1666-1 1718	.2970-1 1676	.5098-1 1637	.2353-2 1601	.2089-1 1566	.4332-1 1534	.1770-1 1503	.5164-4 1475	.1637-1 1447
11	.8843-5 2208	.5428-3 2131	.1096-1 2061	.7629-1 1995	.1640-0 1935	.3779-1 1879	.5354-1 1828	.3085-1 1780	.5472-1 1735	.9607-3 1693	.4822-1 1654	.2665-1 1617	.3679-3 1583	.2831-1 1550	.3556-1 1520	.1150-1 1491
12	.9387-6 2310	.7274-4 2225	.2333-2 2148	.2721-1 2078	.1194-0 2012	.1399-0 1952	.1348-2 1897	.8412-1 1845	.8411-3 1797	.6281-1 1752	.1204-1 1710	.1780-1 1671	.4543-1 1634	.1133-1 1599	.4215-2 1567	.2995-1 1536
13	.1422-8 2419	.9297-5 2327	.3658-3 2243	.6979-2 2166	.5404-1 2095	.1509-0 2030	.8817-1 1970	.1236-1 1914	.7324-1 1862	.1285-1 1814	.3528-1 1769	.4069-1 1727	.4756-4 1688	.3287-1 1651	.3250-1 1616	.2854-2 1584
14	.2962-8 2537	.8884-6 2436	.4328-4 2344	.1293-2 2260	.1653-1 2183	.8734-1 2112	.1595-0 2047	.3212-1 1987	.4921-1 1931	.3452-1 1880	.4498-1 1832	.5364-2 1787	.5031-1 1745	.1289-1 1705	.7935-2 1668	.3627-1 1634
15	.1165-7 2666	.1371-6 2554	.3946-5 2453	.1747-3 2361	.3635-2 2277	.3255-1 2201	.1234-0 2130	.1347-0 2065	.2139-2 2005	.7874-1 1949	.4005-2 1897	.6129-1 1849	.2983-2 1804	.3096-1 1762	.3496-1 1723	.6828-3 1686
16	.1514-7 2806	.8131-8 2682	.3724-6 2571	.1951-4 2470	.5686-3 2379	.8411-2 2295	.5661-1 2219	.1481-0 2148	.9010-1 2083	.7078-2 2023	.7715-1 1967	.4352-2 1916	.4714-1 1867	.2548-1 1822	.6276-2 1780	.4054-1 1741
17	.1275-7 2958	.9154-8 2822	.7331-8 2699	.1909-5 2588	.6443-4 2488	.1519-2 2396	.1718-1 2313	.8495-1 2237	.1543-0 2166	.4282-1 2101	.3631-1 2041	.4892-1 1986	.2903-1 1934	.1786-1 1886	.4570-1 1841	.1225-2 1799
18	.1101-6 3126	.3279-7 2974	.1417-7 2838	.2476-5 2715	.5484-5 2605	.1919-3 2505	.3625-2 2414	.3033-1 2331	.1133-0 2255	.1426-0 2184	.8639-2 2120	.6856-1 2060	.1529-1 2004	.5308-1 1952	.5280-3 1904	.4364-1 1859
19	.1557-7 3311	.8061-8 3140	.4196-8 2989	.9400-8 2854	.4915-6 2732	.2018-4 2622	.5185-3 2523	.7349-2 2432	.4927-1 2349	.1414-0 2273	.1094-0 2203	.6202-3 2138	.8001-1 2078	.1020-3 2023	.5744-1 1971	.7653-2 1923
20	.3210-7 3515	.1190-8 3323	.1193-7 3154	.8834-9 3004	.4305-9 2870	.1726-5 2749	.5238-4 2640	.1207-2 2541	.1368-1 2450	.7386-1 2368	.1549-0 2292	.6843-1 2222	.1707-1 2157	.6688-1 2097	.1017-1 2042	.3821-1 1990

Data is from Benesch et al. [71]. The Deslandres tables have v'' and v' in reverse order as compared with conventional usage. The second entry for each transition is the band wavelength.

TABLE 84. Franck–Condon factors: $B\ ^3\Pi_g - A\ ^3\Sigma_u^+$, $B'\ ^3\Sigma_u^- - B\ ^3\Pi_g$, $C\ ^3\Pi_u - B\ ^3\Pi_g$, $a\ ^1\Pi_g - a'\ ^1\Sigma_u^-$, and $w\ ^1\Delta_u - a\ ^1\Pi_g$.

$B\ ^3\Pi_g$ —— $A\ ^3\Sigma_u^+$

v'' \ v'	0	1	2	3	4	5	6	7	8	9	10	11	12	13	14	15	16	17
0	.4011−0 1.105	.3976−0 .8883	.1617−0 .7732	.3423−1 .6858	.4043−2 6.73	.2680−3 .5622	.1338−4 .5168	.4460−6 .4789	.2788−6 .4468	.1086−6 .4192	.1041−6 .3951	.6958−6 .3744	.7342−7 .3660	.4159−7 .3396	.6675−7 .3250	.5876−8 .3119	.1998−8 .3001	.8729−8 .2894
1	.3300−0 1.123	.2307−2 1.02	.2744−0 .8695	.2757−0 .7606	.9719−1 .6772	.1640−1 .6114	.1408−2 .5582	.6177−4 .5142	.8721−6 .4774	.2812−7 .4460	.4631−9 .4190	.2220−7 .3956	.5979−8 .3751	.4040−7 .3570	.4997−7 .3409	.1650−7 .3265	.4607−8 .3136	.3593−7 .3020
2	.1661−0 1.149	.1593−0 1.19	.6877−1 .9706	.9557−1 .8516	.2976−0 .7484	.1698−0 .6689	.3929−1 .6057	.4318−2 .5543	.2221−3 .5117	.6736−5 .4758	.2166−6 .4451	.5428−6 .4189	.3932−7 .3960	.1350−7 .3758	.1120−7 .3580	.7637−9 .3422	.2000−8 .3280	.8369−8 .3153
3	.6692−1 1.87	.1973−0 1.42	.2208−1 1.15	.1516−0 .9648	.7488−2 .8145	.2425−0 .7368	.2311−0 .6608	.7188−1 .6001	.9946−2 .5505	.6234−3 .5092	.1621−4 .4744	.2478−6 .4446	.5210−9 .4188	.2389−7 .3963	.4085−7 .3766	.9245−8 .3591	.5883−8 .3436	.1692−7 .3297
4	.2384−1 2.51	.1306−0 1.76	.1246−0 1.36	.5122−2 1.11	.1539−0 .9.04	.1046−1 .8181	.1584−0 .7255	.2657−0 .6530	.1118−0 .5947	.1911−1 .5468	.1412−2 .5068	.5410−4 .4729	.7109−6 .4439	.1557−7 .4187	.1891−7 .3968	.1681−9 .3774	.3698−9 .3603	.1021−7 .3450
5	.7992−2 3.75	.6578−1 2.29	.1431−0 1.65	.4236−1 1.30	.5115−1 1.07	.9517−1 .9173	.5839−1 .8024	.7415−1 .7147	.2695−0 .6454	.1564−0 .5894	.3257−1 .5432	.2800−2 .5045	.9588−4 .4716	.1069−5 .4433	.3523−7 .4187	.3426−8 .3972	.4684−8 .3783	.9587−8 .3615
6	.2570−2 7.29	.2833−1 3.25	.1006−0 2.10	.1073−0 1.56	.2213−2 1.25	.9428−1 1.04	.3521−1 .8954	.1057−0 .7874	.1991−1 .7042	.2493−0 .6380	.1990−0 .5847	.5123−1 .5367	.5087−2 .5022	.1913−3 .4702	.3165−5 .4427	.3426−8 .4188	.1257−8 .3978	.3663−7 .3792
7	.8211−3 94.06	.1133−1 5.52	.5608−1 2.87	.1120−0 1.95	.5492−1 1.48	.8782−2 1.20	.1041−0 1.01	.3002−2 .8746	.1278−0 .7931	.1676−3 .6941	.2046−0 .6361	.2376−0 .5792	.7324−1 .5363	.8566−2 .5000	.3660−3 .4690	.3998−5 .4422	.2266−8 .4188	.1958−7 .3983
8	.2605−3 −8.84	.4274−2 17.40	.2724−1 4.44	.8058−1 2.57	.9438−1 1.81	.1409−1 1.41	.3932−1 1.15	.8127−1 .9806	.4815−2 .8548	.1198−0 .7592	.1028−1 .6842	.1516−0 .6259	.2595−0 .5744	.9955−1 .5329	.1343−1 .4978	.6280−3 .4678	.6741−5 .4417	.3053−8 .4190
9	.8249−4 −4.27	.1566−2 −15.79	.1213−1 8.58	.4750−1 3.72	.8949−1 2.32	.5993−1 1.70	.2021−5 1.34	.6737−1 1.11	.4441−1 .9532	.2937−1 .8359	.8951−1 .7455	.3931−1 .6748	.9598−1 .6172	.2722−0 .5696	.1302−0 .5297	.2011−1 .4958	.1036−2 .4666	.1367−4 .4413
10	.2633−4 −2.83	.5696−3 −5.51	.5149−2 −14.17	.2492−1 6.61	.6508−1 3.19	.8204−1 2.12	.2548−1 1.59	.1045−1 1.28	.7705−1 1.07	.1344−1 .9272	.5917−1 .8178	.5171−1 .7331	.7216−1 .6656	.4969−1 .6106	.2728−0 .5649	.1610−0 .5265	.2882−1 .4937	.1644−2 .4695
11	.8487−5 −2.13	.2071−3 −5.37	.2118−2 −7.98	.1209−1 27.46	.4093−1 9.04	.7443−1 2.80	.5945−1 1.05	.4151−2 1.30	.3267−1 1.22	.6552−1 1.04	.2500−3 .9025	.7956−1 .8005	.1982−1 .7267	.9826−1 .6566	.1739−1 .6041	.2571−0 .5604	.1930−0 .5234	.3993−1 .4918
12	.2805−5 −1.72	.7817−4 −2.44	.8598−3 −4.15	.5611−2 −13.25	.2213−1 11.57	.5449−1 4.08	.7086−1 2.40	.3298−1 1.80	.8255−3 1.42	.5192−1 1.17	.4197−1 1.00	.6041−2 .8792	.8327−1 .7858	.2437−2 .7087	.1135−0 .6479	.1725−2 .5979	.2305−0 .5560	.2241−0 .5204
13	.9556−6 −1.45	.2801−4 −1.93	.3444−3 −2.86	.2508−2 −5.42	.1143−1 −44.76	.3467−1 7.32	.6229−1 3.42	.5692−1 2.24	.1101−1 1.68	.1178−1 1.35	.5894−1 1.13	.1769−1 .9721	.4220−1 .8569	.7088−1 .7878	.1597−2 .6970	.1116−0 .6395	.2003−2 .5918	.1963−0 .5516

Table 84.--Continued

$B'^3\Sigma_u^- \longrightarrow B\,^3\Pi_g$

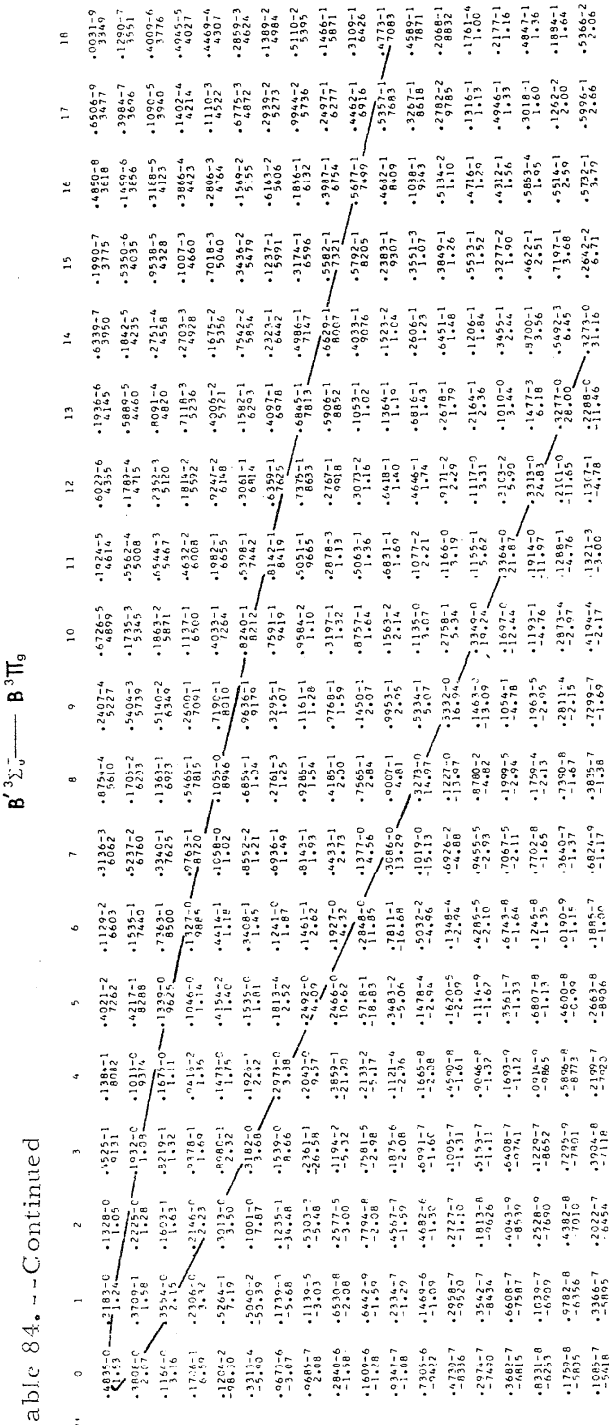

Table 84.--Continued

$C\,^3\Pi_u$ —— $B\,^3\Pi_g$

V'' \ V'	0	1	2	3	4
0	•4527-0 3370	•3949-0 3158	•1330-0 2976	•2038-1 2818	•8808-3 2684
1	•3291-0 3576	•2157-1 3338	•3413-0 3135	•2536-0 ·2961	•5454-1 2812
2	•1462-0 3804	•2033-0 3536	•2384-1 3309	•2117-0 3115	•3367-0 2952
3	•5172-1 4058	•1990-0 3754	•6345-1 3499	•8817-1 3284	•1260-0 3102
4	•1588-1 4343	•1097-0 3997	•1605-0 3709	•4811-2 3468	•1075-0 3266
5	•4540-2 4665	•4663-1 4268	•1393-0 3942	•9426-1 3671	•3908-2 3445
6	•1224-2 5032	•1686-1 4573	•7913-1 4200	•1292-0 3894	•4242-1 3641
7	•3227-3 5452	•5671-2 4917	•3622-1 4489	•9859-1 4140	•1000-0 3856
8	•8436-4 5938	•1780-2 5309	•1460-1 4813	•5520-1 4415	•9929-1 4093
9	•2139-4 6506	•5317-3 5759	•5262-2 5180	•2569-1 4722	•6566-1 4355
10	•5399-5 7180	•1567-3 6281	•1784-2 5599	•1085-1 5067	•3539-1 4647
11	•1324-5 7991	•4367-4 6893	•5608-3 6080	•4144-2 5458	•1622-1 4974
12	•3524-6 8985	•1142-4 7619	•1823-3 6638	•1475-2 5903	•7169-2 5342
13	•8744-7 1.02	•2893-5 8405	•5348-4 7293	•5076-3 6416	•2803-2 5758
14	•1875-7 1.18	•6725-6 9571	•1453-4 8072	•1607-3 7011	•1011-2 6233
15	•2182-8 1.40	•1345-6 1.09	•3614-5 9011	•4558-4 7709	•3480-3 6779
16	•1245-9 1.69	•1692-7 1.27	•6204-6 1.02	•1126-4 8539	•1014-3 7412
17	•2223-8 2.14	•1472-9 1.50	•2673-7 1.16	•1910-5 9540	•2368-4 8154

Table 84.--Continued

$a\,^1\Pi_g$ —— $a'\,^1\Sigma_u^-$

v'' \ v'	0	1	2	3	4	5	6	7	8	9	10	11	12	13	14	15
0	.6011-0 8.125	.2309-0 2.477	.6299-1 2.221	.5291-2 1.653	.1668-3 1.930	.7882-6 1.088	.6502-7 9264	.5718-7 8134	.1304-6 7283	.6151-7 6573	.2265-7 6012	.1769-6 5548	.2546-7 5158	.5001-7 4825	.4923-7 4538	.3429-7 4288
1	.2799-0 33.96	.1471-0 7.29	.4063-0 3.32	.1478-0 2.16	.1782-1 1.611	.7308-3 1.293	.5049-5 1.088	.5808-8 9269	.4330-8 3156	.8913-8 7295	.1933-7 6611	.1169-6 6054	.2593-7 5592	.7284-7 5203	.8994-7 4870	.9109-7 4584
2	.8747-1 5.62	.2779-0 90.49	.8915-2 6.54	.3596-0 3.19	.2266-0 2.12	.3732-1 1.594	.1868-2 1.128	.1546-4 1.071	.3491-6 9277	.1154-7 8180	.2409-7 7329	.8230-7 6651	.9555-8 6097	.1728-8 5638	.4175-8 5249	.1852-7 4918
3	.2322-1 3.08	.1567-0 5.36	.1848-0 144.67	.1233-1 6.95	.2682-0 3.06	.2876-0 2.08	.6300-1 1.581	.3784-2 1.271	.3578-4 1.071	.3170-6 9289	.1356-8 8207	.5693-7 7366	.2616-7 6693	.8602-7 6143	.9069-7 5685	.4558-7 5298
4	.5712-2 2.13	.6020-1 3.32	.1795-0 7.31	.9030-1 40.93	.6185-1 5.467	.1741-0 2.496	.3295-0 2.042	.9280-1 1.562	.6512-2 1.271	.5494-4 1.071	.1255-5 9303	.5363-7 8237	.1908-7 7404	.6737	.8190-8 6190	.2683-7 5734
5	.1310-2 1.83	.1943-1 2.25	.9643-1 3.59	.1632-0 8.52	.2811-1 24.10	.1110-0 5.088	.9688-1 2.486	.3487-0 2.060	.1241-0 1.552	.1001-1 1.261	.8551-4 1.071	.1932-5 9321	.1000-7 8269	.1232-6 7445	.7530-7 6785	.5885-7 6239
6	.3226-3 1.33	.3952-1 2.39	.1190-0 3.90	.1236-0 10.25	.2105-2 17.22	.1410-0 4.746	.6300-1 1.581	.4343-1 2.772	.3512-0 1.972	.1591-0 1.532	.1430-1 1.261	.9635-4 1.071	.6067-5 9343	.4892-7 8304	.7246-9 7480	.1293-7 6831
7	.7490-4 1.12	.1627-2 1.38	.1406-1 1.80	.6126-1 2.54	.1255-0 4.26	.7945-1 12.71	.3491-2 13.48	.1497-0 4.466	.1275-1 2.869	.3415-0 1.944	.1913-0 1.532	.1922-1 1.251	.1250-3 1.007	.1277-4 9368	.1503-7 8343	.1455-6 7535
8	.1795-4 .9818	.4458-3 1.16	.4720-2 1.44	.2600-1 1.89	.8012-1 2.70	.1175-0 4.68	.4126-1 16.59	.2097-1 11.14	.1408-0 4.224	.7342-3 2.622	.3208-0 1.911	.2240-0 1.251	.2415-1 1.251	.1402-3 1.007	.2162-4 9397	.1564-6 8384
9	.4240-5 .8990	.1216-3 1.011	.1475-2 1.521	.9847-2 1.931	.3978-1 1.989	.9121-1 2.489	.9604-1 4.119	.1502-1 23.57	.4340-1 3.453	.1202-0 4.011	.2208-2 2.566	.2976-0 1.886	.2538-0 1.550	.2973-1 1.251	.1045-3 1.007	.3862-4 .9430
10	.1067-5 .7807	.3365-4 .8975	.4477-3 1.04	.3566-2 1.268	.1729-1 1.958	.5345-1 2.09	.9438-1 3.09	.7144-1 5.79	.2358-2 39.83	.6441-1 8.437	.9465-1 3.693	.1217-1 2.502	.2689-0 1.886	.2806-0 1.449	.3535-1 1.251	.8340-4 1.007
11	.3013-6 .7069	.9253-5 .8052	.1336-3 .9275	.1230-2 1.081	.6858-2 1.311	.2630-1 1.652	.6401-1 2.221	.8875-1 3.326	.4529-1 5.631	.5500-3 120.21	.7899-1 7.496	.6869-1 3.674	.2622-1 2.442	.2414-0 1.884	.3107-0 1.482	.4063-1 1.251
12	.1066-6 .6517	.2415-5 .7312	.4325-4 .8307	.4031-3 .9591	.2670-2 1.122	.1178-1 1.356	.3593-1 1.732	.7154-1 2.934	.7341-1 5.258	.2552-1 7.466	.7146-2 126.11	.8666-1 6.860	.4562-1 3.553	.4153-1 2.402	.2150-0 1.822	.2318-0 1.482
13	.3252-7 .6032	.8025-6 .6706	.1251-4 .7534	.1429-3 .8575	.9666-3 .9922	.5044-2 1.162	.1803-1 1.422	.4542-1 1.812	.7486-1 2.648	.6353-1 3.872	.1072-1 8.644	.1826-1 42.31	.8797-1 6.252	.2704-1 3.402	.5600-1 2.352	.1901-0 1.812
14	.6974-8 .5420	.2738-6 .6281	.3789-5 .7767	.4772-4 .8856	.3473-3 .9835	.2019-2 1.022	.8235-2 1.221	.2478-1 1.482	.5303-1 1.902	.7103-1 2.685	.4636-1 4.221	.2397-2 10.23	.3042-1 25.78	.8247-1 5.792	.1375-1 2.291	.6789-1 2.431
15	.5103-9 .5267	.8774-7 .5774	.1326-5 .6378	.1480-4 .7109	.1322-3 .8010	.7769-3 .9151	.3641-2 1.105	.1254-1 1.262	.3213-1 1.552	.5757-1 2.002	.6470-1 2.480	.3077-1 4.602	.6328-5 12.443	.4193-1 18.722	.7328-1 5.422	.5218-2 3.192
16	.1953-9 .4661	.3298-7 .5409	.3554-6 .6935	.5930-5 .8562	.4258-4 .7323	.3284-3 .8265	.1517-2 .9460	.6034-2 1.099	.1797-1 1.311	.3888-1 1.962	.6014-1 2.410	.5547-1 2.498	.1821-1 15.05	.2470-2 15.69	.5114-1 14.82	.6255-1 5.110
17	.4013-9 .4693	.6511-8 .5092	.1227-6 .5556	.1911-5 .6102	.1555-4 .6754	.1220-3 .7548	.6243-3 .8532	.2704-2 .9785	.9204-2 1.113	.2284-1 1.436	.4383-1 1.689	.5738-1 2.222	.4366-1 3.119	.8275-2 5.459	.7688-2 21.04	.5590-1 12.35
18	.0841-9 .4457	.2540-9 .4815	.5043-7 .5228	.5627-6 .5708	.6394-5 .6276	.4297-4 .6955	.2663-3 .7782	.1186-2 .8811	.4382-2 1.000	.1265-1 1.118	.2831-1 1.442	.4680-1 1.777	.5391-1 2.234	.3248-1 3.422	.2469-2 6.222	.1494-1 31.34
19	.0582-9 .4247	.1435-9 .4571	.1972-7 .4941	.1655-6 .5369	.2621-5 .5867	.1467-4 .6457	.1120-3 .7164	.4987-3 .8027	.2345-2 .9104	.6541-2 1.004	.1644-1 1.422	.3232-1 1.848	.4828-1 1.886	.4698-1 2.488	.2131-1 3.688	.1057-3 7.600

Table 84.--Continued $w\ ^1\Delta_u \text{——} a\ ^1\Pi_g$

v'' \ v'	0	1	2	3	4	5	6
0	•6842-0 3.64	•2396-0 2.34	•5930-1 1.73	•1295-1 1.37	•2699-2 1.14	•5671-3 9812	•1200-3 8612
1	•2785-0 9.26	•2662-0 3.82	•2857-0 2.42	•1198-0 1.78	•3678-1 1.41	•9895-2 1.17	•2495-2 1.01
2	•3681-1 -17.90	•3957-0 10.23	•7138-1 4.02	•2426-0 2.51	•1574-0 1.84	•6520-1 1.45	•2191-1 1.20
3	•1817-2 -4.60	•9176-1 -15.78	•4164-0 11.38	•5102-2 4.22	•1695-0 2.61	•1688-0 1.90	•8968-1 1.49
4	•2245-4 -2.66	•6331-2 -4.50	•1527-0 -14.18	•3834-0 12.75	•6189-2 4.44	•9957-1 2.71	•1558-0 1.96
5	•5471-7 -1.87	•1011-3 -2.64	•1382-1 -4.41	•2110-0 -12.96	•3246-0 14.40	•3647-1 4.68	•4689-1 2.81
6	•8810-7 -1.45	•1378-7 -1.88	•2485-3 -2.63	•2427-1 -4.34	•2654-0 -11.99	•2576-0 16.41	•7327-1 4.93
7	•5422-7 -1.19	•2244-8 -1.46	•1156-6 -1.88	•5078-3 -2.62	•3729-1 -4.27	•3087-0 -11.21	•1935-0 18.90
8	•7501-7 -1.01	•2184-7 -1.20	•2883-6 -1.47	•3364-6 -1.89	•8626-3 -2.62	•5181-1 -4.22	•3441-0 -10.58
9	•4370-7 -8884	•1491-7 -1.02	•2243-7 -1.21	•1397-6 -1.48	•2146-5 -1.89	•1260-2 -2.61	•6941-1 -4.17
10	•1623-7 -7889	•2440-7 -8977	•1350-7 -1.03	•2573-7 -1.22	•5016-6 -1.49	•5259-5 -1.90	•1730-2 -2.62
11	•1247-6 -7109	•1521-6 -7980	•3144-7 -9075	•1097-6 -1.04	•8432-7 -1.23	•2530-6 -1.50	•1871-4 -1.91
12	•2529-7 -6480	•3393-7 -7196	•2487-8 -8075	•4388-7 -9178	•2610-8 -1.05	•6761-7 -1.24	•1122-5 -1.51
13	•4368-7 -5963	•8544-7 -6564	•1611-7 -7287	•6791-7 -8174	•1734-7 -9287	•9515-7 -1.06	•7602-7 -1.26
14	•4732-7 -5530	•1002-6 -6043	•2220-7 -6651	•7253-7 -7383	•3382-7 -8279	•5272-7 -9402	•8012-7 -1.08
15	•2040-7 -5163	•8764-7 -5608	•4363-7 -6127	•1734-7 -6743	•5807-7 -7482	•2741-7 -8388	•2021-7 -9523

Data is from Benesch et al. [72]. The Deslandres tables have v'' and v' in reverse order as compared with conventional usage. The second entry for each transition is the band wavelength.

Table 85. Franck-Condon factors for W $^3\Delta_u$ - B $^3\Pi_g$

v' \ v''	0	1	2	3	4	5	6	7	8	9
0	.3301	.4175	.2014	.4635-1	.5169-2	.2561-3	.2151-5	.3959-5	.4864-5	.8988-5
1	.3408	.4976-2	.2161	.3031	.1167	.1792-1	.1404-2	.6735-4	.1172-6	.9251-7
2	.1935	.8808-1	.1102	.4601-1	.3025	.2081	.4763-1	.4335-2	.1451-3	.1173-4
3	.9480-1	.1681	.3533-3	.1572	.4926-3	.2131	.2638	.8855-1	.1056-1	.4041-3
4	.4086-1	.1410	.6983-1	.3315-1	.1131	.3942-1	.1108	.2897	.1384	.2320-1
5	.1589-1	.8952-1	.1144	.9994-2	.8589-1	.4841-1	.9569-1	.3569-1	.2705	.1908
6	.5959-2	.5108-1	.1044	.7856-1	.4460-2	.1131	.4837-2	.1266	.1577-2	.2119
7	.2031-2	.1838-1	.7638-1	.7692-1	.2734-1	.2717-1	.9374-1	.3215-2	.1234	.8443-2
8	.4890-3	.6899-2	.2783-1	.7727-1	.3420-1	.4406-2	.4013-1	.5881-1	.2195-1	.9352-1
9	.1147-3	.2910-2	.9873-2	.5809-1	.3803-1	.2956-1	.1767-3	.6966-1	.2000-1	.5767-1

Data from Benesch (unpublished).

Table 86. Franck-Condon factors for W $^3\Delta_u$ - X $^1\Sigma_g^+$

v' \ v''	0	1	2	3	4	5	6	7	8	9	10
0	1.713-3	1.310-2	4.721-2	1.065-1	1.691-1	2.005-1	1.846-1	1.354-1	8.034-2	3.900-2	1.559-2
1	8.568-3	4.711-2	1.107-1	1.384-1	8.733-2	1.401-2	9.521-3	7.826-2	1.443-1	1.520-1	1.112-1
2	2.295-2	8.741-2	1.204-1	5.727-2	1.253-4	4.533-2	9.516-2	5.355-2	1.093-3	3.407-2	1.119-1
3	4.383-2	1.099-1	7.207-2	1.040-3	4.385-2	7.576-2	1.548-2	1.425-2	7.715-2	6.305-2	4.797-3
4	6.680-2	1.025-1	1.818-2	2.143-2	6.970-2	1.385-2	1.912-2	6.787-2	2.127-2	9.271-3	7.073-2
5	8.696-2	7.284-2	7.807-5	5.735-2	3.075-2	7.809-3	5.891-2	1.536-2	1.653_2	6.249-2	1.615-2
6	1.003-1	3.743-2	1.649-2	5.698-2	5.108-4	4.486-2	2.615-2	8.806-3	5.382-2	8.728-3	2.385-2
7	1.050-1	1.106-2	4.202-2	2.820-2	1.368-2	4.519-2	2.614-5	4.465-2	1.513-2	1.712-2	4.744-2
8	1.020-1	3.046-4	5.511-2	4.007-3	3.909-2	1.477-2	2.141-2	3.225-2	3.756-3	4.475-2	3.523-3
9	9.325-2	3.737-3	4.992-2	1.816-3	4.350-2	1.630-5	4.062-2	2.814-3	3.293-2	1.525-2	1.641-2
10	8.129-2	1.581-2	3.329-2	1.623-2	2.659-2	1.279-2	2.831-2	6.968-3	3.377-2	1.172-3	3.827-2

Data from Saum and Benesch [557].

Table 87. Franck-Condon factors for the A $^2\Pi_u$ - X $^2\Sigma_g^+$ transition in N_2^+

v' \ v''	0	1	2	3	4	5	6	7	8	9
0	.49744	.37183	.11155	.01753						
1	.31903	.04404	.35016	.22447	.05515					
2	.12647	.23639	.01369	.20793	.28991	.10698				
3	.04072	.19369	.09303	.09457	.07921	.29780	.16346			
4	.01184	.09623	.17711	.01178	.15336	.01111	.25940	.21483		
5	.00328	.03802	.13403	.11393	.00420	.15701	.00269	.19482	.25333	
6	.00089	.01333	.07051	.13839	.04839	.03895	.11924	.03221	.12440	
7	.00024	.00439	.00308	.09706	.11252	.00834	.08009	.06730	.07428	.06386

Data taken from Albritton et al. [1], as quoted by Holland and Maier [316].

Table 88. Franck-Condon factors and r centroids for the $B^2\Sigma_u^+ - X^2\Sigma_g^+$ First Negative band system of N_2^+. [a]

v'\v"	0	1	2	3	4	5	6	7	8
0	6.481-1[b]	2.619-1	7.045-2	1.565-2	3.161-3	6.106-4	1.151-4	2.084-5	
	1.1004	1.0529	1.0138	0.9782	0.9458	0.9166	0.8896	0.8611	
1	3.010-1	2.149-1	2.889-1	1.364-1	4.369-2	1.150-2	2.709-3	5.980-4	1.270-4
	1.1522	1.1121	1.0583	1.0192	0.9837	0.9510	0.9205	0.8920	0.8653
2	4.897-2	4.041-1	4.542-2	2.250-1	1.699-1	7.354-2	2.427-2	6.830-3	1.746-3
	1.2152	1.1605	1.1382	1.0636	1.0243	0.9887	0.9560	0.9252	0.8962
3	2.733-3	1.118-1	4.123-1	1.628-3	1.467-1	1.720-1	9.661-2	3.870-2	1.274-2
	1.3111	1.2251	1.1701	1.3312	1.0684	1.0291	0.9932	0.9605	0.9296
4		7.402-3	1.711-1	3.876-1	4.751-3	8.446-2	1.550-1	1.093-1	5.186-2
		1.3335	1.2360	1.1816	0.9478	1.0718	1.0336	0.9970	0.9644
5			1.169-2	2.201-1	3.639-1	1.630-2	4.373-2	1.305-1	1.120-1
			1.3630	1.2483	1.1953	0.9994	1.0707	1.0382	1.0000
6		3.016-5	5.710-5	1.301-2	2.555-1	3.569-1	2.126-2	2.019-2	1.069-1
				1.4072	1.2624	1.2111	0.9793	1.0561	1.0435
7			1.019-4	6.122-4	9.815-3	2.746-1	3.745-1	1.671-2	7.688-3
			1.3047	1.0152	1.4886	1.2787	1.2283	0.8978	0.9952
8				1.985-4	2.535-3	3.289-3	2.691-1	4.198-1	6.311-3
				1.3854	1.1560	1.7423	1.2983	1.2458	0.5943
9				1.496-5	1.836-4	6.484-3	2.832-4	2.268-1	4.867-1
				1.0438	1.5450	1.2392		1.3238	1.2624
10					9.112-5		1.092-2	1.542-2	1.400-1
					1.2115		1.3117	1.0426	1.3639
11						2.420-4	5.502-4	1.026-2	5.938-2
						1.3279	0.9621	1.4073	1.1918
12						2.496-5	2.369-4	3.808-3	2.402-3
						1.0520	1.5088	1.1946	1.7372
13							1.582-4		8.681-3
							1.2516		1.3031
14								2.886-4	1.242-3
								1.4063	1.0790

Table 88. (Continued)

v'\v"	9	10	11	12	13	14	15	16	17
0									
1	2.580-4								
	0.8385								
2	4.186-4	9.377-5	1.849-5						
	0.8690	0.8407	0.8007						
3	3.713-3	9.918-4	2.429-4	5.254-5					
	0.9005	0.8725	0.8422	0.8017					
4	1.959-2	6.426-3	1.899-3	5.081-4	1.215-4	2.558-5			
	0.9335	0.9046	0.8762	0.8448	0.8056	0.7541			
5	6.161-2	2.628-2	9.600-3	3.116-3	9.087-4	2.402-4	5.845-5	1.297-5	
	0.9678	0.9369	0.9084	0.8799	0.8480	0.8109	0.7701	0.7235	
6	1.074-1	6.730-2	3.193-2	1.284-2	4.533-3	1.438-3	4.208-4	1.170-4	3.042-5
	1.0015	0.9705	0.9396	0.9117	0.8830	0.8511	0.8174	0.7859	0.7507
7	8.845-2	9.796-2	6.901-2	3.851-2	1.566-2	5.961-3	2.052-3	6.668-4	2.083-4
	1.0519	1.0003	0.9728	0.9416	0.9146	0.8850	0.8540	0.8256	0.8008
8	1.665-3	7.724-2	8.547-2	6.774-2	3.752-2	1.765-2	7.182-3	2.691-3	9.610-4
	0.7009	1.0673	0.9937	0.9760	0.9421	0.9162	0.8858	0.8580	0.8343
9	2.320-5	4.965-5	7.511-2	7.073-2	6.484-2	3.676-2	1.853-2	8.012-3	3.252-3
			1.0958	0.9756	0.9825	0.9388	0.9172	0.8864	0.8629
10	5.473-1	1.445-2	4.231-3	8.546-2	5.371-2	6.198-2	3.336-2	1.846-2	8.300-3
	1.2764	1.8466	1.9024	1.1417	0.9320	0.9970	0.9270	0.9213	0.8855
11	4.027-2	5.403-1	5.898-2	1.872-2	1.144-1	3.388-2	6.218-2	2.803-2	1.808-2
	1.4660	1.2859	1.5924	1.7112	1.2004	0.8193	1.0289	0.8983	0.9334
12	1.124-1	1.293-3	4.184-1	1.138-1	4.415-2	1.675-1	1.386-2	6.928-2	2.072-2
	1.2618		1.2871	1.5153	1.6673	1.2578		1.0869	0.8263
13	3.481-3	1.174-1	8.231-2	2.129-1	1.334-1	6.797-2	2.419-1	9.413-4	8.766-2
	0.8343	1.3168	1.1953	1.2688	1.4790	1.6707	1.3045		1.1682
14	7.401-3	3.746-2	5.286-2	2.266-1	4.358-2	9.208-2	6.501-2	3.117-1	4.145-3
	1.4343	1.1767	1.3975	1.2595	1.1640	1.4470	1.7208	1.3356	

Data from Jain and Sahni [336]. Grandmontagne et al. [270] have calculated the parameters for higher quantum numbers. Where they overlap the calculations of Jain and Sahni, often very different numbers are obtained.

[a] The first value given for each is the Franck-Condon factor, $q_{v'v''}$; the second the r centroid $\bar{r}_{v'v''}$, units (Å).

[b] The signed digit in each first entry indicates the power of 10 to which the entry should be raised.

Table 89. Franck-Condon factors and r centroids for the $C^2\Sigma_u^+ - X^2\Sigma_g^+$ Second Negative band system of N_2^+.[a]

v'\v''	0	1	2	3	4	5	6	7	8
0	1.319-2[b]	7.599-2	1.917-1	2.755-1	2.460-1	1.388-1	4.794-2	9.087-3	6.776-4
	1.1952	1.2131	1.2323	1.2533	1.2767	1.3039	1.3378	1.3856	1.4784
1	4.876-2	1.568-1	1.569-1	2.711-2	3.217-2	1.889-1	2.311-1	1.242-1	3.073-2
	1.1783	1.1945	1.2105	1.2204	1.2681	1.2831	1.3088	1.3424	1.3913
2	9.637-2	1.530-1	2.594-2	3.898-2	1.179-1	1.794-2	5.811-2	2.265-1	1.961-1
	1.1629	1.1775	1.1883	1.2184	1.2304	1.2290	1.2983	1.3154	1.3476
3	1.354-1	8.326-2	8.036-3	9.677-2	1.255-2	5.608-2	8.184-2	1.708-3	1.667-1
	1.1485	1.1615	1.1887	1.1954	1.1989	1.2377	1.2457	1.4347	1.3254
4	1.519-1	1.911-2	6.120-2	4.203-2	2.457-2	6.885-2	2.084-3	9.034-2	1.282-2
	1.1351	1.1450	1.1660	1.1762	1.2029	1.2105	1.2842	1.2521	1.2166
5	1.449-1	1.875-4	8.147-2	1.501-4	6.885-2	2.997-3	6.262-2	1.377-2	5.433-2
	1.1224	1.1802	1.1504	1.0933	1.1811	1.1716	1.2158	1.2118	1.2594
6	1.224-1	1.892-2	5.272-2	2.323-2	3.893-2	2.349-2	3.753-2	2.144-2	4.511-2
	1.1105	1.1278	1.1360	1.1559	1.1634	1.1874	1.1926	1.2243	1.2245
7	9.412-2	4.888-2	1.543-2	5.514-2	2.260-3	5.420-2	2.416-5	5.371-2	3.228-4
	1.0992	1.1143	1.1208	1.1400	1.1358	1.1678		1.1976	1.3223
8	6.734-2	7.023-2	8.373-5	5.444-2	9.635-3	3.330-2	2.429-2	1.762-2	3.606-2
	1.0886	1.1026		1.1264	1.1475	1.1514	1.1730	1.1759	1.2025
9	4.558-2	7.664-2	8.062-3	3.021-2	3.576-2	3.771-3	4.461-2	1.024-3	3.863-2
	1.0785	1.0919	1.1108	1.1131	1.1307	1.1293	1.1556	1.2009	1.1819
10	2.967-2	7.112-2	2.596-2	7.747-3	4.597-2	3.896-3	2.801-2	2.405-2	7.018-3
	1.0692	1.0819	1.0970	1.0977	1.1178	1.1422	1.1405	1.1604	1.1596

Table 89. (continued)

v'\v''	9	10	11	12	13	14	15	16	17
0									
1	2.583-3		2.585-5						
	1.4903		1.3198						
2	6.289-2	5.801-3		8.370-5					
	1.3970	1.5031		1.3512					
3	2.460-1	1.013-1	1.010-2	2.943-5	2.009-4				
	1.3538	1.4032	1.5163		1.3809				
4	9.818-2	2.713-1	1.423-1	1.500-2	1.479-4	3.886-4		1.285-5	
	1.3419	1.3613	1.4098	1.5307		1.4109		1.4075	
5	4.473-2	4.568-2	2.766-1	1.830-1	2.004-2	4.581-4	6.390-4	1.240-5	2.265-5
	1.2471	1.3726	1.3702	1.4171	1.5461		1.4420		
6	1.715-2	6.712-2	1.474-2	2.685-1	2.223-1	2.482-2	1.082-3	9.212-4	5.129-5
	1.2746	1.2566	1.4451	1.3808	1.4248	1.5628	1.0208	1.4752	
7	5.758-2	6.717-4	7.147-2	1.742-3	2.526-1	2.597-1	2.902-2	2.136-3	1.178-3
	1.2300	1.3930	1.2620	1.7664	1.3934	1.4332	1.5810	1.1022	1.5127
8	8.660-3	4.662-2	4.179-3	6.159-2	5.730-4	2.328-1	2.949-1	3.275-2	3.702-3
	1.1951	1.2351	1.1926	1.2666		1.4084	1.4421	1.6000	1.1594
9	1.071-2	2.775-2	2.537-2	1.768-2	4.454-2	5.736-3	2.113-1	3.288-1	3.606-2
	1.2119	1.2073	1.2422	1.2249	1.2715	1.0024	1.4260	1.4514	1.6197
10	3.819-2	2.609-5	3.925-2	7.584-3	3.137-2	2.679-2	1.333-2	1.885-1	3.613-1
	1.1862	1.4975	1.2128	1.2578	1.2348	1.2785	1.0948	1.4468	1.4614

Data from Jain and Sahni [336].

[a] The first value given for each v',v'' is the Franck-Condon factor, $q_{v'v''}$; the second is the r centroid, $\bar{r}_{v'v''}$, units are (Å).

[b] The sign and final digit indicate the power of 10 to which each entry should be raised.

Table 90. Franck-Condon factors for ionization of the N_2 molecule

Transition v' - v''	$N_2^+(X^2\Sigma_u^+) - N_2(X^1\Sigma_g^+)$		$N_2^+(A^2\Pi_u) - N_2(X^1\Sigma_g^+)$		$N_2^+(B^2\Sigma_u^+) - N_2(X^1\Sigma_g^+)$		$N_2^+(C^2\Sigma_u^+) - N_2(X^1\Sigma_g^+)$	
	$^{14}N_2$	$^{14}N^{15}N$	$^{14}N_2$	$^{14}N^{15}N$	$^{14}N_2$	$^{14}N^{15}N$	$^{14}N_2$	$^{14}N^{15}N$
0 - 0	9.046-1	9.031-1	2.732-1	2.674-1	8.864-1	8.844-1	2.793-3	2.517-3
1 - 0	8.931-2	9.046-2	3.204-1	3.187-1	1.112-1	1.131-1	1.418-2	1.301-2
2 - 0	5.922-3	6.067-3	2.154-1	2.173-1	2.335-3	2.512-3	3.740-2	3.494-2
3 - 0	3.455-4	3.554-4	1.108-1	1.131-1	1.420-5	1.127-5	6.871-2	6.523-2
4 - 0	2.268-5	2.357-5	4.895-2	5.046-2	7.154-6	7.398-6	9.895-2	9.536-2
5 - 0	2.043-6	2.143-6	1.970-2	2.046-2	1.151-7	1.015-7	1.195-1	1.168-1
6 - 0	8.951-8	9.713-8	7.531-3	7.868-3	2.956-8	3.087-8	1.256-1	1.245-1
7 - 0			2.806-3	2.945-3	6.671-8	6.937-8	1.187-1	1.190-1
8 - 0			1.034-3	1.088-3			1.029-1	1.044-1
9 - 0			3.790-4	4.003-4			8.339-2	8.547-2
10 - 0			1.383-4	1.463-4			6.422-2	6.639-2
11 - 0			4.988-5	5.281-5				
12 - 0			1.765-5	1.868-5				

Data from Jain and Sahni [338].

More recently Franck-Condon factors for ionization transition N_2^+ A - N_2 X have been calculated by Albritton et al. [1]; these have been quoted by Holland and Maier [316]. Only values for the v''=0 progression were published. These are:

v'	
0	0.2746
1	.3195
2	.2148
3	.1107
4	.04894
5	.01971
6	.007492
7	.002750

TABLE 91. r-centroids: $A\ ^3\Sigma_u^+ - X\ ^1\Sigma_g^+$, $B\ ^3\Pi_g - X\ ^1\Sigma_g^+$, $B'\ ^3\Sigma_u^- - X\ ^1\Sigma_g^+$, $a'\ ^1\Sigma_u^- - X\ ^1\Sigma_g^+$, $a\ ^1\Pi_g - X\ ^1\Sigma_g^+$, $w\ ^1\Delta_u - X\ ^1\Sigma_g^+$, $C\ ^3\Pi_u - X\ ^1\Sigma_g^+$, $B\ ^3\Pi_g - A\ ^3\Sigma_u^+$, $B'\ ^3\Sigma_u^- - B\ ^3\Pi_g$, $C\ ^3\Pi_u - B\ ^3\Pi_g$, $a\ ^1\Pi_g - a'\ ^1\Sigma_u^-$, $w\ ^1\Delta_u - a\ ^1\Gamma_g$.

$A\ ^3\Sigma_u^+ \longrightarrow X\ ^1\Sigma_g^+$

v'' \ v'	0	1	2	3	4	5	6	7	8	9	10	11	12	13
0	.1185-07 .5992+16	.1175-07 .3579+17	.1165-07 .1134+18	.1155-07 .2552+18	.1146-07 .4554+18	.1137-07 .6619+18	.1129-07 .9210+18	.1120-07 .1123+19	.1113-07 .1262+19	.1105-07 .1326+19	.1098-07 .1325+19	.1091-07 .1266+19	.1084-07 .1111+19	.1077-07 .1047+19
1	.1202-07 .4138+17	.1191-07 .1844+18	.1181-07 .4237+18	.1171-07 .6669+18	.1161-07 .7919+18	.1152-07 .7453+18	.1143-07 .5503+18	.1134-07 .3070+18	.1124-07 .1033+18	.1107-07 .5126+16	.1117-07 .2990+17	.1106-07 .1568+18	.1099-07 .3401+18	.1092-07 .5524+18
2	.1219-07 .1339+18	.1208-07 .4113+18	.1197-07 .6045+18	.1186-07 .5345+18	.1176-07 .2718+18	.1163-07 .4592+17	.1168-07 .1341+17	.1153-07 .1641+18	.1143-07 .3736+18	.1135-07 .5113+18	.1127-07 .5184+18	.1119-07 .4064+18	.1112-07 .2452+18	.1105-07 .9564+17
3	.1237-07 .2704+18	.1225-07 .5049+18	.1213-07 .3532+18	.1200-07 .1757+17	.1201-07 .1707+17	.1186-07 .2039+18	.1175-07 .3717+18	.1165-07 .3525+18	.1155-07 .1872+18	.1143-07 .3440+17	.1156-07 .7372+16	.1137-07 .1067+18	.1119-07 .2680+18	.1121-07 .3936+18
4	.1256-07 .3829+18	.1243-07 .3453+18	.1228-07 .3880+17	.1224-07 .6417+17	.1211-07 .2706+18	.1200-07 .2689+18	.1188-07 .8877+17	.1242-07 .3821+15	.1178-07 .1001+18	.1165-07 .2593+18	.1156-07 .3207+18	.1147-07 .2449+18	.1118-07 .1087+18	.1122-07 .1273+17
5	.1275-07 .4027+18	.1260-07 .9695+17	.1254-07 .4272+17	.1230-07 .2590+18	.1226-07 .1518+18	.1199-07 .3241+16	.1211-07 .8188+17	.1198-07 .2289+18	.1188-07 .2162+18	.1176-07 .8061+17	.1110-07 .4200-15	.1168-07 .5662+17	.1118-07 .1883+18	.1149-07 .2690+18
6	.1294-07 .3281+18	.1075-07 .1308+18	.1270-07 .1821+18	.1255-07 .1197+18	.1271-07 .1512+16	.1236-07 .1345+18	.1224-07 .1857+18	.1210-07 .5987+17	.1225-07 .3353+16	.1199-07 .1044+18	.1188-07 .2061+18	.1178-07 .1810+18	.1167-07 .7311+17	.1136-07 .2408+18
7	.1314-07 .2109+18	.1304-07 .5925+17	.1287-07 .1498+18	.1012-07 .1131+14	.1265-07 .1223+18	.1251-07 .1242+18	.1227-07 .5136+16	.1235-07 .6072+17	.1222-07 .1633+18	.1210-07 .1178+18	.1194-07 .1608+17	.1203-07 .1764+17	.1149-07 .1167+18	.1179-07 .1841+18
8	.1335-07 .1096+18	.1323-07 .1371+18	.1304-07 .3104+17	.1297-07 .7437+17	.1281-07 .1042+18	.1180-07 .1054+15	.1261-07 .8825+17	.1248-07 .1230+18	.1232-07 .2354+17	.1237-07 .1744+17	.1221-07 .1138+18	.1210-07 .1415+18	.1199-07 .8612+17	.1167-07 .2147+16
9	.1357-07 .4590-17	.1343-07 .1431+18	.1339-07 .4567+16	.1315-07 .1086+18	.1287-07 .3204+16	.1292-07 .7568+17	.1276-07 .8213+17	.1227-07 .6758+15	.1259-07 .6210+17	.1246-07 .1143+18	.1232-07 .4560+17	.1223-07 .6161+15	.1212-07 .5066+17	.1210-07 .1253+18
10	.1380-07 .1578+17	.1365-07 .9726+17	.1352-07 .5499+17	.1333-07 .3724+17	.1325-07 .3884+17	.1308-07 .7228+17	.1434-07 .5379+14	.1287-07 .7109+17	.1272-07 .7169+17	.1242-07 .2368+16	.1258-07 .3999+17	.1244-07 .1005+18	.1232-07 .8586+17	.1211-07 .5207+16
11	.1403-07 .4477+16	.1387-07 .4820+17	.1373-07 .8422+17	.1419-07 .1339+15	.1343-07 .3291+17	.1311-07 .2057+16	.1318-07 .5724+17	.1302-07 .4699+17	.1318-07 .1521+16	.1283-07 .6422+17	.1269-07 .6634+17	.1248-07 .6088+16	.1258-07 .2147+17	.1244-07 .8126+17
12	.1427-07 .1041+16	.1410-07 .1816+17	.1395-07 .6780+17	.1382-07 .2834+17	.1361-07 .2713+17	.1353-07 .2839+17	.1335-07 .4443+17	.1342-07 .2343+16	.1313-07 .5978+17	.1296-07 .3206+17	.1309-07 .2496+16	.1281-07 .5530+17	.1267-07 .8327+17	.1251-07 .1233+17
13	.1453-07 .1993+15	.1435-07 .5391+16	.1418-07 .3615+17	.1403-07 .5288+17	.1481-07 .3414+14	.1372-07 .4908+17	.1276-07 .9245+14	.1345-07 .4455+17	.1326-07 .1990+17	.1327-07 .1026+17	.1308-07 .5602+17	.1282-07 .2444+17	.1273-07 .2069+16	.1279-07 .4546+17
14	.1480-07 .3098+14	.1460-07 .1257+16	.1443-07 .1387+17	.1426-07 .4419+17	.1413-07 .1935+17	.1390-07 .1507+17	.1382-07 .2515+17	.1361-07 .2257+17	.1360-07 .8406+16	.1339-07 .4431+17	.1317-07 .7227+16	.1322-07 .1578+17	.1305-07 .5008+17	.1289-07 .2148+17
15	.1510-07 .3856+13	.1487-07 .2341+15	.1468-07 .4024+16	.1450-07 .2332+17	.1435-07 .3493+17	.1442-07 .5487+15	.1401-07 .3163+17	.1408-07 .9944+15	.1373-07 .3504+17	.1347-07 .4011+16	.1351-07 .2041+17	.1333-07 .3542+17	.1305-07 .2368+16	.1319-07 .1760+17
16	.1534-07 .4119+12	.1517-07 .3438+14	.1495-07 .9081+15	.1476-07 .8660+16	.1459-07 .2796+17	.1444-07 .1578+17	.1418-07 .6109+16	.1411-07 .2263+17	.1387-07 .7788+16	.1385-07 .1505+17	.1365-07 .2523+17	.1582-07 .1300+14	.1345-07 .2652+17	.1332-07 .2758+17
17	.1554-07 .3566+11	.1549-07 .3980+13	.1523-07 .1562+15	.1503-07 .2362+16	.1486-07 .1374+17	.1467-07 .2373+17	.1461-07 .1923+16	.1431-07 .1806+17	.1425-07 .4490+16	.1401-07 .2192+17	.1489-07 .5427+14	.1377-07 .2398+17	.1318-07 .1315+17	.1368-07 .2085+16
18	.1511-07 .3480+10	.1598-07 .3343+12	.1550-07 .2157+14	.1532-07 .4813+15	.1511-07 .4644+16	.1492-07 .1658+17	.1477-07 .1336+17	.1443-07 .1213+16	.1441-07 .1815+17	.1403-07 .8583+15	.1412-07 .1735+17	.1390-07 .8669+16	.1393-07 .5074+16	.1371-07 .2371+17
19	.2044-07 .2653+08	.1583-07 .3039+11	.1590-07 .2148+13	.1561-07 .7606+14	.1539-07 .1146+16	.1519-07 .7266+16	.1501-07 .1565+17	.1489-07 .3657+16	.1461-07 .8123+16	.1453-07 .7901+16	.1429-07 .9669+16	.1478-07 .3667+16	.1403-07 .1791+17	.1371-07 .1269+16
20	.9284-08 .8713+07	.1559-07 .2176+10	.1633-07 .1631+12	.1569-07 .9001+13	.1569-07 .2083+15	.1548-07 .2169+16	.1528-07 .9218+16	.1511-07 .1074+17	.1817-07 .2678+13	.1472-07 .1205+17	.1485-07 .3800+15	.1441-07 .1384+17	.1402-07 .6788+15	.1416-07 .1111+17

Table 9I.--Continued

$B\,^3\Pi_0 \rightarrow X\,^1\Sigma_g^+$

v''	0	1	2	3	4	5	6	7	8	9	10	11	12	13	14	15	16	17
0	.1455-07 .1553-07	.1037-07 .1064-07	.1021-07 .1016-07	.1105-07 .1267-09	.1090-07 .2860-08	.1035-07 .1002-07	.1002-07 .1001-07	.1048-07 .8659-08	.1015-07 .5814-08	.1023-07 .3545-08	.1012-07 .1876-08	.1000-07 .9974-17	.9893-08 .5389-17	.9796-08 .2824-17	.9688-08 .1450-11	.9588-08 .7477-16	.9489-08 .3804-16	.9392-08 .1913-16
1	.1179-07 .2617-19	.1160-07 .2302-19	.1141-07 .8683-18	.1018-07 .1018-07	.1115-07 .4266-08	.1084-07 .1084-07	.1069-07 .2936-16	.1046-07 .1879-19	.1016-07 .1879-19	.1043-07 .1546-19	.1031-07 .1165-19	.1019-07 .7245-18	.1008-07 .4687-18	.9972-08 .2855-18	.9868-08 .1677-11	.9768-08 .9780-17	.9671-08 .5764-17	.9575-08 .3090-17
2	.1203-07 .2458-19	.1182-07 .5481-18	.1121-07 .2758-18	.1150-07 .1541-19	.1138-07 .4456-07	.1114-07 .3178-18	.1128-07 .1086-17	.1108-07 .5408-18	.1093-07 .4868-18	.1079-07 .3216-19	.1065-19 .1753-19	.1053-07 .1713-19	.1039-07 .1419-19	.1027-07 .1045-19	.1005-07 .7467-18	.9867-08 .9661-18	.9847-08 .5286-18	.9728-08 .2861-18
3	.1225-07 .1815-19	.1201-07 .1586-18	.1141-07 .3809-18	.1170-07 .1479-18	.1156-07 .4465-07	.1142-07 .8685-18	.1152-07 .1114-19	.1134-07 .5408-18	.1117-07 .3899-17	.1102-07 .1298-18	.1088-07 .6650-18	.1098-07 .1368-17	.1069-07 .9221-18	.1054-07 .8264-18	.1041-07 .1263-11	.1032-07 .1495-19	.1021-07 .1519-19	.1011-07 .1356-19
4	.1256-07 .9110-18	.1232-07 .1032-19	.1183-07 .3803-18	.1203-07 .2603-18	.1190-07 .8460-18	.1159-07 .2949-18	.1159-07 .3263-17	.1134-07 .8734-18	.1117-07 .1087-19	.1102-07 .6441-18	.1084-07 .1429-18	.1098-07 .1368-17	.1069-07 .9221-18	.1054-07 .8264-18	.1041-07 .1263-11	.1032-07 .1495-19	.1021-07 .1519-19	.1011-07 .1356-19
5	.1284-07 .3276-18	.1264-07 .1264-19	.1232-07 .4745-18	.1232-07 .4745-18	.1192-07 .4209-18	.1190-07 .3706-18	.1169-07 .3706-18	.1149-07 .2204-18	.1134-07 .2016-17	.1127-07 .5353-18	.1111-07 .8869-18	.1096-07 .8750-18	.1081-07 .8458-18	.1068-07 .8431-16	.1055-07 .8431-16	.1043-07 .8431-16	.1031-07 .8431-16	.1020-07 .8431-16
6	.1314-07 .4864-07	.1292-07 .1426-08	.1262-07 .5362-18	.1263-07 .1596-18	.1233-07 .4235-18	.1235-07 .3235-18	.1222-07 .3282-18	.1179-07 .6676-18	.1150-07 .2618-18	.1140-07 .1674-17	.1140-07 .3247-17	.1122-07 .4316-18	.1106-07 .9778-18	.1091-07 .8691-18	.1078-07 .3248-11	.1066-07 .4445-11	.1055-07 .3000-17	.1045-07 .3723-18
7	.1345-07 .1761-17	.1321-07 .1586-18	.1286-07 .1439-18	.1307-07 .8781-18	.1258-07 .1368-17	.1255-07 .2628-17	.1219-07 .6000-18	.1198-07 .2405-18	.1177-07 .4024-17	.1170-07 .4240-18	.1152-07 .3551-18	.1133-07 .1325-18	.1148-07 .3605-17	.1122-07 .1121-18	.1102-11 .1064-11	.1088-07 .2758-18	.1078-07 .2118-18	.1065-07 .1708-18
8	.1378-07 .3428-18	.1352-07 .8402-17	.1307-07 .8781-18	.1327-07 .1328-07	.1296-07 .1356-17	.1264-07 .3555-18	.1235-07 .1106-18	.1220-07 .2378-18	.1221-07 .5224-18	.1181-07 .1474-17	.1163-07 .1206-18	.1161-07 .3602-18	.1145-07 .1721-18	.1148-07 .1064-11	.1148-07 .1064-11	.1148-07 .1064-11	.1148-07 .1064-11	.1148-07 .1064-11
9	.1415-07 .5368-17	.1385-07 .1599-17	.1359-07 .1975-18	.1336-07 .8699-18	.1317-07 .2786-18	.1286-07 .2357-18	.1275-07 .2308-18	.1248-07 .3674-18	.1224-07 .2556-18	.1217-07 .3951-18	.1196-07 .3851-18	.1195-07 .1298-17	.1174-07 .7786-18	.1155-07 .5496-18	.1138-01 .1138-01	.1138-01 .1138-01	.1138-01 .1138-01	.1138-01 .1138-01
10	.1457-07 .3074-17	.1418-07 .2578-16	.1392-07 .2636-17	.1367-07 .1368-18	.1344-07 .2682-18	.1338-07 .2922-17	.1297-07 .2793-18	.1298-07 .1026-17	.1273-07 .2859-18	.1231-07 .1770-18	.1231-07 .9673-17	.1177-07 .4460-16	.1158-07 .2860-18	.1180-07 .2180-18	.1158-01 .2180-18	.1158-01 .2180-18	.1158-01 .2180-18	.1158-01 .2180-18
11	.1462-07 .3748-13	.1462-07 .2528-15	.1428-07 .8978-16	.1398-07 .1094-18	.1374-07 .2592-18	.1352-07 .4012-18	.1309-07 .2814-17	.1306-07 .3895-18	.1273-07 .8858-17	.1273-07 .2172-18	.1244-07 .3243-18	.1177-07 .4460-16	.1158-07 .2860-18	.1180-07 .2180-18	.1158-01 .2180-18	.1158-01 .2180-18	.1158-01 .2180-18	.1158-01 .2180-18
12	.1457-07 .1043-12	.1514-07 .1870-14	.1463-07 .1086-16	.1434-07 .2405-17	.1401-07 .1916-18	.1383-07 .4955-18	.1363-07 .1665-18	.1323-07 .1167-18	.1317-07 .1865-18	.1285-07 .2459-18	.1292-07 .2436-17	.1255-07 .3563-18	.1238-07 .1858-17	.1213-07 .5839-17	.1201-07 .3681-18	.1201-07 .3681-18	.1201-07 .3681-18	.1201-07 .3681-18
13	.9527-08 .3766-11	.1466-07 .2226-13	.1511-07 .1106-15	.1472-07 .3757-16	.1441-07 .5193-17	.1415-07 .2785-18	.1390-07 .4388-18	.1380-07 .2165-17	.1330-07 .3041-18	.1328-07 .2422-17	.1298-07 .3201-18	.1258-07 .2610-17	.1267-07 .2335-18	.1244-07 .2644-18	.1213-07 .5839-17	.1201-07 .3681-18	.1201-07 .3681-18	.1201-07 .3681-18
14	.1077-07 .2688-10	.1430-07 .1829-12	.1501-07 .1732-13	.1515-07 .2172-15	.1471-07 .9598-16	.1448-07 .9265-17	.1423-07 .3435-18	.1380-07 .3658-18	.1305-07 .1105-17	.1302-07 .1506-17	.1302-07 .1506-17	.1267-07 .2335-18	.1267-07 .2335-18	.1267-07 .2335-18	.1267-07 .2335-18	.1267-07 .2335-18	.1267-07 .2335-18	.1267-07 .2335-18
15	.1172-07 .1326-11	.1351-07 .1757-11	.1568-07 .5106-12	.1566-07 .3288-14	.1511-07 .1264-16	.1488-01 .2042-17	.1457-07 .1449-18	.1430-07 .3658-18	.1408-07 .1475-18	.1373-07 .6074-17	.1365-07 .1068-16	.1324-07 .2434-17	.1324-07 .2434-17	.1324-07 .2434-17	.1324-07 .2434-17	.1324-07 .2434-17	.1324-07 .2434-17	.1324-07 .2434-17
16	.1183-07 .5086-10	.1160-07 .9618-10	.1619-07 .2134-11	.1563-07 .2623-13	.1584-07 .1156-15	.1528-01 .3116-16	.1489-07 .3843-17	.1465-07 .1965-18	.1430-07 .1465-18	.1427-07 .1465-18	.1381-07 .1068-16	.1375-07 .5662-17	.1340-07 .2142-18	.1340-07 .2142-18	.1340-07 .2142-18	.1340-07 .2142-18	.1340-07 .2142-18	.1340-07 .2142-18
17	.1198-07 .6749-10	.1167-07 .3659-09	.1658-08 .2093-10	.1543-07 .1676-12	.1611-07 .7869-15	.1573-01 .3241-16	.1533-07 .2836-16	.1501-07 .6355-17	.1433-08 .2405-18	.1378-08 .2641-18	.1318-08 .3215-18	.1393-07 .4386-17	.1518-07 .4602-15	.1351-07 .2129-18	.1316-07 .4427-17	.1320-07 .8423-17	.1282-07 .2085-18	.1261-07 .3648-17
18	.1209-07 .2303-11	.1212-07 .2612-10	.1192-07 .1264-11	.1383-07 .2335-11	.1601-07 .1490-12	.1636-07 .2360-14	.1522-07 .8534-15	.1543-07 .1301-17	.1450-07 .2405-18	.1568-08 .2644-18	.1558-08 .3215-18	.1411-07 .4386-17	.1498-07 .4678-18	.1363-07 .3286-17	.1301-07 .1264-18	.1333-07 .1342-16	.1365-07 .4343-16	.1305-07 .1676-18
19	.1205-07 .3372-10	.1182-07 .3928-08	.1211-07 .3611-10	.1313-07 .1193-10	.1809-07 .1605-11	.1827-07 .1707-13	.1683-07 .1707-15	.1585-07 .1707-16	.1533-07 .2515-17	.1489-07 .2620-18	.1517-07 .1560-18	.1470-07 .4629-17	.1478-07 .1062-18	.1416-07 .1011-18	.1381-07 .1060-18	.1382-07 .3285-17	.1346-07 .1771-18	.1306-07 .2596-17
20	.1223-07 .2866-10	.1218-07 .3284-08	.1229-07 .1403-10	.1502-07 .1958-08	.1042-07 .3436-10	.1628-07 .8558-11	.1462-07 .4566-13	.1535-07 .1957-15	.1482-07 .3666-16	.1557-07 .3762-17	.1526-07 .1637-18	.1498-07 .2280-18	.1495-07 .1051-17	.1439-07 .1949-18	.1436-07 .2452-17	.1393-07 .1581-18	.1282-07 .3281-15	.1358-07 .1943-18

Table 91.--Continued

$B'^3\Sigma_u^- \longrightarrow X\,^1\Sigma_g^+$

v', v''	0	1	2	3	4	5	6	7	8	9	10	11	12	13	14	15	16	17	18
0	.1082-07	.1421-08	.2486-08	.1836-09	.1111-09	.2131-09	.3038-09	—.3458-09	—.3485-09	.3450-09	.3088-09	.2683-09	.2476-09	.2196-09	.1960-09	.1854-09	.1047-09	.1041-09	.1035-09
1	.1209-07	.1188-07	.1877-08	.1446-09	.2158-09	.1844-09	.1086-09	.1126-09	.1109-09	.1197-09	.1050-09	.1097-09	.1095-09	.2217-09	.1074-09	.1067-09	.1061-09	.1054-09	.1048-09
2	.1217-07	.1205-07	.1193-07	.1381-08	.1178-09	.1818-09	.1366-09	.1045-09	.1135-09	.1318-09	.1165-09	.1108-09	.1378-08	.1179-09	.1092-09	.1083-09	.1075-09	.1068-09	.1062-09
3	.1236-07	.1223-07	.1210-07	.1385-08	.1182-09	.1180-09	.1168-09	.1157-09	.1144-09	.1165-09	.1136-09	.1126-09	.1117-09	.1109-09	.1100-09	.1092-09	.1083-09	.1076-09	.1069-09
4	.1255-07	.1250-07	.1201-07	.1219-07	.1206-09	.1193-09	.1168-09	.1179-09	.1167-09	.1178-09	.1146-09	.1135-09	.1323-08	.1278-08	.1118-09	.1109-09	.1101-09	.1094-09	.1087-09
5	.1274-07	.1256-07	.1250-07	.1235-07	.1220-09	.1220-09	.1203-09	.1191-09	.1178-09	.1191-09	.1167-09	.1155-09	.1146-09	.1138-08	.1126-09	.1118-09	.1111-09	.1103-09	.1097-09
6	.1294-07	.1287-07	.1267-07	.1250-07	.1246-09	.1230-09	.1218-09	.1203-09	.1191-09	.1203-09	.1177-09	.1166-09	.1156-09	.1148-08	.1146-09	.1136-09	.1127-09	.1118-09	.1111-09
7	.1313-07	.1303-07	.1285-07	.1270-07	.1261-09	.1245-09	.1228-09	.1215-09	.1203-09	.1215-09	.1187-09	.1177-09	.1167-09	.1158-09	.1158-09	.1148-09	.1139-09	.1131-09	.1124-09
8	.1333-07	.1331-07	.1305-07	.1289-07	.1276-09	.1262-09	.1239-09	.1227-09	.1215-09	.1227-09	.1199-09	.1187-09	.1178-09	.1170-09	.1170-09	.1158-09	.1150-09	.1143-09	.1136-09
9	.1356-07	.1344-07	.1327-07	.1310-07	.1308-09	.1286-09	.1265-09	.1251-09	.1239-09	.1251-09	.1221-09	.1211-09	.1201-09	.1193-09	.1193-09	.1181-09	.1172-09	.1164-09	.1158-09
10	.1378-07	.1367-07	.1353-07	.1334-07	.1338-09	.1311-09	.1291-09	.1278-09	.1265-09	.1278-09	.1247-09	.1236-09	.1226-09	.1218-09	.1218-09	.1206-09	.1197-09	.1189-09	.1182-09
11	.1409-07	.1391-08	.1374-07	.1358-07	.1361-09	.1337-09	.1318-09	.1305-09	.1291-09	.1305-09	.1273-09	.1262-09	.1252-09	.1243-09	.1243-09	.1231-09	.1222-09	.1214-09	.1207-09
12	.1443-07	.1429-08	.1402-07	.1383-08	.1387-09	.1367-09	.1345-09	.1332-09	.1318-09	.1332-09	.1300-09	.1288-09	.1278-09	.1269-09	.1269-09	.1257-09	.1248-09	.1240-09	.1233-09
13	.1484-07	.1468-07	.1442-07	.1408-07	.1416-09	.1396-09	.1374-09	.1361-09	.1347-09	.1361-09	.1329-09	.1317-09	.1307-09	.1298-09	.1298-09	.1286-09	.1277-09	.1269-09	.1262-09
14	.1533-07	.1520-07	.1494-07	.1458-07	.1473-09	.1451-09	.1429-09	.1416-09	.1403-09	.1416-09	.1384-09	.1372-09	.1362-09	.1353-09	.1353-09	.1341-09	.1332-09	.1324-09	.1317-09
15	.1597-07	.1589-07	.1564-07	.1528-07	.1548-09	.1527-09	.1505-09	.1492-09	.1479-09	.1492-09	.1460-09	.1448-09	.1438-09	.1429-09	.1429-09	.1417-09	.1408-09	.1400-09	.1393-09
16	.1687-07	.1674-07	.1650-07	.1614-07	.1641-09	.1620-09	.1598-09	.1585-09	.1572-09	.1585-09	.1553-09	.1541-09	.1531-09	.1522-09	.1522-09	.1510-09	.1501-09	.1493-09	.1486-09
17	.1808-07	.1795-07	.1771-07	.1735-07	.1766-09	.1745-09	.1723-09	.1710-09	.1697-09	.1710-09	.1678-09	.1666-09	.1656-09	.1647-09	.1647-09	.1635-09	.1626-09	.1618-09	.1611-09
18	.1968-07	.1955-07	.1931-07	.1895-07	.1926-09	.1905-09	.1883-09	.1870-09	.1857-09	.1870-09	.1838-09	.1826-09	.1816-09	.1807-09	.1807-09	.1795-09	.1786-09	.1778-09	.1771-09
19	.2178-07	.2165-07	.2141-07	.2105-07	.2136-09	.2115-09	.2093-09	.2080-09	.2067-09	.2080-09	.2048-09	.2036-09	.2026-09	.2017-09	.2017-09	.2005-09	.1996-09	.1988-09	.1981-09
20	.2464-07	.2451-07	.2427-07	.2391-07	.2422-09	.2401-09	.2379-09	.2366-09	.2353-09	.2366-09	.2334-09	.2322-09	.2312-09	.2303-09	.2303-09	.2291-09	.2282-09	.2274-09	.2267-09

Table 91.--Continued

$a'^1\Sigma_u^- — X^1\Sigma_g^+$

Table 91.--Continued

$a\,{}^1\Pi_g \longrightarrow X\,\Sigma_g^+$

v'\v''	0	1	2	3	4	5	6	7	8	9	10	11	12	13	14	15
0	.1158-07 .9738+18	.1141-07 .2873+19	.1126-07 .4652+19	.1111-07 .5454+19	.1087-07 .5186+19	.1083-07 .4278+19	.1070-07 .3156+19	.1057-07 .2159+19	.1045-07 .1391+19	.1033-07 .8445+18	.1021-07 .4971+18	.1011-07 .2806+18	.1001-07 .1575+18	.9903-08 .8624+17	.9804-08 .4593+17	.9707-08 .2465+17
1	.1181-07 .3306+19	.1163-07 .4200+19	.1146-07 .2321+19	.1128-07 .3226+18	.1124-07 .1772+18	.1105-07 .1447+19	.1091-07 .2851+19	.1078-07 .3618+19	.1065-07 .3626+19	.1053-07 .3098+19	.1042-07 .2394+19	.1030-07 .1690+19	.1019-07 .1156+19	.1008-07 .7480+18	.9982-08 .4613+18	.9884-08 .2821+18
2	.1204-07 .4270+19	.1185-07 .1513+19	.1181-07 .1726+18	.1125-07 .1743+19	.1139-07 .2425+19	.1123-07 .1278+19	.1103-07 .1348+18	.1104-07 .1859+18	.1086-07 .1178+19	.1073-07 .2287+19	.1061-07 .2976+19	.1049-07 .3071+19	.1038-07 .2795+19	.1027-07 .2287+19	.1016-07 .1716+19	.1006-07 .1240+19
3	.1229-07 .5708+19	.1241-07 .9361+18	.1194-07 .1978+19	.1175-07 .1360+19	.1129-07 .1059+17	.1148-07 .8318+18	.1132-07 .1915+19	.1116-07 .1606+19	.1101-07 .1590+18	.1043-07 .3634+16	.1084-07 .3574+18	.1069-07 .1235+19	.1057-07 .2120+19	.1046-07 .2646+19	.1035-07 .2714+19	.1024-07 .2509+19
4	.1254-07 .2210+19	.1238-07 .1202+19	.1216-07 .1346+19	.1212-07 .7328+17	.1184-07 .1514+19	.1166-07 .1185+19	.1138-07 .5728+17	.1143-07 .4501+18	.1126-07 .1480+19	.1111-07 .1614+19	.1097-07 .8761+18	.1079-07 .1450+18	.1088-07 .4878+17	.1067-07 .5731+18	.1055-07 .1399+19	.1043-07 .2021+19
5	.1281-07 .8545+18	.1262-07 .2326+19	.1202-07 .8775+16	.1225+07 .1478+19	.1203-07 .3697+18	.1198-07 .1745+18	.1175-07 .1303+19	.1158-07 .1019+19	.1134-07 .8835+17	.1138-07 .2628+18	.1120-07 .1136+19	.1106-07 .1490+19	.1092-07 .1064+19	.1078-07 .3636+18	.1032-07 .5730+16	.1067-07 .1914+18
6	.1309-07 .3115+18	.1288-07 .1861+19	.1271-07 .8204+18	.1247-07 .8415+18	.1237-07 .2802+18	.1211-07 .1281+19	.1190-07 .2960+18	.1188-07 .2771+18	.1184-07 .1184+19	.1138-07 .8918+18	.1084-07 .1084+18	.1143-07 .1343+18	.1112-07 .3712+18	.1089-07 .1347+19	.1076-07 .5696+18	.1076-07 .5696+18
7	.1338-07 .7783+17	.1316-07 .9215+18	.1296-07 .1719+19	.1320-07 .8340+16	.1256-07 .1247+19	.1225-07 .8881+17	.1224-07 .8750+18	.1203-07 .9572+18	.1175-07 .1000+17	.1179-07 .3596+18	.1160-07 .1067+19	.1144-07 .7914+18	.1124-07 .1248+18	.1132-07 .8558+17	.1112-07 .8531+18	.1098-07 .1168+19
8	.1369-07 .1508+17	.1345-07 .3185+18	.1324-07 .1414+19	.1305-07 .8410+18	.1277-07 .3612+18	.1266-07 .6284+18	.1242-07 .7152+18	.1252-07 .2842+17	.1213-07 .8629+18	.1193-07 .6577+18	.1140-07 .8849+16	.1171-07 .4074+18	.1154-07 .9766+18	.1138-07 .7252+18	.1119-07 .1432+18	.1133-07 .3893+17
9	.1402-07 .2270+16	.1376-07 .7025+17	.1352-07 .6811+18	.1331-07 .1411+19	.1320-07 .1181+18	.1288-07 .8661+18	.1289-07 .4194+17	.1252-07 .8982+18	.1227-07 .1120+18	.1226-07 .2260+18	.1201-07 .8623+18	.1184-07 .4205+18	.1300-07 .8798+15	.1166-07 .4405+18	.1149-07 .8874+18	.1134-07 .6765+18
10	.1439-07 .2374+15	.1408-07 .1493+17	.1383-07 .2212+18	.1360-07 .1016+19	.1340-07 .8494+18	.1299-07 .4841+17	.1297-07 .8894+18	.1267-07 .1554+18	.1263-07 .4424+18	.1240-07 .6669+18	.1219-07 .1225+17	.1214-07 .4220+18	.1195-07 .7705+18	.1176-07 .2125+18	.1200-07 .1223+17	.1160-07 .4392+18
11	.1493-07 .2858+14	.1444-07 .2118+16	.1415-07 .5185+17	.1380-07 .4388+18	.1368-07 .1114?+17	.1350-07 .3886+18	.1319-07 .4081+18	.1281-07 .1495+18	.1288-07 .3401+17	.1250-07 .6868+18	.1228-07 .3382+18	.1243-07 .2400+17	.1206-07 .9444+18	.1188-07 .6462+18	.1169-07 .1795+18
12	.1474-07 .2424+13	.1484-07 .8917+16	.1449-07 .1271?+18	.1423-07 .6758+18	.1398-07 .2481?+18	.1376-07 .9013+18	.1375-07 .3004+17	.1335-07 .3726+17	.1292-07 .8797+18	.1261-07 .9267+17	.1263-07 .2892+18	.1239-07 .8220+18	.1215-07 .1174?+18	.1221-07 .1138+18	.1199-07 .5857+18
13	.5264-07 .3889+09	.1490-07 .2372+14	.1491-07 .1120+16	.1457-07 .2628+17	.1430-07 .2481+18	.1406-07 .8513+18	.1385-07 .6407+18	.1343-07 .5532+17	.1339-07 .6409+18	.1303-07 .7471+17	.1302-07 .4177+18	.1277-07 .4082+18	.1306-07 .1019+17	.1250-07 .4897+18	.1229-07 .4964+18	.1190-07 .1953+17
14	.8575-08 .9900-10	.1512-07 .1639+13	.1533-07 .1063+15	.1495-07 .3913+16	.1465-07 .6116+17	.1438-07 .3972+18	.1414-07 .8890+18	.1361-07 .3867+18	.1350-07 .3932+18	.1323-07 .3431+18	.1320-07 .8965+17	.1288-07 .3448+18	.1260-07 .1033+18	.1265-07 .1489+18	.1241-07 .5322+18
15	.1134-07 .2269+11	.1398-07 .2501+12	.1578-07 .7595+13	.1539-07 .4231+15	.1501-07 .1074+17	.1473-07 .1140?+18	.1440-07 .5501+18	.1418-07 .1682?+18	.1344-07 .3061+18	.1321-07 .6081+17	.1361-07 .6083+17	.1331-07 .5085+18	.1268-07 .8754+16	.1289-07 .3692+18	.1275-07 .3578+18	.1055-07 .3828+15
16	.1193-07 .2121+11	.9075-08 .7824+10	.1586-07 .5034+12	.1570-07 .3869?+14	.1545-07 .1338+16	.1510-07 .2455+17	.1480-07 .2029+18	.1454-07 .6629+18	.1432-07 .1312+18	.1374-07 .1844+17	.1382-07 .5282+18	.1317-07 .1099+17	.1342-07 .4224+18	.1313-07 .1789+18	.1318-07 .9977+17	.1287-07 .4525+18
17	.1193-07 .1584+11	.1181-07 .1775+11	.1987-07 .6288+10	.1580-07 .2666+13	.1591-07 .1211+15	.1551-07 .3539+16	.1517-07 .4904+17	.1488-07 .3031+18	.1462-07 .9967+18	.1442-07 .2707+18	.1401-07 .1597+18	.1392-07 .3575+18	.1358-07 .1576+18	.1355-07 .1874+18	.1326-07 .3685+18	.1194-07 .1375+16
18	.1207-07 .6220+11	.1217-07 .3596+11	.1116-07 .1843+11	.1453-07 .3382+12	.1644-07 .7821+13	.1601-07 .3529+15	.1557-07 .8158+16	.1526-07 .8618+17	.1497-07 .4034+18	.1471-07 .6377+18	.1453-07 .7358+17	.1415-07 .3311+18	.1406-07 .1357+18	.1372-07 .3292+18	.1388-07 .1806+17	.1337-07 .3819+18
19	.1201-07 .1852+11	.1218-07 .1005+11	.1818-07 .3858+10	.9829-08 .7075+10	.1656+12	.1628-07 .9301+14	.1608-07 .9301+15	.1566-07 .1566+17	.1533-07 .1388+18	.1505-07 .6401+18	.1480-07 .5003+18	.1723-07 .2671+15	.1425-07 .4156+18	.1450-07 .9075+16	.1383-07 .3815+18	.1337-07 .2833+17
20	.1221-07 .1819+11	.1248-07 .5176+09	.1224-07 .9684+10	.1170-07 .3704+10	.3192-07 .9679+00	.1645-07 .1776+13	.1657-07 .9529+14	.1612-07 .2151+16	.1574-07 .1036+17	.1542-07 .2041+18	.1511-07 .5411+18	.1439-07 .3235+18	.1439-07 .9700+17	.1436-07 .3878+18	.1386-07 .2978+17	.1394-07 .2774+18

Table 91.--Continued $w\,^1\Delta_u \longrightarrow X\,^1\Sigma_g^+$

V'' \ V'	0	1	2	3	4	5	6
0	.1178-07 .8094+17	.1167-07 .4051+18	.1155-07 .1089+19	.1145-07 .2086+19	.1134-07 .3181+19	.1124-07 .4152+19	.1115-07 .4762+19
1	.1196-07 .4930+18	.1184-07 .1710+19	.1172-07 .3033+19	.1161-07 .3575+19	.1149-07 .3006+19	.1139-07 .1788+19	.1127-07 .6162+18
2	.1215-07 .1400+19	.1202-07 .2975+19	.1189-07 .2763+19	.1176-07 .1180+19	.1157-07 .6397+17	.1161-07 .3154+18	.1147-07 .1346+19
3	.1234-07 .2466+19	.1220-07 .2568+19	.1205-07 .5723+18	.1203-07 .1129+18	.1185-07 .1260+19	.1173-07 .1842+19	.1161-07 .1145+19
4	.1253-07 .3030+19	.1237-07 .9034+18	.1232-07 .1731+18	.1214-07 .1492+19	.1200-07 .1247+19	.1183-07 .1527+18	.1185-07 .2142+18
5	.1274-07 .2747+19	.1210-07 .2409+16	.1247-07 .1319+19	.1231-07 .9572+18	.2083-07 .1128+14	.1210-07 .7729+18	.1196-07 .1265+19
6	.1295-07 .1918+19	.1283-07 .5478+18	.1265-07 .1220+19	.2968-06 .8180+10	.1240-07 .9172+18	.1225-07 .9110+18	.1200-07 .4633+17
7	.1317-07 .1049+19	.1303-07 .1395+19	.1281-07 .2082+18	.1274-07 .7196+18	.1256-07 .7804+18	.1316-07 .1882+16	.1234-07 .7178+18
8	.1340-07 .4603+18	.1324-07 .1550+19	.1316-07 .1167+18	.1292-07 .9889+18	.1169-07 .7280+15	.1266-07 .7631+18	.1248-07 .5466+18
9	.1364-07 .1613+18	.1347-07 .1082+19	.1333-07 .8075+18	.1310-07 .2281+18	.1302-07 .5664+18	.1282-07 .5147+18	.1285-07 .5274+17
10	.1390-07 .4584+17	.1371-07 .5404+18	.1355-07 .1151+19	.1348-07 .6627+17	.1320-07 .7483+18	.1337-07 .1077+17	.1292-07 .6930+18
11	.1417-07 .1061+17	.1397-07 .2038+18	.1379-07 .8950+18	.1364-07 .6252+18	.1336-07 .1298+18	.1330-07 .5608+18	.1307-07 .2436+18
12	.1445-07 .1981+16	.1424-07 .5906+17	.1404-07 .4608+18	.1387-07 .9154+18	.1377-07 .1013+18	.1349-07 .5206+18	.1345-07 .9093+17
13	.1477-07 .3003+15	.1452-07 .1354+17	.1431-07 .1714+18	.1412-07 .6950+18	.1395-07 .5943+18	.1357-07 .2976+17	.1358-07 .5601+18
14	.1508-07 .3691+14	.1482-07 .2415+16	.1460-07 .4742+17	.1439-07 .3377+18	.1420-07 .7519+18	.1406-07 .1916+18	.1377-07 .2852+18
15	.1566-07 .3133+13	.1513-07 .3443+15	.1492-07 .9983+16	.1467-07 .1162+18	.1447-07 .5049+18	.1428-07 .5921+18	.1471-07 .2832+16
16	.1570-07 .2678+12	.1563-07 .3471+14	.1523-07 .1646+16	.1499-07 .2925+17	.1475-07 .2201+18	.1454-07 .5982+18	.1438-07 .3167+18
17	.1442-07 .4653+11	.1640-07 .2425+13	.1557-07 .2055+15	.1533-07 .5472+16	.1506-07 .6659+17	.1483-07 .3378+18	.1463-07 .5681+18
18	.1268-07 .5327+11	.2503-07 .2135+11	.1577-07 .2129+14	.1571-07 .7561+15	.1541-07 .1444+17	.1514-07 .1242+18	.1491-07 .4351+18
19	.1181-07 .6716+10	.1401-07 .5747+11	.1703-07 .1024+13	.1608-07 .8117+14	.1578-07 .2317+16	.1549-07 .3179+17	.1523-07 .2001+18
20	.1229-07 .1150+11	.1283-07 .1698+11	.1957-07 .2693+11	.1659-07 .6027+13	.1617-07 .2706+15	.1587-07 .5744+16	.1557-07 .6038+17

Table 91.--Continued

$C\,^3\Pi_u \text{——} X\,^1\Sigma_g^+$

V'' \ V'	0	1	2	3	4
0	.1126-07 .3426+20	.1087-07 .2089+20	.1051-07 .7879+19	.1019-07 .2392+19	.9900-08 .6592+18
1	.1172-07 .1956+20	.1138-07 .4999+19	.1096-07 .1804+20	.1060-07 .1320+20	.1030-07 .6116+19
2	.1222-07 .4660+19	.1180-07 .2007+20	.1101-07 .1466+18	.1108-07 .8482+19	.1071-07 .1264+20
3	.1274-07 .6216+18	.1229-07 .9885+19	.1188-07 .1286+20	.1142-07 .4433+19	.1131-07 .1397+19
4	.1330-07 .5241+17	.1280-07 .2125+19	.1236-07 .1314+20	.1197-07 .4923+19	.1155-07 .8801+19
5	.1379-07 .3272+16	.1333-07 .2617+18	.1285-07 .4377+19	.1244-07 .1324+20	.1210-07 .3390+18
6	.1394-07 .2171+15	.1379-07 .2308+17	.1336-07 .7803+18	.1291-07 .7093+19	.1252-07 .9767+19
7	.1364-07 .1979+14	.1406-07 .1888+16	.1378-07 .9876+17	.1338-07 .1853+19	.1298-07 .9257+19
8	.9007-08 .1207+13	.1405-07 .2021+15	.1395-07 .1207+17	.1381-07 .3320+18	.1341-07 .3767+19
9	.1010-07 .6253+12	.1364-07 .2526+14	.1438-07 .1288+16	.1395-07 .5768+17	.1382-07 .9894+18
10	.1157-07 .5046+12	.3076-07 .6568+11	.1368-07 .2836+15	.1434-07 .8888+16	.1397-07 .2482+18
11	.1183-07 .6792+12	.1246-07 .1025+13	.1581-07 .1515+14	.1413-07 .1896+16	.1423-07 .5782+17
12	.1184-07 .2573+12	.1223-07 .5937+12	.1822-07 .6984+12	.1458-07 .2900+15	.1435-07 .1380+17
13	.1182-07 .1006+13	.1118-07 .1054+13	.1217-07 .4872+13	.1572-07 .2978+14	.1456-07 .2928+16
14	.1157-07 .2595+12	.1601-07 .1032+11	.3721-07 .1329+10	.1307-07 .1802+14	.1543-07 .4552+15
15	.1208-07 .2105+12	.1122-07 .2902+12	.1070-07 .3288+12	.2251-07 .2490+12	.1413-07 .1715+15
16	.1204-07 .1112+12	.1159-07 .1454+12	.9882-08 .7152+11	.1231-07 .1305+12	.1717-07 .1185+14
17	.1202-07 .9073+11	.1192-07 .1695+12	.1203-07 .1947+11	.8175-08 .2661+11	.1549-07 .3535+13
18	.1201-07 .2092+12	.1222-07 .7258+12	.1134-07 .2704+12	.1118-07 .9518+12	.1332-07 .2660+13
19	.1182-07 .6915+11	.1254-07 .1041+12	.1077-07 .1585+12	.1085-07 .6474+12	.7034-08 .4313+12
20	.1300-07 .6866+10	.1184-07 .1824+12	.2875-07 .8505+09	.9083-08 .1214+12	.1106-07 .1319+13

Table 91.--Continued

$B\,^3\Pi_g$ — $A\,^3\Sigma_u^+$

v' \ v''	0	1	2	3	4	5	6	7	8	9	10	11	12	13	14	15	16	17
0	.1254-07 .3339+16	.1298-07 .6384+16	.1347-07 .4526+16	.1403-07 .1547+16	.1469-07 .2798+15	.1551-07 .2684+14	.1594-07 .1875+13	.1588-07 .8678+11	.1326-07 .6995+11	.1279-07 .3517+11	.1300-07 .4263+11	.1302-07 .3541+12	.1310-07 .4579+11	.1321-07 .3121+11	.1339-07 .5983+10	.1358-07 .8288+10	.1358-07 .2456+10	.1349-07 .1264+11
1	.1216-07 .1438+16	.1206-07 .2708+14	.1309-07 .4800+16	.1357-07 .8238+16	.1412-07 .4630+16	.1476-07 .1174+16	.1559-07 .1450+15	.1662-07 .8834+13	.1901-07 .1686+12	.1715-07 .7105+10	.4454-08 .2046+08	.1249-07 .9062+10	.1289-07 .3021+10	.1317-07 .2488+11	.1326-07 .3701+11	.1323-07 .1492+11	.1374-07 .4764+10	.1329-07 .4322+11
2	.1183-07 .3376+15	.1227-07 .8011+15	.1257-07 .1167+16	.1327-07 .1817+16	.1367-07 .9483+16	.1423-07 .8443+16	.1486-07 .4920+16	.1565-07 .4575+15	.1673-07 .3239+14	.1754-07 .1314+13	.1623-07 .5511+11	.1289-07 .1761+12	.1318-07 .1599+11	.1343-07 .6768+10	.1358-07 .5569+09	.1341-07 .1727+10	.1330-07 .8464+10	.1351-07 .1363-07
3	.1152-07 .5427+14	.1192-07 .4851+15	.1248-07 .1275+15	.1271-07 .1750+16	.1368-07 .1540+15	.1378-07 .8230+16	.1431-07 .1212-07	.1485-07 .3543+16	.1673-07 .1083+16	.1678-07 .8272+14	.1820-07 .3802+13	.1777-07 .8345+11	.1883-07 .1831+12	.1944-07 .5064+10	.1375-07 .1631+10	.1380-07 .8286+08	.1360-07 .4222+10	.1433+11 .1353-07
4	.1125-07 .6024+13	.1161-07 .1370+15	.1203-07 .3671+15	.1199-07 .3384+14	.1283-07 .1929+16	.1288-07 .2334+15	.1391-07 .5646+16	.1441-07 .1461+17	.1505-07 .8543+16	.1584-07 .2138+16	.1688-07 .2140+15	.1777-07 .1081+14	.1846-07 .1939+14	.1947-07 .2768+12	.1392-07 .1378+10	.1392-07 .2287+10	.1351-07 .2159+09	.7204+10 .1374-07
5	.1100-07 .4032+12	.1134-07 .2369+14	.1171-07 .1912+15	.1181-07 .1468+15	.1236-07 .3854+15	.1296-07 .1344+16	.1321-07 .1408+16	.1407-07 .2843+16	.1452-07 .1553+17	.1514-07 .1296+17	.1593-07 .3741+16	.1700-07 .4323+15	.1846-07 .1939+14	.1947-07 .2768+12	.1097-07 .1146+11	.1392-07 .1378+10	.1342-07 .2287+10	.5615+10 .1374-07
6	.1077-07 .9093+10	.1108-07 .2538+13	.1143-07 .3133+14	.1181-07 .1801+15	.1248-07 .9193+13	.1274-07 .8035+15	.1316-07 .5479+15	.1337-07 .2749+16	.1438-07 .8098+15	.1463-07 .1504+17	.1525-07 .1707+17	.1604-07 .6037+16	.1708-07 .3998+15	.1862-07 .3912+14	.1967-07 .8240+12	.1773-08 .1114+10	.1605-07 .5021+09	.1771+11 .1346-07
7	.1058-07 .1249+08	.1085-07 .1219+12	.1117-07 .2698+13	.1152-07 .7780+14	.1192-07 .1142+15	.1193-07 .1162-07	.1361-07 .1001+16	.1381-07 .3131+16	.1350-07 .3578+16	.1802-07 .7222+13	.1476-07 .1291+17	.1535-07 .2109+17	.1614-07 .8855+16	.1717-07 .1369+16	.1867-07 .7966+14	.2139-07 .1046+13	.3041-07 .7364+09	.7764+10 .1444-07
8	.1036-07 .4252+09	.1063-07 .4664+09	.1093-07 .6994+12	.1126-07 .1861+14	.1162-07 .8734+14	.1213-07 .3593+14	.1219-07 .2218+15	.1275-07 .8788+15	.1251-07 .9020+14	.1363-07 .3604+16	.1353-07 .4695+15	.1600-07 .1000+17	.1546-07 .2385-07	.1825-07 .1254+17	.2180-07 .2186+16	.1884-07 .2197-07	.2197-07 .2671+13	.9452-08 .1490-07
9	.1018-07 .2464+10	.1043-07 .2512+09	.1072-07 .1438+11	.1102-07 .2491+13	.1135-07 .3106+14	.1173-07 .7256+14	.3080-07 .6297+10	.1233-07 .4400+15	.1290-07 .5381+15	.1298-07 .8016+15	.1377-07 .2892+16	.1394-07 .1896+16	.1507-07 .6616+16	.1558-07 .2586+17	.1636-07 .1654+17	.1740-07 .3329+16	.1898-07 .2191+15	.3604+13 .2159-07
10	.9996-08 .4025+10	.1025-07 .6128+10	.1052-07 .1706-07	.1081-07 .1305-12	.1111-07 .8255+13	.1143-07 .4073+14	.1188-07 .3965+14	.1186-07 .3891+14	.1246-07 .5797+15	.1318-07 .1819+15	.1317-07 .1323+16	.1396-07 .3677+16	.1415-07 .3575+16	.1531-07 .2678+17	.1570-07 .2678+17	.1648-07 .2095+17	.1752-07 .4849+16	.3501+15 .1912-07
11	.9822-08 .4018+10	.1034-07 .1589+11	.1061-07 .5746+10	.1089-07 .2126-09	.1121-07 .1212+14	.1126-07 .4124+14	.1210-07 .8181+13	.1252+15	.1207-07 .1252+15	.1260-07 .3651+15	.1267-07 .3767+15	.1332-07 .1938+16	.1422-07 .7385+15	.1431-07 .5340+16	.1575-07 .1306+16	.1583-07 .2607+17	.1660-07 .2671+17	.6826+16 .1765-07
12	.9666-08 .3137+10	.9946-09 .2106+11	.1017-07 .2860+11	.1042-07 .1815+10	.1069-07 .1246+11	.1099-07 .1975+13	.1130-07 .1839+14	.1168-07 .3112+14	.1132-07 .2035+13	.1182-07 .2734+15	.1236-07 .4133+15	.1300-07 .1981+15	.1286-07 .4488+15	.1360-07 .2039-16	.1255-07 .6765+14	.1461-07 .6676+16	.1634+15 .1613-07	.1672-07 .2120+17
13	.9549-08 .2129+10	.9810-08 .1994+11	.1002-07 .5105+11	.1025-07 .2886+11	.1051-07 .2895+08	.1078-07 .1207+12	.1108-07 .4567+13	.1141-07 .2247+14	.1186-07 .1388+14	.1182-07 .3592+14	.1236-07 .3654+15	.1300-07 .1981+15	.1286-07 .4488+15	.1360-07 .2039-16	.1255-07 .6765+14	.1461-07 .6676+16	.1634+15	.1613-07 .2120+17

$B'\,^3\Sigma_u^-$ — $B\,^3\Pi_g$

v' \ v''	0	1	2	3	4	5	6	7	8	9	10	11	12	13	14	15	16	17	18
0	.1250-07 .8875+15	.1297-07 .1329+16	.1170-07 .8509+15	.1138-07 .1108-07	.1108-07 .3243+15	.1082-07 .1446+15	.1058-07 .5943+14	.1035-07 .2323+14	.1014-07 .8838+13	.9939-08 .3224+13	.9739-08 .1168+13	.9573-08 .6246+12	.9516-08 .1661+12	.8595-08 .2665+11	.9421-08 .2605+11	.9309-08 .9799+10	.8751-08 .2829+10	.8806-08 .4452+09	.3114-07 .2490-07
1	.1298-07 .2009+15	.1273-07 .5967+14	.1217-07 .8243+15	.1178-07 .1412+16	.1145-07 .1312+16	.1115-07 .8938+15	.1088-07 .5009+15	.1064-07 .2507+15	.1040-07 .1151+15	.1019-07 .6983+14	.1002-07 .2125+14	.9875-08 .8845+13	.9703-08 .3617+13	.9581-08 .1488+13	.9411-08 .5728+12	.9071-08 .2018+12	.8693-08 .5776+11	.8118-08 .2135+11	.7911-08 .8108+10
2	.1354-07 .1167+14	.1308-07 .1671+15	.1228-07 .2256+14	.1230-07 .2700+15	.1187-07 .1095+16	.1153-07 .1560+16	.1122-07 .1410+16	.1095-07 .6885+15	.1071-07 .2695+15	.1048-07 .3165+15	.1026-07 .1568+15	.1007-07 .7328+14	.9925-08 .3422+14	.9728-08 .1499+14	.9400-08 .2678+13	.9155-08 .1165+13	.8991-08 .1922+12	.8953-08 .1881+13	.9089-08 .9397-08
3	.1421-07 .5027+11	.1363-07 .1891+14	.1320-07 .8631+14	.1276-07 .1154+15	.1197-07 .8107+15	.1160-07 .1380+16	.1133-07 .1689+16	.1102-07 .1466+16	.1028+16	.1055-07 .6371+15	.1034-07 .3556+15	.1013-07 .1856+15	.9986-08 .9486+14	.9828-08 .4582+14	.9632-08 .2136+14	.9531-08 .1010+14	.9349-08 .4446+13	.1881+13	.1298-08 .2490-07
4	.1510-07 .1288+06	.1430-07 .1970+12	.1372-07 .2015+14	.1338-07 .3083+14	.1268-07 .1588+15	.1170-07 .1070+14	.1211-07 .2302+15	.1169-07 .9967+15	.1137-07 .1648+16	.1109-07 .1746+16	.1084-07 .1448+16	.1060-07 .1011+16	.1041-07 .6471+15	.1020-07 .3740+15	.1001-07 .2036+15	.9879-08 .1088+15	.9672-08 .5445+14	.9513-08 .2655+14	.9397-08 .1298+14
5	.1660-07 .2710+09	.1517-07 .9812+07	.1439-07 .2606+12	.1382-07 .1726+14	.1376-07 .8638+15	.1278-07 .2466+15	.1218-07 .1246+15	.1179-07 .3681+14	.1145-07 .1709+15	.1115-07 .1145+16	.1118-07 .1812+16	.1091-07 .1760+16	.1067-07 .1419+16	.1047-07 .1009+16	.1028-07 .4422+15	.1048-07 .3815+15	.9848-08 .2222+15	.9788-08 .6253+14	.9595-08 .4329-07
6	.1518-07 .1081+08	.1662-07 .1664+10	.1528-07 .8758-08	.1448-07 .2748-08	.1393-07 .2523-08	.1393-07 .1016+15	.1290-07 .1271-07	.1233-07 .5398+15	.1187-07 .9836-08	.1162-07 .2501+15	.3154-07 .9646+15	.1126-07 .1626+16	.1098-07 .1881+15	.1078-07 .1724+16	.1063-07 .1363+16	.1036-07 .9606+15	.1014-07 .6241+15	.9977-08 .3801+15	.9864-08 .2752+15
7	.1317-07 .5065+08	.2074-07 .1534+09	.1669-07 .9830+10	.1538-07 .4.72E+09	.1468-07 .2435+12	.1405-07 .8876+13	.1271-07 .3105+13	.1302-07 .5814+14	.1244-07 .1655+15	.1180-07 .4396+14	.4153-07 .8533+14	.1183-07 .5788+15	.1389-07 .1761+13	.1175-07 .2859+15	.1105-07 .9620+15	.1088-07 .1140-07	.1069-07 .1913+16	.1067-07 .1609+16	.1028-07 .1234+16
8	.1277-07 .4428+09	.2249-07 .3140+09	.1678-07 .1484+11	.1469-07 .1675+10	.1469-07 .1937+12	.1419-07 .5543+13	.1319-07 .8021+13	.1307-07 .2607+14	.1254-07 .1352-07	.1202-07 .1058+15	.1389-07 .1761+13	.1214-07 .1496+15	.1132-07 .1689+14	.1194-07 .9812+14	.1147-07 .5943+15	.1121-07 .1278+16	.1095-07 .1995+16	.1073-07 .1960+16	.1054-07 .1823+16
9	.1285-07 .5823+09	.1792-07 .9915+06	.2165-07 .9548+09	.1560-07 .4539+10	.1560-07 .2951+11	.1479-07 .1444+12	.1436-07 .3198+13	.1324-07 .1167+14	.1352-07 .7888+13	.1264-07 .1222+15	.1214-07 .1496+15	.1132-07 .1689+14	.1194-07 .9812+14	.1147-07 .5943+15	.1121-07 .1278+16	.1095-07 .1995+16	.1073-07 .1960+16	.1823+16 .1054-07	.9844-08 .2752+15
10	.1309-07 .6693+09	.1288-07 .8230+08	.1233-07 .6713+08	.1163-07 .9893-08	.1717-07 .2312-07 .1449+10	.1572-07 .5285+11	.1572-07 .1006+11	.1490-07 .9804+11	.1426-07 .1687+13	.1336-07 .1309+14	.1478-07 .7492+12	.1275-07 .8446+14	.1225-07 .1842+15	.1173-07 .6734+14	.1280-14 .1280-14	.1161-07 .3176+15	.1129-07 .9363+15	.1103-07 .1538+16	.1086-07 .1896+16
11	.1303-07 .9265+10	.1280-07 .1016+10	.1308-07 .1684+10	.1470-07 .1037+09	.6452-08 .8726+08	.2460-07 .1944+10	.1743-07 .8268+11	.1583-07 .1941+11	.1501-07 .6513+11	.1488-07 .8092+12	.1347-07 .1277+14	.1088-07 .4481+12	.1288-07 .5684+14	.1234-07 .1608+15	.1188-07 .1156+15	.1178-07 .1312+15	.1138-07 .5623+15	.1110-07 .1196+16	.1148-07 .1398+15
12	.1318-07 .9793+09	.1304-07 .3600+09	.1315-07 .1816+09	.1293-07 .3534+08	.1379-08 .8443+07	.1428-07 .8367+09	.2800-07 .7992+10	.1759-07 .1209+12	.1514-07 .3215+11	.1533-07 .3395+12	.1357-07 .1124+14	.1242-07 .3547+13	.1309-07 .2667+14	.1243-07 .1362+15	.1200-07 .1536+15	.1141-07 .3648+14	.1209-07 .3635+14	.1148-07 .1739+12	.1833-07 .1739+12
13	.1332-07 .9424+09	.1327-07 .6369+09	.1390-07 .3111+08	.1308-07 .3295+09	.1367-07 .2895+08	.1390-06 .1566+06	.1495-07 .2179+10	.1788-07 .1259-07	.1788-07 .1608+12	.1690-07 .4960-07	.2546-07 .1160+13	.1618-07 .9262+13	.1265-07 .1275-07	.1275-07 .6644+13	.1330-07 .1045+14	.1243-07 .1047+15	.1210-07 .1694+15	.1166-07 .9135+14	.1833-07 .1739+12
14	.1338-07 .1706-07	.1395-07 .1605-07	.1401-07 .1116-09	.1374-07 .1116-09	.1391-07 .1095-09	.1282-07 .1255-07	.4022-07 .3686+07	.1503-07 .5508+10	.2303-07 .9184+11	.1941-07 .1944-12	.1622-07 .7658+11	.1548-07 .1467+11	.1539-07 .2593+11	.1238-07 .9238+13	.1783-07 .9783-09	.1283-07 .1160+14	.1221-07 .2591-07	.1218-07 .4523-07	.1178-07 .1178-07
15	.1328-07 .5410-09	.1333-07 .4595-09	.1304-07 .1225-07	.1337-09 .2193-09	.1226-07 .9644-08	.1255-07 .9668-08	.1877-07 .3680+07	.4929-08 .1006+08	.8617-07 .8464+10	.1841-07 .2595+09	.1841-07 .2297-12	.1639-07 .9297+11	.1544-07 .8715+10	.3491-07 .1011+10	.1383-07 .5425+13	.1305-07 .1160+14	.2092-07 .4051-14	.1275-07 .4611-14	.1227-07 .1427-07
16	.1366-07 .1548-09	.1346-07 .5961-09	.1344-07 .1813-09	.1423-07 .1966+08	.1337-07 .9644+08	.1369-07 .1052+06	.3036-07 .1018+06	.1565-07 .6097-07	.1693-07 .9226-07	.1693-07 .1361+11	.4539-10 .4643+10	.2483-12 .1877-07	.1651-07 .1138+12	.5329+10 .5329+10	.1569-07 .2633-08	.1391-07 .3935+13	.1235-07 .1235+14	.1116-07 .7851+12	.1299-07 .2597-14
17	.1348-07 .1258+10	.1355-07 .2785+10	.1355-07 .1164+10	.1300-07 .1520+09	.1354-07 .5567+09	.1375-07 .4231+08	.1362-07 .1776+09	.1036-07 .3564+07	.1763-07 .1015+09	.3726-08 .8649+08	.1770-07 .1852+11	.7844-08 .1613+11	.1920-07 .2476+12	.1666-07 .1320+12	.1586-07 .3472+10	.8517-08 .1305+11	.1399-07 .2776+13	.1325-07 .1202+14	.1213-07 .3005+13

Table 91.--Continued

$C\,^3\Pi_u$ —— $B\,^3\Pi_g$

V'' \ V'	0	1	2	3	4
0	.1184-07 .3509+18	.1228-07 .3971+18	.1278-07 .1697+18	.1342-07 .3230+17	.1469-07 .1708+16
1	.1147-07 .2013+18	.1211-07 .1738+17	.1239-07 .3535+18	.1289-07 .3300+18	.1357-07 .8703+17
2	.1114-07 .6982+17	.1155-07 .1301+18	.1168-07 .1989+17	.1255-07 .2248+18	.1303-07 .4432+18
3	.1083-07 .1907+17	.1121-07 .1002+18	.1165-07 .4231+17	.1183-07 .7582+17	.1283-07 .1360+18
4	.1055-07 .4461+16	.1090-07 .4298+17	.1129-07 .8477+17	.1185-07 .3322+16	.1180-07 .9441+17
5	.1028-07 .9583+15	.1062-07 .1405+17	.1098-07 .5770+17	.1137-07 .5191+17	.1168-07 .2782+16
6	.1003-07 .1909+15	.1035-07 .3855+16	.1069-07 .2543+17	.1104-07 .5619+17	.1148-07 .2412+17
7	.9783-08 .3654+14	.1011-07 .9703+15	.1042-07 .8923+16	.1076-07 .3355+17	.1110-07 .4534+17
8	.9562-08 .6788+13	.9864-08 .2241+15	.1018-07 .2721+16	.1049-07 .1453+17	.1082-07 .3541+17
9	.9336-08 .1194+13	.9639-08 .4835+14	.9944-08 .7310+15	.1024-07 .5171+16	.1054-07 .1828+17
10	.9091-08 .2032+12	.9430-08 .1007+14	.9698-08 .1817+15	.1001-07 .1647+16	.1029-07 .7603+16
11	.8834-08 .3252+11	.9214-08 .1937+13	.9442-08 .4110+14	.9803-08 .4677+15	.1004-07 .2657+16
12	.8696-08 .5426+10	.8863-08 .3397+12	.9262-08 .9414+13	.9531-08 .1217+15	.9843-08 .8833+15
13	.8491-08 .8051+09	.8547-08 .5587+11	.8985-08 .1899+13	.9321-08 .3006+14	.9597-08 .2560+15
14	.8186-08 .9761+08	.8180-08 .8122+10	.8668-08 .3455+12	.9077-08 .6694+13	.9346-08 .6738+14
15	.7007-08 .6107+07	.7655-08 .9769+09	.8299-08 .5587+11	.8699-08 .1306+13	.9110-08 .1665+14
16	.2006-07 .1113+06	.6617-08 .7230+08	.7381-08 .6090+10	.8229-08 .2171+12	.8700-08 .3429+13
17	.1164-07 .9880+06	.5325-07 .6400+05	.2627-08 .1822+09	.7215-08 .2453+11	.8013-08 .5587+12

Table 9I.—Continued

$a\,^1\Pi_g$ —— $a'\,^1\Sigma_u^-$

v'' \ v'	0	1	2	3	4	5	6	7	8	9	10	11	12	13	14	15
0	.1253-07 .1296+13	.1310-07 .2211+14	.1380-07 .2663+14	.1470-07 .7458+13	.1608-07 .5806+12	.2111-07 .3442+10	.1825-07 .8826+09	.1255-07 .1506+10	.1295-07 .3606+10	.1394-07 .3195+10	.1322-07 .1734+10	.1314-07 .1867+11	.1326-07 .3599+10	.1328-07 .9230+10	.1336-07 .1161+11	.1342-07 .1015+11
1	.1201-07 .2101+10	.1269-07 .5211+12	.1330-07 .1337+14	.1388-07 .1243+14	.1479-07 .2640+14	.1619-07 .2650+13	.1679-07 .3757+11	.3101-08 .7868+08	.9534-08 .1046+09	.1179-07 .3146+09	.1293-07 .1012+10	.1296-07 .8703+10	.1315-07 .2652+10	.1333-07 .9941+10	.1340-07 .1598+11	.1339-07 .2064+11
2	.1158-07 .8718+12	.1210-07 .4163+08	.1330-07 .4860+11	.1330-07 .3490+14	.1397-07 .1127+15	.1489-07 .5795+14	.1633-07 .6934+13	.2020-07 .1159+12	.1086-07 .4712+10	.2020-08 .2577+09	.1300-07 .8346+09	.1318-07 .4206+10	.1335-07 .6913+09	.1240-07 .1711+09	.1279-07 .5498+09	.1327-07 .3166+10
3	.1120-07 .2546+13	.1165-07 .9508+12	.1220-07 .4218+07	.1207-07 .9815+11	.1342-07 .3041+14	.1407-07 .1550+15	.1698-07 .1022+15	.1644-07 .1634+14	.2026-07 .2760+12	.1039-07 .4159+10	.3568-07 .2998+08	.1288-07 .1634+10	.1287-07 .5304+10	.1331-07 .6041+10	.1334-07 .8684+10	.1356-07 .5786+10
4	.1088-07 .2720+13	.1127-07 .4960+13	.1172-07 .6259+12	.1233-07 .3217+09	.1248-07 .6897+12	.1357-07 .2280+14	.1816-07 .1816+15	.1508-07 .1588+15	.2656-07 .2516+14	.2124-07 .4164+12	.1178-07 .1875+11	.7506-08 .1165+10	.1347-07 .8347+09	.1038-07 .3849+08	.1282-07 .3579+09	.1283-07 .2481+10
5	.1059-07 .1876+13	.1054-07 .7598+13	.1134-07 .3751+13	.1180-07 .3059+12	.1256-07 .8331+09	.1264-07 .1675+13	.1377-07 .1451+14	.1427-07 .2177+15	.1519-07 .2178+15	.1672-07 .3933+14	.2169-07 .6698+12	.1257-07 .2546+11	.3440-07 .2134+09	.1345-07 .4011+10	.1316-07 .3559+10	.1356-07 .3884+10
6	.1033-07 .1308+13	.1064-07 .8481+13	.1101-07 .1193+14	.1141-07 .3691+13	.1189-07 .1115+12	.1362-07 .2395+09	.1275-07 .2789+13	.1410-07 .7370+13	.1437-07 .2343+15	.1128-07 .2893+15	.1686-07 .5706+14	.2332-07 .7329+12	.1340-07 .3664+11	.2707-07 .1029+10	.2145-08 .2304+08	.1241-07 .5935+09
7	.1006-07 .4575+12	.1039-07 .4310+13	.1070-07 .1320+14	.1107-07 .1453+14	.1148-07 .3773+13	.1200-07 .3034+11	.1130-07 .1057+10	.1285-07 .3785+13	.1480-07 .2431+13	.1449-07 .2423+15	.1530-07 .3587+15	.1702-07 .7762+14	.2388-07 .9603+12	.1403-07 .1658+12	.2045-07 .3103+09	.1448-07 .4514+10
8	.9845-08 .1931+12	.1013-07 .2347+13	.1045-07 .1057+14	.1076-07 .2004+14	.1113-07 .1479+14	.1156-07 .2420+13	.1214-07 .2438+10	.1199-07 .1383+11	.1295-07 .4432+13	.1338-07 .1938+12	.1461-07 .2411+15	.1530-07 .4321+15	.3718-07 .8853+14	.2693-07 .1863+13	.2472-07 .2774+12	.2736-07 .5169+10
9	.9612-08 .7451+11	.9905-08 .1135+13	.1021-07 .6674+13	.1048-07 .1858+14	.1083-07 .2469+14	.1120-07 .1296+14	.1164-07 .1318+13	.1239-07 .4862+09	.1220-07 .5266+11	.1307-07 .4656+13	.1017-07 .5180+12	.1475-07 .2358+15	.1561-07 .5023+15	.1735-07 .1223+15	.2868-07 .7883+12	.1528-07 .4885+12
10	.9411-08 .2870+11	.9780-08 .5189+12	.9956-08 .3649+13	.1027-07 .1383+14	.1055-07 .2758+14	.1089-07 .2729+14	.1127-07 .1021+14	.1173-07 .6314+12	.1320-07 .8170+07	.1233-07 .1313+12	.1318-07 .4419+13	.1216-07 .3133+13	.1489-07 .2236+15	.1573-07 .5683+15	.1753-07 .1464+15	.2218-07 .6252+12
11	.9396-08 .1202+11	.9558-08 .2201+12	.9720-08 .1804+13	.1007-07 .8696+13	.1030-07 .2271+14	.1062-07 .3479+14	.1096-07 .2631+14	.1134-07 .7210+13	.1183-07 .2531+12	.9708-08 .2633+05	.1243-07 .2514+12	.1333-07 .3800+13	.1269-07 .7354+13	.1505-07 .2096+15	.1565-07 .6419+15	.1771-07 .1687+15
12	.9716-08 .6671+10	.9214-08 .8447+11	.9644-08 .9078+12	.9801-08 .4762+13	.1011-07 .1632+14	.1037-07 .3322+14	.1068-07 .3953+14	.1103-07 .2353+14	.1162-07 .4726+13	.1198-07 .8171+11	.1158-07 .2825+06	.1253-07 .4055+12	.1349-07 .2951+13	.1295-07 .1281+14	.1527-07 .1042+15	.1597-07 .6972+15
13	.9600-08 .2455+10	.9343-08 .3965+11	.9317-08 .3882+12	.9722-08 .2641+13	.9851-08 .9867+13	.1017-07 .2660+14	.1044-07 .4313+14	.1074-07 .4136+14	.1109-07 .1955+14	.1150-07 .2190+13	.1221-07 .1910+11	.1181-07 .5697+08	.1262-07 .3783+12	.1371-07 .2018+13	.1311-07 .1828+14	.1541-07 .1785+15
14	.8993-08 .8944+09	.9460-08 .1850+11	.9112-08 .1668+12	.9377-08 .1311+13	.9657-08 .5643+13	.9969-08 .1815+14	.1021-07 .3736+14	.1049-07 .5013+14	.1081-07 .3978+14	.1116-07 .1462+14	.1159-07 .1459+13	.1281-07 .2184-10	.1197-07 .6891+09	.1271-07 .7321+12	.1408-07 .1171+13	.1323-07 .2370+14
15	.5606-08 .6623+08	.9351-08 .7886+10	.9214-08 .8008-11	.9223-08 .5793+12	.9601-08 .3210+13	.9731-08 .1107+14	.1002-07 .2841+14	.1027-07 .4880+14	.1055-07 .5476+14	.1087-07 .3940+14	.1124-07 .1040+14	.1170-07 .6809-12	.7344-08 .2645+07	.1209-07 .3412+10	.8502+12	.1475-07 .5012+12
16	.1853-07 .3221+08	.9650-08 .3851+10	.8551-08 .2863-11	.9460-08 .3196+12	.9137-08 .1479+13	.9723-08 .7034+13	.9770-08 .1893+14	.1007-07 .4082+14	.1034-07 .5982+14	.1061-07 .3563+14	.1093-07 .3014+14	.1132-07 .6900-13	.1185-07 .2770-12	.1099-07 .4061+09	.1219-07 .1660+11	.1288-07 .4227+12
17	.1440-07 .8387+08	.8730-08 .9679+09	.8600-08 .1287-11	.9023-08 .1578+12	.9053-08 .7468+12	.9521-08 .3757+13	.9611-08 .1178+14	.9883-08 .2944+14	.1013-07 .5269+14	.1039-07 .6681+14	.1068-07 .5244+14	.1101-07 .2931-14	.1139-07 .4182+13	.1205-07 .8430-11	.1144-07 .3916+09	.1227-07 .2408+11
18	.1421-07 .2079+08	.8304-09 .4721+08	.9038-08 .8747+10	.8651-08 .5296+11	.9232-08 .4120+12	.9153-08 .1838+13	.9544-08 .7258+13	.9883-08 .1967+14	.9933-08 .4167+14	.1019-07 .6393+14	.1045-07 .6838+14	.1074-07 .4663+14	.1108-07 .1785+14	.1149-07 .2347+13	.1251-07 .1634+11	.1167-07 .1547+09
19	.1144-07 .1787+08	.2168-07 .3286+08	.9344-08 .3305-10	.8012-08 .1991+11	.9427-08 .2210+12	.8721-08 .8436+12	.9513-08 .4250+13	.9471-08 .1201+14	.9764-08 .2076+14	.1002-07 .5612+14	.1023-07 .7143+14	.1050-07 .6618-14	.1081-07 .3001+14	.1115-07 .1231+14	.1158-07 .1153+13	.1583-07 .4387+09

Table 91.--Continued $W\ ^1\Delta_u$ —— $a\ ^1\Pi_g$

V'' \ V'	0	1	2	3	4	5	6
0	.1249-07 .3894+14	.1189-07 .8056+14	.1140-07 .6684+14	.1100-07 .3643+14	.1065-07 .1581+14	.1036-07 .6118+13	.1011-07 .2182+13
1	.1314-07 .3791+12	.1263-07 .1246+14	.1197-07 .8294+14	.1147-07 .1192+15	.1106-07 .9254+14	.1070-07 .5227+14	.1039-07 .2441+14
2	.1398-07 .3576+10	.1324-07 .3609+12	.1288-07 .2741+13	.1205-07 .6075+14	.1154-07 .1382+15	.1112-07 .1467+15	.1077-07 .1043+15
3	.1516-07 .4023+11	.1407-07 .1478+11	.1333-07 .2481+12	.1396-07 .1603+12	.1216-07 .3658+14	.1161-07 .1308+15	.1119-07 .1803+15
4	.1762-07 .4451+10	.1527-07 .1528+12	.1416-07 .3762+11	.1344-07 .1451+12	.1138-07 .1586+12	.1229-07 .1852+14	.1169-07 .1065+15
5	.4011-08 .4342+08	.1769-07 .2047+11	.1537-07 .3606+12	.1425-07 .7464+11	.1356-07 .7552+11	.1220-07 .7609+12	.1248-07 .7509+13
6	.1208-07 .1923+09	.2475-07 .1087+08	.1801-07 .5115+11	.1548-07 .6780+12	.1434-07 .1280+12	.1369-07 .3553+11	.1243-07 .1243+13
7	.1272-07 .2618+09	.2276-07 .4799+07	.8999-08 .9039+08	.1814-07 .1058+12	.1559-07 .1106+13	.1444-07 .1947+12	.1386-07 .1515+11
8	.1301-07 .6944+09	.1217-07 .1023+09	.1477-07 .6026+09	.5665-08 .2600+09	.1835-07 .1812+12	.1571-07 .1619+13	.1454-07 .2735+12
9	.1298-07 .7013+09	.1270-07 .1330+09	.1224-07 .1018+09	.1811-07 .2847+09	.3551-08 .1634+10	.1871-07 .2655+12	.1581-07 .2265+13
10	.1328-07 .4186+09	.1296-07 .3755+09	.1340-07 .1159+09	.1157-07 .1128+09	.1759-07 .9939+09	.5846-08 .3931+10	.1903-07 .3640+12
11	.1319-07 .4880+10	.1300-07 .3748+10	.1337-07 .4634+09	.1277-07 .9045+09	.1254-07 .3565+09	.2329-07 .4861+09	.8915-08 .1369+11
12	.1321-07 .1434+10	.1316-07 .1265+10	.1350-07 .5847+08	.1309-07 .6180+09	.1610-07 .2063+08	.1187-07 .2749+09	.2023-07 .2085+10
13	.1325-07 .3453+10	.1334-07 .4600+10	.1301-07 .5711+09	.1338-07 .1520+10	.1311-07 .2330+09	.1399-07 .7191+09	.1226-07 .2966+09
14	.1328-07 .5056+10	.1340-07 .7504+10	.1313-07 .1134+10	.1338-07 .2440+10	.1321-07 .7198+09	.1358-07 .6745+09	.1199-07 .5778+09
15	.1350-07 .2869+10	.1340-07 .8856+10	.1333-07 .3093+10	.1371-07 .8382+09	.1333-07 .1852+10	.1363-07 .5534+09	.1385-07 .2456+09

Data is from the unpublished supplement to Benesch et al. [69]. The Deslandres tables have v'' and v' in reverse order as compared with conventional usage. The r-centroids are in units of 10^{-7} cm (e.g., .1185-07 = 1.185 Å). The second entry for each band is $^4\sigma_{v'v''}\ q_{v'v''}$.

Table 92. r-centroids for the $W^3\Delta_u$ - $X^1\Sigma_g^+$ transition (Å).

v' \ v''	0	1	2	3	4	5	6	7	8	9	10
0	1.182	1.199	1.217	1.236	1.254	1.274	1.294	1.315	1.337	1.360	1.383
1	1.171	1.188	1.205	1.223	1.240	1.256	1.286	1.303	1.323	1.345	1.367
2	1.160	1.177	1.193	1.210	1.183	1.250	1.267	1.285	1.286	1.333	1.353
3	1.150	1.166	1.182	1.185	1.219	1.235	1.250	1.279	1.295	1.313	1.325
4	1.140	1.156	1.169	1.192	1.206	1.220	1.246	1.261	1.276	1.308	1.322
5	1.131	1.145	1.211	1.179	1.193	1.219	1.231	1.244	1.273	1.287	1.301
6	1.122	1.135	1.155	1.168	1.162	1.203	1.217	1.244	1.256	1.267	1.298
7	1.113	1.125	1.145	1.157	1.179	1.191	1.324	1.227	1.239	1.267	1.280
8	1.105	1.100	1.135	1.143	1.167	1.178	1.201	1.214	1.243	1.251	1.257
9	1.096	1.116	1.126	1.152	1.156	1.302	1.189	1.194	1.224	1.235	1.262
10	1.089	1.105	1.117	1.136	1.146	1.167	1.177	1.202	1.211	1.249	1.247

Data from W. Benesch (unpublished).

Table 93. Oscillator strengths, transition probabilities and band origin wavelengths for the $A^2\Pi_u - X^2\Sigma_g^+$ Meinel system of N_2^+. [a]

v'\v''	0	1	2	3	4	5	6	7	8	9	10	11	12	13	$\tau_v(10^{-6})$ Expt.[b]	Calc.
	1.68-3	8.71-4	1.62-4	1.24-5	1.91-7											
0	4.55+4	1.36+4	1.19+3	2.79+1	1.70-2											16.57
	11086.9	14609.8	21264.9	38560.8	193.4+3											
	1.40-3	1.39-4	7.74-4	3.04-4	3.55-5	5.42-7										
1	5.53+4	3.52+3	1.12+4	2.02+3	6.75+1	2.16-2									13.9±1.0	13.88
	9181.5	11472.4	15210.5	22395.7	41860.3	389.1+3										
	6.90-4	9.87-4	4.43-5	4.32-4	3.66-4	6.20-5	7.12-7									
2	3.73+4	3.67+4	1.05+3	5.73+3	2.19+3	9.92+1	7.67-3								11.9± .4	12.04
	7852.5	9469.9	11879.8	15851.9	23628.7	45679.6	556.5+3									
	2.68-4	1.01-3	3.68-4	2.82-4	1.52-4	3.49-4	8.48-5	1.36-7								
3	1.89+4	5.17+4	1.28+4	6.21+3	1.86+3	1.86+3	1.12+2	1.41-5							10.7± .4	10.70
	6873.6	8081.8	9774.0	12312.2	16540.5	24982.6	50168.0	567.4+4								
	9.18-5	6.08-4	8.85-4	4.27-5	4.32-4	1.84-5	2.79-4	9.88-5								
4	8.17+3	4.07+4	4.26+4	1.40+3	8.82+3	2.05+2	1.33+3	1.07+2							9.7± .4	9.68
	6123.0	7063.7	8323.1	10095.4	12772.5	17282.1	26477.2	55519.8								
	2.94-5	2.84-4	8.13-4	5.42-4	1.72-5	4.16-4	6.38-6	1.91-4	1.02-4							
5	3.20+3	2.39+4	5.14+4	2.46+4	5.28+2	7.90+3	6.51+1	8.06+2	8.85+1						9.1± .4	8.89
	5529.4	6285.2	7263.1	8577.1	10435.5	13263.1	18082.5	28133.0	61996.2							
	9.07-6	1.15-4	5.06-4	8.04-4	2.17-4	1.41-4	2.95-4	5.94-5	1.09-4	9.52-5						
6	1.19+3	1.19+4	4.05+4	4.80+4	9.27+3	4.05+3	5.18+3	5.52+2	4.05+2	6.49+1					8.4± .5	8.25
	5048.3	5671.0	6455.1	7472.6	8844.8	10795.6	13786.3	18946.9	29972.8	69963.1						
	2.77-6	4.32-5	2.56-4	6.70-4	5.26-4	3.41-5	2.73-4	1.53-4	1.25-4	4.80-5	8.12-5					
7	4.26+2	5.38+3	2.52+4	5.08+4	3.53+4	1.37+3	7.28+3	2.48+3	1.05+3	1.56+2	4.24+1				7.8± .5	7.72
	4650.7	5174.1	5819.0	6633.2	7692.6	9127.0	11176.9	14344.4	19881.4	32022.6	79957.8					
	8.43-7	1.55-5	1.15-4	4.20-4	7.17-4	3.78-4	5.06-6	3.32-4	4.78-5	1.69-4	1.27-5	6.33-5				
8	1.51+2	2.28+1	1.36+4	3.93+4	5.15+4	2.01+4	1.90+2	8.26+3	7.14+2	1.29+3	3.61+1	2.45+2			7.3± .5	7.28
	4316.7	4764.0	5305.4	5974.0	6819.9	7923.9	9424.6	11580.9	14940.2	20892.9	34315.0	92818.8				
	2.59-7	5.43-6	4.79-5	2.23-4	5.59-4	6.40-4	1.61-4	7.66-4	3.07-4	2.42-6	1.79-4	3.12-3	4.50-5			
9	5.31+1	9.27+2	6.70+3	2.51+4	4.95+4	4.34+4	8.05+3	2.69+3	7.10+3	3.33+1	1.23+3	7.65-1	1.24+1			6.91
	4032.5	4420.1	4882.4	5442.9	6136.4	7016.0	8167.5	9739.0	12009.9	15577.7	21991.1	36893.7	110.0+3			
	8.04-8	1.88-6	1.91-5	1.07-4	3.52-4	6.31-4	4.79-4	3.17-5	1.76-4	2.24-4	1.01-5	1.59-4	3.87-6	2.88-5		
10	1.87+1	3.68+2	3.10+3	1.43+4	3.76+4	5.29+4	3.06+4	1.49+3	5.28+3	4.81+3	1.28+2	9.88+2	8.14+0	5.35+0	6.2± .4	6.58
	3787.8	4127.9	4528.3	5006.5	5587.3	6307.2	7222.6	8424.8	10072.3	12467.1	16262.8	23190.1	39822.5	134.0+3		

Data from Cartwright [146].

[a] $f_{v'v''}$, $A_{v'v''}$, $\lambda_{v'v''}$ (Å). Entries followed by a + or - quantity are multiplied by ten to that power.

[b] Reference [524] (v' = 1-8), Ref. [435] (v' = 10).

Table 94. Einstein A coefficients, absolute band strengths, and band oscillator strengths for the $B^2\Sigma_u^+ - X^2\Sigma_g^+$ first negative bands of N_2^+.[a]

	v''					
v'	0	1	2	3	4	5
0	9.64 + 6[b]	3.48 + 6	7.75 + 5	1.36 + 5	2.06 + 4	2.83 + 3
	5.69 - 1	2.68 - 1	7.97 - 2	1.91 - 2	4.09 - 3	8.25 - 4
	2.21 - 2	9.53 - 3	2.57 - 3	5.56 - 4	1.06 - 4	1.88 - 5
1	4.87 + 6	3.08 + 6	3.87 + 6	1.53 + 6	3.92 + 5	7.85 + 4
	2.21 - 1	1.78 - 1	2.90 - 1	1.52 - 1	5.27 - 2	1.47 - 2
	9.36 - 3	6.97 - 3	1.04 - 2	4.97 - 3	1.56 - 3	3.89 - 4
2	7.57 + 5	6.36 + 6	5.74 + 5	3.03 + 6	1.94 + 6	6.80 + 5
	2.70 - 2	2.84 - 1	3.25 - 2	2.21 - 1	1.86 - 1	8.76 - 2
	1.24 - 3	1.21 - 2	1.28 - 3	8.00 - 3	6.16 - 3	2.62 - 3
3	2.81 + 4	1.64 + 6	6.24 + 6	3.62 + 3	1.98 + 6	2.00 + 6
	8.06 - 4	5.80 - 2	2.75 - 1	2.01 - 4	1.41 - 1	1.86 - 1
	3.98 - 5	2.67 - 3	1.18 - 2	7.99 - 6	5.15 - 3	6.20 - 3
4		6.23 + 4	2.35 + 6	5.55 + 6	1.54 + 5	1.14 + 6
		1.79 - 3	8.26 - 2	2.42 - 1	8.45 - 3	7.98 - 2
		8.83 - 5	3.82 - 3	1.04 - 2	3.37 - 4	2.93 - 3
5			7.26 + 4	2.78 + 6	4.83 + 6	4.31 + 5
			2.09 - 3	9.77 - 2	2.09 - 1	2.34 - 2
			1.03 - 4	4.51 - 3	9.02 - 3	9.35 - 4

Data from Jain and Sahni [336].

[a] The first value for each v', v'' is the Einstein A coefficient, $A_{v'v''}$ (sec^{-1}), the second the absolute band strength, $p^a_{v'v''}$ (a^2e^2) and the third the band oscillator strength, $f_{v'v''}$.

[b] The sign and final digit indicate the power of 10 to which each entry should be raised.

Table 95. Absolute transition probabilities for the N_2 $C^3\Pi_u$ - $B^3\Pi_g$ system (in units of $10^6 s^{-1}$)

v' \ v''	0	1	2	3	4	5	6	7	8	9	τ
0	13.9	8.88	3.34	.96	.23	.052					3.66(-8)
1	13.8	0.53	5.49	4.62	2.12	.72	.20	.05			3.63(-8)
2	4.81	11.41	1.00	1.65	3.80	2.77	1.27	.46	.14	.038	3.66(-8)
3	.64	8.68	6.40	3.34	.089	2.19	2.66	1.66	.74	.27	3.75(-8)
4		1.48	10.37	3.04	4.28	.17	.90	2.06	1.73	.95	4.00(-8)

Data from relative band strengths of Jain and Sahni [337] rescaled using τ for v'=0 as 3.66(-8)s. A-values from Shemansky and Broadfoot [572], and Johnson and Fowler [362], are not always in agreement.

Table 96. Absolute transition probabilities of the N_2 First Positive System

v' \ v"	0	1	2	3	4	5	6	7	8	9	10	11	12	13	$\Sigma_{v"} A_{v'v"}$	Extrapolated
0	10469.0 6.25+4	12316.6 3.56+4	14894.5 1.12+4	18739.1 2.47+3	25082.9 3.97+2	37522.0 4.24+1									1.12+5	1.12+5
1	8883.4 8.72+4	10179.0 4.12+2	11878.1 1.85+4	14201.7 1.48+4	17569.3 5.69+3	22882.9 1.40+3	32503.7 2.27+2								1.28+5	1.29+5
2	7732.0 4.44+4	8695.3 6.17+4	9905.7 1.25+4	11470.9 2.68+3	13572.1 1.05+4	16538.8 7.29+3	21039.8 2.71+3	28671.4 6.39+2	44417.6 8.87+1						1.42+5	1.43+5
3	6858.3 1.07+4	7605.8 7.73+4	8516.0 2.17+4	9647.7 2.85+4	11092.0 7.97+2	12997.4 3.88+3	15624.1 6.33+3	19473.2 3.68+3	25648.7 1.24+3	37156.2 2.57+2	66039.9 2.54+1				1.54+5	1.54+5
4	6173.1 1.29+3	6772.1 3.02+4	7484.4 8.36+4	8344.7 1.54+3	9403.8 2.94+4	10738.4 7.84+3	12470.6 1.93+2	14806.6 1.52+3	18124.8 3.74+3	23202.8 1.84+3	31932.9 5.44+2	50431.6 9.03+1			1.62+5	1.64+5
5	5621.6 7.42+1	6114.1 5.08+3	6688.7 5.25+4	7367.5 6.86+4	8181.0 3.02+3	9172.9 1.91+4	10407.7 1.52+4	11985.9 1.10+3	14071.2 1.02+3	16951.5 2.81+3	21132.2 2.13+3	27993.4 8.95+2	40756.3 2.24+2		1.72+5	1.73+5
6		5581.6 3.71+2	6056.7 1.19+4	6608.0 7.09+4	7255.0 4.38+4	8024.4 1.58+4	8953.8 7.10+3	10097.6 1.76+4	11538.2 5.11+3	13405.9 ---	15920.7 1.40+3	19483.8 1.93+3	24914.0 1.17+3	34170.0 4.24+2	1.78+5	1.81+5
7			5542.7 1.07+3	6000.9 2.14+4	6529.7 8.10+4	7146.5 2.03+4	7874.4 2.88+4	8745.6 5.09+2	9806.0 1.43+4	11123.1 9.39+3	12800.7 1.12+3	15007.4 2.31+2	18035.1 1.26+3	22434.2 1.22+3	1.81+5	1.88+5
8				5504.9 2.34+3	5946.7 3.25+4	6453.9 8.15+4	7041.8 4.94+3	7730.4 3.50+4	8547.4 1.38+3	9531.1 8.11+3	10736.9 1.15+4	12247.4 3.73+3	14191.7 9.33+1	16781.1 4.62+2	1.82+5	1.95+5
9				5092.2 7.77+1	5468.0 4.29+3	5893.9 4.38+4	6380.3 7.31+4	6940.5 ---	7592.1 3.28+4	8358.3 7.66+3	9271.4 2.44+3	10376.4 1.04+4	11739.1 6.47+3	13456.6 1.17+3	1.82+5	2.01+5
10					5068.2 1.59+2	5432.0 6.92+3	5842.5 5.38+4	6308.8 5.86+4	6842.6 3.99+3	7458.9 2.44+4	8177.6 1.54+4	9025.3 ---	10038.9 6.96+3	11268.9 7.95+3	1.78+5	2.07+5
11						5044.8 2.82+2	5397.0 1.01+4	5792.5 6.11+4	6239.3 4.14+4	8747.7 1.33+4	7330.5 1.38+4	8004.5 2.09+4	8791.8 1.58+3	9721.0 2.98+3	1.65+5	2.13+5
12							5022.1 4.49+2	5362.8 1.38+4	5743.6 6.49+4	6171.7 2.48+4	6655.6 2.37+4	7206.6 4.86+3	7838.5 2.19+4	8568.8 6.03+3	1.60+5	2.18+5

Data from Shemansky and Broadfoot [572].

λ (Å) and $A_{v'v"}$ are given for each v'-v".

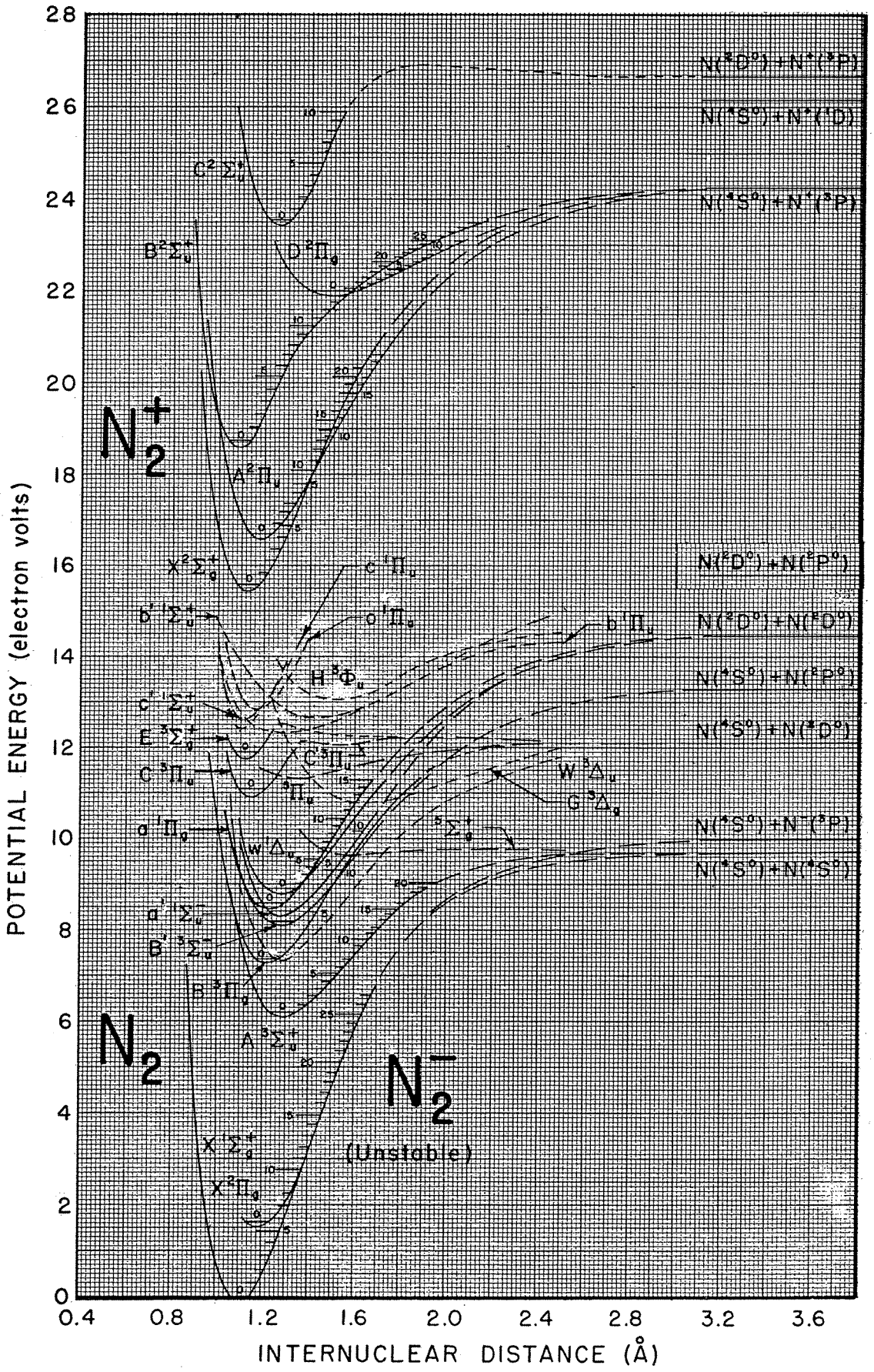

FIGURE 1. Potential energy curves for N_2 and N_2^+.*

* Enlarged copies of figure 1 may be obtained from the authors on request.

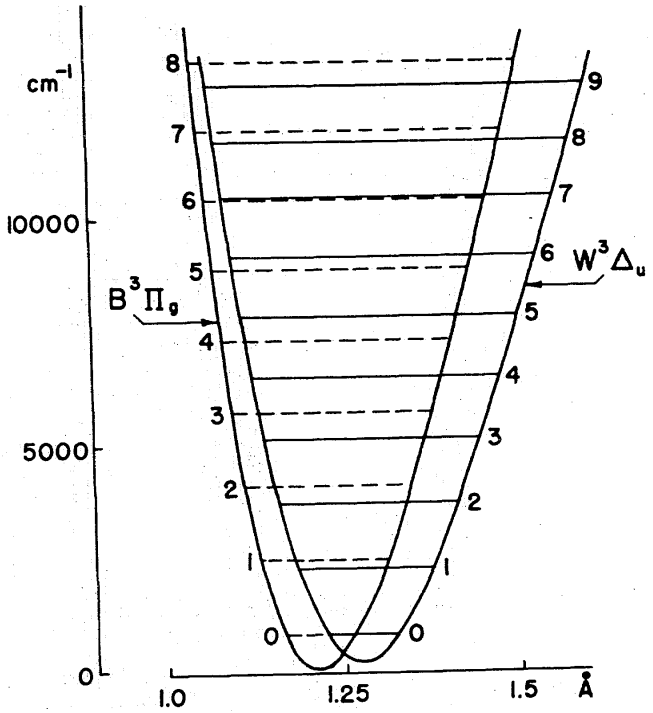

FIGURE 2. Potential energy curves for the $W^3\Delta_u$ and $B^3\Pi_g$ states (from Saum and Benesch [556]). Transitions 4–6 and 4–1, for example, illustrate intrasystem cascade. (See Benesch and Saum [67]). T_0 for the W state lies only about 70 cm^{-1} above that of the B state.

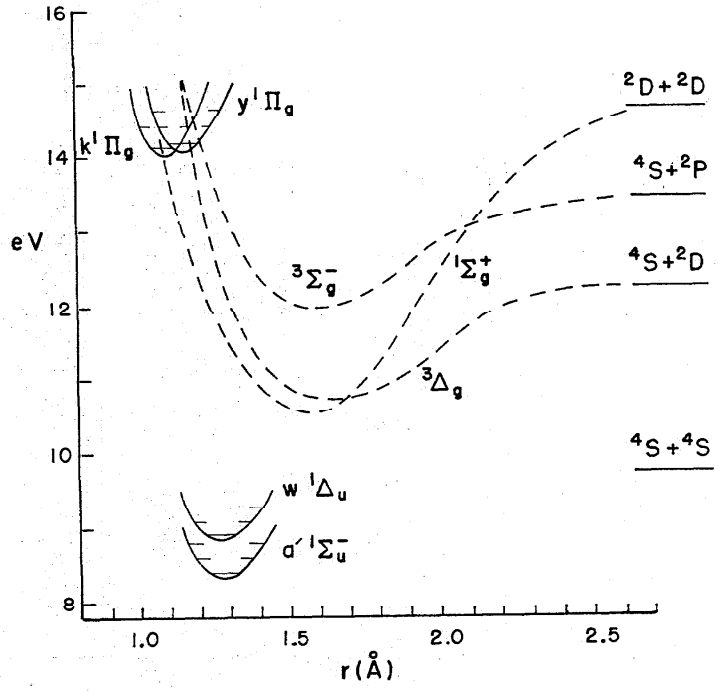

FIGURE 3. Potential curves for states involved in transitions to and interactions with the $k^1\Pi_g$ and $y^1\Pi_g$ states. These are discussed section 8.9.

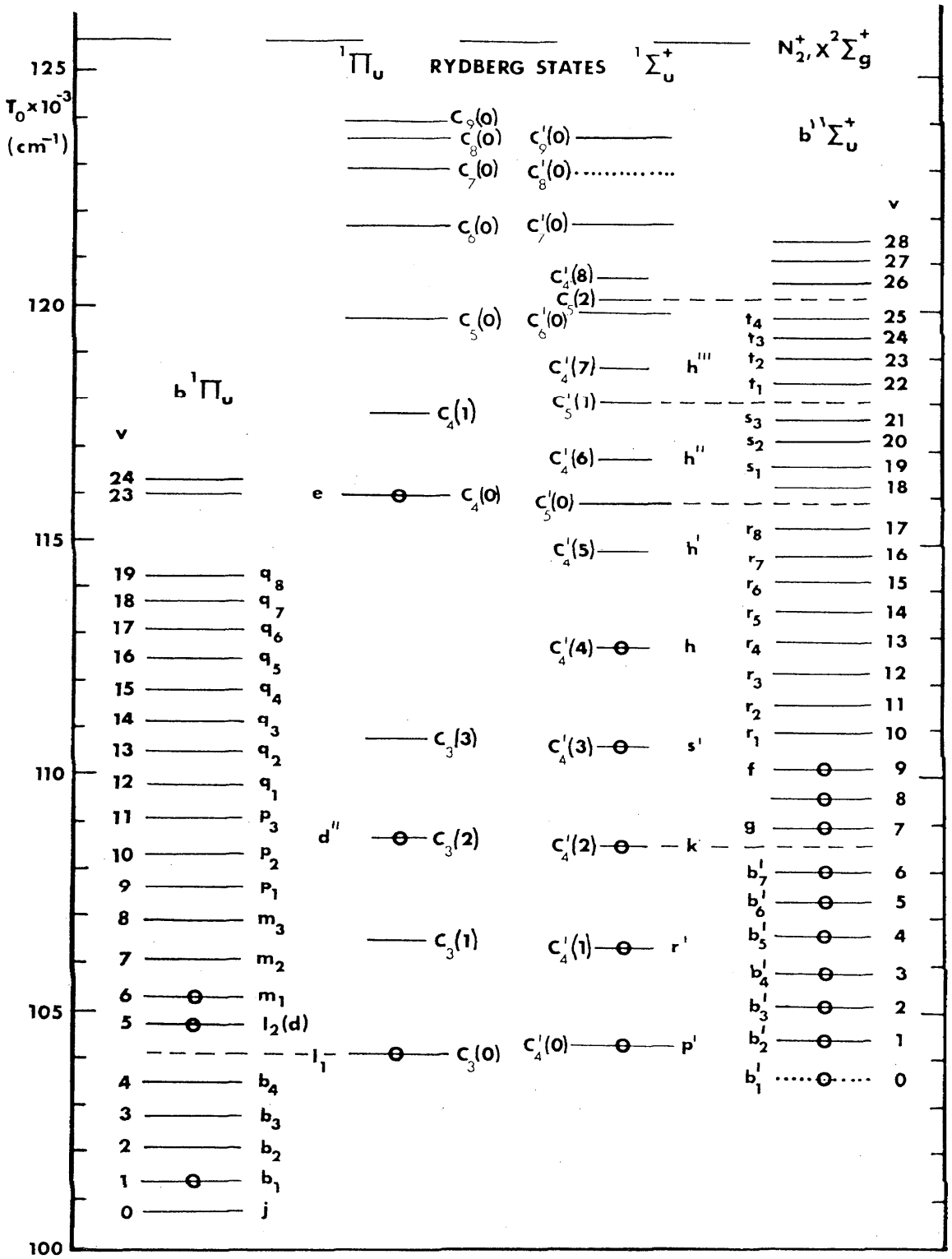

FIGURE 4. Energy level diagram for the highly excited $^1\Sigma_u^+$ and $^1\Pi_u$ states of N_2 arranged according to the new interpretations of Dressler [210] and Carroll and Collins [130]. This figure is taken from the latter work. Successive vibrational levels of the valence states b and b' are also designated according to the old notation, as are the Rydberg states c_n and c_n'. For the Rydberg states, the new notation indicates principal quantum number by a subscript, with vibrational level enclosed in parentheses. Levels observed in emission are identified by a circle.

13. Acknowledgments

Many thanks to Betty King, Gloria Rotter, and Ruth Barber, for their creative typing. We are indebted to P. K. Carroll, K. Yoshino, and J. J. Barrett, and M. Krauss for providing us with material prior to publication and to W. Benesch for providing unpublished material.

14. References

Monographs, Books, Reviews

[1] Albritton, D. L., Schmeltekopf, A. L., and Zare, R. N., Diatomic Intensity Factors (Harper and Row, N.Y., in preparation).

[2] Anketell, J., and Nicholls, R. W., The afterglow and energy transfer mechanisms of active nitrogen. Rep. Prog. Phys. **33**, 269–306 (1970).

[3] Bardsley, J. N., and Mandl, F., Resonant scattering of electrons by molecules. Rep. Prog. Phys. **31**, 471–531 (1968).

[4] Berry, R. S., Electronic spectroscopy by electron electroscopy. Annu. Rev. Phys. Chem. **20**, 357–406 (1969).

[5] Brewer, L., and Searcy, A. W., High temperature chemistry. Annu. Rev. Phys. Chem. **7**, 259–286 (1956).

[6] Chamberlain, J. W., Physics of the Aurora and Airglow (Acad. Press, New York, 1961).

[7] Duncan, A. B. F., Rydberg Series in Atoms and Molecules (Acad. Press, New York, 1971).

[8] Gaydon, A. G., Dissociation Energies and Spectra of Diatomic Molecules, 3rd ed. (Chapman and Hall, London, 1968).

[9] Golde, M. F., and Thrush, B. A. Afterglows. Rep. Prog. Phys. **36**, 1285–1364 (1973).

[10] Goodisman, J., Diatomic Interaction Potential Theory: Vol. 1, Fundamentals, Vol. 2, Applications (Acad. Press, New York, 1973).

[11] Hasted, J. B., Electron scattering spectroscopy. Contemp. Phys. **14**, 357–387 (1973).

[12] Herzberg, G., Spectra of Diatomic Molecules, 2d ed. (Van Nostrand, New York, 1950).

[13] Herzberg, G., Forbidden transitions in diatomic molecules. Mem. Soc. R. Sci. Liege, Collect. 8 **17**, 121–55 (1969).

[14] Herzberg, G., Spectra and structures of molecular ions. Chem. Soc. Lond. Q. Rev. **25**, 201–222 (1971).

[15] Hudson, R. D., Critical review of ultraviolet photoabsorption cross sections for molecules of astrophysical and aeronomic interest. Rev. Geophys: Space Phys. **9**, 305–406 (1971). Reprinted as Natl. Bur. Stand. (U.S.) Monogr. NSRDS–NBS 38 (1971).

[16] Kayser, H., Handbuch der Spectroscopie. 5. (Hirzel, Leipzig, 1910).

[17] Kranendonk, J. Van, Intermolecular spectroscopy. Physica **73**, 156–173 (1974).

[18] Krauss, M., Compendium of ab initio Calculations of Molecular Energies and Properties. Natl. Bur. Stand. (U.S.) Technical Note 438, Washington, D.C. (1967).

[19] Krishnaji, V. P., Evaluation of molecular quadrupole moments. Rev. Mod. Phys. **38**, 690–709 (1966).

[20] Lofthus, A., The molecular spectrum of nitrogen. Spectroscopic Report No. 2, Department of Physics, University of Oslo (1960).

[21] Lyman, T., The Spectroscopy of The Extreme Ultraviolet (Longmans Green, London, 1928).

[22] Mannella, G. G., Active nitrogen. Chem. Rev. **63**, 1–20 (1963).

[23] McCormac, B. M., (ed.), The Radiating Atmosphere (Reidel, Dordrecht, Holland, 1971).

[24] Mitra, S. K., Active Nitrogen: A New Theory. (Association for the Cultivation of Science, Calcutta, 1945).

[25] Moore, C. E., Ionization potentials and ionization limits derived from the analyses of optical spectra. Natl. Bur. Stand. (U.S.), Natl. Stand. Ref. Data Ser., NSRDS–NBS 34 (1970).

[26] Pearse, R. W. B. and Gaydon, A. G., The Identification of Molecular Spectra (Chapman & Hall, London, 1963).

[27] Richards, W. G., Walker, T. E. H., and Hinkley, R. K., A Bibliography of Ab Initio Molecular Wave Functions (Clarendon Press, Oxford, 1971).

[28] Richards, W. G., Walker, T. E. H., Farnell, L. and Scott, P. R., Bibliography of Ab Initio Molecular Wave Functions: Supplement for 1970–1973 (Clarendon Press, Oxford, 1974).

[29] Rosen, B., (ed.) Donnees Spectroscopiques Relatives aux Molecules Diatomiques. Spectroscopic Data Relative to Diatomic Molecules. (Tables Internationales de Constantes Selectionnees, No. 17) (Pergamon, Oxford. 1970).

[30] Schaefer, H. F. III, The Electronic Structure of Atoms and Molecules: A Survey of Rigorous Quantum Mechanical Results (Addison-Wesley, Reading, Mass., 1972).

[31] Schulz, G. J., Resonances in electron impact on diatomic molecules, Rev. Mod. Phys. **45**, 423–486 (1973). Reprinted as Natl. Bur. Stand. (U.S.) Monogr. NSRDS–NBS 50 (1973).

[32] Siegbahn, K. et al., ESCA; Atomic, Molecular and Solid State Structure Studied by Means of Electron Spectroscopy (Almqvist and Wiksells, Uppsala, 1967); Siegbahn, K. et al., ESCA; Applied to Free Molecules (North-Holland Publ. Co., Amsterdam and London, 1969).

[33] Tatum, J. B., The interpretation of intensities in diatomic molecular spectra, Astrophys. J. Suppl. No. 124, **16**, 21–56 (1967).

[34] Tilford, S. G., Wilkinson, P. G., Franklin, V. B., Naber, R. H., Benesch, W., and Vanderslice, J. T., Summary of observed absorption lines of room-temperature molecular nitrogen between 1060 and 1520 Å. Astrophys. J. Suppl. No. 115, **13**, 31–64 (1966).

[35] Trajmar, S., Rice, J. K., and Kuppermann, A., Electron impact spectroscopy. Adv. Chem. Phys. **18**, 15–90 (1970).

[36] Turner, D. W., Baker, C., Baker, A. D., and Brundle, C. R., Molecular Photoelectron Spectroscopy (Wiley-Interscience, London, New York, 1970).

[37] Tyte, D. C., and Nicholls, R. W., Identification Atlas of Molecular Spectra. 2. The N_2 $C^3\Pi_u$–$B^3\Pi_g$ Second Positive System. Department of Physics, The University of Western Ontario, London, Ontario (October, 1964).

[38] Tyte, D. C., and Nicholls, R. W., Identification Atlas of Molecular Spectra. 3. The N_2^+ $B\ ^2\Sigma_u^+$–$X\ ^2\Sigma_g^+$ First Negative System of Nitrogen. Department of Physics, The University of Western Ontario, London, Ontario (April 1965).

[39] Vallance Jones, A., Auroral spectroscopy. Space Sci. Rev. **11**, 776–826 (1971).

[40] Wallace, L., A collection of the band-head wavelengths of N_2 and N_2^+. Astrophys. J. Suppl. No. 62, **6**, 445–480 (1962).

[41] Weber, A., High resolution Raman studies of gases, Chapt. 9 in A. Anderson (ed.), The Raman Effect, Vol. 2 (Dekker, N.Y., 1973).

[42] Whiting, E. E., and Nicholls, R. W., Reinvestigation of rotational-line intensity factors in diatomic spectra. Astrophys. J. Suppl. No. 235, **27**, 1–20 (1974).
[43] Wright, A. N., and Winkler, C. A., Active Nitrogen (Acad. Press, New York, 1968).

Individual Papers

[44] Albritton, D. L., Schmeltekopf, A. L., and Ferguson, E. E., Mechanism of the reaction of He^+ and N_2, presented at 6th Int. Conf. on Physics of Electronic and Atomic Collisions (1969), held at M.I.T.
[45] Allen, L., Jones, D. G. C., and Swaram, B. M., The interaction of the ultraviolet and near infrared laser systems of molecular nitrogen. Phys. Lett. **25A**, 280–281 (1967).
[46] Anderson, A., Sun, T. S., and Donkersloot, M. C. A., Raman spectra and lattice dynamics of the α phases of nitrogen and carbon monoxide crystals. Can. J. Phys. **48**, 2265–2271 (1970).
[47] Andersen, A., and Thulstrup, E. W., Configuration interaction studies of the low-lying quartet states of N_2^+. J. Phys. B **6**, L211–L213 (1973).
[48] Andrade, O., Gallards, M., and Bockasten, K., New lines in a pulsed N_2 laser. Appl. Opt. **6**, 2006 (1967).
[49] Anton, H., Luminescence of some molecular gases excited by fast electrons I, II. Ann. Phys. (Leipzig) **16**, 17–29 (1966); **18**, 178–193 (1966).
[50] Appell, J., Durup, J., Fehsenfeld, F. C., and Fournier, P., Double charge transfer spectroscopy of diatomic molecules. J. Phys. B **6**, 197–205 (1973).
[51] Appleton, J. P., and Steinberg, M., Vacuum-ultraviolet absorption of shock-heated vibrationally excited nitrogen. J. Chem. Phys. **46**, 1521–1529 (1967).
[52] Appleyard, E. T. S., Electronic structure of the a–X band system of N_2. Phys. Rev. **41**, 254–255 (1932).
[53] Archibald, T. W., and Sabin, J. R., Theoretical investigation of the electronic structure and properties of N_3^-, N_3 and N_3^+. J. Chem. Phys. **55**, 1821–1829 (1971).
[54] Åsbrink, L., and Fridh, C., The C state of N_2^+, studied by photoelectron spectrosocopy. Phys. Scripta **9**, 338–340 (1974).
[55] Asundi, R. K., Schulz, G. J., and Chantry, P. J., Studies of N_4^+ and N_3^+ ion formation in nitrogen using high-pressure mass spectrometry. J. Chem. Phys. **47**, 1584–1591 (1967).
[56] Baer, P., and Miescher, E., Band spectra in the Schumann region of NO and N_2^+ with enriched nitrogen-15. Nature (London) **169**, 581 (1952).
[57] Baer, P., and Miescher, E., NO, NO^+, and N_2^+ emission spectra in the Schumann region. Helv. Phys. Acta **26**, 91–110 (1953).
[58] Baker, M. R., Anderson, C. H., and Ramsey, N. F., Nuclear magnetic antishielding of nuclei in molecules. Magnetic moments of F^{19}, N^{14} and N^{15}. Phys. Rev. **133**, A1533–A1536 (1964).
[59] Barrett, J. J., and Adams, N. I., III, Laser-excited rotation-vibration Raman scattering in ultra-small gas samples. J. Opt. Soc. Amer. **58**, 311–319 (1968).
[60] Barrett, J. J., and Harvey, A. B., Vibrational and rotational-translational temperatures in N_2 by interferometric measurement of the pure rotational Raman effect. J. Opt. Soc. Amer. **65**, 392–398 (1975).
[61] Bass, A. M., Absorption spectrum of the pink afterglow of nitrogen in the vacuum ultraviolet. J. Chem. Phys. 40, 695–700 (1964).
[62] Bass, A. M., and Broida, H. P., Stablization of free radicals at low temperatures: Summary of the NBS Free Radicals Research Program. Natl. Bur. Stand. (U.S.) NBS Monograph 12, 1960.
[63] Bass, A. M., and Broida, H. P., Color phenomena associated with energy transfer in afterglows and, atomic flames. J. Res. Natl. Bur. Stand. (U.S.) **67A**, 379–388 (1963).
[64] Bayes, K. D., and Kistiakowsky, G. B., On the mechanism of the Lewis-Rayleigh nitrogen afterglow. J. Chem. Phys. **32**, 992–1000 (1960).
[65] Becker, K. H., Fink, E. H., Groth, W., Jud, W., and Kley, D., N_2 formation in the Lewis-Rayleigh afterglow. Faraday Disc. Chem. Soc. (Lond.) No. 53, 35–51 (1972).
[66] Bendtsen, J., The rotational and rotation-vibrational Raman spectra of $^{14}N_2$, $^{14}N^{15}N$ and $^{15}N_2$. J. Raman Spectrosc. **2**, 133–145 (1974).
[67] Benesch, W. M., and Saum, K. A., The $W\,^3\Delta_u$ state of molecular nitrogen. J. Phys. B **4**, 732–738 (1971).
[68] Benesch, W., Vanderslice, J. T., and Tilford, S. G., Excitation and photon emission rates of the auroral nitrogen first positive group. J. Atmos. Terr. Phys. **29**, 251–258 (1967).
[69] Benesch, W., Vanderslice, J. T., and Tilford, S. G., r-centroid calculations for observed and permitted transitions in N_2. J. Mol. Spectrosc. **36**, 464–467 (1970).
[70] Benesch, W., Vanderslice, J. T., Tilford, S. G., and Wilkinson, P. G., Potential curves for the observed states of N_2 below 11 eV. Astrophys. J. **142**, 1227–1240 (1965).
[71] Benesch, W., Vanderslice, J. T., Tilford, S. G., and Wilkinson, P. G., Franck-Condon factors for observed transitions in N_2 above 6 eV. Astrophys. J. **143**, 236–252 (1966).
[72] Benesch, W., Vanderslice, J. T., Tilford, S. G., and Wilkinson, P. G., Franck-Condon factors for permitted transitions in N_2. Astrophys. J. **144**, 408–418 (1966).
[73] Bennett, R. G., and Dalby, F. W., Experimental determination of the oscillator strength of the first negative bands of N_2^+. J. Chem. Phys. **31**, 434–441 (1959).
[74] Benson, S. W., Kinetic and spectroscopic constraints on the origin of the N_2 afterglow. J. Chem. Phys. **48**, 1765–1768 (1968).
[75] Berkowitz, J., and Chupka, W. A., Photoelectron spectroscopy of autoionization peaks. J. Chem. Phys. **51**, 2341–2354 (1969).
[76] Bernard, R., Excitation of Vegard-Kaplan bands by electronic bombardment of a mixture of argon and nitrogen. C. R. Acad. Sci. (Paris) **200**, 2074–2076 (1935).
[77] Betts, T., and McKoy, V., Rydberg states of diatomic and polyatomic molecules using model potentials. J. Chem. Phys. **54**, 113–123 (1971).
[78] Billingsley, F. P., II, and Krauss, M., Quadrupole moment of CO, N_2 and NO^+. J. Chem. Phys. **60**, 2767–2772. (1974).
[79] Birge, R. T., The first Deslandres' group of the positive band spectrum of nitrogen, under high dispersion. Astrophys. J. **39**, 50–88 (1914).
[80] Birge, R. T., The band spectrum of nitrogen, and its theoretical interpretation. Phys. Rev. **23**, 294–295 (1924).
[81] Birge, R. T., and Hopfield, J. J., The quantum analysis of new nitrogen bands in the ultra-violet. Nature (London) **116**, 15 (1925).
[82] Birge, R. T., and Hopfield, J. J., The ultra-violet band spectra of nitrogen. Phys. Rev. **29**, 356 (1927).
[83] Birge, R. T., and Hopfield, J. J., The ultra-violet band spectrum of nitrogen. Astrophys. J. **68**, 257–278 (1928).
[84] Birkenbeil, H., Spectra of a carbon arc in the red spectral region. Z. Phys. 88, 1–13 (1934).

[85] Birtwistle, D. T., and Herzenberg, A., Vibrational excitation of N_2 by resonance scattering of electrons. J. Phys. B **4**, 53–70 (1971).

[86] Bleekrode, R., Intensity alternations in the second positive bands ($C^3\Pi_u$–$B^3\Pi_g$) of $^{14}N_2$ and $^{15}N_2$. Physica **41**, 24–26 (1969).

[87] Bloom, M., Oppenheim, I., Lipsicas, M., Wade, C. G., and Yarnell, C. F., Nuclear spin relaxation in gases and liquids. IV. Interpretation of experiments in gases. J. Chem. Phys. **43**, 1036–1047 (1965).

[88] Borst, W. L., and Zipf, E. C., Lifetimes of metastable CO and N_2 molecules. Phys. Rev. A **3**, 979–989 (1971).

[89] Bosomworth, D. R., and Gush, H. P., Collision-induced absorption of compressed gases in the far infrared. Can. J. Phys. **43**, 751–769 (1965).

[90] Boursey, E., and Roncin, J., Experimental deperturbation of the $b^1\Pi_u \leftarrow X^1\Sigma_g^+$ transition of N_2 in the solid state, pure and trapped in Ne and CF_4 matrices at low temperature. Phys. Rev. Lett. **26**, 308–11 (1971).

[91] Breene, R. G., Jr., Oscillator strengths in certain air molecule systems II. The N_2 first positive system. J. Quant. Spectrosc. Radiat. Transfer **11**, 169–173 (1971).

[92] Bridge, N. J., and Buckingham, A. D., Polarization of laser light scattered by gases. J. Chem. Phys. **40**, 2733–2734 (1964).

[93] Bridge, N. J., and Buckingham, A. D., The polarization of laser light scattered by gases. Proc. R. Soc. Lond. **A295**, 334–349 (1966).

[93a] Briggs, J. S., and Hayns, M. R., Molecular orbital calculations for close atomic collisions: The N_2 system. J. Phys. B **6**, 514–20 (1973).

[94] Briglia, D. D., Mass spectrometer studies of ionization processes in nitrogen. Scientific Report No. 1, Physics Department, University of California, Los Angeles, California (Jan. 1964).

[95] Brith, M., Ron, A., and Schnepp, O., Raman spectrum of α-N_2. J. Chem. Phys. **51**, 1318–1323 (1969).

[96] Brith, M., and Schnepp, O., The absorption spectra of solid CO and N_2. Mol. Phys. **9**, 473–489 (1965).

[97] Broadfoot, A. L., Resonance scattering by N_2^+. Planet. Space Sci. **15**, 1801–1815 (1967).

[98] Broadfoot, A. L., and Hunten, D. M., Excitation of N_2 band systems in aurora. Can. J. Phys. **42**, 1212–1230 (1964).

[99] Broadfoot, A. L., and Maran, S. P., Electronic transition moment for the N_2 Vegard-Kaplan bands. J. Chem. Phys. **51**, 678–681 (1969).

[100] Brömer, H. H., Fette, K., and Hirsch, J., The $D^2\Pi_g$–$A^2\Pi_u$ band system of N_2^+ in the "Pink Afterglow". Z. Naturforsch. **20a**, 643–646 (1965).

[101] Brolley, J. E., Porter, L. E., Sherman, R. H., Theobald, J. K., and Fong, J. C., Photoabsorption cross sections of H_2, D_2, N_2, O_2, Ar, Kr and Xe at the 584Å line of neutral helium. J. Geophys. Res. **78**, 1627–1632 (1973).

[102] Brons, H. H., Perturbations in the (9,8) $^2\Sigma$–$^2\Sigma$ N_2^+-band. Physica **1**, 739–744 (1934).

[103] Brons, H. H., On perturbations in the $^2\Sigma \rightarrow {}^2\Sigma$ bands of of N_2^+. Proc. K. Akad. Wet. Amsterdam **38**, 271–280 (1935).

[104] Brook, N., New studies of nitrogen afterglow. Sci. Rep. No. 2, Inst. of Geophys., University of California, Los Angeles, Calif. (1953).

[105] Brown, W. A., and Landshoff, R. K., The electronic transition moment of the N_2^+ first negative system. J. Quant. Spectrosc. Radiat. Transfer **11**, 1143–1145 (1971).

[106] Budó, A., On the triplet-band term formulas for the general intermediate case and their application to the $B^3\Pi$ and $C^3\Pi$ terms of the N_2 molecule. Z. Phys. **96**, 219–229 (1935).

[107] Bullock, L. E., and Hause, C. D., Molecular constants of the $B^3\Pi_g$ and $A^3\Sigma_u^+$ states of N_2. J. Mol. Spectrosc. **39**, 519–520 (1971).

[108] Buontempo, U., Cunsolo, S., and Jacucci, G., Far-infrared absorption in N_2—Air liquid mixtures. Mol. Phys. **21**, 381–383 (1971).

[109] Burns, D. J., Simpson F. R., and McConkey, J. W., Absolute cross sections for electron excitation of the second positive bands of nitrogen. J. Phys. B **2**, 52–64 (1969).

[110] Butcher, R. J., and Jones, W. J., Study of the rotational Raman spectra of $^{14}N^{15}N$ and $^{15}N_2$, using a Fabry-Perot etalon. J. Chem. Soc. Faraday Trans. II **70**, 560–563 (1974).

[111] Butcher, R. J., Willetts, D. V., and Jones, W. J., On the use of a Fabry-Perot etalon for the determination of rotational constants of simple molecules—the pure rotational Raman spectra of oxygen and nitrogen. Proc. R. Soc. Lond. **A234**, 231–245 (1971).

[112] Büttenbender, C., and Herzberg, G., On the structure of the second positive nitrogen group and the predissociation of the N_2 molecule. Ann. Phys. (Leipzig) (5) **21**, 577–610 (1934).

[113] Buxton, R. A. H., and Duley, W. W., Reflection spectrum of solid nitrogen in the vaccum ultraviolet. Phys. Rev. Lett. **25**, 801–803 (1970).

[114] Cade, P. E., Sales, K. D., and Wahl, A. C., Electronic structure of diatomic molecules. III. A. Hartree-Fock wavefunctions and energy quantities for N_2 ($X^1\Sigma_g^+$) and N_2^+ ($X^2\Sigma_g^+$, $A^2\Pi_u$, $B^2\Sigma_u^+$) molecular ions. J. Chem. Phys. **44**, 1973–2003 (1966).

[115] Cahill, J. E., and Leroi, G. E. Raman spectra of solid CO_2, N_2O, N_2 and CO. J. Chem. Phys. **51**, 1324–1332 (1969).

[116] Calo, J. M., and Axtmann, R. C., Vibrational relaxation and electronic quenching of the $C^3\Pi_u$ ($v'=1$) state of nitrogen. J. Chem. Phys. **54**, 1332–1341 (1971).

[117] Campbell, I. M., and Thrush, B. A., Some new vacuum ultra-violet emissions of active nitrogen. Trans. Faraday Soc. **65**, 32–40 (1968).

[118] Carbonneau, R., and Marmet, P., Autoionizing levels of N_2 converging to the $A^2\Pi_u$ and $B^2\Sigma_u^+$ limits. Int. J. Mass Spectrom. Ion Phys. **10**, 143–155 (1972/73).

[119] Carleton, N. P., and Oldenberg, O., Lifetime of the lowest excited level of N_2. J. Chem. Phys. **36**, 3640–3463 (1962).

[120] Carleton, N. P., and Papaliolios, C., Measured variation of the electronic transition moment of Vegard-Kaplan bands in N_2. J. Quant. Spectrosc. Radiat. Transfer **2**, 241–244 (1962).

[121] Carlson, T. A., Angular dependence of vibrational structure in the photoelectron spectra of N_2 and O_2. Chem. Phys. Lett. **9**, 23–26 (1971).

[122] Carlson, T. A., Moddeman, W. E., Pullen, B. P., and Krause, M. O., Identification of high energy lines in the K–LL Auger spectrum of N_2. Chem. Phys. Lett. **5**, 390–392 (1970).

[123] Carroll, P. K., Rotational structure of the (1, 0), (2, 1) and (3, 2) bands of the nitrogen first positive system. Proc. R. Irish Acad. **54A**, 369–397 (1952).

[124] Carroll, P. K., A new transition in molecular nitrogen. Can. J. Phys. **36**, 1585–1587 (1958).

[125] Carroll, P. K., The C–X system of N_2^+. Can. J. Phys. **37**, 880–889 (1959).

[126] Carroll, P. K., Note on the $^5\Sigma_g^+$ state of N_2. J. Chem. Phys. **37**, 805–809 (1962).

[127] Carroll, P. K., The spectrum of N_2 in the far ultraviolet. J. Quant. Spectrosc. Radiat. Transfer **2**, 417–419 (1962).

[128] Carroll, P. K., The structure of the Goldstein-Kaplan bands of N_2. Proc. R. Soc. (Lond.) **A272**, 270–283 (1963).

[129] Carroll, P. K., Band structures in N_2 Rydberg complexes. J. Chem. Phys. **58**, 3597–3604 (1973).

[130] Carroll, P. K., and Collins, C. P., High resolution absorption studies of the $b^1\Pi_u$–$X^1\Sigma_g^+$ system of nitrogen. Can. J. Phys. **47**, 563–589 (1969).

[131] Carroll, P. K., Collins, C. C., and Murnaghan, J. T., Rotational studies of the Gaydon-Herman (green) bands of N_2. J. Phys. B **5**, 1634–1654 (1972).

[132] Carroll, P. K., Collins, C. P., and Yoshino, K., The high energy $^1\Sigma_u^+$ states of N_2. J. Phys. B **3**, L127–L131 (1970).

[133] Carroll, P. K., and Doheny, A. P., The Herman-Kaplan system of N_2: High resolution studies. J. Mol. Spectrosc. **50**, 257–265 (1974).

[134] Carroll, P. K., and Hurley, A. C., Identification of an electronic transition of N_2^{2+}. J. Chem. Phys. **35**, 2247–2248 (1961).

[135] Carroll, P. K., and Mahon-Smith, D., Isotope shifts in some ultraviolet systems of N_2. J. Chem. Phys. **39**, 237–238 (1963).

[136] Carroll. P. K., and Mulliken, R. S., $^3\Pi$ levels and predissociations of N_2 near the 12.135 eV dissociation limit. J. Chem. Phys. **43**, 2170–2179 (1965).

[137] Carroll, P. K., and Rubalcava, H. E., Near infrared system of nitrogen. Nature (London) **184**, 119–120 (1959).

[138] Carroll, P. K., and Rubalcava, H. E., Rotational analysis of the 5–1 band of the B'–B system of N_2. Proc. Phys. Soc. (Lond). **76**, 337–345 (1960).

[139] Carroll, P. K., and Sayers, N. D., The band spectrum of nitrogen: New studies of the triplet systems. Proc. Phys. Soc. (Lond.) **64**, 1138–1144 (1953).

[140] Carroll, P. K., and Subbaram. K. V., Two new band systems in the ultraviolet spectrum of N_2. Can. J. Phys. **53**, 2198–2209 (1975).

[141] Carroll, P. K., and Yoshino, K., New Rydberg series of N_2. J. Chem. Phys. **47**, 3073–3074 (1967).

[142] Carroll, P. K., and Yoshino, K., The $c_n{}^1\Pi_u$ and $c_n{}'\ ^1\Sigma_u^+$ Rydberg states of N_2; high resolution studies. J. Phys. B **5**, 1614–1633 (1972).

[143] Carter, V. L., High-resolution N_2 absorption study from 730 to 980 Å. J. Chem. Phys. **56**, 4195–4205 (1972).

[144] Carter, V. L., and Berkowitz, J., Photoionization yields in N_2 in the band series from 734 to 796 Å. J. Chem. Phys. **59**, 4573–4577 (1973).

[145] Cartwright, D.C., Total cross sections for the excitation of the triplet states in molecular nitrogen. Phys. Rev. A **2**, 1331–1348 (1970).

[146] Cartwright, D. C., Transition probabilities for the Meinel band system of N_2^+. J. Chem. Phys. **58**, 178–185 (1973).

[147] Cartwright, D. C., and Dunning, T. H., Jr., Vibrational matrix elements of the quadrupole moment of N_2 ($X^1\Sigma_g^+$). J. Phys. B **7**, 1776–1781 (1974).

[148] Cartwright, D. C., and Dunning, T. H., Jr., New electronic states of N_2^+. J. Phys. B **8**, L100–L104 (1975).

[149] Cartwright, D. C., Trajmar, S., and Williams W., Vibrational population of the $A^3\Sigma_u^+$ and $B^3\Pi_g$ states of N_2 in normal auroras. J. Geophys. Res. **76**, 8368–8377 (1971).

[150] Cartwright, D. C., Trajmar, S., and Williams, W. Reply. J. Geophys. Res. **78**, 2365–2373 (1973). (See also papers cited therein.)

[151] Cartwright, D. C., Trajmar, S., Williams, W., and Huestis, D. L., Selection rules for $\Sigma^+ \longleftrightarrow \Sigma^-$ transitions in electron-molecule collisions. Phys. Rev. Lett. **27**, 704–707 (1971).

[152] Cermak, V., Detection of long-lived excited states of molecules by Penning ionization. J. Chem. Phys. **44**, 1318–1323 (1966).

[153] Cermak, V., Penning ionization electron spectroscopy. Spectroscopy of excited long-lived molecular states. Chem. Phys. Lett. **4**, 515–517 (1970).

[154] Cermak, V., and Herman, Z., On the existence of a $^4\Sigma$ excited state of N_2^+. Collect. Czech. Chem. Commun. **27**, 1493–1495 (1962).

[154a] Cermak, V., and Herman, Z., Mass spectrometric study of the formation of N_3^+ and C_2O^+ ions. Collect. Czech. Chem. Commun. **30**, 1343–1357 (1965).

[154b] Chakraborty, B., Pan, Y. K., and Chang, T. Y., On the Franck-Condon factor and band strength calculations with vibration-rotation interaction for Morse oscillators. J. Chem. Phys. **55**, 5147–8 (1971).

[155] Chan, S. I., Baker, M. R., and Ramsey, N. F., Molecular-beam magnetic-resonance studies of the nitrogen molecule. Phys. Rev. **136A**, 1224–1228 (1964).

[156] Chandraiah, G., and Shepherd, G. G., Intensity measurements in emission of 18 Vegard-Kaplan bands of N_2. Can. J. Phys. **46**, 221–226 (1968).

[157] Childs, W. H. J., Perturbations and rotation constants of some first negative nitrogen bands. Proc. R. Soc. (Lond.) **A137**, 641–661 (1932).

[158] Ching, B. K., Cook, G. R., and Becker, R. A., Oscillator strengths of the a, w, and C bands of N_2. J. Quant. Spectrosc. Radiat. Transfer **7**, 323–330 (1967).

[159] Chiu, Y. N., Electric-quadrupole and magnetic-dipole radiation in linear molecules. Applications to $^1\Pi$–$^3\Pi$ transitions. J. Chem. Phys. **42**, 2671–2681 (1965).

[160] Chutjian, A., Cartwright, D. C., and Trajmar, S., Excitation of the $W^3\Delta_u$, $w^1\Delta_u$, $B'^3\Sigma_u^-$, and $a'^1\Sigma_u^-$ states of N_2 by electron impact. Phys. Rev. Lett. **30**, 195–198 (1973).

[161] Clerc, M., and Lesigne, B., Absorption spectra of the CO_2^+ ($X^2\Pi_g$) and N_2^+ ($X^2\Sigma_g^+$) ions, in their ground state, produced by pulsed radiolysis of CO_2 and N_2. J. Chim. Phys. (Paris) **67**, 701–703 (1970).

[162] Codling, K., Structure in the photo-ionization continuum of N_2 near 500 Å. Astrophys. J. **143**, 552–558 (1966).

[163] Collin, J. E., and Natalis, P., Ionic states and photon impact-enhanced vibrational excitation in diatomic molecules by photoelectron spectroscopy. Photoelectron spectra of N_2, CO, and O_2. Int. J. Mass Spectrom. Ion Phys. **2**, 231–245 (1969).

[164] Comer, J., and Harrison, M., Observation of the effects of rotational transitions in the resonant scattering of electrons from N_2. J. Phys. B **6**, L70–L72 (1973).

[165] Comer, J., and Read, F. H., Electron impact studies of a resonant state of N_2^-. J. Phys. B **4**, 1055–1062 (1971).

[166] Comes, F. J., and Speier, F., Luminescence of diatomic molecular ions. I. Franck-Condon factors and collision deactivation. Z. Naturforsch. **26a**, 1998–2007 (1971).

[167] Cook, G. R., and McNeal, R. J., Photoionization of vibrationally excited nitrogen. J. Chem. Phys. **56**, 1388–1399 (1972).

[168] Cook, G. R., and Metzger, P. H., Photoionization and absorption cross sections of O_2 and N_2 in the 600 to 1000 Å region. J. Chem. Phys. **41**, 321–336 (1964).

[169] Cook, G. R., and Ogawa, M., Photoionization of N_2 in the 734–805 Å region. Can. J. Phys. **43**, 256–267 (1965).

[170] Cook, G. R., and Ogawa, M., Oscillator strengths of the Hopfield absorption series of N_2. J. Chem. Phys. **53**, 1292–1293 (1970).

[171] Cook, G. R., Ogawa, M., and Carlson, R. W., Photodissociation continuums of N_2 and O_2. J. Geophys. Res. **78**, 1663–1667 (1973).

[172] Cooper, D. M., Spectral intensity measurements from high-pressure nitrogen plasmas. J. Quant. Spectrosc. Radiat. Transfer **12**, 1175–1189 (1972).

[173] Coster, D., and Brons, H. H., On several "tail bands" of the negative nitrogen group. Z. Phys. **70**, 492–497 (1931).

[174] Coster, D., and Brons, H. H., The negative nitrogen bands. Z. Phys. **73**, 747–774 (1932).

[175] Coster, D., Brons, F., and van der Ziel, A., The so called second positive nitrogen spectrum. Z. Phys. **84**, 304–334 (1933).

[176] Coster, D., van Dijk, E. W., and Lameris, A. J., Predissociation in the upper level of the second positive group of nitrogen. Physica **2**, 267–272 (1935).

[177] Coughran, W, Rose, J., Shibuya, T., and McKoy, V., Equations of motion method: Potential energy curves for N_2, CO, and C_2H_4. J. Chem. Phys. **58**, 2699–2709 (1973).

[178] Courtois, D., and Jouve, P., Electric field induced infrared spectrum of nitrogen. Vibrational polarizability matrix elements. J. Mol. Spectrosc. **55**, 18–27 (1975).

[179] Courtois, D., Thiebeaux, C., and Jouve, P., Infrared absorption of the nitrogen molecule induced by an electric field. C. R. Acad. Sci. (Paris) **274B**, 744–746 (1972).

[180] Covey, R., Saum, K. A., and Benesch, W., Transition probabilities for the $W^3\Delta_u$–$B^3\Pi_g$ system of molecular nitrogen. J. Opt. Soc. Amer. **63**, 592–596 (1973).

[181] Cramarossa, F., and Ferraro, G., Evaluation of the rotational temperature of $N_2^+(B^2\Sigma_u^+)$ in an r.f. discharge at moderate pressure in nitrogen: A comparison of methods. J. Quant. Spectrosc. Radiat. Transfer **14**, 159–163 (1974).

[182] Cramarossa, F., Ferraro, G., and Molinari, E., Spectroscopic diagnostics of r.f. discharges at moderate pressure and chemical applications. I. Pure nitrogen. J. Quant. Spectrosc. Radiat. Transfer **14**, 419–436 (1974).

[183] Crawford, F. H., and Tsai, P. M., New bands of the ionized nitrogen molecule. Proc. Amer. Acad. Arts. Sci. **69**, 407–437 (1935).

[184] Crawford, M. F., Welsh, H. L., and Harrold, J. H., Rotational wings of Raman bands and free rotation in liquid oxygen, nitrogen and methane. Can. J. Phys. **30**, 81–98 (1952).

[185] Crawford, M. F., Welsh, H. L., and Locke, J. L., Infrared absorption of oxygen and nitrogen induced by intermolecular forces. Phys. Rev. **75**, 1607 (1949).

[186] Cress, M. C., Becker, P. M., and Lampe, F. W., Pulsed mass-spectrometric study of the bimolecular formation of N_3^+. J. Chem. Phys. **44**, 2212–2213 (1966).

[187] Crosswhite, H. M., Zipf, E. C., Jr., and Fastie, W. G., Far-ultraviolet auroral spectra. J. Opt. Soc. Amer. **52**, 643–648 (1962).

[188] Cunio, R. E., and Jansson, R. E. W., The electronic transition moment of the N_2 first positive system. J. Quant. Spectrosc. Radiat. Transfer **8**, 1763–1771 (1968).

[189] Dalby, F. W., and Douglas, A. E., Laboratory observation of the $A\,^2\Pi$–$X\,^2\Sigma$ bands of the N_2^+ molecule. Phys. Rev. **84**, 843 (1951).

[190] Davidson, G., and O'Neil, R., Optical radiation from nitrogen and air at high pressure excited by energetic electrons. J. Chem. Phys. **41**, 3946–3955 (1964).

[191] de la Vega, J. R., and Hameka, H. F., Calculation of magnetic susceptibilities of diatomic molecules. VIII. Anisotropies and rotational magnetic moments. J. Chem. Phys. **47**, 1834–1836 (1967).

[192] De Santis, D, Lurio, A., Miller, T. A., and Freund, R. S., Radiofrequency spectrum of metastable $N_2(A^3\Sigma_u^+)$: II. Fine structure, magnetic hyperfine structure, and electric quadupole constants in the lowest 13 vibrational levels. J. Chem. Phys. **58**, 4625–4665. (1973).

[193] Desesquelles, J., Dufay, M., and Poulizac, M. C., Lifetime measurement of molecular states with an accelerated ion beam. Phys. Lett. **27A**, 96–97 (1968).

[194] Deslandres, H., On the band spectra of nitrogen. C. R. Acad. Sci. (Paris) **134**, 747–750 (1902).

[195] Deslandres, H., and d'Azambuja, L., A law relating to the structure of band spectra and the perturbations of their arithmetical series. C. R. Acad. Sci. (Paris) **157**, 671–678 (1913).

[196] Dieke, G. H., and Heath, D. F., The first and second positive bands of N_2. Johns Hopkins Spectroscopic Report No. 17, Department of Physcs, The Johns Hopkins University, Baltimore (1959).

[197] Dieke, G. H., and Heath, D. F., Structure of the infrared Y bands of N_2. J. Chem. Phys. **33**, 432–436 (1960).

[198] d'Incan, J., Contribution a l'etude du spectre de la molecule d'azote ionizee N_2^+. Thesis, Universite de Lyon, (1959).

[199] d'Incan, J., and Topouzkhanian, A., A new band system of N_2^+ excited from impact by hydrogen ions on a nitrogen target. Z. Naturforsch. **29a**, 1377–1378 (1974).

[200] d'Incan, J., and Topouzkhanian, A., High resolution analysis of collision-induced N_2^+ spectrum. J. Chem. Phys. **63**, 2683–2689 (1975).

[201] Ditchburn, R. W., Bradley, J. E. S., Cannon, C. G., and Munday, G., Absorption cross-sections for Lyman α and neighboring lines., p. 327–34 in Rocket Exploration of the Upper Atmosphere, R. L. F. Boyd, M. J. Seaton, and H. S. W. Massey (eds.) (Interscience, Lond., 1954).

[202] Dorman, F. H., and Morrison, J. D., Ionization potentials of doubly charged oxygen and nitrogen. J. Chem. Phys. **39**, 1906–1907 (1963).

[203] Dotchin, L. W., Chupp, E. L., and Pegg, D. J., Radiative lifetimes and pressure dependence of the relaxation rates of some vibronic levels in N_2^+, N_2, CO^+, and CO. J. Chem. Phys. **59**, 3960–3967 (1973).

[204] Douglas, A. E., The near ultraviolet bands of N_2^+ and the dissociation energies of the N_2^+ and N_2 molecules. Can. J. Phys. **30**, 302–313 (1952).

[205] Douglas, A. E., Analysis of the $^2\Pi$–$^2\Sigma$ bands of the N_2^+ molecule. Astrophys. J. **117**, 380–386 (1953).

[206] Douglas, A. E., and Herzberg, G., Predissociation and dissociation of the N_2 molecule. Can. J. Phys. **29**, 294–300 (1951).

[207] Douglas, A. E., and Jones, W. J., The 2700 Å bands of the N_3 molecule. Can. J. Phys. **43**, 2216–2221 (1965).

[208] Dressler, K., Absorption spectrum of vibrationally excited N_2 in active nitrogen. J. Chem. Phys. **30**, 1621–1622 (1959).

[209] Dressler, K., Absorption spectroscopy of condensed gases at low temperatures. J. Quant. Spectrosc. Radiat. Transfer **2**, 683–688 (1962).

[210] Dressler, K., The lowest valence and Rydberg states in the dipole-allowed absorption spectrum of nitrogen. A survey of their interactions. Can. J. Phys. **47**, 547–561 (1969).

[211] Dressler, K., Matrix isolation spectroscopy. Mem. Soc. R. Sci. (Liege) Ser. 5 **20**, 357–374 (1970).

[212] Dressler, K., and Lutz, B. L., Optical identification of the 12.28 eV quadrupole transition in molecular nitrogen. Phys. Rev. Lett. **19**, 1219–1221 (1967).

[213] Dufayard, J., Negre, J. M., and Nedelec, O., Perturbation effects on lifetimes in N_2^+. J. Chem. Phys. **61**, 3614–3618 (1974).

[214] Duncan, A. B. F., Theory of Rydberg terms of the nitrogen molecule. J. Chem. Phys. **42**, 2453–2457 (1965).
[215] Duncan, A. B. F., and Damiani, A., Calculations on $\pi_u np$ Rydberg terms of the nitrogen molecule. J. Chem. Phys. **45**, 1245–1250 (1966).
[216] Duncan, D. C., The excitation of the spectra of nitrogen by electron impacts. Astrophys. J. **62**, 145–167 (1925).
[217] Edqvist, O., Lindholm, E., Selin, L. E., and Åsbrink, L., The photoelectron spectra of O_2, N_2, and CO. Phys. Lett. **31A**, 292–293 (1970).
[218] Ehrhardt, H., and Willmann, K., Angular dependence of resonance scattering of low-energy electrons in N_2. Z. Phys. **204**, 462–473 (1967).
[219] Eliezer, I., and Moualem, A., Stabilization calculations on a N_2^- resonance. J. Chem. Phys. **58**, 1147–1148 (1973).
[220] El-Sherbini, T. M., and van der Wiel, M. J., Ionization of N_2 and CO by 10 keV electrons as a function of the energy loss. I. Valence electrons. II. Inner-shell electrons. Physica **59**, 433–452, 453–462 (1972).
[221] Fano, U., Effects of configuration interaction on intensities and phase shifts. Phys. Rev. **124**, 1866–1878 (1961).
[222] Fassbender, M., Studies on the negative nitrogen band spectrum. Z. Phys. **30**, 73–92 (1924).
[223] Feast, M. W., Rotational analysis of the (1, 0) band of the N_2 first positive system. Proc. Phys. Soc. (Lond.) **63**, 568–574 (1950).
[224] Fedorova, N. I., Determining the relative populations of vibrational levels and rotational temperature of the system of bands $A^2\Pi - X^2\Sigma$ of N_2^+. Aurorae and Airglow, V. I. Krasovskiy (ed.) Report (NASA TTF-204) p. 140–166 (1964).
[225] Fenner, W. R., Hyatt, H. A., Kellam, J. M., and Porto, S. P. S., Raman cross section of some simple gases. J. Opt. Soc. Amer. **63**, 73–77 (1973).
[226] Fink, E., and Welge, K. H., Lifetime of the electronic states $N_2(C^3\Pi_u)$, $N_2^+(B^2\Sigma_u^+)$, $NH(A^3\Pi)$, $NH(c^1\Pi)$, PH ($^3\Pi$). Z. Naturforsch. **19a**, 1193–1201 (1964).
[227] Fishburne, E. S., Lazdinis, S. S., and Seibert, G. L., The N_2 second positive system excited by impact with a metastable argon atom. J. Mol. Spectrosc. **23**, 100–103 (1967).
[228] Fiutak, J., and Van Kranendonk, J., Impact theory of Raman line broadening. Can. J. Phys. **40**, 1085–1100 (1962).
[229] Fiutak, J., and Van Kranendonk, J., Theory of the impact broadening of Raman lines due to anisotropic intermolecular forces. Can. J. Phys. **41**, 21–32 (1963).
[230] Fournier, P. G., Govers, T. R., Van de Runstraat, C. A., Schopman, J., and Los, J., Translational spectroscopy of the unimolecular dissociation $N_2^+ \rightarrow N^+ + N$. J. Phys. (Paris) **33**, 755–759 (1972).
[231] Fournier, P., Ozenne, J. B., and Durup, J., Vibrational structure of predissociating molecular states: Velocity spectrum of N^+ fragments from fast N_2^+ ions. J. Chem. Phys. **53**, 4095–4096 (1970).
[232] Fournier, P., Pernot, A., and Durup, J. Collisions of N_2^+ ions on noble gas atoms. I. Collision induced dissociation of N_2^+. J. Phys. (Paris) **32**, 533–541 (1971).
[233] Fournier, P., Van de Runstraat, C. A., Govers, T. R., Schopman, J., de Heer, F. J., and Los, J., Collision-induced dissociation of 10 keV N_2^+ ions: evidence for predissociation of the $C^2\Sigma_u^+$ state. Chem. Phys. Lett. **9**, 426–428 (1971)
[234] Fowler, A., and Strutt, R. J., spectroscopic investigations in connection with the active modification of nitrogen. I. Spectrum of the afterglow. Proc. R. Soc. (Lond.) **85**, 377–388 (1911).
[235] Fowler, R. G., Basic research on optical properties. Air Force Weapons Lab., Air Force Systems Command, Kirtland Air Force Base, New Mexico. (Tech. Rep. AFWL-TR-70-112) (1971).
[236] Fowler, R. G., and Holzberlein, T. M., Transition probabilities for H_2, D_2, N_2, N_2^+, and CO. J. Chem. Phys. **45**, 1123–1125 (1966).
[237] Frackowiak, M., Predissociation in $C^3\Pi_u$ state of $^{15}N_2$. Bull. Acad. Polon. Sci., Ser. Sci., Math, Astron., Phys. **12**, 361–367 (1964).
[238] Freund, R. S., Molecular-beam measurements of the emission spectrum and radiative lifetime of N_2 in the metastable $E^3\Sigma_g^+$ state. J. Chem. Phys. **50**, 3734–3740 (1969).
[239] Freund, R. S., Electron-impact excitation functions for metastable states of N_2. J. Chem. Phys. **51**, 1979–1982 (1969).
[240] Freund, R. S., Radiative lifetime of $N_2(a^1\Pi_g)$ and the formation of metastable $N_2(a'^1\Sigma_u^-)$. J. Chem. Phys. **56**, 4344–4351 (1972).
[241] Freund, R. S., Miller, T. A., De Santis, D., and Lurio, A Radio-frequency spectrum of metastable $N_2(A^3\Sigma_u^+)$. I. Magnetic hyperfine and electric quadrupole constants. J. Chem. Phys. **53**, 2290–2303 (1970).
[242] Frost, D. C., McDowell, C. A., and Vroom, D. A., Photoelectron kinetic energy analysis in gases by means of a spherical analyzer. Proc. R. Soc. (Lond.) **A296**, 566–579 (1967).
[243] Gardner, J. L., and Samson, J. A. R., 304 Å photoelectron spectra of CO, N_2, O_2 and CO_2. J. Electron Spectrosc. Related Phenom. **2**, 259–266 (1973).
[244] Gardner, J. L., and Samson, J. A. R., Photoelectron spectroscopy of N_2 and CO with dispersed Ne I radiation. Chem., Phys. Lett. **26**, 240–242 (1974).
[245] Gardner, J. L., and Samson, J. A. R., Experimental vibrational intensity distributions for continuum photoionization to the $X^2\Sigma^+$, $A^2\Pi$, and $B^2\Sigma^+$ states of CO^+ and N_2^+. J. Chem. Phys. **60**, 3711–3712 (1974).
[246] Garstang, R. H., Forbidden transitions in excitation by electron impact. J. Chem. Phys. **44**, 1308–1309 (1966).
[247] Gaydon, A. G., A new band spectrum associated with nitrogen. Nature (Lond.) **151**, 167–168 (1943).
[248] Gaydon, A. G., The band spectrum of N_2: Weak system in the visible region. Proc. Phys. Soc. (Lond.) **56**, 85–95 (1944).
[249] Gaydon, A. G., The band spectrum of nitrogen: New singlet systems. Proc. R. Soc. (Lond.) **A182**, 286–301 (1944).
[250] Gaydon, A. G., and Herman, R., Band systems in the spectrum of nitrogen. Proc. Phys. Soc. (Lond.) **58**, 292–296 (1946).
[251] Gaydon, A. G., and Worley, R. E., Singlet terms in the spectrum of molecular nitrogen. Nature (Lond.) **153**, 747 (1944).
[252] Gebbie, H. A., Stone, N. W. B., and Williams, D., An interferometric study of the far infrared spectum of compressed nitrogen. Mol. Phys. **6**, 215–217 (1963).
[253] Geiger, J., and Schröder, B., Intensity perturbations due to configuration interaction observed in the electron energy-loss spectrum of N_2. J. Chem. Phys. **50**, 7–11 (1969).
[254] Geiger, J., and Stickel, W., Energy losses of fast electrons in nitrogen. J. Chem. Phys. **43**, 4535–4536 (1965).
[255] Generosa, J. I., Harris, R. A., and Sullo, L. R., Franck-Condon factors for various air species. Air Force Weapons Lab., Air Force Systems Command, Kirtland Air Force Base, New Mexico. (Tech. Rep. AFWL-TR-70-108) (1971).

[256] Gerö, L., and Schmid, R., On the interpretation of perturbations in nitrogen bands. Z. Phys. **116**, 246–248 (1940).

[257] Gerö, L., and Schmid, R., Rotational analysis of fourth positive bands of the N_2 molecule. Z. Phys. **116**, 598–603 (1940).

[258] Gilmore, F. R., Potential energy curves for N_2, NO, O_2, and corresponding ions. J. Quant. Spectrosc. Radiat. Transfer **5**, 369–390 (1965).

[259] Girardeau-Montaut, J. P., Ultraviolet molecular nitrogen lasers. Nouv. Rev. Opt. **5**, 367–377 (1974).

[260] Goddard, W. A., Huestis, D. L., Cartwright, D. C., and Trajmar, S., Group theoretical selection rules for electron-impact spectroscopy. Chem. Phys. Lett. 11, 329–333 (1971).

[261] Golde, M. F., and Thrush, B. A., Vacuum ultraviolet emission by active nitrogen. I. The formation and removal of $N_2(a^1\Pi_g)$. II. The excitation of singlet and triplet states of carbon monoxide by active nitrogen. III. The absolute rates of population of $N_2(a^1\Pi_g)$ and $CO(A^1\Pi)$. IV. The kinetic behavior of $N_2(B'^3\Sigma_u^-)$. Proc. R. Soc. (Lond.) **A330**, 79–130 (1972).

[262] Golden, D. E., Burns, D. J., and Sutcliffe, V. C., Jr., Role of resonances in the electron-impact excitation functions of the $C^3\Pi_u$ and $E^3\Sigma_g^+$ states of N_2. Phys. Rev. **A10**, 2123–2130 (1974).

[263] Goldstein, E., On electric discharge phenomena and their spectra. Z. Phys. **6**, 14–17 (1905).

[264] Gombas, P., The bonding of the nitrogen molecule as given by the statistical theory. Z. Phys. **152**, 397–401 (1958),

[265] Gombas, P., Statistical treatment of the N_2 molecule. Acta. Phys. Acad. Sci. (Hung.) **9**, 461–469 (1959).

[266] Govers, T. R., Fehsenfeld, F. C., Albritton, D. L., Fournier, P. G., and Fournier, J., Molecular isotope effects in the thermal-energy charge exchange between He^+ and N_2. Chem. Phys. Lett. **26**, 134–137 (1974).

[267] Govers, T. R., van de Runstraat, C. A., and de Heer, F. J., Isotope effects in the predissociation of the $C^2\Sigma_u^+$ state of N_2^+. J. Phys. B **6**, L73–L75 (1973).

[268] Grandmontagne, R., d'Incan, J., and Janin, J., Band intensities of the $D^2\Pi_g$–$A^2\Pi_u$ system of the N_2^+ molecule. J. Phys. Radium 20, 59S–60S (1959).

[269] Grandmontagne, R., and Eido, R., Potential curve of the $B^2\Sigma_u^+$ state of the molecule N_2^+. C. R. Acad. Sci. (Paris) **249**, 306–308 (1959).

[270] Grandmontagne, R., Jorus, A. M., and Vincent, F., Theoretical calculation of band intensities for the first negative system of nitrogen. J. Phys. (Paris) **31**, 749–753 (1970).

[271] Gray, D., Morack, J. L., and Roberts, T.D., Radiative lifetime of the $A^2\Pi_u$ ($v'=2$) level of N_2^+. Phys. Lett. **37A**, 25–26 (1971).

[272] Gray, D. D., Roberts, T. D., and Morack, J. L., Measured lifetimes of some $A^2\Pi_u$ vibrational levels of N_2^+ molecules. J. Chem. Phys. **57**, 4190–4193 (1972).

[273] Grün, A. E., The Gaydon bands of N_2. Z. Naturforsch. **9a**, 1017–1019 (1954).

[274] Guerin-Bartholin, F., Theoretical evaluation of the potential energy distribution of the electronic state $D^2\Pi_g$ of the N_2^+ ion. C. R. Acad. Sci. (Paris) **B262**, 693–695 (1966).

[275] Guerin, F., Valence states $^2\Pi$ and $^2\Delta$ of isoelectronic molecules N_2^+, CN, and CO^+. Theor. Chim. Acta **17**, 97–108 (1970).

[276] Guntsch, A., On the structure of the second positive nitrogen group. Z. Phys. **86**, 262–273 (1933).

[277] Haensel, R., Koch, E. E., Kosuch, N., Nielsen, U., and Skibowski, M. Vacuum ultraviolet reflectivity of solid nitrogen and oxygen. Chem. Phys. Lett. **9**, 548–550 (1971).

[278] Halevi, P., An improved formula for the vibrational transition probabilities of diatomic molecules. Proc. Phys. Soc. (Lond.) **86**, 1051–1054 (1965).

[279] Hall, R. I., Mazeau, J., Reinhardt, J., and Schermann, C., Electron impact threshold excitation of N_2 by the trapped-electron method. J. Phys. B **3**, 991–998 (1970).

[280] Halmann, M., and Laulicht, F., Isotope effects on vibrational transition probabilities. II. Electronic transitions of isotopic nitrogen, nitric oxide and oxygen molecules. J. Chem. Phys. **43**, 438–448 (1965).

[281] Halmann, M., and Laulicht, I., Isotope effects on vibrational transition probabilities. III. Ionization of isotopic H_2, N_2, O_2, NO, CO, and HCl molecules. J. Chem. Phys. **43**, 1503–1509 (1965).

[282] Halmann, M., and Laulicht, I., Isotope effects on Franck-Condon factors. V. Electronic transitions of isotopic O_2, N_2, C_2, and H_2 molecules. J. Chem. Phys. **44**, 2398–2405 (1966).

[283] Halmann, M., and Laulicht, I., Isotope effects on Franck-Condon factors. VII. Vibrational intensity distribution in the H_2 Lyman, H_2 Werner, O_2 Schuman-Runge, N_2 first positive, N_2 Vegard-Kaplan, and LiH (A–X) system based on RKR potentials. J. Chem. Phys. **46**, 2684–2689 (1967); Supplementary tables (unpublished).

[284] Hamada, H., Bands at 4450 and 4180 Å in the spectra of the night sky and of the aurora. Nature (Lond.) **134**, 851 (1934).

[285] Hamada, H., On the energy of metastable nitrogen molecules. Phil. Mag. **23**, 25–33 (1937).

[286] Hartfuss, H. J., and Schmillen, A., Decay of the first positive group of N_2 and the Asundi bands of CO. Z. Naturforsch. **23a**, 722–726 (1968).

[287] Hazi, A. U., and Rice, S. A., Use of model potentials in the study of molecular Rydberg states. J. Chem. Phys. **48**, 495–502 (1968).

[288] Heastie, R., and Martin, D. H., Collision-induced absorption of sub-millimeter radiation by non-polar atmospheric gases. Can. J. Phys. **40**, 122–127 (1962).

[289] Heath, D. F., New data on the emission spectrum of air. Los Alamos Scientific Lab. of the University of California (Los Alamos Spectroscopic Report LA–2335) (Jan. 1959).

[290] Head, C. E., Radiative lifetimes of the $B^2\Sigma_u^+$ $v'=0$ and $v'=1$ levels of N_2^+. Phys. Lett. **34A**, 92–93 (1971).

[291] Hébert, C. R., and Nicholls, R. W., Franck-Condon factors for the $v'=0$ progression of the N_2 fourth positive band system. J. Phys. B **2**, 626–627 (1969).

[292] Heideman, H. G. M., Kuyatt, C. E., and Chamberlain, G. E., Resonances in the elastic and inelastic electron scattering from N_2. J. Chem. Phys. **44**, 355–358 (1966).

[293] Hepner, G., and Herman, L., Spectra of nitrogen from 0.9μ to 2.6μ. Ann. Geophys. (Paris) **13**, 242–248 (1957).

[294] Herman, R., A new forbidden transition of the neutral nitrogen molecule. C. R. Acad. Sci. (Paris) **217**, 141–143 (1943).

[295] Herman, R., Contribution to the study of the spectra of the nitrogen molecule. Ann. Phys. (Paris) (11) **20**, 241–291 (1945).

[296] Herman, R., Extension of the A–X band system of the nitrogen molecule. C. R. Acad. Sci. (Paris) **222**, 1226–1227 (1946).

[297] Herman, R., A new forbidden transition of the N_2 molecule. C. R. Acad. Sci. (Paris) **233**, 738 (1951).

[298] Herman, R., and Gaydon, A. G., Band systems of the neutral nitrogen molecule. J. Phys. Radium (8) **7**, 121–123 (1946).

[299] Herman, R., and Herman, L., Extension of the Lyman-Birge-Hopfield system of the nitrogen molecule. Ann. Astrophys. **5**, 71–81 (1942).

[300] Herman, R., and Herman, L., Spectra of nitrogen in an atmosphere of xenon. J. Phys. Radium (8) **7**, 203–208 (1946).

[301] Herman, R., and Weniger, C., Excitation of high rotational levels of the first positive system $B^3\Pi_g$–$A^3\Sigma_u^+$ of N_2. C. R. Acad. Sci. (Paris) **234**, 928–930 (1952).

[302] Herzberg, G., Structure of the negative nitrogen bands. Ann. Phys. (Leipzig) **86**, 189–213 (1928).

[303] Herzberg, G., The nitrogen isotope of mass 15. Z. Phys. Chem. **B9**, 43 (1930).

[304] Herzberg, G., Predissociation and related phenomena. Ergeb. Exakten Naturwiss. **10**, 207–284 (1931).

[305] Herzberg, G., On the electronic structure of the nitrogen molecule. Phys. Rev. **69**, 362–365 (1946).

[306] Herzberg, G., and Herzberg, L., Production of nitrogen atoms in the upper atmosphere. Nature (Lond.) **161**, 283 (1948).

[307] Herzenberg. A., Oscillator energy dependence of resonant electron-molecule scattering. J. Phys. B **1**, 548–558 (1968).

[308] Herzfeld, C. M., and Broida, H. P., Interpretation of spectra of atoms and molecules in solid nitrogen condensed at 4.2° K. Phys. Rev. **101**, 606–611 (1956).

[309] Hesser, J. E., Absolute transition probabilities in ultraviolet molecular spectra. J. Chem. Phys. **48**, 2518–2535 (1968).

[310] Hesser, J. E., and Dressler, K., Radiative lifetimes of ultraviolet molecular transitions. J. Chem. Phys. **45**, 3149–3150 (1966).

[311] Heurlinger, T., Atomic oscillations and molecular spectra. Z. Phys. **1**, 82–91 (1920).

[312] Hicks, P. J., Comer, J., and Read, F. H., Autoionizing transitions in N_2 and H_2 produced by electron impact. J. Phys. B **6**, L65–L69 (1973).

[313] Ho, W., Kaufman, I. A., and Thaddeus, P., Pressure-induced microwave absorption in N_2. J. Chem. Phys. **49**, 3627–3631 (1968).

[314] Holland, R. F., Excitation of nitrogen by electrons: The Lyman-Birge-Hopfield system of N_2. J. Chem. Phys. **51**, 3940–3950 (1969).

[315] Holland, R. F., and Maier, W. B., II., Production of light by collisions of 2.5 −490 eV He^+ with N_2: N_1, N_2^+ second negative, and unresolved emissions between 1200 and 3200 Å. J. Chem. Phys. **55**, 1299–1314 (1971).

[316] Holland, R. F., and Maier, W. B., II, Study of the $A \rightarrow X$ transitions in N_2^+ and CO^+. J. Chem. Phys. **56**, 5229–5246 (1972); Erratum, **58**, 2672–2673 (1973).

[317] Holland, R. F., and Maier, W. B., II, Emission from long-lived states of N_2^+. A new interpretation of $N_2^+ + N_2 \rightarrow N_3^+ + N$. J. Chem. Phys. **57**, 4497–4498 (1972).

[318] Hollstein, M., Lorents, D. C., Peterson, J. R., and Sheridan, J. R., Time of flight measurement of N_2 and N_2^+ lifetimes. Can. J. Chem. **47**, 1858–1861 (1969).

[319] Hopfield, J. J., New spectra in nitrogen. Phys. Rev. **36**, 789–90 (1930).

[320] Hori, T., and Endo, Y., Predissociation in the second positive nitrogen group. Proc. Phys. Math. Soc. Japan **23**, 834–842 (1941).

[321] Huber, L. M., and Thorson, W. R., $X^1\Sigma_g^+$–$A^3\Sigma_u^+$ excitation energy in N_2. J. Chem. Phys. **41**, 1829–1832 (1964).

[322] Hudson, R. D., and Carter, V. L., Predissociation in N_2 and O_2. Can. J. Chem. **47**, 1840–1845 (1969); Atmospheric implications of predissociation in N_2. J. Geophys Res.: Space Phys. **74**, 393–395 (1969).

[323] Huffman, R. E., Absorption cross-sections of atmospheric gases for use in aeronomy. Can. J. Chem. **47**, 1823–1834 (1969).

[324] Huffman, R. E., Larrabee. J. C., and Tanaka, Y., Absorption spectrum of activated nitrogen in the 600–1100 Å region. J. Chem. Phys. **45**, 3205–3213 (1966).

[325] Huffman, R. E., Tanaka, Y., and Larrabee, J. C., Fluorescence and pre-ionization in nitrogen excited by vacuum ultraviolet radiation. J. Chem. Phys. **38**, 1920–1926 (1963).

[326] Huffman, R. E., Tanaka, Y., and Larrabee, J. C., Absorption coefficients of nitrogen in the 1000–580 Å wavelength region. J. Chem. Phys. **39**, 910–925 (1963).

[327] Hulthen, E., and Johansson, G., Study of the second positive nitrogen spectrum. Measurement of bands 3536, 3755, 3805. Z. Phys. **26**, 308–322 (1924).

[328] Hurley, A. C., Potential energy curves for doubly positive diatomic ions. Part II. Predicted states and transitions of N_2^{2+}, O_2^{2+} and NO_2^{2+} [NO^{2+}]. J. Mol. Spectrosc. **9**, 18–29 (1962).

[329] Hurley, A. C., and Maslen, V. W., Potential curves for doubly positive diatomic ions. J. Chem. Phys. **34**, 1919–1925 (1961).

[330] Hyatt, H. A., Cherlow, J. M., Fenner, W. R., and Porto, S. P. S., Cross section for the Raman effect in molecular nitrogen gas. J. Opt. Soc. Amer. **63**, 1604–1606 (1973).

[331] Imhof, R. E., and Read, F. H., Measured lifetimes of the $C^3\Pi_u$ state of N_2 and the $a^3\Sigma_g^+$ state of H_2. J. Phys. B **4**, 1063–1069 (1971).

[332] Inn, E. C. Y., Charge transfer between He^+ and N_2. Planet. Space Sci. **15**, 19–25 (1967).

[333] Ittmann, G. P., Theory of perturbations in band spectra. Z. Phys. **71**, 616–626 (1931).

[334] Jain, D. C., Potential energy curves of some electronic states of the N_2 molecule. Proc. Phys. Soc. (Lond.) **83**, 17–21 (1964).

[335] Jain, D. C., Transition moment variation in the first and second positive band systems of N_2. J. Quant. Spectrosc. Radiat. Transfer **12**, 759–762 (1972).

[336] Jain, D. C., and Sahni, R. C., Einstein A coefficients, oscillator strengths, and absolute band strengths for the first negative system, and Franck-Condon factors for the second negative system of N_2^+. Int. J. Quantum Chem. **1**, 721–729 (1967).

[337] Jain, D. C., and Sahni, R. C., Variation of electronic transition moment in some band systems of the N_2 molecule. J. Quant. Spectrosc. Radiat. Transfer **7**, 475–482 (1967).

[338] Jain, D. C., and Sahni, R. C., Transition probabilities for the ionization of N_2, O_2, NO, and CO molecules. Int. J. Quantum Chem. **2**, 325–332 (1968).

[339] James, T. C., The analysis of intensity data in diatomic molecules. A criticism of the r-centroid approach. J. Mol. Spectrosc. **20**, 77–87 (1966).

[340] Jammu, K. S., St. John, G. E., and Welsh, H. L., Pressure broadening of the rotational Raman lines of some simple gases. Can. J. Phys. **44**, 797–814 (1966).

[341] Janin, J., New band spectra of nitrogen. Cah. Phys. **3** (16), 73–74 (1943).

[342] Janin, J., Study of emission spectra of nitrogen. C. R. Acad. Sci. (Paris) **217**, 392–393 (1943).

[343] Janin, J., New band system of the nitrogen molecule. C. R. Acad. Sci. (Paris) **220**, 218–220 (1945).

[344] Janin, J., Spectroscopic study of the luminescence from the silent discharge in nitrogen. Ann. Phys. (Paris) (12) **1**, 538–606 (1946).

[345] Janin, J., Identification of some transitions in the molecular spectrum of nitrogen. C. R. Acad. Sci. (Paris) **223**, 321–322 (1946).

[346] Janin, J., Certain singlet systems of the nitrogen molecule. J. Rech. Cent. Natl. Rech. Sci. **3** (12), 156–163 (1950).

[347] Janin, J., and Crozet, A., Excitation of the nitrogen spectrum by an electric discharge through ammonia gas. C. R. Acad. Sci. (Paris) **223**, 1114–1115 (1946).

[348] Janin, J., and d'Incan, J., Observation of a new band system of the nitrogen ion molecule. C. R. Acad. Sci. (Paris) **246**, 3436–3439 (1958).

[349] Janin, J., and d'Incan, J., Analysis of bands of a new system attributed to the molecule N_2^+. Revue Universelle des Mines **15** (5), 1–4 (1959).

[350] Janin, J, d'Incan, J., and Marchand, J., State $A^2\Pi_u$ and perturbations in the system $B^2\Sigma_u^+$–$X^2\Sigma_g^+$ of N_2^+. Ann. Univ. Lyon: Sci. B No. 12, 29–42 (1959).

[351] Janin, J., d'Incan, J., and Roux, A., Analysis of bands of higher vibrational quantum numbers belonging to the negative nitrogen system. Ann. Univ. Lyon: Sci. B No. 10, 7–48 (1957).

[352] Janin, J., d'Incan, J., Stringat, R., and Magnaval, J., New analysis of the system $D^2\Pi_g$–$A^2\Pi_u$ of the N_2^+ molecule. Rev. Opt. **42**, 120–128 (1963).

[353] Janin, J., and Eyraud, I., Red degraded bands of the negative system of nitrogen. J. Phys. Radium **15**, 88S–90S (1954).

[354] Jansson, R. E. W., Relative transition probabilities for the $B^3\Pi$–$A^3\Sigma$ system of nitrogen. Proc. Phys. Soc. (Lond.) **87**, 851–854 (1966).

[355] Jansson, R. E. W., and Cunio, B. E., Application of Halevi's correction to the Einstein coefficients of the N_2 first positive system (N_2 1PG). J. Quant. Spectrosc. Radiat. Transfer **8**, 1747–1762 (1968).

[356] Jeunehomme, M., Oscillator strengths of the first negative and second positive systems of nitrogen. J. Chem. Phys. **44**, 2672–2677 (1966).

[357] Jeunehomme, M., Transition moment of the first positive band system of nitrogen. J. Chem. Phys. **45**, 1805–1811 (1966).

[358] Jeunehomme, M., and Duncan, A. B. F., Lifetime measurements of some excited states of nitrogen, nitric oxide and formaldehyde. J. Chem. Phys. **41**, 1692–1699 (1964).

[359] Jeunehomme, M., and Schwenker, R. P., Focused laser-beam experiment and the oscillator strength of the Swan system. J. Chem. Phys. **42**, 2406–2408 (1965).

[360] Johns, J. W. C., and Lepard, D. W., Calculation of rotation-electronic energies and relative transition intensities in diatomic molecules. J. Mol. Spectrosc. **55**, 374–406 (1975).

[361] Johnson, A. W., Measured lifetimes of electronic, vibrational and rotational levels of the nitrogen molecule. Ph. D. Thesis, Department of Physics, University of Oklahoma (1968).

[362] Johnson, A. W., and Fowler, R. G., Measured lifetimes of rotational and vibrational levels of electronic states of N_2. J. Chem. Phys. **53**, 65–72 (1970).

363] Jones, W. J., On the use of a Fabry-Perot interferometer for the study of Raman spectra of gases under high resolution. Contemp. Phys. **13**, 419–439 (1972).

[364] Jorus-Bony, A. M., Vincent, F., and Grandmontagne, R., Franck-Condon factors and r-centroids for the vibration bands of the first negative system of the N_2^+ molecule determined at high quantum numbers. C. R. Acad. Sci. (Paris) **B270**, 491–493 (1970).

[365] Joshi, K. C., Potential energy curves for the $C^2\Sigma_u^+$ and $X^2\Sigma_g^+$ states of N_2^+. J. Quant. Spectrosc. Radiat. Transfer **6**, 211–213 (1966).

[366] Joshi, K. C., The spectrum of the C–X system of N_2^+. Proc. Phys. Soc. (Lond.) **87**, 285–292 (1966).

[367] Joshi, K. C., The $C^2\Sigma_u^+$–$X^2\Sigma_g^+$ system of $^{15}N_2^+$. Proc. Phys. Soc. (Lond.) **87**, 561–568 (1966).

[368] Joyez, G., Hall, R. I., Reinhardt, J., and Mazeau, J., Low energy electron spectroscopy of N_2 in the 11.8–13.8 eV energy range. J. Electron Spectrosc. Relat. Phenom. **2**, 183–190 (1973).

[369] Judge, D. L., and Weissler, G. L., Fluorescence spectra of the excited ion N_2^+ resulting from vacuum-ultraviolet photon impact on N_2. J. Chem. Phys. **48**, 4590–4596 (1968).

[370] Kaplan, J., Repulsive energy levels in band spectra. Phys. Rev. **37**, 1406–1411 (1931).

[371] Kaplan, J., Forced predissociation in nitrogen. Phys. Rev. **38**, 373–374 (1931).

[372] Kaplan, J., Products of dissociation in nitrogen. Phys. Rev. **42**, 97–100 (1932).

[373] Kaplan, J., New band system in nitrogen. Phys. Rev. **45**, 675–677, 898–899 (1934).

[374] Kaplan, J., New bands in nitrogen. Phys. Rev. **46**, 534, 631 (1934).

[375] Kaplan, J., Light of the night sky. Phys. Rev. **47**, 193 (1935).

[376] Kaplan, J., A new system of nitrogen bands. Phys. Rev. **47**, 259 (1935).

[377] Kaplan, J., A new afterglow spectrum in nitrogen. Phys. Rev. **48**, 800–801 (1935).

[378] Kaslin, V. M., and Petrash, G. G., Rotational structure of ultraviolet generation of molecular nitrogen. JETP Lett. **3**, 55–57 (1966).

[379] Kasuya, T., and Lide, D. R., Jr., Measurements on the molecular nitrogen pulsed laser. Appl. Opt. **6**, 69–80 (1967).

[380] Kaufman, F., and Kelso, J. R., Vibrationally excited ground-state nitrogen in active nitrogen. J. Chem. Phys. **28**, 510–511 (1958).

[381] Keck, J. C., Allen, R. A., and Taylor, R. L., Electronic transition moments for air molecules. J. Quant. Spectrosc. Radiat. Transfer **3**, 335–353 (1963).

[382] Kenty, C., Evidence for a long-lived metastable state of N_2 at about 8 eV. J. Chem. Phys. **35**, 2267–2268 (1961); **37**, 1567–1568 (1962).

[383] Kenty, C., New evidence for the importance of $N_2(^3\Delta_u)$ in discharge and afterglows in N_2 plus a rare gas. J. Chem. Phys. **41**, 3996–3997 (1964); Erratum, **42**, 4062 (1965).

[384] Ketelaar, J. A. A., and Rettschnick, R. P. H., The quadrupole moment of nitrogen deduced from the pressure-induced rotational spectrum of nitrogen. Mol. Phys. **7**, 191–193 (1963).

[385] Khvostikov, I. A., and Megrelishvili, T. G., New bands and lines in the twilight sky spectrum. Nature (Lond.) **183**, 811 (1959).

386] Kiselyovskii, L. I., and Shimanovich, V. D., Experimental determination of the matrix elements of the electronic transition dipole moment in the first negative band system of the N_2^+ molecule using an arc filament in an axial-vortex air flow. Opt. Spectrosc. (USSR) **24**, 266–269 (1968).

[387] Kistiakowsky, G. B., and Warneck, P., Lewis-Rayleigh nitrogen afterglow. J. Chem. Phys. **27**, 1417–1418 (1957).

[388] Klose, J. Z., The mean life of the $v'=0$ level of the $B^2\Sigma_u^-$ state in N_2^+. (Unpublished manuscript, 1972).

[389] Klynning, L., On the 6895.5 Å and 8937 Å bands of N_2. Spectrosc. Lett. **6**, 291–2 (1973).

[390] Klynning, L., and Pages, P., On the first negative system of N_2^+. Phys. Scripta **6**, 195–199 (1972).

[391] Koppe, V. T., Koval, A. G., Gritsyna, V. V., and Fogel, Y. M., Dependence of the electronic transition moment R_e upon the internuclear spacing r for the Meinel band system of the N_2^+ ion. Opt. Spectrosc. (USSR) **24**, 440–441 (1968).

[392] Kotani, M., A formal theory of Rydberg series of molecules. Molecular Orbitals in Chemistry, Physics and Biology, P.O. Lowdin and B. Pullman (eds.) (Academic Press, New York, 1964). pp. 539–545.

[393] Kovacs, I., On the anomalous splitting of the multiplet Σ states in diatomic molecules. Acta Phys. (Budapest) **15**, 1–10, 337–340 (1962–3).

[394] Kovacs, I., On an intercombination transition of the N_2 molecule. Opt. Spectrosc. (USSR) **28**, 239–240 (1970).

[395] Krauss, M., and Mies, F. H., Molecular-orbital calculation of the shape resonance in N_2^-. Phys. Rev. **A1**, 1592–1598 (1970).

[396] Krauss, M., and Neumann, D., Valence resonance states of N_2^-. J. Res. Natl. Bur. Stand. (U.S.) **77A**, 411–412 (1973).

[397] Krupenie, P. H., and Benesch, W., Electronic transition moment integrals for first ionization of CO and the A–X transition in CO^+. Some limitations on the use of the r-centroid approximation. J. Res. Natl. Bur. Stand. (U.S.) **72A**, 495–503 (1968).

[398] Kupriyanova, E. B., Kolesnikov, V. N., and Sobolev, N. N., Electronic band strengths of the first positive system of nitrogen and of the Meinel system of N_2^+ II. J. Quant. Spectrosc. Radiat. Transfer **9**, 1025–1032 (1969).

[399] Kurzweg, L., Egbert, G. T., and Burns, D. J., Lifetime of the $D^3\Sigma_u^+$ state of N_2. J. Chem. Phys. **59**, 2641–2645 (1973).

[400] Lassettre, E. N., Inelastic scattering of high energy electrons by atmospheric gases. Can. J. Chem. **47**, 1733–1774 (1969).

[401] Lassettre, E. N., Skerbele, A., and Meyer, V. D., Quadrupole-allowed transitions in the electron-impact spectrum of N_2. J. Chem. Phys. **45**, 3214–3226 (1966).

[402] LaVilla, R. E., K α emission spectrum of gaseous N_2. J. Chem. Phys. **56**, 2345–2349 (1972).

[403] Lawrence, G. M., Quenching and radiation rates of CO($a^3\Pi$). Chem. Phys. Lett. **9**, 575–577 (1971).

[404] Lawrence, G. M., Mickey, D. L., and Dressler, K., Absolute oscillator strengths of the strongest bands within the dipole-allowed absorption spectrum of nitrogen. J. Chem, Phys. **48**, 1989–1994 (1968).

[405] Laws, E. A., Stevens, R. M., and Lipscomb, W. N., Magnetic properties of AlH and N_2 from coupled Hartree-Fock theory. J. Chem. Phys. **54**, 4269–4278 (1971).

[406] Lazdinis, S. S., and Carpenter, R. F., Perturbations in electron beam induced spectra of the first negative system of N_2^+. J. Chem. Phys. **59**, 5203–5204 (1973).

[407] LeBlanc, F., Tanaka, Y., and Jursa, A., New band system, in the afterglow of nitrogen. J. Chem. Phys. **28**, 979–981 (1958).

[408] Ledbetter, J. W., Jr., New Rydberg bands in the visible region and identification of the lowest $^1\Sigma_g^+$ Rydberg state of the N_2 molecule. J. Mol. Spectrosc. **42**, 100–111 (1972).

[409] Lee, L. C., Carlson, R. W., Judge, D. L., and Ogawa, M., The absorption cross sections of N_2, O_2, CO, NO, CO_2, N_2O, CH_4, C_2H_4, C_2H_6, and C_4H_{10} from 180 to 700 Å. J. Quant. Spectrosc. Radiat. Transfer **13**, 1023–1031 (1973).

[410] Lee, L. C., Carlson, R. W., Judge, D. L., and Ogawa, M., Vacuum ultraviolet fluorescence from photodissociation fragments of O_2 and N_2. J. Chem, Phys. **61**, 3261–3269 (1974).

[411] Lee, L. C., and Judge, D. L., The electronic transition moment of the N_2^+ ($B^2\Sigma_u^+ \rightarrow X^2\Sigma_g^+$) system. J. Phys. B **6**, L121–L123 (1973).

[412] Lefebver-Brion, H., Theoretical study of homogeneous perturbations. II. Least-squares fitting method to obtain "deperturbed" crossing Morse curves. Application to the perturbed $^1\Sigma_u^+$ states of N_2. Can. J. Phys. **47**, 541–545 (1969).

[413] Lefebvre-Brion, H., and Moser, C. M., Calculation of Rydberg levels in the nitrogen molecule. J. Chem. Phys. **43**, 1394–1399 (1965).

[414] Leoni, M. W., Nuclear dynamics in coupled electronic states of the N_2 molecule. Dr. Sci. Thesis, Eidgenossische Technische Hochschule. (Zurich, 1972).

[415] Leoni, M., and Dressler, K., Predissociation probabilities and determination of a repulsive potential in the N_2 molecule. Z. Angew. Math. Phys. **22**, 794–797 (1971).

[416] Leoni, M., and Dressler, K., Deperturbation of the Worley-Jenkins Rydberg series. Helv. Phys. Acta **45**, 959–961 (1972).

[417] Lichten, W., Lifetime measurements of metastable states in molecular nitrogen. J. Chem. Phys. **26**, 306–313 (1957).

[418] Lindau, P., Structure of the second positive group of nitrogen bands. Z. Phys. **25**, 247–252 (1924); **26**, 343–370 (1924); **30**, 187–199 (1924).

[419] Lindholm, E., Rydberg series in small molecules. I–V. Arkiv Fys. **40**, 97–131 (1969).

[420] Liu, I. D., The vibrational numbering of the $A^2\Pi$–$X^2\Sigma$ bands of N_2^+. Astrophys. J. **129**, 516–517 (1959).

[421] Lofthus, A., Emission band spectra of nitrogen. The Lyman-Birge-Hopfield system. Can. J. Phys. **34**, 780–789 (1956).

[422] Lofthus, A., Emission band spectra of nitrogen. The fifth positive system. J. Chem. Phys. **25**, 494–497 (1956).

[423] Lofthus, A., Emission band spectra of nitrogen. A study of some singlet systems. Can. J. Phys. **35**, 216–234 (1957).

[424] Lofthus, A., A new predissociation in nitrogen. Nature (Lond.) **186**, 302–303 (1960).

[425] Lofthus, A., and Mulliken, R. S., Emission band spectra of nitrogen. Kaplan's first and second systems. J. Chem. Phys. **26**, 1010–1017 (1957).

[426] Long, C. A., Henderson, G., and Ewing, G. E., The infrared spectrum of the $(N_2)_2$ van der Waals molecule. Chem Phys. **2**, 485–489 (1973).

[427] Lorquet, J. C., and Desouter, M., Excited states of gaseous ions. Transitions to and predissociation of the $C^2\Sigma_u^+$ state of N_2^+. Chem. Phys. Lett. **16**, 136–140 (1972).

[428] Lorquet, A. J., and Lorquet, J. C., Isotopic effects in accidental predissociation. The case of the $C^2\Sigma_u^+$ state of N_2^+. Chem. Phys. Lett. **26**, 138–143 (1974).

[429] Lutz, B. L., Pressure-induced $a''\,^1\Sigma_g^+$–$X\,^1\Sigma_g^+$ absorption in the vacuum ultraviolet spectrum of molecular nitrogen. J. Chem. Phys. **51**, 706–716 (1969).

[430] Lyman, T., The spectra of some gases in the Schumann region. Astrophys. J. **33**, 98–107 (1911).

[431] Mahon-Smith, D., and Carroll, P. K., Isotope shifts and the vibrational structure in some weaker systems of N_2. J. Chem. Phys. **41**, 1377–1382 (1964).

[432] Maier, W. B., II., Reactions between isotopically labeled N_2^+ and N_2 for primary ion energies below 45 eV. J. Chem. Phys. **61**, 3459–3470 (1974).

[433] Maier, W. B., II, and Holland, R. F., Emission from metastable states in a nitrogen ion beam. J. Chem. Phys. **52**, 2997–3001 (1970).

[434] Maier, W. B., II, and Holland, R. F., Spectrum of emission from long-lived states in a nitrogen ion beam. J. Chem. Phys. **55**, 2602–2603 (1971).

[435] Maier, W. B., II, and Holland, R. F., A study of visible and near ultraviolet radiation from long-lived states of N_2^+. Bull. Amer. Phys. Soc. **17** (5), 695–696 (1972).

[436] Maier, W. B., II., and Holland, R. F., Visible and near ultraviolet light produced by the radiative decay of long-lived states in a nitrogen ion beam. J. Chem. Phys. **59**, 4501–4534 (1973).

[436a] Marchetti, M. A., and La Paglia, S. R., Theoretical $^1\Sigma_g^+$–$^1\Sigma_u^+$ dipole strengths of some homonuclear diatomic molecules: Configuration interaction. J. Chem Phys. **48**, 434–9 (1968).

[437] Massone, C. A., Garavaglia, M., and Gallardo, M., New IR lines in a N_2 pulsed discharge. IEEE J. Quantum Electron. **5**, 553–554 (1969).

[438] Massone, C. A., Garavaglia, M., Gallardo, M., Calatroni, J. A. E., and Tagliaferri, A. A., Investigation of a pulsed molecular nitrogen laser at low temperature. Appl. Opt. **11**, 1317–1328 (1972).

[439] Mathai, P. M., and Allin, E. J., Low frequency Raman spectra of α-$^{16}O_2$, α-$^{18}O_2$, and α-N_2. Can. J. Phys. **49**, 1973–1975 (1971).

[440] Mathias, L. E. S., and Parker, J. T., Stimulated emission in the band spectrum of nitrogen. Appl. Phys. Lett. **3**, 16–18 (1963).

[441] May, A. D., Stryland, J. C., and Varghese, G., Collisional narrowing of the vibrational Raman band of nitrogen and carbon monoxide. Can. J. Phys. **48**, 2331–2335 (1970).

[442] Mazeau, J., Gresteau, F., Hall, R. I., Joyez, G., and Reinhardt, J., Electron impact excitation of N_2. I. Resonant phenomena associated with the $A^3\Sigma_u^+$ and $B^3\Pi_g$ valence states. J. Phys. B **6**, 862–872 (1973).

[443] Mazeau, J., Hall, R. I., Joyez, G., Landau, M., and Reinhardt, J., Electron excitation of N_2. II. Resonant phenomena associated with Rydberg states. J. Phys. B **6**, 873–880 (1973).

[444] McConkey, J. W., Woolsey, J. M., and Burns, D. J., Absolute cross section for electron impact excitation of 3914 Å N_2^+. Planet. Space Sci. **19**, 1192 (1971).

[445] McEwen, D. J., Intensity measurements of the Lyman-Birge-Hopfield system of nitrogen. Ph. D. Thesis, The University of Western Ontario, London, Canada (1965).

[446] McEwen, D. J., and Nicholls, R. W., Intensity distribution of the Lyman-Birge-Hopfield system of N_2. Nature (Lond.) **209**, 902 (1966).

[447] McFarlane, R. A., Observation of a $^1\Pi$–$^1\Sigma^-$ transition in the N_2 molecule. Phys. Rev. **140A**, 1070–1071 (1965).

[448] McFarlane, R. A., Precision spectroscopy of new infrared emission systems of molecular nitrogen. IEEE J. Quantum Electron. **2**, 229–232 (1966).

[449] McFarlane, R. A., Measurements on the $w^1\Delta_u$–$a^1\Pi_g$ transition in molecular nitrogen. Phys. Rev. **146**, 37–39 (1966).

[450] McFarlane, R. A., Stimulated-emission spectroscopy of some diatomic molecules. Physics of Quantum Electronics. P. L. Kelly, B. Lax, and P. E. Tannenwald (eds) (McGraw Hill, New York, 1966) p. 655 62

[451] Mecke, R., and Lindau, P., On the second positive group of nitrogen bands. Z. Phys. **25**, 277–278 (1924).

[452] Meinel, A. B., A new band system of N_2^+ in the infrared auroral spectrum. Astrophys. J. **112**, 562–563 (1950).

[453] Meinel, A. B., New bands of N_2^+ in the auroral infrared spectra. C. R. Acad. Sci. (Paris) **231**, 1049–1050 (1950).

[454] Meinel, A. B., The auroral spectrum from 6200 to 8900 Å. Astrophys. J. **113**, 583–588 (1951).

[455] Meinel, A. B., The analysis of auroral emission bands from the $A^2\Pi$ state of N_2^+. Astrophys. J. **114**, 431–437 (1951).

[456] Merton, T. R., and Pilley, J. G., On an extension of the negative band spectrum of nitrogen. Phil. Mag. **50**, 195–199 (1925).

[457] Meyer, J. A., Klosterboer, D. H., and Setser, D. W., Energy transfer reactions of $N_2(A^3\Sigma_u^+)$. IV. Measurements of the radiative lifetime and study of the interactions with olefins and other molecules. J. Chem. Phys. **55**, 2084–91 (1971).

[457a] Meyer, V. D., and Lassettre, E. N., Weak transitions in excitation of N_2 by electron impact and comparison with excitation by absorption of radiation. J. Chem. Phys. **44**, 2535–6 (1966).

[458] Michels, H. H., Identification of two low-lying non-Rydberg states of the nitrogen molecule. J. Chem. Phys. **53**, 841–842 (1970).

[459] Michels, H. H., Unpublished potential curves for N_2 valence states. (1971).

[460] Miller, C. E., A note on the Raman spectra of nitrogen. J. Chem. Phys. **6**, 902–904 (1938).

[461] Miller, K. J., and Green, A. E. S., Energy levels and potential energy curves for H_2, N_2 and O_2 with an independent particle model. J. Chem. Phys. **60**, 2617–2626 (1974).

[462] Miller, R. E., High-resolution emission Vegard-Kaplan bands of nitrogen. J. Chem. Phys. **43**, 1695–1701 (1965).

[463] Miller, R. E., The absolute energy of the $A^3\Sigma_u^+$ state of nitrogen. J. Mol. Spectrosc. **19**, 185–187 (1966).

[464] Miller, R. E., High-resolution emission Lyman-Birge-Hopfield bands of nitrogen. J. Opt. Soc. Amer. **60**, 171–176 (1970).

[465] Miller, R. E., Rotational line intensities in $^3\Sigma^+$–$^1\Sigma^+$ electronic transitions. Phys. Rev. **A1**, 590–594 (1970).

[466] Miller, R. E., Fastie, W. G., and Isler, R. C., Rocket studies of far-ultraviolet radiation in an aurora. J. Geophys. Res.: Space Phys. **73**, 3353–3365 (1968).

[467] Millet, P., Salermo, Y., Brunet, H., Galy, J., Blanc, D., and Teyssier, J. L. De-excitation of $N_2(C^3\Pi_u; v'=0$ and 1) levels in mixtures of oxygen and nitrogen. J. Chem. Phys. **58**, 5839–5841 (1973).

[468] Moddeman, W. E., Carlson, T. A., Krause, M. O., and Pullen, B. P., Determination of the *K-LL* Auger spectra of N_2, O_2, CO, NO, H_2O, and CO_2. J. Chem. Phys. **55**, 2317–2336 (1971).

[469] Mohamed, K. A., and Khanna, B. N., Franck-Condon factors and *r*-centroids for the $H^3\Phi_u$–$G^3\Delta_g$ (Gaydon-Herman) green band system of N_2. Indian J. Pure Appl. Phys. **12**, 77–78 (1974).

[470] Moore, G. E., and Hansen, H. H., Direct observation of the thermal dissociation of molecular nitrogen. J. Chem. Phys. **54**, 399–404 (1971).

[471] Mulliken, R. S., The interpretation of band spectra. Rev. Mod. Phys. **2**, 60–115 (1930); **2**, 506–508 (1930); **3**, 89–155 (1931); **4**, 1–86 (1932).

[471a] Mulliken, R. S., Hopfield's Rydberg series and the ionization potential and heat of dissociation of N_2. Phys. Rev. **46**, 144–6 (1934).

[472] Mulliken, R. S., Intensities of electronic transitions in molecular spectra. J. Chem. Phys. **7**, 14–20 (1939).

[473] Mulliken, R. S. The energy levels of the nitrogen molecule. The threshold of space, M. Zelikoff (ed.) (Pergamon Press, New York, 1957). p. 169–79.

[474] Mulliken, R. S., Some neglected subcases of predissociation in diatomic molecules. J. Chem. Phys. **33**, 247–252 (1960).

[475] Mulliken, R. S., Low-energy $^5\Sigma_g^+$ states of the nitrogen molecule. J. Chem. Phys. **37**, 809–813 (1962).

[476] Mulliken, R. S., The Rydberg states of molecules. Parts I–VI. J. Amer. Chem. Soc. **86**, 3183–3197 (1964); **88**, 1849–1861 (1966).

[477] Mulliken, R. S., The bonding characteristics of diatomic MO's. Quantum Theory of Atoms, Molecules and the Solid State, P. O. Lowdin (ed.) (Acad. Press, New York, 1966). pp. 231–241.

[478] Mulliken, R. S., The nitrogen molecule correlation diagram. Chem. Phys. Lett. **14**, 137–140 (1972).

[479] Mulliken, R. S., Rydberg and valence-shell character as functions of internuclear distance in some excited states of CH, NH, H_2 and N_2. Chem. Phys. Lett. **14**, 141–144 (1972).

[480] Mulliken, R. S., Molecular orbitals of nitrogen at small internuclear distances. Int. J. Quantum Chem. **8**, 817–821 (1974).

[481] Nakamura, M., et al., Absorption structure near the K edge of the nitrogen molecule. Phys. Rev. **178**, 80–82 (1969).

[482] Namioka, T., Yoshino, K., and Tanaka, Y., Isotope bands and vibration assignment of the $D^2\Pi_g - A^2\Pi_u$ system of N_2^+. J. Chem. Phys. **39**, 2629–2633 (1963).

[483] Natalis, P., Delwiche, J., and Collin, J. E., Enhancement of vibrational level population of N_2^+ and CO^+ by photoelectron spectrometry. Chem. Phys. Lett. **13**, 491–495 (1972).

[484] Naudé, S. M., Quantum analysis of the rotational structure of the first positive bands of nitrogen. Proc. R. Soc. (Lond.) **136**, 114–144 (1932).

[485] Nelson, L. Y., Saunders, A. W., Jr., Harvey, A. B., and Neely, G. O., Detection of vibrationally excited homonuclear diatomic molecules by Raman spectroscopy. J. Chem. Phys. **55**, 5127–5128 (1971).

[486] Nesbet, R. K., Approximate Hartree-Fock calculations on small molecules. Adv. Quantum Chem. **3**, P. O. Lowdin (ed.) (Acad. Press, New York, 1967). p. 1–24.

[487] Newton, A. S., and Sciamanna, A. F., Metastable peaks in the mass spectrum of N_2 and NO. J. Chem. Phys. **50**, 4868–4877 (1969).

[488] Nicholls, R. W., Franck-Condon factors to high vibrational quantum numbers. I. N_2 and N_2^+. J. Res. Natl. Bur. Stand. (U.S.) **65A**, 451–460 (1961).

[489] Nicholls, R. W., Franck-Condon factors and r-centroids to high quantum numbers for bands of the $^2\Pi_g - A^2\Pi_u$ system of N_2^+. Can. J. Phys. **40**, 523–527 (1962).

[490] Nicholls, R. W., Laboratory astrophysics. J. Quant. Spectrosc. Radiat. Transfer **2**, 433–439 (1962).

[491] Nicholls, R. W., Franck-Condon factors for the Gaydon-Green band system of N_2. J. Chem. Phys. **42**, 804–805 (1965).

[492] Nicholls, R. W., Aeronomically important transition probability data. Can. J. Chem. **47**, 1847–1856 (1969).

[493] Nichols, L. L., and Wilson, W. E., Optical lifetime measurements using a positive ion van de Graff accelerator. Appl. Opt. **7**, 167–170 (1968).

[494] Noxon, J. F., Active nitrogen at high pressure. J. Chem. Phys. **36**, 926–940 (1962).

[495] Ogawa, M., Vibrational isotope shifts of absorption bands of N_2 in the spectral region 720–830 Å. Can. J. Phys. **42**, 1087–1096 (1964).

[496] Ogawa, M., and Cairns, R. B., The absorption of hydrogen Lyman gamma radiation by molecular nitrogen. Planet. Space Sci. **12**, 656–657 (1964).

497] Ogawa, M., and Tanaka, Y., New emission bands of N_2 in the vacuum ultraviolet region. J. Chem. Phys. **30**, 1354–1355 (1959).

[498] Ogawa, M., and Tanaka, Y., New emission bands of forbidden systems of nitrogen in the vacuum ultraviolet region. J. Chem. Phys. **32**, 754–758 (1964).

[499] Ogawa, M., and Tanaka, Y., Rydberg absorption series of N_2. Can. J. Phys. **40**, 1593–1607 (1962).

[500] Ogawa, M., Tanaka, Y., and Jursa, A. S., Isotope shift of the nitrogen absorption bands in the vacuum ultraviolet region. Can. J. Phys. **42**, 1716–1729 (1964).

[501] Ogawa, M., Tanaka, Y., and Jursa, A. S., Absorption spectrum of electrically excited nitrogen molecules in the vacuum-uv region. J. Chem. Phys. **41**, 3351–3356 (1964).

[502] Ogawa, M., Tanaka, Y., and Yoshino, K., Rydberg absorption series of N_2, $A^2\Pi_u \leftarrow X^1\Sigma_g$. (Draft, 1974). (See Note Added in Proof).

[503] Okuda, M., and Jonathan, N., Forbidden bands in the photoelectron spectra of diatomic molecules. J. Electron Spectrosc. Relat. Phenom. **3**, 19–25 (1974).

[504] Oldenberg, O., A theory of the auroral afterglow of nitrogen. Air Force Cambridge Research Laboratories, L. G. Hanscom Field, Bedford, Massachusetts. Report AFCRL-67-0252 (1967).

[505] Oldenberg, O., Mechanism of the short-duration nitrogen afterglow. J. Opt. Soc. Amer. **61**, 1092–1098 (1971).

[506] Oldenberg, O., Reversal of relative intensities of band systems of nitrogen. J. Opt. Soc. Amer. **61**, 1098–1100 (1971).

[507] Olmsted, J., III, Excitation of nitrogen triplet states by electron impact. Radiat. Res. **31**, 191–200 (1967).

[508] Olmsted, J., III, Newton, A. S., and Street, K., Jr., Determination of the excitation functions for formation of metastable states of some rare gases and diatomic molecules by electron impact. J. Chem. Phys. **42**, 2321–2327 (1965).

[509] Omholt, A., Spectroscopy and excitation. Ann. Geophys. (Paris) **24**, 1–12 (1968).

[510] O'Neil, R., and Davidson, G., The fluorescence of air and nitrogen excited by energetic electrons. Copies available from National Technical Information Service, Springfield Va. 22151. (AD 673995, Report issued Jan. 1968; period covered, Mar. 1964–Feb. 1967).

[511] Öpik, U., and Thomas, T. H., An application of the Pariser-Parr approximation to the nitrogen molecule. Mol. Phys. **10**, 289–296 (1966).

[512] Ortenberg, F. S., and Antropov, E. T., Probability of electron-vibrational transitions in diatomic molecules. Sov. Phys.-Usp. **9**, 717–742 (1967).

[513] Oxholm, M. L., and Williams, D., Infrared absorption by homonuclear diatomic molecules. Phys. Rev. **76**, 151–152 (1949).

[514] Pankhurst, R. C., Note on the second positive band system of nitrogen. Proc. Phys. Soc. (Lond.) **52**, 388–389 (1940).

[515] Pannetier, G., Marsigny, L., and Guenebaut, H., Second positive system of nitrogen in reactions of atomic nitrogen with aliphatic amines. Assignment of a newly-identified band as (5,5). C. R. Acad. Sci. (Paris) **252**, 1753–1755 (1961).

[516] Parker, A. E., Zeeman effect for perturbed N_2^+ terms. Phys. Rev. **44**, 84–89 (1933).

[517] Parker, A. E., Rotational analysis of the perturbed (13,15) $^2\Sigma$–$^2\Sigma$ N_2^+ band. Phys. Rev. **44**, 90–91 (1933).

[518] Parker, A. E., Further analysis of the N_2^+ bands. Phys. Rev. **44**, 914–918 (1933).

[519] Parks, J. H., Rao, D. R., and Javan, A., A high-resolution study of the $C^3\Pi_u$–$B^3\Pi_g$ (0,0) stimulated transitions in N_2. Appl. Phys. Lett. **13**, 142–144 (1968).

[520] Pavlovic, Z., Boness, M. J. W., Herzenberg, A, and Schulz, G. J. Vibrational excitation in N_2 by electron impact in the 15–35 eV region. Phys. Rev. **6A**, 676–685 (1972).

[521] Peck, E. R., and Khanna, B. N., Dispersion of nitrogen. J. Opt. Soc. Amer. **56**, 1059–1063 (1966).

[522] Pendleton, W. R., and O'Neil, R. R., Departure of $N_2^+(B^2\Sigma_u^+, v'=2$ and 3) vibrational populations from Franck-Condon predictions in the case of energetic e-N_2 ($X^1\Sigma_g^+$, $v=0$) collisions. J. Chem. Phys. **56**, 6260–6262 (1972).

[523] Penney, C. M., St. Peters, R. L., and Lapp, M., Absolute rotational Raman cross sections for N_2, O_2, and CO_2. J. Opt. Soc. Amer. **64**, 712–716 (1974).

[524] Peterson, J. R., and Moseley, J. T., Time-of-flight determination of lifetimes of N_2^+ ($A^2\Pi_u$)—the Meinel band system. J. Chem. Phys. **58**, 172–177 (1973).

[525] Petrie, W., and Small, R., The auroral spectrum in the wavelength range 3300–8900 Å. Astrophys. J. **116**, 433–441 (1952).

[526] Phillips, L. F., The lifetime of the $A^3\Sigma_u^+$ state of N_2. Can. J. Chem. **43**, 369–374 (1965).

[527] Pilling, M. J., Bass, A. M., and Braun, W., A curve of growth determination of the *f*-values for the Fourth Positive system of CO and the Lyman-Birge-Hopfield system of N_2. J. Quant. Spectrosc. Radiat. Tranfer **11**, 1593–1604 (1971).

[528] Pillow, M. E., and Smallwood, S. E. F., Intensity ratios in a v'' progression of the second positive system of N_2. Proc. Phys. Soc. (Lond.) **80**, 560 (1962).

[529] Pinter, F., Dependence of the width of the rotational Raman lines of N_2 and CO_2 on the quantum number j. Opt. Spectrosc. (USSR) **17**, 428–429 (1964).

[530] Pleiter, D., Spectral observations on a radio-frequency excited nitrogen jet. Can. J. Phys. **41**, 1245–1251 (1963).

[531] Poetker, A. H., The infrared radiation of nitrogen. Phys. Rev. **30**, 812–824 (1927).

[532] Polak, L. S., Slovetskii, D. L., and Sokolov, A. S., Predissociation and quenching probabilities for the vibrational levels of the $B^3\Pi_g$ state of molecular nitrogen. Opt. Spectrosc. (USSR) **32**, 247–251 (1972).

[533] Poll, J. D., Determination of the quadrupole moment of N_2 from induced absorption in the far infrared. Phys. Lett. **7**, 32–33 (1963).

[534] Poll, J. D., and Van Kranendonk, J., Theory of translational absorption in gases. Can. J. Phys. **39**, 189–204 (1961).

[535] Popkie, H. E., and Henneker, W. H., Theoretical electronic transition probabilities in diatomic molecules II. 13-electron sequence. J. Chem. Phys. **55**, 617–628 (1971).

[536] Potts, A. W., and Williams, T. A., The observation of "forbidden" transitions in He II photoelectron spectra. J. Electron Spectrosc. Relat. Phenom. **3**, 3–17 (1974).

[537] Raich, J. C., $k=0$ vibrational spectrum for solid α-N_2. J. Chem. Phys. **56**, 2395–2401 (1972).

[538] Rajan, K. J., The 1–0 band of the $b^1\Pi_u - a^1\Pi_g$ transition and the 1–10 and 2–12 bands of the fifth positive system of N_2: Rotational analyses. Proc. R. Irish Acad. **74A**, 17–22 (1974).

[539] Rasetti, F., Selection rules in the Raman effect. Nature (Lond.) **123**, 757–759 (1929).

[540] Rasetti, F., Incoherent scattered radiation in diatomic molecules. Phys. Rev. **34**, 367–371 (1929).

[541] Recknagel, A., Calculation of electronic terms of the nitrogen molecule. Z. Phys. **87**, 375–398 (1934).

[542] Reddy, S. P., and Cho, C. W., Induced infrared absorption of nitrogen and nitrogen-foreign gas mixtures. Can. J. Phys. **43**, 2331–2343 (1965).

[543] Reis, V. H., Oscillator strengths for the N_2 second positive and N_2^+ first negative systems from observations of shock layers about hypersonic projectiles. J. Quant. Spectrosc. Radiat. Transfer **4**, 783–792 (1964).

[544] Roche, A. L., and Lefebvre-Brion, H., Some ab initio calculations related to the predissociation of the $C\ ^2\Sigma_u^+$ state of N_2^+. Chem. Phys. Lett. **32**, 155–158 (1975).

[545] Roncin, J. Y., Electronic transitions of CO, N_2 and NO molecules trapped in solid rare gas matrices: Qualitative discussion. J. Mol. Spectrosc. **26**, 105–110 (1968).

[546] Roncin, J. Y., Damany, N., and Romand, J., Far ultraviolet absorption spectra of atoms and molecules trapped in rare gas matrices at low temperature. J. Mol. Spectrosc. **22**, 154–164 (1967).

[547] Rose, J. Shibuya, T., and McKoy, V., Application of the equations-of-motion method to the excited states of N_2, CO, and C_2H_4. J. Chem. Phys. **58**, 74–83 (1973)

[548] Rowell, R. L., Aval, G. M., and Barrett, J. J., Rayleigh Raman depolarization of laser light scattered by gases. J. Chem. Phys. **54**, 1960–1964 (1971).

[549] Runstraat, C. A., van de, Govers, T. R., Fournier, P. G. and de Heer, F. J., Ion-impact excitation and lifetim of the $C^2\Sigma_u^+$ state of N_2^+. Electronic and Atomi Collisions: Abstracts of papers of the VIIth Inter national Conference on the Physics of Electronic anc Atomic Collisions, Branscomb, L. M., et al. (ed.) pp. 382–3. (North Holland, Amsterdam, 1971).

[550] Runstraat. C. A., van de, Govers, T. R., Maier, W. B., II and Holland, R. F., Extension of the Meinel systen of N_2^+ to high vibrational levels of the $A^2\Pi_u$ state Chem. Phys. Lett. **18**, 549–552 (1973).

[551] Runstraat, C. A., van de, de Heer, F. J., and Govers T. R. Excitation and decay of the $C^2\Sigma_u^+$ state o N_2^+ in the case of electron impact on N_2. Chem Phys. **3**, 431 450 (1974).

[552] Ryan, K. R., Ionic collision processes in gaseous nitrogen. J. Chem. Phys. **51**, 570–576 (1969).

[553] Samson, J. A. R., Angular distributions of photoelectrons and partial photoionization cross sections. Phil. Trans. R. Soc. (Lond.) **A268**, 141–146 (1970).

[553a] Samson, J. A. R., and Cairns, R. B., Absorption and photoionization cross sections of O_2 and N_2 at intense solar emission lines. J. Geophys. Res. **69**, 4583–4590 (1964).

[554] Samson, J. A. R., and Cairns, R. B., Total absorption cross sections of H_2, N_2, and O_2 in the region 550–200 Å. J. Opt. Soc. Amer. **55**, 1035 (1965).

[555] Sanche, L., and Schulz, G. J., Electron transmission spectroscopy: Core-excited resonances in diatomic molecules. Phys. Rev. **A6**, 69–86 (1972); Erratum, **A6**, 2500 (1972).

[556] Saum, K. A., and Benesch, W. M., Infrared electronic emission spectrum of nitrogen. Appl. Opt. **9**, 195–200 (1970).

[557] Saum, K. A., and Benesch, W. M., $W\ ^3\Delta_u - X\ ^1\Sigma_g^+$ system of N_2. Phys. Rev. **2**, 1655–1659 (1970).

[558] Sawada, T., and Kamada, H., Radiative lifetime measurements of some excited states of N_2^+ and CH. Bull. Chem. Soc. Japan **43**, 325–330 (1970).

[559] Sawada, T., and Kamada, H., Radiative lifetime measurements of $N_2(C^3\Pi_u)$, $NH(A^3\Pi)$ and $NH(c^1\Pi)$. Bull. Chem. Soc. Japan **43**, 331–334 (1970).

[560] Sayers, N. D., Meinel's infra-red auroral bands. Proc. Phys. Soc. (Lond.) **A65**, 152–153 (1952).

[561] Sayers, N. D., Taylor, G. R., and Emeleus, K. G., Laboratory production of the Vegard-Kaplan bands. Nature (Lond.) **175**, 254 (1955).

[562] Schadee, A., The relation between the electronic oscillator strength and the wavelength for diatomic molecules. J. Quant. Spectrosc. Radiat. Transfer **7**, 169–183 (1967).

[563] Schnepp, O., The spectra of molecular solids. Adv. At. Mol. Phys. **5**, 155–200 (1969).

[564] Schoen, R. I., and Doolittle, P. H., Energies of electrons and ions released in photoionization. V. Int. Conf. on the Physics of Electronic and Atomic Collisions, held in Leningrad, (July, 1967) pp. 613–615.

[565] Schulz, G. J., Vibrational excitation of N_2, CO, and H_2 by electron impact. Phys. Rev. **A135**, 988–994 (1964).
[566] Schumann, V., Ultraviolet band spectrum of nitrogen. Smithsonian Institute, Smithsonian Contributions to Knowledge. No. 1413 (1903).
[567] Sebacher, D. I., Study of collision effects between the constituents of a mixture of helium and nitrogen gases when excited by a 10 keV electron beam. J. Chem. Phys. **42**, 1368–1372 (1965).
[568] Setlow, R. B., High energy states of N_2^+ and N_2. Phys. Rev. **74**, 153–162 (1948).
[569] Shapiro, M. M., and Gush, H. P., The collision-induced fundamental and first overtone bands of oxygen and nitrogen. Can. J. Phys. **44**, 949–963 (1966).
[570] Shemansky, D. E., N_2 Vegard-Kaplan system in absorption. J. Chem. Phys. **51**, 689–700 (1969).
[571] Shemansky, D. E., Transition probabilities and collision broadening cross section of the N_2 Lyman-Birge-Hopfield system. J. Chem. Phys. **51**, 5487–5494 (1969).
[572] Shemansky, D. E., and Broadfoot, A. L., Excitation of N_2 and N_2^+ systems by electrons: I. Absolute transition probabilities. II. Excitation cross sections and N_2 1PG low pressure afterglow. J. Quant. Spectrosc. Radiat. Transfer **11**, 1385–1400, 1401–1439 (1971).
[573] Shemansky, D. E., and Carleton, N. P., Lifetime of the N_2 Vegard-Kaplan system. J. Chem. Phys. **51**, 682–688 (1969).
[574] Sheng, De T., and Ewing, G. E., Collision induced infrared absorption of gaseous nitrogen at low temperature. J. Chem. Phys. **55**, 5425–5430 (1971).
[575] Shumaker, J. B., Jr., Franck-Condon factors for high rotational levels of nitrogen. J. Quant. Spectrosc. Radiat. Transfer **9**, 153–156 (1969).
[576] Shvangiradze, R. R., Oganezov, K. A., and Chikhladze, B. Y., Isotopic band shifts in the electronic-vibrational spectra of some diatomic molecules. Opt. Spectrosc. (USSR) **8**, 239–242 (1960).
[577] Silverman, S. M., and Lassettre, E. N., Generalized oscillator strengths and electronic collision cross sections for nitrogen at excitation energies above 10 eV. J. Chem. Phys. **42**, 3420–3429 (1965).
[578] Singh, R. B., and Rai, D. K., Potential-energy curves for O_2^+, N_2^+, and CO^+. J. Mol. Spectrosc. **19**, 424–434 (1966).
[579] Spinks, J. W. T., Rotational structure of the Birge-Hopfield bands of N_2. Can. J. Res. **20A**, 1–5 (1942).
[580] Sponer, H., The absorption bands of nitrogen. Z. Phys. **41**, 611–618 (1927).
[581] Sroka, W., Light emission in the vacuum ultraviolet by electron-impact excitation. Part. B. Experiments with nitrogen. Z. Naturforsch. **24a**, 398–403 (1969).
[582] Stalherm, D., Cleff, B., Hillig, H., and Melhorn, W., Energies of excited states of doubly ionized molecules by means of Auger electron spectroscopy. Part I. Electronic states of N_2^{2+}. Z. Naturforsch. **24a**, 1728–1733 (1969).
[583] Stallcop, J. R., N_2^+ potential-energy curves. J. Chem. Phys. **54**, 2602–2605 (1971).
[584] Stedman, D. H., and Setser, D. W., Energy pooling by triplet nitrogen ($A^3\Sigma_u^+$) molecules. J. Chem. Phys. **50**, 2256–2258 (1969).
[585] Stewart, D. T., Electron excitation function of the first negative bands of N_2^+. Proc. Phys. Soc. (Lond.) **A69**, 437–440 (1956).
[586] Stewart, D. T., and Gabathuler, E., Some electron collision cross sections for nitrogen and oxygen. Proc. Phys. Soc. (Lond.) **72**, 287–289 (1958).
[587] Stoebner, A., Delbourgo, R., and Laffitte, P., Observation and characterization of new bands of the nitrogen systems ($C^3\Pi$–$B^3\Pi$) and ($^2\Sigma$–$^2\Sigma$) in the high voltage discharge spectrum of a methane-nitrogen mixture. C. R. Acad. Sci. (Paris) **255**, 1936–1938 (1962).
[588] Stoebner, A., Delbourgo, R., and Laffitte, P., Observation and characterization of a band of the $B^2\Sigma_u^+$–$X^2\Sigma_g^+$ first negative system of nitrogen. C. R. Acad. Sci. (Paris) **259**, 1318–1320 (1964).
[589] Stogryn, D. E., and Stogryn, A. P., Molecular multipole moments. Mol. Phys. **11**, 371–393 (1966).
[590] Stoicheff, B. P., High resolution Raman spectroscopy of gases. III. Raman spectrum of nitrogen. Can. J. Phys. **32**, 630–634 (1954).
[591] Stolterfoht, N., Production of intense satellite lines in Auger spectra of nitrogen by slow proton impact. Phys. Lett. **41A**, 400–402 (1972).
[592] Streets, D. G., Potts, A. W., and Price, W. C., Electron-molecule interactions in photoelectron spectroscopy. Int. J. Mass Spectrom. Ion Phys. **10**, 123–131 (1972–3).
[593] Sullivan, J. O., and Holland, A. C., A congeries of absorption cross sections for wavelengths less than 3000 Å. NASA CR–371 (1966).
[594] Takamine, T., Suga, T., and Tanaka, Y., On the band spectra of nitrogen. Sci. Pap. Inst. Phys. Chem. Res. (Tokyo) **34**, 854–864 (1938).
[595] Takamine, T., Suga, T., and Tanaka, Y., On the shift of intensity in N_2^+ bands excited in helium and neon. Sci. Pap. Inst. Phys. Chem. Res. (Tokyo) **36**, 437–448 (1939).
[596] Tanaka, Y., Extension of the N_2^+ (C–X) bands in the far ultraviolet region. J. Chem. Phys. **21**, 1402–1403 (1953).
[597] Tanaka, Y., Absorption spectrum of nitrogen in the region from 1075 to 1650 Å. J. Opt. Soc. Amer. **45**, 663–664 (1955).
[598] Tanaka, Y., Absorption spectra of nitrogen molecule in the region 600–1500 Å. Mem. Soc. R. Sci. (Liege), Ser. 5 **4**, 198–201 (1961).
[599] Tanaka, Y., Innes, F. R., Jursa. A. S., and Nakamura, M., Absorption spectra of the pink and Lewis-Rayleigh afterglows of nitrogen in the vacuum-uv region. J. Chem. Phys. **42**, 1183–1198 (1965).
[600] Tanaka, Y., and Jursa, A. S., a new method for producing the auroral afterglow of nitrogen and its spectrum. J. Opt. Soc. Amer. **51**, 1239–1245 (1961).
[601] Tanaka, Y., Le Blanc, F., and Jursa, A., Second positive bands in the Lewis-Rayleigh afterglow of nitrogen. J. Chem. Phys. **30**, 1624–1625 (1959).
[602] Tanaka, Y., and Nakamura, M., Selective enhancement of the $b'^1\Sigma_u^+$–$X^1\Sigma_g^+$ and $g^1\Sigma_u^+$–$X^1\Sigma_g^+$ band systems of N_2 in the vacuum ultraviolet region. Sci. Light **16**, 73–90 (1967).
[603] Tanaka, Y., Namioka, T., and Jursa, A. S., New emission bands of N_2^+, $^2\Pi_g$–$A^2\Pi_u$. Can. J. Phys. **39**, 1138–1145 (1961).
[604] Tanaka, Y., Ogawa, M., and Jursa, A. S., Forbidden absorption-band systems of N_2 in the vacuum-ultraviolet region. J. Chem. Phys. **40**, 3690–3700 (1964).
[605] Tanaka, Y., and Takamine, T., Vibrational structure of the $^2\Sigma_g^+$–$^1\Sigma_g^+$ Rydberg series of N_2. Sci. Pap. Inst. Phys. Chem. Res. (Tokyo) **39**, 427–436 (1942).
[606] Tellinghuisen, J., and Albritton, D. L., Predissociation of the $C^2\Sigma_u^+$ state of N_2^+. Chem. Phys. Lett. **31**, 91–96 (1975).
[607] Thrush, B. A., The detection of free radicals in the high intensity photolysis of hydrogen azide. Proc. R. Soc. (Lond.) **A235**, 143–147 (1956).
[608] Thulstrup, E. W., and Andersen, A., Configuration interaction studies of bound, low-lying states of N_2^-, N_2, N_2^+, and N_2^{2+}. J. Phys. B **8**, 965–976 (1975).

[609] Tilford, S. G., and Simmons, J. D., Re-examination of the vacuum ultraviolet emission spectrum of CO in the 950–1200 Å region. J. Mol. Spectrosc. **53**, 436–442 (1974).

[610] Tilford, S. G., Vanderslice, J. T., and Tanaka, Y., A pressure induced electronic transition in N_2. The $w^1\Delta_u - X^1\Sigma_g^+$ system. (Unpublished draft, 1973.)

[611] Tilford, S. G., Vanderslice, J. T., and Wilkinson, P. G., The high resolution absorption spectrum of nitrogen from 1060 to 1520 Å. III. The $B'^3\Sigma_u^- - X^1\Sigma_g^+$ system. Astrophys. J. **141**, 1226–1265 (1965).

[612] Tilford, S. G., Vanderslice, J. T., and Wilkinson, P. G., The high resolution absorption spectrum of nitrogen from 1060 to 1250 Å. V. The $C^3\Pi_u - X^1\Sigma_g^+$ system. Astrophys. J. **142**, 1203–1226 (1965).

[613] Tilford, S. G., and Wilkinson, P. G., The emission spectrum of molecular nitrogen in the region 900–1130 Å. J. Mol. Spectrosc. **12**, 231–288 (1964).

[614] Tilford, S. G., and Wilkinson, P. G., An inverse predissociation in molecular nitrogen. J. Mol. Spectrosc. **12**, 347–359 (1964).

[615] Tilford, S. G., Wilkinson, P. G., and Vanderslice, J. T., The high resolution absorption spectrum of nitrogen from 1060 to 1520 Å. II. The $a'^1\Sigma_u^- - X^1\Sigma_g^+$ system. Astrophys. J. **141**, 427–443 (1965).

[616] Tinti, D. S., and Robinson, G. W., Spectroscopic evidence for slow vibrational and electronic relaxation in solids. The Vegard-Kaplan and second positive systems of N_2 in solid rare gases. J. Chem. Phys. **49**, 3229–3245 (1968).

[617] Tocho, J. O., Ranea Sandoval, H. F., Tagliaferri, A. A., Garavaglia, M., Gallardo, M., and Massone, C. A., Spectroscopic analysis of the crossed field excited $C^3\Pi_u - B^3\Pi_g$ (0–0) UV laser band of N_2 at low temperature. Nouv. Rev. Opt. **5**, 319–322 (1974).

[618] Tschulanowsky, W. M., Rotational structure of the nitrogen band system ($b'-X$) in the Schumann region. Bull. Acad. Sci. (SSR), Classe des Sciences Math. et Nat., Ser. 7, No. 10, 1313–1353 (1935).

[619] Turner, R. G., and Nicholls, R. W., An experimental study of band intensities in the first positive system of N_2. I. Vibrational transition probabilities. II. The transition moment. Can. J. Phys. **32**, 468–474, 475–479 (1954).

[620] Tyte, D. C., Intensity measurements on the nitrogen second positive system in a low temperature discharge. Proc. Phys. Soc. (Lond.) **60**, 1347–1353 (1962).

[621] Tyte, D. C., The effect of helium on the intensity of the second positive system of nitrogen. Proc. Phys. Soc. (Lond.) **80**, 1354–1363 (1962).

[622] Tyte, D. C., Intensity variations of the nitrogen first negative system in nitrogen-helium mixtures. Proc. Phys. Soc. (Lond.) **80**, 1364–1369 (1962).

[623] Tyte, D. C., Some observations on the nitrogen first negative system. Proc. Phys. Soc. (Lond.) **81**, 163–170 (1963).

[624] Tyte, D. C., The effect of environmental conditions on band strength. J. Quant. Spectrosc. Radiat. Transfer **5**, 545–547 (1965).

[625] Vanderslice. J. T., Mason, E. A., and Lippincott, E. R., Interactions between ground-state nitrogen atoms and molecules. The N–N, N–N_2, and N_2–N_2 interactions. J. Chem. Phys. **30**, 129–136 (1959).

[626] Vanderslice, J. T., Mason, E. A., Maisch, W. G., and Lippincott, E. R., Potential curves for N_2, NO, and O_2. J. Chem. Phys. **33**, 614–615 (1960).

[627] Vanderslice, J. T., Tilford, S. G., and Wilkinson, P. G., The high resolution absorption spectrum of nitrogen from 1060–1520 Å. I. The $a\,^1\Pi_g - X\,^1\Sigma_g^+$ system. Astrophys. J. **141**, 395–426 (1965).

[628] Vanderslice, J. T., Tilford, S. G., and Wilkinson, P. G., The high resolution absorption spectrum of nitrogen from 1060 to 1520 Å. IV. The $a\,^1\Pi_g - X\,^1\Sigma_g^+$ system of $N^{14}N^{15}$. Astrophys. J. **142**, 84–93 (1965).

[629] Vanderslice, J. T., Wilkinson, P. G., and Tilford, S. G., Magnetic-dipole and electric-quadrupole transition moments for the $a\,^1\Pi_g - X\,^1\Sigma_g^+$ transition in N_2. J. Chem. Phys. **42**, 2681–2683 (1965).

[629a] van der Wiel, M. J., El-Sherbini, T. M., and Brion, C. E., *K*-shell excitation of nitrogen and carbon monoxide by electron impact. Chem. Phys. Lett. **7**, 161–4 (1970).

[630] van der Ziel, A., Predissociation in the first positive group of N_2 and its bearing on the electronic level diagram of the nitrogen molecule. Physica **1**, 353–362 (1934).

[631] van der Ziel, A., A new band system of nitrogen. Physica **1**, 513–517 (1934).

[632] van der Ziel, A., On the level scheme and band spectra of N_2 and N_2^+. Physica **4**, 373–378 (1937).

[633] Vegard, L., New types of emission spectra. Nature (Lond.) **125**, 14 (1930).

[634] Vegard, L., Continued investigations on light emission from solidified gases. Relations between electronic terms and afterglow of gaseous nitrogen. Z. Phys. **75**, 30–62 (1932).

[635] Vegard, L., and Kvifte, G., Spectral investigations of aurora and twilight. Geofys. Publikasjoner, Norske Videnskaps-Akad. Oslo **16** (7), 3–29 (1945).

[636] Veseth, L., Fine structure of $^3\Pi$ and $^3\Sigma^-$ states in diatomic molecules. J. Phys. B **5**, 229–241 (1972).

[637] Veseth, L., On the calculation of molecular parameters for triplet states in diatomic molecules. The $G\,^3\Delta_g$ and $H\,^3\Phi_u$ states of N_2. Mol. Phys. **26**, 101–107 (1973).

[638] Vinogradov, A. S., Shlarbaum, B., and Zimkina, T. M., *K*-absorption spectrum of nitrogen in the N_2 molecule. Opt. Spectrosc. (USSR) **36**, 383–385 (1974).

[639] Vinogradov, A. S., Zimkina, T. M., Akimov, V. N., and Shlarbaum, B., Structure of absorption spectra of the molecules N_2, O_2, and NF_3 near the ionization thresholds of the inner atomic shells. Bull. Acad. Sci. (USSR), Phys. Ser. **38**, 69–75 (1974).

[640] von der Helm, R., Long-wavelength part of the nitrogen band spectrum. Z. Wiss. Photogr. Photophys. Photochem. **8**, 405–432 (1910).

[641] Wagner, K. H., Afterglow of Ar, N_2, and N_2 plus CH_4 after impact excitation by electron avalanches. Z. Naturforsch. **19a**, 716–721 (1964).

[642] Wallace, L. V., and Nicholls, R. W., The interpretation of intensity distributions in the N_2 second positive and N_2^+ first negative band systems. J. Atmos. Terr. Phys. **7**, 101–105 (1955); Erratum, **24**, 749 (1962).

[643] Watson. J. K. G., Rotational line intensities in $^3\Sigma$–$^1\Sigma$ electronic transitions. Can. J. Phys. **46**, 1637–1643 (1968).

[644] Watson, W. S., Lang, J., and Stewart, D. T., Photoabsorption coefficients of molecular nitrogen in the 300–700 Å region. J. Phys. B **6**, L148–L151 (1973).

[645] Watson, W. W., and Koontz, P. G., Nitrogen molecular spectra in the vacuum untraviolet. Phys. Rev. **46**, 32–37 (1934).

[646] Weeks, J. D., Hazi, A. and Rice, S. A., On the use of pseudopotentials in the quantum theory of atoms and molecules. Adv. Chem. Phys. **16**, 283–342 (1969).

[647] Weiss, A. W., and Krauss, M., Bound-state calculation of scattering resonance energies. J. Chem. Phys. **52**, 4363–4368 (1970).

[648] Weissler, G. L., Lee, P., and Mohr, E. I., Absolute absorption coefficients of nitrogen in the vacuum ultraviolet. J. Opt. Soc. Amer. **42**, 84–90 (1952).

[649] Wentink, T., Jr., Isaacson, L., and Spindler, R. J., Research on the opacity of low temperature air: Oscillator strengths and transition moments of band systems of N_2, O_2, and NO. Air Force Weapons Lab., Air Force Systems Command, Kirtland Air Force Base, New Mexico. (Tech. Rep. AFWL-TR-65-139) (1965).

[650] Wentink, T., Jr., Marram, E. P., and Isaacson, L., Research on the opacity of low temperature air: Oscillator strengths and transition moments of molecular band systems. Air Force Weapons Lab., Air Force Systems Command, Kirtland Air Force Base, New Mexico. (Tech. Rep. AFWL-TR-67-6) (1967).

[651] Werme, L. O., Grennberg, B., Nordgren, J., Nordling, C., and Siegbahn, K. Observation of vibrational fine structure in X-ray emission lines. Phys. Rev. Lett. **30**, 523-524 (1973).

[652] Whalen, J. E., and Green, A. E. S., Analytic independent particle model for molecules. Amer. J. Phys. **40**, 1484-1489 (1972).

[653] Wight, G. R., Brion, C. E., and Van der Wiel, M. J., *K*-shell energy loss spectra of 2.5 keV electrons in N_2 and CO. J. Electron Spectrosc. Related Phenom. **1**, 457-469 (1972-3).

[654] Wilkinson, P. G., The far ultraviolet (C-X) bands of N_2^+. Can. J. Phys. **34**, 250-255 (1956).

[655] Wilkinson, P. G., High resolution absorption spectra of nitrogen in the vacuum ultraviolet. Astrophys. J. **126**, 1-9 (1957).

[656] Wilkinson, P. G., Forbidden band systems in nitrogen. I. The Vegard-Kaplan system in absorption. J. Chem. Phys. **30**, 773-776 (1959).

[657] Wilkinson, P. G., Forbidden band systems in nitrogen. III. The $Y\,^3\Sigma_u^- - X\,^1\Sigma_g^+$ system in absorption. J. Chem. Phys. **32**, 1061-1065 (1960).

[658] Wilkinson, P. G., Refractive dispersion of nitrogen in the vacuum ultraviolet. J. Opt. Soc. Amer. **50**, 1002-1005 (1960).

[659] Wilkinson, P. G., Some unsolved problems in the vacuum ultraviolet. J. Quant. Spectrosc. Radiat. Transfer **2**, 343-348 (1962).

[660] Wilkinson, P. G., and Houk, N. B., Emission spectra of nitrogen in the vacuum ultraviolet. J. Chem. Phys. **24**, 528-534 (1956).

[661] Wilkinson, P. G., and Mulliken, R. S., An electric quadrupole electronic band system in molecular nitrogen. Astrophys. J. **126**, 10-13 (1957).

[662] Wilkinson, P. G., and Mulliken, R. S., Forbidden band systems in nitrogen. II. The $a'\,^1\Sigma_u^- - X\,^1\Sigma_g^+$ system in absorption. J. Chem. Phys. **31**, 674-679 (1959).

[663] Williams, A. J., III, and Doering, J. P., An experimental survey of the low energy electron scattering spectrum of nitrogen. Planet. Space Sci. **17**, 1527-1537 (1969).

[664] Wood, R. W., and Dieke, G. H., The negative bands of $N^{14}N^{15}$. J. Chem. Phys. **6**, 734-739 (1938).

[665] Wood, R. W., and Dieke, G. H., The negative bands of heavy nitrogen molecules. J. Chem. Phys. **8**, 351-361 (1940).

[666] Worley, R. E., Absorption spectrum of N_2 in the extreme ultraviolet. Phys. Rev. **64**, 207-224 (1943).

[667] Worley, R. E., A third Rydberg series of N_2. Phys. Rev. **89**, 863-864 (1953).

[668] Worley, R. E., and Jenkins, F. A., A new Rydberg series in N_2. Phys. Rev. **54**, 305 (1938).

[669] Wray, K. L., and Connolly, T. J., Electronic *f*-number of the N_2^+ (1-) band system. J. Quant. Spectrosc. Radiat. Transfer **5**, 633-635 (1965).

[670] Wu, H. L., and Benesch, W., Evidence for the $^3\Delta_u$-$B^3\Pi_g$ transition in N_2. Phys. Rev. **172**, 31-35 (1968); Erratum, **176**, 423 (1968).

[671] Wulf, O. R., and Melvin, E. H., Band spectra in nitrogen at atmospheric pressure. A source of band spectra excitation. Phys. Rev. **55**, 687-691 (1939).

[672] Wurster, W. H., Measured transition probability for the first positive band system of nitrogen. J. Chem. Phys. **36**, 2111-2117 (1962).

[673] Wurster, W. H., Quantitative spectroscopic studies with the shock tube. J. Quant. Spectrosc. Radiat. Transfer **3**, 355-364 (1963).

[674] Yoshino, T., and Bernstein, H. J., Intensity in the Raman effect. VI. The photoelectrically recorded Raman spectra of some gases. J. Mol. Spectrosc. **2**, 213-240 (1958).

[675] Yoshino, K., Tanaka, Y., Carroll, P. K., and Mitchell, P., High resolution absorption spectrum of N_2 in the vacuum-uv region, $o_{3,4}\,^1\Pi_u \leftarrow X\,^1\Sigma_g^+$ bands. J. Mol. Spectrosc. **54**, 87-109 (1975).

[676] Young, R. A., New theory of active nitrogen. J. Chem. Phys. **60**, 5050-5053 (1974).

[677] Zamanskii, V. M., Stepanov, P. I., Kuzyakov, Yu. Ya., and Moskvitina, E. N. The spectroscopic study of photochemical decomposition of HN_3. Vestnik Moskovaskogo Universiteta; Khimiia **14**, 412-415 (1973).

[678] Zare, R. H., Larsson, E. O., and Berg, R. A., Franck-Condon factors for electronic band systems of molecular nitrogen. J. Mol. Spectrosc. **15**, 117-139 (1965).

[679] Zipf, E. C., Jr., Measurement of the diffusion coefficient and radiative lifetime of nitrogen molecules in the $A\,^3\Sigma_u^+$ state. J. Chem. Phys. **38**, 2034-2035 (1963); Erratum, **39**, 3534 (1963).

Appendix A: Notation and Terminology

The spectroscopic notation used in this report is that adopted in Herzberg's book [12] as modified by recommendations of the Triple Commission on Spectroscopy [J. Opt. Soc. Amer. **43**, 425-30 (1953); **52**, 476-7 (1962); **53**, 883-5 (1963)]. A number of specific conventions used are itemized below.

(1) Wavenumber in cm^{-1} is denoted by σ; ν is reserved for frequency in Hz.

(2) N is total angular momentum of electrons and nuclei exclusive of spin (case b, b', d), formerly denoted by K.

(3) Rotational angular momentum of the nuclei, formerly denoted N, is now denoted by R.

(4) Dissociation energy is written as D° or D^e centrifugal distortion constants (for the zero level or equilibrium value, respectively) are denoted as usual by D_0 and D_e.

(5) A transition is always represented with a dash, as $^2\Pi$-$^2\Sigma$ transition. The upper state is always written first. $\leftarrow$ means absorption; $\rightarrow$ means emission, for an electronic, vibration-rotation, or rotational transition.

(6) A perturbation by one state of another is indicated as e. g., $(^1\Delta\,^1\Pi)$ perturbation, following an early notation of Kovács. (Conventions used in some early papers include $^1\Delta \times\,^1\Pi$ or $^1\Delta$, $^1\Pi$.)

(7) A progression of bands is indicated as follows:
(a) $v''=0$ progression
(b) $(v'-0)$ progression

(8) Reciprocal dispersion is given in Å/mm. However, following the colloquial use of many spectroscopists this quantity is referred to as dispersion.

(9) In the tables, wavelengths above 2000 Å are air wavelengths unless otherwise specified; below 2000 Å vacuum wavelengths are listed.

(10) The known band degradation is indicated by R (red-degraded) or V (violet-degraded) in the headings of section 3 and in the contents.

(11) Rotational constants in the tables are given in units of cm^{-1}.

(12) First negative system is abbreviated as (1–), etc. An alternate abbreviation used in the literature is 1NG, etc.

(13) Powers of 10 as, e.g., 3×10^{-4} can also be found written as $3(10^{-4})$ or, especially in tables, as 3(–4).

(14) Following universal spectroscopic practice, the principal molecular constants are defined so as to have units of cm^{-1}. The actual energy levels may be calculated from the expression

$$E_{v,J}=hc[T_e+G(v)+F_v(J)],$$

where T_e, $G(v)$, and $F_v(J)$ have units of cm^{-1}, h is Plancks constant, and c is the speed of light. $G(v)$ and $F_v(J)$ are defined in terms of the molecular constants in the introduction to table 1.

Appendix B: Physical Constants[1,2,3] and Conversion Factors

$c=2.99792458(1.2)\times10^{10}$ cm·s^{-1}
$h=6.626176(36)\times10^{-34}$ J·s
$N_A=6.022045(31)\times10^{23}$ mol^{-1}
1 eV $\doteq 8065.479(21)$ cm^{-1}
$R_\infty=1.097373177(83)\times10^5$ cm^{-1}
$R(^{14}N_2)=1.097287202\times10^5$ cm^{-1}
$m_e=5.4858026(21)\times10^{-4}$ u
$\mu=\mu_A/N_A$ in g
$^{14}N=14.00307440$ u
$^{15}N=15.0001093$ u
$\mu_A(^{14}N_2)=7.00153720$
$\mu_A(^{14}N^{15}N)=7.242227222$
$\mu_A(^{15}N_2)=7.500054650$
$\mu_A(^{14}N_2^+)=7.00140005$
$r_e(^{14}N_2)=1.55167786\sqrt{\frac{1}{B_e}}$ (B_e in cm^{-1}; r_e in Å)
$r_e(^{14}N_2^+)=1.55169306\sqrt{\frac{1}{B_e}}$

[1] The molecular reduced masses are calculated from the data of Wapstra and Gove. The 1971 atomic mass evaluation. Nuclear Data Tables 9, 265–468 (1971).

[2] The fundamental physical constants and conversion factors are from Cohen and Taylor, The 1973 Least-Squares Adjustment of the Fundamental Constants, J. Phys. Chem. Ref. Data 2, 663–734 (1973).

[3] The uncertainties in parentheses represent one standard deviation in the last digits quoted.